

Tunable Reactivity in Transition Metal-Catalyzed Group Transfer Reactions and Subsequent  
Cyclization Reactions

By

Alicia Marie Phelps

A dissertation submitted in partial fulfillment of  
the requirements for the degree of

Doctor of Philosophy  
(Chemistry)

at the

UNIVERSITY OF WISCONSIN-MADISON

2015

Date of final oral examination: 10/28/2015

The dissertation is approved by the following members of the Final Oral Committee:

Jennifer M. Schomaker, Associate Professor, Chemistry

Weiping Tang, Associate Professor, Pharmacy

Steven D. Burke, Professor, Chemistry

Tehshik P. Yoon, Professor, Chemistry

Daniel C. Fredrickson, Associate Professor, Chemistry

## Abstract

### Tunable Reactivity in Transition Metal-Catalyzed Group Transfer Reactions and Subsequent Cyclization Reactions

Alicia M. Phelps

Under the Supervision of Jennifer M. Schomaker

At the University of Wisconsin – Madison

Controlling the outcome of transition metal-catalyzed group transfer reactions represents a powerful strategy for assembling complex synthesis targets. Herein, we describe two such selective methods, as well as a further method for the functionalization of allene products. First, a carbene transfer in an allene substrate that is controlled by selection of transition metal catalyst is described. These products represent the building blocks of complex frameworks, and a gold-catalyzed carbocyclization from these products is described that leads to fully functionalized cyclopentane rings in only a few steps from the allene substrate. Finally, a silver-catalyzed C-H insertion method that can select between different types of C-H bonds is shown. This methodology complements the others as a strategy for late-stage functionalization of the constructed scaffolds.

## Acknowledgements

Like everything else in life, it really “takes a village” to complete a Ph.D. thesis, and I truly can’t say enough about everyone who helped me during this journey.

First, I would like to thank the members of the Schomaker group for being an inspiring and encouraging group of colleagues. “The Six” were a great bunch to work with for my first few years and I could not have asked for better colleagues than Drs. David Grigg, Jared Rigoli, Cale Weatherly, and Chris Adams. I need to thank Julie Alderson and Nicholas Dolan for experimental work, as well as Dr. Ryan Van Hoveln for constant insight. All three together need to be thanked for creating a welcoming and friendly office to work in. More recently, Ryan Reeves contributed a great deal of experimental work to the Au catalysis project and will continue the work on it moving forward.

None of this work would have been possible without the support of my research advisor Jennifer Schomaker. She is one of the hardest working people I have ever met, and I could not have asked to learn from a better scientist. Helping to establish her group was extremely exciting, and I can’t wait to see what comes from the group in the future.

In my past scientific career, I need to thank my high school science teacher Larry Montgomery, for believing that kids from the middle of the cornfield could do good science and move on to greater heights. At Butler, my advisor Prof. John Esteb was incredibly patient in teaching me the fundamentals of organic research, and Profs. LuAnne McNulty and Stacy O’Reilly were great role models and mentors to me.

On the non-science side, I need to thank my parents, Tim and Ellie Phelps, for believing I could finish, even when they didn’t understand anything about what I do or how grad school

works. My sister Amber went through significant struggles of her own while I was in grad school, and seeing her come out the other side helped keep me going as well. My nieces, Jayden and Addisyn, never failed to cheer me up when I felt like nothing else was going right. My extended family never forgot to include me, even when I was far away for long periods of time, and talking to them always reminded me that there is life outside of lab.

My roleplaying gaming group deserves special mention as well, because sometimes when labwork doesn't go well you need to pretend to smash things with a five foot hammer. They were likewise patient with me falling asleep during night sessions and I will miss the creative interaction with them.

Most of all, I can firmly say that I would not have been able to finish this degree without the support of my partner DJ. He has put up with more tears than either of us ever expected, doing more than his fair share of the chores, and seeing me very little for the last five and a half years. Through all this, his constant refrain has been, "What can I do to help you graduate?" I'm looking forward to helping him find his dream career, since he has put everything on hold for mine.



## Table of Contents

Abstract .....	i
Acknowledgements .....	ii
Table of Contents .....	iv
List of Abbreviations .....	vi
List of Figures, Tables, and Schemes .....	x
Chapter 1 .....	1
1.1. Introduction to Allene Functionalization with Carbenes .....	2
1.2 Reactions of Alkenes with Carbenes .....	3
1.2.1. Intramolecular carbene addition to alkenes .....	5
1.2.2. Intermolecular carbene addition to alkenes .....	8
1.2.3. Conclusions .....	11
1.3. Reactions of Allenes with Carbenes .....	12
1.3.1. Work by the Singleton Group .....	12
1.3.2. Work by the Lautens Group .....	13
1.3.3. Work by the Gregg Group .....	14
1.3.4. Application to one-pot rearrangement .....	16
1.3.5. Examples of C-H insertion reactions .....	17
1.3.6. Conclusions .....	17
1.4. Methods of Allene Synthesis .....	17
1.4.1. Orthoester Johnson-Claisen .....	18
1.4.2. $S_N2'$ cuprate addition to activated alcohols .....	19
1.4.3 Mitsunobu displacement of propargyl alcohols .....	20
1.5 Previous work in the Schomaker group .....	20
1.6 Results and Discussion .....	23
1.6.1. Activation of allenic C-H bonds .....	23
1.6.2. Synthesis of bicyclic methylene cyclopropanes .....	27
1.6.3. Conclusions .....	30
1.7 Experimental section .....	31
1.7.1 General .....	31

1.7.2. General preparation of diazo compounds.....	32
1.7.3. General procedure for allenic C-H insertion reactions .....	37
1.7.4. General procedure for allene reductions .....	42
1.7.5. General procedure for cyclopropanation reactions .....	42
1.8. Bibliography .....	46
Chapter 2.....	51
2.1 Introduction to Gold-Catalyzed Carbocyclization .....	52
2.1.1 Gold Carbocyclizations of Alkynes .....	53
2.1.2 Previous work with allenes .....	56
2.1.3 Previous work with silver-free systems .....	60
2.1.4 Conclusions.....	62
2.2 Results and Discussion .....	63
2.3 Experimental Section .....	73
2.3.1 General procedure for gold reactions .....	74
2.4 Bibliography .....	81
Chapter 3.....	85
3.1. Background.....	86
3.1.1. Previous approaches to selective C-H amination .....	87
3.1.2. Previous work from Schomaker Group.....	93
3.2 Results and Discussion .....	97
3.2.1 Conclusions.....	105
3.3 Experimental Section .....	106
3.3.1 Synthesis of Sulfamate Substrates .....	106
3.3.2. Investigation of Counteranion Effects.....	131
3.3.3 Synthesis of C-H Insertion Products .....	131
3.3.4 Stereochemical Probe .....	154
3.4 Bibliography .....	159
Appendix I. Selected $^1\text{H}$ and $^{13}\text{C}$ NMR Spectra.....	163

## List of Abbreviations

Å	angstrom(s)
Bn	benzyl
br d	broad doublet
br s	broad singlet
Bu	normal-butyl
C	Celsius
cat.	catalyst
COSY	correlation spectroscopy
Cy	cyclohexyl
d	doublet
dd	doublet of doublets
ddd	doublet of doublets of doublets
dq	doublet of quartets
<i>dr</i>	diastereomeric ratio
dt	doublet of triplets
EI	electron ionization

equiv	equivalent
ESI	electrospray ionization
Et	ethyl
EtOAc	ethyl acetate
g	gram
h	heptet
h	hour
HRMS	high resolution mass spectrometry
Hz	hertz
<sup>i</sup> Pr	<i>iso</i> -propyl
<i>J</i>	spin-spin coupling in hertz
M	molar
m	multiplet
Me	methyl
mg	milligram
min	minute
mL	milliliter

mM	millimolar
mmol	millimole
mol	moles
MS	molecular sieves
NMR	nuclear magnetic resonance spectroscopy
OAc	acetate
OBn	benzoate
OMe	methoxy
Ph	phenyl
phen	1,10-phenanthroline
PPh <sub>3</sub>	triphenylphosphine
ppm	parts per million
Pr	normal-propyl
q	quartet
qd	quartet of doublets
R <sub>f</sub>	retention factor
rt	room temperature

s	singlet
TBS	<i>tert</i> -butyldimethylsilyl
<sup>t</sup> Bu	<i>tert</i> -butyl
td	triplet of doublets
THF	tetrahydrofuran
TLC	thin layer chromatography
tt	triplet of triplets
δ	chemical shift in ppm
μL	microliter
μmol	micromol

## List of Figures, Tables, and Schemes

<b>Scheme 1.1.</b> Possible modes of reactivity between carbenes and alkenes.	2
<b>Scheme 1.2.</b> General mechanism of carbene C-H bond insertion.	4
<b>Scheme 1.3.</b> General mechanism of carbene cyclopropanation.	4
<b>Scheme 1.4.</b> Rh(II) lantern complex ligand control of chemoselectivity.	5
<b>Scheme 1.5.</b> Selectivity between allylic C-H and tertiary alkene with rhodium acetate dimer.	6
<b>Table 1.1.</b> Chemoselectivity using enantioenriched Rh(II) catalysts.	7
<b>Scheme 1.6.</b> Selectivity for cyclopropanation using copper(II) catalysis.	8
<b>Scheme 1.7.</b> Reactivity vs. selectivity of carbene precursors.	9
<b>Table 1.2.</b> Intermolecular carbene reactivity with <i>trans</i> alkenes.	10
<b>Scheme 1.8.</b> Intermolecular carbene reactivity with dihydronaphthalenes.	11
<b>Scheme 1.9.</b> Carbene reactivity with allenes.	12
<b>Scheme 1.10.</b> Intermolecular cyclopropanation of silylallenes.	12
<b>Scheme 1.11.</b> Radical annulations of methylenecyclopropanes.	13
<b>Scheme 1.12</b> Simmon-Smith cyclopropanation of $\beta$ -allenic alcohols.	13
<b>Table 1.3.</b> Intramolecular carbene addition to allenes.	14
<b>Scheme 1.13.</b> Enantioselective intermolecular cyclopropanation of simple allenes.	15
<b>Scheme 1.14.</b> Intermolecular enantioselective cyclopropanation of 1,3-disubstituted allenes.	15
<b>Scheme 1.15.</b> Combined cyclopropanation/rearrangement of allenes.	16
<b>Scheme 1.16.</b> C-H insertion in photochemical allene reaction.	17
<b>Scheme 1.17.</b> Orthoester Claisen rearrangement with propargyl alcohols.	18
<b>Scheme 1.18.</b> Gold-catalyzed vinyl ether rearrangement to allenes.	19
<b>Scheme 1.19.</b> Cuprate addition to propargyl tosylates.	19

<b>Scheme 1.20</b> Mitsunobu displacement of propargyl alcohols.	20
<b>Table 1.4.</b> C-H amination with homoallenic carbamates.	21
<b>Table 1.5.</b> Conversion of homoallenic sulfamates to stereotriads.	21
<b>Scheme 1.21.</b> Transfer of axial chirality to stereotriad.	22
<b>Scheme 1.22.</b> Further transformation of C-H amination products.	22
<b>Scheme 1.23.</b> Divergent reactivity of diazo-containing allene substrates.	23
<b>Table 1.6.</b> Rh-catalyzed optimization of C-H insertion.	24
<b>Table 1.7.</b> Scope of the Rh-catalyzed C-H insertion.	26
<b>Scheme 1.24.</b> Verifying the <i>trans</i> stereochemistry of <b>1.79</b> .	27
<b>Table 1.6.</b> Optimization of Cu-catalyzed allene cyclopropanation.	28
<b>Table 1.7.</b> Scope of cyclopropanation of allenes.	29
<b>Table 2.1.</b> Hydration of alkynones with palladium and gold catalysis.	52
<b>Scheme 2.1.</b> Conia-ene cyclization of alkynes.	53
<b>Scheme 2.2.</b> Possible mechanistic pathways for alkyne cyclization.	54
<b>Table 2.2.</b> 5- <i>endo-dig</i> carbocyclization of alkynes.	55
<b>Scheme 2.3.</b> Cyclopentene annulation using allenyltriphenylstannane.	55
<b>Scheme 2.4.</b> Use of alkyne carbocyclization in the synthesis of (+)-lycopoladine A.	56
<b>Scheme 2.5.</b> Cyclization of silyl enol ether onto 1,1-disubstituted allene.	56
<b>Table 2.3.</b> Au-catalyzed cyclization of 2-(2',3'-allenyl)acetylacetates	57
<b>Table 2.4.</b> Hydroarylation of allenes using pyrrole nucleophiles.	58
<b>Scheme 2.6.</b> Gold-catalyzed hydroarylation of allenes with indole nucleophiles.	59
<b>Scheme 2.7.</b> Intramolecular hydroarylation of electron-rich aryl allenes.	60



<b>Scheme 2.8.</b> Use of copper salts as Au(I) halide scavenger.	61
<b>Table 2.5.</b> Effects of various two-component catalyst systems on hydroalkylation.	62
<b>Scheme 2.9.</b> Extension of previous C-H insertion chemistry to form cyclopentanes.	63
<b>Scheme 2.10.</b> Highly substituted cyclopentane natural products.	64
<b>Table 2.6.</b> Initial screening of gold carbocyclization conditions.	65
<b>Table 2.7.</b> Catalyst screening for Au-catalyzed carbocyclization.	66
<b>Figure 2.1.</b> Possible coordination geometries of gold to allene.	67
<b>Scheme 2.11.</b> Epimerization of cyclopentene products.	68
<b>Table 2.8.</b> Screening of chiral ligands and acids for diastereoselectivity.	69
<b>Table 2.9.</b> Exploration of Au:Cu ratio for increased diastereoselectivity.	70
<b>Table 2.10.</b> Substrate scope of Au-catalyzed carbocyclization.	71
<b>Scheme 2.12.</b> Further reactivity of carbocyclization products.	72
<b>Scheme 3.1.</b> Selective nitrene insertion into C-H bonds.	86
<b>Table 3.1.</b> Catalyst influence on sulfamate C-H amination selectivity.	88
<b>Scheme 3.2.</b> Intermolecular amination using a variety of sulfamates.	89
<b>Table 3.2.</b> Oxidation of sulfamate esters with rhodium and ruthenium catalysts.	90
<b>Table 3.3.</b> Reactivity trends for C-H allylic amination.	92
<b>Table 3.4.</b> Intramolecular C-H amination with Fe(qpy) catalyst.	93
<b>Table 3.5.</b> Chemoselective Ag-catalyzed aziridination vs. C-H amination	94
<b>Table 3.6.</b> Chemoselective amination of allenes using silver catalysis.	95
<b>Table 3.7.</b> Chemoselective amination of alkenes using silver catalysis.	96

<b>Table 3.8.</b> Ligand-controlled, silver-catalyzed C–H amination.	98
<b>Table 3.9.</b> Investigation of steric effects on selectivity.	100
<b>Table 3.10.</b> Further study of site-selectivity.	101
<b>Table 3.11.</b> Exploration of electronic effects.	102
<b>Figure 3.1.</b> Hammett plots using ( <sup>t</sup> Bubipy) <sub>2</sub> AgOTf and (tpa)AgOTf.	103
<b>Scheme 3.3.</b> Mechanistic studies of nitrene transfer.	104
<b>Table 3.10.</b> Insight into future catalyst design.	105

## Chapter 1

### Divergent Reactivity of Allene-Containing $\alpha$ -Diazoesters using Cu and Rh Catalysis

Parts of this work are reproduced from:

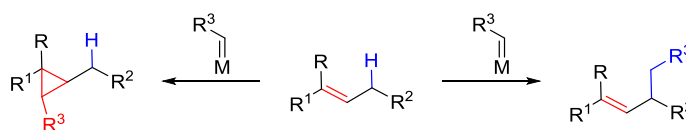
Phelps, A. M.; Dolan, N. S.; Connell, N. T.; Schomaker, J. M. *Tetrahedron*, **2013**, 69, 5614.

with permission from Elsevier.

## 1.1. Introduction to Allene Functionalization with Carbenes

The formation of new C-C bonds through the use of carbenes is a field with a long and productive history, with the first recorded synthesis of a diazocarbonyl compound dating back to the 1880's.<sup>1</sup> One particularly intriguing class of substrates in carbene reactions has been alkenes.<sup>2</sup> Alkenes have the possibility to undergo two different reactions with carbenes: direct interaction with the alkene yields cyclopropanes (Scheme 1.1, left), while C-H insertion at the activated allylic position yields elaborated carbon scaffolds (Scheme 1.1, right). Both of these reactions are synthetically powerful. Cyclopropanes are common structural subunits in biologically active products,<sup>3</sup> and interest in cyclopropanes as synthetic intermediates is still growing.<sup>4</sup> The power of C-H insertion as a method cannot be overstated; the direct formation of carbon-carbon bonds selectively in a complex chemical environment is a distinct departure from the traditional strategy of functionalizing pre-existing groups, and advances in this field can fundamentally change the way target synthesis is approached.<sup>5</sup>

**Scheme 1.1.** Possible modes of reactivity between carbenes and alkenes.



In many cases, the greatest challenge of using alkenes as substrates has been regiocontrol between competing cyclopropanation and C-H insertion at the activated allylic position. This obstacle is of prime importance if the methods are going to be useful for complex synthesis, as sites of unsaturation are ubiquitous in natural products. This means that any carbene method that is to be applied to complex intermediates must be able to perform one of the two reactions

selectivity, to avoid mixtures of products in complex chemical environments. The problem of has been addressed with varying levels of success for different classes of alkenes.

An extension of this carbene chemistry is the addition of carbenes to allene substrates. Allenes provide several advantages over alkenes. They allow for functionalization of three contiguous carbons over two, often avoiding the problems that result from stereochemical mismatching in alkenes containing an adjacent stereocenter.<sup>6</sup> In addition, allenenes are easily synthesized in an enantioenriched fashion, and the axial chirality can be transferred into point chirality during the course of the reaction.<sup>7</sup>

This chapter will focus on strategies which lead to chemoselectivity between C-H insertion and cyclopropanation in the reactions of carbenes with alkenes, previous studies of carbenes with allenenes, and our work with chemoselective carbene transfer to allenenes.

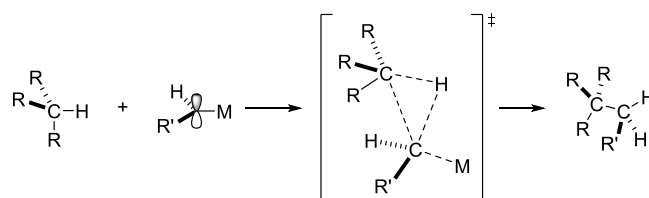
## 1.2 Reactions of Alkenes with Carbenes

The reactivity of transition metal carbenoid species with alkenes is a wide field, and several reviews have covered this topic.<sup>2a,8</sup> Relevant to allene studies is the regioselectivity between two possible modes of reactivity: cyclopropanation through carbene addition to the double bond (Scheme 1.1, left) and insertion into the activated allylic C-H bond (Scheme 1.1, right).

There are a variety of factors to be considered in these transformations; however, a basic study of the accepted mechanism of each is instructive. This discussion will focus on reactions catalyzed by rhodium(II) lantern complexes, as these are one of the most commonly used classes of catalysts. The C-H insertion is thought to proceed in a concerted but asynchronous manner, as

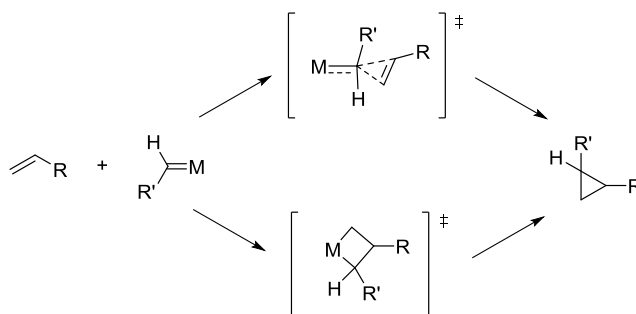
shown in Scheme 1.2. This process is initiated by the overlap of the p-orbital of the metal carbene with the  $\sigma$ -bond of the reacting C-H bond.<sup>9</sup> The reaction then proceeds through a three center interaction, in which C-C and C-H bond formation occur as the metal species dissociates to deliver the C-H insertion product. The degree to which the C-C bond has formed when the C-H bond is broken depends on the structure of both the C-H insertion substrate and the carbene precursor that is used.<sup>10</sup>

**Scheme 1.2.** General mechanism of carbene C-H bond insertion.



Cyclopropanation is also considered to be an asynchronous concerted reaction.<sup>10</sup> As shown in Scheme 1.3, there are two possible mechanisms that could be envisioned: a concerted reaction (top) and a discrete metalocycle that undergoes reductive elimination to the product (bottom). Experimental Hammett and KIE studies, as well as several computational studies favor the concerted mechanism.

**Scheme 1.3.** General mechanism of carbene cyclopropanation.

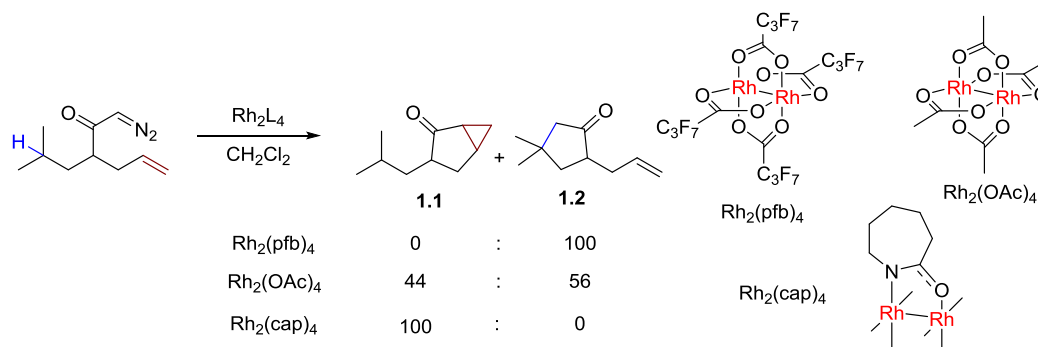


Both mechanisms begin with the formation of the same metal carbene species, meaning a variety of factors can control the selectivity of the reaction, including the transition metal used, the ligand on the metal, as well as both electronic and steric features of the substrate. This chemistry has been investigated in both intra- and intermolecular reactions, and each will be examined in more detail below.

### 1.2.1. Intramolecular carbene addition to alkenes

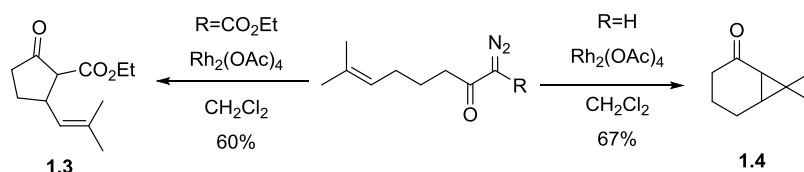
Since the first report by Teyssie in the 1970s<sup>11</sup> rhodium catalysts have generally been the catalyst of choice for diazo decomposition reactions. Most studies of chemoselectivity focus on tuning the properties of Rh(II) lantern catalysts to achieve the desired product. One very striking example comes from the Padwa group,<sup>12</sup> which demonstrated a complete switch in chemoselectivity through tuning of the carboxylate or carboxamide ligands on the rhodium catalyst (Scheme 1.4). It was noted that an increase in electron density at the metal center, accomplished by switching the ligand from the electron withdrawing perfluorobutyrate to the comparatively electron rich caprolactam ligand, corresponds to a direct increase in the amount of cyclopropanation product **1.1**; however, this control is very substrate dependent.

**Scheme 1.4.** Rh(II) lantern complex ligand control of chemoselectivity.



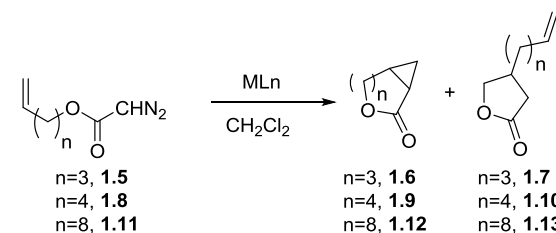
For example, trisubstituted olefins exhibited a lesser degree of catalyst control and substrate preferences became dominant.<sup>13</sup> As seen in Scheme 1.5, the same  $\text{Rh}_2(\text{OAc})_4$  catalyst that previously gave a mixture of products is very selective for C-H insertion product **1.3** when  $\alpha$ -diazo- $\beta$ -ketoesters are the substrate, and similarly selective for the cyclopropanation product **1.4** when  $\alpha$ -diazo ketones are used.

**Scheme 1.5.** Selectivity between allylic C-H and tertiary alkene with rhodium acetate dimer.



These results imply that rhodium selectivity is complex, and depends on a variety of factors. Moving to a more synthetically relevant system bears out that observation. The Doyle group demonstrated an example in which a C-H insertion reaction is possible and poor selectivity is observed with a variety of enantioenriched Rh catalysts (Table 1.1, entries 1-6),<sup>14</sup> though intriguingly, a copper catalyst with these same substrates shows a strong preference for cyclopropanation over C-H insertion (entry 7). It is important to note that in both examples, the C-H insertion results in a five-membered ring. This preference of rhodium carbenoid species to form five membered rings is well-precedented<sup>15</sup> and informs substrate design for reactions of this type.

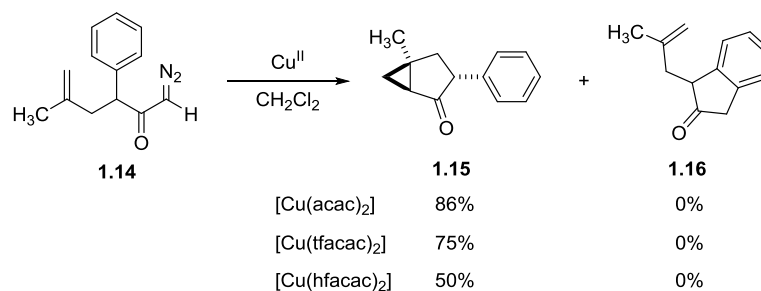


**Table 1.1.** Chemoselectivity using enantioenriched Rh(II) catalysts.


Entry	Catalyst	1.6:1.7	1.9:1.10	1.12:1.13
1	Rh <sub>2</sub> (OAc) <sub>4</sub>	>99:1	84:16	68:32
2	Rh <sub>2</sub> (5S-MEPY) <sub>4</sub>	42:58	14:86	4:96
3	Rh <sub>2</sub> (4S-MEOX) <sub>4</sub>	19:81	9:91	1:99
4	Rh <sub>2</sub> (4S-MPPIM) <sub>4</sub>	47:53	13:87	2:98
5	Rh <sub>2</sub> (4S-IBAZ) <sub>4</sub>	92:8	50:50	18:82
6	Rh <sub>2</sub> (5S-TBPRO) <sub>4</sub>	>99:1	82:18	79:21
7	Cu(box)PF <sub>6</sub>	>99:1	>99:1	86:14

<sup>a</sup> Ratios were obtained by GC (SBP-5 column).

Copper catalysts show a marked preference for cyclopropanation over C-H insertion in many cases. For example, the Padwa group did a similar selectivity study using a copper catalyst and substrate **1.14** (Scheme 1.6),<sup>16</sup> which compares propensity for cyclopropanation or insertion into an aromatic C-H bond. In contrast to rhodium, all copper catalysts were completely selective for cyclopropanation over C-H insertion, despite significant changes in the electronic structure of the ligand. In comparison to the Rh-catalyzed C-H insertion reactions, the copper cyclopropanation reaction is somewhat less selective for a particular ring size, though five and six-membered rings are generally favored.

**Scheme 1.6.** Selectivity for cyclopropanation using copper(II) catalysis.

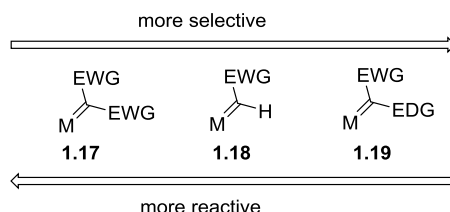
In conclusion, rhodium catalysis can often be harnessed to change the chemoselective outcome of intramolecular carbenoid reactions. Both electronic and steric control plays a role, and a variety of carboxylate and carboxamide catalysts can be utilized for both racemic and enantioenriched transformations. In addition, copper systems show selectivity for cyclopropanation that is distinct from the rhodium catalysts.

### 1.2.2. Intermolecular carbene addition to alkenes

One aspect of carbene chemistry that must be discussed is the role of the carbene precursor that is used. Most of the intramolecular chemistry utilizes more reactive precursors containing one or more electron withdrawing groups of the diazo group, such as **1.17** and **1.18** in Scheme 1.7. These groups make the resulting metal-carbene species more electrophilic, thereby promoting reactivity. However, the use of “donor-acceptor” carbenes like **1.19**, containing one electron donating group along with one electron withdrawing group, was pioneered by Huw Davies and co-workers,<sup>17, 18</sup> and this discovery was crucial to the application of carbene chemistry in an intermolecular sense. These carbenes can be thought of as lying on a dual spectrum of reactivity and selectivity, where the more electron-poor precursors generally are

more reactive, but the electron-rich precursors tend to be more selective due to their attenuated reactivity.<sup>19</sup>

**Scheme 1.7.** Reactivity vs. selectivity of carbene precursors.



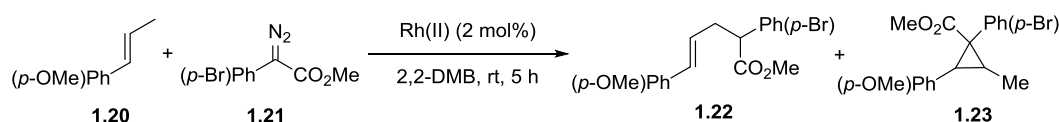
The less reactive nature of the so-called “donor-acceptor” carbenes has enabled significant advances to be made in intermolecular reactivity; the reduced reactivity leads to higher selectivities. One point of note in comparing the use of the donor-acceptor groups, in comparison to acceptor-acceptor groups, is the inclusion of the aryl or vinyl group in the final product. Many of the acceptor groups are carbonyl derived groups that can either be hydrolyzed or through a decarboxylation; the donor groups are more difficult to remove if they are not desired as part of the final structure.

Nonetheless, the reaction of carbenes with allylic substrates has been pursued intermolecularly, providing some interesting insights. In general, the tendency of donor-acceptor carbenes to perform C-H insertion or cyclopropanation is controlled by the sterics of the substrate, with the less hindered alkenes undergoing cyclopropanation, and more hindered alkenes undergoing C-H insertion.<sup>20</sup> However, there are a few cases where neither C-H insertion or cyclopropanation are especially favored, and these cases allow for study of the factors leading to chemoselectivity.<sup>21</sup> In Table 1.2, the substrate **1.20** contains a *trans* substituted alkene and a primary allylic C-H bond. Neither of C-H insertion nor cyclopropanation of these groups is

especially favorable, as the *trans* alkene is sterically hindered and the primary C-H bond cannot support buildup of positive charge as well as a secondary allylic position would.

When using the standard catalyst of choice,  $\text{Rh}_2(\text{S-DOSP})_4$ , some selectivity for the C-H insertion is achieved but the racemic catalysts tested showed no preference between the two sites of reactivity. High selectivity for C-H insertion was eventually achieved using the very bulky  $\text{Rh}_2(\text{O}_2\text{CCPh}_3)_4$ . Selectivity for cyclopropanation is achieved with the  $\text{Rh}_2(\text{esp})_2$  catalyst pioneered by the DuBois group, but no rationale for this selectivity is given.

**Table 1.2.** Intermolecular carbene reactivity with *trans* alkenes.

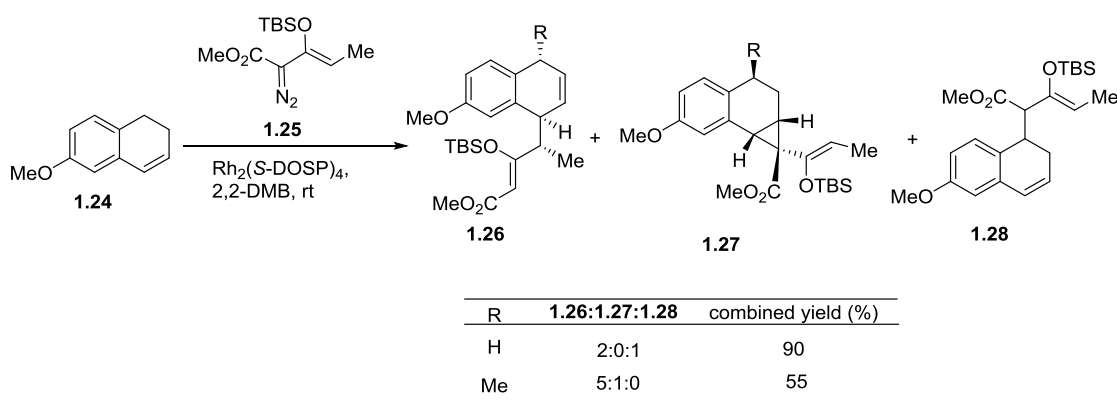


Catalyst	Ratio	yield <b>1.22</b>	yield <b>1.23</b>
$\text{Rh}_2(\text{S-DOSP})_4$	3:1	62%	22%
$\text{Rh}_2(\text{OAc})_4$	1:1	19%	16%
$\text{Rh}_2(\text{O}_2\text{CCF}_3)_4$	1:1	18%	12%
$\text{Rh}_2(\text{O}_2\text{CCMe}_3)_4$	1:4	10%	48%
$\text{Rh}_2(\text{O}_2\text{CCPh}_3)_4$	>15:1	74%	0%
$\text{Rh}_2(\text{esp})_2$	1:>15	0%	74%

A more recent example showed the further difficulties that arise when applying intermolecular carbene chemistry to complex natural products.<sup>22</sup> In the example demonstrated in Scheme 1.8, the authors attempted to access the combined C-H insertion/Cope rearrangement product **1.26** while trying to synthesize analogs of (+)-erogorgianene. However, very poor regioselectivity was observed when electron rich substrates such as **1.24** were used. The reaction of OTBS-substituted carbene **1.25** was known to give superior results in previous work,<sup>23</sup> and this was successful when  $\text{Rh}_2(\text{S-DOSP})_4$  was used, in that only C-H insertion products were obtained; however, there was still no control between the desired allylic C-H insertion that would

results in **1.26** and simple benzylic insertion to result in **1.28**. Due to the sensitivity of donor-acceptor carbenes to steric effects, the addition of a methyl group at the benzylic insertion position shut down formation of that product, allowing for a higher proportion of **1.26** to be formed, though the overall yield suffered.

**Scheme 1.8.** Intermolecular carbene reactivity with dihydronaphthalenes.



These examples demonstrate that the intermolecular reactivity of alkenes still faces regioselectivity challenges, and that there is still much to learn about how to obtain selective reactivity with rhodium lantern catalysts and donor-acceptor carbene precursors.

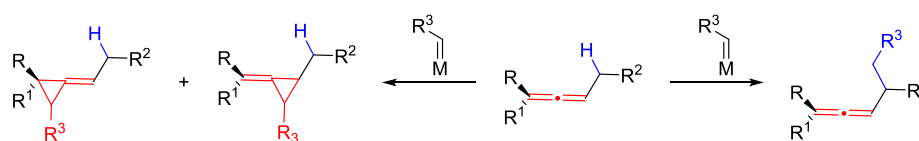
### 1.2.3. Conclusions

In summary, the chemistry of carbenes derived from diazocarbonyl species reacting with alkenes has been explored widely by a variety of groups. Generally, rhodium catalysts can be modulated to provide some amount of chemoselectivity between C-H insertion and cyclopropanation. However, the chemoselectivity does not always translate well between different groups of substrates and must often be reevaluated for each new set of substrates that is used.

### 1.3. Reactions of Allenes with Carbenes

While reactivity of carbenes has been extensively investigated with alkenes (see Part 1.2), much less attention has been focused on the use of this approach with allenes. In addition to the chemoselectivity between cyclopropanation and C-H insertion, allenes also have the additional regiochemical challenge of selecting for one double bond over the other (Scheme 1.9).

**Scheme 1.9.** Carbene reactivity with allenes.

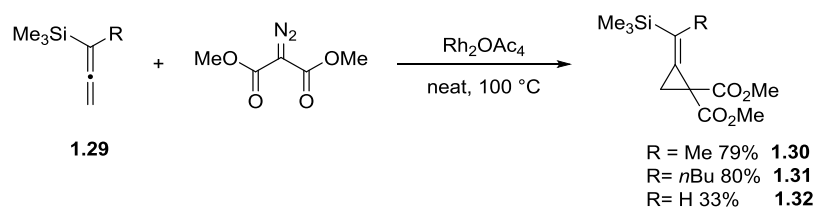


Initial investigations of the reaction of carbenes with allenes were most successful with dihalocarbenes<sup>24</sup>, as the first attempts to use diazo compounds as precursors<sup>25</sup> showed poor selectivity and often resulted in the generation of spiropentanes.

#### 1.3.1. Work by the Singleton Group

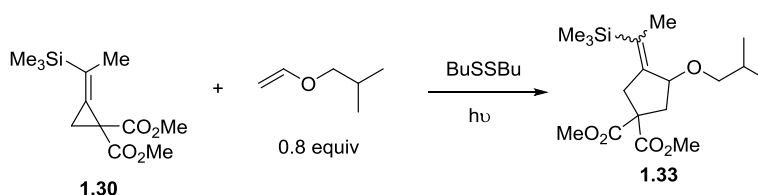
New interest into the reactions of allenes with diazo compounds emerged in the 1990s, and along with it came a second generation of reaction conditions. The Singleton group first synthesized methylene cyclopropanes **1.30-1.32** by reaction of dimethyldiazomalonate with the unsymmetrical allene **1.29** using rhodium (II) acetate as a catalyst.<sup>26</sup>

**Scheme 1.10.** Intermolecular cyclopropanation of silylallenes.



The selectivity for the bond distal to the silyl group is likely to be due to the  $\beta$ -silicon effect stabilizing the developing partial positive charge in the transition state. Singleton went on to demonstrate the utility of the methylenecyclopropane products in radical annulations with alkenes to form five membered rings as shown in Scheme 1.11, but did not further explore the scope of methylenecyclopropanes.

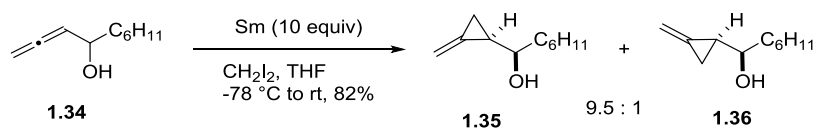
**Scheme 1.11.** Radical annulations of methylenecyclopropanes.



### 1.3.2. Work by the Lautens Group

The Lautens group demonstrated a Simmons-Smith cyclopropanation of  $\alpha$ -allenic alcohols that showed high chemoselectivity for methylenecyclopropane carbinols, in addition to high diastereoselectivity (Scheme 1.12).<sup>27</sup> Previous attempts at Simmons-Smith functionalization of allenes resulted in a mixture of products.<sup>28</sup> However, a modification of a procedure used for geraniol<sup>29</sup> enabled directed cyclopropanation of allenic alcohols to give selective hydroxyl-directed cyclopropanation at the double bond adjacent to the alcohol, in moderate yields (30-82%) and high diastereoselectivities.

**Scheme 1.12** Simmons-Smith cyclopropanation of  $\beta$ -allenic alcohols.



Following their success with allenic alcohols, the Lautens group investigated an alternative route to methylenecyclopropanes,<sup>30</sup> using a copper(II) catalyst to promote intramolecular cyclopropanation of an allene, as shown in Table 1.3. Only terminal allenes were used, and the best results were obtained with silyl-substituted allene starting materials. While the  $\beta$ -silicon effect directs reactivity to the bond further away from the silyl group in Scheme 1.10, the selectivity in the intramolecular case is presumably driven by selectivity for the 5-membered ring formation. The complete selectivity for cyclopropanation (no C-H insertion product was reported) echoed the earlier results when copper was used with diazo precursors.<sup>16</sup>

**Table 1.3.** Intramolecular carbene addition to allenes.

Entry	n	R1	R2	R3	yield	dr
1	0	-(CH <sub>2</sub> ) <sub>5</sub> -		H	94%	--
2	1	Me	Me	H	76%	--
3	2	H	H	H	-- (Complex mixture)	
4	0	H	Ph	H	84%	50/50
5	0	H	cHex	H	82%	55/45
6	1	H	tBu	H	83%	53/47
7	0	H	cHex	Me	89%	65/35
8	0	H	cHex	Me <sub>3</sub> Si	90%	80/20
9	0	H	Ph	Me <sub>3</sub> Si	90%	85/15
10	0	H	tBu	Me <sub>3</sub> Si	78%	94/6
11	0	H	cHex	tBuPh <sub>2</sub> Si	60%	90/10

a) Cu(TBS)<sub>2</sub> = bis-(N-tert-butylsalicylaldehyde)copper(II). b) Isolated yields of analytically pure products. c) Diastereomeric ratio measured on the <sup>1</sup>H NMR spectra of the crude reaction mixture.

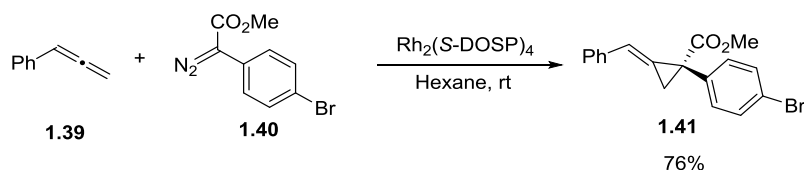
### 1.3.3. Work by the Gregg Group

The Gregg group has demonstrated successful intermolecular enantioselective cyclopropanation of allenes<sup>31</sup> using the Rh<sub>2</sub>(S-DOSP)<sub>4</sub> catalyst developed by the Davies group. The general transformation is shown in Scheme 1.13. Simple mono- and 1,1-disubstituted



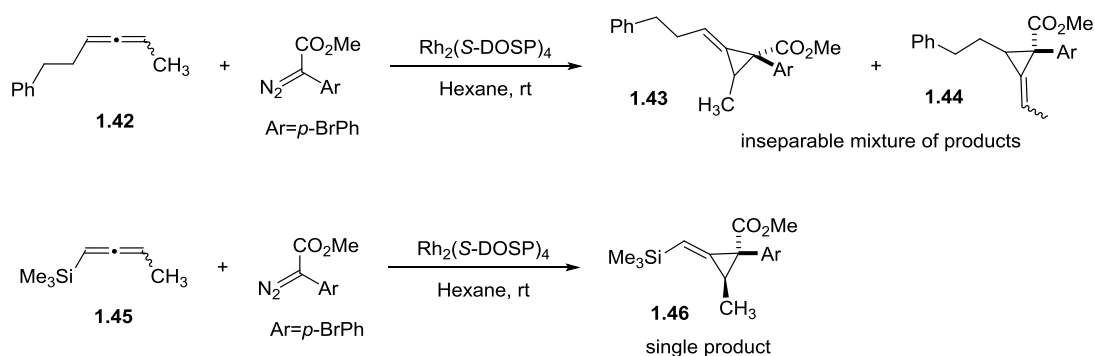
allenes can be transformed into the appropriate methylenecyclopropane in moderate yields, and with high *ee*'s.

**Scheme 1.13.** Enantioselective intermolecular cyclopropanation of simple allenes.



However, in further investigations using 1,3-disubstituted allenes,<sup>32</sup> regioselectivity proved quite difficult. As shown in Scheme 1.14, 1,3-disubstituted allenes gave complex mixtures of the possible cyclopropanation products **1.43** and **1.44**, except in the case of silyl-substituted allenes, in which only **1.46**, the product of distal cyclopropanation is observed. This echoes the observation made by Singleton earlier, and suggests that the  $\beta$ -silicon effect accelerates reaction at that position. In addition, only one diastereomer is observed.

**Scheme 1.14.** Intermolecular enantioselective cyclopropanation of 1,3-disubstituted allenes.

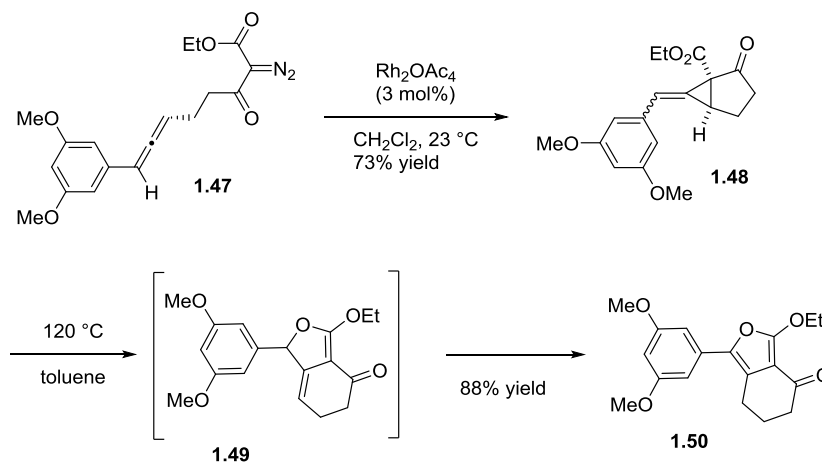


Overall, these results suggest that the regioselectivity of intermolecular cyclopropanation will be difficult to control in the context of a complex target.

### 1.3.4. Application to one-pot rearrangement

Though only a few methodologies have been developed with allenes, their utility can clearly be seen in a demonstration by the Sarpong group,<sup>33</sup> which showed a formal [3+2] cycloaddition/isomerization sequence that yields tetrasubstituted furans (Scheme 1.15). The method begins with diazoallene **1.47**, undergoes a cyclopropanation of the proximal double bond using  $\text{Rh}_2(\text{OAc})_4$ . The methylenecyclopropane can then rearrange to the tetrasubstituted furan **1.50** upon heating in toluene.

**Scheme 1.15.** Combined cyclopropanation/rearrangement of allenes.

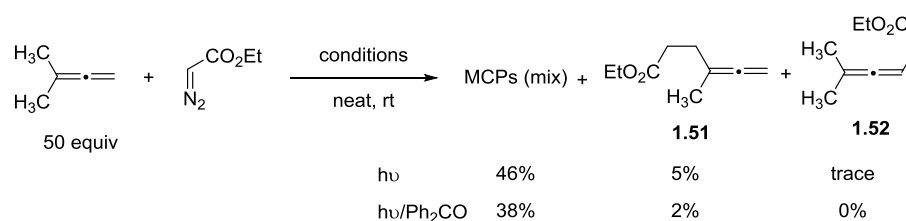


This protocol uses the power of carbene-allene chemistry to access a substitution pattern that is otherwise difficult to synthesize, and shows the potential of this chemistry to be used for highly functionalized products. These types of transformations are outside the realm of possibility for simple alkene-carbene chemistry, and demonstrate how allenes in particular allow new modes of access to chemical space.

### 1.3.5. Examples of C-H insertion reactions

In comparison to the wealth of cyclopropanation examples, almost no mention is made of C-H insertion products with allenic substrates. Creary mentions observing small amounts (approximately 5%)<sup>24b</sup> of C-H insertion products as byproducts when using photochemical methods of promoting allene/carbene reactions (Scheme 1.16), but beyond this no explorations of allenic C-H insertion had been performed in the chemical literature.

**Scheme 1.16.** C-H insertion in photochemical allene reaction.



### 1.3.6. Conclusions

In summary, allene chemistry with carbenes represents a powerful strategy for construction of carbon skeletons and the utility of the method is still being expanded. Many of the methods thus far have been tested on simple terminal allenes without extraneous functionality, and have focused exclusively on cyclopropanation. No examples existed previously wherein an allene could be used to either form a C-H insertion product or a methylene cyclopropane selectively in an intramolecular reaction. This approach opens up the possibility of building a complex carbocyclic skeleton rapidly, and will be the subject of Section 1.5.

## 1.4. Methods of Allene Synthesis

Many discussions of allene chemistry are dismissed due to the perceived difficulty of installing the allene initially. A wealth of information exists on the synthesis of many different

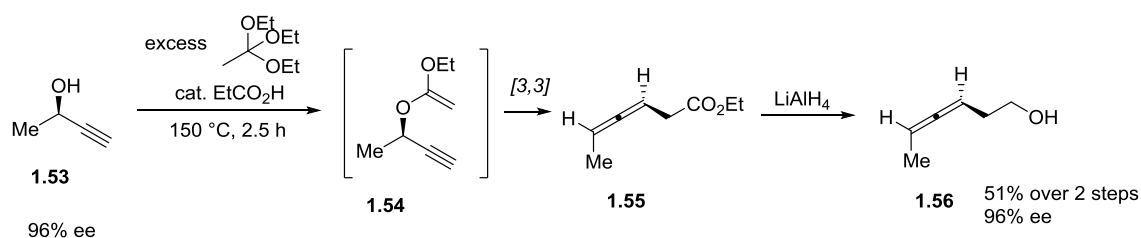
types of functionalized allenes;<sup>34</sup> the methods most commonly used by the Schomaker group will be discussed here.

#### 1.4.1. Orthoester Johnson-Claisen

Propargyl alcohol groups are a very common starting material for allene synthesis for several reasons. Synthesis of propargyl alcohols *via* addition of an acetylide to an aldehyde or ketone is simple to carry out in both racemic and enantioselective variants. Most important to allene synthesis is the fact that the absolute stereochemistry imparted to the propargyl alcohol can be preserved over the course of the stereospecific Claisen reaction.

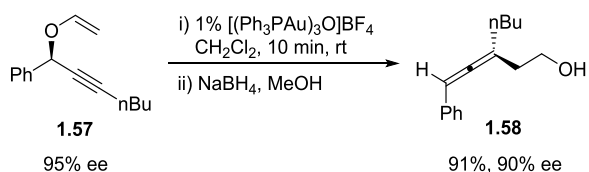
To access  $\beta$ -allenic alcohols, a propargyl vinyl ether can be used with an orthoester reagent as shown in Scheme 1.17.<sup>35</sup> High temperatures are used, both to promote the sigmatropic rearrangement and to drive off ethanol, pushing the equilibrium towards the products. While these high temperatures, in combination with the propionic acid catalyst, can cause problems with certain substrate classes, this is an effective and efficient protocol for a wide variety of propargyl alcohols. In addition, the rearrangement is stereospecific, allowing synthesis of highly enantioenriched allenes. From the Johnson-Claisen product **1.55**, the homoallenic alcohol **1.56** is easily accessed *via* reduction with lithium aluminum hydride.

**Scheme 1.17.** Orthoester Claisen rearrangement with propargyl alcohols.



For substrates that cannot be synthesized under the standard orthoester Claisen conditions, such as phenyl-substituted or acid-sensitive substrates,<sup>35</sup> a milder gold-catalyzed reaction, developed by the Toste group, can be used.<sup>36</sup> The Au catalyst coordinates strongly to the alkyne, activating it for the rearrangement. While a small amount of *ee* is lost during the course of the reaction, this is still a useful approach for aryl-substituted allenes.

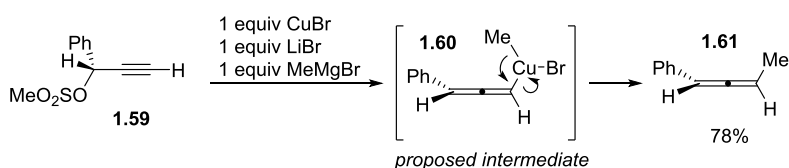
**Scheme 1.18.** Gold-catalyzed vinyl ether rearrangement to allenes.



#### 1.4.2. *S<sub>N</sub>2'* cuprate addition to activated alcohols

An alternative method is the addition of cuprates to activated propargyl alcohols (Scheme 1.19).<sup>38</sup> This reaction proceeds *via* an *S<sub>N</sub>2'* mechanism to deliver the allene, and is particularly useful for highly substituted allenes. One equivalent of Grignard reagent is used when using enantioenriched starting material, as the dicuprate has been shown to racemize the final allene.<sup>39</sup> The mesylate can be substituted for a variety of different activating groups, including acetates, ethers, and epoxides.<sup>33b</sup>

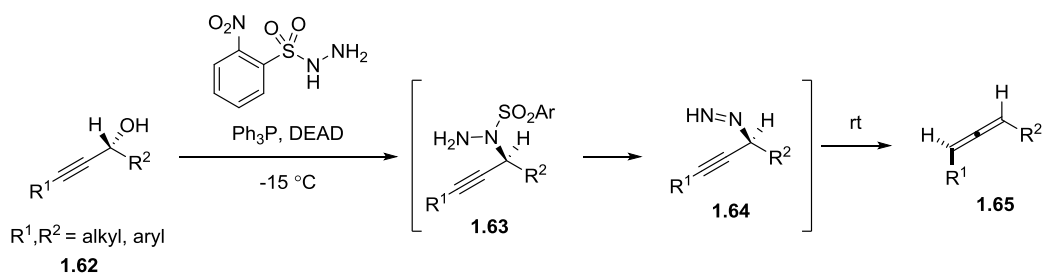
**Scheme 1.19.** Cuprate addition to propargyl tosylates.



### 1.4.3 Mitsunobu displacement of propargyl alcohols

A final method using propargyl alcohols for allene synthesis proceeds through a sequential Mitsunobu displacement/rearrangement to yield allenes (Scheme 1.20).<sup>39</sup> First, the alcohol is displaced with *o*-nitrobenzenesulfonyl hydrazine (NBSH), which decomposes to the diazine **1.64** when the reaction is warmed to room temperature. This intermediate undergoes a [3,3] sigmatropic rearrangement to yield the allene **1.65** as the final product. This method can be used for both terminal allenes, as well as a variety of 1,3-disubstituted allenes containing a range of functional groups.

**Scheme 1.20** Mitsunobu displacement of propargyl alcohols.



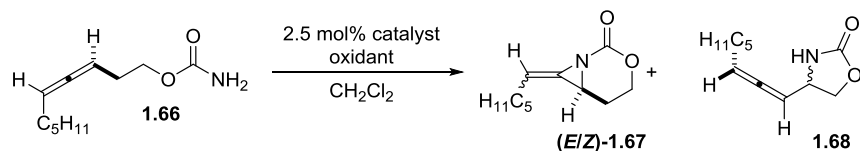
While this is only a small sampling of the variety of methods that can be used to make allenes, these methods allow access to most substrates of interest to our group.

## 1.5 Previous work in the Schomaker group

Previous work in our group has focused on the chemoselective amination of allenes, and exploration of these substrates faced the same issues of competing pi-bond reactivity as discussed in the carbene case. Our initial studies began with homoallenic carbamates (Table 1.4)<sup>40</sup> and these substrates showed generally poor selectivity between aziridination of the proximal alkene to yield **1.67** and nitrene insertion into the activated allenic C–H bond to yield

**1.68.** In this case, the best results were obtained with the  $\text{Rh}_2\text{TPA}_4$  catalyst (entry 4). While this selectivity was later increased using silver catalysis (see Chapter 3), these results demonstrate the difficulty of achieving chemoselectivity with these systems.

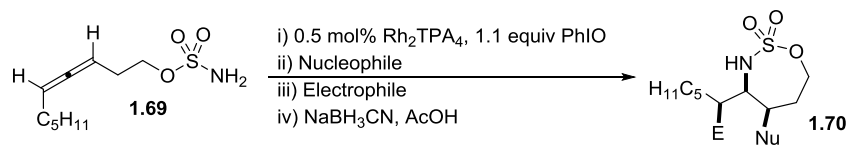
**Table 1.4.** C-H amination with homoallenlic carbamates.



entry	catalyst	oxidant	additive	temp (°C)	%MA ( <i>E</i> : <i>Z</i> )	%CH
1	$\text{Rh}_2(\text{esp})_2$	$\text{PhI}(\text{OAc})_2$	2.6 eq. MgO	35	46% (1.5:1)	44%
2	$\text{Rh}_2(\text{esp})_2$	$\text{PhI}(\text{OPiv})_2$	2.6 eq. MgO	35	42% (4.1:1)	45%
3	$\text{Rh}_2(\text{esp})_2$	PhIO	4 Å MS	rt	66% (3.0:1)	16%
4	$\text{Rh}_2(\text{TPA})_4$	PhIO	4 Å MS	rt	80% (4.0:1)	15%

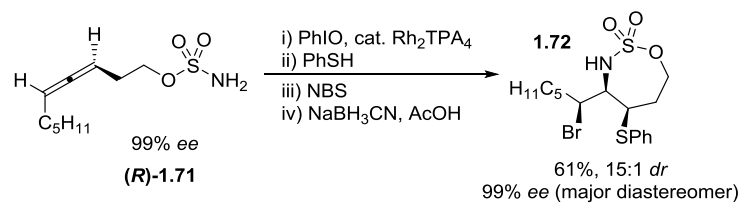
When the carbamate group was replaced with a sulfamate as the nitrene precursor, high selectivity for aziridination was obtained.<sup>41</sup> This allowed the development of a one-pot conversion of the allene, through the intermediacy of the methylene aziridine, to highly substituted and stereodefined products of the type **1.70** containing a wide variety of functional groups.

**Table 1.5.** Conversion of homoallenlic sulfamates to stereotriads.

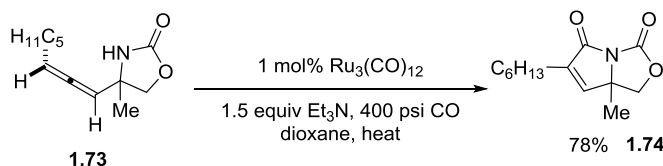


entry	nucleophile (Nu)	electrophile (E)	% yield	dr
1	AcOH (OAc)	NBS (Br)	61	20:1
2	MeOH (OMe)	NBS (Br)	58	2.6:1
3	MeOH (OMe)	DIAD ( $\text{NNH}(\text{CO}_2^i\text{Pr})_2$ )	64	4.6:1
4	MeOH (OMe)	PhSCI (SPh)	74	2.6:1

In addition, it was demonstrated that the axial chirality in **1.71** could be transferred to point chirality in stereotriad **1.72** with no loss of enantioenrichment observed during the course of the reaction (Scheme 1.21).

**Scheme 1.21.** Transfer of axial chirality to stereotriad.

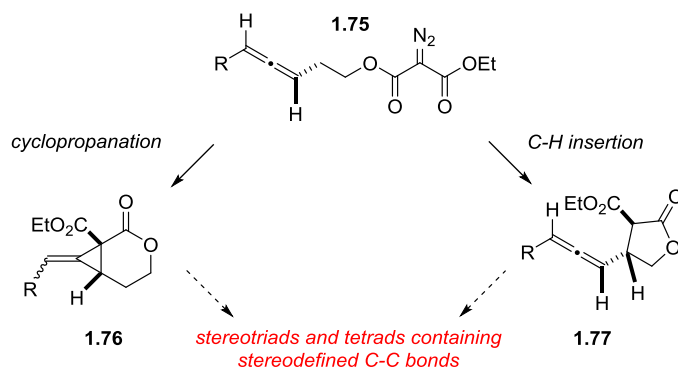
Not only did the products of aziridination prove useful, but the C-H amination products, were shown to be an interesting scaffold from which a variety of interesting structures could be synthesized.<sup>42</sup> In Scheme 1.22, the C-H amination product is carried through a cyclocarbonylation to yield an interesting heterocyclic scaffold, including a quaternary carbon.

**Scheme 1.22.** Further transformation of C-H amination products.

This result demonstrated that both products of the nitrene insertion proved to be convenient precursors to permit facile access to a diverse array of amine-containing scaffolds. Further work in the group to utilize these scaffolds in the synthesis of biologically active natural products and their unnatural analogs is ongoing.

These C-N bond formations inspired the investigation of a similar scaffold using carbene chemistry. Starting from an activated acceptor-acceptor allenic diazo compound such as **1.75**, we hoped to develop conditions that would selectively lead to bicyclic methylenecyclopropanes or functionalized allenes (Scheme 1.23).



**Scheme 1.23.** Divergent reactivity of diazo-containing allene substrates.

These intermediates could be further transformed into valuable stereodefined motifs for the construction of biologically active molecules. In the case of allene cyclopropanation, transfer of the axial chirality of the substrate to the methylene cyclopropane could produce chiral intermediates poised for further manipulation to enantioenriched stereotriads and tetrads.

This chapter describes the identification of catalysts that can be employed to promote divergent reactivity of allenic diazomalonates. Our goal was to permit selective transformation of a single substrate *via* either intramolecular C-H activation or cyclopropanation. The promotion of successful chemoselective C-H activation of allenes to generate new C-C bonds required us to address many of the same issues that faced us in our studies on the amination of allenes.

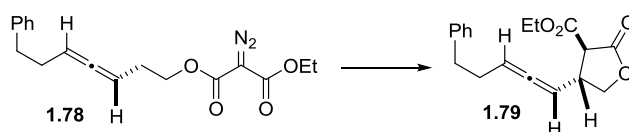
## 1.6 Results and Discussion

### 1.6.1. Activation of allenic C-H bonds

Our first goal was to investigate the surprising neglect of allenes as substrates for C-H activation (Scheme 1.22, **1.75** to **1.77**). Investigations of common Rh-based catalysts employing **1.78** as the allene precursor (Table 1.6) showed that the bulky  $\text{Rh}_2(\text{TPA})_4$  catalyst (TPA = triphenylacetate), which gave good results in previous studies on allene amination,<sup>37</sup> did not

perform well in the C-C bond-forming reaction. The addition of molecular sieves to remove any adventitious water did improve the reaction (compare entries 1 and 2), but the yield was still low. No product was observed when using  $\text{Rh}_2(\text{esp})_2$  in the absence of an additive or using  $\text{MgSO}_4$  (entries 3 and 4), but the inclusion of 4 Å molecular sieves (entry 5) gave the desired product **1.79** in moderate yield. One exciting development was that no increase in dimerization was observed when the final molarity of **1a** was increased from 0.01 M to 0.1 M (entry 6), as this allowed significantly less solvent to be used, and is not always possible in carbene chemistry of this type. Benzene and dichloroethane were also suitable solvents (entries 7 and 8), but gave no advantage over  $\text{CH}_2\text{Cl}_2$ . Additional molecular sieves (entry 9) decreased the yield of **1.79** and  $\text{Rh}_2(\text{OAc})_4$  also gave inferior results (entry 10) as compared to  $\text{Rh}_2(\text{esp})_2$ ; thus, the conditions utilized in entry 8 were adopted as the standard conditions for future studies. Finally, a control experiment was carried out (entry 11) to ensure the reaction was not being catalyzed by the molecular sieves.

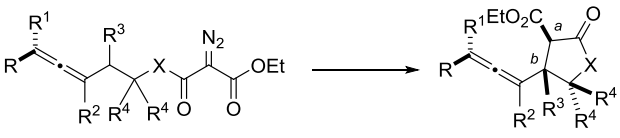
**Table 1.6.** Rh-catalyzed optimization of C-H insertion.

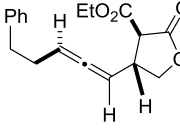
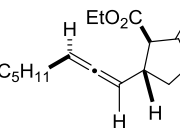
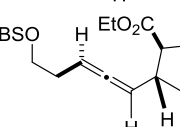
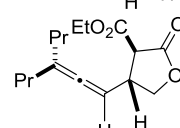
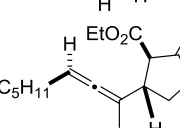
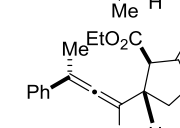
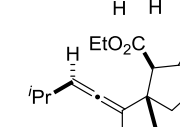
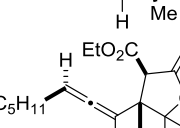
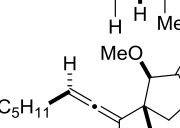


entry	catalyst	solvent (M)	additive <sup>a</sup>	addn time	yield
1	$\text{Rh}_2(\text{TPA})_4$	$\text{CH}_2\text{Cl}_2$ (0.01)	none	6h	0%
2	$\text{Rh}_2(\text{TPA})_4$	$\text{CH}_2\text{Cl}_2$ (0.01)	4Å MS	6h	43%
3	$\text{Rh}_2(\text{esp})_2$	$\text{CH}_2\text{Cl}_2$ (0.01)	none	6h	0%
4	$\text{Rh}_2(\text{esp})_2$	$\text{CH}_2\text{Cl}_2$ (0.01)	$\text{MgSO}_4$	6h	0%
5	$\text{Rh}_2(\text{esp})_2$	$\text{CH}_2\text{Cl}_2$ (0.01)	4Å MS	6h	57%
6	$\text{Rh}_2(\text{esp})_2$	$\text{CH}_2\text{Cl}_2$ (0.1)	4Å MS	3h	80%
7	$\text{Rh}_2(\text{esp})_2$	$\text{C}_6\text{H}_6$ (0.1)	4Å MS	3h	58%
8	$\text{Rh}_2(\text{esp})_2$	$(\text{CH}_2)_2\text{Cl}_2$ (0.1)	4Å MS	3h	79%
9	$\text{Rh}_2(\text{OAc})_4$	$\text{CH}_2\text{Cl}_2$ (0.1)	4Å MS	3h	70%
10	$\text{Rh}_2(\text{esp})_2$	$\text{CH}_2\text{Cl}_2$ (0.1)	4Å MS <sup>b</sup>	3h	60%
11	none	$\text{CH}_2\text{Cl}_2$ (0.1)	4Å MS	3h	0%

<sup>a</sup> 100 mg/0.1 mmol **1.78**. <sup>b</sup> 200 mg/0.1 mmol **1.78**.

The scope of the reaction was explored (Table 1.7) using acceptor-acceptor carbenoid precursors, as donor-acceptor carbenoids led to competing side reactions. The reported *dr* refers to the stereochemical relationship between the protons labeled *a* and *b* in the product lactone. The *dr* between these newly formed stereocenters and the axial chirality of the allene was essentially 1:1. In the case of 1,3-disubstituted allenes (entries 1-3), good yields and *dr* of the products were obtained with both Rh<sub>2</sub>(OAc)<sub>4</sub> and Rh<sub>2</sub>(esp)<sub>2</sub>. When the allene precursor was the 1,3,3-trisubstituted **1.84** (entry 4) or 1,1,3-trisubstituted **1.86** (entry 5), the less sterically demanding Rh<sub>2</sub>(OAc)<sub>4</sub> gave improved yields over the bulky Rh<sub>2</sub>(esp)<sub>2</sub>. However, this appeared to extend only to alkyl-substituted substrates, as the substitution of a Ph group for an alkyl group resulted in greatly decreased yields of **1.89**, even when Rh<sub>2</sub>(OAc)<sub>4</sub> was employed (entry 6). The stereoselectivity of the C-H insertion was explored by employing a diastereoenriched diazoallene **1.90** (*dr* = 86:14). The product was obtained in with *dr* of 4.7:2.7:1.5:1 (entry 7). Reduction of the allene functionality of **1.91** yielded the lactone with a *dr* of 1.5:1. The β,β-dimethyl substituted allene **1.92** (entry 8) gave good to excellent yields of **1.93**, with Rh<sub>2</sub>(esp)<sub>2</sub> superior to Rh<sub>2</sub>(OAc)<sub>4</sub> in this case. The malonate-type diazo precursor could be replaced by the β-ketoester precursor **1.94** to give the cyclopentanone **1.95** in excellent yield and *dr*.

**Table 1.7.** Scope of the Rh-catalyzed C-H insertion.


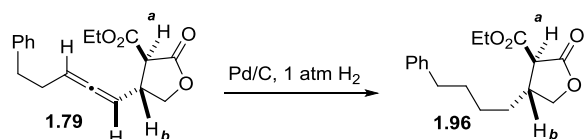
entry	R, R <sup>1</sup> , R <sup>2</sup> , R <sup>3</sup> , R <sup>4</sup> , X	catalyst	product	yield	dr <sup>a</sup>
1	Ph(CH <sub>2</sub> ) <sub>2</sub> , H, H, H, H, O <b>1.78</b>	Rh <sub>2</sub> (OAc) <sub>4</sub> Rh <sub>2</sub> esp <sub>2</sub>		70% 80% <b>1.79</b>	10:1 10:1
2	C <sub>5</sub> H <sub>11</sub> , H, H, H, H, O <b>1.80</b>	Rh <sub>2</sub> (OAc) <sub>4</sub>		73% <b>1.81</b>	10:1
3	TBSO(CH <sub>2</sub> ) <sub>2</sub> , H, H, H, H, O <b>1.82</b>	Rh <sub>2</sub> (OAc) <sub>4</sub>		76% <b>1.83</b>	6:1
4	Pr, Pr, H, H, H, O <b>1.84</b>	Rh <sub>2</sub> esp <sub>2</sub> Rh <sub>2</sub> (OAc) <sub>4</sub>		65% 88% <b>1.85</b>	> 10:1 > 10:1
5	C <sub>5</sub> H <sub>11</sub> , H, Me, H, H, O <b>1.86</b>	Rh <sub>2</sub> (OAc) <sub>4</sub>		74% <b>1.87</b>	> 10:1
6	Ph, Me, H, H, H, O <b>1.88</b>	Rh <sub>2</sub> (OAc) <sub>4</sub>		34% <b>1.89</b>	4.4:1
7	<sup>i</sup> Pr, H, H, Me, H, O <b>1.90</b>	Rh <sub>2</sub> (OAc) <sub>4</sub>		80% <b>1.91</b>	4.7:2.7:1.5:1
8	C <sub>5</sub> H <sub>11</sub> , H, H, H, Me, O <b>1.92</b>	Rh <sub>2</sub> (OAc) <sub>4</sub> Rh <sub>2</sub> esp <sub>2</sub>		70% 97% <b>1.93</b>	> 10:1 > 10:1
9	C <sub>5</sub> H <sub>11</sub> , H, H, H, H, C <b>1.94</b>	Rh <sub>2</sub> (OAc) <sub>4</sub>		92% <b>1.95</b>	> 14:1

<sup>a</sup> The dr of the chiral centers at a and b.

To further ensure that the observed diastereomers were due to a 1:1 stereochemistry at the allene, the allene functionality was removed. Full hydrogenation of the allene functionality of

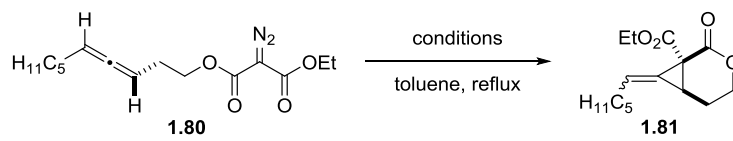
**1.79** gave **1.96** as a single diastereomer. The coupling constant between  $H_a$  and  $H_b$  in **1.96** was 9.1 Hz, further supporting the assignment of a *trans* relationship between these two newly formed stereocenters (Scheme 1.24).

**Scheme 1.24.** Verifying the *trans* stereochemistry of **1.79**.

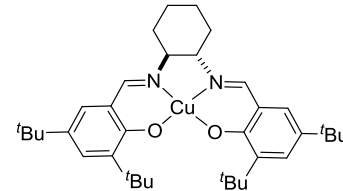


### 1.6.2. Synthesis of bicyclic methylene cyclopropanes

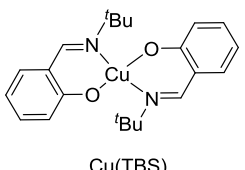
We then turned our attention to the chemoselective conversion of allenes to methylenecyclopropanes, which has been previously studied using both Rh- and Cu-based catalysts (see Section 1.3). However, these substrates were either minimally substituted or did not contain axial chirality. While previous studies (see Section 1.2) indicated that ligand design could tune the chemoselectivity using rhodium catalysts using alkenes, all rhodium catalysts that were used gave solely the C-H insertion product with our allene substrates. Thus, Cu-based catalysts in combination with acceptor-acceptor carbenoid precursors were explored to cleanly access the desired methylenecyclopropanes (Table 1.6).

**Table 1.6.** Optimization of Cu-catalyzed allene cyclopropanation.


entry	catalyst	mol%	addn time	yield	<i>E</i> : <i>Z</i>
1	Cu(salen)	10	12 h	70%	5.9:1
2	Cu(salen)	10	16 h	69%	6.7:1
3	Cu(TBS) <sub>2</sub>	10	12 h	58%	5.9:1
4	Cu(OTf) <sub>2</sub>	10	12 h	24%	8.3:1
5	CuOTf-toluene	10	18 h	0%	-
6	Cu(OAc) <sub>2</sub>	10	12 h	48%	8.3:1
7	Cu(OAc) <sub>2</sub>	10	24 h	59%	6.8:1
8	Cu(OAc) <sub>2</sub>	20	12 h	23%	7.6:1
9	CuI	10	18 h	67%	6.7:1



Cu(salen)

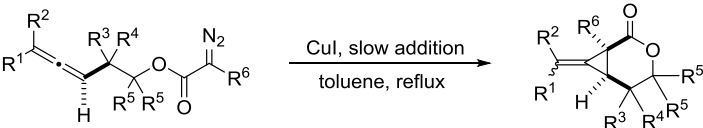
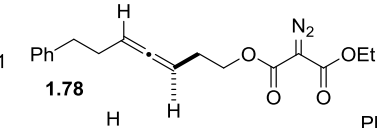
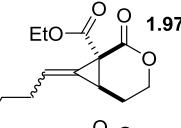
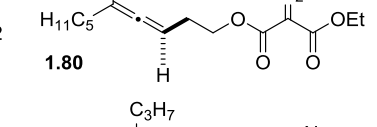
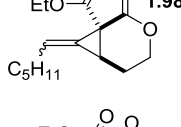
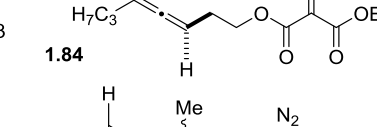
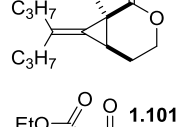
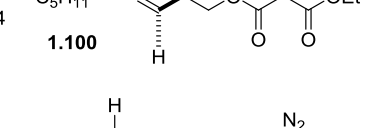
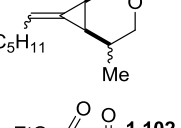
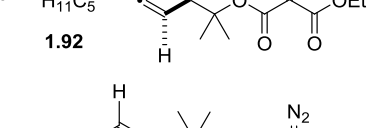
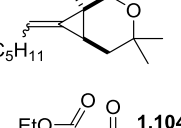
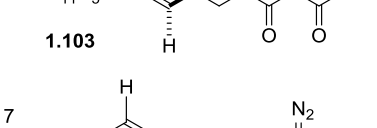
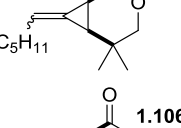
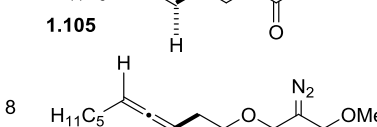
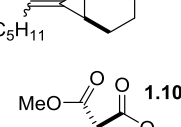
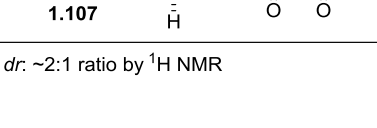
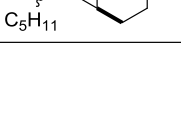


Cu(TBS)

Initial promising results employed a salen ligand for a Cu(II) catalyst, although slow addition of **1.80** to a solution of the catalyst was necessary to minimize dimerization of the substrate, and reflux temperatures were required for complete conversion. Both Cu(salen)<sup>43</sup> and Cu(TBS)<sub>2</sub><sup>43</sup> catalysts performed moderately well in the reaction (entries 1-3), although the identity of the ligand did not influence the *E*:*Z* ratio of the methylenecyclopropane to any great extent. Commercially available Cu(I) and Cu(II) salts gave varying yields of the desired **1.81**, with triflate counterions giving poor results (entries 4 and 5), possibly due to generation of small amounts of TfOH during the course of the reaction. Copper (II)acetate performed better, but still gave only moderate yields of **1.81** (entries 6, 7). While longer addition times moderately improved the yield (entry 6 vs. entry 7), increasing the catalyst loading led to increased carbene dimerization and a correspondingly lower yield of the desired product (entry 8). Finally, the

simple and commercially available copper(I) iodide salt gave the best combination of yield and *E:Z* selectivity (entry 9).

**Table 1.7.** Scope of cyclopropanation of allenes.

				
entry	substrate	product	yield	<i>E:Z</i>
1	 1.78	 1.97	77%	7.9:1
2	 1.80	 1.98	67%	6.7:1
3	 1.84	 1.99	23%	NA
4	 1.100	 1.101	68% <sup>a</sup>	>20:1
5	 1.92	 1.102	18%	19:1
6	 1.103	 1.104	30%	24:1
7	 1.105	 1.106	68%	2.3:1
8	 1.107	 1.108	30%	9.3:1

<sup>a</sup> *dr*: ~2:1 ratio by <sup>1</sup>H NMR

A 10 mol% loading of CuI was utilized in the exploration of the substrate scope of the reaction (Table 4). In all cases, only one diastereomer was observed by <sup>1</sup>H NMR and was postulated to be

the *cis* diastereomer resulting from *syn* addition of the metal carbenoid species to the allene.<sup>2a</sup> The success of the cyclopropanation was quite sensitive to the steric environment of the allene. Yields were high for the 1,3-substituted substrates **1.97** and **1.98** (entries 1 and 2), while the 1,3,3-trisubstituted allene **1.84** gave a poor yield of **1.99** (entry 3). The *E*:*Z* ratios were on the order of 7-8:1. Interestingly, additional substitution in the tether between the allene and the diazo group greatly increased the *E*:*Z* ratios (entries 4-6), although too much steric congestion was detrimental to the reaction (entries 5 and 6). Using the diazo precursor **1.105** (entry 7) instead of the malonate lowered the selectivity for the *E* alkene, but gave a moderate yield of the desired methylenecyclopropane **1.106**. Finally, replacement of the ethyl ester of the carbene precursor with a methyl ester resulted in lowered yields in the conversion of **1.107** to **1.108** (entry 8) due to demethylation of the ester under the reaction conditions.

Previous studies in our group on the amination of allenes have demonstrated that the axial chirality of the allene can be effectively transferred to point chirality in the product.<sup>41</sup> We fully expect this to be the case for the cyclopropanation of allene-containing diazoesters which would allow the transformation of these building blocks into enantioenriched stereotriads and tetrads.

### 1.6.3. Conclusions

In conclusion, we have demonstrated that by judicious choice of a transition metal catalyst, the intramolecular reaction of allene-containing diazomalonates can be diverted to one of two different pathways. The use of dinuclear Rh catalysts promotes a C-H activation pathway that generates an allene bearing a pendant lactone or cyclopentanone, depending on the carbene source that is employed. The reaction is completely chemoselective and yields excellent *trans* diastereoselectivity between the two newly formed stereocenters. On the other hand, the utilization of a simple CuI catalyst shows complete chemoselectivity for cyclopropanation of the



allene to yield a bicyclic methylenecyclopropane. Continuing work will focus on elaboration of the allenic lactone and bicyclic methylenecyclopropanes into useful complex stereotriads and tetrads.

## 1.7 Experimental section

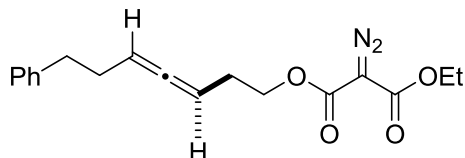
### 1.7.1 General

All glassware was either oven-dried overnight at 130 °C or flame-dried under a stream of dry nitrogen prior to use. Unless otherwise specified, reagents were used as obtained from the vendor without further purification. Tetrahydrofuran and diethyl ether were freshly distilled from purple Na/benzophenone ketyl. Dichloromethane, acetonitrile and toluene were dried over CaH<sub>2</sub> and freshly distilled prior to use. All other solvents were purified in accordance with "Purification of Laboratory Chemicals".<sup>44</sup> Air- and moisture-sensitive reactions were performed using standard Schlenk techniques under an atmosphere of nitrogen. Analytical thin layer chromatography (TLC) was performed utilizing pre-coated silica gel 60 F254 plates containing a fluorescent indicator, while preparative chromatography was performed using SilicaFlash P60 silica gel (230-400 mesh) via Still's method. Unless otherwise stated, the mobile phases for column chromatography were mixtures of hexanes/ethyl acetate. Columns were typically run using a gradient method, beginning with 100% hexanes and gradually increasing the polarity using ethyl acetate. Various stains were used to visualize reaction products, including *p*-anisaldehyde, KMnO<sub>4</sub>, ceric ammonium molybdate (CAM stain) and iodine powder. <sup>1</sup>H NMR and <sup>13</sup>C NMR spectra were obtained using Bruker-300, Varian-300, Varian Inova-500, or Varian Unity-500 spectrometers. For <sup>1</sup>H NMR, chemical shifts are reported relative to residual protiated solvent peaks ( $\delta$  7.26, 2.49, 7.15 and 7.09 ppm for CDCl<sub>3</sub>, (CD<sub>3</sub>)<sub>2</sub>SO, C<sub>6</sub>D<sub>6</sub> and CD<sub>3</sub>C<sub>6</sub>D<sub>5</sub> respectively).

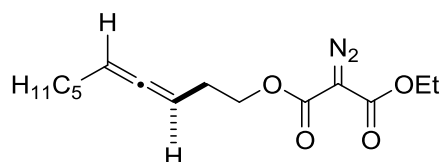
$^{13}\text{C}$  NMR spectra were measured at either 125 MHz or 75 MHz on the same instruments noted above for recording  $^1\text{H}$  NMR spectra. Chemical shifts were again reported in accordance to residual protiated solvent peaks ( $\delta$  77.2, 39.5, 128.0 and 137.9 ppm for  $\text{CDCl}_3$ ,  $(\text{CD}_3)_2\text{SO}$ ,  $\text{C}_6\text{D}_6$ , and  $\text{CD}_3\text{C}_6\text{D}_5$ , respectively). IR spectra were acquired on a Bruker Tensor 27. Melting ranges were measured on a DigiMelt MPA 160. Optical rotations were measured in  $\text{CH}_2\text{Cl}_2$  on an AUTOPOL III automatic polarimeter. High-pressure liquid chromatography (HPLC) analyses were performed at 215 and 225 nm using a Shimadzu HPLC, Model LC-20AB. Accurate mass measurements were acquired at the University of Wisconsin-Madison using a Micromass LCT (electrospray ionization, time-of flight analyzer or electron impact methods). When two or more significant isotopes were present in the molecule, a monoisotopic approach was used, focusing on the isotope with the lowest mass ( $^{35}\text{Cl}$  and  $^{79}\text{Br}$ ). The NMR and Mass Spectrometry facilities are funded by the NSF (CHE 9974839, CHE-9304546, CHE-9208463, CHE-9629688) and the University of Wisconsin, as well as the NIH (RR08389-01).

#### 1.7.2. General preparation of diazo compounds

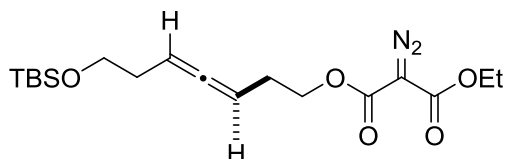
The malonic ester or acetoacetate (1 equiv), *p*-toluenesulfonyl azide (1.05 equiv) and triethylamine (2.2 equiv) were dissolved in acetonitrile (0.3 M) and stirred at room temperature until TLC indicated complete consumption of the starting material. The reaction was then concentrated *in vacuo* and the resulting solid residue was dissolved in a minimum amount of ethyl acetate with the aid of sonication. Hexane was added to the solution to precipitate the  $\text{TsNH}_2$  byproduct. The mixture was filtered through Celite and the filtrate concentrated *in vacuo* gave a pale yellow oil. The crude product was purified by flash column chromatography (slow gradient of 1% to 5% ethyl acetate in hexanes) to give the products as colorless to pale yellow oils.



**Compound 1.78.**  $^1\text{H}$  NMR (400 MHz,  $\text{CDCl}_3$ )  $\delta$  7.34–7.23 (m, 2H), 7.23–7.14 (m, 3H), 5.18 (app qt,  $J$  = 6.4, 2.8 Hz, 1H), 5.07 (app qt,  $J$  = 6.4, 3.0 Hz, 1H), 4.29 (q,  $J$  = 7.1 Hz, 2H), 4.23 (t,  $J$  = 6.7 Hz, 2H), 2.71 (t,  $J$  = 7.7 Hz, 2H), 2.37–2.23 (m, 4H), 1.30 (t,  $J$  = 7.1 Hz, 3H).  $^{13}\text{C}$  NMR (101 MHz,  $\text{CDCl}_3$ )  $\delta$  204.8, 161.0, 160.9, 141.6, 128.5, 128.3, 125.9, 91.3, 86.8, 64.6, 61.7, 35.3, 30.4, 28.4, 14.4. HRMS  $m/z$   $[\text{M} + \text{H}]^+$  predicted, 329.1496; observed, 329.1483.

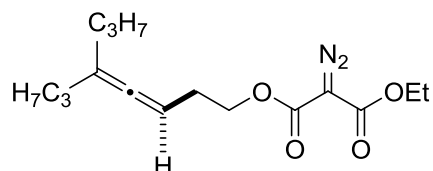


**Compound 1.80.**  $^1\text{H}$  NMR (400 MHz,  $\text{CDCl}_3$ )  $\delta$  5.13 (app qt,  $J$  = 6.5, 2.9 Hz, 1H), 5.06 (app qt,  $J$  = 6.4, 3.0 Hz, 1H), 4.43–4.17 (m, 4H), 2.36 (app qd,  $J$  = 6.7, 2.9 Hz, 2H), 1.97 (app qd,  $J$  = 7.0, 3.0 Hz, 2H), 1.49–1.17 (m, 9H), 0.9 –0.79 (m, 3H).  $^{13}\text{C}$  NMR (101 MHz,  $\text{CDCl}_3$ )  $\delta$  204.6, 161.1, 160.9, 92.0, 86.2, 64.7, 61.7, 31.3, 28.8, 28.7, 28.5, 22.5, 14.4, 14.1. HRMS  $m/z$   $[\text{M} + \text{H}]^+$  predicted, 295.1653; observed, 295.1642.

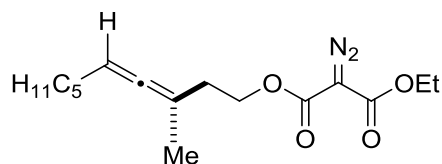


**Compound 1.82.**  $^1\text{H}$  NMR (500 MHz,  $\text{CDCl}_3$ )  $\delta$  5.15 (app tt,  $J$  = 6.9, 4.1 Hz, 1H), 5.07 (app dtd,  $J$  = 9.0, 6.7, 2.4 Hz, 1H), 4.30 (dt,  $J$  = 11.9, 6.9 Hz, 3H), 3.65 (t,  $J$  = 6.7 Hz, 2H), 2.36 (app qd,  $J$  = 6.6, 2.7 Hz, 2H), 2.20 (app qd,  $J$  = 6.8, 2.6 Hz, 2H), 1.32 (t,  $J$  = 7.1 Hz, 3H), 0.89 (s, 9H), 0.05 (d,  $J$  = 1.8 Hz, 6H).  $^{13}\text{C}$  NMR (126 MHz,  $\text{CDCl}_3$ )  $\delta$  205.2, 161.0, 160.9, 88.5, 86.1, 64.6, 62.8,

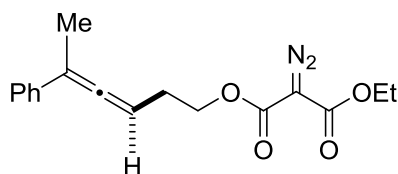
61.7, 32.5, 28.3, 25.9, 18.3, 14.4, -5.3. HRMS  $m/z$   $[M + NH_4]^+$  predicted, 400.2263; observed, 400.2260.



**Compound 1.84.**  $^1H$  NMR (500 MHz,  $CDCl_3$ )  $\delta$  5.05 (tp,  $J = 5.6, 2.7$  Hz, 1H), 4.30 (dq,  $J = 8.6, 7.0$  Hz, 4H), 2.35 (q,  $J = 6.8$  Hz, 2H), 1.93 – 1.82 (m, 4H), 1.41 (m, 4H), 1.31 (t,  $J = 7.2$  Hz, 3H), 0.90 (t,  $J = 7.4$  Hz, 6H).  $^{13}C$  NMR (126 MHz,  $CDCl_3$ )  $\delta$  201.7, 161.1, 160.9, 129.8, 127.9, 105.1, 86.0, 66.8, 65.0, 61.7, 34.7, 29.0, 20.8, 14.7, 14.4, 13.9. HRMS  $m/z$   $[M + NH_4]^+$  predicted, 326.2075; observed, 326.2071.

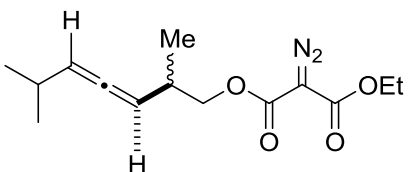


**Compound 1.86.**  $^1H$  NMR (400 MHz,  $CDCl_3$ )  $\delta$  5.05 (app tq,  $J = 6.3, 2.9$  Hz, 1H), 4.31 (m, 4H), 2.30 (td,  $J = 6.8, 2.8$  Hz, 2H), 2.01–1.88 (m, 2H), 1.70 (d,  $J = 2.9$  Hz, 3H), 1.44 – 1.17 (m, 9H), 0.88 (t,  $J = 6.8$  Hz, 3H).  $^{13}C$  NMR (101 MHz,  $CDCl_3$ )  $\delta$  201.4, 161.1, 160.9, 95.0, 91.4, 63.8, 61.7, 33.1, 31.4, 29.1, 28.9, 22.5, 19.5, 14.4, 14.1. HRMS  $m/z$   $[M + H]^+$  predicted, 309.1809; observed, 309.1819.

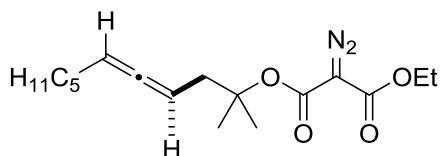


**Compound 1.88.**  $^1H$  NMR (400 MHz,  $CDCl_3$ )  $\delta$  7.41 – 7.36 (m, 2H), 7.34 – 7.25 (m, 2H), 7.23 – 7.15 (m, 2H), 5.44 (app dq,  $J = 6.5, 3.2$  Hz, 1H), 4.31 (q,  $J = 7.1$  Hz, 4H), 2.49 (app qd,  $J = 6.5,$

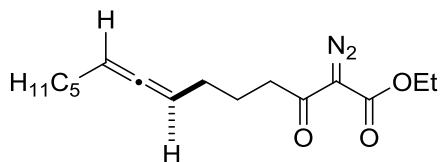
1.9 Hz, 2H), 2.09 (d,  $J = 2.9$  Hz, 3H), 1.32 (t,  $J = 7.1$  Hz, 3H).  $^{13}\text{C}$  NMR (101 MHz,  $\text{CDCl}_3$ )  $\delta$  204.8, 161.1, 161.0, 137.0, 131.6, 128.3, 126.7, 125.7, 102.8, 101.6, 88.6, 64.5, 61.6, 35.7, 28.5, 17.0, 14.4. HRMS  $m/z$   $[\text{M} + \text{Na}]^+$  predicted, 337.1159; observed, 337.1153.



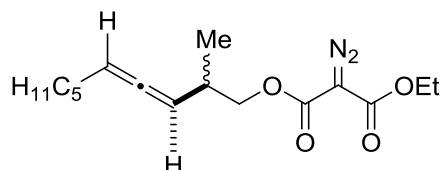
**Compound 1.90.**  $^1\text{H}$  NMR (300 MHz,  $\text{CDCl}_3$ )  $\delta$  5.22 (app td,  $J = 6.0, 3.0$  Hz, 1H), 5.15 (app td,  $J = 6.1, 3.1$  Hz, 1H), 4.31 (q,  $J = 7.1$  Hz, 2H), 4.24–4.00 (m, 2H), 2.6–2.41 (m, 2H), 2.27 (m, 1H), 1.32 (t,  $J = 7.1$  Hz, 3H), 1.06 (d,  $J = 6.8$  Hz, 3H), 1.00 (dd,  $J = 6.8, 1.0$  Hz, 6H).  $^{13}\text{C}$  NMR (101 MHz,  $\text{CDCl}_3$ )  $\delta$  202.0, 201.9, 161.1, 161.0, 130.3, 129.8, 127.9, 127.6, 100.4, 100.4, 93.9, 77.4, 77.3, 77.1, 76.7, 69.6, 69.6, 61.7, 53.5, 32.9, 32.8, 27.8, 27.8, 23.0, 22.5, 22.4, 21.8, 21.7, 16.8, 16.7, 14.7, 14.4. HRMS  $m/z$   $[\text{M} + \text{H}]^+$  predicted, 281.1496; observed, 281.1485.



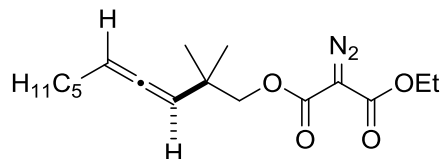
**Compound 1.92.**  $^1\text{H}$  NMR (400 MHz,  $\text{CDCl}_3$ )  $\delta$  5.18–4.92 (m, 1H), 4.29 (q,  $J = 7.1$  Hz, 2H), 2.55–2.42 (m, 2H), 1.97 (app qd,  $J = 7.0, 2.9$  Hz, 2H), 1.53 (s, 6H), 1.31 (t,  $J = 7.2$  Hz, 7H), 0.95–0.82 (m, 3H).  $^{13}\text{C}$  NMR (101 MHz,  $\text{CDCl}_3$ )  $\delta$  205.8, 161.4, 159.7, 90.6, 85.4, 84.7, 61.5, 41.3, 31.3, 28.9, 28.7, 25.9, 25.7, 22.5, 14.4, 14.0. HRMS  $m/z$   $[\text{M} + \text{H}]^+$  predicted, 323.1966; observed, 323.1965.



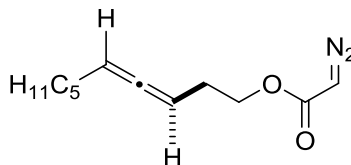
**Compound 1.94.**  $^1\text{H}$  NMR (500 MHz,  $\text{CDCl}_3$ )  $\delta$  5.13 – 5.00 (m, 2H), 3.84 (s, 3H), 2.89 (t,  $J$  = 7.5 Hz, 2H), 2.10 – 1.90 (m, 4H), 1.76 (p,  $J$  = 7.4 Hz, 2H), 1.44 – 1.24 (m, 7H), 0.92 – 0.84 (m, 3H).  $^{13}\text{C}$  NMR (126 MHz,  $\text{CDCl}_3$ )  $\delta$  204.0, 192.6, 161.8, 91.4, 90.0, 52.1, 39.6, 31.3, 28.9, 28.9, 28.4, 23.7, 22.5, 14.1. HRMS  $m/z$   $[\text{M} + \text{Na}]^+$  predicted, 301.1523; observed, 301.1526.



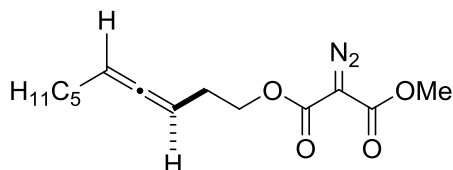
**Compound 1.100.**  $^1\text{H}$  NMR (300 MHz,  $\text{CDCl}_3$ )  $\delta$  5.17 (tdd,  $J$  = 6.6, 2.9, 1.3 Hz, 1H), 5.08 (dddt,  $J$  = 7.9, 4.9, 3.1, 1.7 Hz, 1H), 4.31 (qd,  $J$  = 7.1, 1.3 Hz, 2H), 4.22 – 4.02 (m, 2H), 2.64 – 2.41 (m, 1H), 2.08 – 1.88 (m, 2H), 1.48 – 1.19 (m, 10H), 1.06 (dd,  $J$  = 6.8, 1.2 Hz, 3H), 0.94 – 0.83 (m, 3H).  $^{13}\text{C}$  NMR (126 MHz,  $\text{CDCl}_3$ )  $\delta$  203.5, 161.1, 160.9, 93.0, 93.0, 92.6, 69.6, 66.8, 61.7, 32.9, 31.4, 31.3, 28.9, 28.8, 28.8, 22.5, 21.6, 16.8, 16.74, 14.7, 14.4, 14.1. HRMS  $m/z$   $[\text{M} + \text{H}]^+$  predicted, 309.1809; observed, 309.1808.



**Compound 1.103.**  $^1\text{H}$  NMR (400 MHz,  $\text{CDCl}_3$ )  $\delta$  5.20 (app q,  $J$  = 6.6 Hz, 1H), 5.05 (app dt,  $J$  = 6.2, 3.0 Hz, 1H), 4.31 (q,  $J$  = 7.1 Hz, 2H), 4.01 (s, 2H), 2.09 – 1.87 (m, 2H), 1.46 – 1.23 (m, 10H), 1.06 (s, 6H), 0.98 – 0.79 (m, 3H).  $^{13}\text{C}$  NMR (101 MHz,  $\text{CDCl}_3$ )  $\delta$  202.3, 161.0, 97.9, 93.7, 73.3, 61.7, 35.4, 31.4, 28.9, 28.9, 28.9, 24.9, 24.9, 22.5, 14.4, 14.1. HRMS  $m/z$  predicted  $[\text{M} + \text{NH}_4]^+$ : 340.2231, observed 340.2225.



**Compound 1.105.**  $^1\text{H}$  NMR (400 MHz,  $\text{CDCl}_3$ )  $\delta$  5.13 (m, 1H), 5.05 (app qt,  $J = 6.0, 3.4$  Hz, 1H), 4.73 (s, 1H), 4.22 (t,  $J = 6.8$  Hz, 2H), 2.32 (app qd,  $J = 6.7, 2.9$  Hz, 2H), 1.98 (app qd,  $J = 7.0, 3.0$  Hz, 2H), 1.46-1.22 (m, 7H), 0.94 – 0.85 (m, 3H).  $^{13}\text{C}$  NMR (101 MHz,  $\text{CDCl}_3$ )  $\delta$  204.6, 91.9, 86.4, 64.1, 31.3, 28.8, 28.7, 28.6, 22.5, 14.1. HRMS  $m/z$   $[\text{M} + \text{NH}_4]^+$  predicted, 240.1707; observed, 240.1710.

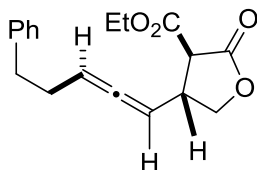


**Compound 1.107.**  $^1\text{H}$  NMR (500 MHz,  $\text{CDCl}_3$ )  $\delta$  5.13 (app qt,  $J = 6.3, 2.7$  Hz, 1H), 5.06 (m, 1H), 4.30 (t,  $J = 6.8$  Hz, 2H), 3.85 (s, 3H), 2.36 (qd,  $J = 6.6, 2.6$  Hz, 2H), 1.97 (qd,  $J = 7.0, 2.6$  Hz, 2H), 1.44 – 1.23 (m, 7H), 0.94 – 0.84 (m, 3H).  $^{13}\text{C}$  NMR (126 MHz,  $\text{CDCl}_3$ )  $\delta$  203.6, 160.6, 159.7, 91.0, 85.1, 63.7, 51.5, 30.3, 27.8, 27.7, 27.4, 21.5, 21.4, 13.1. HRMS  $m/z$   $[\text{M} + \text{H}]^+$  predicted, 281.1496; observed, 281.1490.

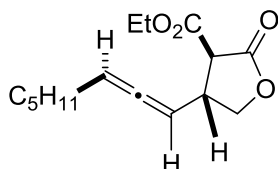
### 1.7.3. General procedure for allenic C-H insertion reactions

A 0.1 M solution of diazomalonate in dichloromethane was added at a rate of 1.0 mmol/hour by syringe pump to a vigorously stirred mixture of  $\text{Rh}_2(\text{OAc})_4$  or  $\text{Rh}_2(\text{esp})_2$  (3.0 mol %) and activated 4Å molecular sieves (100 mg/0.1 mmol) in dichloromethane (0.1 M) under an atmosphere of nitrogen. After the addition was complete, the reaction was monitored by TLC. Upon completion, the reaction mixture was filtered through Celite, concentrated *in vacuo* and

purified by column chromatography (gradient 2% to 10% ethyl acetate in hexanes) to yield the products. All products isolated as mixture of diastereomers resulting from chirality of allene; reported *dr* based on  $^1\text{H}$  NMR data, when peak separation is observed.



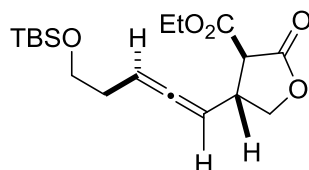
**Compound 1.79.** *dr*  $\approx$  1:1  $^1\text{H}$  NMR (500 MHz,  $\text{CDCl}_3$ )  $\delta$  7.32–7.24 (m, 3H), 7.23–7.14 (m, 4H), 5.42–5.32 (m, 1H), 5.19–5.12 (m, 1H), 4.40 (dd,  $J$  = 8.9, 7.6 Hz, 0.5H), 4.37 (dd,  $J$  = 8.9, 7.5 Hz, 0.5H), 4.31–4.16 (m, 2H), 3.84 (m, 1H), 3.51–3.39 (m, 1H), 3.28 (d,  $J$  = 9.1 Hz, 0.5H), 3.25 (d,  $J$  = 8.9 Hz, 0.5H), 2.79–2.64 (m, 2H), 2.45–2.25 (m, 2H), 1.30 (td,  $J$  = 7.2, 2.3 Hz, 3H).  $^{13}\text{C}$  NMR (125.8 MHz,  $\text{CDCl}_3$ ):  $\delta$  203.9, 171.6, 171.5, 167.2, 141.2, 141.2, 128.6, 128.6, 128.5, 126.3, 126.3, 94.7, 94.6, 89.2, 89.1, 71.4, 71.3, 62.4, 62.3, 52.2, 52.0, 39.3, 39.2, 35.1, 35.0, 30.2, 30.1, 14.3. HRMS (ESI)  $m/z$   $[\text{M} + \text{Na}]^+$  predicted, 323.1254; observed, 323.1246.



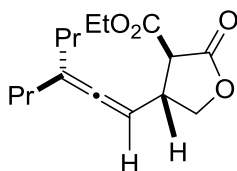
**Compound 1.81.** *dr*  $\approx$  1.5:1  $^1\text{H}$  NMR (300 MHz,  $\text{CDCl}_3$ )  $\delta$  5.44–5.28 (app qdd,  $J$  = 6.6, 2.7, 1.4 Hz, 1H), 5.18 (app ttd,  $J$  = 6.1, 3.0, 1.2 Hz, 1H), 4.54 (ddd,  $J$  = 8.9, 7.5, 2.9 Hz, 1H), 4.27 (tdd,  $J$  = 7.2, 6.6, 1.0 Hz, 2H), 4.03 (ddd,  $J$  = 8.9, 7.9, 4.3 Hz, 1H), 3.58–3.47 (m, 1H), 3.44 (d,  $J$  = 6.9 Hz, 0.6H), 3.42 (d,  $J$  = 6.6 Hz, 0.4H), 2.00 (app qd,  $J$  = 7.6, 2.8 Hz, 2H), 1.39–1.20 (m, 8H), 0.97–0.86 (m, 3H).  $^{13}\text{C}$  NMR (126 MHz,  $\text{CDCl}_3$ )  $\delta$  206.2, 206.1, 197.4, 174.2, 174.1, 169.7, 169.7, 132.5, 130.5, 98.2, 98.2, 98.1, 96.7, 91.4, 91.3, 88.0, 80.0, 79.7, 79.5, 74.1, 74.1, 73.9,



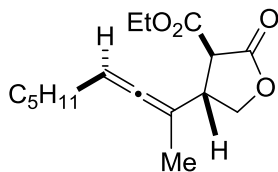
69.5, 64.9, 64.8, 64.5, 54.7, 54.7, 53.7, 42.0, 41.9, 41.8, 34.0, 33.9, 33.8, 31.2, 31.2, 31.1, 31.1, 31.0, 25.1, 25.1, 25.0, 17.4, 16.7, 16.7, 16.6. HRMS (ESI)  $m/z$   $[M + NH_4]^+$  predicted, 284.1857; observed, 284.1857.



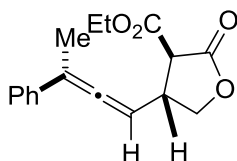
**Compound 1.83.**  $dr \approx 1.5:1$   $^1H$  NMR (500 MHz,  $CDCl_3$ )  $\delta$  5.38 (dddd,  $J = 10.7, 6.8, 3.4, 2.6$  Hz, 1H), 5.21-5.16 (m, 1H), 4.53 (dd,  $J = 8.9, 3.0$  Hz, 1H), 4.30–4.23 (m, 2H), 4.07 (dd,  $J = 8.9, 2.2$  Hz, 1H), 3.66 (t,  $J = 6.5$  Hz, 1H), 3.66 (t,  $J = 6.5$  Hz, 1H), 3.57-3.50 (m, 1H), 3.44 (d,  $J = 3.4$  Hz, 0.6H), 3.42 (d,  $J = 3.7$  Hz, 0.4H), 2.23 (app qd,  $J = 6.7, 2.7$  Hz, 2H), 1.32 (t,  $J = 7.2$  Hz, 3H), 0.89 (s, 9H), 0.06 (d,  $J = 0.7$  Hz, 6H).  $^{13}C$  NMR (75.4 MHz,  $CDCl_3$ )  $\delta$  204.3, 204.2, 171.6, 167.2, 92.4, 88.9, 88.8, 71.6, 71.5, 62.6, 62.4, 52.3, 52.2, 39.3, 32.5, 26.1, 18.5, 14.3, -5.1. HRMS  $m/z$   $[M+H]^+$  predicted, 355.1936; observed 355.1935.



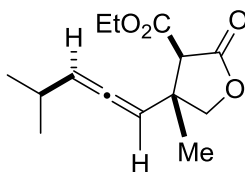
**Compound 1.85.**  $^1H$  NMR (500 MHz,  $CDCl_3$ )  $\delta$  5.17 (dp,  $J = 5.9, 3.0$  Hz, 1H), 4.52 (dd,  $J = 8.8, 7.6$  Hz, 1H), 4.26 (qd,  $J = 7.1, 2.6$  Hz, 2H), 4.02 (dd,  $J = 8.8, 8.0$  Hz, 1H), 3.62–3.48 (m, 1H), 3.42 (d,  $J = 9.0$  Hz, 1H), 2.00–1.84 (m, 4H), 1.4–1.34 (m, 4H), 1.31 (t,  $J = 7.1$  Hz, 3H), 0.91 (t,  $J = 7.4$  Hz, 2H), 0.91 (t,  $J = 7.4$  Hz, 4H).  $^{13}C$  NMR (125.8 MHz,  $CDCl_3$ )  $\delta$  200.8, 171.9, 167.4, 109.3, 89.5, 71.9, 62.3, 52.3, 40.2, 34.7, 34.6, 20.9, 20.8, 14.2, 14.0, 13.9. HRMS  $m/z$   $[M + Na]^+$  predicted, 303.1567; observed, 303.1559.



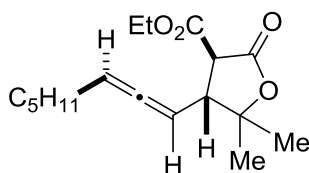
**Compound 1.87.**  $^1\text{H}$  NMR (500 MHz,  $\text{CDCl}_3$ )  $\delta$  5.32–5.22 (m, 1H), 4.54 (dd,  $J = 8.8, 7.3$  Hz, 1H), 4.26 (qd,  $J = 7.0, 5.0$  Hz, 2H), 4.12–4.03 (m, 1H), 3.53–3.38 (m, 2H), 2.02–1.92 (m, 2H), 1.72 (d,  $J = 2.9$  Hz, 3H), 1.42–1.23 (m, 8H), 0.89 (t, 3H).  $^{13}\text{C}$  NMR (75.4 MHz,  $\text{CDCl}_3$ )  $\delta$  200.3, 200.2, 171.9, 167.6, 97.4, 97.3, 95.1, 95.0, 71.2, 62.3, 51.9, 43.4, 43.3, 31.5, 31.4, 29.0, 28.9, 28.8, 28.7, 22.6, 18.1, 18.0, 14.2, 14.1. HRMS  $m/z$   $[\text{M}+\text{NH}_4]^+$  predicted, 298.2013; observed, 298.2001.



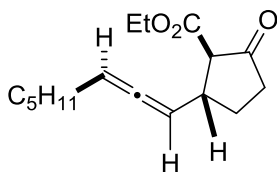
**Compound 1.89.** Major diastereomer:  $^1\text{H}$  NMR (300 MHz,  $\text{CDCl}_3$ )  $\delta$  5.44–5.28 (m, 1H), 5.25–5.08 (m, 1H), 4.54 (ddd,  $J = 9.0, 7.4, 1.6$  Hz, 1H), 4.36–4.19 (m, 2H), 4.11–4.00 (m, 1H), 3.64–3.47 (m, 1H), 3.48–3.35 (m, 1H), 2.10–1.88 (m, 3H), 1.3–1.20 (m, 8H), 0.97–0.86 (m, 3H).  $^{13}\text{C}$  NMR (101 MHz,  $\text{CDCl}_3$ )  $\delta$  204.0, 203.9, 171.4, 171.30, 167.0, 166.9, 164.3, 162.6, 135.7, 135.5, 128.5, 128.4, 128.3, 127.4, 127.4, 125.8, 125.7, 105.1, 105.0, 90.7, 90.6, 71.5, 71.4, 71.2, 70.1, 62.5, 62.3, 62.3, 62.2, 61.7, 58.4, 52.1, 51.8, 40.1, 39.9, 19.8, 17.1, 17.0, 16.6, 14.2, 14.1, 14.0, 13.9, 1.1. HRMS  $m/z$   $[\text{M}+\text{NH}_4]^+$  predicted, 304.1544; observed, 304.1550.



**Compound 1.91.**  $dr = 83:17$ .  $^1\text{H}$  NMR (500 MHz, Chloroform- $d$ )  $\delta$  5.47 – 5.41 (m, 1H), 5.36 (q,  $J = 6.0$  Hz, 1H), 4.44 (dd,  $J = 8.8, 2.5$  Hz, 1H), 4.30 – 4.15 (m, 5H), 4.00 (d,  $J = 8.7$  Hz, 1H), 3.46 (s, 0.13H), 3.43 (s, 0.49H), 3.26 (s, 0.30H), 3.24 (s, 0.08H), 2.32 (ddt,  $J = 13.4, 9.4, 6.7$  Hz, 2H), 1.39 – 1.20 (m, 12H), 1.07 – 0.96 (m, 10H).  $^{13}\text{C}$  NMR (126 MHz,  $\text{CDCl}_3$ )  $\delta$  201.9, 201.8, 200.4, 200.2, 172.1, 172.0, 171.9, 171.8, 166.8, 166.7, 166.3, 104.1, 104.0, 102.6, 102.5, 97.9, 97.8, 93.1, 93.0, 61.9, 58.5, 58.2, 56.7, 56.2, 44.4, 44.0, 43.9, 43.7, 29.7, 29.4, 27.9, 27.9, 27.8, 27.8, 27.7, 25.7, 25.4, 22.4, 22.3, 22.2, 22.2, 22.1, 22.1, 22.0, 20.4, 20.3, 17.6, 14.3, 14.2, 14.1. HRMS  $m/z$  ( $\text{M}+\text{H}^+$ ) predicted, 270.1700; observed, 270.1694.



**Compound 1.93.**  $dr \approx 1.7:1$   $^1\text{H}$  NMR (500 MHz,  $\text{CDCl}_3$ )  $\delta$  5.37–5.27 (m, 1H), 5.06 (tq,  $J = 5.8, 2.9$  Hz, 1H), 4.34–4.18 (m, 2H), 3.62 (d,  $J = 12.5$  Hz, 0.63H), 3.58 (d,  $J = 12.4$  Hz, 0.37H), 3.38–3.30 (m, 1H), 1.99 (overlapping qd,  $J = 7.1, 2.9$  Hz, 2H), 1.52 (s, 3H), 1.46–1.23 (m, 9H), 0.93 – 0.82 (m, 3H).  $^{13}\text{C}$  NMR (75.4 MHz,  $\text{CDCl}_3$ )  $\delta$  204.7, 170.4, 167.4, 94.7, 94.6, 86.4, 86.3, 85.8, 85.7, 62.1, 62.0, 51.8, 51.7, 49.7, 49.5, 31.5, 31.4, 28.8, 28.7, 28.6, 27.1, 23.3, 22.6, 14.3, 14.2. HRMS  $m/z$  [ $\text{M}+\text{H}]^+$  predicted, 295.1904; observed, 295.1915.

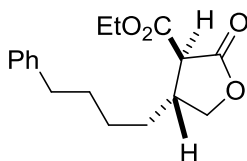


**Compound 1.95.**  $^1\text{H}$  NMR (500 MHz,  $\text{CDCl}_3$ )  $\delta$  5.31–5.22 (m, 2H), 3.76 (s, 3H), 3.25–3.14 (m, 1H), 3.09 (d,  $J = 10.8$  Hz, 1H), 2.53–2.24 (m, 3H), 2.02–1.93 (m, 3H), 1.78–1.64 (m, 1H), 1.46–1.25 (m, 8H), 0.93–0.86 (m, 3H).  $^{13}\text{C}$  NMR (125.8 MHz,  $\text{CDCl}_3$ )  $\delta$  211.2, 203.1, 202.9, 169.3,

94.6, 94.4, 92.5, 92.4, 61.1, 60.9, 52.6, 40.3, 40.1, 38.4, 38.3, 31.6, 31.5, 28.9, 28.8, 27.9, 27.8, 22.7, 22.6, 14.2. HRMS  $m/z$   $[M+H]^+$  predicted, 251.1642; observed, 251.1634.

#### 1.7.4. General procedure for allene reductions

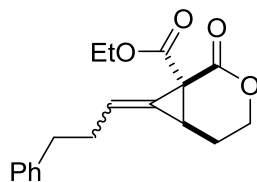
To a 0.1 M solution of allene in THF was added 5% Pd/C. Reaction purged with N<sub>2</sub> for 15 minutes, placed under static vacuum, then placed under 1 atm H<sub>2</sub> gas *via* balloon. After 24 h, the balloon was removed and reaction mixture evaporated under reduced pressure. The resulting residue was purified by column chromatography (using a gradient of 0% to 10% ethyl acetate in hexanes) to yield the products as a colorless oil.



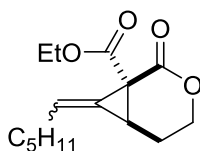
**Compound 1.96.** <sup>1</sup>H NMR (300 MHz, CDCl<sub>3</sub>) δ 7.35 – 7.10 (m, 7H), 4.49 (ddd,  $J$  = 8.7, 7.7, 0.8 Hz, 1H), 4.30 – 4.20 (m, 2H), 3.88 (t,  $J$  = 8.6 Hz, 1H), 3.21 (dd,  $J$  = 9.2, 0.8 Hz, 1H), 3.05 – 2.81 (m, 1H), 2.67 – 2.52 (m, 3H), 1.75 – 1.17 (m, 15H). <sup>13</sup>C NMR (75 MHz, CDCl<sub>3</sub>) δ 172.4, 168.0, 142.6, 128.6, 128.5, 126.0, 72.3, 62.4, 52.9, 40.4, 36.0, 32.5, 31.4, 29.2, 27.1, 14.3.

#### 1.7.5. General procedure for cyclopropanation reactions

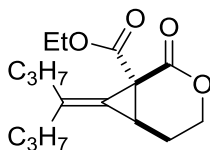
A 0.1 M solution of the diazo compound in toluene was added over a period of 12 to 24 h to a vigorously stirring mixture of CuI (5.0 mol %) in dichloromethane (0.1 M) under an atmosphere of nitrogen. When TLC indicated complete consumption of the starting material, the reaction mixture was concentrated *in vacuo*. The resulting residue was purified by column chromatography (using a gradient of 5% to 25% ethyl acetate in hexanes) to yield the products as colorless or yellow oils. All products were isolated as inseparable mixtures of *E* and *Z* isomers.



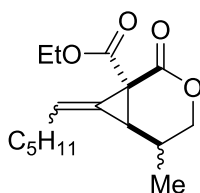
**Compound 1.97.**  $^1\text{H}$  NMR (300 MHz,  $\text{CDCl}_3$ )  $\delta$  7.34–7.11 (m, 5H), 6.33 (ddd,  $J = 8.0, 6.1, 2.3$  Hz, 0.89H), 6.10 (t,  $J = 6.5$  Hz, 0.11H), 4.21 (q,  $J = 7.1$  Hz, 2H), 3.96 (ddt,  $J = 11.5, 4.7, 1.9$  Hz, 1H), 3.46 (ddd,  $J = 12.6, 11.5, 2.9$  Hz, 1H), 2.94–2.45 (m, 5H), 2.17–1.86 (m, 1H), 1.78 (app dq,  $J = 14.2, 2.5$  Hz, 1H), 1.28 (t,  $J = 7.1$  Hz, 3H).  $^{13}\text{C}$  NMR (75 MHz,  $\text{CDCl}_3$ )  $\delta$  176.1, 166.8, 166.7, 165.6, 165.4, 141.1, 141.0, 128.8, 128.7, 128.6, 128.5, 126.4, 126.3, 126.0, 125.9, 120.7, 120.5, 100.6, 64.9, 64.8, 62.1, 35.0, 34.9, 33.4, 33.1, 32.9, 32.8, 25.9, 25.4, 21.2, 21.2, 14.3, 14.2. HRMS  $m/z$   $[\text{M} + \text{H}]^+$  predicted, 301.1435; observed, 301.1428.



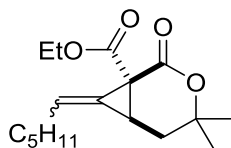
**Compound 1.98.**  $^1\text{H}$  NMR (300 MHz,  $\text{CDCl}_3$ )  $\delta$  6.34 (*E*) (td,  $J = 6.7, 2.3$  Hz, 0.87H), 6.14 (td,  $J = 7.2, 2.1$  Hz, 0.13H), 4.27–4.16 (m, 3H), 4.15–3.96 (m, 1H), 2.80 (dd,  $J = 3.7, 1.9$  Hz, 1H), 2.31–2.17 (m, 3H), 2.10–1.95 (m, 1H), 1.49 (q,  $J = 6.6$  Hz, 1H), 1.39–1.22 (m, 8H), 0.99–0.81 (m, 3H).  $^{13}\text{C}$  NMR (101 MHz,  $\text{CDCl}_3$ )  $\delta$  166.8, 165.5, 127.2, 119.3, 65.0, 61.9, 32.7, 31.4, 31.3, 28.2, 25.7, 22.4, 21.2, 14.2, 14.0, 0.1. HRMS  $m/z$   $[\text{M} + \text{H}]^+$  predicted, 267.1591; observed, 267.1598.



**Compound 1.99.**  $^1\text{H}$  NMR (300 MHz,  $\text{CDCl}_3$ )  $\delta$  4.21 (m, 3H), 4.04 (ddd,  $J = 12.7, 11.3, 3.0$  Hz, 1H), 2.87–2.73 (m, 1H), 2.34–2.12 (m, 4H), 1.62–1.40 (m, 4H), 1.28 (t,  $J = 7.1$  Hz, 3H), 0.94 (t,  $J = 7.3$  Hz, 3H), 0.87 (t,  $J = 7.3$  Hz, 3H).  $^{13}\text{C}$  NMR (75 MHz,  $\text{CDCl}_3$ )  $\delta$  167.4, 166.1, 139.6, 114.3, 110.0, 100.6, 65.2, 61.9, 37.0, 36.4, 32.6, 26.6, 22.9, 21.8, 20.9, 20.8, 14.3, 14.2, 14.1. HRMS  $m/z$   $[\text{M} + \text{H}]^+$  predicted, 281.1748; observed, 281.1738.

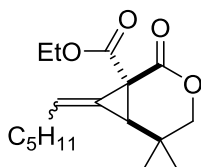


**Compound 1.101.** as a 97:3 mixture of *E*:*Z* isomers.  $dr \approx 2:1$ .  $^1\text{H}$  NMR (300 MHz,  $\text{CDCl}_3$ )  $\delta$  6.37–6.21 (m, 0.97H), 6.20–6.05 (m, 0.03H), 4.28–4.17 (m, 2H), 4.13 (dd,  $J = 11.3, 2.9$  Hz, 1H), 3.98 (dt,  $J = 11.3, 2.0$  Hz, 1H), 2.58 (q,  $J = 2.0$  Hz, 1H), 2.37–2.13 (m, 3H), 1.57–1.42 (m, 4H), 1.42–1.18 (m, 8H), 1.11 (d,  $J = 6.7$  Hz, 0.8H), 1.04 (d,  $J = 6.6$  Hz, 0.2 H), 1.04–0.77 (m, 3H).  $^{13}\text{C}$  NMR (75 MHz,  $\text{CDCl}_3$ )  $\delta$  187.0, 167.1, 165.8, 165.6, 127.5, 126.5, 120.7, 119.0, 70.6, 70.4, 62.0, 32.6, 32.5, 32.1, 31.6, 31.4, 29.1, 28.4, 26.6, 26.3, 22.6, 16.5, 15.6, 14.2, 14.1. HRMS  $m/z$   $[\text{M} + \text{H}]^+$  predicted, 281.1748; observed, 281.1762.

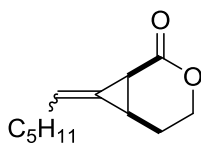


**Compound 1.102.**  $^1\text{H}$  NMR (400 MHz,  $\text{CDCl}_3$ )  $\delta$  6.03 (td,  $J = 6.8, 2.4$  Hz, 0.86H), 5.95 (td,  $J = 7.3, 2.1$  Hz, 0.11H), 4.16 (m, 2H), 2.56 (tt,  $J = 5.7, 2.1$  Hz, 1H), 2.27–2.03 (m, 3H), 1.64 (dd,  $J =$

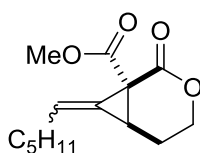
14.1, 5.4 Hz, 1H), 1.43 (s, 3H), 1.30 (s, 3H), 1.27–1.14 (m, 8H), 0.82 (t,  $J = 6.9$  Hz, 3H).  $^{13}\text{C}$  NMR (101 MHz,  $\text{CDCl}_3$ )  $\delta$  176.6, 168.4, 168.3, 165.2, 165.0, 127.3, 127.2, 122.9, 122.6, 83.2, 61.9, 61.8, 35.4, 35.1, 31.4, 31.3, 31.0, 30.8, 29.1, 28.6, 28.5, 28.4, 28.1, 26.4, 26.3, 24.3, 24.0, 22.5, 22.4, 14.2, 14.1, 14.0, 14.0, 13.9, 1.0. HRMS (ESI)  $m/z$   $[\text{M} + \text{Na}]^+$  predicted, 317.1724; observed, 317.1741.



**Compound 1.104.**  $^1\text{H}$  NMR (400 MHz,  $\text{CDCl}_3$ )  $\delta$  6.23 (td,  $J = 7.5, 2.3$  Hz, 1H), 6.13 (td,  $J = 7.2, 2.0$  Hz, 0H), 4.21 (q,  $J = 7.1$  Hz, 2H), 3.81 (d,  $J = 11.1$  Hz, 1H), 3.70 (dd,  $J = 11.1, 2.4$  Hz, 1H), 2.48 (t,  $J = 2.0$  Hz, 1H), 2.27 (qd,  $J = 7.4, 1.4$  Hz, 2H), 1.48 (qt,  $J = 6.9, 4.2$  Hz, 2H), 1.39 – 1.19 (m, 10H), 1.13 (s, 3H), 0.93 – 0.83 (m, 3H).  $^{13}\text{C}$  NMR (101 MHz,  $\text{CDCl}_3$ )  $\delta$  186.1, 166.8, 165.6, 126.6, 121.9, 120.3, 74.7, 61.8, 53.5, 36.9, 33.2, 31.9, 31.4, 29.6, 28.9, 23.9, 23.8, 22.5, 22.4, 14.1, 14.0, 13.9. HRMS (ESI)  $m/z$   $[\text{M} + \text{H}]^+$  predicted, 295.1904; observed, 295.1910.



**Compound 1.106.** as a 66:34 mixture of *E*:*Z* isomers.  $^1\text{H}$  NMR (300 MHz,  $\text{CDCl}_3$ )  $\delta$  6.20 (tt,  $J$  = 6.7, 2.1 Hz, 0.66H), 6.08 (tt,  $J$  = 7.0, 2.1 Hz, 0.34H), 4.22–3.99 (m, 2H), 2.52–2.41 (m, 2H), 2.36 (ddt,  $J$  = 7.3, 3.4, 1.7 Hz, 1H), 2.27–2.15 (m, 1H), 1.40–1.19 (m, 8H), 0.89 (overlapping t,  $J$  = 6.9, 3H).  $^{13}\text{C}$  NMR (75 MHz,  $\text{CDCl}_3$ )  $\delta$  170.2, 170.1, 118.9, 118.6, 100.7, 64.4, 64.3, 31.7, 31.6, 28.8, 28.6, 22.7, 22.6, 21.5, 21.4, 20.8, 20.5, 18.7, 18.6, 14.2. HRMS (ESI)  $m/z$   $[\text{M} + \text{H}]^+$  predicted, 195.1380; observed, 195.1383.



**Compound 1.108.**  $^1\text{H}$  NMR (300 MHz,  $\text{CDCl}_3$ )  $\delta$  6.34 (td,  $J$  = 6.7, 2.2 Hz, 0.9H), 6.22–6.10 (m, 0.1H), 4.24 (m, 1H), 4.15–3.96 (m, 3H), 3.77 (s, 3H), 2.82 (dq,  $J$  = 3.7, 2.1 Hz, 1H), 2.34–2.13 (m, 3H), 1.49 (q,  $J$  = 6.8 Hz, 2H), 1.43–1.13 (m, 6H), 1.01–0.80 (m, 3H).  $^{13}\text{C}$  NMR (126 MHz,  $\text{CDCl}_3$ )  $\delta$  167.3, 167.2, 165.4, 165.3, 127.4, 127.0, 119.4, 119.2, 65.0, 64.9, 52.9, 52.8, 32.5, 32.3, 31.5, 31.3, 31.2, 31.2, 31.1, 28.8, 28.7, 28.4, 28.1, 26.1, 25.9, 22.5, 22.4, 22.3, 21.1, 21.0, 14.1, 14.0, 13.9, 13.8. HRMS (ESI)  $m/z$   $[\text{M} + \text{H}]^+$  predicted, 253.1435; observed, 253.1436.

## 1.8. Bibliography

1. (a) Curtius, T. *Ber.* **1883**, 16, 2230. (b) Curtius, T. *J. Prakt. Chem.* **1888**, 38, 396.
2. (a) Doyle, M. P.; McKervey, M. A.; Ye, T. *Modern Catalytic Methods for Organic Synthesis with Diazo Compounds: From Cyclopropanes to Ylides.*; John Wiley & Sons: New York, 1998. pp. 163-279. (b) H. M. L. Davies, E. Antoulinakis, *Org. React.* **2001**, 57, 1 – 326. (c) M. P. Doyle, D. C. Forbes, “Recent Advances in Asymmetric Catalytic Metal Carbene Transformations” *Chem. Rev.* **1998**, 98, 911 – 935.



3. Chen, D. Y.-K.; Pouwer, R. H.; Richard, J.-A. *Chem. Soc. Rev.* **2012**, *41*, 4631.
4. Tang, P.; Qin, Y. *Synthesis* **2012**, *44*, 2969.
5. (a) Davies, H. M. L.; Manning, J. R. *Nature* **2008**, *451*, 417. (b) Colby, D. A.; Bergman, R. G.; Ellman, J. A. *Chem. Rev.* **2010**, *110*, 704. (c) *C-H Activation*, eds. Yu, J.-Q; Shi, Z.; Wiley-VCH Verlag, Heidelberg, 2010.
6. For classical examples of stereochemical match/mismatch in more complex aldol reactions: (a) Masamune, S.; Choy, W.; Petersen, J. S.; Rita, L. R. *Angew. Chem. Int. Ed.* **1985**, *24*, 1. (b) Evans, D. A.; Dart, M. J.; Duffy, J. L.; Rieger, D. L. *J. Am. Chem. Soc.* **1995**, *117*, 9073.
7. Recent reviews demonstrating the generation and transfer of allene axial chirality: (a) Hoffman-Röder, A.; Krause, N. *Angew. Chem., Int. Ed.* **2004**, *43*, 1196. (b) Yu, S.; Ma, S. *Angew. Chem., Int. Ed.* **2012**, *51*, 3074. (c) Allen, A. D.; Tidwell, T. T. *Chem. Rev.* **2013**, *113*, 7287. (d) Campolo, D.; Gastaldi, S.; Roussel, C.; Bertrand, M. P.; Nacheb, M. *Chem. Soc. Rev.* **2013**, *42*, 8434.
8. Burke, S. D.; Grieco, P. A. *Org. React.* **1979**, *26*, 361.
9. Doyle, M. P.; Westrum, L. J.; Wolthuis, W. N.; See, M. M.; Boone, W. P.; Bagheri, V.; Pearson, M. M. *J. Am. Chem. Soc.* **1993**, *115*, 958.
10. (a) Fraile, J. M.; García, J. I.; Martínez-Merino, V.; Mayoral, J. A.; Salvatella, L. *J. Am. Chem. Soc.* **2001**, *123*, 7616. (b) Rasmussen, T.; Jensen, J. F.; Østergaard, N.; Tanner, D.; Ziegler, O.; Norrby, O. *Chem. Eur. J.* **2002**, *8*, 177. (c) Hansen, J.; Autschbach, J.; Davies, H. M. L. *J. Org. Chem.* **2009**, *74*, 6555.
11. Paulissenen, R.; Reimlinger, H.; Hayez, E.; Hubert, A. J.; Teyssie, P. *Tetrahedron Lett.* **1973**, *24*, 2233.

12. Padwa, A.; Austin, D. J.; Price, A. T.; Semones, M. A.; Doyle, M. P.; Protopopova, M. N.; Winchester, W. R.; Tran, A. *J. Am. Chem. Soc.* **1993**, *115*, 8669.
13. Ceccherelli, P.; Curini, M.; Marcotullio, M. C.; Rosati, O. *Tetrahedron* **1992**, *48*, 9767.
14. Doyle, M. P.; Phillips, I. M. *Tetrahedron Lett.* **2001**, *42*, 3155.
15. Taber, D. F., "Carbon-Carbon Bond Formation by C-H Insertion," in *Comprehensive Organic Synthesis: Selectivity, Strategy, and Efficiency in Modern Organic Chemistry*; Trost, B. M.; Fleming, I., Eds.; Pergamon Press: New York, 1991; Vol. 3, Chapter 4.2.
16. Padwa, A.; Austin, D. J. *Angew. Chem. Int. Ed. Engl.* **1994**, *33*, 1797.
17. Davies, H. M. L.; Denton, J. R. *Chem. Soc. Rev.* **2009**, *38*, 3061.
18. Beckwith, R. E. J.; Davies, H. M. L. *Chem. Rev.* **2003**, *103*, 2861.
19. Davies, H. M. L.; Morton, D. *Chem. Soc. Rev.* **2011**, *40*, 1857.
20. Davies, H. M. L.; Coleman, M. G.; Ventura, D. L. *Org. Lett.* **2007**, *9*, 4971.
21. Nadeua, E.; Ventura, D. L.; Brekan, J. A.; Davies, H. M. L. *J. Org. Chem.* **2010**, *75*, 1927.
22. (a) Rahman, W.; Kuivila, H.G. *J. Org. Chem.*, **1966**, *31*, 772. (b) Ball, W. J.; Landor, S. *R. Proc. Chem. Soc.* **1961**, 246.
23. (a) Reddy, R. P.; Davies, H. M. L. *J. Am. Chem. Soc.* **2007**, *129*, 10312. (b) Schwartz, B. D.; Denton, J. R.; Lian, Y.; Davies, H. M. L.; Williams, C. M. *J. Am. Chem. Soc.* **2009**, *131*, 8329.
24. (a) Noyori, R.; Takaya, H.; Nakanisi, Y.; Nozaki, H. *Can. J. Chem.* **1969**, *47*, 1242. (b) Creary, X. *J. Org. Chem.*, **1978**, *43*, 1777.
25. Huval, C. C.; Singleton, D. A. *J. Org. Chem.* **1994**, *59*, 2020.
26. Lautens, M.; Delanghe, P. H. M. *J. Org. Chem.* **1993**, *58*, 5037

27. (a) Bertrand, M.; Maurin, R. *Bull. Soc. Chim. Fr.* **1967**, 2779. (b) Maurin, R.; Bertrand, M. *Bull. Soc. Chim. Fr.* **1961**, 2261.
28. Molander, G. A.; Harring, L. S. *J. Org. Chem.* **1989**, *54*, 3525.
29. Lautens, M.; Meyer, C.; van Oeveren, A. *Tetrahedron Lett.* **1997**, *38*, 3833.
30. Gregg, T. M.; Farrugia, M. K.; Frost, J. R. *Org. Lett.* **2009**, *11*, 4434.
31. Gregg, T. M.; Algera, R. F.; Frost, J. R.; Hassan, F.; Stewart, R. J. *Tetrahedron Lett.* **2010**, *51*, 6429.
32. Yao, T.; Hong, A.; Sarpong, R. *Synthesis* **2006**, *21*, 3605.
33. (a) Yu, S.; Ma, S. *Chem Commun.* **2011**, *47*, 5384. (b) *Modern Allene Chemistry*, ed N. Krause and A. S. K. Hashmi, Wiley-VCH, Weinheim, Germany, 2004.
34. Tejedor, D.; Méndez-Abt, G.; Cotos, L.; García-Tellado, F. *Chem. Soc. Rev.* **2013**, *42*, 458.
35. Henderson, M. A.; Heathcock, C. H. *J. Org. Chem.* **1988**, *53*, 4736.
36. Sherry, B. D.; Toste, F. D. *J. Am. Chem. Soc.* **2004**, *126*, 15978.
37. N. Krause and A. Hoffmann-Röder, *Tetrahedron* **2004**, *60*, 11671.
38. Elsevier, C. J.; Vermeer, P. *J. Org. Chem.* **1989**, *54*, 3726.
39. Myers, A. G.; Zheng, B. *J. Am. Chem. Soc.* **1996**, *118*, 4492.
40. (a) Weatherly, C.D.; Rigoli, J.W.; Schomaker, J.M. *Org. Lett.* **2012**, *14*, 1704. (b) Rigoli, J.W.; Boralsky, L.A.; Hershberger, J.C.; Meis, A.R.; Guzei, I.A.; Schomaker, J.M. *J. Org. Chem.* **2012**, *77*, 2446.
41. Adams, C. S.; Boralsky, L. A.; Guzei, I. A.; Schomaker, J. M. *J. Am. Chem. Soc.*, **2012**, *134*, 10807.
42. Grigg, R.D.; Schomaker, J.M.; Timokhin, V. *Tetrahedron* **2011**, *67*, 4318.

43. Nozaki, H.; Takaya, H.; Moriuti, S. *Tetrahedron* **1968**, 24, 3655.
44. Armarego, W.L.F.; Chai, C.L.L. *Purification of Laboratory Chemicals* 6th ed., Elsevier: Burlington, MA, 2009.

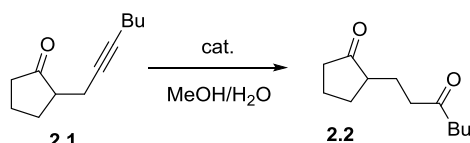
## **Chapter 2:**

# **Au-Catalyzed Carbocyclization of Allenes to form Fully Substituted Cyclopentanes**

## 2.1 Introduction to Gold-Catalyzed Carbocyclization

Homogenous gold catalysis as a field of study has seen explosive growth in the last twenty years.<sup>1</sup> Gold catalysts are ideally suited to coordinate to multiple C-C bonds as a  $\pi$ -acid due to relativistic effects.<sup>2</sup> In comparison to other Group 11 metals, gold catalysts are less nucleophilic and less likely to undergo oxidative addition, preferring instead to act as “soft” Lewis acids. This activation of normally electron-rich, unsaturated species for nucleophilic attack was demonstrated first by the Utimoto group, in which a gold catalyst was demonstrated to show comparable activity to palladium catalysts for the addition of water to alkynones (Table 2.1).<sup>3</sup>

**Table 2.1.** Hydration of alkynones with palladium and gold catalysis.



The reaction scheme shows the hydration of alkynone **2.1** to ketone **2.2**. **2.1** is 1-(but-1-en-3-yn-1-yl)cyclopentan-1-one. The reaction conditions are a catalyst (cat.) in a mixture of methanol and water (MeOH/H<sub>2</sub>O). The product **2.2** is 1-(butan-1-onyl)cyclopentan-1-one.

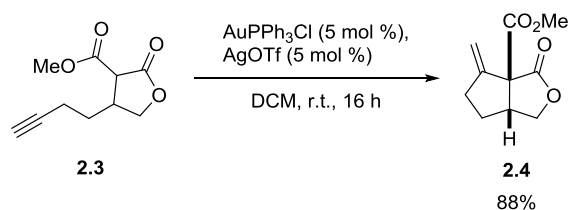
Catalyst (mol%)	time (h)	yield (%)
(MeCN) <sub>2</sub> PdCl <sub>2</sub> (5)	10	96
NaAuCl <sub>4</sub> ·2H <sub>2</sub> O (3)	5.5	91

Since these initial results, gold activation of double and triple bonds has become an incredibly active field of study.<sup>4</sup> A wide variety of nucleophiles have been used to attack the activated bonds, including nitrogen,<sup>5</sup> oxygen,<sup>6</sup> and halogens,<sup>7</sup> but the possibility for the formation of carbon-carbon bonds is particularly exciting. The utility of this has been exploited in a range of carbocyclization reactions that have been developed to allow for new strategies of carbon skeleton construction.

### 2.1.1 Gold Carbocyclizations of Alkynes

A large body of work exists in connection with gold catalyzed carbocyclizations. The Conia-ene cyclizations represent a subgroup which is more relevant to the allene cyclizations discussed here. The Toste group developed the reaction shown in Scheme 2.1, in which a 1,3-dicarbonyl species can be used for direct nucleophilic attack onto the alkyne.<sup>8</sup> The gold-catalyzed Conia-ene reaction allows formation of the *exo*-methylenecyclopropane **2.4** in good yield. Deuteration studies suggested that this reaction proceeds through an enol addition to the gold-activated alkyne.

**Scheme 2.1.** Conia-ene cyclization of alkynes.

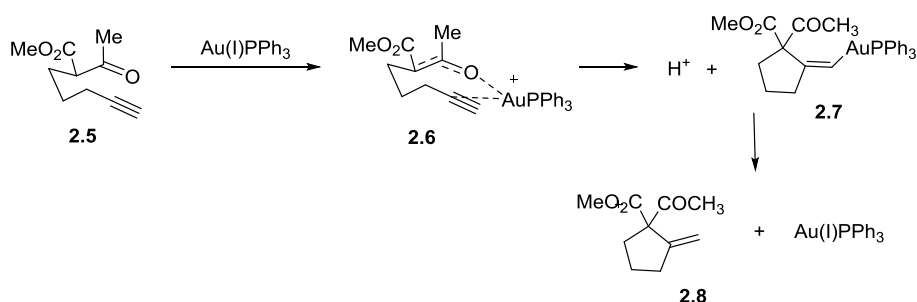


The proposed possible mechanisms for this Conia-ene reaction could proceed were investigated computationally (Scheme 2.2).<sup>9</sup> Pathway 1 begins with the coordination of the cationic Au(I) species to the alkyne and the ketone to form gold enolate **2.6**. The cyclization of this enolate results in vinyl gold intermediate **2.7**, which undergoes protodeauration to yield the product **2.8**. Pathway 2 begins with formation of the enol **2.9** *before* coordination of the gold catalyst. When the gold catalyst does coordinate, it does so to the alkyne exclusively to give intermediate **2.10**. The cycloisomerization reaction occurs and is followed quickly by the spontaneous protonation of the vinyl gold intermediate **2.11** to yield the products. The computations indicated that pathway 2 is more likely, as was suggested originally by Toste. It was found that the triflate counterion can participate as a proton shuttle and lower the energy

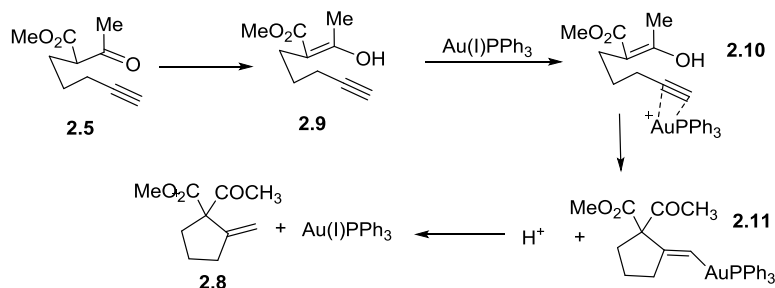
barrier of keto-enol tautomerization. In addition, the gold cation always showed a preference for coordination to the triple bond as in **2.10**. An intermediate Au-enolate such as **2.6** could not be located computationally.

**Scheme 2.2.** Possible mechanistic pathways for alkyne cyclization.

**Pathway 1:**

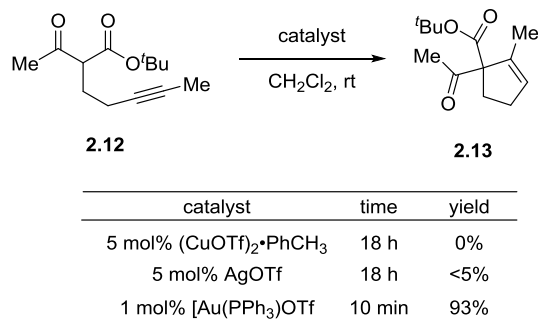


**Pathway 2:**

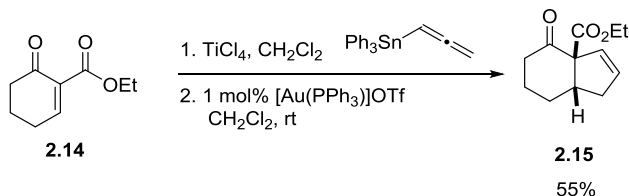


Further work from the Toste group expanded the methodology to internal alkynes, simply by switching to a 5-*endo-dig* cyclization (Table 2.2).<sup>10</sup> In comparison to the *exo* reaction, the *endo* Conia-ene avoids a significant 1,3-allylic strain in the transition state. Working from the previous assumption that the alkyne was exclusively activated by gold catalysts, they showed that copper and silver were unable to perform the conversion of internal alkynes such as **2.12** to cyclopentenones (Table 2.2, entries 1 and 2), demonstrating the singularity of gold in these types of reactions.

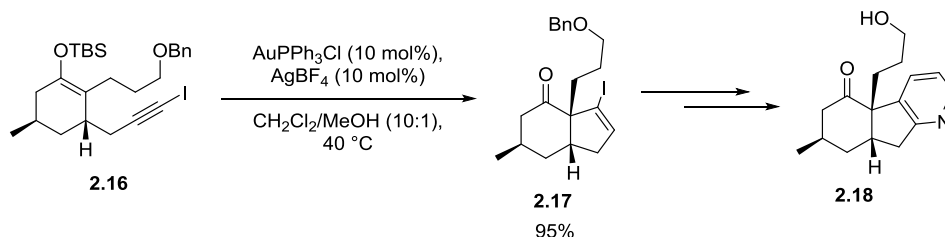


**Table 2.2.** 5-*endo-dig* carbocyclization of alkynes.

Interestingly, the group generated bicyclic substrates using allenyl organometallic species (Scheme 2.3).<sup>10</sup> Conjugate addition of the allenyltriphenylstannane to **2.14** could then be followed by gold-catalyzed cyclization to result in cyclopentene **2.15** as a single diastereomer.

**Scheme 2.3.** Cyclopentene annulation using allenyltriphenylstannane.

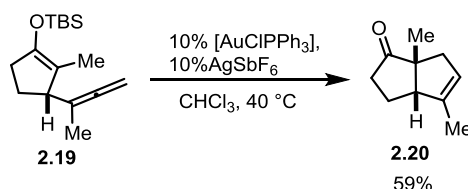
Between the two methods, a wide variety of substituted cyclopentane rings could be synthesized quickly and easily. The methodology proved so useful that it was almost immediately applied to natural product synthesis by the Toste group. As part of the first total synthesis of (+)-lycopoladine A (Scheme 2.4),<sup>10</sup> iodoalkyne **2.16** was efficiently cyclized using AuPPh<sub>3</sub>Cl, under slightly elevated catalyst loading and reaction temperature. This method led to a very efficient total synthesis of (+)-lycopoladine A, delivering the desired structure in eight steps and 16.5% overall yield.

**Scheme 2.4.** Use of alkyne carbocyclization in the synthesis of (+)-lycopoladine A.

In conclusion, direct cyclization reactions of alkynes laid the groundwork for further studies using gold. Mechanistic investigations in this reaction strongly suggest that the main mechanism of action is *via* activation of alkynes by the gold- $\pi$  bond interaction. The development of the mild cationic gold activation conditions opened new avenues of investigation into carbon nucleophile attack on sites of unsaturation.

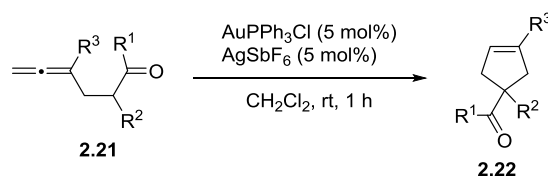
### 2.1.2 Previous work with allenes

While cyclization reactions resulting from the addition of heteroatoms to allenes using gold catalysis is became well known around the year 2000,<sup>11</sup> attack of a carbon nucleophile on a gold-activated allene was not demonstrated until the Toste group showed an example in 2006.<sup>12</sup> The 5-*endo-trig* cyclization of a silyl enol ether onto a terminal allene was demonstrated to provide a hexahydroindenone derivative (Scheme 2.5). This transformation was not explored fully; only two examples were shown at the end of a publication focusing on the analogous reaction with alkynes.

**Scheme 2.5.** Cyclization of silyl enol ether onto 1,1-disubstituted allene.

In contrast, the Ma group more fully developed a cyclization from allenic  $\beta$ -keto esters (Table 2.3).<sup>13</sup> This cyclization showed moderate to good yields (43-93%) for a variety of 1,1-disubstituted allenes; however, the variation in functional groups was comparatively small, and only terminal allenes were attempted, leading to relatively simple products. In contrast to previous work, however, the reactions required no external heating and were finished in a relatively short time. Substrates containing simple alkyl groups and esters worked moderately well (entries 1-3), though use of a more electron-donating phenyl group instead of the ester showed the best yield of the substrates tried (entry 4). More substituted alkyl chains (entry 5) and aryl-containing groups (entries 6 and 7) were tolerated on the ketone, as well as on the allene itself (entry 8). Interestingly, palladium catalysts, which are known to promote Conia-ene reactivity with alkenes,<sup>14</sup> favored oxymetallation-allylation to result in dihydrofuran products instead of the Conia-ene reaction.

**Table 2.3.** Au-catalyzed cyclization of 2-(2',3'-allenyl)acetylacetates

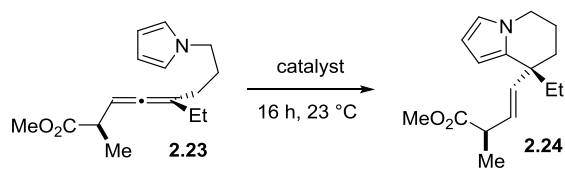


Entry	R <sup>1</sup>	R <sup>2</sup>	R <sup>3</sup>	yield
1	Me	CO <sub>2</sub> Et	H	68%
2	Me	CO <sub>2</sub> Me	H	51%
3	Et	CO <sub>2</sub> Et	H	42%
4	nPr	Ph	H	93%
5	iPr	CO <sub>2</sub> Me	H	76%
6	Bn	CO <sub>2</sub> Me	H	71%
7	Ph	CO <sub>2</sub> Me	H	67%
8	Me	CO <sub>2</sub> Et	Bn	73%

In addition to malonate-type moieties, electron-rich aromatic rings can be used as nucleophiles.<sup>15</sup> As shown in Table 2.4, pyrrole nucleophiles were used to perform hydroarylation on the proximal double bond of the allene, forming six-membered rings. Palladium catalysts

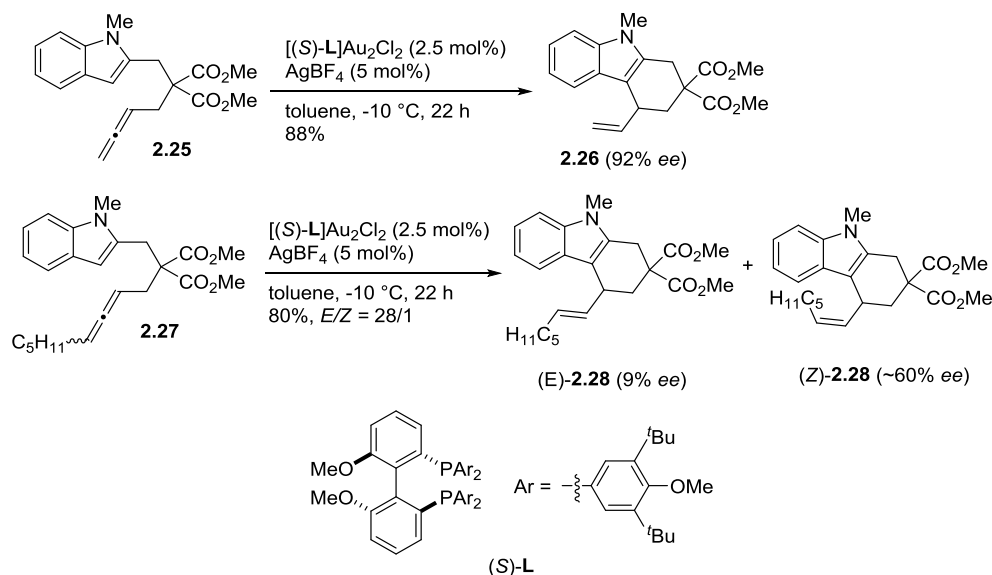
showed poor reactivity (entry 1), and gold (III) catalysts showed poor conversion (entry 2). High diastereoselectivity is only achieved with gold (I) catalysts in conjunction with a silver halide scavenger (entry 4), and this is presumed to be due to the internal carbonyl group directing coordination to the cationic gold catalyst.

**Table 2.4.** Hydroarylation of allenes using pyrrole nucleophiles.

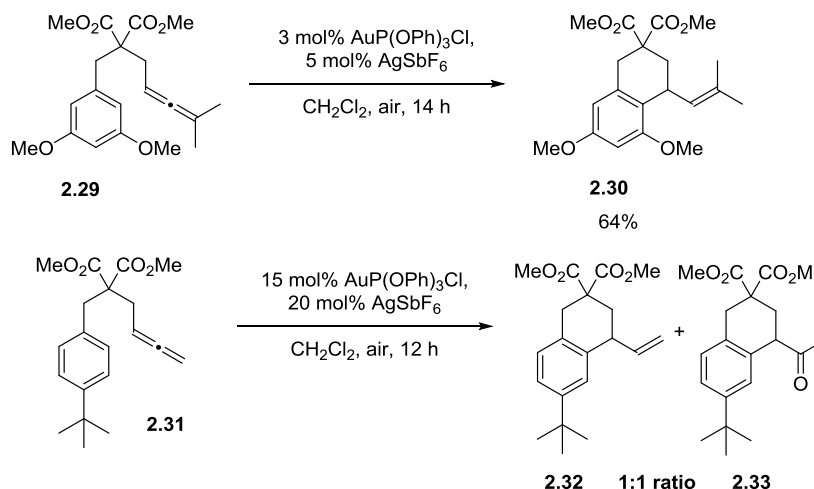


Catalyst (mol%)	yield (%)	<i>dr</i>
(MeCN) <sub>2</sub> PdCl <sub>2</sub> (30)	83	67:33
AuCl <sub>3</sub> (10)	27	92:8
AuCl <sub>3</sub> (5): AgOTf (20)	82	92:8
PPh <sub>3</sub> AuOTf (5)	92	97:3

Indoles can also be used as internal nucleophiles for allenes. As shown in Scheme 2.6, tetrahydrocarbazoles can be formed easily.<sup>16</sup> Starting from achiral allenes such as **2.25**, the hydroarylation can occur to give tetrahydrocarbazole products such as **2.26** in good yields and high enantioselectivities, even when using trisubstituted allenes or forming seven membered rings. However, when 1,3-disubstituted allenes such as **2.27** are used, the products *E/Z*-**2.28** are obtained with low enantioselectivity, even at low temperatures and long reaction times. This substrate control of stereoselectivity suggests that the chiral catalyst binds *trans* to the homoallylic ester group, so poor discrimination of the *si* and *re* faces of the allene is obtained.

**Scheme 2.6.** Gold-catalyzed hydroarylation of allenes with indole nucleophiles.

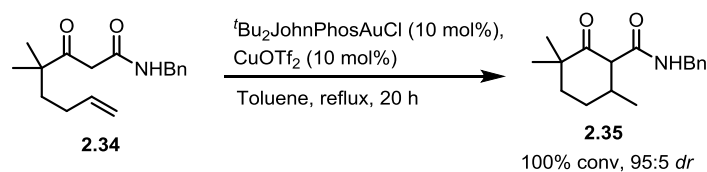
One final class of nucleophiles that has been explored with allenes are electron-rich aromatic rings.<sup>17</sup> Selective 6-*exo-trig* cyclization of aryl allenes is demonstrated in Scheme 2.7. This investigation was undertaken to find the full range of nucleophiles that can be freely used with allenes, based on nucleophilicity parameters.<sup>18</sup> While electron-rich aromatic rings such as **2.29** worked quite well, moving to less activated substrates such as **2.31** results in significant amounts of the allene hydration product methyl ketone **2.33**. Only allene hydration products are produced when more electron-poor substrates are subjected to the reaction conditions, and all attempts to reduce the hydration product only led to poor conversion. This gives a helpful guideline of Mayr N values of  $\sim -4$  as the lower limit of  $\pi$ -nucleophilicity that is required to attack the gold-activated allene.<sup>19</sup>

**Scheme 2.7.** Intramolecular hydroarylation of electron-rich aryl allenes.

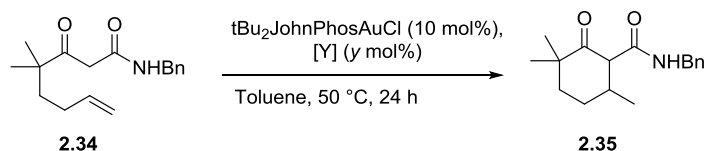
### 2.1.3 Previous work with silver-free systems

While most of the previous systems focused exclusively on gold catalysts paired with silver halide scavengers as an activating group, this approach has more recently been shown to be somewhat problematic. Several groups have found that silver additives can have non-innocent roles in gold catalysis, affecting the reaction in unexpected ways, including formation of mixed gold-silver complexes and changing the rates and selectivities of the reaction.<sup>15</sup> In addition, the  $\text{Au}^+$  cation generated when the halide is removed is fragile, and prone to decomposing into  $\text{Au}(0)$  or other nonreactive complexes. For these reasons, the Gandon group has investigated the possibility of using other metals for the activation of gold complexes.

Their first reported reaction using a silver-free system used a gold catalyst with a variety of copper salts,<sup>20</sup> to produce cyclized product from the ene- $\beta$ -ketoamide **2.34**, as seen in Scheme 2.8. The use of a copper salt instead of a silver salt is hypothesized to allow a more gradual delivery of the cationic gold species into solution. This leads to slower degradation of the catalyst, allowing the reaction to take place at high temperatures for long reaction times without loss of activity.

**Scheme 2.8.** Use of copper salts as Au(I) halide scavenger.

In addition to copper, the Gandon group extended the possible halide scavengers to include other Lewis acids including zinc, indium and bismuth (Table 2.5).<sup>21</sup> These catalysts provided several benefits, including higher diastereoselectivity and lowered catalyst loading, but not just any Lewis acid could be used as the partner to gold. The triflates of early transition metals did not catalyze the reaction (entries 1 and 2). While zinc, aluminum and gallium triflates did promote the reaction (entries 3,4,6), the respective chlorides of these metals did not, possibly due to a reduced capacity to act as a proton shuttle in the reaction.<sup>22</sup> In addition, the inactivity of triflic acid alone (entries 13 and 14) points to a mechanism other than simple hydrolysis of the triflate group.

**Table 2.5.** Effects of various two-component catalyst systems on hydroalkylation.

Entry	[Y]	y [mol%]	Conv. [%]	dr
1	Sc(OTf) <sub>3</sub>	10	0	--
2	Yb(OTf) <sub>3</sub>	10	0	--
3	Zn(OTf) <sub>2</sub>	10	83	73:27
4	Al(OTf) <sub>3</sub>	10	26	72:28
5	AlCl <sub>3</sub>	10	0	--
6	Ga(OTf) <sub>3</sub>	10	traces	n.d.
7	GaCl <sub>3</sub>	10	0	--
8	In(OTf) <sub>3</sub>	10	100	74:26
9	In(OTf) <sub>3</sub>	1	100	73:27
10	Me <sub>3</sub> SiOTf	10	100	73:27
11	Bi(OTf) <sub>3</sub>	10	60%	90:10
12	Bi(OTf) <sub>3</sub>	1	100	72:28
13	TfOH	1	0	--
14	TfOH	10	0	--

### 2.1.4 Conclusions

In conclusion, there is a wide body of literature demonstrating that gold catalysis is particularly effective at activating positions of unsaturation in cyclization reactions for nucleophilic attack. Direct carbocyclization of this type has been explored most fully with alkyne substrates. Some work with allenes has been done, but much of the work has used simple terminal allene substrates, yielding comparatively unfunctionalized products. One interesting aspect to this chemistry has been the development of Au chemistry using halide scavengers other than silver, which became a key component of the method described in this chapter.

Two specific gaps that our method sought to address are the lack of 1,3-disubstituted allenes and malonates used in previous reports. A new stereocenter at the site of C-C bond formation can be installed by using an unsymmetrical allene starting material, assuming the reaction can be made diastereoselective. Our previous C-H insertion reaction was developed to

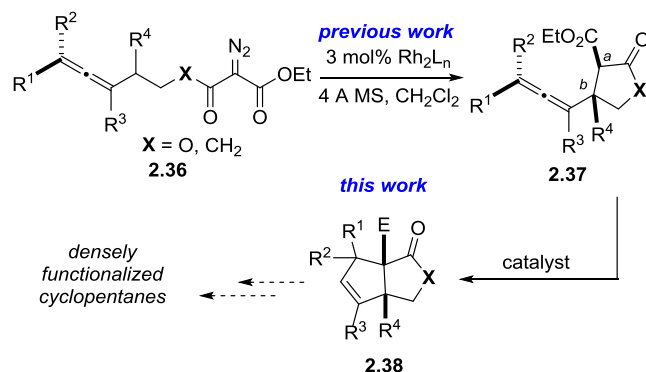


form *gamma*-lactones and these substrates are known to be more difficult to cyclized in Conia-ene type reactions than the  $\beta$ -ketoesters used in previous work. The development of such a diastereoselective system and its application in the synthesis of fully substituted cyclopentane rings is the focus of the work described in this chapter.

## 2.2 Results and Discussion

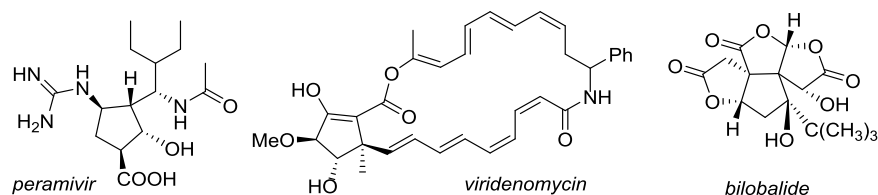
Our group has previously described Rh(II)-catalyzed, chemoselective insertions of metal carbenoids into allenic C-H bonds<sup>23</sup> (Scheme 2.9, see Chapter 1) to yield products poised for subsequent carbocyclization to substituted cyclopentanes containing up to six contiguous stereocenters.

**Scheme 2.9.** Extension of previous C-H insertion chemistry to form cyclopentanes.



These motifs occur in a host of biologically important natural products, examples of which are shown in Scheme 2.10. However, these highly substituted cyclopentanes are often difficult to synthesize in a straightforward manner.<sup>24</sup>

**Scheme 2.10.** Highly substituted cyclopentane natural products.



Intramolecular examples of C-C bond formation through the addition of carbon nucleophiles to allenes are known using Au catalysts (see Section 2.1.2). However, these approaches require the use of pre-functionalized silyl enol ethers and do not take advantage of the axial chirality of the allene to achieve the diastereoselective syntheses of fully substituted five-membered ring systems. To our knowledge, no examples using 1,3-disubstituted allenes in this chemistry have been reported. Therefore, we sought to develop a system that would address these issues.

Transition metal catalysis for the carbocyclization of allenes **2.39** and **2.40** was investigated using the well-known combination of a Au(I) halide and Ag(I) halide scavenger (Table 2.6.). For  $\beta$ -ketoester substrate **2.39**, simple conditions using AuPPh<sub>3</sub>Cl and a range of silver sources enabled complete conversion to the cyclopentene **2.41** (entries 1-4). Copper catalysts did not facilitate the reaction adequately (entries 5 and 6). However, the gold/silver conditions optimized for the  $\beta$ -ketoester substrate **2.39** were not adequate for the malonate substrate **2.40** (entry 7). Palladium conditions used for the analogous alkyne systems were adequate (entry 8), but showed no induction of diastereoselectivity. A variety of acids were tested as additives (entries 9-11). The optimal conditions used AgOTf as a halide scavenger and TfOH as an additive (entries 12 and 13). However, these conditions oddly only worked with AuPPh<sub>3</sub>Cl; all other gold sources gave little or no conversion. In addition, the conditions were difficult to reproduce even when the same source of AuPPh<sub>3</sub>Cl was used. When a new bottle of

AuPPh<sub>3</sub>Cl was obtained, the same conditions optimized in Table 2.6 failed and no conversion of **2.40** was observed.

**Table 2.6.** Initial screening of gold carbocyclization conditions.

entry	R, X	catalyst	additive	conversion	dr
1	Me, CH <sub>2</sub>	(Ph <sub>3</sub> P)AuCl	AgOTf	100%	1:1
2	Me, CH <sub>2</sub>	(Ph <sub>3</sub> P)AuCl	AgBF <sub>4</sub>	100%	1:1
3	Me, CH <sub>2</sub>	(Ph <sub>3</sub> P)AuCl	AgSbF <sub>6</sub>	100%	1:1
4	Me, CH <sub>2</sub>	(Ph <sub>3</sub> P)AuCl	AgClO <sub>4</sub>	100%	1:1
5	Me, CH <sub>2</sub>	Cu(OTf) <sup>+</sup> toluene	Et <sub>3</sub> N	trace	---
6	Me, CH <sub>2</sub>	Cu(MeCN) <sub>4</sub> PF <sub>6</sub>	Et <sub>3</sub> N	trace	---
7	Et, O	(Ph <sub>3</sub> P)AuCl	AgOTf	0%	---
8	Et, O	Pd <sub>2</sub> dba <sub>3</sub> /dppe	NaOMe	100%	1:1
9	Et, O	(Ph <sub>3</sub> P)AuCl	AgOTf, Tf <sub>2</sub> NH	0%	---
10	Et, O	(Ph <sub>3</sub> P)AuCl	AgOTf, CSA	10%	1:1
11	Et, O	(Ph <sub>3</sub> P)AuCl	AgOTf, Bi(OTf) <sub>3</sub>	100%	1:1
12	Et, O	(Ph <sub>3</sub> P)AuCl	AgOTf, TfOH	90%	2.5:1
13	Me, CH <sub>2</sub>	(Ph <sub>3</sub> P)AuCl	AgOTf, TfOH	100%	1:1

We proposed that the allene might be interacting with the active cationic gold species in a reductive manner to yield either Au(0) or inactive (PPh<sub>3</sub>)<sub>2</sub>Au<sup>+</sup>.<sup>25</sup> This meant that the original gold source had been contaminated with a small amount of some other compound, most likely metallic, that had been preventing the decomposition of the Au and accelerating the reaction. With this in mind, we screened a variety of additives in an attempt to restore the reactivity.

We found that Cu(OTf)<sub>2</sub> as an additive, inspired by the previous report from Gandon,<sup>20</sup> reinstated the reactivity of a variety of gold sources (Table 2.7) with *dr* ranging from 1:1 to 1.6:1, provided the reaction was run at reflux; lower temperatures did not effectively promote the reaction. A wide variety of gold catalysts were able to facilitate the cyclization, but very bulky catalysts (entry 7) and electron-poor catalysts (entry 9) showed lower conversion to product. In addition, gold(III) chloride was not an effective catalyst (entry 10). As expected, Cu sources with coordinating anions did not promote the reaction (entry 11). While Cu(I)OTf-toluene complex

promoted the reaction (entry 12), it did not result in any increased *dr*. Additionally, using gold or copper alone (entry 13 and 14 respectively) did not yield the desired product.

**Table 2.7.** Catalyst screening for Au-catalyzed carbocyclization.

**2.40** **2.42**

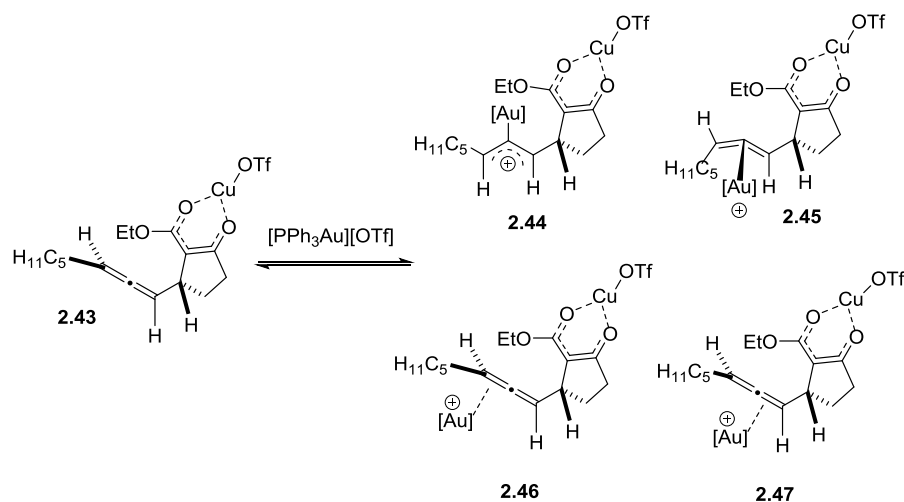
entry	Au source	Cu source	NMR yield <sup>a</sup>	<i>dr</i>
1	(Ph <sub>3</sub> P)AuCl	Cu(OTf) <sub>2</sub>	100%	1.1:1
2	dppm(AuCl) <sub>2</sub>	Cu(OTf) <sub>2</sub>	100%	1.1:1
3	AuPrCl	Cu(OTf) <sub>2</sub>	88%	1.3:1
4	<sup>t</sup> Bu <sub>2</sub> JohnPhosAuCl	Cu(OTf) <sub>2</sub>	81%	1:1
5	Cy <sub>2</sub> JohnPhosAuCl	Cu(OTf) <sub>2</sub>	100%	1:1
6	<sup>t</sup> Bu <sub>3</sub> PAuCl	Cu(OTf) <sub>2</sub>	100%	1:1
7	( <i>o</i> -tolyl) <sub>3</sub> PAuCl	Cu(OTf) <sub>2</sub>	70%	1:1
8	Cy <sub>3</sub> PAuCl	Cu(OTf) <sub>2</sub>	85%	1.3:1
9	(PhO) <sub>3</sub> PAuCl	Cu(OTf) <sub>2</sub>	55%	1.6:1
10	AuCl <sub>3</sub>	Cu(OTf) <sub>2</sub>	0%	--
11	(Ph <sub>3</sub> P)AuCl	Cu(OAc) <sub>2</sub>	0%	--
12	(Ph <sub>3</sub> P)AuCl	(CuOTf) <sub>2</sub> •toluene	82%	1:1
13	(Ph <sub>3</sub> P)AuCl	none	0%	--
14	none	Cu(OTf) <sub>2</sub>	0%	--

<sup>a</sup>Yield determined by relative integration to mesitylene internal standard

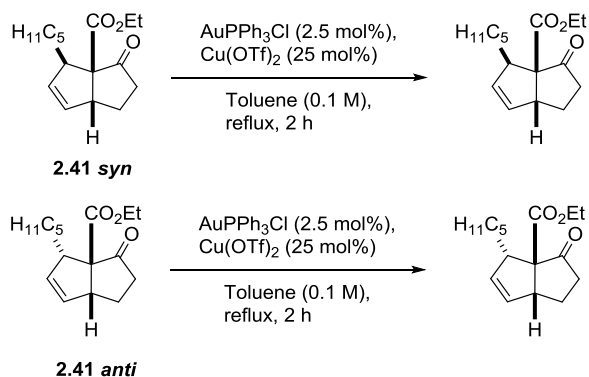
With a reproducible carbocyclization method in hand, the next goal was to improve the *dr* in the addition of the proposed copper enolate intermediate to the allene (Figure 2.1). Control of the facial selectivity is challenging due to several factors, including the planar nature of the enolate, the distance between the catalyst complex and the site of bond formation, and the lack of substantial steric differentiation between the nucleophilic and electrophilic portions of the molecule. The formation of the copper enolate **2.43** negates the stereochemistry of the dicarbonyl carbon, and the coordination of gold to the allene can go through one of several structures.<sup>26</sup> A structure such as  $\alpha$ -allylic cation **2.44** would destroy stereochemical information from the allene, while a “bent allene” structure (**2.45**) or either of the possible  $\eta^2$  forms (**2.46** or **2.47**) would

retain that stereochemistry. Even within the coordination types that would retain stereochemistry, the degree of retention will depend on the size and type of ligands on the gold catalyst. To make matters even more complicated, Widenhoefer has shown that allenes can equilibrate between different types of coordination during the course of a reaction,<sup>27</sup> so nailing down the exact intermediate is difficult.

**Figure 2.1.** Possible coordination geometries of gold to allene.



While poor selectivity may be observed initially, an epimerization to the most stable product could theoretically yield a higher selectivity for one product. The *dr* was observed over the course of the reaction in order to determine if the final *dr* was the result of equilibration to the most stable product. For several different conditions (see experimental), the *dr* stayed consistent over the course of the reaction. This indicates that the stereochemistry set at the time of attack sets the *dr*, and epimerization over the course of the reaction is not a major factor in the final stereoselectivity that is observed. A second piece of evidence for this conclusion is that separated diastereomers of the cyclopentene **2.41** do not undergo epimerization to the other isomer, as shown in Scheme 2.11.

**Scheme 2.11.** Epimerization of cyclopentene products.

A wide variety of reaction conditions were explored to try to increase the diastereoselectivity of the initial attack, including solvents, temperatures and reaction times, chiral acid additives and chiral ligands. Some common bulky chiral gold dimer complexes were screened for activity; however, these catalysts gave no conversion on their own (entries 1 and 2). The monomer chiral ligand MonoPhos gave moderate conversion alone (entry 3). The addition of the chiral acid additive **A** slightly increased the *dr* with  $\text{AuPPh}_3\text{Cl}$  (entry 4), but the dimeric catalysts still showed poor conversion even with the additive (entry 5). The combination of MonoPhos and **A** gave a good balance of conversion and *dr* (entry 6), but a small mismatch effect of the different enantiomers of MonoPhos was observed (entry 7). The acid additive could be reduced to a catalytic amount without much loss of yield or *dr* (entry 8). However, the distance of the Au catalyst from the site of reactivity hindered attempts to influence the stereoselectivity of the cyclization event any further.

**Table 2.8.** Screening of chiral ligands and acids for diastereoselectivity.

entry	Au source	additive	NMR yield	dr
1	<i>R</i> -DTBM-SEGPHOS(AuCl) <sub>2</sub>	none	0%	--
2	<i>R</i> -SEGPHOS(AuCl) <sub>2</sub>	none	0%	--
3	<i>S</i> -MonoPhosAuCl	none	46%	1.6:1
4	AuPPh <sub>3</sub> Cl	1 equiv. <b>A</b>	76%	1.6:1
5	dppm(AuCl) <sub>2</sub>	1 equiv. <b>A</b>	22%	1.5:1
6	<i>S</i> -MonoPhosAuCl	1 equiv. <b>A</b>	83%	1.8:1
7	<i>R</i> -MonoPhosAuCl	1 equiv. <b>A</b>	53%	1.5:1
8	<i>S</i> -MonoPhosAuCl	5 mol% <b>A</b>	76%	1.7:1

<sup>a</sup> dr of the stereocenter *a*

**A:**

*S*-MonoPhos:

As the reaction conditions shown in Table 2.8 were not very practical, we sought an alternative solution. While the Cu(OTf)<sub>2</sub> additive is postulated to cause a slow release of the active cationic gold species,<sup>20</sup> not much is known about any other roles it might be playing in the reaction mixture. Therefore, we sought to improve the *dr* by changing the relative amounts of gold and copper catalysts in the reaction, a strategy which was successful in obtaining diastereoselectivity comparable to the chiral catalysts used in Table 2.8. When the ratio of Au:Cu was changed to 1:5, the *dr* increased significantly, while the conversion was poorer due to the lower amount of gold catalyst that was used (entry 2). However, even when the ratio was kept at 1:5 and the amount of gold was raised back to 5 mol% (entry 3), conversion was still poor under the normal 2 hour reaction time. Raising the ratio of Au:Cu up to 1:10 increased the *dr* slightly (entries 4 and 5), but increasing it further resulted in poorer *dr* and the high amount of copper made isolation more difficult (entries 6 and 7). To alleviate the poor conversion while still maintaining high *dr*, a 1:10 ratio of Au:Cu was used with a higher gold loading of 2.5 mol%

and the reaction time was extended to 24 hours (entry 8). Because of the extended reaction time, we hypothesized that catalyst decomposition could become a problem, and tried a more electron-rich gold catalyst to better support the cationic species (entry 9). Excitingly, this gave a much improved yield in conjunction with high diastereoselectivity.

**Table 2.9.** Exploration of Au:Cu ratio for increased diastereoselectivity.

$\text{H}_{11}\text{C}_5$   $\text{EtO}_2\text{C}$   $\text{O}$   $\text{X mol\% AuPPh}_3\text{Cl}$   $\text{H}_{11}\text{C}_5$   $\text{EtO}_2\text{C}$   $\text{O}$   
 $\text{dr 1:1}$   $\text{Y mol\% Cu(OTf)}_2$   $\text{2.42}$   
 $\text{2.40}$   $\text{toluene, reflux}$

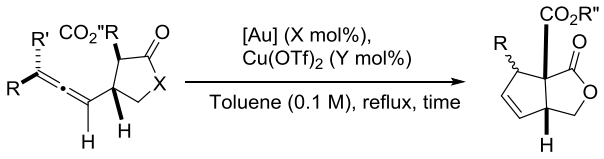
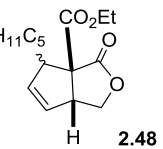
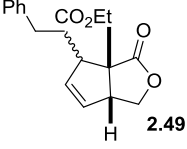
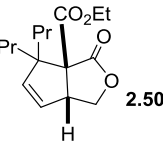
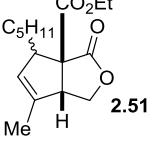
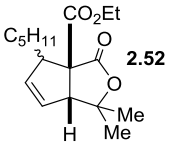
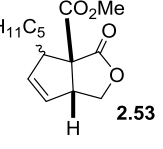
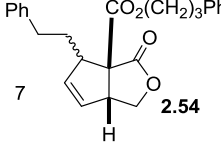
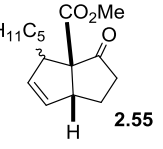
entry	X	Y	time (h)	NMR yield <sup>a</sup>	dr
1	5	5	2	72%	1.3:1
2	1	5	2	35%	1.7:1
3	5	25	2	41%	1.8:1
4	1	10	2	34%	2.0:1
5	1	10	12	50%	1.9:1
6	1	25	2	36%	1.4:1
7	1	100	2	58%	1:1
8	2.5	25	24	68%	1.6:1
9 <sup>b</sup>	2.5	25	24	93%	1.8:1

<sup>a</sup>Yield determined by relative integration to mesitylene internal standard.  
<sup>b</sup> AuPCy<sub>3</sub>Cl used in place of AuPPh<sub>3</sub>Cl.

Using the optimized reaction conditions, the substrate scope of the cyclization was explored. Substitution on the distal position of the allene was well tolerated (entries 1 and 2), including trisubstituted allenes (entry 3). Substitution could also be introduced at the proximal end of the allene with no loss of *dr* (entry 4). A gem-dimethyl group on the lactone ring can be used (entry 5) and substitutions on the ester were also tolerated (entry 6 and 7). As expected, the  $\beta$ -keto ester converted quite well under these conditions, but control of diastereoselectivity was never obtained (entry 8).



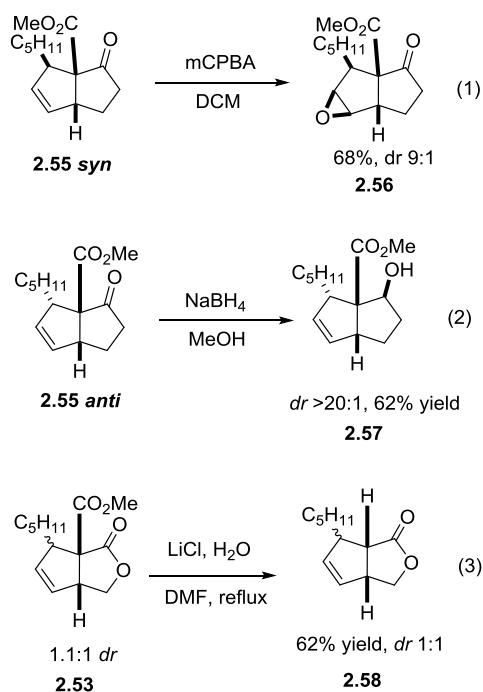
**Table 2.10.** Substrate scope of Au-catalyzed carbocyclization.

						
entry	product	[Au]	X:Y	time	yield <sup>a</sup>	dr
1	 <b>2.48</b>	AuPPh <sub>3</sub> Cl	2.5:25	24 h	68%	1.6:1
		AuPCy <sub>3</sub> Cl	2.5:25	24 h	93%	1.8:1
2	 <b>2.49</b>	AuPPh <sub>3</sub> Cl	1:5	2 h	72%	2.1:1
		AuPPh <sub>3</sub> Cl	2.5:25	24 h	67%	1.2:1
3	 <b>2.50</b>	AuPPh <sub>3</sub> Cl	5:5	2h	62%	N/A
4	 <b>2.51</b>	AuPPh <sub>3</sub> Cl	2.5:25	24h	54%	2.0:1
5	 <b>2.52</b>	AuPPh <sub>3</sub> Cl	2.5:25	24 h	70%	2.6:1
		AuPCy <sub>3</sub> Cl	2.5:25	24 h	89%	6.6:1
6	 <b>2.53</b>	AuPPh <sub>3</sub> Cl	5:5	2 h	68%	2.0:1
7	 <b>2.54</b>	AuPPh <sub>3</sub> Cl	5:5	18 h	43%	1.0:1
		AuPPh <sub>3</sub> Cl	2.5:25	24 h	74%	1.2:1
8	 <b>2.55</b>	AuPPh <sub>3</sub> Cl	5:5	2 h	95%	1.0:1
		AuPPh <sub>3</sub> Cl	2.5:25	2 h	71%	1.0:1

<sup>a</sup> NMR yields relative to mesitylene standard.

The cyclopentene product was carried forward to the fully substituted cyclopentane ring *via* alkene functionalization. Simple epoxidation of the alkene with mCPBA works quite well, with high diastereoselectivity for the convex face of the bicyclic system (Scheme 2.12, eq 1). Reduction of the ketone in an all carbon substrate proceeds with high selectivity for one diastereomer, leading to the possibility of 6 adjacent stereocenters if the alkene is also functionalized (Scheme 2.12, eq 2). If the ester moiety is not needed, the methyl ester can be easily removed using Krapcho decarbocyclization conditions as shown in Scheme 2.12, equation 3. This facile removal is a marked advantage of using an acceptor-substituted carbene precursor in the initial C-H insertion reaction.

**Scheme 2.12.** Further reactivity of carbocyclization products.



In conclusion, we have demonstrated that highly complex cyclopentane scaffolds can be accessed in only a few steps from an allene precursor. Equilibrium control of a copper enolate addition to the activated allene drives stereocontrol of a Conia-ene carbocyclization. This high

energy transformation is enabled by the slow delivery of the fragile cationic gold species via triflate exchange with the copper source. Subsequent transformations of the alkene products show the variety of functionalization patterns that can be accessed *via* this methodology.

Future work on this project will involve broader exploration of the substrate scope, as well as demonstrating more functionalization reactions of the final product. The power of this modular method to access fully substituted cyclopentane rings can be applied to a wide variety of interesting molecules and will hopefully inspire further investigation into the exciting realm of gold catalysis of allenes.

## 2.3 Experimental Section

All glassware was either oven-dried overnight at 130 °C or flame-dried under a stream of dry nitrogen prior to use. Unless otherwise specified, reagents were used as obtained from the vendor without further purification. Tetrahydrofuran and diethyl ether were freshly distilled from purple Na/benzophenone ketyl. Dichloromethane, acetonitrile and toluene were dried over  $\text{CaH}_2$  and freshly distilled prior to use. All other solvents were purified in accordance with “Purification of Laboratory Chemicals”.<sup>1</sup> Air- and moisture- sensitive reactions were performed using standard Schlenk techniques under an atmosphere of nitrogen. Analytical thin layer chromatography (TLC) was performed utilizing pre-coated silica gel 60 F<sub>254</sub> plates containing a fluorescent indicator, while preparative chromatography was performed using SilicaFlash P60 silica gel (230-400 mesh) via Still’s method.<sup>2</sup> Unless otherwise stated, the mobile phases for column chromatography were mixtures of hexanes/ethyl acetate. Columns were typically run using a gradient method, beginning with 100% hexanes and gradually increasing the polarity

using ethyl acetate. Various stains were used to visualize reaction products, including *p*-anisaldehyde,  $\text{KMnO}_4$ , ceric ammonium molybdate (CAM stain) and iodine powder.

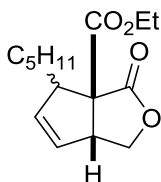
$^1\text{H}$  NMR and  $^{13}\text{C}$  NMR spectra were obtained using Bruker-300, Varian-300, Varian Inova-500, or Varian Unity-500 spectrometers. For  $^1\text{H}$  NMR, chemical shifts are reported relative to residual protiated solvent peaks ( $\delta$  7.26, 2.49, 7.15 and 7.09 ppm for  $\text{CDCl}_3$ ,  $(\text{CD}_3)_2\text{SO}$ ,  $\text{C}_6\text{D}_6$  and  $\text{CD}_3\text{C}_6\text{D}_5$  respectively).  $^{13}\text{C}$  NMR spectra were measured at either 125 MHz or 75 MHz on the same instruments noted above for recording  $^1\text{H}$  NMR spectra. Chemical shifts were again reported in accordance to residual protiated solvent peaks ( $\delta$  77.2, 39.5, 128.0 and 137.9 ppm for  $\text{CDCl}_3$ ,  $(\text{CD}_3)_2\text{SO}$ ,  $\text{C}_6\text{D}_6$ , and  $\text{CD}_3\text{C}_6\text{D}_5$ , respectively). High-pressure liquid chromatography (HPLC) analyses were performed at 215 and 225 nm using a Shimadzu HPLC, Model LC-20AB. Further details are given in Section VII. Accurate mass measurements were acquired at the University of Wisconsin, Madison using a Micromass LCT (electrospray ionization, time-of-flight analyzer or electron impact methods) or a Waters Micromass Autospec (electron impact, high sector, direct probe). The NMR and Mass Spectrometry facilities are funded by the NSF (CHE-9974839, CHE-9304546, CHE-9208463, CHE-9629688) and the University of Wisconsin, as well as the NIH (RR08389-01).

Substrate lactones were synthesized as described previously<sup>19</sup> and characterization matched previous literature values.

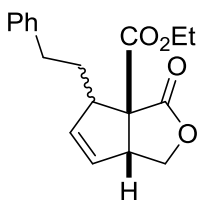
### 2.3.1 General procedure for gold reactions

A 10 mL round bottom flask was charged with  $\text{AuPPh}_3\text{Cl}$  (0.38 mmol) and  $\text{Cu}(\text{OTf})_2$  (0.095 mmol) in 1.9 mL toluene and allowed to stir for ~15 minutes under  $\text{N}_2$ . Allene substrate (0.38 mmol) in 1.9 mL toluene is then added, and reaction heated to reflux. After 2 hours, reaction cooled to room temperature, vacuum filtered through silica to remove excess metal salts,

plug washed with ethyl acetate, then solvent removed under reduced pressure. The resulting residue was purified *via* column chromatography, using hexanes:ethyl acetate gradients.

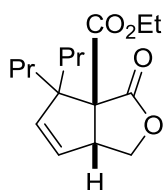


**Compound 2.48.**  $^1\text{H}$  NMR (500 MHz,  $\text{CDCl}_3$ ), Major isomer:  $\delta$  5.84 (dt,  $J = 5.5, 2.0$  Hz, 1H), 5.53 (dt,  $J = 5.3, 2.3$  Hz, 1H), 4.44 (dd,  $J = 8.7, 7.3$  Hz, 1H), 4.26 (q,  $J = 6.8$  Hz, 2H), 4.17 (dd,  $J = 8.9, 1.8$  Hz, 1H), 3.80 (dt,  $J = 7.1, 2.1$  Hz, 1H), 3.51 (ddd,  $J = 9.2, 5.4, 2.4$  Hz, 1H), 2.01 – 1.92 (m, 1H), 1.48 – 1.17 (m, 10H), 0.96 – 0.82 (m, 3H). Minor isomer:  $\delta$  5.89 (dt,  $J = 5.3, 2.4$  Hz, 1H), 5.63 (dt,  $J = 5.8, 1.5$  Hz, 1H), 4.41 (dd,  $J = 9.1, 6.0$  Hz, 1H), 4.26 (q,  $J = 6.8$  Hz, 2H), 4.23 (m, 1H), 4.02 – 3.94 (m, 1H), 3.37 – 3.27 (m, 1H), 1.58 (dt,  $J = 11.0, 4.2$  Hz, 1H), 1.50 – 1.18 (m, 10H), 0.91 – 0.86 (m, 3H).  $^{13}\text{C}$  NMR (126 MHz,  $\text{CDCl}_3$ )  $\delta$  175.5, 173.1, 169.6, 166.8, 136.3, 136.0, 129.2, 127.5, 70.3, 70.2, 63.8, 62.2, 62.2, 61.7, 53.4, 52.1, 51.4, 49.1, 31.9, 31.8, 31.6, 30.0, 28.4, 26.3, 22.6, 22.5, 14.1, 14.1, 14.0. HRMS (ESI)  $m/z$  calculated for  $\text{C}_{15}\text{H}_{22}\text{O}_4$   $[\text{M} + \text{H}]^+$  267.1591, found 267.1595.

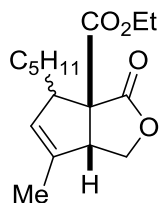


**Compound 2.49.**  $^1\text{H}$  NMR (500 MHz,  $\text{CDCl}_3$ ) Major isomer:  $\delta$  7.30 – 7.21 (m, 3H), 7.21 – 7.11 (m, 2H), 5.82 (dt,  $J = 5.7, 2.0$  Hz, 1H), 5.55 (dt,  $J = 5.8, 2.4$  Hz, 1H), 4.44 (overlapping t,  $J = 6.4$  Hz, 1H), 4.29 – 4.21 (m, 2H), 4.19 (dd,  $J = 8.9, 1.7$  Hz, 1H), 3.80 (dt,  $J = 7.1, 2.0$  Hz, 1H), 3.57 (ddq,  $J = 8.7, 6.3, 2.3$  Hz, 1H), 2.86 – 2.73 (m, 1H), 2.59 (dd,  $J = 9.2, 7.5$  Hz, 1H), 2.31 (ddt,  $J = 13.3, 9.8, 6.5$  Hz, 1H), 1.75 (dtd,  $J = 13.8, 9.4, 5.7$  Hz, 1H). Minor isomer:  $\delta$  7.30 – 7.21 (m, 3H),

7.21 – 7.11 (m, 2H), 5.96 (dt,  $J = 5.8, 2.4$  Hz, 1H), 5.69 (dt,  $J = 5.8, 1.5$  Hz, 1H), 4.44 (overlapping t,  $J = 6.4$  Hz, 1H), 4.29 – 4.21 (m, 3H), 4.02 (dt,  $J = 5.8, 2.0$  Hz, 1H), 3.41 (ddq,  $J = 9.3, 3.5, 1.8$  Hz, 1H), 2.86 – 2.73 (m, 1H), 2.59 (dd,  $J = 9.2, 7.5$  Hz, 1H), 1.94 (dtd,  $J = 12.9, 8.6, 8.0, 4.3$  Hz, 1H), 1.67 – 1.58 (m, 1H).  $^{13}\text{C}$  NMR (126 MHz,  $\text{CDCl}_3$ )  $\delta$  175.3, 173.1, 169.5, 166.7, 141.9, 141.5, 135.9, 135.7, 134.2, 134.1, 129.8, 129.3, 129.2, 128.5, 128.5, 128.3, 128.2, 127.9, 126.0, 125.8, 70.3, 70.1, 63.7, 62.3, 62.3, 61.7, 53.4, 51.9, 50.9, 49.2, 34.9, 33.7, 33.0, 31.9, 14.1, 14.0. HRMS (ESI)  $m/z$  calculated for  $\text{C}_{18}\text{H}_{20}\text{O}_4$   $[\text{M} + \text{NH}_4]^+$  318.1700, found 318.1699.

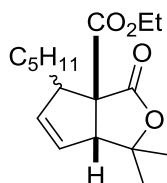


**Compound 2.50.**  $^1\text{H}$  NMR (500 MHz,  $\text{CDCl}_3$ )  $\delta$  5.65 (dd,  $J = 5.9, 2.3$  Hz, 1H), 5.56 (dd,  $J = 5.9, 1.8$  Hz, 1H), 4.32 (dd,  $J = 8.8, 6.5$  Hz, 1H), 4.31 – 4.17 (m, 2H), 4.14 (dd,  $J = 8.8, 1.1$  Hz, 1H), 4.04 (dtd,  $J = 6.6, 2.1, 1.1$  Hz, 1H), 1.91 – 1.74 (m, 2H), 1.67 (tqd,  $J = 12.2, 7.1, 5.0$  Hz, 1H), 1.51 – 1.45 (m, 2H), 1.32 (t,  $J = 7.1$  Hz, 3H), 1.29 – 1.16 (m, 2H), 1.15 – 1.03 (m, 1H), 0.93 (t,  $J = 7.2$  Hz, 3H), 0.85 (t,  $J = 7.2$  Hz, 3H).  $^{13}\text{C}$  NMR (126 MHz,  $\text{CDCl}_3$ )  $\delta$  172.6, 167.6, 139.9, 127.3, 69.2, 66.2, 62.1, 58.4, 50.9, 39.0, 36.8, 18.6, 17.4, 14.9, 14.7, 14.0. HRMS (ESI)  $m/z$  calculated for  $\text{C}_{18}\text{H}_{20}\text{O}_4$   $[\text{M} + \text{H}]^+$  281.1747, found 281.1744.

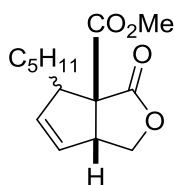


**Compound 2.51.**  $^1\text{H}$  NMR (500 MHz,  $\text{CDCl}_3$ ), Major isomer:  $\delta$  5.46 (q,  $J = 1.7$  Hz, 1H), 4.41 – 4.19 (m, 4H), 3.61 (dt,  $J = 7.5, 1.8$  Hz, 1H), 3.44 (ddd,  $J = 9.8, 5.2, 2.5$  Hz, 1H), 1.98 – 1.87 (m,

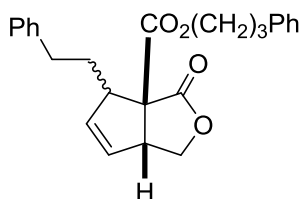
1H), 1.72 (dt,  $J = 2.5, 1.3$  Hz, 3H), 1.36 – 1.22 (m, 10H), 0.93 – 0.82 (m, 3H). Minor isomer:  $\delta$  5.52 (q,  $J = 1.9$  Hz, 1H), 4.41 – 4.19 (m, 4H), 3.80 (ddt,  $J = 5.0, 2.7, 1.4$  Hz, 1H), 3.24 – 3.18 (m, 1H), 1.97 – 1.88 (m, 1H), 1.76 (q,  $J = 1.4$  Hz, 3H), 1.36 – 1.18 (m, 10H), 0.93 – 0.83 (m, 3H).  $^{13}\text{C}$  NMR (126 MHz,  $\text{CDCl}_3$ )  $\delta$  175.7, 173.3, 169.7, 167.0, 136.5, 134.9, 130.2, 130.1, 68.1, 68.0, 64.2, 62.1, 62.1, 62.0, 56.0, 51.7, 51.0, 50.6, 31.9, 31.9, 31.8, 30.5, 28.4, 26.3, 22.6, 22.5, 14.1, 14.1, 14.1, 14.0. HRMS (ESI)  $m/z$  calculated for  $\text{C}_{16}\text{H}_{24}\text{O}_4$   $[\text{M} + \text{H}]^+$  calculated: 281.1747 found: 281.1749.



**Compound 2.52.**  $^1\text{H}$  NMR (500 MHz,  $\text{CDCl}_3$ ), Major isomer:  $\delta$  5.83 (dt,  $J = 5.8, 2.1$  Hz, 1H), 5.54 (dt,  $J = 5.8, 2.4$  Hz, 1H), 4.27 (q,  $J = 7.1$  Hz, 2H), 3.64 (q,  $J = 2.1$  Hz, 1H), 3.45 (ddq,  $J = 9.8, 5.8, 2.1$  Hz, 1H), 1.97 (m, 1H), 1.50 (s, 3H), 1.40 (d,  $J = 7.2$  Hz, 3H), 1.36 – 1.24 (m, 10H), 0.93 – 0.84 (m, 3H). Minor isomer:  $^1\text{H}$  NMR (500 MHz,  $\text{CDCl}_3$ )  $\delta$  5.86 (dt,  $J = 5.9, 2.3$  Hz, 1H), 5.65 (dt,  $J = 5.9, 1.7$  Hz, 1H), 4.28 (q,  $J = 7.2$  Hz, 2H), 3.82 (q,  $J = 2.1$  Hz, 1H), 3.36 (dtt,  $J = 10.9, 4.3, 1.9$  Hz, 1H), 1.97 (m, 1H), 1.50 (s, 3H), 1.40 (d,  $J = 7.2$  Hz, 3H), 1.36 – 1.24 (m, 10H), 0.92 – 0.84 (m, 3H).  $^{13}\text{C}$  NMR (126 MHz,  $\text{CDCl}_3$ )  $\delta$  174.8, 171.7, 170.9, 168.5, 135.4, 135.4, 127.4, 125.8, 84.9, 84.0, 65.7, 64.5, 62.5, 62.3, 62.2, 58.6, 53.8, 53.4, 32.1, 31.9, 31.8, 30.8, 29.6, 28.8, 28.1, 26.8, 25.2, 24.9, 22.5, 22.5, 22.5, 14.2, 14.0, 14.0. HRMS (ESI)  $m/z$  calculated for  $\text{C}_{17}\text{H}_{26}\text{O}_4$   $[\text{M} + \text{H}]^+$  295.1904, found 295.1901.



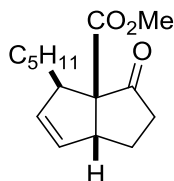
**Compound 2.53.**  $^1\text{H}$  NMR (500 MHz,  $\text{CDCl}_3$ ) Major isomer:  $\delta$  5.85 (dt,  $J$  = 5.8, 2.0 Hz, 1H), 5.54 (dt,  $J$  = 5.7, 2.3 Hz, 1H), 4.44 (dd,  $J$  = 9.0, 7.3 Hz, 1H), 4.16 (dd,  $J$  = 8.9, 2.0 Hz, 1H), 3.83 – 3.81 (m, 1H), 3.80 (s, 3H), 3.51 (ddt,  $J$  = 9.5, 5.1, 2.4 Hz, 1H), 2.01 – 1.90 (m, 1H), 1.48 – 1.17 (m, 8H), 0.91 – 0.86 (m, 3H). Minor isomer:  $\delta$  5.90 (dt,  $J$  = 5.8, 2.4 Hz, 1H), 5.63 (dt,  $J$  = 5.8, 1.5 Hz, 1H), 4.43 (s, 1H), 4.24 (d,  $J$  = 9.2 Hz, 1H), 4.02 – 3.97 (m, 1H), 3.80 (s, 3H), 3.33 (dtd,  $J$  = 9.4, 3.7, 1.8 Hz, 1H), 1.55 – 1.47 (m, 1H), 1.49 – 1.17 (m, 8H), 0.96 – 0.73 (m, 3H).  $^{13}\text{C}$  NMR (126 MHz,  $\text{CDCl}_3$ )  $\delta$  175.4, 173.0, 170.2, 167.3, 136.2, 135.9, 129.2, 127.6, 70.3, 70.2, 63.8, 61.6, 53.3, 53.2, 52.9, 52.4, 51.6, 49.1, 31.9, 31.8, 31.7, 30.0, 28.4, 26.4, 22.6, 22.5, 14.1, 13.9. HRMS (ESI)  $m/z$  calculated for  $\text{C}_{14}\text{H}_{20}\text{O}_4$  [ $\text{M} + \text{NH}_4$ ] $^+$  270.1700, found 270.1696.



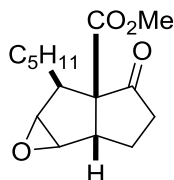
**Compound 2.54.**  $^1\text{H}$  NMR (500 MHz,  $\text{CDCl}_3$ ) Major isomer:  $\delta$  7.36 – 7.03 (m, 10H), 5.82 (dt,  $J$  = 5.8, 2.1 Hz, 1H), 5.55 (dt,  $J$  = 5.7, 2.4 Hz, 1H), 4.43 (dt,  $J$  = 9.1, 6.6 Hz, 1H), 4.20 (d,  $J$  = 2.1 Hz, 2H), 4.20 – 4.15 (m, 1H), 3.78 (dp,  $J$  = 6.3, 2.1 Hz, 1H), 3.57 (ddq,  $J$  = 8.6, 6.4, 2.3 Hz, 1H), 2.79 (qdd,  $J$  = 13.7, 9.7, 6.1 Hz, 1H), 2.68 (td,  $J$  = 8.2, 7.7, 2.5 Hz, 2H), 2.60 (dd,  $J$  = 9.7, 7.0 Hz, 1H), 2.33 (ddt,  $J$  = 13.2, 9.9, 6.5 Hz, 1H), 2.02 – 1.93 (m, 2H), 1.76 (dtd,  $J$  = 13.8, 9.4, 5.6 Hz, 1H). Minor diastereomer:  $\delta$  7.31 – 7.07 (m, 10H), 5.97 (dt,  $J$  = 5.8, 2.4 Hz, 1H), 5.70 (dt,  $J$  = 5.9, 1.5 Hz, 1H), 4.43 (dt,  $J$  = 9.1, 6.6 Hz, 2H), 4.26 (d,  $J$  = 9.2 Hz, 1H), 4.22 – 4.15 (m, 2H), 4.02 – 3.96 (m, 1H), 3.43 (ddd,  $J$  = 9.7, 4.1, 2.0 Hz, 1H), 2.79 (qdd,  $J$  = 13.7, 9.7, 6.1 Hz, 1H), 2.68 (td,  $J$  = 8.2, 7.7, 2.5 Hz, 2H), 2.60 (dd,  $J$  = 9.7, 7.0 Hz, 1H), 2.03 – 1.93 (m, 2H), 1.94 – 1.90 (m, 1H), 1.65 – 1.55 (m, 1H).  $^{13}\text{C}$  NMR (126 MHz,  $\text{CDCl}_3$ )  $\delta$  175.1, 172.9, 169.5, 166.7, 141.8, 141.4, 140.7, 140.7, 135.9, 135.7, 129.8, 128.5, 128.5, 128.5, 128.4, 128.4, 128.3, 128.2, 127.9,



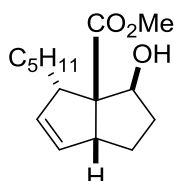
126.1, 126.1, 126.1, 125.9, 70.2, 70.1, 65.4, 65.4, 63.8, 61.7, 53.4, 51.9, 50.9, 49.2, 34.9, 33.8, 33.1, 31.9, 31.9, 30.0, 29.9. HRMS (ESI)  $m/z$  calculated for  $C_{18}H_{20}O_4$   $[M + NH_4]^+$  408.2169, found 408.2167.



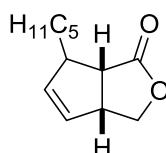
**Compound 2.55.**  $^1H$  NMR (500 MHz,  $CDCl_3$ )  $\delta$  5.74 (dt,  $J = 5.7, 2.1$  Hz, 1H), 5.50 (dt,  $J = 5.8, 2.3$  Hz, 1H), 3.74 (dt,  $J = 7.4, 2.2$  Hz, 1H), 3.71 (s, 3H), 3.42 (ddq,  $J = 11.0, 4.6, 2.2$  Hz, 1H), 2.37 – 2.31 (m, 1H), 2.24 – 2.08 (m, 2H), 1.92 – 1.88 (m, 1H), 1.77 – 1.68 (m, 1H), 1.45 – 1.23 (m, 6H), 1.00 (dddd,  $J = 13.3, 10.7, 9.5, 5.5$  Hz, 1H), 0.92 – 0.83 (m, 3H).  $^{13}C$  NMR (126 MHz,  $CDCl_3$ )  $\delta$  213.8, 172.1, 134.1, 130.2, 66.8, 54.4, 52.5, 52.1, 38.3, 31.9, 30.9, 28.3, 24.9, 22.6, 14.1. HRMS (ESI)  $m/z$  calculated for  $C_{15}H_{22}O_3$   $[M + H]^+$  251.1642, found 251.1648.



**Compound 2.56.**  $^1H$  NMR (500 MHz,  $CDCl_3$ )  $\delta$  3.70 (s, 3H), 3.56 (dd,  $J = 2.8, 1.7$  Hz, 1H), 3.48 (dd,  $J = 2.8, 1.2$  Hz, 1H), 2.94 (dt,  $J = 6.4, 1.4$  Hz, 1H), 2.84 (ddd,  $J = 10.3, 4.7, 1.2$  Hz, 1H), 2.81 – 2.69 (m, 1H), 2.33 – 2.20 (m, 3H), 1.94 (ddt,  $J = 14.4, 11.1, 5.4$  Hz, 1H), 1.59 – 1.42 (m, 2H), 1.42 – 1.28 (m, 5H), 0.90 (td,  $J = 5.7, 4.8, 3.4$  Hz, 3H).  $^{13}C$  NMR (126 MHz,  $CDCl_3$ )  $\delta$  212.6, 171.4, 62.0, 59.7, 59.1, 52.8, 49.9, 48.9, 37.8, 31.9, 28.5, 25.9, 25.8, 22.6, 22.6, 14.1. HRMS (ESI)  $m/z$  calculated for  $C_{15}H_{22}O_3$   $[M + NH_4]^+$  284.1857, found 284.1846.



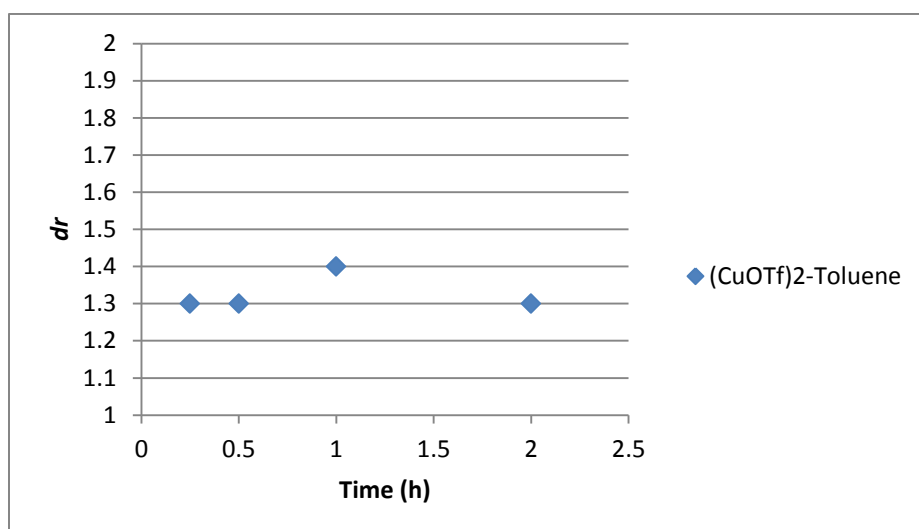
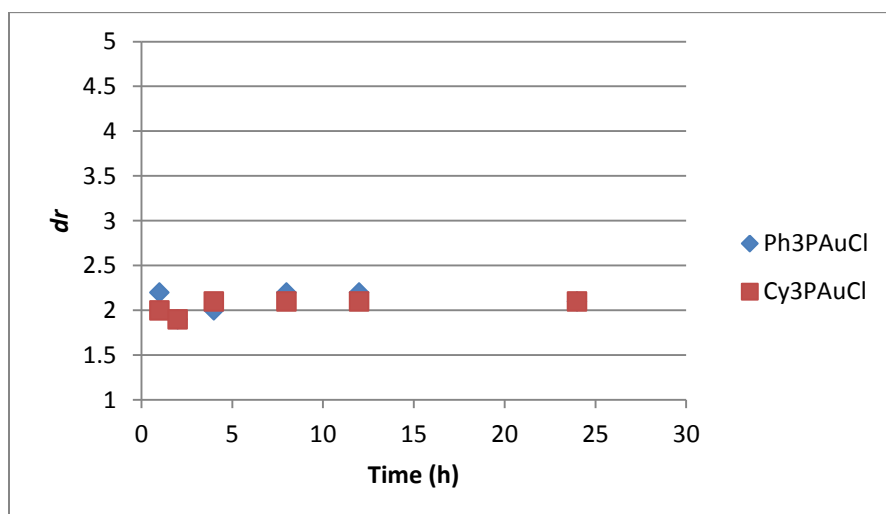
**Compound 2.57.**  $^1\text{H}$  NMR (500 MHz,  $\text{CDCl}_3$ )  $\delta$  5.70 (dt,  $J = 5.5, 1.9$  Hz, 1H), 5.56 (dt,  $J = 5.3, 2.5$  Hz, 1H), 4.36 (ddd,  $J = 11.1, 5.7, 3.0$  Hz, 1H), 3.70 (s, 3H), 3.48 (dp,  $J = 8.3, 1.8$  Hz, 1H), 3.28 – 3.16 (m, 1H), 2.33 (p,  $J = 2.6$  Hz, 1H), 1.80 (dt,  $J = 11.4, 5.7$  Hz, 1H), 1.71 – 1.58 (m, 1H), 1.56 – 1.46 (m, 1H), 1.44 – 1.37 (m, 2H), 1.37 – 1.19 (m, 6H), 1.18 – 1.06 (m, 1H), 0.87 (t,  $J = 6.9$  Hz, 3H).  $^{13}\text{C}$  NMR (126 MHz,  $\text{CDCl}_3$ )  $\delta$  176.8, 132.7, 132.5, 64.1, 52.5, 51.5, 48.8, 32.2, 32.1, 29.9, 28.2, 26.9, 22.6, 14.1. HRMS (ESI)  $m/z$  calculated for  $\text{C}_{15}\text{H}_{22}\text{O}_3$   $[\text{M} + \text{H}]^+$  253.1799, found 253.1791.



**Compound 2.58.**  $^1\text{H}$  NMR (500 MHz,  $\text{CDCl}_3$ ) Major isomer:  $\delta$  5.85 (dt,  $J = 5.6, 2.0$  Hz, 1H), 5.63 (m, 2H), 4.34 (dd,  $J = 9.0, 7.7$  Hz, 1H), 4.10 (dd,  $J = 9.1, 2.7$  Hz, 1H), 3.61 (dtt,  $J = 12.5, 7.3, 2.2$  Hz, 1H), 3.17 (t,  $J = 8.5$  Hz, 1H), 3.03 (dtq,  $J = 8.7, 6.4, 2.1$  Hz, 1H), 1.99 – 1.87 (m, 1H), 1.49 – 1.23 (m, 8H), 0.92 – 0.85 (m, 3H). Minor isomer:  $\delta$  5.87 (dt,  $J = 5.3, 2.4$  Hz, 1H), 5.63 (m, 1H), 4.39 (dd,  $J = 9.2, 7.1$  Hz, 1H), 4.21 (dd,  $J = 9.2, 1.6$  Hz, 1H), 3.61 (dtt,  $J = 12.5, 7.3, 2.2$  Hz, 1H), 3.03 (dtq,  $J = 8.7, 6.4, 2.1$  Hz, 1H), 2.81 (dd,  $J = 7.6, 1.2$  Hz, 1H), 1.48 – 1.24 (m, 8H), 0.93 – 0.85 (m, 3H).  $^{13}\text{C}$  NMR (126 MHz,  $\text{CDCl}_3$ )  $\delta$  180.4, 177.3, 137.1, 136.9, 129.8, 129.8, 71.4, 70.9, 50.2, 48.2, 47.7, 46.9, 45.5, 44.3, 35.4, 31.9, 31.8, 30.3, 28.5, 27.0, 22.6, 22.6, 14.1, 14.0. HRMS (ESI)  $m/z$  calculated for  $\text{C}_{12}\text{H}_{18}\text{O}_2$   $[\text{M} + \text{H}]^+$  195.1380, found 195.1378.

#### Monitoring of $dr$ over the course of the reaction:

The standard reaction was set up as normal, then 0.1 mL aliquots of solution were taken at each time point, concentrated under pressure, and NMR spectra taken. The  $dr$  shown is the ratio of  $^1\text{H}$  NMR peaks.



## 2.4 Bibliography

1. *Modern Gold-Catalyzed Synthesis* Hashmi, A. S. K.; Toste, F. D.; Eds. Wiley-VCH, Weinheim, **2012**.
2. Gorin, D. J.; Toste, F. D. *Nature* **2007**, *446*, 395.
3. Imi, K.; Imai, K.; Utimoto, K. *Tetrahedron Lett.* **1987**, *28*, 3127.

4. (a) Fürstner, A. *Acc. Chem. Res.* **2014**, *47*, 925. (b) Hashmi, A. S. K. *Gold. Bull.* **2004**, *37*, 51. (c) Chiarucci, M.; Bandini, M. *Beilstein J. Org. Chem.* **2013**, *9*, 2586.
5. (a) Li, Z.; Capretto, D. A.; He, C. *Modern Gold-Catalyzed Synthesis* Hashmi, A. S. K.; Toste, F. D.; Eds. Wiley-VCH, Weinheim, **2012**, pp. 297-302.
6. (b) Li, Z.; Capretto, D. A.; He, C. *Modern Gold-Catalyzed Synthesis* Hashmi, A. S. K.; Toste, F. D.; Eds. Wiley-VCH, Weinheim, **2012**, pp. 303-307.
7. (a) Conte, M.; Hutchings, G. J. Li, Z.; Capretto, D. A.; He, C. *Modern Gold-Catalyzed Synthesis* Hashmi, A. S. K.; Toste, F. D.; Eds. Wiley-VCH, Weinheim, **2012**, pp. 1-26.
8. (a) de Monedoza, P; Echavarren, A. M. *Modern Gold-Catalyzed Synthesis* Hashmi, A. S. K.; Toste, F. D.; Eds. Wiley-VCH, Weinheim, **2012**, pp. 135-152. (b) Hubbert, C.; Hashmi, A. S. K. *Modern Gold-Catalyzed Synthesis* Hashmi, A. S. K.; Toste, F. D.; Eds. Wiley-VCH, Weinheim, **2012**, pp. 237-261.
9. Kennedy-Smith, J. J.; Staben, S. T.; Toste, F. D. *J. Am. Chem. Soc.*, **2004**, *126*, 4526.
10. Yin, Y.; Wang, M.; Wang, J.; Zhou, L.; Duan, W. *Chin. J. Chem.* **2011**, *29*, 2320.
11. Staben, S. T.; Kennedy-Smith, J. J.; Toste, F. D. *Angew. Chem. Int. Ed.* **2004**, *43*, 5350.
12. a) Butler, K. L.; Tragni, M.; Widenhoefer, R. A. *Angew. Chem. Int. Ed.* **2012**, *51*, 5175.  
b) Zhang, Z.; Liu, C.; Kinder, R. E.; Han, X.; Qian, H.; Widenhoefer, R. A. *J. Am. Chem. Soc.* **2006**, *128*, 9066. c) *Modern Gold-Catalyzed Synthesis* Hashmi, A. S. K.; Toste, F. D.; Eds. Wiley-VCH, Weinheim, **2012**, p363-381.

13. Staben, S. T.; Kennedy-Smith, J. J.; Huang, D.; Corkey, B. K.; LaLonde, R. B.; Toste, F. D. *Angew. Chem. Int. Ed.* **2006**, *45*, 5991.
14. (a) Corkey, B. K.; Toste, F. D. *J. Am. Chem. Soc.* **2005**, *127*, 17168. (b) Lomberget, T.; Bouyssi, D.; Balme, G. *Synthesis* **2005**, 311. (c) Pei, T.; Wang, X.; Widenhoefer, R. A. *J. Am. Chem. Soc.* **2003**, *125*, 648.
15. Jiang, X.; Ma, X.; Zheng, Z.; Ma, S. *Chem. Eur. J.* **2008**, *14*, 8572.
16. Liu, Z.; Wasmuth, A. S.; Nelson, S. G. *J. Am. Chem. Soc.* **2006**, *128*, 10352.
17. Liu, C.; Widenhoefer, R. A. *Org. Lett.* **2007**, *9*, 1935.
18. Tarselli, M. A.; Gagné, M. R. *J. Org. Chem.* **2008**, *73*, 2439.
19. Mayr, H.; Kempf, B.; Ofial, A. R. *Acc. Chem. Res.* **2003**, *36*, 66.
20. (a) Homs, A.; Escofet, I.; Echavarren *Org. Lett.* **2013**, *15*, 5782. (b) Zhu, Y.; Day, C. S.; Zhang, L.; Hauser, K. J.; Jones, A. C. *Chem. Eur. J.* **2013**, *19*, 12264. Wang, D.; Cai, R.; Sharma, S.; Jirak, J.; Thummanapelli, S. K.; Akhmedov, N. G.; Zhang, H.; Liu, X.; Petersen, J. L.; Shi, X. *J. Am. Chem. Soc.* **2012**, *134*, 9012. Weber, D.; Gagné, M. R. *Org. Lett.* **2009**, *11*, 4962.
21. Guerinot, A.; Fang, W.; Sircoglou, M.; Bour, C.; Bezzenine-Lafollee, S.; Gandon, V. *Angew. Chem. Int. Ed.*, **2013**, *52*, 5848.
22. Fang, W.; Presset, M.; Guérinot, A.; Bour, C.; Bezzenine-Lafolleé, S.; Gandon, V. *Chem. Eur. J.* **2014**, *20*, 5439.
23. Zhang, J.; Shen, W.; Li, L.; Li, M. *Organometallics* **2009**, *28*, 3129.

24. Phelps, A. M.; Dolan, N. S.; Connell, N. T.; Schomaker, J. M. *Tetrahedron*, **2013**, *69*, 5614.
25. (a) Jia, F.; Hong, J.; Sun, P.; Chen, J.; Chem, W. *Synth. Comm.* **2013**, *43*, 2641. (b) Mineno, T.; Miller, M. J. *J. Org. Chem.* **2003**, *68*, 6591. (c) Corey, E. J.; Su, W. G. *J. Am. Chem. Soc.* **1987**, *109*, 7534. (d) Crimmins, M. T.; Jung, D. K.; Gray, J. L. *J. Am. Chem. Soc.* **1993**, *115*, 3146. (e) Mulholland, N. P.; Pattenden, G. *Tetrahedron Lett.* **2005**, *46*, 937.
26. (a) Wang, W.; Hammond, G. B.; Xu, B. *J. Am. Chem. Soc.* **2012**, *134*, 5697. (b) Lemi re, G.; Gandon, V.; Agenet, N.; Goddard, J.-P., de Kozak, A.; Aubert, C.; Fensterbank, L.; Malacria, M. *Angew. Chem. Int. Ed.* **2006**, *45*, 7596. (c) Gandon, V.; Lemi re, G.; Hours, A.; Fensterbank, L.; Malacria, M. *Angew. Chem. Int. Ed.* **2008**, *47*, 7534.
27. Brown, T. J.; Sugie, A.; Leed, M. G. D.; Widenhoefer, R. A. *Chem. Eur. J.* **2012**, *22*, 6959.

### **Chapter 3:**

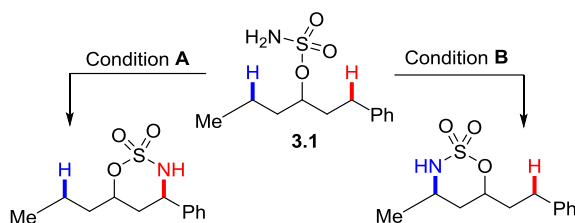
## **Ligand-controlled, tunable silver-catalyzed C-H amination**

Parts of this work are reproduced with permission from Alderson, J. M.\*; Phelps, A. M.\*; Scamp, R. S.\*; Dolan, N. S.; Schomaker, J. M. *J. Am. Chem. Soc.* **2014**, *136*, 16720. \*Equal contributors. Copyright 2014 American Chemical Society

### 3.1. Background

Nitrogenated natural products represent some of the most potent biologically active compounds known, and the strategies for their synthesis have been a matter of considerable study.<sup>1</sup> One of the most direct methods for nitrogen incorporation into a molecule is the insertion of a nitrene or metal nitrenoid into a carbon-hydrogen bond. As with all C-H functionalizations of this type, a persistent obstacle to this vision is regioselectivity: the ability to selectively functionalize different types of C-H bonds in similar chemical environments.<sup>2</sup> In comparison to chemoselectivity, where one of two different reactions is occurring, regioselectivity is often more difficult to obtain. A simple example of nitrene regioselectivity is shown in Scheme 3.1, in which a sulfamate, one of several classes of functional groups often used as a nitrene precursor, selectively inserts into one of two different C-H bonds under two different sets of reaction conditions.

**Scheme 3.1.** Selective nitrene insertion into C-H bonds.



In many reactions of this type, the identity of the substrate controls the reaction outcome completely,<sup>3</sup> meaning the nitrene can only insert into C-H bonds in a specific steric or electronic environment and selectivity for other positions cannot be obtained with that system. While methods that rely on substrate control can be useful in specific circumstances, they can be difficult to apply to new chemical systems. The use of directing groups on the substrate is one solution that has been investigated to override inherent reactivity preferences in a molecule and



can be very powerful for the functionalization of a specific C–H bond,<sup>4</sup> but is not ideal if the aim is to achieve tunable and site-selective transformations in the presence of multiple possible reactive sites. One set of reagents that can be applied across a wide variety of substrates with predictable, selective catalyst control would be the most versatile and practical solution to this problem. Progress towards reagent control, or even more preferably, catalyst control in direct C–H aminations will be discussed in this chapter.

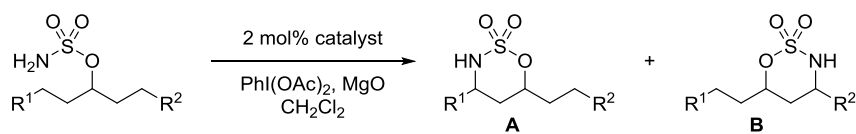
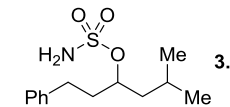
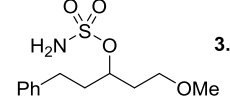
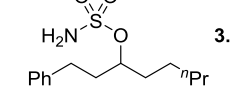
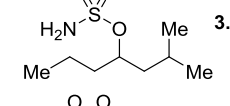
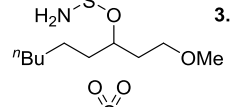
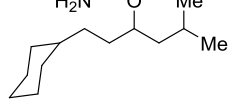
### 3.1.1. Previous approaches to selective C–H amination

The development of tunable C–H aminations in different steric and electronic environments *via* nitrene transfer has focused mainly on dinuclear Rh(II) complexes, an approach pioneered by the DuBois group.<sup>5</sup> However, the rigid structure of the lantern catalysts has hindered attempts to control insertion into C–H bonds simply by changing ligand sets. Such catalysts can show excellent selectivity in the presence of multiple reactive sites, but the transformations are primarily substrate-controlled: changing the nature of the ligand generally does not permit tunable C–H functionalization (*vide infra*).<sup>6</sup>

In a study investigating the mechanistic factors that lead to selectivity,<sup>7</sup> the DuBois group compared a set of rhodium catalysts that perform intramolecular C–H amination of sulfamates. As seen in Table 3.1, the dirhodium catalysts favor alkyl insertion in most cases, with varying degrees of control. A variety of the most common dirhodium catalysts were used in the reaction of **3.2**, and while the degree of selectivity changed, the position selected for did not; all of the catalyst showed some amount of selectivity for the more electron-rich tertiary C–H bond (entry 1). Likewise, the activated bond next to the ether in **3.3** is favored in both cases (entry 2). The simplest complex, Rh<sub>2</sub>(OAc)<sub>4</sub>, gives high selectivity with some substrates (entries 3–5) with a slight increase in control when bulky catalysts are used at sterically hindered insertion positions

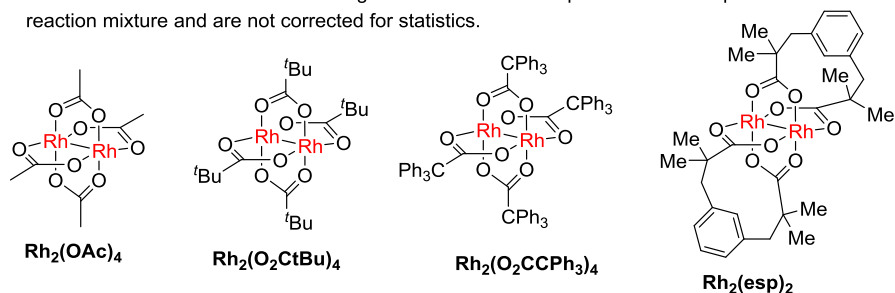
(entry 4). Only entry 3 showed a change in selectivity, as the  $\text{Rh}_2(\text{OAc})_4$  catalyst was unable to activate the secondary C-H bond but the very bulky  $\text{Rh}_2(\text{O}_2\text{CCPh}_3)_4$  favored the secondary C-H bond due to the lack of steric hindrance.

**Table 3.1.** Catalyst influence on sulfamate C-H amination selectivity.

			
Entry	Substrate	Catalyst <sup>a</sup>	A:B <sup>b</sup>
1	 <b>3.2</b>	$\text{Rh}(\text{OAc})_4$	1:1.5
		$\text{Rh}_2(\text{O}_2\text{CtBu})_4$	1:1.5
		$\text{Rh}_2(\text{esp})_2$	1:7
		$\text{Rh}_2(\text{O}_2\text{CCPh}_3)_4$	1:14
2	 <b>3.3</b>	$\text{Rh}(\text{OAc})_4$	1:1
		$\text{Rh}_2(\text{O}_2\text{CCPh}_3)_4$	1:15
3	 <b>3.4</b>	$\text{Rh}(\text{OAc})_4$	8:1
		$\text{Rh}_2(\text{O}_2\text{CCPh}_3)_4$	1:1.5
4	 <b>3.5</b>	$\text{Rh}(\text{OAc})_4$	1:20
		$\text{Rh}_2(\text{O}_2\text{CCPh}_3)_4$	1:4.5
5	 <b>3.6</b>	$\text{Rh}(\text{OAc})_4$	1:11
		$\text{Rh}_2(\text{O}_2\text{CCPh}_3)_4$	1:14
6	 <b>3.7</b>	$\text{Rh}(\text{OAc})_4$	1:2
		$\text{Rh}_2(\text{O}_2\text{CtBu})_4$	1:2
		$\text{Rh}_2(\text{O}_2\text{CCPh}_3)_4$	1:6

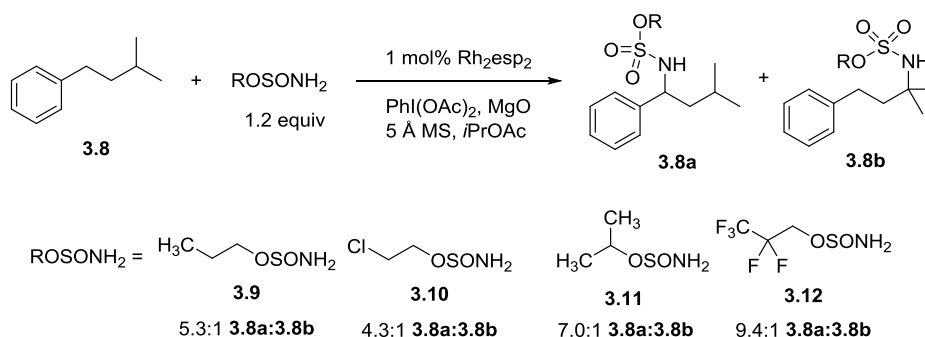
<sup>a</sup> Reactions performed in  $\text{CH}_2\text{Cl}_2$  at 23 °C using 1.1 equiv of  $\text{PhI}(\text{OAc})_2$ , 2.3 equiv of  $\text{MgO}$ , and 2 mol% of the indicated catalyst.

<sup>b</sup> Product ratios are based on the integration of the  $^1\text{H}$  NMR spectrum of the unpurified reaction mixture and are not corrected for statistics.



Having investigated intramolecular reactivity, the group worked to ascertain if the same principles of selectivity held for intermolecular reactivity as well.<sup>3a,e</sup> Intriguingly, the same sets of catalysts that gave tertiary selectivity in intramolecular reactivity (Table 3.1, entry 1) show selectivity for benzylic positions in intermolecular reactions (Scheme 3.2). This difference is proposed to be due to a different mechanism involving a mixed Rh(II,III) species, but the specifics are still under investigation.<sup>6g</sup> Competition studies between a benzyl and tertiary C-H bond were performed, with the results shown in Scheme 3.2. In these cases, control of chemoselectivity is obtained by changing the substitution present on the sulfamate precursor, not the rhodium catalyst.

**Scheme 3.2.** Intermolecular amination using a variety of sulfamates.



While structural modification of rhodium catalysts often did not impact the selectivity, the DuBois group has demonstrated that switching between rhodium and ruthenium catalysts could allow some modest changes in selectivity between different types of C-H amination sites (Table 3.2).<sup>8</sup> The ruthenium tetra-2-oxypyridinate dimer  $\text{Ru}_2(\text{hp})_4\text{Cl}$  demonstrated a distinct selectivity for the benzylic C-H bond over a tertiary alkyl C-H bond that was not observed with either of the rhodium catalysts used or the  $\text{Ru}_2(\text{esp})_2$  dimer (entry 1). When the competition in the substrate was between a benzyl position and an allylic position, the  $\text{Ru}_2(\text{hp})_4\text{Cl}$  again showed unique reactivity. In entry 2, both the catalysts with esp ligands showed a higher selectivity for

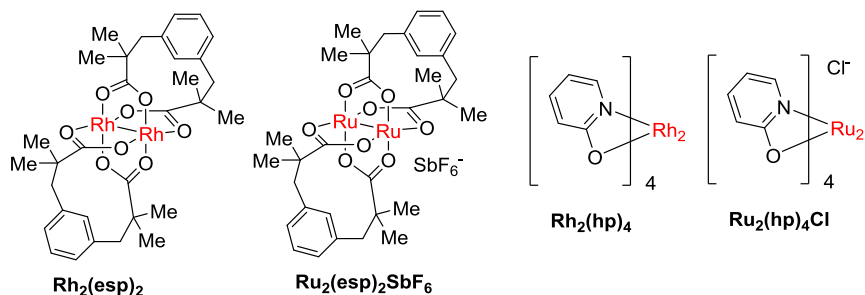
aziridination over C-H insertion. While  $\text{Rh}_2(\text{hp})_4$  showed a lower ratio of aziridination, it was still competitive with C-H insertion, whereas no aziridination was observed with  $\text{Ru}_2(\text{hp})_4\text{Cl}$  (entry 2). Mechanistic studies show that the diruthenium catalysts show this greater selectivity for allylic and benzylic positions due to a change in mechanism; the diruthenium catalysts are believed to progress through a stepwise pathway involving a short-lived diradical intermediate.<sup>8</sup> This is in contrast to the widely accepted mechanism concerted nitrene transfer for dirhodium catalysts.

**Table 3.2.** Oxidation of sulfamate esters with rhodium and ruthenium catalysts.

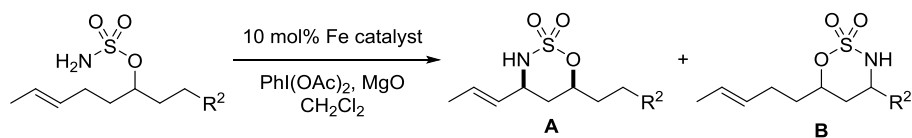
Entry	Substrate	Catalyst <sup>a</sup>	A:B:C		
1	 3.2	[Rh <sub>2</sub> (esp) <sub>2</sub> ] [Ru <sub>2</sub> (esp) <sub>2</sub> SbF <sub>6</sub> ] [Rh <sub>2</sub> (hp) <sub>4</sub> ] [Ru <sub>2</sub> (hp) <sub>4</sub> ]Cl	<b>A</b> <b>B</b>		
			1.0	7.0	
			1.0	6.0	
			1.0	1.2	
			1.5	1.0	
2	 3.14	[Rh <sub>2</sub> (esp) <sub>2</sub> ] [Ru <sub>2</sub> (esp) <sub>2</sub> SbF <sub>6</sub> ] [Rh <sub>2</sub> (hp) <sub>4</sub> ] [Ru <sub>2</sub> (hp) <sub>4</sub> ]Cl	<b>A</b> <b>B</b> <b>C</b>		
			0.2	1.0	0.5
			--	1.0	1.5
			0.6	1.0	1.0
			0.3	1.0	--

<sup>a</sup> Reactions performed in  $\text{CH}_2\text{Cl}_2$  at 23 °C using 1.1 equiv of  $\text{PhI}(\text{OAc})_2$ , 2.3 equiv of  $\text{MgO}$ , and 2 mol% of the indicated catalyst.

<sup>b</sup> Product ratios are based on the integration of the  $^1\text{H}$  NMR spectrum of the unpurified reaction mixture and are not corrected for statistics.



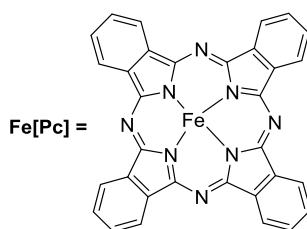
Several alternatives to the rhodium complexes have been developed.<sup>9</sup> The White group has developed an iron phthalocyanine catalyst that favors allylic insertion over insertion at all other sites (Table 3.3).<sup>10</sup> It is highly selective for allylic C-H insertion over tertiary C-H bonds (entry 1), benzylic C-H bonds (entry 2), and C-H bonds activated by an adjacent heteroatom (entry 3). To select between two different allylic C-H bonds, it was determined that the most electron-rich bond would be favored (entry 4). In addition, steric factors could be used to guide the bulky catalyst to the least hindered position (entry 5). However, both entries 4 and 5 required a portionwise addition of an increased amount of catalyst (12 mol% total) over the course of the reaction. Mechanistic probes indicated a radical rebound mechanism, similar to the diruthenium catalysts above.<sup>10</sup>

**Table 3.3.** Reactivity trends for C-H allylic amination.

Entry	Substrate	Catalyst <sup>a</sup>	A:B <sup>b</sup>	% yield major
1	<b>3.13</b>	Fe[Pc]Cl <sup>c</sup>	>20:1	72
2	<b>3.14</b>	Fe[Pc]Cl <sup>c</sup>	5:1	62
3	<b>3.15</b>	Fe[Pc]Cl <sup>c</sup>	7:1	71
4	<b>3.17</b>	Fe[Pc]SbF <sub>6</sub> <sup>d</sup>	14:1	55
5	<b>3.18</b>	Fe[Pc]SbF <sub>6</sub> <sup>d</sup>	7:1	53

<sup>a</sup>Determined by <sup>1</sup>H NMR analysis of the crude reaction mixture (dr ≈ 3:1 unless otherwise noted) <sup>b</sup>Isolated yields (syn + anti; *E/Z* >20:1 in all cases). <sup>c</sup>Conditions: 0.10 equiv of Fe[Pc]Cl, 0.10 equiv of PhI(OPiv)<sub>2</sub>, 4:1 PhMe/MeCN, rt, 6 h.

<sup>d</sup>Conditions: 4 x (0.03 equiv of FePcCl, 0.03 equiv of AgSbF<sub>6</sub>), 2 equiv of PhI(OPiv)<sub>2</sub>, 4:1 PhMe/MeCN, rt, 8 h.



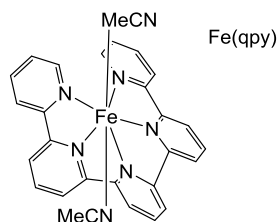
A recently developed iron catalyst<sup>11</sup> used a more flexible pentapyridine ligand to demonstrate high selectivity for benzylic positions, even when compared to allylic positions (entry 1). The benzylic selectivity remains high when comparing benzylic and tertiary alkyl C-H bonds in 5- and 6-membered rings (entries 2 and 3). This system also shows high reactivity for amination when no benzylic position is present (entry 4), favoring the tertiary C-H bond over the

secondary C-H bond. No alterations to the ligand scaffolds were demonstrated, so no changes in the selectivity were explored.

**Table 3.4.** Intramolecular C-H amination with Fe(qpy) catalyst.

Entry	Substrate	Product yield (%)
1	<b>3.19</b>	<b>3.19a</b> 59 (9:1) <sup>d</sup> <b>3.19b</b> 21 (2.5:1) <sup>d</sup>
2	<b>3.20</b>	<b>3.20a</b> 89 (3:1) <sup>d</sup>
3	<b>3.21</b>	<b>3.21a</b> 68 <sup>a</sup> <b>3.21b</b> 21
4	<b>3.22</b>	<b>3.22a</b> 82 <sup>a</sup> <b>3.22b</b> 8
5	<b>3.23</b>	<b>3.23a</b> 86

<sup>a</sup>Reaction conditions: substrate/Fe(qpy)/PhI(OAc)<sub>2</sub>/MgO = 1:0.05:1.4:2.3, MeCN, 80 °C, 12 h; substrate conversion: 100%. <sup>b</sup>Isolated yield. <sup>c</sup>Substrate/Fe(qpy)/PhI(OAc)<sub>2</sub>/MgO = 1.0:0.05:1.8:2.5 <sup>d</sup>*cis/trans* ratio. <sup>e</sup>*cis* only.

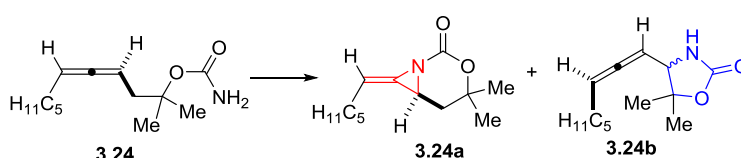


### 3.1.2. Previous work from Schomaker Group

Members of the Schomaker group previously developed a silver catalyzed nitrene insertion that showed remarkable chemoselectivity,<sup>12</sup> demonstrating a complete reversal of

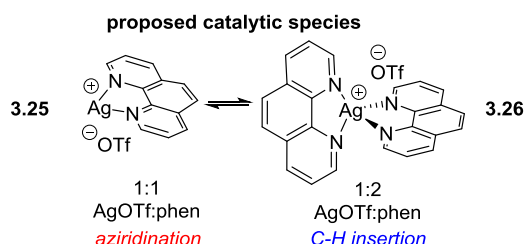
selectivity between aziridination and C-H amination of allene substrates simply by changing the ratio of silver precursor and nitrogenated ligand (Table 3.5). The ability to tune the reactivity between C=C and C-H groups was shown to be due to a dynamic equilibrium established between the two different catalyst species **3.25** and **3.26**. While aminations using silver catalysts had been demonstrated previously,<sup>13</sup> both the impressive degree of selectivity and novel method of dynamic catalysis differentiated this work from earlier efforts.

**Table 3.5.** Chemoselective Ag-catalyzed aziridination vs. C-H amination



entry <sup>a</sup>	equiv AgOTf/phen	<b>3.24a</b> : <b>3.24b</b>	Total yield <sup>b</sup>
1	0.2 / 0.1	5:1	72%
2	0.2 / 0.2	5.8:1	88%
<b>3</b>	<b>0.2 / 0.25</b>	<b>6.2:1</b>	<b>93%</b>
4	0.2 / 0.3	5.8:1	82%
5	0.2 / 0.4	1:4	90%
<b>6</b>	<b>0.2 / 0.6</b>	<b>1:38</b>	<b>78%</b>

<sup>a</sup> Reactions were carried out at 0.125 M substrate in CH<sub>2</sub>Cl<sub>2</sub>, 2 equiv PhIO, AgOTf/phen, rt. <sup>b</sup> NMR yields with mesitylene as the internal standard.



The system showed excellent catalyst control, demonstrating selectivity across a wide variety of allenic substrates (Table 3.6), including trisubstituted allenes (entries 1 and 5), those with substitution next to the carbamate (entries 2 and 3), and sterically hindered substrates (entry 4). In all cases, the silver catalysts showed much higher selectivity than the relevant dirhodium complexes. Most importantly, the selectivity was driven by catalyst control, with the 1:1.25



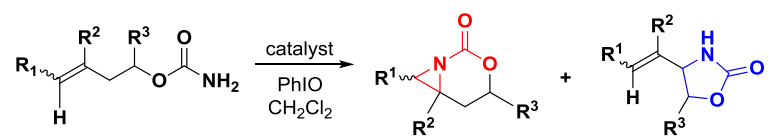
AgOTf:phen complex always favoring aziridination, and the 1:3 AgOTf:phen complex always favoring C-H amination.

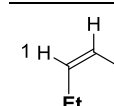
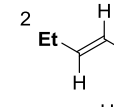
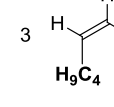
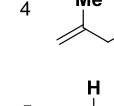
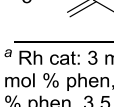
**Table 3.6.** Chemoselective amination of allenes using silver catalysis.

entry	allene	AgOTf:phen <sup>a,b</sup>	I:A <sup>d</sup>	Total yield
1		1:1.25	<b>1:20</b>	83%
		1:3	<b>100:0</b>	81%
		Rh <sub>2</sub> (esp) <sub>2</sub>	<b>1:2</b>	52%
2		1:1.25	<b>1:5.9</b>	92%
		1:3	<b>76:1</b>	77%
3		1:1.25	<b>1:9</b>	89%
		1:3	<b>100:0</b>	76%
		Rh <sub>2</sub> (esp) <sub>2</sub>	<b>1:1</b>	68%
4		1:1.25 <sup>c</sup>	<b>1:3.7</b>	85%
		1:3	<b>100:0</b>	83%
5		1:1.25	<b>1:11.5</b>	94%
		1:3	<b>100:0</b>	88%
		Rh <sub>2</sub> (esp) <sub>2</sub>	<b>1.3:1</b>	78%

a: Aziridination: 20 mol% AgOTf, 25 mol% phen, 2 equiv PhIO, 4 Å MS, CH<sub>2</sub>Cl<sub>2</sub>. b: C-H insertion: 10 mol% AgOTf, 30 mol% phen, 3.5 equiv PhIO, 4 Å MS, CH<sub>2</sub>Cl<sub>2</sub>. c: 2,2'-bipyridine ligand. d: I = insertion, A = aziridination. e: 10 mol% BHT added.

Not only was the silver catalyst system highly selective for the allenic systems originally tested by the group, but also for allylic systems (Table 3.7). Again, the chemistry showed high selectivity for a variety of substitution patterns and alkene geometries in the substrates. In each case, the 1:1.25 AgOTf:phen conditions demonstrated higher selectivity for aziridination than Rh<sub>2</sub>(OAc)<sub>4</sub>, though the difference in entry 5 is quite small. In addition, each substrate was able to undergo selective C-H insertion simply by switching the silver:ligand ratio to 1:3. The flexibility and power of this system inspired us to push further and see if regioselectivity between two different types of C-H bonds could be achieved with a similar silver system.

**Table 3.7.** Chemoselective amination of alkenes using silver catalysis.


entry	substrate	catalyst <sup>a,b,c</sup>	A:I	2	3	dr (cis:trans)
1		Rh <sub>2</sub> (OAc) <sub>4</sub> 1:1.25 AgOTf:phen 1:3 AgOTf:phen	3.2:1 16.8:1 0:100	58% 2a 67% 2a 0% 2a	18% 3a 4% 3a 93% 3a	(100:0) --- ---
2		Rh <sub>2</sub> (OAc) <sub>4</sub> 1:1.25 AgOTf:phen 1:3 AgOTf:phen	4.9:1 29:1 1:6.6	68% 2c 88% 2c 11% 2c	14% 3c 3% 3c 73% 3c	(0:100) --- ---
3		Rh <sub>2</sub> (esp) <sub>2</sub> 1:1.25 AgOTf:phen 1:3 AgOTf:phen	1.8:1 9.9:1 1:22	45% 2b 89% 2b 4% 2a	25% 3b <sup>d</sup> 9% 3b 87% 3b	nd 3.2:1 3:1
4		Rh <sub>2</sub> (OAc) <sub>4</sub> 1:1.25 AgOTf:phen 1:3 AgOTf:phen	7:1 99:1 1:2.9	35% 2d 85% 2d 23% 2d	5% 3d <1% 3d 66% 3d	--- --- ---
5		Rh <sub>2</sub> (esp) <sub>2</sub> 1:1.25 AgOTf:phen 1:3 AgOTf:phen	1.2:1 1.4:1 0:100	25% 2e 54% 2e 0% 2e	21% 3e <sup>d</sup> 39% 3e <sup>d</sup> 68% 3e	nd nd 2.4:1

<sup>a</sup> Rh cat: 3 mol %, 2 equiv PhIO, 4 Å MS, CH<sub>2</sub>Cl<sub>2</sub>. <sup>b</sup> Aziridination: 20 mol % AgOTf, 25 mol % phen, 2 equiv PhIO, 4 Å MS, CH<sub>2</sub>Cl<sub>2</sub>. <sup>c</sup> C-H insertion: 10 mol % AgOTf, 30 mol % phen, 3.5 equiv PhIO, 4 Å MS, CH<sub>2</sub>Cl<sub>2</sub>. <sup>d</sup> NMR yields, mesitylene internal standard.

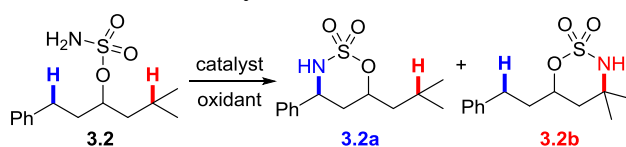
Our group is interested in developing inexpensive, *catalyst-controlled* methods for late-stage C–H oxidation chemistries, with the ultimate goal of reshaping current synthetic strategies towards complex molecules. In this chapter, we describe our progress in promoting tunable silver-catalyzed nitrene transfer reactions where the selectivity of C–H amination is controlled solely by the identity of the ligand.

As described above, our previous work with silver catalysts had demonstrated the power of exploiting the myriad different coordination geometries that the metal can adopt,<sup>14</sup> and we were curious if the changes in the coordination geometries of silver complexes enforced by different types of ligands could be translated into tunable, site-selective amination between C–H bonds in different chemical environments. This would represent a more versatile approach to C–H amination. Ideally, the system would be applicable in a wide variety of complex environments with predictable catalyst control.

## 3.2 Results and Discussion

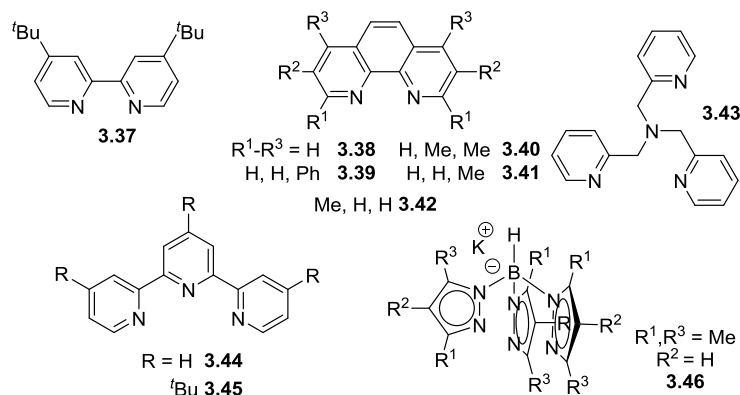
Sulfamate **3.2** (Table 3.8) was used to compare reactivity between a benzylic C–H bond (**Bn**) and an electron-rich 3° C–H bond (**T**) when a variety of different transition metals were used as catalysts. As expected, the amination of **3.2** with dinuclear Rh(II) catalysts (Table 3.8, entries 1-4) favors reaction at **T** to yield **3.2b**, even when the steric bulk of the catalyst is increased (entry 4).<sup>4c</sup> Consistent with known reactivity, activation of **Bn** was favored using Ru- and Fe-based catalysts. (entries 5-6).<sup>7</sup>

While initial screens of silver catalysts focused on control of regioselectivity through silver:ligand ratios, this approach did not work. However, the modularity and breadth of ligands that could be employed with AgOTf enabled catalyst control of the nitrene transfer by changing the coordination geometry of silver through ligands. The substituted 2,2'-bipyridine (<sup>t</sup>Bubipy, **3.37**, entry 8) preferred activation of **T**, as did ligands **3.38** and **3.39** (entries 9-10). Phenanthroline-derived ligands **3.40-3.41** (entries 11-12), 2, 2', 2''-terpyridines **3.44-3.45** (entries 15-16) and Tp ligand **3.46** (entry 17).<sup>13f-j</sup> all showed reduced selectivity in favor of **3.2b**. Surprisingly, a silver catalyst supported by tris(2-pyridylmethyl)amine (tpa, **3.43**, entry 13) preferred activation of **Bn**, indicating that Ag-catalyzed C–H amination is tunable through the ligand.

**Table 3.8.** Ligand-controlled, silver-catalyzed C–H amination.

entry	cat <sup>a-c</sup>	Ag:L	3.2a:3.2b	yield <sup>d</sup>
1 <sup>c</sup>	Rh <sub>2</sub> (OAc) <sub>4</sub>	---	1:1.6	98%
2	Rh <sub>2</sub> (OPiv) <sub>4</sub>	---	1:1.5	---
3	Rh <sub>2</sub> (esp) <sub>2</sub>	---	1:7	99%
4	Rh <sub>2</sub> (O <sub>2</sub> CPh <sub>3</sub> ) <sub>4</sub>	---	1:14	92%
5	Ru <sub>2</sub> (hp) <sub>4</sub> Cl	---	1.4:1	74%
6	[FePc]Cl	---	1:0	58%
7	Cu(MeCN) <sub>4</sub> PF <sub>6</sub>	---	---	0%
8	<b>3.37</b>	<b>1:3</b>	<b>1:2.8</b>	<b>76%</b>
9	<b>3.38</b>	1:3	1:1.6	72%
10	<b>3.39</b>	1:3	1:2.2	77%
11	<b>3.40</b>	1:3	1:1.1	84%
12	<b>3.41</b>	1:3	1:1.1	82%
13	<b>3.42</b>	1:1.2	---	0%
14	<b>3.43</b>	<b>1:1.2</b>	<b>2.4:1</b>	<b>84%</b>
15	<b>3.44</b>	1:1.2	1:1.4	67%
16	<b>3.45</b>	1:1.2	1:1.5	93%
17	<b>3.46</b>	1:1.2	1:1.6	84%

<sup>a</sup>C–H insertion: 10 mol% AgOTf, 10–30 mol% ligand, 3.5 equiv PhIO, 4 Å MS, 0.05 M CH<sub>2</sub>Cl<sub>2</sub>. <sup>b</sup>Rh cat: 2 mol%, 1.1 equiv PhI(OAc)<sub>2</sub>, 2.3 equiv MgO, CH<sub>2</sub>Cl<sub>2</sub>. <sup>c</sup>See SI for the conditions for entries 5–7. <sup>d</sup>Total NMR yield. Average of 2 runs, mesitylene internal standard.



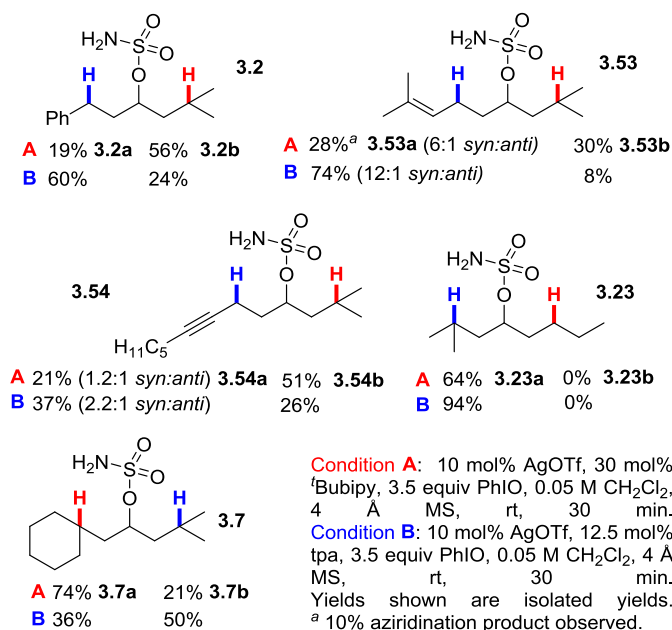
Based on these initial results, <sup>t</sup>Bubipy **3.37** (Condition A) and the tpa ligand **3.43** (Condition B) were chosen to compare the reactivity between a **Bn** and various **T** bonds. Substrates in Table 3.9 were designed to elucidate the relationship between the steric environment around **T** and the site-selectivity. The moderate preference for insertion into **T** over **Bn** in **3.2** using (<sup>t</sup>Bubipy)<sub>2</sub>AgOTf parallels the reactivity of Rh(II) catalysts in intramolecular

aminations.<sup>5c</sup> Moving from the isopropyl group of **3.2** to a cyclopropyl group in **3.47** gave exclusive **Bn** activation with both catalysts; however, the yield was superior using (tpa)AgOTf. The high bond dissociation energy (BDE) of the cyclopropyl C–H in **3.47** (~106 kcal/mol) compared to **Bn** (~89 kcal/mol) may preclude the formation of **3.47b**.<sup>15</sup> For comparison, the BDE of the tertiary position of **3.2** is ~96 kcal/mol.<sup>15</sup> The two catalysts responded differently to increasing the size of the alkyl group. For (<sup>t</sup>Bubipy)<sub>2</sub>AgOTf, the selectivity for amination at **T** vs. **Bn** improved as the size of the alkyl group was increased from the cyclopropyl of **3.47** to the cyclohexyl of **3.51** (**3.51b**:**3.51a** = 8:1). This indicates that moderate steric bulk does not hinder C–H insertion; however, further steric congestion in **3.52** lowered the **T**:**Bn** selectivity to 2.6:1, similar to the ratio observed for **3.2**. In contrast, (tpa)AgOTf reveals selective functionalization of **Bn** over **T** for all substrates in Table 3.9. When **T** was contained in a cyclic alkane, (tpa)AgOTf appeared to favor **Bn** to a greater extent as the size of the ring increased, with the exception of **3.50**, where lower selectivity was observed. This could be due to the lower BDE of the cyclopentyl C–H bond of **3.50** (~96 kcal/mol)<sup>11</sup> compared to the other substrates. Substrates **3.49** and **3.52**, containing acyclic alkyl groups, showed higher selectivity for the benzylic position as the steric bulk increased. In general, it appears that steric effects influence the selectivity of (tpa)AgOTf to a greater extent than (<sup>t</sup>Bubipy)<sub>2</sub>AgOTf, which tends to promote reaction at the most electron-rich C–H bond.

**Table 3.9.** Investigation of steric effects on selectivity.

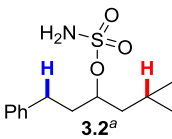
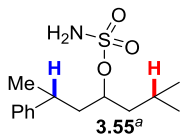
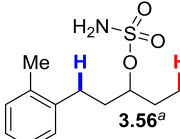
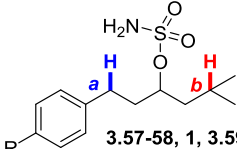
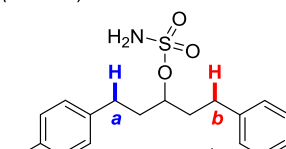
 <b>3.2</b> <b>A</b> <sup>a</sup> 19% <b>3.2a</b> 56% <b>3.2b</b> <b>B</b> 60% 24%	 <b>3.47</b> <b>A</b> 28% <b>3.47a</b> 0% <b>3.47b</b> <b>B</b> 63% 0%	 <b>3.48</b> <b>A</b> 27% <b>3.48a</b> 30% <b>3.48b</b> <b>B</b> 64% 21%
 <b>3.49</b> <b>A</b> 13% <b>3.49a</b> 68% <b>3.49b</b> <b>B</b> 65% 22%	 <b>3.50</b> <b>A</b> 14% <b>3.50a</b> 67% <b>3.50b</b> <b>B</b> 54% 38%	 <b>3.51</b> <b>A</b> 9% <b>3.51a</b> 72% <b>3.51b</b> <b>B</b> 73% 20%
 <b>3.52</b> <b>A</b> 21% <b>3.52a</b> 54% <b>3.52b</b> <b>B</b> 63% 0%	<p><b>Condition A:</b> 10 mol% AgOTf, 30 mol% <sup>t</sup>Bubipy, 3.5 equiv PhIO, 0.05 M CH<sub>2</sub>Cl<sub>2</sub>, 4 Å MS, rt, 30 min.</p> <p><b>Condition B:</b> 10 mol% AgOTf, 12.5 mol% tpa, 3.5 equiv PhIO, 0.05 M CH<sub>2</sub>Cl<sub>2</sub>, 4 Å MS, rt, 30 min.</p> <p>Yields shown are isolated yields.</p> <p><sup>a</sup> In all cases, the <i>syn</i> diastereomer was produced in &gt; 19:1 <i>dr</i>.</p>	

The reactivity of the isopropyl 3° C–H bond **T** was further compared to other types of C–H bonds (Table 3.10). Reaction of **3.53** with (tpa)AgOTf resulted in predominant formation of the allylic C–H insertion product, while **3.54** with (<sup>t</sup>Bubipy)<sub>2</sub>AgOTf favored **T** over the propargylic C–H bond. The higher BDE of the propargylic C–H of **3.54** (87.3 kcal/mol),<sup>11</sup> as compared to the allylic C–H of **3.53** (83.4 kcal/mol),<sup>11</sup> might be responsible for the decreased selectivity with (tpa)AgOTf. As expected, amination of **3.23** gave **3.23a** as the exclusive product, as 2° C–H bonds are generally less reactive than 3° C–Hs. Amination of **3.23** with (tpa)AgOTf again gave exclusive insertion at the 3° C–H bond, but with an improved yield compared to (<sup>t</sup>Bubipy)<sub>2</sub>AgOTf. Finally, the amination of **3.7** shows selectivity between two similar 3° C–H bonds is achievable. This intriguing result demonstrates that even slight differences in sterics and electronics can yield moderate site-selectivity with silver catalysis.

**Table 3.10.** Further study of site-selectivity.

Further exploration of the impact of substrate electronics on the selectivity of the nitrene transfer was carried out (Table 3.11). In **3.55**, the additional Me group increases the electron density of the 3° **Bn** C–H, resulting in lower selectivity using (*t*Bubipy)<sub>2</sub>AgOTf. In contrast, the steric congestion at **Bn** in **3.55** decreased the preference of (tpa)AgOTf for benzylic amination. A methyl group in the *ortho* position as in **3.56** again shows high selectivity with (tpa)AgOTf (compare **3.2** and **3.56**), further supporting the observation that steric effects influence the behavior of (tpa)AgOTf to a greater extent than (*t*Bubipy)<sub>2</sub>AgOTf, which tends to be more sensitive to the electron density at the C–H bond.

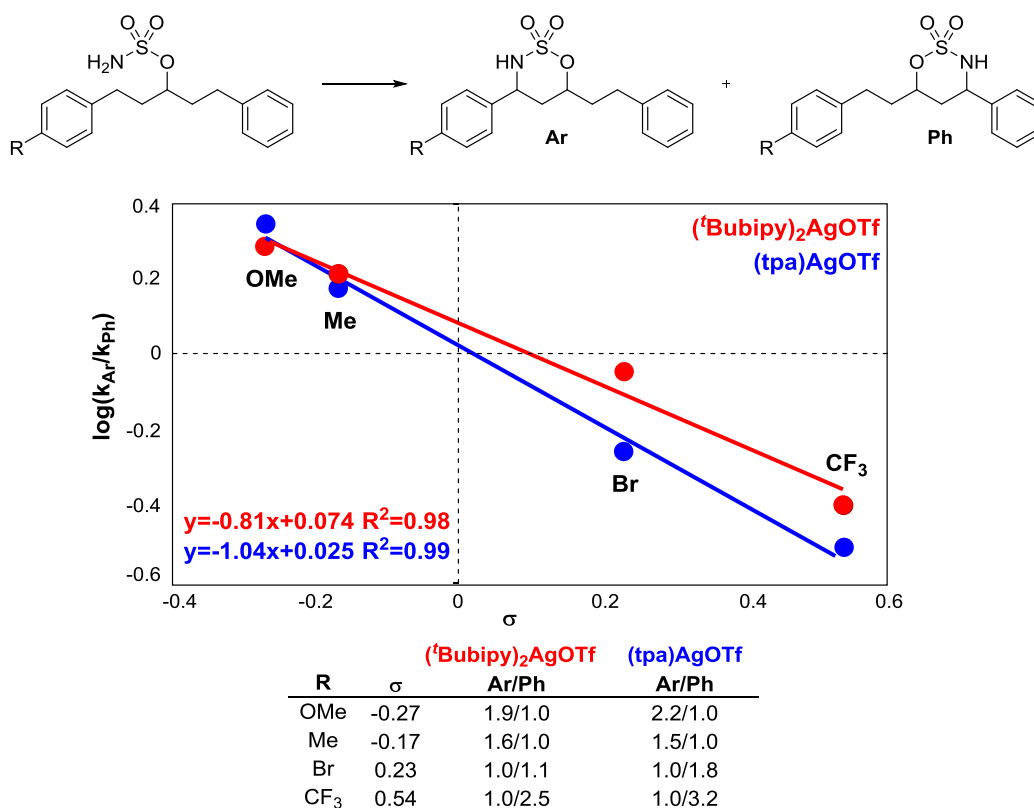
**Table 3.11.** Exploration of electronic effects.

		
<b>3.2<sup>a</sup></b>	<b>3.55<sup>a</sup></b>	<b>3.56<sup>a</sup></b>
<b>A</b> 19% <b>3.2a</b> 56% <b>3.2b</b>	<b>A</b> 35% <b>3.55a</b> 58% <b>3.55b</b>	<b>A</b> 32% <b>3.56a</b> 45% <b>3.56b</b>
<b>B</b> 60%	( <i>dr</i> 1.5:1) 48% 51%	<b>B</b> 65% 20%
	( <i>dr</i> 2.5:1) ( <i>dr</i> 1.6:1)	
		
<b>3.57-58, 1, 3.59-60<sup>b</sup></b>	<b>3.61-64<sup>b</sup></b>	
<b>R</b>	<b>a</b>	<b>b</b>
OMe	<b>A</b> 31% <b>3.57a</b> 38% <b>3.57b</b>	
	<b>B</b> 70%	15%
Me	<b>A</b> 25% <b>3.58a</b> 52% <b>3.58b</b>	
	<b>B</b> 66%	15%
H	<b>A</b> 20% <b>3.2a</b> 56% <b>3.2b</b>	
	<b>B</b> 60%	25%
Br	<b>A</b> 16% <b>3.59a</b> 44% <b>3.59b</b>	
	<b>B</b> 55%	33%
CF <sub>3</sub>	<b>A</b> 11% <b>3.60a</b> 69% <b>3.60b</b>	
	<b>B</b> 42%	54%
<b>R</b>	<b>a</b>	<b>b</b>
OMe	<b>A</b> 44% <b>3.61a</b> 23% <b>3.61b</b>	
	<b>B</b> 51%	23%
Me	<b>A</b> 39% <b>3.62a</b> 28% <b>3.62b</b>	
	<b>B</b> 45%	31%
Br	<b>A</b> 34% <b>3.63a</b> 37% <b>3.63b</b>	
	<b>B</b> 33%	58%
CF <sub>3</sub>	<b>A</b> 21% <b>3.64a</b> 53% <b>3.64b</b>	
	<b>B</b> 19%	61%

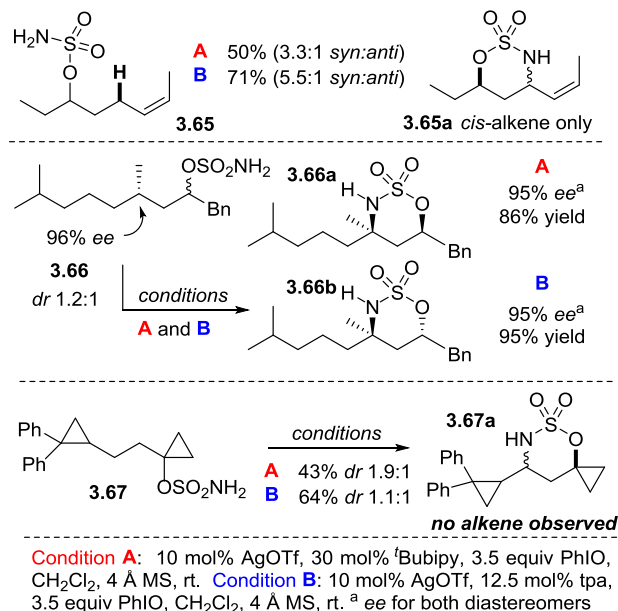
**Condition A:** 10 mol% AgOTf, 30 mol% <sup>t</sup>Bubipy, 3.5 equiv PhIO, CH<sub>2</sub>Cl<sub>2</sub>, 4 Å MS, rt. **Condition B:** 10 mol% AgOTf, 12.5 mol% tpa, 3.5 equiv PhIO, CH<sub>2</sub>Cl<sub>2</sub>, 4 Å MS, rt. <sup>a</sup> Isolated yields. <sup>b</sup> Average of two runs; NMR yields using mesitylene as the internal standard.

The sensitivity of (<sup>t</sup>Bubipy)<sub>2</sub>AgOTf for activation of the most electron-rich C–H bond was further supported by substrates **3.57-3.60**. Interestingly, the same trend held true for (tpa)AgOTf, indicating that the two catalysts react similarly to changes in the electronics of the substrate. Insight into the nature of the transition state was obtained through Hammett correlations using the diaryls **3.61-3.64**. Because selectivity occurs during the product-determining step, the ratio of the isomeric products offers a direct measure of  $k_{Ar}/k_{Ph}$  and does not require knowledge of the rate-determining step.<sup>5a,c,8</sup> Hammett plots of both catalysts (Figure 3.1) support the build-up of positive charge at the carbon undergoing reaction.<sup>8</sup>

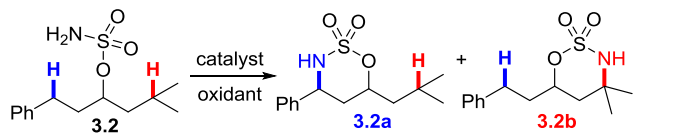


**Figure 3.1.** Hammett plots using (*t*Bubipy)<sub>2</sub>AgOTf and (tpa)AgOTf.

Further exploration of the mechanistic pathway of silver-promoted nitrene transfer was carried out (Scheme 3.3). No isomerization of the double bond of **3.65** was noted using either catalyst. A stereochemical probe **3.66** resulted in no loss in *ee* in the products **3.66a** or **3.66b** with either catalyst. Finally, employing the radical clock **3.67** yielded no alkene products with either (*t*Bubipy)<sub>2</sub>AgOTf or (tpa)AgOTf. All three of these experiments argue against the presence of long-lived radical species in the reaction pathway.

**Scheme 3.3.** Mechanistic studies of nitrene transfer.

Our initial empirical results for catalyst-controlled tunable amination suggest design principles for developing more selective catalysts. The sensitivity of the bipy-supported catalyst to the electron density of the C-H bond prompted us to briefly explore the impact of the ligand electronics on the site-selectivity of nitrene transfer. We were pleased to find that installing an electron-donating *p*-OMe group on the bipy ligand increased the selectivity for **3.2b:3.2a** from 1.6:1 in the unsubstituted ligand **3.37** to 4.0:1 in **3.70**. In contrast, the tpa-supported catalysts were not as sensitive to ligand electronics (Table 5, compare catalysts **3.43**, **3.71** and **3.72**). Interestingly, installing a Me group *ortho* to the pyridines of **3.73** reversed the selectivity to again favor **T**, while replacing a pyridine with a phenyl ring in **3.74** also eroded selectivity, suggesting future studies of tpa-based ligand should focus on the steric features of the catalyst and the oxidant. Indeed, replacing PhIO with PhI(OPiv)<sub>2</sub> increased both the yield and the selectivity (Table 3.10, entry 10). The behavior of tpa-derived catalysts is likely influenced by the substitution of the tpa scaffold and studies to determine how this design feature impacts selectivity are currently underway.

**Table 3.10.** Insight into future catalyst design.


entry	catalyst <sup>a</sup>	R	3.2a:3.2b	yield <sup>b</sup>
1	3.37	<sup>t</sup> Bu	1:2.8	76%
2	3.68	H	1:1.6	81%
3	3.69	Me	1:2.8	73%
4	3.70	OMe	1:4.0	76%

entry	catalyst	R <sup>1</sup> , R <sup>2</sup>	3.2a:3.2b	yield
5	3.43	H, H	2.8:1	76%
6	3.71	H, NMe <sub>2</sub>	2.2:1	85%
7	3.72	H, Cl	2.5:1	91%
8	3.73	Me, H	1:2.1	72%
9	3.74 <sup>c</sup>	H, H	1:1.4	57%
10	3.43 <sup>d</sup>	H, H	3.3:1	94%

<sup>a</sup> 10 mol% catalyst, 30% bipy or 12.5% tpa, 3.5 equiv PhIO, 4 Å MS, CH<sub>2</sub>Cl<sub>2</sub>. <sup>b</sup> Total NMR yield, mesitylene internal standard. <sup>c</sup> One of the pyridines of the ligand was replaced with a phenyl group. <sup>d</sup> The oxidant was Ph(OPiv)<sub>2</sub> instead of PhIO.

### 3.2.1 Conclusions

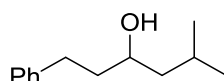
In conclusion, we have developed two silver catalyst systems capable of promoting tunable, regioselective amination of C–H bonds in different chemical environments. Silver catalysts supported by <sup>t</sup>Bubipy appear to prefer amination of the most electron-rich C–H bond, while silver supported by a tpa ligand is more sensitive to the steric environment around the C–H bond, as well as the bond dissociation energy. Preliminary mechanistic work indicates that if radical intermediates are formed in either pathway, they undergo rapid rebound, as no loss of stereochemical information is noted.<sup>12</sup> Computational studies are currently underway to obtain a more detailed mechanistic picture of both reaction pathways and gain a better understanding of how the ligand identity affects the electronic and steric nature of the purported silver nitrene intermediate. Further investigation is utilizing these initial results to parameterize features of both the silver-nitrenes and the substrates to develop predictive models for site-selectivity in complex substrates.

### 3.3 Experimental Section

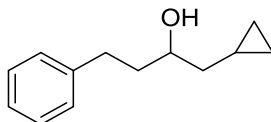
#### 3.3.1 Synthesis of Sulfamate Substrates

##### General procedure for synthesis of alcohols:

A 250 mL round bottom flask with condenser was charged with 30 mL of diethyl ether and 0.97 g (40 mmol, 2 equiv) of Mg turnings. Alkyl bromide (40 mmol, 2 equiv) was added dropwise so as to keep a constant reflux, and the mixture was allowed to stir for 30 min. The reaction mixture was cooled to -78 °C in a dry ice/acetone bath and aldehyde (20 mmol, 1 equiv) in 30 mL of was added slowly via cannula. The reaction mixture was stirred 1 h at -78 °C, and was then quenched with gradual addition of aqueous 0.25 M HCl (60 mL). The layers were separated and the aqueous layer was extracted with two 30 mL portions of diethyl ether. The organic layers were combined, dried over MgSO<sub>4</sub>, and concentrated *in vacuo*. The crude residue was purified via column chromatography with an ethyl acetate/hexane gradient to give the pure alcohol product.

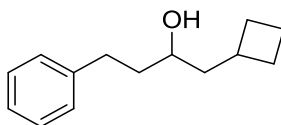


**5-methyl-1-phenylhexan-3-ol.** The product was purified by column chromatography using a 0→30% gradient of EtOAc in hexanes with 5% increments. The resulting colorless oil was obtained in 80% yield from 3-phenylpropionaldehyde. Characterization data was consistent with a previously reported synthesis.<sup>3</sup> <sup>1</sup>H NMR (500 MHz, CDCl<sub>3</sub>) δ 7.35 – 7.23 (m, 2H), 7.23 – 7.13 (m, 3H), 3.71 (tt, *J* = 8.8, 4.7 Hz, 1H), 2.79 (ddd, *J* = 13.8, 9.9, 5.7 Hz, 1H), 2.67 (ddd, *J* = 13.7, 9.8, 6.4 Hz, 1H), 1.85 – 1.64 (m, 3H), 1.41 (ddd, *J* = 14.1, 8.8, 5.4 Hz, 1H), 1.36 (s, 1H), 1.28 (ddd, *J* = 13.5, 8.8, 4.2 Hz, 1H), 0.91 (t, *J* = 7.1 Hz, 6H). <sup>13</sup>C NMR (126 MHz, CDCl<sub>3</sub>) δ 142.2, 128.4, 125.8, 69.5, 46.8, 39.7, 32.1, 24.6, 23.5, 22.1.



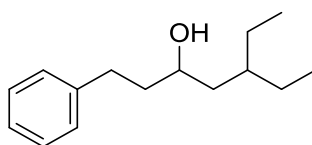
**1-cyclopropyl-4-phenylbutan-2-ol.** The alcohol was prepared from 1-phenyl-5-hexen-3-ol, which had been synthesized according to a previous procedure.<sup>4</sup>

A Schlenk flask was charged with 2.6 g (40 mmol, 3.1 equiv.) zinc powder and 3.9 g (40 mmol, 3.1 equiv.) copper(I) chloride. The flask was fitted with a condenser, sealed with a rubber septum, and flushed with N<sub>2</sub> to create an inert atmosphere. Diethyl ether (20 mL) was added and the suspension was stirred 30 min at reflux. 1-phenyl-5-hexen-3-ol (2.4 g, 13 mmol, 1 equiv.) was added, followed by 11 g (40 mmol, 3.1 equiv.) diiodomethane. The mixture was left to stir at reflux overnight. The mixture was filtered through Celite and concentrated *in vacuo* to yield a dark oil. The product was purified by column chromatography using a 0→30% gradient of EtOAc in hexanes with 5% increments. The resulting colorless oil was obtained in 42% yield. <sup>1</sup>H NMR (400 MHz, CDCl<sub>3</sub>) δ 7.29 (t, *J* = 7.4 Hz, 2H), 7.24 – 7.16 (m, 3H), 3.75 (tq, *J* = 8.3, 4.3 Hz, 1H), 2.81 (ddd, *J* = 13.7, 9.7, 5.8 Hz, 1H), 2.68 (ddd, *J* = 13.8, 9.7, 6.7 Hz, 1H), 1.89 – 1.72 (m, 2H), 1.67 (d, *J* = 4.1 Hz, 1H), 1.47 – 1.33 (m, 2H), 0.81 – 0.68 (m, 1H), 0.48 (tddd, *J* = 13.0, 9.4, 8.2, 4.5 Hz, 2H), 0.13 (dtd, *J* = 9.4, 4.8, 3.4 Hz, 1H), 0.09 – 0.01 (m, 1H). <sup>13</sup>C NMR (101 MHz, CDCl<sub>3</sub>) δ 142.2, 128.4, 128.4, 125.8, 71.9, 42.3, 38.8, 32.1, 7.4, 4.5, 3.7. HRMS (EI) *m/z* calculated for C<sub>13</sub>H<sub>18</sub>O [M]<sup>+</sup> 190.1353, found 190.1357.

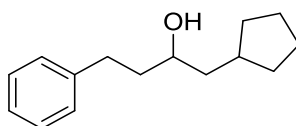


**1-cyclobutyl-4-phenylbutan-2-ol.** The product was purified by column chromatography using a 0→30% gradient of EtOAc in hexanes with 5% increments. The resulting colorless oil was obtained in 73% yield from 3-phenylpropionaldehyde.  $^1\text{H}$  NMR (500 MHz,  $\text{CDCl}_3$ )  $\delta$  7.34 – 7.25 (m, 2H), 7.22 – 7.15 (m, 3H), 3.59 (dp,  $J = 7.8, 4.0$  Hz, 1H), 2.78 (ddd,  $J = 13.7, 9.9, 5.8$  Hz, 1H), 2.65 (ddd,  $J = 13.7, 9.8, 6.6$  Hz, 1H), 2.44 (hept,  $J = 7.9$  Hz, 1H), 2.06 (dtd,  $J = 11.1, 8.0, 2.8$  Hz, 2H), 1.93 – 1.61 (m, 6H), 1.61 – 1.56 (m, 2H), 1.31 (s, 1H).  $^{13}\text{C}$  NMR (126 MHz,  $\text{CDCl}_3$ )  $\delta$  142.2, 128.4, 128.4, 125.8, 70.2, 44.8, 39.2, 32.9, 32.1, 29.0, 28.6, 18.9.

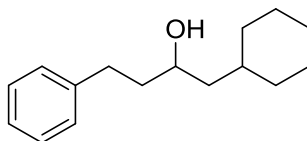
HRMS (EI)  $m/z$  calculated for  $\text{C}_{14}\text{H}_{18} [\text{M}-\text{H}_2\text{O}]^+$  186.1404, found 186.1407.



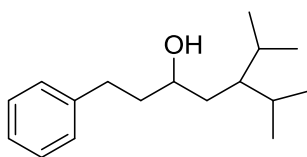
**5-ethyl-1-phenylheptan-3-ol.** The product was purified by column chromatography using a 0→30% gradient of EtOAc in hexanes with 5% increments. The resulting colorless oil was obtained in 49% yield from 3-phenylpropionaldehyde.  $^1\text{H}$  NMR (500 MHz,  $\text{CDCl}_3$ )  $\delta$  7.31 – 7.25 (m, 2H), 7.22 – 7.16 (m, 3H), 3.72 (tt,  $J = 7.9, 4.1$  Hz, 1H), 2.80 (ddd,  $J = 13.8, 10.1, 5.7$  Hz, 1H), 2.67 (ddd,  $J = 13.7, 9.9, 6.4$  Hz, 1H), 1.86 – 1.66 (m, 2H), 1.45 – 1.21 (m, 8H), 0.85 (t,  $J = 7.4$  Hz, 3H), 0.85 (t,  $J = 7.4$  Hz, 3H).  $^{13}\text{C}$  NMR (126 MHz,  $\text{CDCl}_3$ )  $\delta$  142.2, 128.4, 125.8, 69.5, 41.4, 39.8, 36.7, 32.1, 25.9, 25.0, 10.8, 10.5. HRMS (EI)  $m/z$  calculated for  $\text{C}_{15}\text{H}_{24}\text{O} [\text{M}]^+$  220.1822, found 220.1824.



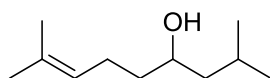
**1-cyclopentyl-4-phenylbutan-2-ol.** The product was purified by column chromatography using a 0→30% gradient of EtOAc in hexanes with 5% increments. The resulting colorless oil was obtained in 49% yield from cyclohexylacetaldehyde.  $^1\text{H}$  NMR (500 MHz,  $\text{CDCl}_3$ )  $\delta$  = 7.28 (t,  $J=7.5$  Hz, 2H), 7.22 – 7.16 (m, 3H), 3.67 (tt,  $J=8.3$ , 4.3 Hz, 1H), 2.80 (ddd,  $J=13.8$ , 10.0, 5.7 Hz 1H), 2.67 (ddd,  $J=13.7$ , 9.9, 6.4 Hz 1H), 1.92 (tdd,  $J=15.7$ , 8.6, 6.8 Hz 1H), 1.85 – 1.69 (m, 4H), 1.60 (ddt,  $J=13.5$ , 10.3, 4.5 Hz 2H), 1.57 – 1.49 (m, 3H), 1.45 (ddd,  $J=13.4$ , 8.4, 4.5 Hz, 1H), 1.40 – 1.32 (m, 1H), 1.16 – 1.01 (m, 2H).  $^{13}\text{C}$  NMR (126 MHz,  $\text{CDCl}_3$ )  $\delta$  142.2, 128.4, 128.4, 125.8, 70.8, 44.0, 39.5, 36.8, 33.2, 32.6, 32.1, 25.1, 24.9. HRMS (EI)  $m/z$  calculated for  $\text{C}_{15}\text{H}_{22}\text{O}$   $[\text{M}]^+$  218.1666, found 218.1667.



**1-cyclohexyl-4-phenylbutan-2-ol.** The product was purified by column chromatography using a 0→30% gradient of EtOAc in hexanes with 5% increments. The resulting colorless oil was obtained in 77% yield from 3-phenylpropionaldehyde.  $^1\text{H}$  NMR (500 MHz,  $\text{CDCl}_3$ )  $\delta$  7.28 (t,  $J = 7.6$  Hz, 2H), 7.22 – 7.12 (m, 3H), 3.74 (tt,  $J = 8.3$ , 4.3 Hz, 1H), 2.78 (ddd,  $J = 13.7$ , 9.9, 5.8 Hz, 1H), 2.66 (ddd,  $J = 13.7$ , 9.8, 6.5 Hz, 1H), 1.81 – 1.61 (m, 7H), 1.40 (dddd,  $J = 27.3$ , 13.8, 8.5, 4.3 Hz, 3H), 1.30 (ddd,  $J = 13.6$ , 8.6, 4.2 Hz, 1H), 1.23 (ddt,  $J = 12.4$ , 9.2, 3.2 Hz, 2H), 1.20 – 1.08 (m, 1H), 0.99 – 0.89 (m, 1H), 0.84 (tdd,  $J = 12.4$ , 10.8, 3.3 Hz, 1H).  $^{13}\text{C}$  NMR (126 MHz,  $\text{CDCl}_3$ )  $\delta$  142.2, 128.4, 125.8, 68.8, 45.5, 39.7, 34.2, 34.1, 32.9, 32.1, 26.6, 26.4, 26.2. HRMS (EI)  $m/z$  calculated for  $\text{C}_{16}\text{H}_{24}\text{O}$   $[\text{M}]^+$  232.1822, found 232.1813.

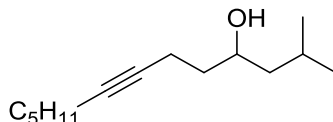


**6-methyl-1-phenyl-5-(propan-2-yl)heptan-3-ol.** The product was purified by column chromatography using a 0→30% gradient of EtOAc in hexanes with 5% increments. The resulting colorless oil was isolated in 48% yield from 3-isopropyl-4-methylpentanal (synthesized according to literature procedure).<sup>5</sup> <sup>1</sup>H NMR (500 MHz, CDCl<sub>3</sub>) δ 7.28 (dd, *J* = 8.0, 7.1 Hz, 2H), 7.23 – 7.16 (m, 3H), 3.65 (tdd, *J* = 8.4, 4.9, 3.8 Hz, 1H), 2.83 (ddd, *J* = 13.7, 10.2, 5.4 Hz, 1H), 2.67 (ddd, *J* = 13.7, 10.1, 6.4 Hz, 1H), 1.83 (dddd, *J* = 14.0, 10.3, 6.4, 3.8 Hz, 1H), 1.79 – 1.66 (m, 3H), 1.43 – 1.31 (m, 2H), 1.10 (dq, *J* = 6.4, 4.6 Hz, 1H), 0.89 (d, *J* = 6.9 Hz, 3H), 0.87 (d, *J* = 6.9 Hz, 3H), 0.85 (d, *J* = 6.9 Hz, 3H), 0.82 (d, *J* = 6.8 Hz, 3H). <sup>13</sup>C NMR (126 MHz, CDCl<sub>3</sub>) δ 142.2, 128.4, 125.8, 71.4, 46.0, 39.7, 36.0, 32.3, 29.7, 29.0, 21.8, 21.2, 19.7, 19.0. HRMS (EI) *m/z* calculated for C<sub>17</sub>H<sub>28</sub>O [M]<sup>+</sup> 248.2140, found 248.2137.

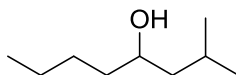


**2,8-dimethylnon-7-en-4-ol.** The product was purified by column chromatography using a 0→30% gradient of EtOAc in hexanes with 5% increments. The resulting colorless oil was obtained in 78% yield from isovaleraldehyde. <sup>1</sup>H NMR (500 MHz, CDCl<sub>3</sub>) δ 5.20 – 5.08 (m, 1H), 3.68 (dq, *J* = 8.1, 4.0 Hz, 1H), 2.10 (dt, *J* = 22.0, 14.7, 7.4 Hz, 2H), 1.85 – 1.72 (m, 1H), 1.70 (s, 3H), 1.63 (s, 3H), 1.54 – 1.47 (m, 1H), 1.47 – 1.42 (m, 1H), 1.42 – 1.37 (m, 1H), 1.36 (d, *J* = 5.2 Hz, 1H), 1.23 (ddd, *J* = 13.7, 8.8, 4.1 Hz, 1H), 0.92 (t, *J* = 6.5 Hz, 6H). <sup>13</sup>C NMR (126 MHz, CDCl<sub>3</sub>) δ 132.0, 124.2, 69.8, 46.8, 37.9, 25.7, 24.6, 24.4, 23.5, 22.1, 17.7. HRMS (EI) *m/z* calculated for C<sub>11</sub>H<sub>22</sub>O [M]<sup>+</sup> 170.1666, found 170.1662.

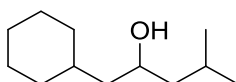




**2-methyltridec-7-yn-4-ol.** The product was purified by column chromatography using a 0→14% gradient of EtOAc in hexanes with 2% increments. The resulting colorless liquid was obtained in 46% yield.  $^1\text{H}$  NMR (500 MHz, Chloroform-*d*)  $\delta$  3.84 (tq,  $J$  = 8.5, 4.2 Hz, 1H), 2.37 – 2.24 (m, 2H), 2.14 (tt,  $J$  = 7.1, 2.4 Hz, 2H), 1.83 – 1.76 (m, 1H), 1.75 (s, 1H), 1.64 (dtd,  $J$  = 14.3, 7.2, 3.5 Hz, 1H), 1.55 (ddd,  $J$  = 13.7, 6.9, 1.9 Hz, 1H), 1.52 – 1.46 (m, 2H), 1.42 (ddd,  $J$  = 14.1, 8.8, 5.5 Hz, 1H), 1.38 – 1.27 (m, 4H), 1.23 (ddd,  $J$  = 13.5, 8.7, 4.3 Hz, 1H), 0.93 (d,  $J$  = 3.0 Hz, 3H), 0.92 (d,  $J$  = 2.9 Hz, 3H), 0.89 (t,  $J$  = 7.1 Hz, 3H).  $^{13}\text{C}$  NMR (126 MHz,  $\text{CDCl}_3$ )  $\delta$  81.3, 79.6, 69.4, 46.6, 36.6, 31.1, 28.8, 24.6, 23.4, 22.2, 22.1, 18.7, 15.4, 14.0. HRMS (EI)  $m/z$  calculated for  $\text{C}_{14}\text{H}_{26}\text{O}$   $[\text{M}]^+$  210.1979, found 210.1979.

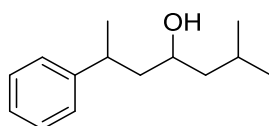


**2-methyloctan-4-ol.** Prepared according to a previous synthesis.<sup>6</sup> The product was purified by column chromatography using a 0→30% gradient of EtOAc in hexanes with 5% increments. The resulting colorless oil was obtained in 60% yield from valeraldehyde. Characterization data was consistent with the previously reported synthesis.<sup>6</sup>

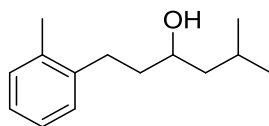


**1-cyclohexyl-4-methylpentan-2-ol.** The product was purified by column chromatography using a 0→30% gradient of EtOAc in hexanes with 5% increments. The resulting colorless oil was obtained in 78% yield from isovaleraldehyde.  $^1\text{H}$  NMR (500 MHz,  $\text{CDCl}_3$ )  $\delta$  = 3.79 (tt,  $J$ =8.6, 4.2

Hz, 1H), 1.85 – 1.73 (m, 2H), 1.73 – 1.61 (m, 4H), 1.45 (tdd,  $J=11.2, 8.3, 5.1$  Hz, 1H), 1.40 – 1.10 (m, 8H), 1.06 – 0.77 (m, 8H).  $^{13}\text{C}$  NMR (126 MHz,  $\text{CDCl}_3$ )  $\delta$  67.3, 47.4, 46.0, 34.3, 34.1, 32.9, 26.6, 26.4, 26.2, 24.6, 23.5, 22.1. HRMS (EI)  $m/z$  calculated for  $\text{C}_{16}\text{H}_{22}$   $[\text{M}-\text{H}_2\text{O}]^+$  166.1717, found 166.1719.

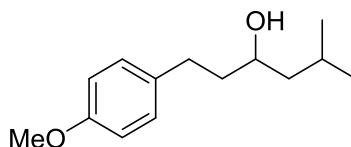


**2-methyl-6-phenylheptan-4-ol.** The product was purified by column chromatography using a 0→30% gradient of EtOAc in hexanes with 5% increments. The resulting colorless oil was obtained in as a 1.2:1 mixture of diastereomers in 64% yield from 3-phenylbutylaldehyde.  $^1\text{H}$  NMR (500 MHz, Chloroform- $d$ ):  $\delta$  7.30 (t,  $J = 7.6$  Hz, 2H), 7.24 – 7.16 (m, 3H), 3.69 (tt,  $J = 8.5, 4.3$  Hz, 0.45H), 3.44 – 3.38 (m, 0.55H), 3.00 (dq,  $J = 10.1, 7.0, 4.8$  Hz, 0.55H), 2.91 (h,  $J = 7.1$  Hz, 0.45H), 1.79 – 1.61 (m, 3H), 1.35 (dddd,  $J = 16.9, 14.1, 8.6, 5.5$  Hz, 1H), 1.27 (dd,  $J = 7.0, 4.6$  Hz, 3H), 1.19 (ddd,  $J = 13.5, 8.3, 4.7$  Hz, 1H), 0.91 (d,  $J = 6.7$  Hz, 1H), 0.86 (d,  $J = 6.6$  Hz, 1H), 0.81 (dd,  $J = 6.6, 1.6$  Hz, 3H).  $^{13}\text{C}$  NMR (126 MHz,  $\text{CDCl}_3$ )  $\delta$  147.7, 146.9, 128.7, 128.6, 127.2, 127.0, 126.3, 126.2, , 68.5, 68.0, 47.5, 47.2, 47.0, 46.3, 36.9, 36.6, 29.9, 24.8, 24.7, 23.7, 23.5, 23.3, 22.4, 22.2, 22.1. HRMS (EI)  $m/z$  calculated for  $\text{C}_{14}\text{H}_{20}$   $[\text{M}-\text{H}_2\text{O}]^+$  188.1560, found 188.1566.

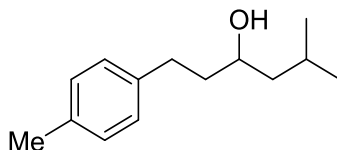


**5-methyl-1-(2-methylphenyl)hexan-3-ol.** The product was purified by column chromatography using a 0→25% gradient of EtOAc in hexanes with 5% increments. The resulting colorless oil was obtained in 80% yield from 3-(2-methylphenyl)propanal.  $^1\text{H}$  NMR (500 MHz, Chloroform-

*d*)  $\delta$  7.21 – 7.07 (m, 4H), 3.78 – 3.72 (m, 1H), 2.79 (ddd,  $J$  = 13.8, 10.6, 5.5 Hz, 1H), 2.65 (ddd,  $J$  = 13.8, 10.4, 6.0 Hz, 1H), 2.32 (s, 3H), 1.83 – 1.62 (m, 3H), 1.43 (ddd,  $J$  = 14.0, 8.8, 5.4 Hz, 1H), 1.30 (ddd,  $J$  = 13.8, 8.8, 4.2 Hz, 1H), 0.92 (dd,  $J$  = 6.7, 4.6 Hz, 6H).  $^{13}\text{C}$  NMR (126 MHz,  $\text{CDCl}_3$ )  $\delta$  140.6, 136.0, 130.4, 128.9, 126.1, 69.9, 46.9, 38.6, 29.6, 24.8, 22.3, 19.4. HRMS (EI)  $m/z$  calculated for  $\text{C}_{14}\text{H}_{22}\text{O}$   $[\text{M}]^+$  206.1666, found 206.1663.

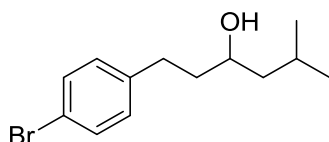


**1-(4-methoxyphenyl)-5-methylhexan-3-ol.** The product was purified by column chromatography using a 10→25% EtOAc in hexanes using 5% increments. The resulting product was isolated in 48% yield from 3-(4-methoxyphenyl)propanal.  $^1\text{H}$  NMR (300 MHz, Chloroform-*d*)  $\delta$  7.12 (d,  $J$  = 8.7 Hz, 2H), 6.83 (d,  $J$  = 8.6 Hz, 2H), 3.79 (s, 3H), 3.70 (tt,  $J$  = 8.4, 4.4 Hz, 1H), 2.79 – 2.56 (m, 2H), 1.84 – 1.65 (m, 3H), 1.47 – 1.35 (m, 1H), 1.33 – 1.22 (m, 2H), 0.91 (dd,  $J$  = 6.6, 4.6 Hz, 6H).  $^{13}\text{C}$  NMR (126 MHz,  $\text{CDCl}_3$ )  $\delta$  157.7, 134.2, 129.3, 129.3, 113.8, 113.8, 76.8, 69.5, 55.3, 46.8, 39.9, 31.1, 30.9, 24.6, 23.5, 22.1. HRMS (ESI)  $m/z$  calculated for  $\text{C}_{14}\text{H}_{22}\text{O}_2$   $[\text{M} + \text{NH}_4]^+$  240.1959, found 240.1966.

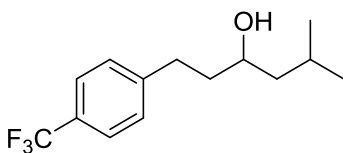


**5-methyl-1-(4-methylphenyl)hexan-3-ol.** The product was purified by column chromatography using a 10→25% gradient of EtOAc in hexanes with 5% increments. The resulting colorless oil was isolated in 50% yield from 3-(4-methylphenyl)propanal.  $^1\text{H}$  NMR (400 MHz, Chloroform-*d*)  $\delta$  7.09 (s, 4H), 3.71 (tt,  $J$  = 8.4, 4.2 Hz, 1H), 2.75 (ddd,  $J$  = 13.7, 9.8, 5.9 Hz, 1H), 2.63 (ddd,  $J$  =

13.7, 9.7, 6.5 Hz, 1H), 2.32 (s, 3H), 1.85 – 1.63 (m, 3H), 1.41 (ddd,  $J = 14.1, 8.7, 5.4$  Hz, 1H), 1.31 – 1.24 (m, 2H), 0.91 (t,  $J = 6.4$  Hz, 6H).,  $^{13}\text{C}$  NMR (126 MHz,  $\text{CDCl}_3$ )  $\delta$  139.2, 135.4, 129.2, 128.4, 69.7, 46.9, 39.9, 31.8, 31.1, 24.8, 23.6, 22.3, 21.1. HRMS (ESI)  $m/z$  calculated for  $\text{C}_{14}\text{H}_{20} [\text{M}-\text{H}_2\text{O}]^+$  188.1560, found 188.1561.

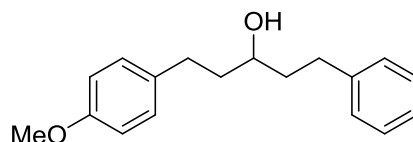


**1-(4-bromophenyl)- 5-methylhexan-3-ol.** The product was purified by column chromatography using a 0→30% gradient of EtOAc in hexanes with 6% increments. The resulting colorless oil was isolated in 73% yield from 3-(4-bromophenyl)propanal.  $^1\text{H}$  NMR (500 MHz, Chloroform- $d$ )  $\delta$  7.39 (d,  $J = 8.3$  Hz, 2H), 7.08 (d,  $J = 8.3$  Hz, 2H), 3.72 – 3.64 (m, 1H), 2.75 (ddd,  $J = 13.8, 9.9, 5.7$  Hz, 1H), 2.64 (tdd,  $J = 13.8, 9.5, 7.0$  Hz, 1H), 1.81 – 1.64 (m, 3H), 1.45 – 1.38 (m, 1H), 1.27 (ddd,  $J = 13.9, 8.7, 4.2$  Hz, 1H), 0.91 (dd,  $J = 8.4, 6.6$  Hz, 6H).,  $^{13}\text{C}$  NMR (126 MHz,  $\text{CDCl}_3$ )  $\delta$  141.3, 131.6, 130.3, 119.6, 69.4, 47.0, 39.6, 31.6, 24.8, 23.6, 22.2. HRMS (ESI)  $m/z$  calculated for  $\text{C}_{13}\text{H}_{18}\text{BrO} [\text{M}-\text{H}]^+$  269.0536, found 269.0535.

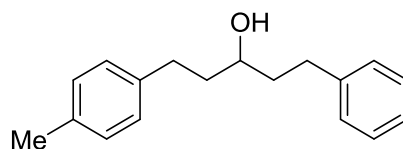


**5-methyl-1-[4-(trifluoromethyl)phenyl]hexan-3-ol.** The product was purified by column chromatography using a 0→25% gradient of EtOAc in hexanes with 5% increments. The resulting colorless oil was isolated in 69% yield from 3-[4-(trifluoromethyl)phenyl]propanal.  $^1\text{H}$  NMR (500 MHz, Chloroform- $d$ )  $\delta$  7.54 (d,  $J = 8.0$  Hz, 2H), 7.31 (d,  $J = 7.9$  Hz, 2H), 3.71 (dp,  $J = 8.4, 3.8$  Hz, 1H), 2.87 (ddd,  $J = 13.8, 10.0, 5.6$  Hz, 1H), 2.74 (ddd,  $J = 13.8, 9.9, 6.5$  Hz, 1H),

1.83 – 1.66 (m, 3H), 1.43 (ddd,  $J = 14.0, 8.8, 5.4$  Hz, 1H), 1.34 – 1.22 (m, 2H), 0.92 (dd,  $J = 8.3, 6.6$  Hz, 6H).  $^{13}\text{C}$  NMR (126 MHz,  $\text{CDCl}_3$ )  $\delta$  146.6, 128.9, 128.3 (q,  $J = 32.4$  Hz), 125.4 (q,  $J = 3.6$  Hz), 124.5 (q,  $J = 271.8$  Hz), 69.4, 47.1, 39.5, 32.0, 24.8, 23.6, 22.2. HRMS (EI)  $m/z$  calculated for  $\text{C}_{14}\text{H}_{17}\text{F}_3 [\text{M}-\text{H}_2\text{O}]^+$  242.1277, found 242.1273.

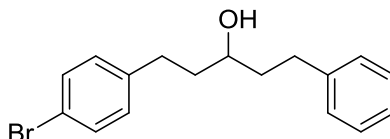


**1-(4-methoxyphenyl)-5-phenylpentan-3-ol.** The product was purified by column chromatography using a 0→25% gradient of EtOAc in hexanes with 5% increments. The resulting white solid was isolated in 59% yield from 3-(4-methoxyphenyl)propanal.  $^1\text{H}$  NMR (500 MHz, Chloroform- $d$ )  $\delta$  7.31 – 7.26 (m, 2H), 7.19 (dt,  $J = 6.0, 1.7$  Hz, 3H), 7.10 (d,  $J = 8.5$  Hz, 2H), 6.83 (d,  $J = 8.6$  Hz, 2H), 3.79 (s, 3H), 3.66 (tt,  $J = 8.2, 4.4$  Hz, 1H), 2.82 – 2.59 (m, 4H), 1.87 – 1.70 (m, 4H).  $^{13}\text{C}$  NMR (126 MHz,  $\text{CDCl}_3$ )  $\delta$  157.9, 142.2, 134.2, 129.4, 128.6, 128.6, 127.4, 126.0, 114.0, 114.0, 71.0, 55.4, 39.6, 39.4, 32.2, 31.3. HRMS (EI)  $m/z$  calculated for  $\text{C}_{18}\text{H}_{22}\text{O}_2 [\text{M}]^+$  270.1615, found 270.1626.

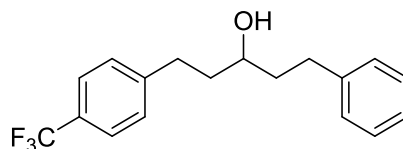


**1-(4-methylphenyl)-5-phenylpentan-3-ol.** The product was purified by column chromatography using a 0→25% gradient of EtOAc in hexanes with 5% increments. The resulting colorless oil was isolated in 61% yield from 3-(4-methylphenyl)propanal.  $^1\text{H}$  NMR (500 MHz, Chloroform- $d$ )  $\delta$  7.28 (dd,  $J = 8.2, 7.0$  Hz, 2H), 7.21 – 7.17 (m, 3H), 7.09 (d,  $J = 1.6$  Hz, 4H), 3.73 – 3.60 (m, 1H), 2.77 (dddd,  $J = 20.4, 13.7, 9.6, 6.0$  Hz, 2H), 2.65 (dddd,  $J = 16.2, 13.7, 9.6, 6.6$  Hz, 2H), 2.32 (s, 3H), 1.87 – 1.71 (m, 4H).  $^{13}\text{C}$  NMR (126 MHz,  $\text{CDCl}_3$ )  $\delta$  142.2, 139.1, 135.5, 129.3,

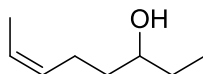
128.6, 128.6, 128.4, 125.9, 71.0, 39.5, 39.4, 32.2, 31.8, 21.1. HRMS (ESI)  $m/z$  calculated for  $C_{18}H_{26}NO$   $[M+NH_4]^+$  272.2009, found 272.2017.



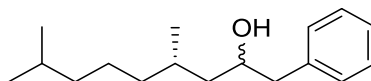
**1-(4-bromophenyl)-5-phenylpentan-3-ol.** The product was purified by column chromatography using a 0→25% gradient of EtOAc in hexanes with 5% increments. The resulting white solid was isolated in 80% yield from 3-(4-bromophenyl)propanal.  $^1H$  NMR (500 MHz, Chloroform- $d$ )  $\delta$  7.39 (d,  $J$  = 8.4 Hz, 2H), 7.31 – 7.26 (m, 2H), 7.19 (tt,  $J$  = 7.9, 1.4 Hz, 3H), 7.05 (d,  $J$  = 8.3 Hz, 2H), 3.68 – 3.59 (m, 1H), 2.76 (dddd,  $J$  = 19.5, 13.7, 9.4, 6.0 Hz, 2H), 2.65 (dddd,  $J$  = 22.9, 13.8, 9.4, 6.9 Hz, 2H), 1.86 – 1.69 (m, 4H).  $^{13}C$  NMR (126 MHz,  $CDCl_3$ )  $\delta$  142.0, 141.1, 131.6, 130.3, 128.6, 128.5, 126.1, 119.7, 70.7, 39.4, 39.2, 32.2, 31.6. HRMS (EI) calculated for  $C_{17}H_{17}Br$   $[M-H_2O]^+$  300.0509, found 300.0518.



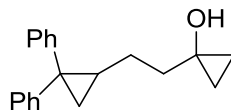
**1-phenyl-5-[4-(trifluoromethyl)phenyl]pentan-3-ol.** The product was purified by column chromatography using a 0→25% gradient of EtOAc in hexanes with 5% increments. The resulting white solid was isolated in 53% yield from 3-[4-(trifluoromethyl)phenyl]propanal.  $^1H$  NMR (500 MHz, Chloroform- $d$ )  $\delta$  7.53 (d,  $J$  = 8.0 Hz, 2H), 7.31 – 7.26 (m, 4H), 7.23 – 7.15 (m, 3H), 3.65 (tq,  $J$  = 8.5, 4.5 Hz, 1H), 2.91 – 2.62 (m, 4H), 1.88 – 1.73 (m, 4H).  $^{13}C$  NMR (126 MHz,  $CDCl_3$ )  $\delta$  146.4, 141.9, 128.9, 128.6, 128.5, 126.1, 125.5 (q,  $J$  = 3.6 Hz), 124.5 (q,  $J$  = 271.4 Hz), 70.7, 39.4, 39.0, 32.2, 32.0. HRMS (EI)  $m/z$  calculated for  $C_{18}H_{17}F_3$   $[M-H_2O]^+$  290.1277, found 290.1267.



**(6-Z)-oct-6-en-3-ol.** The product was purified by column chromatography using a 0→30% gradient of EtOAc in hexanes with 5% increments. The resulting colorless oil was obtained in 10% yield from 4-hexen-1-al, which was used crude from a Swern oxidation<sup>7</sup> of (Z)-4-hexen-1-ol. <sup>1</sup>H NMR (500 MHz, CDCl<sub>3</sub>) δ 5.52 – 5.44 (m, 1H), 5.41 (dtd, *J* = 10.7, 7.0, 1.6 Hz, 1H), 3.55 (tt, *J* = 8.0, 4.5 Hz, 1H), 2.24 – 2.08 (m, 2H), 1.66 – 1.60 (m, 3H), 1.58 – 1.41 (m, 4H), 1.40 (s, 1H), 0.95 (t, *J* = 7.5 Hz, 3H). <sup>13</sup>C NMR (126 MHz, CDCl<sub>3</sub>) δ 130.2, 124.4, 73.1, 36.6, 30.2, 23.2, 12.8, 9.9. HRMS (EI) *m/z* calculated for C<sub>8</sub>H<sub>17</sub>O [M+H]<sup>+</sup> 129.1279, found 129.1282.



**(4S)-4,8-dimethyl-1-phenylnonan-2-ol.** The alcohol was purified by column chromatography using a 0→10% gradient of EtOAc in hexanes with 2% increments. The resulting colorless oil was isolated in 93% yield and 1.2:1 *dr*. <sup>1</sup>H NMR (500 MHz, Chloroform-*d*) δ 7.36 – 7.28 (m, 2H), 7.25 – 7.20 (m, 3H), 3.99 – 3.84 (m, 1H), 2.84 (major, dd, *J* = 13.7, 4.0 Hz, 0.6H), 2.80 (minor, dd, *J* = 13.6, 4.3 Hz, 0.5H), 2.66 (major, dd, *J* = 13.6, 8.4 Hz, 0.6H), 2.60 (minor, dd, *J* = 13.6, 8.6 Hz, 0.5H), 1.73 – 1.61 (m, 1H), 1.58 – 1.47 (m, 2H), 1.47 – 1.38 (m, 2H), 1.38 – 1.20 (m, 3H), 1.20 – 1.04 (m, 3H), 0.93 (minor, d, *J* = 6.7 Hz, 1.3H), 0.89 (major, d, *J* = 6.6 Hz, 1.6H), 0.86 (dd, *J* = 6.6, 1.8 Hz, 5.9H). <sup>13</sup>C NMR (126 MHz, CDCl<sub>3</sub>) δ 138.8, 138.8, 129.6, 129.6, 128.7, 126.6, 70.9, 70.5, 45.0, 44.7, 44.5, 44.4, 39.4, 39.4, 38.2, 36.9, 29.8, 29.4, 28.1, 24.9, 24.7, 22.9, 22.9, 22.8, 22.7, 20.5, 19.4. HRMS (ESI) *m/z* calculated for C<sub>17</sub>H<sub>32</sub>NO [M+NH<sub>4</sub>]<sup>+</sup> 266.2479, found 266.2472.



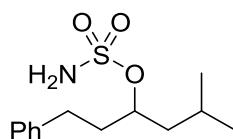
**1-(1-Hydroxycyclopropyl)-2-(2,2-diphenylcyclopropyl)ethane.** A 50 mL round bottom flask with condenser under N<sub>2</sub> was charged with 2.88 g (22.4 mmol) ethyl-4-pentenoate and 5 mL benzene. Diazodiphenylmethane (30 mmol) in 10 mL benzene was added via syringe pump overnight (1.5 mL/h) to the ester solution at reflux. The solution was then cooled to room temperature and diluted with 60 mL hexane to precipitate undesired side products. The filtrate was concentrated and diluted with 20 mL EtOH. The mixture was filtered again and the filtrate concentrated *in vacuo* to yield 1.322g crude ethyl-3-(2,2-diphenylcyclopropyl)propanoate. The residue was carried on to the next step without further purification.

Titanium isopropoxide (0.14 mL, 0.46 mol) was added to the crude ester in 15 mL diethyl ether under N<sub>2</sub> at room temperature. 6.1 mL of 1.5 M ethylmagnesium bromide in diethyl ether was added dropwise over 1 hr with a darkening of the solution over the course of the addition. The mixture was stirred for an additional 15 min and then poured into 50 mL ice cold 5% H<sub>2</sub>SO<sub>4</sub>. The aqueous mixture was extracted with 3 x 15 mL diethyl ether and the combined organic layers were washed with 25 mL brine, and then dried with MgSO<sub>4</sub>, filtered, and concentrated *in vacuo*. The product was purified by column chromatography using 1% MeOH in CH<sub>2</sub>Cl<sub>2</sub> to yield the alcohol in 9% yield (2 steps). <sup>1</sup>H NMR (400 MHz, CDCl<sub>3</sub>) δ 7.34 – 7.28 (m, 4H), 7.25 – 7.16 (m, 6H), 1.77 – 1.56 (m, 5H), 1.25 – 1.19 (m, 2H), 1.13 – 1.00 (m, 1H), 0.71 – 0.59 (m, 2H), 0.41 – 0.34 (m, 1H), 0.34 – 0.26 (m, 1H). <sup>13</sup>C NMR (101 MHz, CDCl<sub>3</sub>) δ 147.3, 141.6, 130.5, 128.2, 127.8, 126.3, 125.6, 55.6, 38.0, 35.6, 27.2, 26.1, 20.6, 13.7, 13.5. HRMS (EI) *m/z* calculated for C<sub>20</sub>H<sub>22</sub>O [M]<sup>+</sup> 278.1664, found 278.1668.

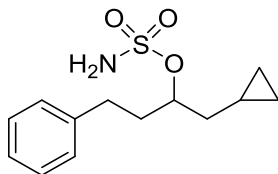


**General procedure for the synthesis of sulfamates.** Formic acid (0.49 mL, 13 mmol, 2.5 equiv) was added dropwise to chlorosulfonyl isocyanate (3.0 equiv) in an ice bath with vigorous stirring. Gas was evolved and the reaction mixture solidified within 5 min. To the solid was added 10.4 mL of CH<sub>3</sub>CN and the resulting clear solution was stirred in an ice bath for 30 minutes and allowed to warm to room temperature and stir at room temperature for four hours. The flask was placed in an ice bath and to the cold solution was added 5.2 mmol alcohol substrate in 8.7 mL of dimethylacetamide. The solution was warmed to room temperature and the mixture was stirred for 1 h. The reaction was quenched with the addition of 10 mL of H<sub>2</sub>O. The aqueous layer was extracted with 3 x 50 mL of Et<sub>2</sub>O. The combined organic layers were washed with 5 x 20 mL H<sub>2</sub>O, 1 x 25 mL saturated aqueous sodium chloride, dried over MgSO<sub>4</sub>, filtered and concentrated under reduced pressure. The crude products were purified by silica gel column chromatography using a hexane/EtOAc gradient.

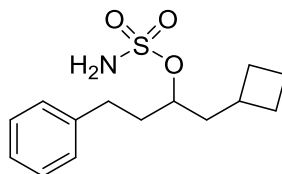
**Compounds 3.61, 3.63, and 3.64** were synthesized according to previously reported procedures.<sup>8</sup>



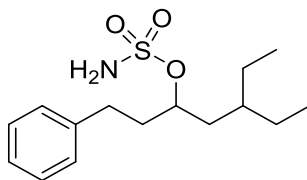
**Compound 3.2.** The product was purified by column chromatography using a 0→30% gradient of EtOAc in hexanes with 5% increments. The resulting yellow oil was obtained in 76% yield from the corresponding alcohol. <sup>1</sup>H NMR (400 MHz, CDCl<sub>3</sub>) δ 7.35 – 7.23 (m, 2H), 7.19 (d, *J* = 7.3 Hz, 3H), 4.91 (bs, 2H), 4.69 (dq, *J* = 7.0, 5.6 Hz, 1H), 2.83 – 2.63 (m, 2H), 2.15 – 1.93 (m, 2H), 1.82 – 1.65 (m, 2H), 1.49 (hept, *J* = 5.6 Hz, 1H), 0.92 (dd, *J* = 9.2, 6.1 Hz, 6H). <sup>13</sup>C NMR (101 MHz, CDCl<sub>3</sub>) δ 141.3, 128.6, 128.5, 126.2, 83.5, 43.3, 36.1, 31.1, 24.5, 22.8, 22.6. HRMS (ESI) *m/z* calculated for C<sub>13</sub>H<sub>25</sub>N<sub>2</sub>O<sub>3</sub>S [M+NH<sub>4</sub>]<sup>+</sup> 289.1581, found 289.1581.



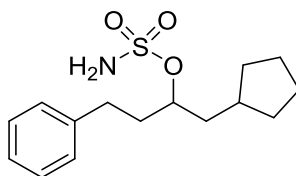
**Compound 3.47.** The product was purified by column chromatography using a 0→30% gradient of EtOAc in hexanes with 5% increments. The resulting clear oil was obtained in 25% yield from the corresponding alcohol.  $^1\text{H}$  NMR (500 MHz, Chloroform-*d*)  $\delta$  7.29 (td,  $J = 7.1$ , 1.6 Hz, 2H), 7.23 – 7.16 (m, 3H), 4.89 (s, 2H), 4.70 (dddd,  $J = 6.4$ , 5.9 Hz, 1H), 2.78 (ddd,  $J = 13.8$ , 9.7, 6.9 Hz, 1H), 2.78 (ddd,  $J = 14.2$ , 9.7, 6.2 Hz, 1H), 2.17 – 2.06 (m, 2H), 1.76 – 1.62 (m, 2H), 0.76 (dddd,  $J = 15.1$ , 10.1, 5.1, 2.3 Hz, 1H), 0.50 (dq,  $J = 8.0$ , 1.2 Hz, 2H), 0.12 (qdd,  $J = 11.3$ , 4.8, 2.0 Hz, 2H).  $^{13}\text{C}$  NMR (126 MHz,  $\text{CDCl}_3$ )  $\delta$  141.1, 128.5, 128.4, 128.4, 126.1, 84.9, 38.9, 35.6, 31.3, 6.8, 4.6, 4.5. . HRMS (ESI)  $m/z$  calculated for  $\text{C}_{13}\text{H}_{23}\text{N}_2\text{O}_3\text{S}$   $[\text{M}+\text{NH}_4]^+$  287.1424, found 287.1414.



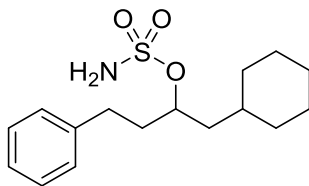
**Compound 3.48.** The product was purified by column chromatography using a 0→30% gradient of EtOAc in hexanes with 5% increments. The resulting clear oil was obtained in 27% yield from the corresponding alcohol.  $^1\text{H}$  NMR (500 MHz,  $\text{CDCl}_3$ )  $\delta$  7.29 (dd,  $J = 8.2$ , 7.0 Hz, 2H), 7.20 (td,  $J = 5.8$ , 5.4, 2.4 Hz, 3H), 4.59 (s, 1H), 4.57 (p,  $J = 6.0$  Hz, 2H), 2.84 – 2.63 (m, 2H), 2.44 (hept,  $J = 7.9$  Hz, 1H), 2.14 – 2.03 (m, 2H), 2.01 (td,  $J = 8.0$ , 5.8 Hz, 2H), 1.97 – 1.77 (m, 4H), 1.68 (dp,  $J = 12.1$ , 9.0 Hz, 2H).  $^{13}\text{C}$  NMR (126 MHz,  $\text{CDCl}_3$ )  $\delta$  141.1, 128.5, 128.4, 126.1, 83.6, 41.1, 35.7, 32.1, 31.2, 28.8, 28.5, 18.7. HRMS (ESI)  $m/z$  calculated for  $\text{C}_{14}\text{H}_{25}\text{N}_2\text{O}_3\text{S}$   $[\text{M}+\text{NH}_4]^+$  301.1581, found 301.1581.



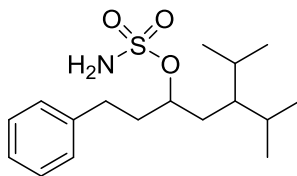
**Compound 3.49.** The product was purified by column chromatography using a 0→30% gradient of EtOAc in hexanes with 5% increments. The resulting clear oil was obtained in 27% yield from the corresponding alcohol.  $^1\text{H}$  NMR (500 MHz, Chloroform-*d*)  $\delta$  7.33 – 7.24 (m, 2H), 7.24 – 7.16 (m, 3H), 4.73 (p,  $J$  = 6.2 Hz, 1H), 4.59 (s, 2H), 2.85 – 2.67 (m, 2H), 2.14 – 1.97 (m, 2H), 1.78 (dt,  $J$  = 14.4, 6.2 Hz, 1H), 1.58 (dt,  $J$  = 14.4, 6.3 Hz, 1H), 1.34 (dddd,  $J$  = 19.1, 11.3, 6.3, 2.9 Hz, 5H), 0.86 (m, 6H).  $^{13}\text{C}$  NMR (126 MHz,  $\text{CDCl}_3$ )  $\delta$  141.1, 128.5, 128.4, 126.1, 83.6, 37.7, 36.5, 36.0, 31.1, 25.2, 10.5, 10.4. HRMS (ESI)  $m/z$  calculated for  $\text{C}_{15}\text{H}_{29}\text{N}_2\text{O}_3\text{S}$   $[\text{M}+\text{NH}_4]^+$  317.1894, found 317.1895.



**Compound 3.50.** The product was purified by column chromatography using a 0→30% gradient of EtOAc in hexanes with 5% increments. The resulting clear oil was obtained in 56% yield from the corresponding alcohol.  $^1\text{H}$  NMR (500 MHz,  $\text{CDCl}_3$ )  $\delta$  7.32 – 7.26 (m, 2H), 7.22 – 7.17 (m, 3H), 4.75 (s, 2H), 4.66 (p,  $J$  = 6.0 Hz, 1H), 2.80 – 2.69 (m, 2H), 2.13 – 1.98 (m, 2H), 1.95 – 1.80 (m, 3H), 1.80 – 1.66 (m, 2H), 1.66 – 1.57 (m, 2H), 1.56 – 1.47 (m, 2H), 1.11 (tq,  $J$  = 12.2, 8.2 Hz, 2H).  $^{13}\text{C}$  NMR (126 MHz,  $\text{CDCl}_3$ )  $\delta$  141.1, 128.5, 128.4, 126.1, 84.4, 40.4, 36.1, 35.9, 32.9, 32.7, 31.1, 25.1, 24.9. HRMS (ESI)  $m/z$  calculated for  $\text{C}_{15}\text{H}_{27}\text{N}_2\text{O}_3\text{S}$   $[\text{M}+\text{NH}_4]^+$  315.1737, found 315.1729.

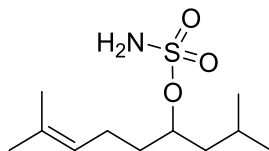


**Compound 3.51.** The product was purified by column chromatography using a 0→30% gradient of EtOAc in hexanes with 5% increments. The resulting clear oil was obtained in 71% yield from the corresponding alcohol.  $^1\text{H}$  NMR (500 MHz,  $\text{CDCl}_3$ )  $\delta$  7.31 – 7.26 (m, 2H), 7.20 (d,  $J$  = 7.0 Hz, 3H), 4.79 – 4.70 (m, 3H), 2.82 – 2.65 (m, 2H), 2.04 (tq,  $J$  = 6.7, 2 Hz, 2H), 1.82 – 1.61 (m, 6H), 1.52 (ddd,  $J$  = 13.9, 7.2, 6.0 Hz, 1H), 1.41 (dtp,  $J$  = 14.1, 6.7, 3.3 Hz, 1H), 1.28 – 1.09 (m, 3H), 1.00 – 0.84 (m, 2H).  $^{13}\text{C}$  NMR (126 MHz,  $\text{CDCl}_3$ )  $\delta$  141.1, 128.4, 126.1, 82.9, 41.8, 36.1, 33.8, 33.4, 33.2, 31.0, 26.4, 26.1. HRMS (ESI)  $m/z$  calculated for  $\text{C}_{16}\text{H}_{29}\text{N}_2\text{O}_3\text{S}$   $[\text{M}+\text{NH}_4]^+$  329.1894, found 329.1889.

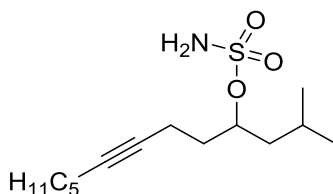


**Compound 3.52.** The product was purified by column chromatography using a 0→30% gradient of EtOAc in hexanes with 5% increments. The resulting clear oil was obtained in 75% yield from the corresponding alcohol.  $^1\text{H}$  NMR (500 MHz, Chloroform- $d$ )  $\delta$  7.30 (td,  $J$  = 7.3, 1.5 Hz, 2H), 7.23 – 7.17 (m, 3H), 4.76 – 4.66 (m, 1H), 4.66 – 4.53 (m, 2H), 2.87 – 2.68 (m, 2H), 2.11 (dddd,  $J$  = 14.6, 9.8, 6.3, 4.9 Hz, 1H), 2.03 (ddt,  $J$  = 14.4, 9.8, 6.3 Hz, 1H), 1.82 – 1.70 (m, 3H), 1.54 (ddd,  $J$  = 14.7, 6.4, 5.4 Hz, 1H), 1.10 (p,  $J$  = 5.2 Hz, 1H), 0.90 (d,  $J$  = 2.8 Hz, 3H), 0.89 (d,  $J$  = 2.7 Hz, 3H), 0.86 (d,  $J$  = 1.7 Hz, 3H), 0.85 (d,  $J$  = 1.7 Hz, 3H).  $^{13}\text{C}$  NMR (126 MHz,  $\text{CDCl}_3$ )  $\delta$

141.2, 128.5, 128.4, 126.1, 85.4, 45.6, 36.0, 32.6, 31.1, 29.4, 29.1, 21.4, 19.3, 19.2. HRMS (ESI)  $m/z$  calculated for  $C_{17}H_{33}N_2O_3S$   $[M+NH_4]^+$  345.2207, found 345.2210.

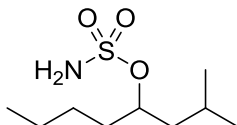


**Compound 3.53.** The product was purified by column chromatography using a 0→30% gradient of EtOAc in hexanes with 5% increments. The resulting clear oil was obtained in 50% yield from the corresponding alcohol. <sup>1</sup>H NMR (500 MHz, CDCl<sub>3</sub>) δ 5.16 – 5.04 (m, 1H), 4.73 (s, 2H), 4.67 (dq,  $J$  = 7.5, 5.7 Hz, 1H), 2.08 (h,  $J$  = 7.8 Hz, 2H), 1.83 – 1.66 (m, 7H), 1.61 (d,  $J$  = 1.3 Hz, 3H), 1.46 (ddd,  $J$  = 14.0, 7.7, 5.4 Hz, 1H), 0.94 (dd,  $J$  = 7.6, 6.5 Hz, 6H). <sup>13</sup>C NMR (126 MHz, CDCl<sub>3</sub>) δ 132.7, 123.0, 83.9, 43.1, 34.5, 25.7, 24.4, 23.4, 22.8, 22.4, 17.8. HRMS (ESI)  $m/z$  calculated for  $C_{11}H_{27}N_2O_3S$   $[M+NH_4]^+$  267.1737, found 267.1738.

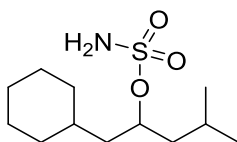


**Compound 3.54.** The product was purified by column chromatography using a 0→20% gradient of EtOAc in hexanes with 4% increments. The resulting clear liquid was obtained in 80% yield from the corresponding alcohol. <sup>1</sup>H NMR (500 MHz, Chloroform-*d*) δ 4.82 (p,  $J$  = 6.3 Hz, 1H), 4.78 (s, 2H), 2.32 (tt,  $J$  = 7.0, 2.4 Hz, 2H), 2.15 (tt,  $J$  = 7.2, 2.4 Hz, 2H), 1.87 (q,  $J$  = 6.8 Hz, 2H), 1.74 (ddt,  $J$  = 13.6, 10.9, 6.7 Hz, 2H), 1.55 – 1.43 (m, 3H), 1.39 – 1.28 (m, 4H), 0.97 (d,  $J$  = 6.3 Hz, 3H), 0.94 (d,  $J$  = 6.3 Hz, 3H), 0.90 (t,  $J$  = 7.0 Hz, 3H). <sup>13</sup>C NMR (126 MHz, CDCl<sub>3</sub>)

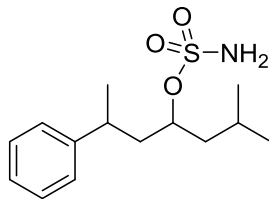
$\delta$  82.7, 82.2, 78.5, 43.5, 33.5, 31.1, 28.7, 24.5, 22.6, 22.5, 22.2, 18.6, 14.9, 13.9. HRMS (ESI)  $m/z$  calculated for  $C_{14}H_{27}NO_3S$   $[M+NH_4]^+$  307.2050, found 307.2047.



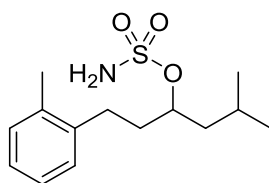
**Compound 3.23.** The product was purified by column chromatography using a 0→30% gradient of EtOAc in hexanes with 5% increments. The resulting clear oil was obtained in 76% yield from the corresponding alcohol.  $^1H$  NMR (500 MHz,  $CDCl_3$ )  $\delta$  4.76 (s, 2H), 4.67 (dq,  $J$  = 7.4, 5.7 Hz, 1H), 1.71 (dddd,  $J$  = 22.1, 13.9, 7.9, 6.3 Hz, 4H), 1.44 (ddd,  $J$  = 13.7, 7.7, 5.3 Hz, 1H), 1.41 – 1.28 (m, 4H), 0.97 – 0.88 (m, 9H).  $^{13}C$  NMR (126 MHz,  $CDCl_3$ )  $\delta$  84.2, 43.2, 34.2, 26.8, 24.4, 22.9, 22.6, 22.4, 13.9. HRMS (ESI)  $m/z$  calculated for  $C_9H_{25}N_2O_3S$   $[M+NH_4]^+$  241.1581, found 241.1584.



**Compound 3.7.** The product was purified by column chromatography using a 0→30% gradient of EtOAc in hexanes with 5% increments. The resulting clear oil was obtained in 71% yield from the corresponding alcohol.  $^1H$  NMR (500 MHz,  $CDCl_3$ )  $\delta$  4.81 (s, 2H), 4.75 (ddd,  $J$  = 12.7, 7.1, 5.6 Hz, 1H), 1.86 – 1.78 (m, 1H), 1.79 – 1.60 (m, 7H), 1.46 (qdd,  $J$  = 14.6, 9.4, 4.7 Hz, 3H), 1.30 – 1.10 (m, 3H), 1.01 – 0.85 (m, 8H).  $^{13}C$  NMR (126 MHz,  $CDCl_3$ )  $\delta$  82.5, 43.8, 42.3, 33.8, 33.4, 33.2, 26.4, 26.1, 26.1, 24.5, 22.7, 22.5. HRMS (ESI)  $m/z$  calculated for  $C_{12}H_{29}N_2O_3S$   $[M+NH_4]^+$  281.1894, found 281.1892.

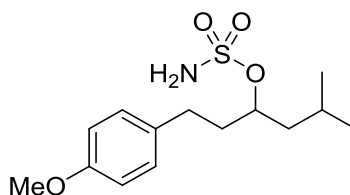


**Compound 3.55.** The product was purified by column chromatography using a 0→30% gradient of EtOAc in hexanes with 6% increments. The resulting yellow oil was obtained in 77% yield from the corresponding alcohol as a 1.2:1 mixture of diastereomers.  $^1\text{H}$  NMR (500 MHz, Chloroform-*d*)  $\delta$  7.31 (t,  $J$  = 7.6 Hz, 2H), 7.24 – 7.18 (m, 3H), 4.55 – 4.45 (m, 2H), 4.43 (bs, 2H), 2.97 (dp,  $J$  = 8.9, 6.9 Hz, 0.55H), 2.85 (dp,  $J$  = 8.9, 6.8 Hz, 0.45H), 2.19 (ddd,  $J$  = 14.1, 8.8, 6.5 Hz, 0.45H), 2.05 – 1.94 (m, 0.1H), 1.88 (dt,  $J$  = 14.2, 6.3 Hz, 0.55H), 1.76 – 1.61 (m, 2H), 1.51 – 1.41 (m, 1H), 1.28 (dd,  $J$  = 11.0, 7.0 Hz, 4H), 0.91 (dd,  $J$  = 11.5, 6.4 Hz, 3H), 0.82 (d,  $J$  = 6.4 Hz, 1H), 0.77 (d,  $J$  = 6.2 Hz, 1H).  $^{13}\text{C}$  NMR (126 MHz,  $\text{CDCl}_3$ )  $\delta$  146.3, 146.2, 128.8, 128.7, 127.3, 127.2, 126.6, 82.8, 82.7, 43.9, 43.7, 42.8, 42.7, 36.9, 36.3, 24.7, 24.4, 23.4, 23.1, 23.1, 22.9, 22.4, 22.3. HRMS (ESI)  $m/z$  calculated from  $\text{C}_{14}\text{H}_{27}\text{N}_2\text{O}_3\text{S}$   $[\text{M}+\text{NH}_4]^+$  303.1737, found 303.1731.

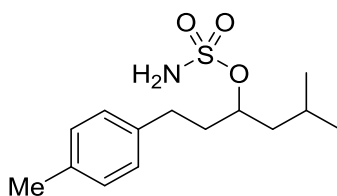


**Compound 3.56.** The product was purified by column chromatography using a 0→30% gradient of EtOAc in hexanes with 5% increments. The resulting white solid was obtained in 78% yield from the corresponding alcohol.  $^1\text{H}$  NMR (500 MHz, Chloroform-*d*)  $\delta$  7.17 – 7.08 (m, 4H), 4.79 – 4.73 (m, 1H), 4.70 (bs, 2H), 2.79 – 2.66 (m, 2H), 2.32 (s, 3H), 2.07 – 1.92 (m, 2H), 1.82 – 1.71 (m, 2H), 1.56 – 1.48 (m, 1H), 0.97 (d,  $J$  = 6.4 Hz, 3H), 0.95 (d,  $J$  = 6.3 Hz, 3H).

$^{13}\text{C}$  NMR (126 MHz,  $\text{CDCl}_3$ )  $\delta$  139.5, 136.0, 130.5, 128.9, 126.3, 83.8, 43.3, 35.0, 28.5, 24.7, 22.9, 22.6, 19.4. HRMS (ESI)  $m/z$  calculated for  $\text{C}_{14}\text{H}_{27}\text{N}_2\text{O}_3\text{S}$   $[\text{M}+\text{NH}_4]^+$  303.1737, found 303.1729.



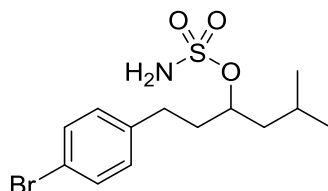
**Compound 3.57.** The product was purified by column chromatography using a 10 $\rightarrow$ 25% gradient EtOAc in hexanes with 5% increments. The resulting white solid was obtained in 69% yield from the corresponding alcohol.  $^1\text{H}$  NMR (500 MHz, Chloroform- $d$ )  $\delta$  7.12 (d,  $J$  = 8.5 Hz, 2H), 6.83 (d,  $J$  = 8.6 Hz, 2H), 4.70 (dq,  $J$  = 7.2, 5.6 Hz, 1H), 4.64 (bs, 2H), 3.79 (s, 3H), 2.74 – 2.63 (m, 2H), 2.07 – 1.98 (m, 2H), 1.81 – 1.69 (m, 2H), 1.50 (hept,  $J$  = 5.6 Hz, 1H),  $\delta$  0.94 (d,  $J$  = 6.3 Hz, 3H), 0.92 (d,  $J$  = 6.2 Hz, 3H).  $^{13}\text{C}$  NMR (126 MHz,  $\text{CDCl}_3$ )  $\delta$  158.1, 133.2, 129.4, 114.1, 83.6, 55.4, 43.4, 36.4, 30.3, 24.6, 22.9, 22.6. HRMS (ESI)  $m/z$  calculated for  $\text{C}_{14}\text{H}_{27}\text{N}_2\text{O}_4\text{S}$   $[\text{M}+\text{NH}_4]^+$  319.1687, found 319.1687.



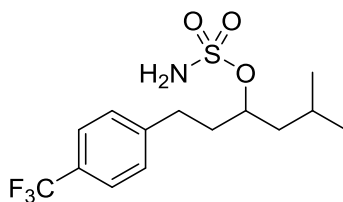
**Compound 3.58.** The product was purified by column chromatography using a 10 $\rightarrow$ 25% gradient of EtOAc in hexanes with 5% increments. The resulting yellow oil was obtained in 69% yield from the corresponding alcohol.  $^1\text{H}$  NMR (500 MHz, Chloroform- $d$ )  $\delta$  7.09 (s, 4H), 4.78 (bs, 2H), 4.70 (dt,  $J$  = 7.1, 5.7 Hz, 1H), 2.69 (m, 2H), 2.31 (s, 3H), 2.02 (dtd,  $J$  = 11.0, 5.9, 3.1 Hz, 2H), 1.79 – 1.69 (m, 2H), 1.50 (hept,  $J$  = 5.7 Hz, 1H),  $\delta$  0.94 (d,  $J$  = 6.3 Hz, 3H), 0.92 (d,  $J$  =



6.3 Hz, 3H).  $^{13}\text{C}$  NMR (126 MHz,  $\text{CDCl}_3$ )  $\delta$  138.1, 135.7, 129.3, 128.4, 83.6, 43.3, 36.3, 30.7, 24.6, 22.9, 22.6, 21.1 HRMS (ESI)  $m/z$  calculated for  $\text{C}_{14}\text{H}_{27}\text{N}_2\text{O}_3\text{S}$   $[\text{M}+\text{NH}_4]^+$  303.1737, found 303.1732.

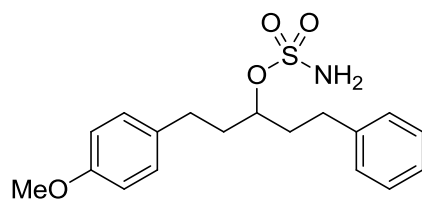


**Compound 3.59.** The product was purified by column chromatography using a 10→25% gradient of EtOAc in hexanes with 5% increments. The resulting white solid was obtained in 60% yield from the corresponding alcohol.  $^1\text{H}$  NMR (500 MHz, Chloroform-*d*)  $\delta$  7.40 (d,  $J$  = 8.3 Hz, 2H), 7.08 (d,  $J$  = 8.3 Hz, 2H), 4.79 (s, 2H), 4.69 (dt,  $J$  = 7.1, 5.6 Hz, 1H), 2.76 – 2.63 (m, 2H), 2.09 – 1.93 (m, 2H), 1.80 – 1.68 (m, 2H), 1.54 – 1.44 (m, 1H), 0.94 (d,  $J$  = 6.3 Hz, 3H), 0.92 (d,  $J$  = 6.3 Hz, 3H).  $^{13}\text{C}$  NMR (126 MHz,  $\text{CDCl}_3$ )  $\delta$  140.2, 131.7, 130.3, 120.0, 83.2, 43.3, 36.1, 30.5, 24.6, 22.9, 22.6. HRMS (ESI)  $m/z$  calculated for  $\text{C}_{13}\text{H}_{23}\text{BrN}_2\text{O}_3\text{S}$   $[\text{M}+\text{NH}_4]^+$  367.0686, found 367.0696.

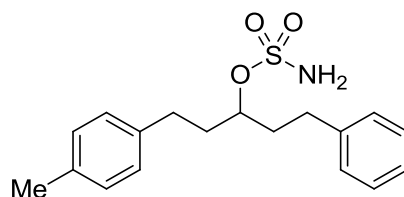


**Compound 3.60.** The product was purified by column chromatography using a 0→30% gradient of EtOAc in hexanes with 6% increments. The resulting white solid was obtained in 71% yield from the corresponding alcohol.  $^1\text{H}$  NMR (500 MHz, Chloroform-*d*)  $\delta$  7.55 (d,  $J$  = 8.0 Hz, 2H), 7.32 (d,  $J$  = 8.0 Hz, 2H), 4.76 – 4.69 (m, 1H), 4.66 (s, 2H), 2.81 (dt,  $J$  = 9.3, 6.2 Hz, 2H), 2.12 – 1.99 (m, 2H), 1.81 – 1.70 (m, 2H), 1.54 – 1.46 (m, 1H), 0.95 (d,  $J$  = 6.4 Hz, 3H), 0.93 (d,  $J$  = 6.3 Hz, 3H).  $^{13}\text{C}$  NMR (126 MHz,  $\text{CDCl}_3$ )  $\delta$  145.4, 129.1, 128.8, 128.7 (q,  $J$  = 32.8 Hz), 125.6 (q,  $J$  =

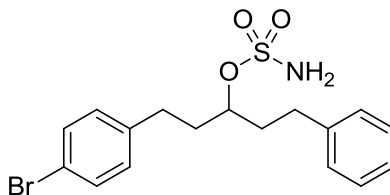
3.7 Hz), 124.4 (q,  $J = 271.7$  Hz) 83.1, 43.3, 36.0, 30.9, 24.7, 22.8, 22.6. HRMS (ESI)  $m/z$  calculated for  $C_{14}H_{24}F_3N_2O_3S$   $[M+NH_4]^+$  357.1455, found 357.1465.



**Compound 3.61.** The product was purified by column chromatography using a 0→30% gradient of EtOAc in hexanes with 6% increments. The resulting oil was obtained in 69% yield from the corresponding alcohol. Characterization was consistent with a previously reported synthesis.<sup>8</sup>

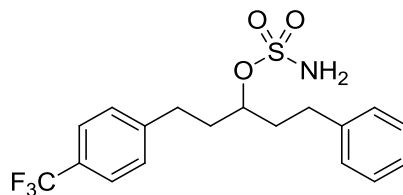


**Compound 3.62.** The product was purified by column chromatography using a 0→30% gradient of EtOAc in hexanes with 6% increments. The resulting white solid was obtained in 83% yield from the corresponding alcohol. Characterization was consistent with a previously reported synthesis.<sup>8</sup>

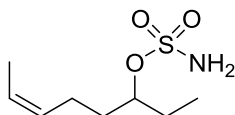


**Compound 3.63.** The product was purified by column chromatography using a 0→30% gradient of EtOAc in hexanes with 6% increments. The resulting white solid was obtained in 87% yield from the corresponding alcohol.  $^1H$  NMR (500 MHz, Chloroform- $d$ )  $\delta$  7.40 (d,  $J = 8.3$  Hz, 2H), 7.32 – 7.27 (m, 2H), 7.23 – 7.15 (m, 3H), 7.05 (d,  $J = 8.4$  Hz, 2H), 4.69 – 4.62 (m, 1H), 4.58 (bs, 2H), 2.81 – 2.61 (m, 4H), 2.19 – 1.96 (m, 4H).  $^{13}C$  NMR (126 MHz,  $CDCl_3$ )  $\delta$  140.9, 139.9,

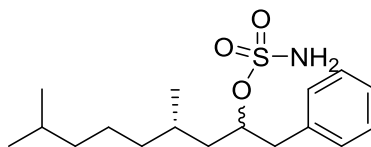
131.8, 130.3, 128.7, 128.5, 126.4, 120.1, 83.7, 35.8, 35.8, 31.3, 30.6. HRMS (ESI)  $m/z$  calculated for  $C_{17}H_{24}BrN_2O_3S$   $[M+NH_4]^+$  415.0686, found 415.0688.



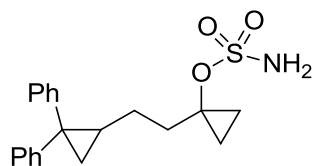
**Compound 3.64.** The product was purified by column chromatography using a 0→30% gradient of EtOAc in hexanes with 6% increments. The resulting colorless oil was obtained in 76% yield from the corresponding alcohol. Characterization data was consistent with a previously reported synthesis.<sup>8</sup>



**Compound 3.65.** The product was purified by column chromatography using a 0→30% gradient of EtOAc in hexanes with 5% increments. The resulting clear oil was obtained in 25% yield from the corresponding alcohol.  $^1H$  NMR (500 MHz, Chloroform- $d$ )  $\delta$  5.56 – 5.43 (m, 1H), 5.37 (dtq,  $J$  = 10.7, 7.2, 1.8 Hz, 1H), 4.63 (s, 2H), 4.61 – 4.55 (m, 1H), 2.16 (p,  $J$  = 7.6 Hz, 2H), 1.87 – 1.68 (m, 4H), 1.62 (ddt,  $J$  = 6.9, 1.9, 1.0 Hz, 3H), 0.99 (t,  $J$  = 7.4 Hz, 3H).  $^{13}C$  NMR (126 MHz,  $CDCl_3$ )  $\delta$  128.9, 125.1, 86.1, 33.2, 26.9, 22.4, 12.8, 9.1. HRMS (ESI)  $m/z$  calculated for  $C_{17}H_{24}BrN_2O_3S$   $[M+NH_4]^+$  225.1268, found 225.1262.



**Compound 3.66.** The product was purified by column chromatography using a 0→25% gradient of EtOAc in hexanes with 5% increments. The resulting colorless oil was obtained in 81% yield from the corresponding alcohol as an inseparable mixture of diastereomers (1.2:1 *dr*).  $^1\text{H}$  NMR (500 MHz, Chloroform-*d*)  $\delta$  7.37 – 7.31 (m, 2H), 7.29 – 7.26 (m, 3H), 4.87 (major, dddd,  $J$  = 8.6, 7.3, 5.8, 4.1 Hz, 0.6H), 4.84 – 4.78 (minor, m, 0.5H), 3.97 (major, bs, 1H), 3.91 (minor, bs, 0.8H), 3.07 – 2.98 (m, 1.7H), 2.92 (minor, dd,  $J$  = 14.1, 8.2 Hz, 0.5H), 1.79 (major, ddd,  $J$  = 14.2, 8.7, 4.5 Hz, 0.6H), 1.66 (tdd,  $J$  = 11.2, 8.1, 5.3 Hz, 2H), 1.51 (dtd,  $J$  = 13.3, 6.7, 4.5 Hz, 1H), 1.39 (ddd,  $J$  = 14.2, 9.1, 4.0 Hz, 0.7H), 1.35 – 1.19 (m, 3H), 1.19 – 1.06 (m, 3H), 0.95 (minor, d,  $J$  = 6.1 Hz, 1.3H), 0.92 (major, d,  $J$  = 6.5 Hz, 1.7H), 0.86 (dd,  $J$  = 6.6, 3.2 Hz, 6H).  $^{13}\text{C}$  NMR (126 MHz,  $\text{CDCl}_3$ )  $\delta$  137.5, 137.5, 129.9, 128.8, 127.2, 84.9, 84.7, 42.4, 42.2, 41.8, 41.1, 39.3, 39.3, 37.7, 37.0, 29.5, 29.1, 28.1, 24.7, 24.5, 22.8, 22.8, 22.7, 19.9, 19.5. HRMS (ESI)  $m/z$  calculated for  $\text{C}_{17}\text{H}_{33}\text{N}_2\text{O}_3\text{S}$   $[\text{M}+\text{NH}_4]^+$  345.2207, found 345.2205.



**Compound 3.67.** The product was purified by column chromatography using a 10→40% gradient of  $\text{Et}_2\text{O}$  in hexanes in two portions. The resulting colorless oil was obtained in 66% yield from the corresponding alcohol.  $^1\text{H}$  NMR (500 MHz,  $\text{CDCl}_3$ )  $\delta$  7.37 – 7.10 (m, 10H), 4.45 (s, 2H), 1.97 (ddd,  $J$  = 15.6, 10.8, 5.3 Hz, 1H), 1.89 (s, 1H), 1.72 – 1.61 (m, 1H), 1.58 – 1.43 (m, 1H), 1.35 – 1.13 (m, 7H), 0.93 – 0.78 (m, 1H), 0.62 – 0.47 (m, 2H).  $^{13}\text{C}$  NMR (126 MHz,  $\text{CDCl}_3$ )  $\delta$  147.06, 141.64, 130.50, 128.22, 128.20, 128.05, 126.26, 125.81, 71.50, 67.18, 35.75, 35.10, 26.61, 25.71, 20.01, 11.80, 11.79.

### 3.3.2. Investigation of Counteranion Effects

**Table SI. Counteranion effects on regioselectivity.**

entry	counteranion (X)	Ligand (L) <sup>a,b</sup>	3.2a:3.2b	yield <sup>c</sup>
1	OTf	<sup>t</sup> Bubipy	1:2.8	76%
2	OTf	tpa	2.4:1	84%
3	NO <sub>3</sub>	<sup>t</sup> Bubipy	1:3.3	68%
4	NO <sub>3</sub>	tpa	2.4:1	82%
5	OAc	<sup>t</sup> Bubipy	1:2.3	76%
6	OAc	tpa	2.5:1	85%
7	BF <sub>4</sub>	<sup>t</sup> Bubipy	1:1.6	59%
8	BF <sub>4</sub>	tpa	2.4:1	89%
9	CO <sub>2</sub> CF <sub>3</sub>	<sup>t</sup> Bubipy	1:2.8	76%
10	CO <sub>2</sub> CF <sub>3</sub>	tpa	2.4:1	68%

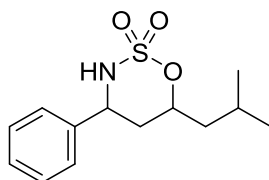
<sup>a</sup>10 mol% AgX, 30 mol% <sup>t</sup>Bubipy, 3.5 equiv PhIO, 4 Å MS, 0.05 M CH<sub>2</sub>Cl<sub>2</sub>. <sup>b</sup>10 mol% AgX, 12.5 mol% tpa, 3.5 equiv PhIO, 4 Å MS, 0.05 M CH<sub>2</sub>Cl<sub>2</sub>. <sup>c</sup>Total NMR yield, mesitylene internal standard.

### 3.3.3 Synthesis of C-H Insertion Products

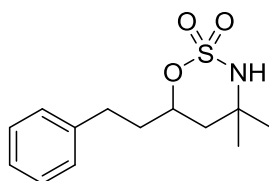
For best results, the silver to ligand ratio needs to be exact. Both silver triflate and phenanthroline are highly hygroscopic and will not give good results if they are not completely dry. Silver reagents should be stored in a dry box and phenanthroline in a standard dessicator. Alternatively, the reaction can be carried out in a glove box, although this is not necessary as long as the quality of the reagents is properly maintained.

**General procedure for Ag-catalyzed C–H amination.** A pre-dried reaction flask was charged with silver triflate (6.6 mg, 0.025 mmol, 0.1 equiv) and ligand (20.1 mg <sup>t</sup>Bubipy, 0.075 mmol, 0.3 equiv or 9.1 mg tpa, 0.031 mmol, 0.125 equiv). Dichloromethane (2.5 mL) was added and the mixture was stirred vigorously for 30 minutes. Then, 4Å molecular sieves (1 mmol substrate/g of sieves) were added, followed by a solution of the sulfamate substrate (0.25 mmol,

1 equiv) in dichloromethane (2.5 mL). Iodosobenzene (194 mg, 0.88 mmol, 3.5 equiv) was added in one portion and the reaction mixture was allowed to stir at room temperature for 30 minutes. The reaction mixture was filtered through a glass frit with dichloromethane and the filtrate was concentrated under reduced pressure. The crude products were purified by silica gel column chromatography using an EtOAc/hexane gradient (0→30% EtOAc/hexane unless otherwise specified). The reported yields were from the higher-yielding conditions for each product.

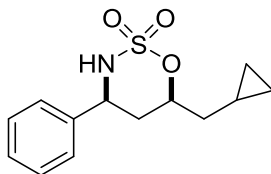


**Compound 3.2a.** The product was obtained in 60% yield.  $^1\text{H}$  NMR (400 MHz,  $\text{CDCl}_3$ )  $\delta$  7.45 – 7.29 (m, 5H), 4.94 (dddd,  $J = 11.3, 8.9, 4.2, 2.2$  Hz, 1H), 4.80 (ddd,  $J = 12.2, 9.3, 2.9$  Hz, 1H), 4.31 (d,  $J = 9.4$  Hz, 1H), 2.03 (dt,  $J = 14.3, 2.6$  Hz, 1H), 1.96 – 1.84 (m, 2H), 1.78 (ddd,  $J = 14.4, 8.9, 5.6$  Hz, 1H), 1.43 (ddd,  $J = 13.9, 8.5, 4.2$  Hz, 1H), 0.96 (dd,  $J = 9.3, 6.6$  Hz, 6H).  $^{13}\text{C}$  NMR (101 MHz,  $\text{CDCl}_3$ )  $\delta$  138.3, 129.3, 128.9, 126.5, 82.9, 58.4, 44.3, 36.8, 23.9, 23.0, 21.9. HRMS (ESI)  $m/z$  calculated for  $\text{C}_{13}\text{H}_{23}\text{N}_2\text{O}_3\text{S}$   $[\text{M}+\text{NH}_4]^+$  287.1424, found 287.1427.

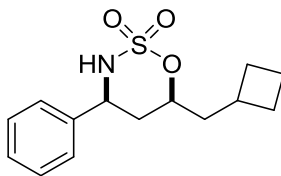


**Compound 3.2b.** The product was isolated in 56% yield.  $^1\text{H}$  NMR (500 MHz,  $\text{CDCl}_3$ )  $\delta$  7.31 (t,  $J = 7.5$  Hz, 2H), 7.24 – 7.17 (m, 3H), 4.88 – 4.78 (m, 1H), 4.03 (bs, 1H), 2.85 (ddd,  $J = 14.5, 9.6, 5.2$  Hz, 1H), 2.75 (ddd,  $J = 13.8, 9.2, 7.2$  Hz, 1H), 2.06 (dtd,  $J = 14.2, 9.1, 5.3$  Hz, 1H), 1.96 – 1.82 (m, 1H), 1.63 (d,  $J = 6.3$  Hz, 2H), 1.47 (s, 3H), 1.30 (s, 3H).  $^{13}\text{C}$  NMR (126 MHz,  $\text{CDCl}_3$ )  $\delta$

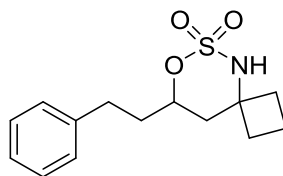
140.46, 128.47, 126.29, 80.19, 55.88, 41.56, 37.10, 32.00, 30.76, 25.13. HRMS (ESI)  $m/z$  calculated for  $C_{13}H_{23}N_2O_3S$   $[M+NH_4]^+$  287.1424, found 287.1430.



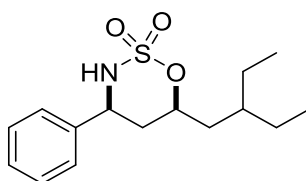
**Compound 3.47a.** The product was isolated in 63% yield.  $^1H$  NMR (500 MHz,  $CDCl_3$ )  $\delta$  7.45 – 7.32 (m, 5H), 4.97 (dtd,  $J$  = 11.7, 6.3, 2.1 Hz, 1H), 4.82 (ddd,  $J$  = 12.2, 9.3, 2.8 Hz, 1H), 4.17 (d,  $J$  = 9.3 Hz, 1H), 2.17 (ddd,  $J$  = 14.3, 2.8, 2.1 Hz, 1H), 1.95 (dt,  $J$  = 14.3, 12.0 Hz, 1H), 1.83 (dt,  $J$  = 13.8, 6.6 Hz, 1H), 1.53 (ddd,  $J$  = 14.0, 7.5, 6.0 Hz, 1H), 0.89 – 0.77 (m, 1H), 0.60 – 0.49 (m, 2H), 0.17 (ddd,  $J$  = 10.6, 4.8, 2.0 Hz, 1H), 0.11 (ddd,  $J$  = 12.3, 4.8, 2.1 Hz, 1H).  $^{13}C$  NMR (126 MHz,  $CDCl_3$ )  $\delta$  138.1, 129.2, 128.9, 126.3, 84.6, 58.3, 40.1, 36.0, 6.4, 4.5, 4.5. HRMS (ESI)  $m/z$  calculated for  $C_{13}H_{21}N_2O_3S$   $[M+NH_4]^+$  285.1268, found 285.1274.



**Compound 3.48a.** The product was isolated in 64% yield.  $^1H$  NMR (500 MHz, Chloroform- $d$ )  $\delta$  = 7.41 – 7.36 (m, 2H), 7.36 – 7.31 (m, 3H), 4.90 – 4.67 (m, 2H), 4.42 (d,  $J$ =9.5 Hz, 1H), 2.49 (hept,  $J$ =8.0 Hz, 1H), 2.09 (dtt,  $J$ =19.1, 7.9, 4.0 Hz, 2H), 1.98 (dt,  $J$ =14.3, 2.7 Hz, 1H), 1.96 – 1.77 (m, 4H), 1.77 – 1.60 (m, 3H).  $^{13}C$  NMR (126 MHz,  $CDCl_3$ )  $\delta$  = 138.1, 129.1, 128.7, 126.3, 83.3, 58.3, 42.2, 36.2, 31.6, 28.5, 28.4, 18.7. HRMS (ESI)  $m/z$  calculated for  $C_{14}H_{23}N_2O_3S$   $[M+NH_4]^+$  299.1424, found 299.1419.

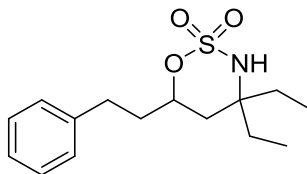


**Compound 3.48b.** The product was obtained in 30% yield.  $^1\text{H}$  NMR (500 MHz, Chloroform-*d*)  $\delta$  7.31 (t,  $J=7.5$  Hz, 2H), 7.25 – 7.16 (m, 3H), 4.73 (dddd,  $J=12.2, 8.6, 4.0, 1.9$  Hz, 1H), 4.17 (s, 1H), 2.85 (ddd,  $J=14.5, 9.7, 5.3$  Hz, 1H), 2.74 (ddd,  $J=13.8, 9.4, 7.0$  Hz, 1H), 2.59 – 2.45 (m, 1H), 2.13 – 1.95 (m, 6H), 1.91 (dddd,  $J=14.1, 9.6, 7.1, 4.0$  Hz, 1H), 1.87 – 1.79 (m, 1H), 1.66 (ddd,  $J=13.9, 11.8, 1.6$  Hz, 1H).  $^{13}\text{C}$  NMR (126 MHz,  $\text{CDCl}_3$ )  $\delta$  = 140.5, 128.6, 128.5, 126.3, 80.8, 58.9, 39.2, 36.9, 34.1, 31.9, 30.8, 14.9. HRMS (ESI)  $m/z$  calculated for  $\text{C}_{14}\text{H}_{23}\text{N}_2\text{O}_3\text{S}$   $[\text{M}+\text{NH}_4]^+$  299.1424, found 299.1423.

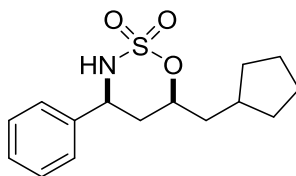


**Compound 3.49a.** The product was isolated in 65% yield.  $^1\text{H}$  NMR (500 MHz, Chloroform-*d*)  $\delta$  7.43 – 7.33 (m, 5H), 4.95 (dddd,  $J = 10.9, 8.7, 4.0, 2.1$  Hz, 1H), 4.81 (ddd,  $J = 12.2, 9.2, 2.9$  Hz, 1H), 4.13 (d,  $J = 9.2$  Hz, 1H), 2.06 (dt,  $J = 14.3, 2.5$  Hz, 1H), 1.90 (dt,  $J = 14.3, 11.8$  Hz, 1H), 1.81 (t,  $J = 8.8$  Hz, 1H), 1.58 – 1.49 (m, 2H), 1.48 – 1.26 (m, 4H), 0.87 (td,  $J = 7.4, 1.3$  Hz, 6H).  $^{13}\text{C}$  NMR (126 MHz,  $\text{CDCl}_3$ )  $\delta$  = 138.1, 129.2, 128.9, 126.3, 82.8, 58.3, 38.9, 36.9, 35.7, 25.4, 24.7, 10.6, 10.3. HRMS (ESI)  $m/z$  calculated for  $\text{C}_{15}\text{H}_{27}\text{N}_2\text{O}_3\text{S}$   $[\text{M}+\text{NH}_4]^+$  315.1737, found 315.1729.

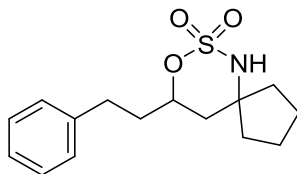




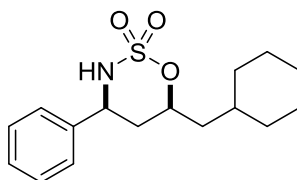
**Compound 3.49b.** The product was isolated in 68% yield.  $^1\text{H}$  NMR (500 MHz, Chloroform-*d*)  $\delta$  7.30 (t,  $J = 7.5$  Hz, 2H), 7.25 – 7.16 (m, 3H), 4.83 (dddd,  $J = 11.1, 8.7, 4.0, 2.2$  Hz, 1H), 3.84 (s, 1H), 2.85 (ddd,  $J = 14.4, 9.5, 5.3$  Hz, 1H), 2.74 (ddd,  $J = 13.8, 9.2, 7.1$  Hz, 1H), 2.13 (dq,  $J = 14.4, 7.2$  Hz, 1H), 2.06 (ddd,  $J = 14.2, 9.8, 5.2$  Hz, 1H), 1.88 (dddd,  $J = 13.9, 9.4, 7.2, 3.9$  Hz, 1H), 1.64 (dd,  $J = 14.4, 2.1$  Hz, 1H), 1.61 – 1.48 (m, 3H), 1.41 (dt,  $J = 14.0, 7.4$  Hz, 1H), 0.89 (td,  $J = 7.5, 1.4$  Hz, 6H).  $^{13}\text{C}$  NMR (126 MHz,  $\text{CDCl}_3$ )  $\delta$  140.5, 128.6, 128.5, 126.3, 79.8, 61.2, 38.5, 37.2, 32.5, 30.8, 25.3, 7.5, 7.0. HRMS (ESI)  $m/z$  calculated for  $\text{C}_{15}\text{H}_{27}\text{N}_2\text{O}_3\text{S}$   $[\text{M}+\text{NH}_4]^+$  315.1737, found 315.1734.



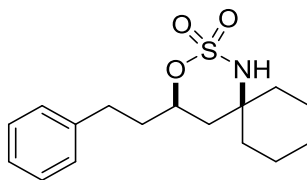
**Compound 3.50a.** The product was isolated in 54% yield.  $^1\text{H}$  NMR (500 MHz, Chloroform-*d*)  $\delta$  7.39 (dd,  $J = 8.4, 6.1$  Hz, 2H), 7.36 – 7.32 (m, 3H), 4.89 (dddd,  $J = 10.8, 8.3, 4.7, 2.1$  Hz, 1H), 4.79 (ddd,  $J = 12.3, 9.4, 2.9$  Hz, 1H), 4.38 (d,  $J = 9.5$  Hz, 1H), 2.05 (dt,  $J = 14.4, 2.6$  Hz, 1H), 2.03 – 1.95 (m, 1H), 1.95 – 1.83 (m, 3H), 1.79 (td,  $J = 11.6, 6.8$  Hz, 1H), 1.69 – 1.57 (m, 3H), 1.54 (dp,  $J = 8.3, 4.7, 4.2$  Hz, 2H), 1.11 (dp,  $J = 12.1, 8.2$  Hz, 2H).  $^{13}\text{C}$  NMR (126 MHz,  $\text{CDCl}_3$ )  $\delta$  138.2, 129.1, 128.8, 126.3, 84.1, 58.3, 41.4, 36.6, 35.6, 32.8, 32.4, 25.0, 24.8. HRMS (ESI)  $m/z$  calculated for  $\text{C}_{15}\text{H}_{25}\text{N}_2\text{O}_3\text{S}$   $[\text{M}+\text{NH}_4]^+$  313.1581, found 313.1591.



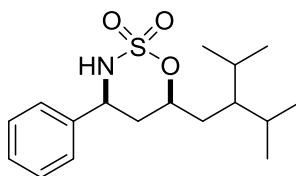
**Compound 3.50b.** The product was obtained in 67% yield.  $^1\text{H}$  NMR (500 MHz,  $\text{CDCl}_3$ )  $\delta$  7.30 (t,  $J = 7.5$  Hz, 2H), 7.23 – 7.15 (m, 3H), 4.78 (dddd,  $J = 12.2, 8.7, 4.1, 1.8$  Hz, 1H), 4.27 (s, 1H), 2.84 (ddd,  $J = 14.6, 9.6, 5.3$  Hz, 1H), 2.73 (ddd,  $J = 13.8, 9.4, 7.0$  Hz, 1H), 2.44 (ddd,  $J = 13.5, 8.4, 4.7$  Hz, 1H), 2.05 (dtd,  $J = 14.3, 9.1, 5.3$  Hz, 1H), 1.94 – 1.84 (m, 2H), 1.83 – 1.73 (m, 2H), 1.73 – 1.63 (m, 4H), 1.60 (dd,  $J = 14.3, 1.9$  Hz, 1H), 1.55 (dt,  $J = 14.0, 7.8$  Hz, 1H).  $^{13}\text{C}$  NMR (126 MHz,  $\text{CDCl}_3$ )  $\delta$  140.5, 128.6, 128.5, 126.2, 81.4, 66.4, 42.4, 39.7, 37.1, 35.3, 30.7, 24.1, 22.4. HRMS (ESI)  $m/z$  calculated for  $\text{C}_{15}\text{H}_{25}\text{N}_2\text{O}_3\text{S}$   $[\text{M}+\text{NH}_4]^+$  313.1581, found 313.1583.



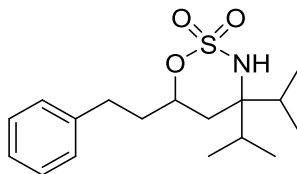
**Compound 3.51a.** The product was isolated in 73% yield.  $^1\text{H}$  NMR (500 MHz, Chloroform-*d*)  $\delta$  7.47 – 7.31 (m, 5H), 4.99 (dddd,  $J = 11.3, 9.0, 4.2, 2.1$  Hz, 1H), 4.81 (ddd,  $J = 12.1, 9.2, 2.9$  Hz, 1H), 4.11 (d,  $J = 9.2$  Hz, 1H), 2.10 – 2.00 (m, 1H), 1.94 – 1.64 (m, 7H), 1.58 (ddt,  $J = 11.5, 5.4, 3.0$  Hz, 1H), 1.47 (ddd,  $J = 14.2, 8.4, 4.2$  Hz, 1H), 1.26 (dddd,  $J = 14.8, 11.6, 8.9, 2.8$  Hz, 2H), 1.15 (qt,  $J = 12.8, 3.5$  Hz, 1H), 1.02 – 0.86 (m, 2H).  $^{13}\text{C}$  NMR (126 MHz,  $\text{CDCl}_3$ )  $\delta$  138.1, 129.2, 128.9, 126.3, 82.3, 58.2, 42.9, 36.8, 33.6, 33.0, 32.6, 26.3, 26.1, 25.9. HRMS (ESI)  $m/z$  calculated for  $\text{C}_{16}\text{H}_{27}\text{N}_2\text{O}_3\text{S}$   $[\text{M}+\text{NH}_4]^+$  327.1737, found 327.1737.



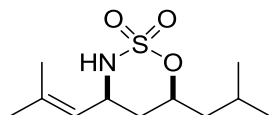
**Compound 3.51b.** The product was obtained in 72% yield.  $^1\text{H}$  NMR (500 MHz,  $\text{CDCl}_3$ )  $\delta$  7.30 (t,  $J = 7.5$  Hz, 2H), 7.24 – 7.16 (m, 3H), 4.92 – 4.76 (m, 1H), 3.91 (s, 1H), 2.84 (ddd,  $J = 14.4$ , 9.6, 5.2 Hz, 1H), 2.78 – 2.69 (m, 1H), 2.40 (d,  $J = 13.1$  Hz, 1H), 2.05 (dtd,  $J = 14.2$ , 8.9, 5.4 Hz, 1H), 1.87 (dtt,  $J = 13.7$ , 7.1, 4.0 Hz, 1H), 1.72 – 1.59 (m, 4H), 1.57 (d,  $J = 4.1$  Hz, 1H), 1.49 (ddd,  $J = 31.0$ , 11.3, 4.7 Hz, 4H), 1.39 – 1.22 (m, 2H).  $^{13}\text{C}$  NMR (126 MHz,  $\text{CDCl}_3$ )  $\delta$  140.5, 128.6, 128.5, 126.3, 79.4, 57.9, 41.3, 40.5, 37.2, 32.8, 30.8, 25.5, 21.1, 20.8. HRMS (ESI)  $m/z$  calculated for  $\text{C}_{16}\text{H}_{27}\text{N}_2\text{O}_3\text{S}$   $[\text{M}+\text{NH}_4]^+$  327.1737, found 327.1742.



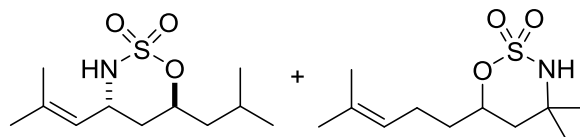
**Compound 3.52a.** The product was obtained in 63% yield.  $^1\text{H}$  NMR (500 MHz, Chloroform- $d$ )  $\delta$  7.43 – 7.38 (m, 2H), 7.38 – 7.32 (m, 3H), 4.88 (dddd,  $J = 10.9$ , 8.3, 4.8, 2.0 Hz, 1H), 4.78 (ddd,  $J = 12.1$ , 9.2, 2.8 Hz, 1H), 4.22 (d,  $J = 9.3$  Hz, 1H), 2.10 (dt,  $J = 14.3$ , 2.5 Hz, 1H), 1.92 – 1.83 (m, 1H), 1.82 – 1.70 (m, 3H), 1.54 (ddd,  $J = 14.9$ , 6.5, 4.8 Hz, 1H), 1.24 (dq,  $J = 6.3$ , 4.8 Hz, 1H), 0.91 (d,  $J = 6.8$  Hz, 6H), 0.89 (d,  $J = 6.8$  Hz, 3H), 0.85 (d,  $J = 6.8$  Hz, 3H).  $^{13}\text{C}$  NMR (126 MHz,  $\text{CDCl}_3$ )  $\delta$  138.2, 129.1, 128.8, 126.3, 84.8, 58.3, 45.0, 36.8, 33.8, 29.3, 28.9, 21.5, 21.2, 19.5, 18.9. HRMS (ESI)  $m/z$  calculated for  $\text{C}_{17}\text{H}_{31}\text{N}_2\text{O}_3\text{S}$   $[\text{M}+\text{NH}_4]^+$  343.2050, found 343.2058.



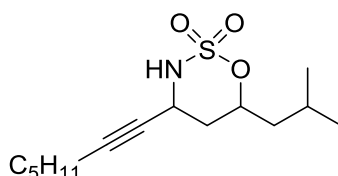
**Compound 3.52b.** Compound isolated by column chromatography on silica gel using a 0  $\rightarrow$  6% gradient of EtOAc in hexanes. The product was obtained in 54% yield.  $^1\text{H}$  NMR (500 MHz, Chloroform-*d*)  $\delta$  7.30 (t,  $J$  = 7.5 Hz, 2H), 7.23 – 7.16 (m, 3H), 4.77 (ddt,  $J$  = 10.1, 8.1, 3.9 Hz, 1H), 3.99 (s, 1H), 2.87 (ddd,  $J$  = 14.6, 9.6, 5.3 Hz, 1H), 2.74 (ddd,  $J$  = 13.9, 9.4, 7.0 Hz, 1H), 2.54 (hept,  $J$  = 7.1 Hz, 1H), 2.11 (dtd,  $J$  = 14.2, 8.9, 5.3 Hz, 1H), 1.99 – 1.86 (m, 2H), 1.78 – 1.71 (m, 2H), 1.09 (d,  $J$  = 6.8 Hz, 3H), 0.98 (d,  $J$  = 6.9 Hz, 6H), 0.95 (d,  $J$  = 7.1 Hz, 3H).  $^{13}\text{C}$  NMR (126 MHz,  $\text{CDCl}_3$ )  $\delta$  140.5, 128.6, 128.4, 126.3, 80.1, 65.9, 37.3, 34.3, 32.4, 32.2, 30.9, 18.4, 18.3, 17.9, 17.5. HRMS (ESI)  $m/z$  calculated for  $\text{C}_{17}\text{H}_{31}\text{N}_2\text{O}_3\text{S}$   $[\text{M}+\text{NH}_4]^+$  343.2050, found 343.2039.



**Compound 3.53a.** The *syn* product was obtained in 68% yield.  $^1\text{H}$  NMR (500 MHz,  $\text{CDCl}_3$ )  $\delta$  4.96 (dp,  $J$  = 8.1, 1.5 Hz, 1H), 4.83 (dddd,  $J$  = 11.4, 9.0, 4.2, 2.1 Hz, 1H), 4.42 (dtd,  $J$  = 11.8, 8.6, 3.0 Hz, 1H), 3.79 (d,  $J$  = 9.6 Hz, 1H), 1.95 – 1.81 (m, 1H), 1.75 (s, 6H), 1.74 – 1.67 (m, 2H), 1.49 (dt,  $J$  = 14.5, 11.8 Hz, 1H), 1.36 (ddd,  $J$  = 14.2, 8.6, 4.2 Hz, 1H), 0.94 (dd,  $J$  = 8.0, 6.6 Hz, 6H).  $^{13}\text{C}$  NMR (126 MHz,  $\text{CDCl}_3$ )  $\delta$  139.7, 139.6, 121.7, 82.5, 53.1, 44.2, 36.7, 36.6, 25.5, 23.7, 22.9, 21.8, 18.6. HRMS (ESI)  $m/z$  calculated for  $\text{C}_{11}\text{H}_{21}\text{NO}_3\text{S}$   $[\text{M}+\text{NH}_4]^+$  265.1581, found 265.1578.

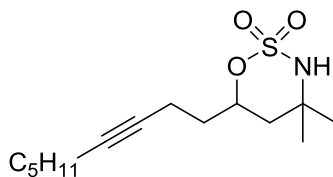


**Compound 3.53b.** The product was isolated in 19% yield, as mixture of *anti* allylic insertion and 3° insertion product.  $^1\text{H}$  NMR (300 MHz,  $\text{CDCl}_3$ )  $\delta$  5.58 (dp,  $J = 8.4, 1.4$  Hz, 1H, *anti*), 5.13 – 5.01 (m, 1H, 3°), 4.95 (tt,  $J = 9.0, 4.0$  Hz, 1H, *anti*), 4.81 (tt,  $J = 8.9, 4.7$  Hz, 1H, 3°), 4.56 (d,  $J = 6.9$  Hz, 1H, *anti*), 4.42 (dq,  $J = 12.6, 5.6$  Hz, 1H, *anti*), 4.27 (s, 1H, 3°), 2.15 (q,  $J = 7.5$  Hz, 2H, 3°), 1.99 – 1.80 (m, 4H), 1.77 (s, 4H), 1.74 – 1.67 (m, 7H), 1.63 (s, 4H), 1.49 (s, 3H), 1.30 (s, 3H), 0.95 (dd,  $J = 6.5, 4.0$  Hz, 6H).  $^{13}\text{C}$  NMR (126 MHz,  $\text{CDCl}_3$ )  $\delta$  137.2, 133.4, 122.3, 121.7, 81.3, 80.7, 55.8, 51.3, 43.4, 41.4, 35.3, 34.7, 31.8, 25.7, 25.6, 25.1, 24.0, 23.1, 22.9, 21.7, 18.2, 17.7. HRMS (ESI)  $m/z$  calculated for  $\text{C}_{11}\text{H}_{21}\text{NO}_3\text{S}$   $[\text{M}+\text{NH}_4]^+$  265.1581, found 265.1580.

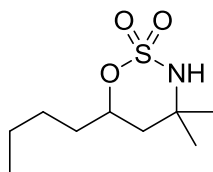


**Compound 3.54a.** The product was isolated in 37% yield. Major isomer (*syn*):  $^1\text{H}$  NMR (500 MHz,  $\text{CDCl}_3$ )  $\delta$  4.77 (dddd,  $J = 11.4, 9.0, 4.3, 2.1$  Hz, 1H), 4.48 (ddt,  $J = 12.3, 7.2, 2.5, 2.5$  Hz, 1H), 4.04 (d,  $J = 10.4$  Hz, 1H), 2.18 (td,  $J = 7.2, 7.1, 2.1$  Hz, 2H), 1.99 (ddd,  $J = 14.5, 3.0, 2.1$  Hz, 1H), 1.92 – 1.81 (m, 1H), 1.76 – 1.67 (m, 2H), 1.54 – 1.45 (m, 2H), 1.42 – 1.27 (m, 5H), 0.94 (d,  $J = 4.5$  Hz, 3H), 0.93 (d,  $J = 4.6$  Hz, 3H), 0.90 (t,  $J = 7.2, 7.0$  Hz, 3H).  $^{13}\text{C}$  NMR (126 MHz,  $\text{CDCl}_3$ )  $\delta$  86.9, 82.1, 75.6, 47.2, 43.9, 37.5, 30.9, 27.9, 23.7, 22.8, 22.1, 21.8, 18.5, 13.9. HRMS (ESI)  $m/z$  calculated for  $\text{C}_{14}\text{H}_{29}\text{N}_2\text{O}_3\text{S}$   $[\text{M}+\text{NH}_4]^+$  305.1894, found 305.1897. The minor

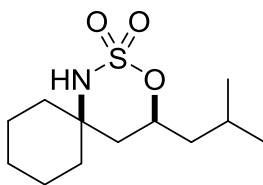
isomer (*anti*) coelutes with **3.54b** and was identified based on peak patterns observed in the crude NMR for **3.54b**.



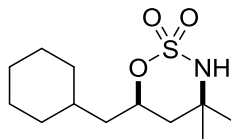
**Compound 3.54b.** Compound co-elutes with minor isomer of **3.54a**, and an amount sufficient for characterization was isolated in 95% purity with a gradient of 0→30% ethyl acetate/hexanes on silica impregnated with AgNO<sub>3</sub> as a 5% solution in acetonitrile. <sup>1</sup>H NMR (500 MHz, CDCl<sub>3</sub>) δ 5.00 (dddd, *J* = 12.2, 8.3, 4.4, 2.0 Hz, 1H), 3.99 (s, 1H), 2.35 (tdt, *J* = 6.3, 4.2, 2.4 Hz, 2H), 2.14 (tt, *J* = 7.1, 2.4 Hz, 2H), 1.98 – 1.89 (m, 1H), 1.77 (dtd, *J* = 14.1, 7.6, 4.5 Hz, 1H), 1.70 (dd, *J* = 14.3, 2.0 Hz, 1H), 1.63 – 1.55 (m, 2H), 1.52 (s, 3H), 1.47 (p, *J* = 7.2 Hz, 2H), 1.40 – 1.27 (m, 3H), 1.31 (s, 3H), 0.90 (t, *J* = 7.0 Hz, 3H). <sup>13</sup>C NMR (126 MHz, CDCl<sub>3</sub>) δ 81.8, 79.9, 77.7, 55.9, 41.3, 34.5, 32.0, 31.1, 28.7, 25.1, 22.2, 18.7, 14.4, 14.0. HRMS (ESI) *m/z* calculated for C<sub>14</sub>H<sub>29</sub>N<sub>2</sub>O<sub>3</sub>S [M+NH<sub>4</sub>]<sup>+</sup> 305.1894, found 305.1897.



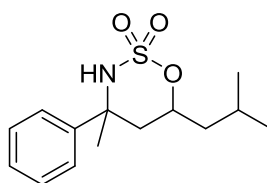
**Compound 3.23a.** The product was obtained in 94% yield. <sup>1</sup>H NMR (500 MHz, CDCl<sub>3</sub>) δ 4.82 (dddd, *J* = 11.5, 7.9, 4.7, 2.2 Hz, 1H), 3.92 (bs, 1H), 1.75 (dddd, *J* = 14.5, 9.8, 7.9, 5.0 Hz, 1H), 1.70-1.54 (m, 3H), 1.50 (s, 3H), 1.45-1.31 (m, 4H), 1.30 (s, 3H), 0.92 (t, *J* = 7.2 Hz, 3H). <sup>13</sup>C NMR (126 MHz, CDCl<sub>3</sub>) δ 81.2, 55.8, 41.6, 34.9, 32.1, 26.7, 25.1, 22.3, 13.9. HRMS (ESI) *m/z* calculated for C<sub>9</sub>H<sub>19</sub>NO<sub>3</sub>S [M+NH<sub>4</sub>]<sup>+</sup> 239.1424, found 239.1416.



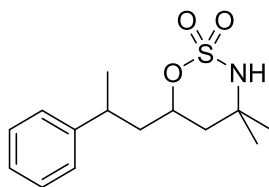
**Compound 3.7a.** The product was purified by column chromatography using a 5→20% gradient of EtOAc in hexanes, using 5% increments. The product was isolated in 74% yield.  $^1\text{H}$  NMR (500 MHz,  $\text{CDCl}_3$ )  $\delta$  4.91 (dddd,  $J = 11.8, 8.9, 4.3, 1.9$  Hz, 1H), 3.76 (bs, 1H), 2.45 (dd,  $J = 11.4, 6.9$  Hz, 1H), 1.94 – 1.81 (m, 1H), 1.78 – 1.56 (m, 5H), 1.56 – 1.45 (m, 5H), 1.35 (qdd,  $J = 16.4, 10.5, 3.1$  Hz, 3H), 0.95 (d,  $J = 6.6$  Hz, 3H), 0.93 (d,  $J = 6.7$  Hz, 3H).  $^{13}\text{C}$  NMR (126 MHz,  $\text{CDCl}_3$ )  $\delta$  78.7, 57.9, 44.2, 40.6, 32.9, 25.6, 23.8, 22.9, 21.9, 21.1, 20.8. HRMS (ESI)  $m/z$  calculated for  $\text{C}_{12}\text{H}_{27}\text{N}_2\text{O}_3\text{S}$   $[\text{M}+\text{NH}_4]^+$  279.1737, found 279.1745.



**Compound 3.7b.** The product was isolated in 50% yield.  $^1\text{H}$  NMR (500 MHz,  $\text{CDCl}_3$ )  $\delta$  4.93 (dddd,  $J = 10.7, 8.9, 4.2, 2.9$  Hz, 1H), 4.08 (bs, 1H), 1.81 (ddt,  $J = 12.1, 4.8, 2.2$  Hz, 1H), 1.73 – 1.62 (m, 5H), 1.62 – 1.59 (m, 2H), 1.50 (s, 3H), 1.42 – 1.35 (m, 2H), 1.29 (s, 3H), 1.25 (dddd,  $J = 13.1, 11.6, 8.7, 4.5$  Hz, 2H), 1.19 – 1.11 (m, 1H), 1.01 – 0.84 (m, 2H).  $^{13}\text{C}$  NMR (126 MHz,  $\text{CDCl}_3$ )  $\delta$  79.1, 55.9, 42.9, 42.0, 33.6, 33.0, 32.6, 31.9, 30.6, 26.4, 26.1, 26.0, 25.2. HRMS (ESI)  $m/z$  calculated for  $\text{C}_{12}\text{H}_{23}\text{NO}_3\text{S}$   $[\text{M}+\text{NH}_4]^+$  279.1737, found 279.1745.



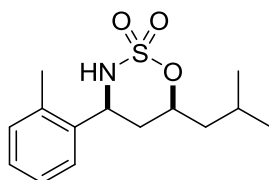
**Compound 3.55a.** The product was purified by column chromatography using a 0→25% gradient of EtOAc in hexanes with 5% increments. The resulting colorless oil was obtained in 48% yield as a mixture of diastereomers with *dr* (2.5:1). Major diastereomer:  $^1\text{H}$  NMR (500 MHz, Chloroform-*d*)  $\delta$  7.46 – 7.38 (m, 4H), 7.35 – 7.31 (m, 1H), 5.07 (dddd,  $J = 11.2, 9.0, 4.1, 2.0$  Hz, 1H), 4.28 (s, 1H), 2.14 (dd,  $J = 14.1, 2.0$  Hz, 1H), 2.08 – 2.01 (m, 1H), 1.95 (dddd,  $J = 15.2, 12.2, 7.7, 6.1$  Hz, 1H), 1.86 – 1.82 (m, 1H), 1.81 (d,  $J = 0.8$  Hz, 3H), 1.47 (ddd,  $J = 14.1, 8.6, 4.1$  Hz, 1H), 0.99 (dd,  $J = 13.7, 6.6$  Hz, 6H).  $^{13}\text{C}$  NMR (126 MHz,  $\text{CDCl}_3$ )  $\delta$  146.1, 129.2, 128.3, 124.1, 79.3, 60.8, 44.4, 40.4, 27.4, 23.9, 23.1, 22.0. HRMS (ESI)  $m/z$  calculated for  $\text{C}_{14}\text{H}_{25}\text{N}_2\text{O}_3\text{S}$   $[\text{M}+\text{NH}_4]^+$  301.1581, found 301.1574. Minor diastereomer:  $^1\text{H}$  NMR (500 MHz, Chloroform-*d*)  $\delta$  7.50 – 7.46 (m, 2H), 7.41 – 7.36 (m, 2H), 7.33 – 7.28 (m, 1H), 4.71 (dddd,  $J = 11.6, 8.7, 4.6, 1.5$  Hz, 1H), 4.38 (s, 1H), 2.65 (dd,  $J = 15.0, 1.5$  Hz, 1H), 1.92 – 1.81 (m, 2H), 1.76 (ddd,  $J = 14.5, 8.7, 6.0$  Hz, 1H), 1.48 (s, 3H), 1.47 – 1.42 (m, 1H), 0.92 (dd,  $J = 13.1, 6.6$  Hz, 6H).  $^{13}\text{C}$  NMR (126 MHz,  $\text{CDCl}_3$ )  $\delta$  161.1, 149.2, 141.4, 128.7, 127.8, 125.7, 120.9, 118.4, 80.2, 61.7, 44.3, 40.1, 35.5, 30.8, 24.0, 23.0, 22.1. HRMS (ESI)  $m/z$  calculated for  $\text{C}_{14}\text{H}_{25}\text{N}_2\text{O}_3\text{S}$   $[\text{M}+\text{NH}_4]^+$  301.1581, found 301.1583.



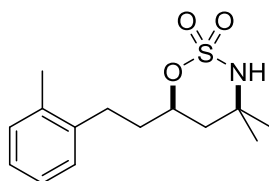
**Compound 3.55b.** The product was purified by column chromatography using a 0→25% gradient of EtOAc in hexanes with 5% increments. The resulting colorless oil was obtained in 58% yield as a mixture of diastereomers with *dr* (2.1:1).  $^1\text{H}$  NMR (500 MHz, Chloroform-*d*)  $\delta$  7.35 – 7.29 (m, 3H), 7.25 – 7.17 (m, 4H), 4.82 (dddd,  $J = 11.7, 8.5, 5.0, 2.0$  Hz, 0.4H), 4.60 – 4.52 (m, 1H), 3.96 (s, 0.4H), 3.93 (s, 1H), 3.07 (ddq,  $J = 13.6, 6.8, 3.4, 2.5$  Hz, 1H), 3.04 – 2.96



(m, 0.4H), 2.09 (ddd,  $J = 14.5, 8.5, 6.3$  Hz, 0.4H), 2.02 (ddd,  $J = 14.1, 9.5, 4.5$  Hz, 1H), 1.81 – 1.76 (m, 0.4H), 1.73 (ddd,  $J = 14.1, 10.6, 3.3$  Hz, 1H), 1.66 (dd,  $J = 14.3, 2.0$  Hz, 0.4H), 1.46 – 1.41 (m, 2H), 1.39 (s, 1H), 1.33 (d,  $J = 2.2$  Hz, 3H), 1.31 (d,  $J = 3.3$  Hz, 2H), 1.29 (d,  $J = 4.9$  Hz, 3H), 1.24 (s, 3H).  $^{13}\text{C}$  NMR (126 MHz,  $\text{CDCl}_3$ )  $\delta$  146.1, 145.3, 128.9, 127.3, 126.8, 126.8, 126.7, 79.6, 79.2, 56.0, 55.9, 44.4, 43.6, 42.0, 41.8, 35.4, 34.9, 32.2, 32.1, 30.8, 25.2, 22.4, 21.2. HRMS (ESI)  $m/z$  calculated for  $\text{C}_{14}\text{H}_{25}\text{N}_2\text{O}_3\text{S}$   $[\text{M}+\text{NH}_4]^+$  301.1581, found 301.1582.

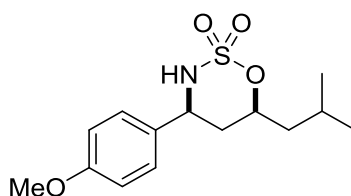


**Compound 3.56a.** The product was purified by column chromatography using a 0→30% gradient of EtOAc in hexanes with 5% increments. The resulting white solid was obtained in 65% yield.  $^1\text{H}$  NMR (500 MHz, Chloroform- $d$ )  $\delta$  7.32 – 7.17 (m, 4H), 4.96 (dddt,  $J = 15.8, 8.9, 4.2, 2.4$  Hz, 2H), 4.13 (d,  $J = 9.8$  Hz, 1H), 2.43 (s, 3H), 2.03 (dt,  $J = 14.3, 11.7$  Hz, 1H), 1.96 – 1.84 (m, 2H), 1.80 (ddd,  $J = 14.5, 9.0, 5.6$  Hz, 1H), 1.45 (ddd,  $J = 14.1, 8.5, 4.2$  Hz, 1H), 0.96 (dd,  $J = 12.3, 6.6$  Hz, 6H).  $^{13}\text{C}$  NMR (126 MHz,  $\text{CDCl}_3$ )  $\delta$  136.9, 135.9, 131.3, 128.8, 126.7, 124.8, 82.9, 54.8, 44.3, 35.5, 23.9, 23.0, 21.9, 19.2. HRMS (ESI)  $m/z$  calculated for  $\text{C}_{14}\text{H}_{25}\text{N}_2\text{O}_3\text{S}$   $[\text{M}+\text{NH}_4]^+$  301.1581, found 301.1571.

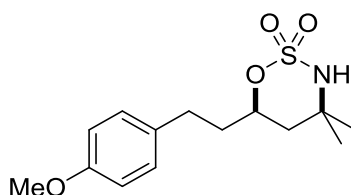


**Compound 3.56b.** The product was purified by column chromatography using a 0→30% gradient of EtOAc in hexanes with 5% increments. The resulting colorless oil was obtained in 45% yield.  $^1\text{H}$  NMR (500 MHz, Chloroform- $d$ )  $\delta$  7.17 – 7.10 (m, 4H), 4.86 (dtd,  $J = 8.6, 7.0, 3.8$

Hz, 1H), 4.13 (s, 1H), 2.86 (ddd,  $J = 13.9, 10.1, 5.0$  Hz, 1H), 2.71 (ddd,  $J = 14.0, 9.9, 6.7$  Hz, 1H), 2.32 (s, 3H), 2.06 – 1.95 (m, 1H), 1.84 (dddd,  $J = 14.1, 10.3, 6.7, 3.8$  Hz, 1H), 1.64 (d,  $J = 6.3$  Hz, 2H), 1.49 (s, 3H), 1.30 (s, 3H).  $^{13}\text{C}$  NMR (126 MHz,  $\text{CDCl}_3$ )  $\delta$  138.8, 136.0, 130.6, 129.1, 126.6, 126.3, 80.6, 56.0, 41.7, 35.9, 32.1, 28.2, 25.3, 19.4. HRMS (ESI)  $m/z$  calculated for  $\text{C}_{14}\text{H}_{25}\text{N}_2\text{O}_3\text{S}$   $[\text{M}+\text{NH}_4]^+$  301.1581, found 301.1573.

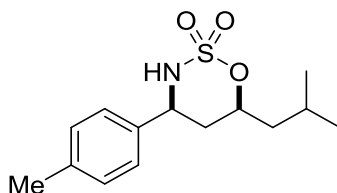


**Compound 3.57a.** The product was purified by column chromatography using a 0→25% gradient of EtOAc in hexanes with 5% increments. The resulting colorless oil was obtained in 70% yield based on NMR integrations using mesitylene as an internal standard.  $^1\text{H}$  NMR (500 MHz,  $\text{CDCl}_3$ )  $\delta$  7.30 – 7.23 (m, 2H), 6.95 – 6.87 (m, 2H), 4.93 (dddd,  $J = 11.2, 8.9, 4.2, 2.1$  Hz, 1H), 4.75 (ddd,  $J = 12.1, 9.2, 2.9$  Hz, 1H), 4.13 (d,  $J = 9.2$  Hz, 1H), 3.81 (s, 3H), 2.03 – 1.97 (m, 1H), 1.95 – 1.83 (m, 2H), 1.79 (ddd,  $J = 14.5, 9.0, 5.6$  Hz, 1H), 1.43 (ddd,  $J = 14.2, 8.6, 4.2$  Hz, 1H), 0.96 (dd,  $J = 9.8, 6.6$  Hz, 6H).  $^{13}\text{C}$  NMR (126 MHz,  $\text{CDCl}_3$ )  $\delta$  159.9, 130.2, 127.6, 114.4, 82.7, 57.8, 55.4, 44.2, 36.7, 23.8, 22.9, 21.9. HRMS (ESI)  $m/z$  calculated for  $\text{C}_{14}\text{H}_{21}\text{NO}_4\text{S}$   $[\text{M}+\text{NH}_4]^+$  317.1530, found 317.1533.

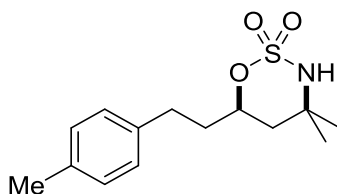


**Compound 3.57b.** The product was purified by column chromatography using a 0→25% gradient of EtOAc in hexanes with 5% increments. The resulting colorless oil was obtained in

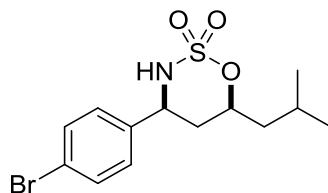
38% yield based on NMR integrations using mesitylene as an internal standard.  $^1\text{H}$  NMR (500 MHz, Chloroform- $d$ )  $\delta$  7.29 – 7.23 (m, 2H), 6.91 (d,  $J$  = 8.8 Hz, 2H), 4.93 (dddd,  $J$  = 11.2, 8.9, 4.2, 2.1 Hz, 1H), 4.75 (ddd,  $J$  = 12.1, 9.1, 2.9 Hz, 1H), 4.13 (d,  $J$  = 9.2 Hz, 1H), 3.81 (s, 3H), 2.05 – 1.97 (m, 1H), 1.95 – 1.86 (m, 2H), 1.79 (ddd,  $J$  = 14.5, 9.0, 5.6 Hz, 1H), 1.43 (ddd,  $J$  = 14.1, 8.5, 4.2 Hz, 1H), 0.96 (dd,  $J$  = 9.8, 6.6 Hz, 6H).  $^{13}\text{C}$  NMR (126 MHz,  $\text{CDCl}_3$ )  $\delta$  157.0, 131.4, 128.4, 112.9, 79.1, 66.9, 54.9, 54.2, 40.5, 36.3, 30.9, 28.8, 24.6, 24.1. HRMS (ESI)  $m/z$  calculated for  $\text{C}_{14}\text{H}_{21}\text{NO}_4\text{S}$   $[\text{M}+\text{NH}_4]^+$  317.1530, found 317.1534.



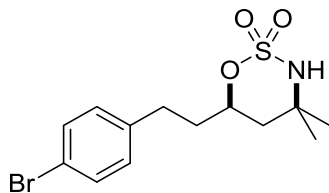
**Compound 3.58a.** The product was purified by column chromatography using a 0→20% gradient of EtOAc in hexanes with 5% increments. The resulting colorless oil was obtained in 66% yield based on NMR integrations using mesitylene as an internal standard.  $^1\text{H}$  NMR (500 MHz, Chloroform- $d$ )  $\delta$  7.24 – 7.19 (m, 4H), 4.94 (dddd,  $J$  = 11.4, 9.0, 4.2, 2.1 Hz, 1H), 4.78 (ddd,  $J$  = 12.2, 9.2, 2.9 Hz, 1H), 4.06 (d,  $J$  = 9.2 Hz, 1H), 2.36 (s, 3H), 2.03 (ddd,  $J$  = 14.4, 2.9, 2.1 Hz, 1H), 1.94 – 1.86 (m, 2H), 1.84 – 1.76 (m, 1H), 1.43 (ddd,  $J$  = 14.1, 8.6, 4.2 Hz, 1H), 0.97 (dd,  $J$  = 9.2, 6.6 Hz, 6H).  $^{13}\text{C}$  NMR (126 MHz,  $\text{CDCl}_3$ )  $\delta$  138.9, 135.3, 129.9, 126.3, 82.9, 58.2, 44.3, 36.9, 23.9, 23.1, 22.0, 21.3. HRMS (ESI)  $m/z$  calculated for  $\text{C}_{14}\text{H}_{25}\text{N}_2\text{O}_3\text{S}$   $[\text{M}+\text{NH}_4]^+$  301.1581, found 301.1578.



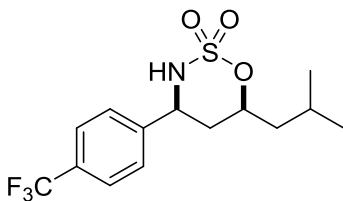
**Compound 3.58b.** The product was purified by column chromatograph using a 0→20% gradient of EtOAc in hexanes with 5% increments. The resulting colorless oil was obtained in 52% yield based on NMR integrations using mesitylene as an internal standard.  $^1\text{H}$  NMR (500 MHz, Chloroform-*d*)  $\delta$  7.13 – 7.05 (m, 4H), 4.83 (dtd,  $J$  = 8.6, 6.9, 3.9 Hz, 1H), 4.10 (s, 1H), 2.80 (ddt,  $J$  = 14.3, 9.6, 4.6 Hz, 1H), 2.70 (ddd,  $J$  = 13.8, 9.2, 7.1 Hz, 1H), 2.32 (s, 3H), 2.04 (dtd,  $J$  = 14.2, 9.0, 5.3 Hz, 1H), 1.89 – 1.81 (m, 1H), 1.62 (d,  $J$  = 6.8 Hz, 2H), 1.46 (s, 3H), 1.29 (s, 3H).  $^{13}\text{C}$  NMR (126 MHz,  $\text{CDCl}_3$ )  $\delta$  137.5, 135.9, 129.4, 128.5, 80.4, 56.0, 41.7, 37.4, 32.1, 30.4, 25.3, 21.1. HRMS (ESI)  $m/z$  calculated for  $\text{C}_{14}\text{H}_{25}\text{N}_2\text{O}_3\text{S}$   $[\text{M}+\text{NH}_4]^+$  301.1581, found 301.1584.



**Compound 3.59a.** The product was purified by column chromatography using a 0→25% gradient of EtOAc in hexanes with 5% increments. The resulting white solid was obtained in 55% yield based on NMR integrations using mesitylene as an internal standard.  $^1\text{H}$  NMR (500 MHz, Chloroform-*d*)  $\delta$  7.53 (d,  $J$  = 8.4 Hz, 2H), 7.23 (d,  $J$  = 8.4 Hz, 2H), 4.93 (dddd,  $J$  = 11.3, 9.0, 4.2, 2.1 Hz, 1H), 4.77 (ddd,  $J$  = 12.2, 9.3, 2.8 Hz, 1H), 4.29 (d,  $J$  = 9.3 Hz, 1H), 2.02 (dt,  $J$  = 14.3, 2.4 Hz, 1H), 1.92 – 1.83 (m, 2H), 1.83 – 1.74 (m, 1H), 1.43 (ddd,  $J$  = 14.1, 8.5, 4.2 Hz, 1H), 0.96 (dd,  $J$  = 10.0, 6.6 Hz, 6H).  $^{13}\text{C}$  NMR (126 MHz,  $\text{CDCl}_3$ )  $\delta$  137.2, 132.4, 128.2, 123.0, 82.9, 57.9, 44.2, 36.6, 23.9, 23.0, 21.9. HRMS (ESI)  $m/z$  calculated for  $\text{C}_{13}\text{H}_{22}\text{BrN}_2\text{O}_3\text{S}$   $[\text{M}+\text{NH}_4]^+$  365.0530, found 365.0527.

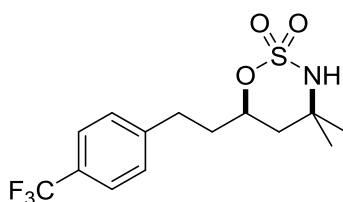


**Compound 3.59b.** The product was purified by column chromatography using a 0→25% gradient of EtOAc in hexanes with 5% increments. The resulting white solid was obtained in 44% yield based on NMR integrations using mesitylene as an internal standard.  $^1\text{H}$  NMR (500 MHz, Chloroform-*d*)  $\delta$  7.42 (d,  $J$  = 8.3 Hz, 2H), 7.07 (d,  $J$  = 8.3 Hz, 2H), 4.80 (dddd,  $J$  = 9.2, 7.7, 6.0, 3.6 Hz, 1H), 4.01 (s, 1H), 2.81 (ddd,  $J$  = 14.3, 9.5, 5.1 Hz, 1H), 2.71 (ddd,  $J$  = 13.9, 9.1, 7.4 Hz, 1H), 2.03 (dtd,  $J$  = 14.2, 9.1, 5.1 Hz, 1H), 1.84 (dddd,  $J$  = 14.3, 9.4, 7.4, 3.6 Hz, 1H), 1.63 (d,  $J$  = 1.8 Hz, 1H), 1.57 (s, 1H), 1.47 (s, 3H), 1.30 (s, 3H).  $^{13}\text{C}$  NMR (126 MHz,  $\text{CDCl}_3$ )  $\delta$  139.5, 131.9, 130.4, 120.3, 79.9, 56.0, 41.7, 37.0, 32.2, 30.3, 25.3. HRMS (ESI)  $m/z$  calculated for  $\text{C}_{13}\text{H}_{22}\text{BrN}_2\text{O}_3\text{S}$   $[\text{M}+\text{NH}_4]^+$  365.0530, found 365.0530.

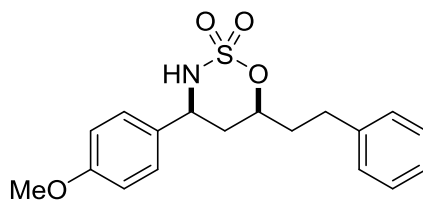


**Compound 3.60a.** The product was purified by column chromatography using a 0→30% gradient of EtOAc in hexanes with 6% increments. The resulting white solid was obtained in 42% yield based on NMR integrations using mesitylene as an internal standard.  $^1\text{H}$  NMR (500 MHz, Chloroform-*d*)  $\delta$  7.67 (d,  $J$  = 8.1 Hz, 2H), 7.49 (d,  $J$  = 8.1 Hz, 2H), 4.96 (dddd,  $J$  = 11.3, 9.0, 4.2, 2.1 Hz, 1H), 4.88 (ddd,  $J$  = 12.2, 9.4, 2.8 Hz, 1H), 4.47 (d,  $J$  = 9.4 Hz, 1H), 2.06 (dt,  $J$  = 14.3, 2.5 Hz, 1H), 1.94 – 1.83 (m, 2H), 1.79 (ddd,  $J$  = 14.4, 9.0, 5.6 Hz, 1H), 1.44 (ddd,  $J$  = 14.1,

8.5, 4.1 Hz, 1H), 0.96 (dd,  $J = 11.8, 6.6$  Hz, 6H).  $^{13}\text{C}$  NMR (126 MHz,  $\text{CDCl}_3$ )  $\delta$  141.9, 131.2 (q,  $J = 32.7$  Hz), 126.9, 126.3 (q,  $J = 3.8$  Hz), 123.9 (q,  $J = 272.2$  Hz), 83.0, 58.0, 44.2, 36.6, 23.9, 22.9, 21.9. HRMS (ESI)  $m/z$  calculated for  $\text{C}_{14}\text{H}_{22}\text{F}_3\text{N}_2\text{O}_3\text{S}$   $[\text{M}+\text{NH}_4]^+$  355.1298, found 355.1300.

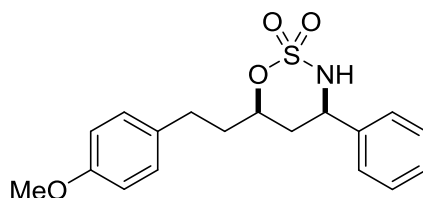


**Compound 3.60b.** The product was purified by column chromatography using a 0→30% gradient of EtOAc in hexanes with 6% increments. The resulting white solid was obtained in 69% yield based on NMR integrations using mesitylene as an internal standard.  $^1\text{H}$  NMR (500 MHz, Chloroform- $d$ )  $\delta$  7.56 (d,  $J = 8.0$  Hz, 2H), 7.31 (d,  $J = 7.9$  Hz, 2H), 4.82 (ddt,  $J = 10.4, 9.1, 3.5$  Hz, 1H), 4.24 (s, 1H), 2.92 (ddd,  $J = 14.4, 9.7, 5.1$  Hz, 1H), 2.81 (ddd,  $J = 13.9, 9.3, 7.2$  Hz, 1H), 2.06 (dtd,  $J = 14.3, 9.2, 5.1$  Hz, 1H), 1.94 – 1.85 (m, 1H), 1.70 – 1.59 (m, 2H), 1.47 (s, 3H), 1.31 (s, 3H).  $^{13}\text{C}$  NMR (126 MHz,  $\text{CDCl}_3$ )  $\delta$  144.7, 128.9, 128.6 (q,  $J=32.4$  Hz), 125.7 (q,  $J=3.52$  Hz), 124.4 (q,  $J=271.81$  Hz), 80.0, 56.0, 41.6, 36.8, 31.9, 30.7, 25.3. HRMS (ESI)  $m/z$  calculated for  $\text{C}_{14}\text{H}_{22}\text{F}_3\text{N}_2\text{O}_3\text{S}$   $[\text{M}+\text{NH}_4]^+$  355.1298, found 355.1308.

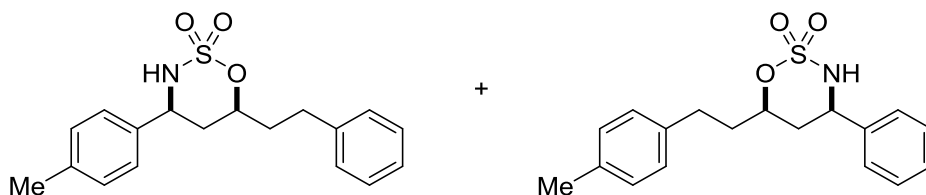


**Compound 3.61a.** The product was purified by column chromatography using 10% EtOAc in hexanes. The resulting colorless oil was obtained in 51% yield based on NMR integrations using mesitylene as an internal standard.  $^1\text{H}$  NMR (500 MHz, Chloroform- $d$ )  $\delta$  7.35 – 7.28 (m, 2H), 7.26 – 7.18 (m, 5H), 6.91 (d,  $J = 8.8$  Hz, 2H), 4.88 – 4.81 (m, 1H), 4.72 (ddd,  $J = 12.0, 9.1, 3.0$

Hz, 1H), 4.08 (d,  $J = 9.1$  Hz, 1H), 3.81 (s, 3H), 2.87 (ddd,  $J = 14.2, 9.2, 5.2$  Hz, 1H), 2.78 (ddd,  $J = 13.9, 8.9, 7.6$  Hz, 1H), 2.14 (dtd,  $J = 14.1, 8.8, 5.0$  Hz, 1H), 2.01 (dt,  $J = 14.4, 2.6$  Hz, 1H), 1.98 – 1.87 (m, 2H).  $^{13}\text{C}$  NMR (126 MHz,  $\text{CDCl}_3$ )  $\delta$  160.1, 140.5, 130.2, 128.8, 128.7, 127.7, 126.5, 114.6, 83.2, 57.8, 55.5, 37.2, 36.4, 30.8, 29.9. HRMS (ESI)  $m/z$  calculated for  $\text{C}_{18}\text{H}_{25}\text{N}_2\text{O}_4\text{S}$   $[\text{M}+\text{NH}_4]^+$  365.1530, found 365.1527.

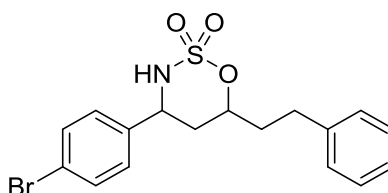


**Compound 3.61b.** The product was purified by column chromatography using 10% EtOAc in hexanes. The resulting colorless oil was obtained in 23% yield based on NMR integrations using mesitylene as an internal standard.  $^1\text{H}$  NMR (500 MHz, Chloroform- $d$ )  $\delta$  7.43 – 7.34 (m, 3H), 7.34 – 7.30 (m, 2H), 7.13 (d,  $J = 8.5$  Hz, 2H), 6.86 (d,  $J = 8.6$  Hz, 2H), 4.85 (tdd,  $J = 9.0, 3.9, 1.9$  Hz, 1H), 4.78 (ddd,  $J = 12.1, 9.2, 2.9$  Hz, 1H), 4.13 (dd,  $J = 8.2, 6.7$  Hz, 1H), 3.80 (s, 3H), 2.81 (ddd,  $J = 14.0, 8.9, 5.2$  Hz, 1H), 2.73 (dt,  $J = 14.0, 8.1$  Hz, 1H), 2.12 (dtd,  $J = 14.0, 8.7, 5.1$  Hz, 1H), 2.06 – 2.01 (m, 1H), 1.98 – 1.88 (m, 2H).  $^{13}\text{C}$  NMR (126 MHz,  $\text{CDCl}_3$ )  $\delta$  158.3, 138.1, 132.4, 129.6, 129.3, 129.1, 126.4, 114.2, 83.2, 58.3, 55.4, 37.4, 36.5, 29.9. HRMS (ESI)  $m/z$  calculated for  $\text{C}_{18}\text{H}_{25}\text{N}_2\text{O}_4\text{S}$   $[\text{M}+\text{NH}_4]^+$  365.1530, found 365.1526.

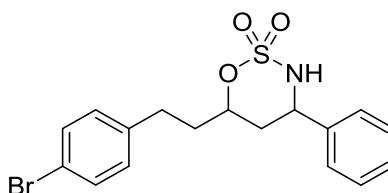


**Compound 3.62a and 3.62b.** The product mixture was inseparable by column chromatography. The yields were based on NMR integrations using mesitylene as an internal standard. Compound **3.62a** formed in 45% yield and **3.62b** formed in 31% yield.  $^1\text{H}$  NMR (500 MHz, Chloroform- $d$ )

$\delta$  7.42 – 7.34 (m, 3H), 7.34 – 7.29 (m, 3H), 7.25 – 7.17 (m, 5H), 7.11 (q,  $J$  = 8.1 Hz, 4H), 4.86 (dddd,  $J$  = 11.3, 8.7, 3.8, 2.3 Hz, 1.8H), 4.75 (dddd,  $J$  = 17.0, 12.2, 9.2, 3.0 Hz, 1.8H), 4.17 (d,  $J$  = 9.3 Hz, 1H), 4.13 (d,  $J$  = 9.3 Hz, 0.8H), 2.91 – 2.70 (m, 4H), 2.35 (s, 2.4H), 2.33 (s, 3H), 2.13 (dtdd,  $J$  = 14.0, 8.7, 6.8, 5.2 Hz, 2H), 2.02 (ddt,  $J$  = 15.4, 10.2, 2.7 Hz, 2H), 1.98 – 1.88 (m, 4H).  $^{13}\text{C}$  NMR (126 MHz,  $\text{CDCl}_3$ )  $\delta$  140.5, 139.0, 138.1, 137.3, 136.0, 135.2, 129.9, 129.5, 129.4, 129.3, 129.1, 128.8, 128.7, 128.6, 126.5, 126.4, 126.3, 83.3, 83.2, 77.2, 58.3, 58.1, 37.3, 37.2, 36.4. HRMS (ESI)  $m/z$  calculated for  $\text{C}_{18}\text{H}_{25}\text{N}_2\text{O}_3\text{S}$   $[\text{M}+\text{NH}_4]^+$  349.1581, found 349.1587.

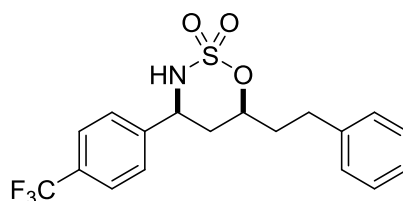


**Compound 3.63a.** The product was purified by column chromatography using 10% EtOAc in hexanes. The resulting colorless oil was obtained in 34% yield based on NMR integrations using mesitylene as an internal standard.  $^1\text{H}$  NMR (500 MHz, Chloroform- $d$ )  $\delta$  7.53 (d,  $J$  = 8.4 Hz, 2H), 7.32 (t,  $J$  = 7.5 Hz, 2H), 7.25 – 7.18 (m, 5H), 4.89 – 4.81 (m, 1H), 4.74 (ddd,  $J$  = 12.1, 9.2, 2.8 Hz, 1H), 4.19 (d,  $J$  = 9.2 Hz, 1H), 2.87 (ddd,  $J$  = 14.0, 9.0, 5.1 Hz, 1H), 2.77 (dt,  $J$  = 13.8, 8.2 Hz, 1H), 2.14 (dtd,  $J$  = 14.1, 8.8, 5.2 Hz, 1H), 2.05 – 2.00 (m, 1H), 2.00 – 1.85 (m, 2H).  $^{13}\text{C}$  NMR (126 MHz,  $\text{CDCl}_3$ )  $\delta$  140.3, 137.1, 132.5, 128.8, 128.7, 128.1, 126.6, 123.1, 83.2, 57.7, 37.1, 36.2, 30.7. HRMS (ESI)  $m/z$  calculated for  $\text{C}_{17}\text{H}_{22}\text{BrN}_2\text{O}_3\text{S}$   $[\text{M}+\text{NH}_4]^+$  413.0530, found 413.0535.

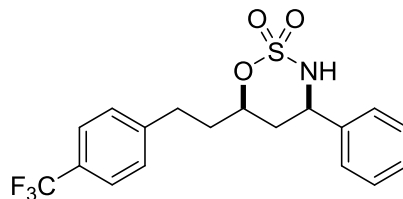




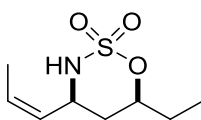
**Compound 3.63b.** The product was purified by column chromatography using 10% EtOAc in hexanes. The resulting colorless oil was obtained in 58% yield based on NMR integrations using mesitylene as an internal standard.  $^1\text{H}$  NMR (500 MHz, Chloroform-*d*)  $\delta$  7.43 (d,  $J$  = 8.3 Hz, 2H), 7.41 – 7.30 (m, 5H), 7.08 (d,  $J$  = 8.3 Hz, 2H), 4.87 – 4.80 (m, 1H), 4.77 (ddd,  $J$  = 12.1, 9.3, 3.1 Hz, 1H), 4.23 (d,  $J$  = 9.3 Hz, 1H), 2.83 (ddd,  $J$  = 14.0, 9.1, 5.0 Hz, 1H), 2.74 (dt,  $J$  = 13.9, 8.2 Hz, 1H), 2.11 (dtd,  $J$  = 14.1, 8.9, 5.0 Hz, 1H), 2.02 (dt,  $J$  = 14.3, 2.5 Hz, 1H), 1.97 – 1.86 (m, 2H).  $^{13}\text{C}$  NMR (126 MHz,  $\text{CDCl}_3$ )  $\delta$  139.3, 138.0, 131.9, 130.4, 129.3, 129.1, 126.4, 120.3, 82.9, 58.3, 36.9, 36.4, 30.2. HRMS (ESI)  $m/z$  calculated for  $\text{C}_{17}\text{H}_{22}\text{BrN}_2\text{O}_3\text{S}$   $[\text{M}+\text{NH}_4]^+$  413.0530, found 413.0528.



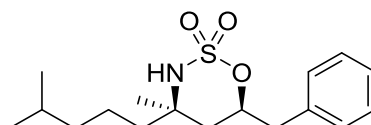
**Compound 3.64a.** The product was purified by column chromatography using 10% EtOAc in hexanes. The resulting colorless oil was obtained in 21% yield based on NMR integrations using mesitylene as an internal standard.  $^1\text{H}$  NMR (500 MHz, Chloroform-*d*)  $\delta$  7.60 (d,  $J$  = 8.1 Hz, 2H), 7.40 (d,  $J$  = 8.1 Hz, 2H), 7.25 (dd,  $J$  = 8.2, 6.8 Hz, 2H), 7.18 – 7.12 (m, 3H), 4.86 – 4.74 (m, 2H), 4.17 (d,  $J$  = 9.2 Hz, 1H), 2.81 (ddd,  $J$  = 14.0, 9.0, 5.1 Hz, 1H), 2.72 (dt,  $J$  = 13.8, 8.2 Hz, 1H), 2.09 (dtd,  $J$  = 14.1, 8.8, 5.2 Hz, 1H), 2.00 (dt,  $J$  = 14.2, 2.5 Hz, 1H), 1.95 – 1.81 (m, 2H).  $^{13}\text{C}$  NMR (126 MHz,  $\text{CDCl}_3$ )  $\delta$  141.8, 140.2, 131.4 (q,  $J$ =32.7 Hz), 128.9, 128.7, 126.9, 126.6, 126.3 (q,  $J$ =3.7 Hz), 123.8 (q,  $J$ =272.1 Hz), 83.2, 57.8, 37.1, 36.3, 30.7. HRMS (ESI)  $m/z$  calculated for  $\text{C}_{18}\text{H}_{22}\text{F}_3\text{N}_2\text{O}_3\text{S}$   $[\text{M}+\text{NH}_4]^+$  403.1298, found 403.1302.



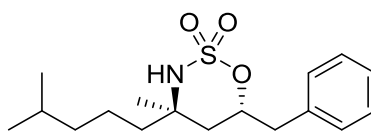
**Compound 3.64b.** The product was purified by column chromatography using 10% EtOAc in hexanes. The resulting colorless oil was obtained in 61% yield based on NMR integrations using mesitylene as an internal standard.  $^1\text{H}$  NMR (500 MHz, Chloroform-*d*)  $\delta$  7.57 (d,  $J$  = 8.0 Hz, 2H), 7.43 – 7.35 (m, 3H), 7.35 – 7.30 (m, 4H), 4.84 (ddt,  $J$  = 11.8, 9.2, 3.0 Hz, 1H), 4.78 (ddd,  $J$  = 12.2, 9.3, 3.1 Hz, 1H), 4.28 (d,  $J$  = 9.3 Hz, 1H), 2.94 (ddd,  $J$  = 14.1, 9.2, 5.0 Hz, 1H), 2.84 (dt,  $J$  = 13.9, 8.3 Hz, 1H), 2.14 (dtd,  $J$  = 14.2, 9.0, 5.0 Hz, 1H), 2.03 (dt,  $J$  = 14.3, 2.8 Hz, 1H), 2.00 – 1.91 (m, 2H).  $^{13}\text{C}$  NMR (126 MHz,  $\text{CDCl}_3$ )  $\delta$  144.5, 137.9, 129.4, 129.1, 129.0, 126.4, 125.7 (q,  $J$ =3.8Hz), 124.4 (q,  $J$ =272 Hz), 82.9, 58.3, 36.8, 36.4, 30.6. HRMS (ESI)  $m/z$  calculated for  $\text{C}_{18}\text{H}_{22}\text{F}_3\text{N}_2\text{O}_3\text{S}$   $[\text{M}+\text{NH}_4]^+$  403.1298, found 403.1298.



**Compound 3.65a.** The product was obtained in 71% yield. Major isomer:  $^1\text{H}$  NMR (500 MHz,  $\text{CDCl}_3$ )  $\delta$  5.74 (dq,  $J$  = 10.8, 7.0, 1.2 Hz, 1H), 5.22 (ddq,  $J$  = 10.4, 8.4, 1.8 Hz, 1H), 4.72 (dddd,  $J$  = 12.2, 7.3, 5.1, 2.1 Hz, 1H), 4.60 – 4.48 (m, 1H), 3.90 (d,  $J$  = 9.7 Hz, 1H), 1.83 – 1.65 (m, 6H), 1.53 (dt,  $J$  = 14.4, 11.9 Hz, 1H), 1.02 (t,  $J$  = 7.5 Hz, 3H).  $^{13}\text{C}$  NMR (126 MHz,  $\text{CDCl}_3$ )  $\delta$  130.6, 127.0, 85.4, 51.8, 35.5, 28.4, 13.6, 9.0. HRMS (ESI)  $m/z$  calculated for  $\text{C}_8\text{H}_{19}\text{N}_2\text{O}_3\text{S}$   $[\text{M}+\text{NH}_4]^+$  223.1111, found 223.1114.



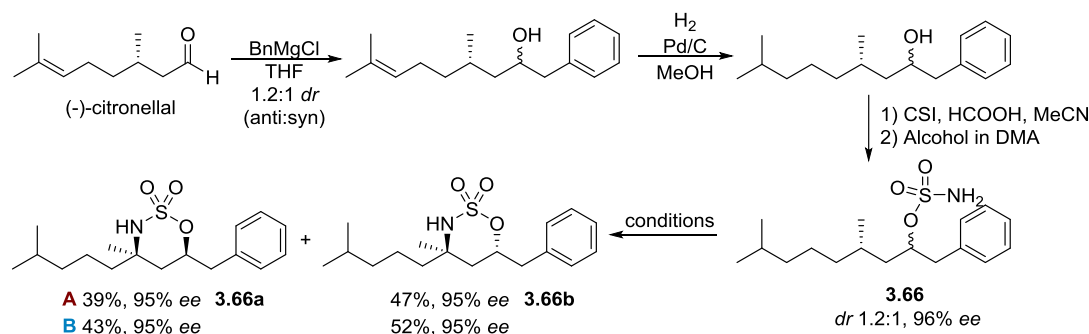
**Compound 3.66a.** The product was purified by column chromatography using a 0→25% gradient of EtOAc in hexanes with 5% increments. The resulting white solid was the minor diastereomer obtained in 38% yield and 95% *ee* from the corresponding sulfamate.  $^1\text{H}$  NMR (500 MHz, Chloroform-*d*)  $\delta$  7.32 (dd,  $J$  = 8.0, 6.5 Hz, 2H), 7.30 – 7.23 (m, 1H), 7.23 – 7.19 (m, 2H), 5.06 (dtd,  $J$  = 9.9, 6.4, 3.1 Hz, 1H), 3.95 (s, 1H), 3.12 (dd,  $J$  = 14.1, 6.3 Hz, 1H), 2.90 (dd,  $J$  = 14.1, 6.5 Hz, 1H), 1.61 – 1.48 (m, 3H), 1.45 – 1.40 (m, 5H), 1.40 – 1.23 (m, 2H), 1.15 (q,  $J$  = 7.0 Hz, 2H), 0.87 (d,  $J$  = 6.6 Hz, 6H).  $^{13}\text{C}$  NMR (126 MHz,  $\text{CDCl}_3$ )  $\delta$  135.3, 129.6, 128.9, 127.3, 80.9, 58.5, 45.3, 41.7, 39.9, 39.1, 27.9, 22.7, 22.7, 22.6, 20.4. HRMS (ESI)  $m/z$  calculated for  $\text{C}_{17}\text{H}_{31}\text{N}_2\text{O}_3\text{S}$   $[\text{M}+\text{NH}_4]^+$  343.2050, found 343.2049.



**Compound 3.66b.** The product was purified by column chromatography using a 0→25% gradient of EtOAc in hexanes with 5% increments. The resulting white solid was the major diastereomer, obtained in 47% yield and 95% *ee* from the corresponding sulfamate.  $^1\text{H}$  NMR (500 MHz, Chloroform-*d*)  $\delta$  7.32 (dd,  $J$  = 8.1, 6.6 Hz, 2H), 7.26 (t,  $J$  = 3.6 Hz, 1H), 7.23 – 7.19 (m, 2H), 5.04 (dtd,  $J$  = 12.0, 6.5, 1.9 Hz, 1H), 3.93 (s, 1H), 3.13 (dd,  $J$  = 14.0, 6.2 Hz, 1H), 2.88 (dd,  $J$  = 14.0, 6.8 Hz, 1H), 2.05 (ddd,  $J$  = 13.7, 11.2, 4.0 Hz, 1H), 1.67 (dd,  $J$  = 14.4, 1.9 Hz, 1H), 1.59 – 1.40 (m, 3H), 1.38 – 1.30 (m, 1H), 1.22 – 1.07 (m, 6H), 0.84 (dd,  $J$  = 6.5, 1.3 Hz, 6H).  $^{13}\text{C}$  NMR (126 MHz,  $\text{CDCl}_3$ )  $\delta$  135.3, 129.6, 128.9, 127.3, 80.7, 58.5, 41.7, 40.6, 39.1, 36.6, 28.9, 27.9, 22.7, 22.7, 21.5. HRMS (ESI)  $m/z$  calculated for  $\text{C}_{17}\text{H}_{31}\text{N}_2\text{O}_3\text{S}$   $[\text{M}+\text{NH}_4]^+$  343.2050, found 343.2047.

### 3.3.4 Stereochemical Probe

The stereochemical probe containing a defined 3° C–H bond was synthesized from (-)-citronellal as shown below. The same synthesis was completed starting from racemic citronellol after oxidation to the aldehyde. The Grignard addition resulted in a 1.2:1 mixture of diastereomers that was confirmed by both  $^1\text{H}$  NMR and HPLC analysis, and the two diastereomers could be separated via column chromatography.

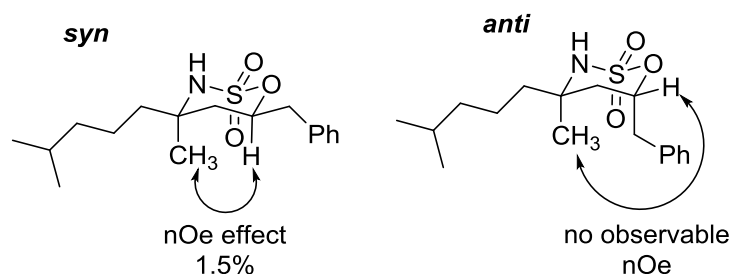


Condition A: 10 mol%  $\text{AgOTf}$ , 30 mol%  $^t\text{Bubipy}$ , 3.5 equiv  $\text{PhIO}$ , 0.5 M  $\text{CH}_2\text{Cl}_2$ , 4 Å MS, rt, 30 min.

Condition B: 10 mol%  $\text{AgOTf}$ , 12.5 mol%  $\text{tpa}$ , 3.5 equiv  $\text{PhIO}$ , 0.5 M  $\text{CH}_2\text{Cl}_2$ , 4 Å MS, rt, 30 min.

NMR yields, average of two runs, mesitylene internal standard. ee's determined by HPLC

The relative configurations of the products were confirmed based on nOe  $^1\text{H}$  NMR experiments (500 MHz,  $\text{CDCl}_3$ ) and matched previously published nOe data for a similar citronellol-derived substrate.<sup>10</sup>



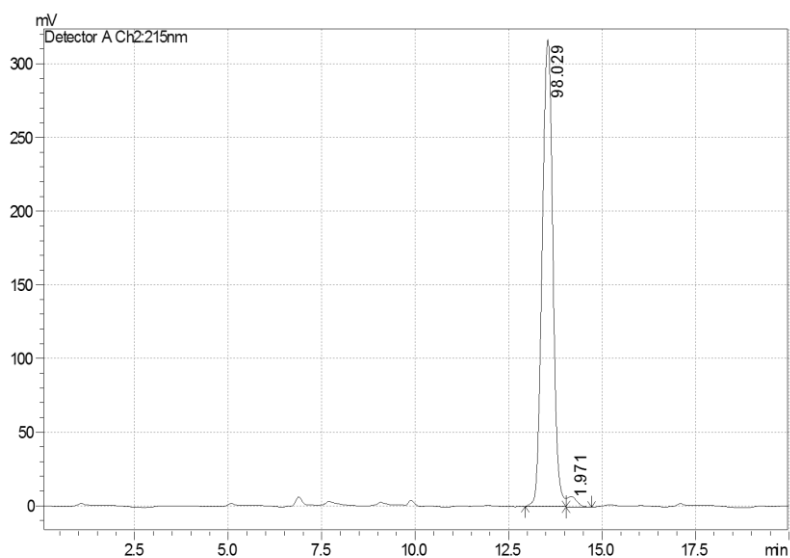
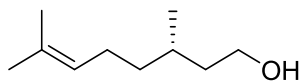
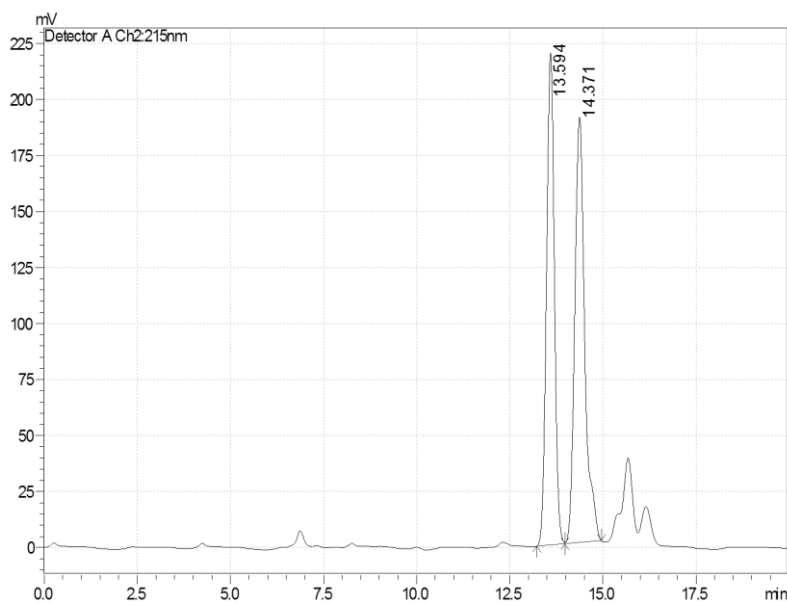
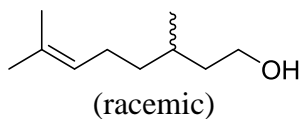
Quantitative determination of stereoretention was accomplished via achiral HPLC analysis.

Racemic citronellol was used to determine the initial enantioselectivity of (-)-citronellal after it had been reduced to the alcohol and was measured to be 96% ee. The racemic version of

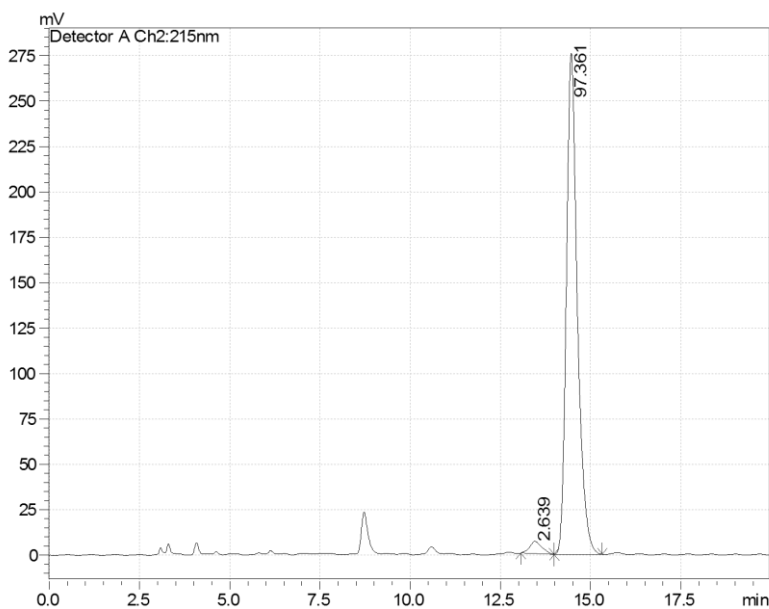
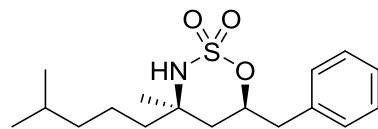
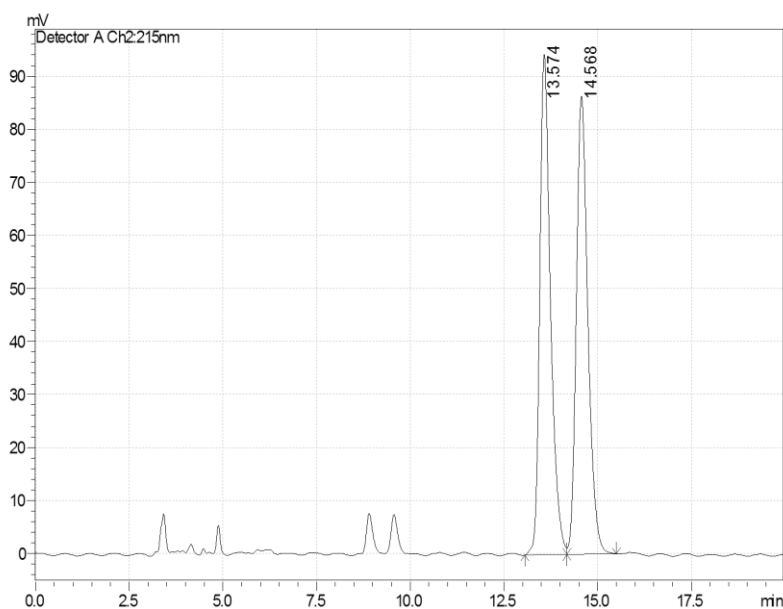
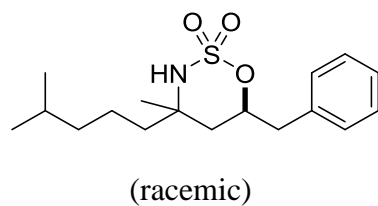
substrate **3.66** was subjected to the standard reaction conditions with <sup>t</sup>Bubipy or tpa and the diastereomers at the ether position were first separated via column chromatography. Each diastereomer and its enantiomer were resolved via achiral HPLC analysis and used as a baseline separation for the enantioenriched products.

After the enantioenriched substrate was subjected to the standard reaction conditions, the diastereomers of the product (**3.66a** and **3.66b**) were separated via column chromatography and then run on the HPLC to determine if any enantiomer was present in either of the two HPLC traces. If the stereochemistry at the 3° position was destroyed, the enantiomer would be present in the other diastereomer's HPLC trace. The reactions were performed twice and an average enantioselectivity was reported for each transformation. Sample HPLC traces can be seen below. The small differences in enantioselectivity between substrate **3.66** and the products **3.66a** and **3.66b** are within experimental error and suggest there are no long-lived radical intermediates.

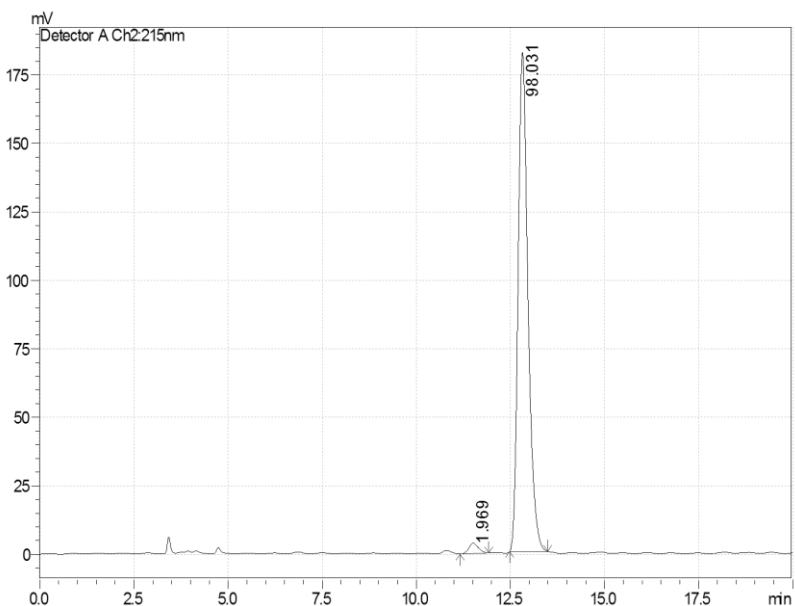
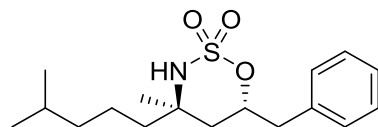
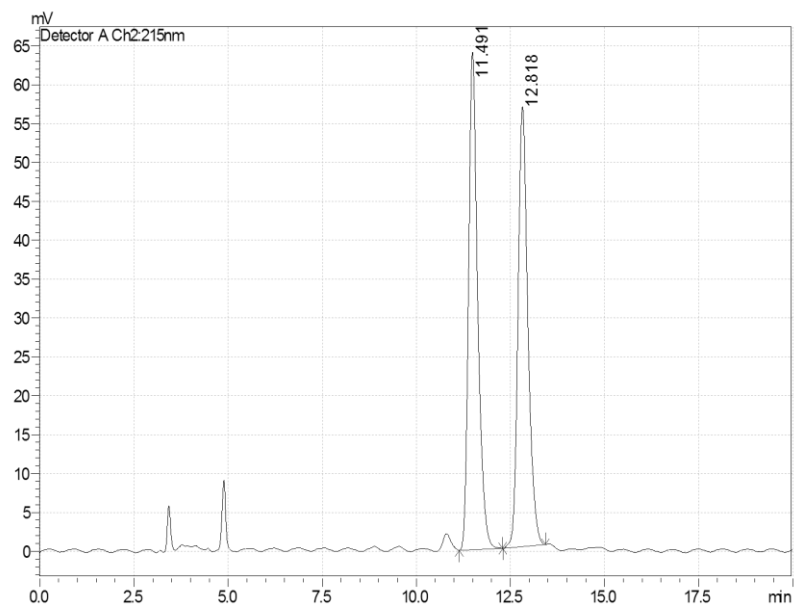
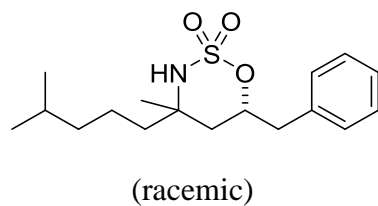
## HPLC Traces

**Citronellol:**

**Conditions:** Chromatograms were acquired on a Shimadzu Prominence HPLC equipped with a Chiracel OJ-H column. Flow rate: 0.5 mL/min.; Oven temp: 25.0 °C; Solvent: isocratic 1.0% *i*PrOH in hexanes; Detector: UV @ 215 nm

**Compound 36a:**

**Conditions:** Chromatograms were acquired on a Shimadzu Prominence HPLC equipped with a Chiracel AD-H column. Flow rate: 1.0 mL/min.; Oven temp: 40.0 °C; Solvent: isocratic 3% *i*PrOH in hexanes; Detector: UV @ 215 nm

**Compound 36b:**

**Conditions:** Chromatograms were acquired on a Shimadzu Prominence HPLC equipped with a Chiracel AD-H column. Flow rate: 1.0 mL/min.; Oven temp: 40.0 °C; Solvent: isocratic 3% *i*PrOH in hexanes; Detector: UV @ 215 nm



### 3.4 Bibliography

1. (a) Lawrence, S. A. *Amines: Synthesis, Properties and Applications*: Cambridge University Press: New York, NY, 2004. (b) Nugent, T. C.; El-Shazly, M. *Adv. Synth. Catal.* **2010**, 352, 753. (c) Smith, M. B. *Compendium of Organic Synthetic Methods*: Wiley: New York, NY, 2009; Vol. 12. (d) Emerson, W. S. The Preparation of Amines by Reductive Alkylation. In *Organic Reactions*; Wiley: New York, NY, 2004. (e) Afagh, N. A.; Yudin, A. K. *Angew. Chem. Int. Ed.* **2010**, 49, 262.
2. For selected reviews on C–H functionalization strategies, see: (a) Godula, K.; Sames, D. *Science* **2006**, 312, 67. (b) Neufeldt, S. R.; Sanford, M. S. *Acc. Chem. Res.* **2012**, 45, 936. (c) Bruckl, T.; Baxter, R. D.; Ishihara, Y.; Baran, P. S. *Acc. Chem. Res.* **2012**, 45, 826.
3. For selected references on selective C–H functionalizations, see: (a) Roizen, J. L.; Harvey, M. E.; Du Bois, J. *Acc. Chem. Res.* **2012**, 45, 911. (b) Lescot, C.; Darses, B.; Collet, F.; Retailleau, P.; Dauban, P. *J. Org. Chem.* **2012**, 77, 7232. (c) Newhouse, T.; Baran, P. S. *Angew. Chem., Int. Ed.* **2011**, 50, 3362. (d) Collet, F.; Lescot, C.; Liang, C.; Dauban, P. *Dalton Trans.* **2010**, 39, 10401. (e) Bess, E. N.; DeLuca, R. J.; Tindall, D. J.; Oderinde, M. S.; Roizen, J. L.; Du Bois, J.; Sigman, M. S. *J. Am. Chem. Soc.* **2014**, 136, 5783. (f) Chen, M. S.; White, M. C. *Science* **2007**, 318, 783. (g) Chen, M. S.; White, M. C. *Science* **2010**, 327, 566. (h) White, M. C. *Science* **2012**, 335, 807. (i) Bagchi, V.; Paraskevopoulou, P.; Das, P.; Chi, L.; Wang, Q.; Choudhury, A.; Mathieson, J. S.; Cronin, L.; Pardue, D. B.; Cundari, T. R.; Mitrikas, G.; Sanakis, Y.; Stavropoulos, P. *J. Am. Chem. Soc.* **2014**, 136, 11362.

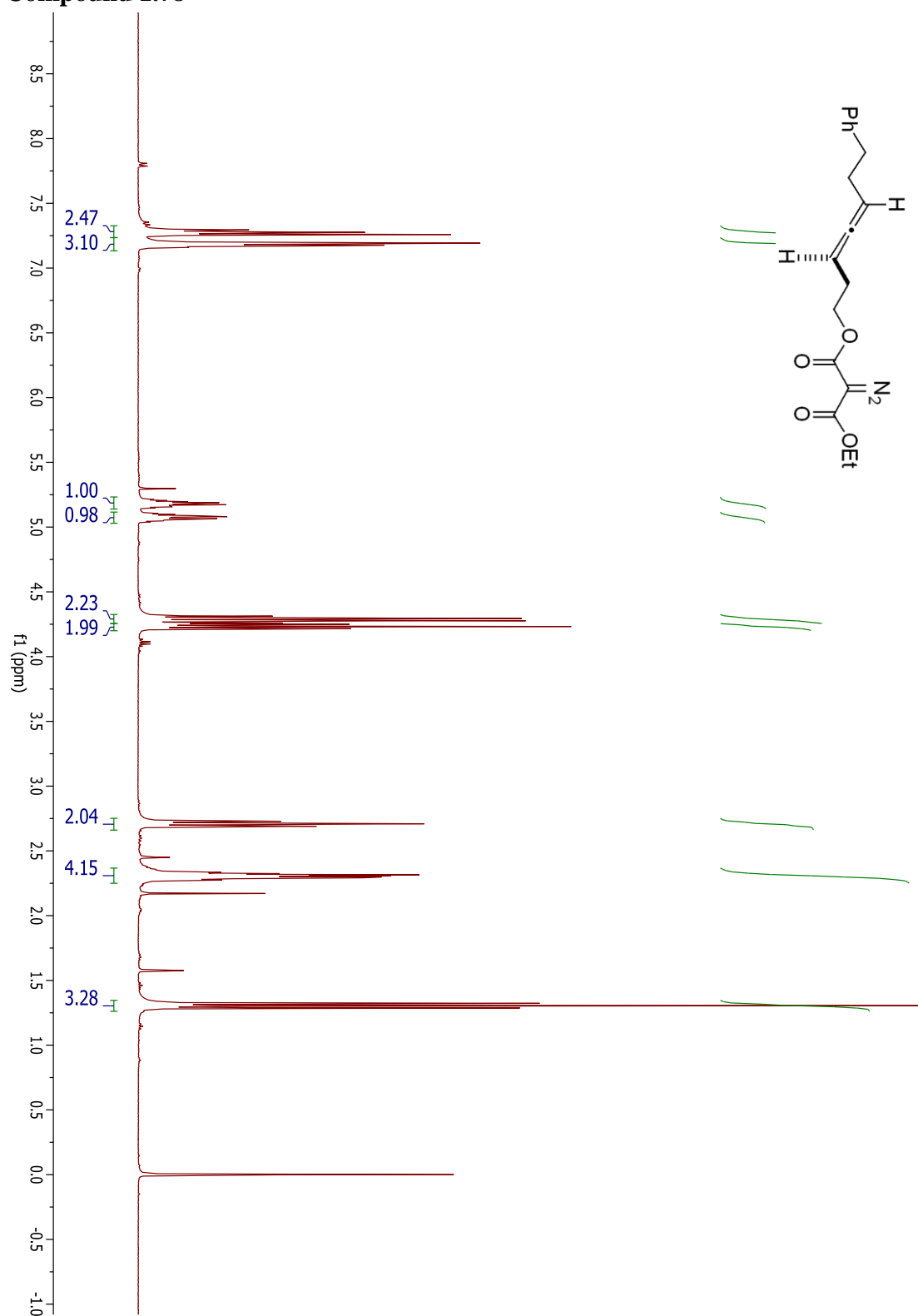
4. For selected examples of directing groups used in conjunction with Ir catalysts, see: (a) Kim, H. J.; Ajitha, M. J.; Ryu, J.; Kim, J.; Lee, Y.; Jung, Y.; Chang, S. *J. Am. Chem. Soc.* **2014**, *136*, 1132. (b) Kang, T.; Kim, Y.; Lee, D.; Wang, Z.; Chang, S. *J. Am. Chem. Soc.* **2014**, *136*, 4141. (c) Simmons, E. M.; Hartwig, J. F. *Nature* **2012**, *483*, 71. For examples involving Pd, see: (d) Shao, J.; Chen, W.; Giulianotti, M. A.; Houghten, R. A.; Yu, Y. *Org. Lett.* **2012**, *14*, 5452. (e) Musaev, D. G.; Kaledin, A.; Shi, B.; Yu, J. *J. Am. Chem. Soc.* **2012**, *134*, 1690. (f) Desai, L. V.; Stowers, K. J.; Sanford, M. S. *J. Am. Chem. Soc.* **2008**, *130*, 13285. For examples involving Ru, see: (g) Allu, S.; Swamy, K. C. K. *J. Org. Chem.* **2014**, *79*, 3963.
5. (a) Espino, C. G.; Wehn, P. M.; Chow, J.; Du Bois, J. *J. Am. Chem. Soc.* **2001**, *123*, 6935. (b) Collet, F.; Dodd, R. H.; Dauban, P. *Chem. Commun.* **2009**, 5061. (c) Norder, A.; Warren, S. A.; Herdtweck, E.; Huber, S. M.; Bach, T. *J. Am. Chem. Soc.* **2012**, *134*, 13524.
6. (a) Nguyen, Q.; Sun, K.; Driver, T. G. *J. Am. Chem. Soc.* **2012**, *134*, 7262. (b) Tang, C.; Yuan, Y.; Cui, Y.; Jiao, N. *Eur. J. Org. Chem.* **2013**, 7480. (c) Beltran, A.; Lescot, C.; Díaz-Requejo, M.; Perez, P. J.; Dauban, P. *Tetrahedron* **2013**, *69*, 4488. (d) Ryu, J.; Shin, K.; Park, S. H.; Kim, Y.; Chang, S. *Angew. Chem., Int. Ed.* **2012**, *51*, 9904. (e) Lebel, H.; Trudel, C.; Spitz, C. *Chem. Commun.* **2012**, 48, 7799. (f) Hayes, C. J.; Beavis, P. W.; Humphries, L. A. *Chem. Commun.* **2006**, 4501. (g) Kornecki, K. P.; Berry, J. F. *Eur. J. Inorg. Chem.* **2012**, *3*, 562.
7. Fiori, K. W.; Espino, C. G.; Brodsky, B. H.; Du Bois, J. *Tetrahedron* **2009**, *65*, 3042.
8. Harvey, M. E.; Musaev, D. G.; Du Bois, J. *J. Am. Chem. Soc.* **2011**, *133*, 17207.
9. Collet, F.; Lescot, C.; Dauban, P. *Chem. Soc. Rev.* **2011**, *40*, 1926.
10. Paradine, S. M.; White, M. C. *J. Am. Chem. Soc.* **2012**, *134*, 2036.

11. Liu, Y.; Guan, X.; Wong, E. L.; Liu, P.; Huang, J.; Che, C. *J. Am. Chem. Soc.* **2013**, *135*, 7194.
12. Rigoli, J. W.; Weatherly, C. D.; Alderson, J. M.; Vo, B. T.; Schomaker, J. M. *J. Am. Chem. Soc.* **2013**, *135*, 17238.
13. For selected examples of aminations mediated by silver catalysis, see: (a) Cui, Y.; He, C. *J. Am. Chem. Soc.* **2003**, *125*, 16202. (b) Cui, Y.; He, C. *Angew. Chem., Int. Ed.* **2004**, *43*, 4210. (c) Li, Z.; Capretto, D. A.; Rahaman, R. H.; He, C. *Angew. Chem., Int. Ed.* **2007**, *46*, 5184. (d) *Silver in Organic Chemistry*; Harmata, M., Ed.; John Wiley & Sons: Hoboken, NJ, 2010. (e) Llaveria, J.; Beltran, A.; Diaz-Requejo, M. M.; Matheu, M. I.; Castillon, S.; Perez, P. J. *Angew. Chem., Int. Ed.* **2010**, *49*, 7092. (f) Frutos, M. R.; Trofimenko, S.; Diaz-Requejo, M. M.; Perez, P. J. *J. Am. Chem. Soc.* **2006**, *128*, 11784. (g) Braga, A. A. C.; Maseras, F.; Urbano, J.; Caballero, A.; Diaz-Requejo, M. M.; Perez, P. J. *Organometallics* **2006**, *25*, 5292. (h) Maestre, L.; Sameera, W. M. C.; Diaz-Requejo, M. M.; Maseras, F.; Perez, P. J. *J. Am. Chem. Soc.* **2013**, *135*, 1338. (i) Arenas, I.; Fuentes, M. Á.; Álvarez, E.; Díaz, Y.; Caballero, A.; Castillon, S.; Pérez, P. J. *Inorg. Chem.* **2014**, *53*, 3991. (j) Gomez-Emeterio, B. P.; Urbano, J.; Díaz-Requejo, M. M.; Perez, P. J. *Organometallics* **2008**, *27*, 4126.
14. For selected examples illustrating the various coordination geometries that can be adopted by silver complexes, see: (a) Hung-Low, F.; Renz, A.; Klausmeyer, K. K. *Polyhedron* **2009**, *28*, 407. (b) HungLow, F.; Renz, A.; Klausmeyer, K. K. *J. Chem. Cryst.* **2011**, *41*, 1174. (c) Du, J.-L.; Hu, T.-L.; Zhang, S.-M.; Zeng, Y.-F.; Bu, X.-H. *CrystEngComm* **2008**, *10*, 1866. (d) Hung-Low, F.; Renz, A.; Klausmeyer, K. K. *J. Chem. Cryst.* **2009**, *39*, 438. (e) Levason, W.; Spicer, M. D. *Coord. Chem. Rev.* **1987**, *76*, 45.

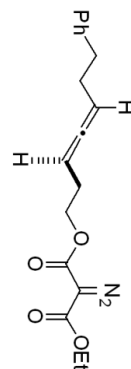
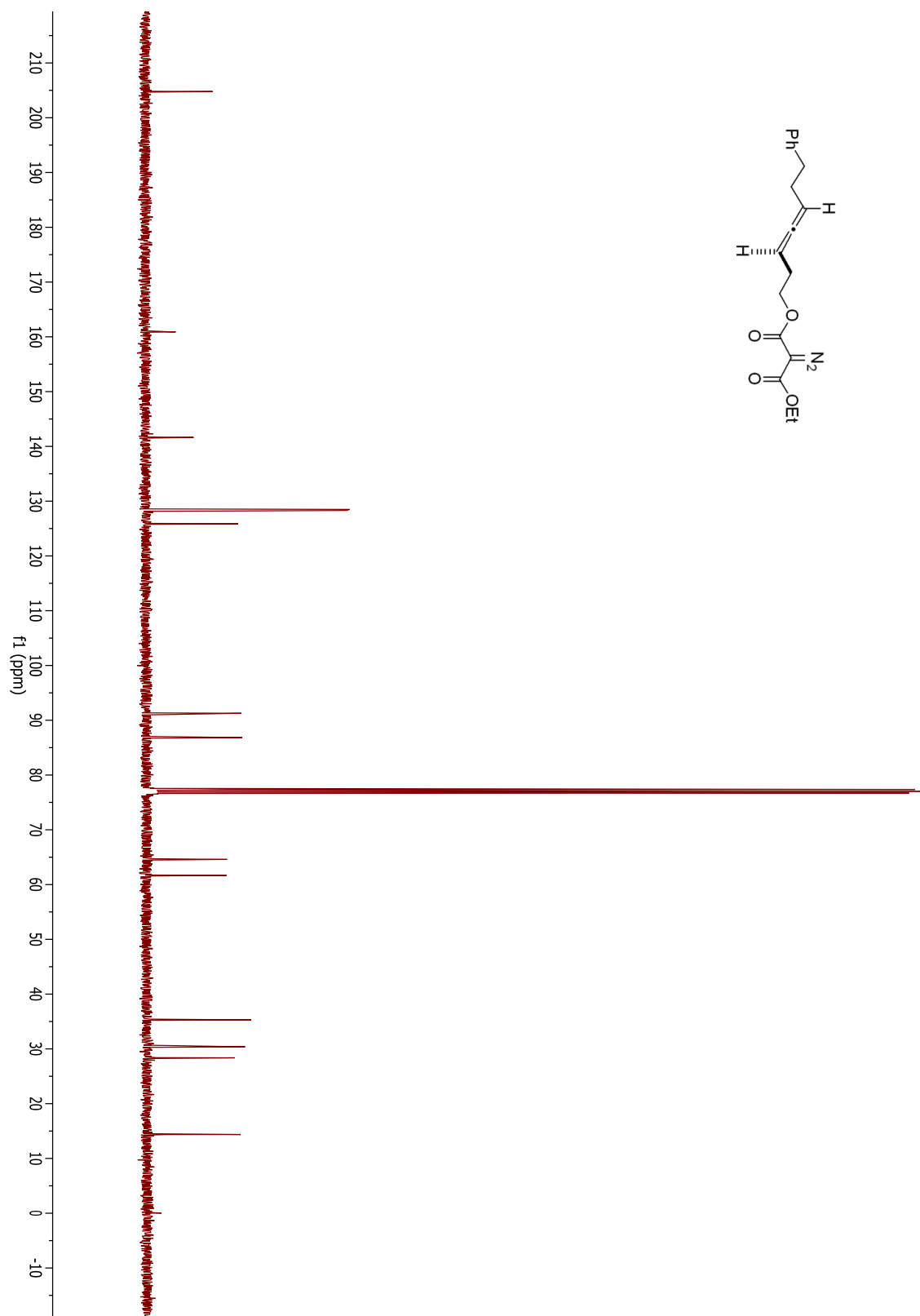
15. (a) Yao, Y.-R. *Handbook of Bond Dissociation Energies in Organic Compounds*; CRC Press: Boca Raton, FL, 2003. (b) *CRC Handbook of Chemistry and Physics*, 85th ed.; Lide, D. R., Ed.; CRC Press: Boca Raton, FL, 2004.

## **Appendix I. Selected $^1\text{H}$ and $^{13}\text{C}$ NMR Spectra**

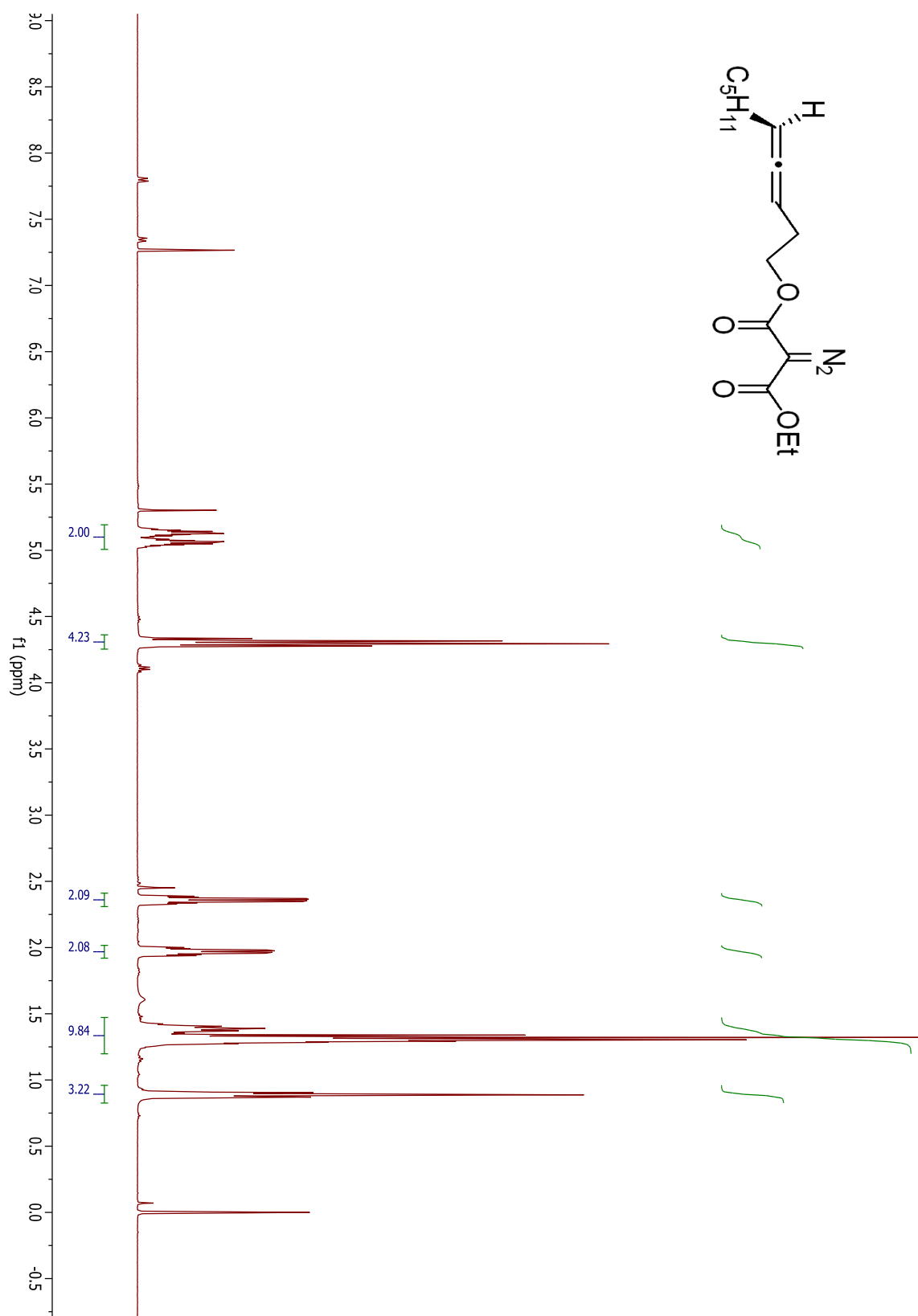
## Compound 1.78



## Compound 1.78

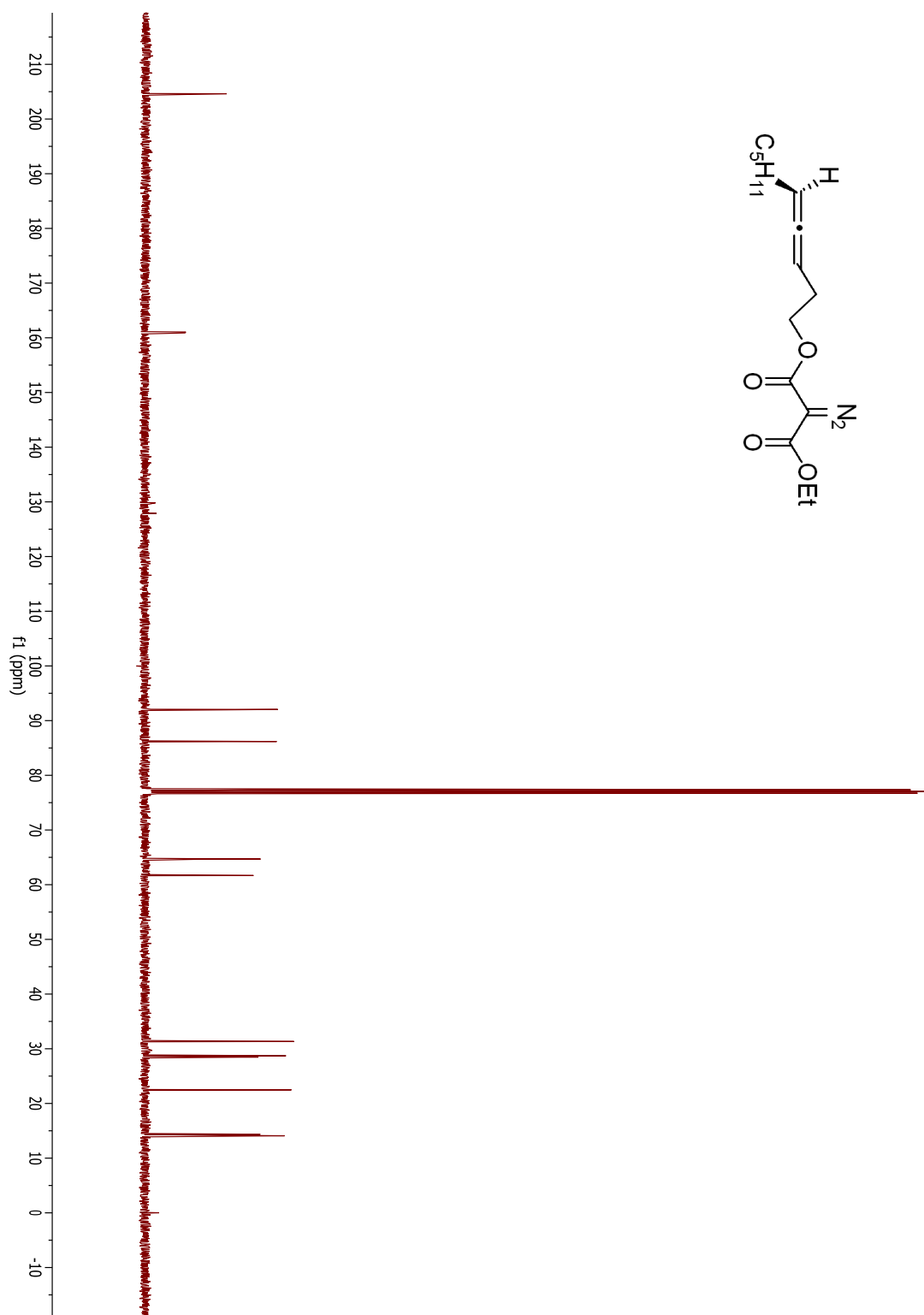


## Compound 1.80

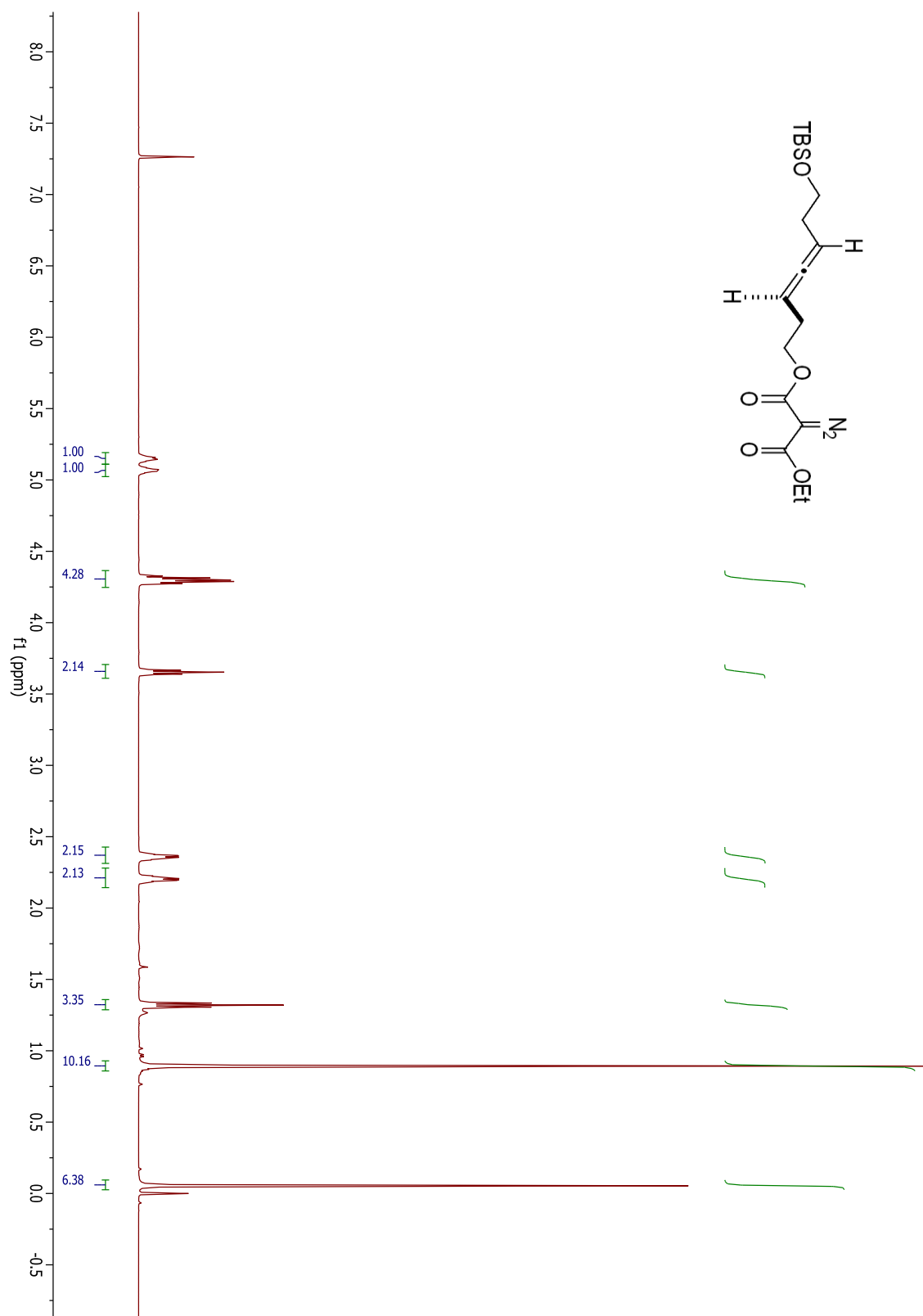




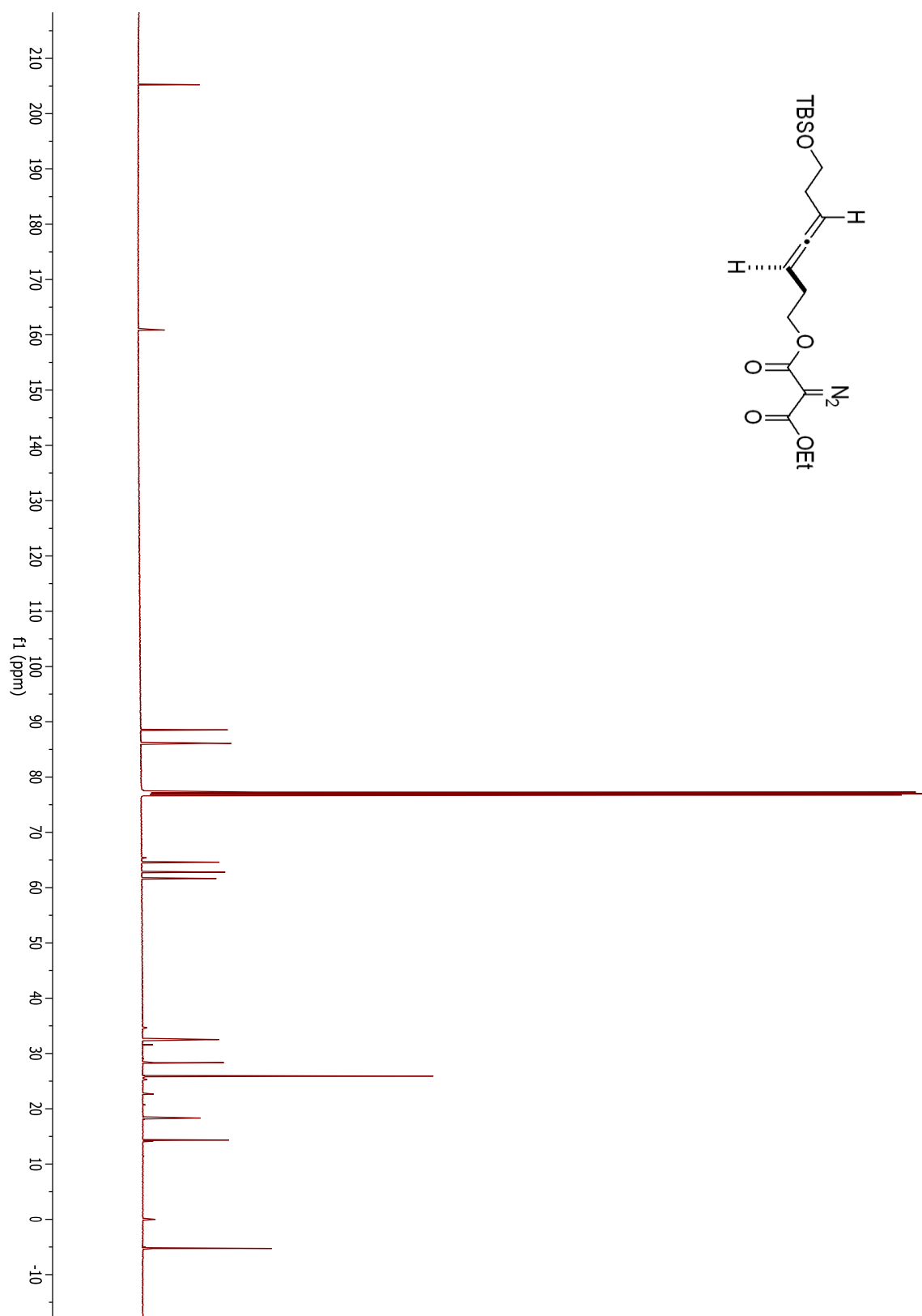
## Compound 1.80



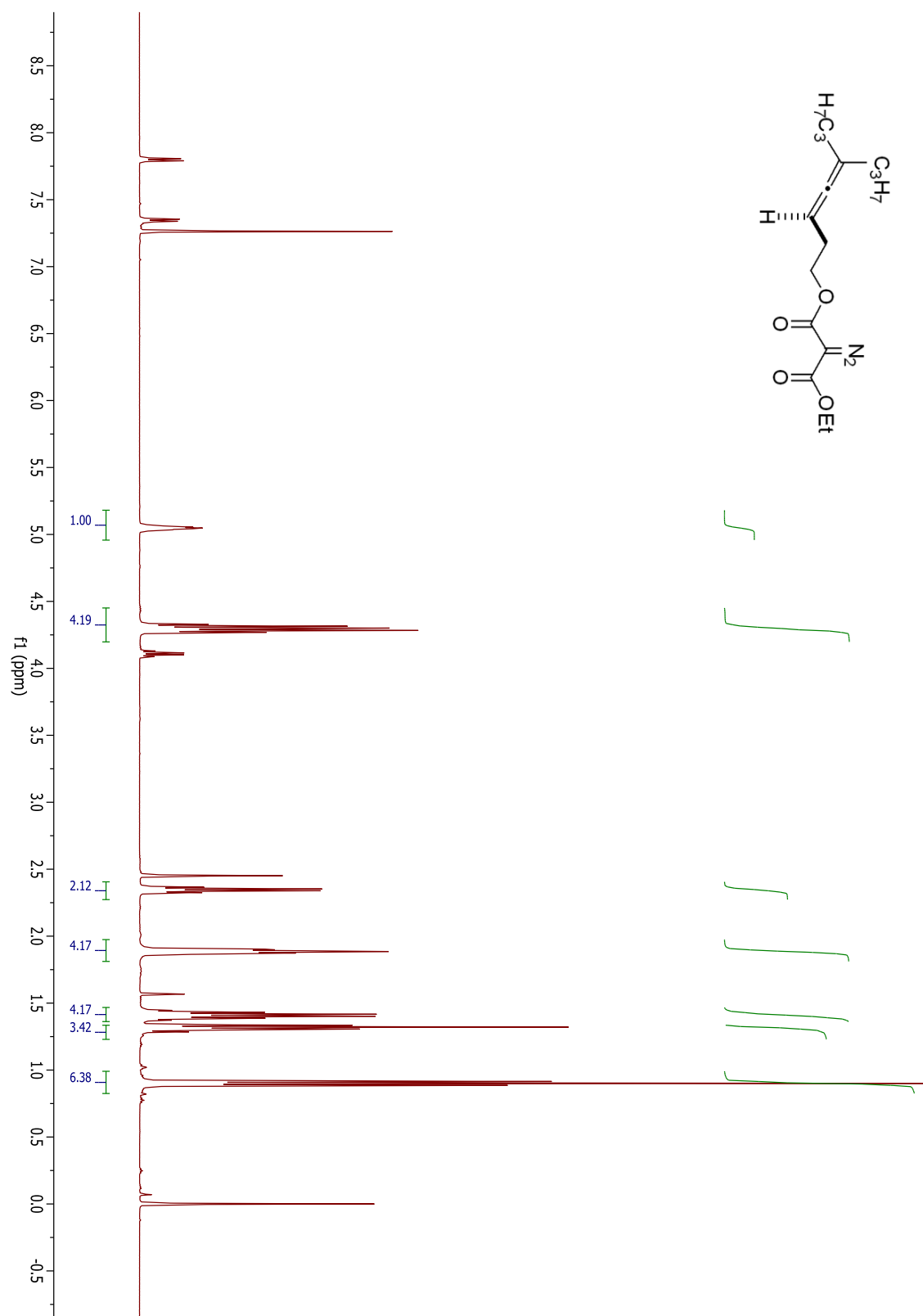
## Compound 1.82



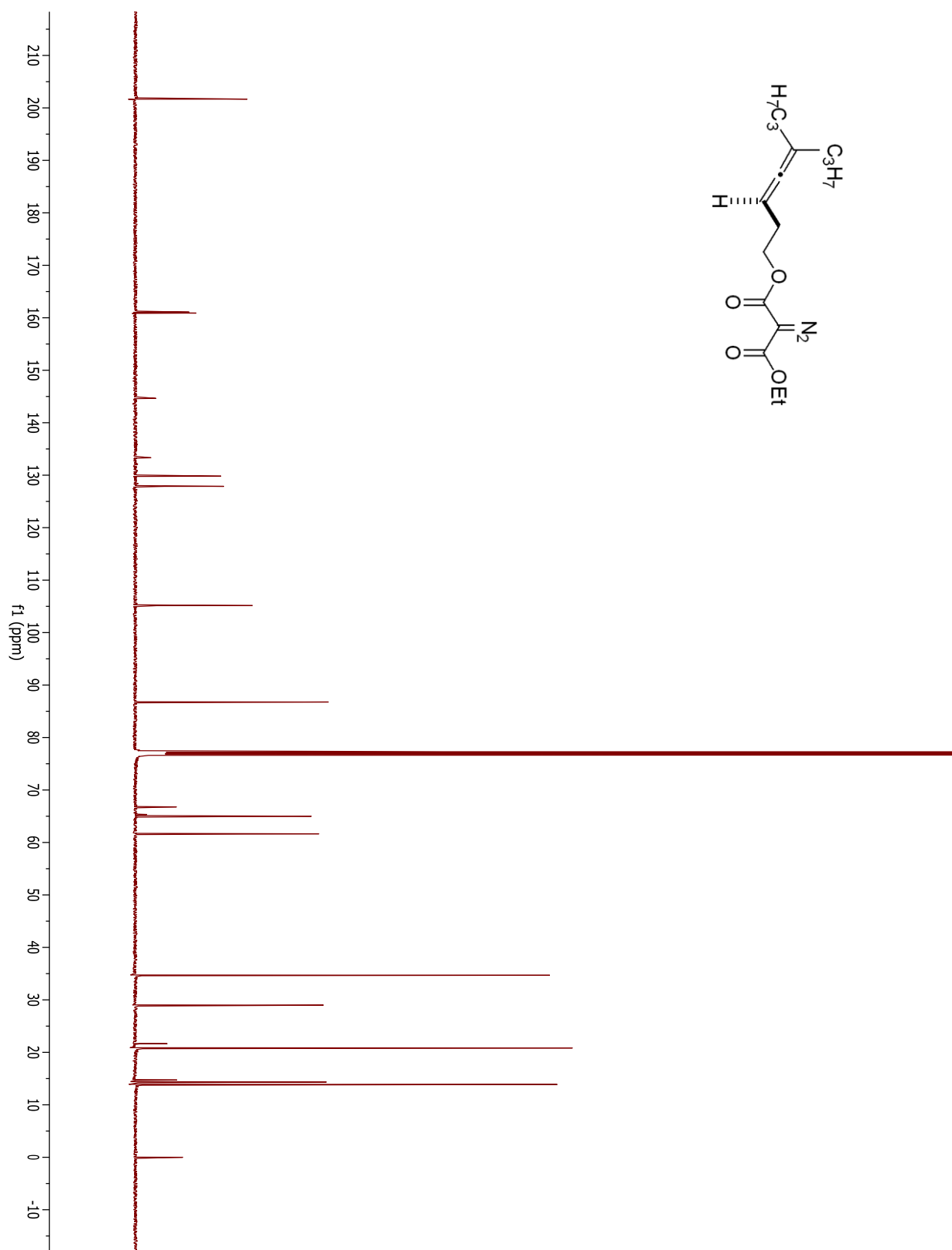
## Compound 1.82



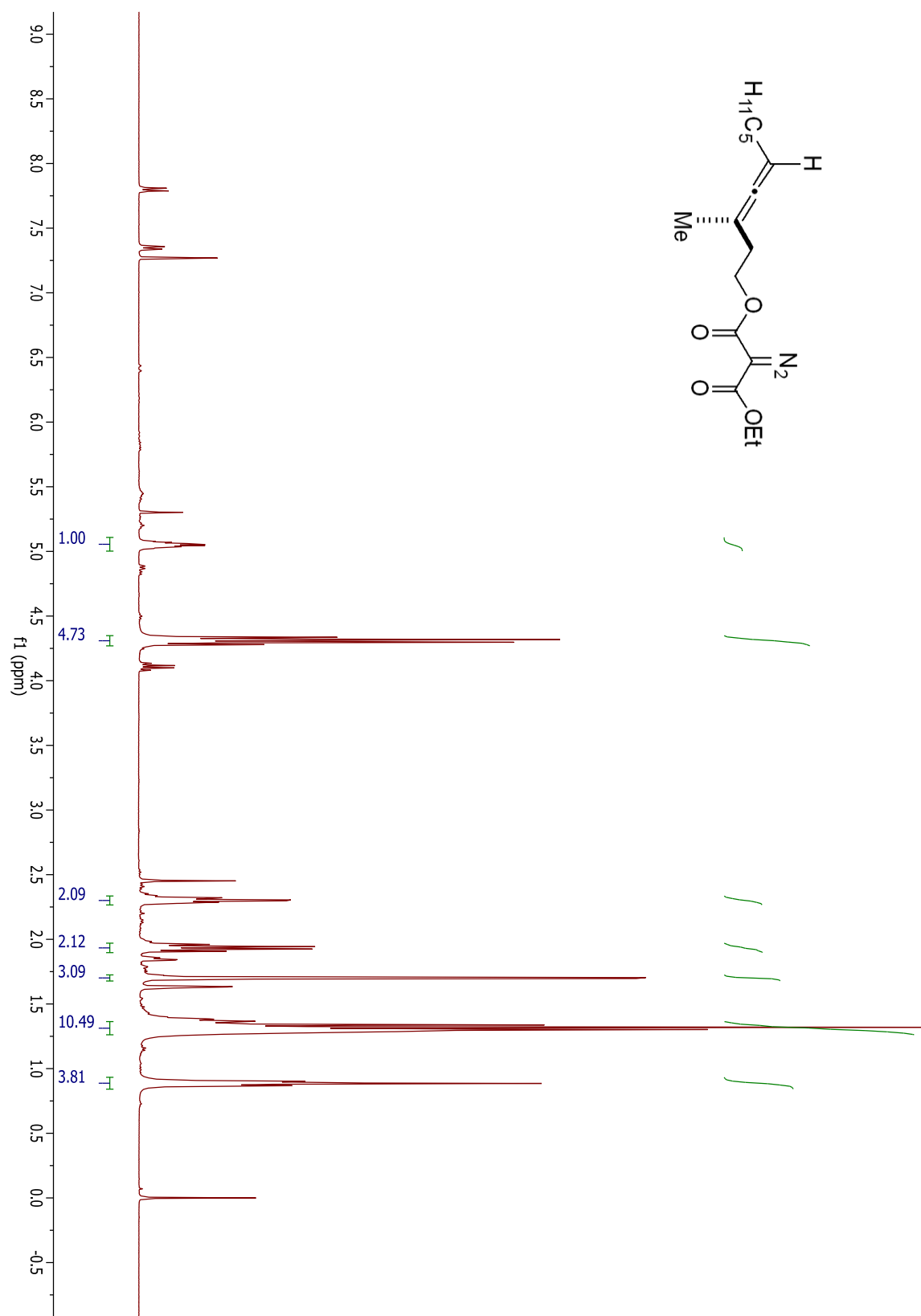
## Compound 1.84



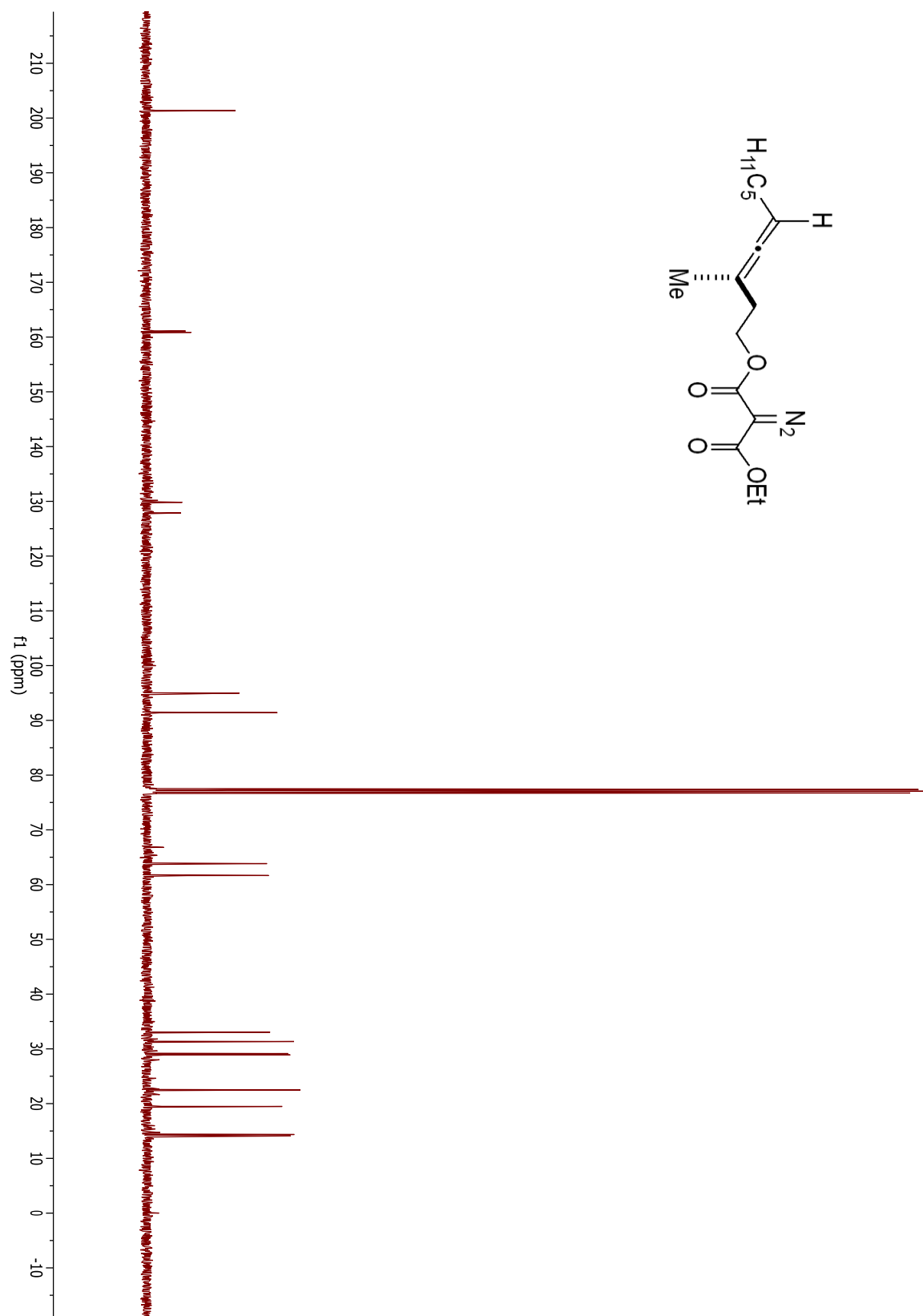
## Compound 1.84

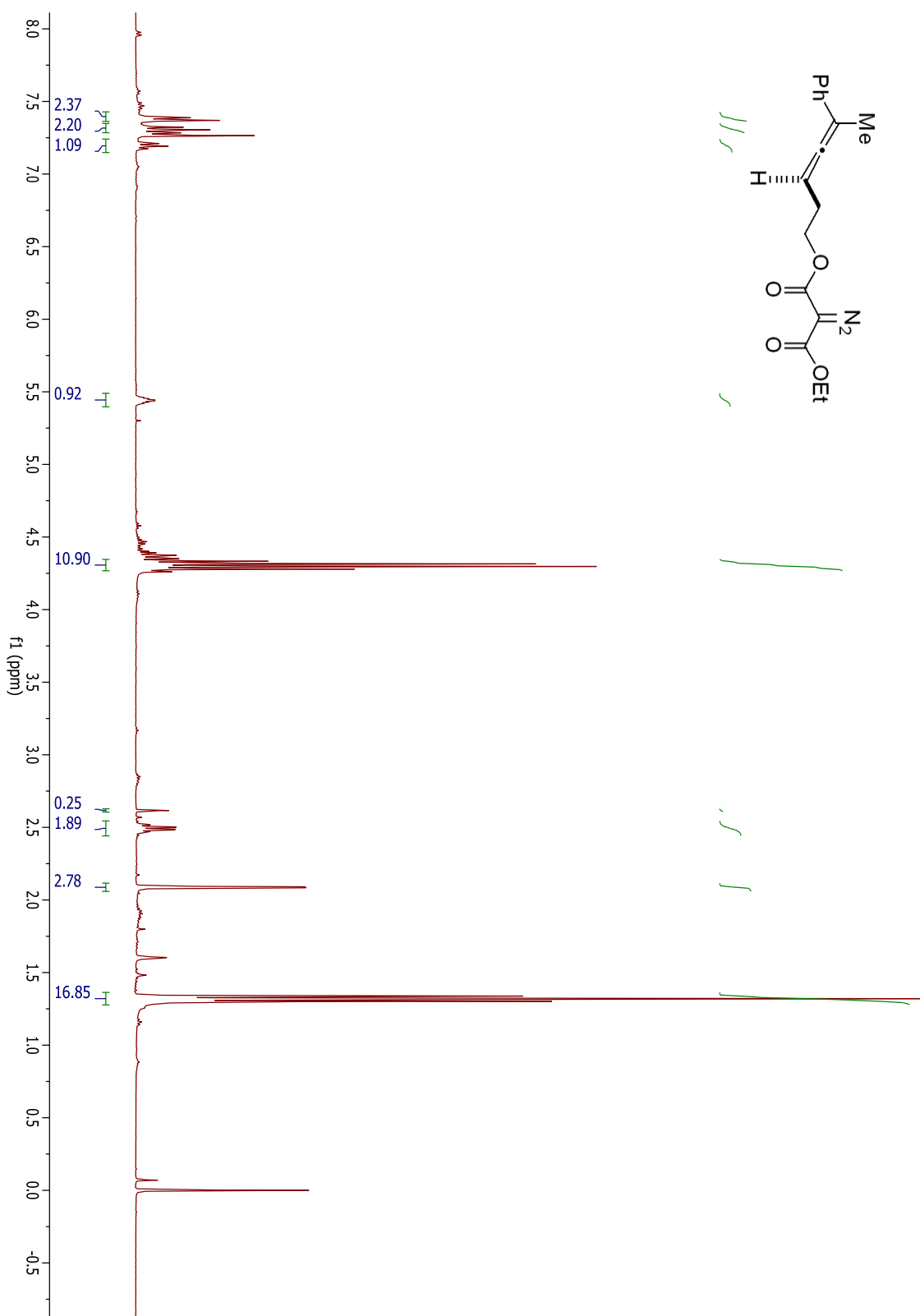


## Compound 1.86



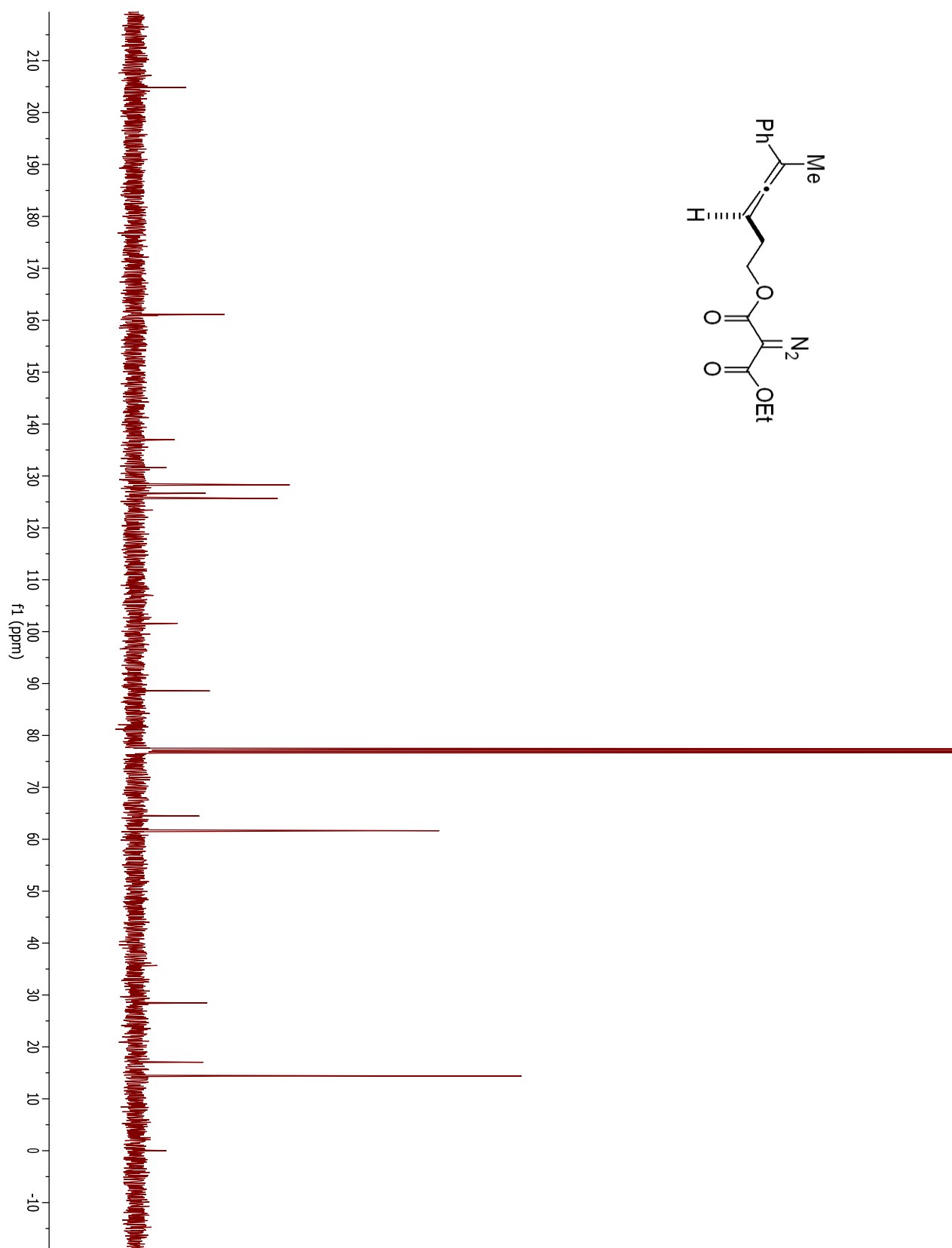
## Compound 1.86



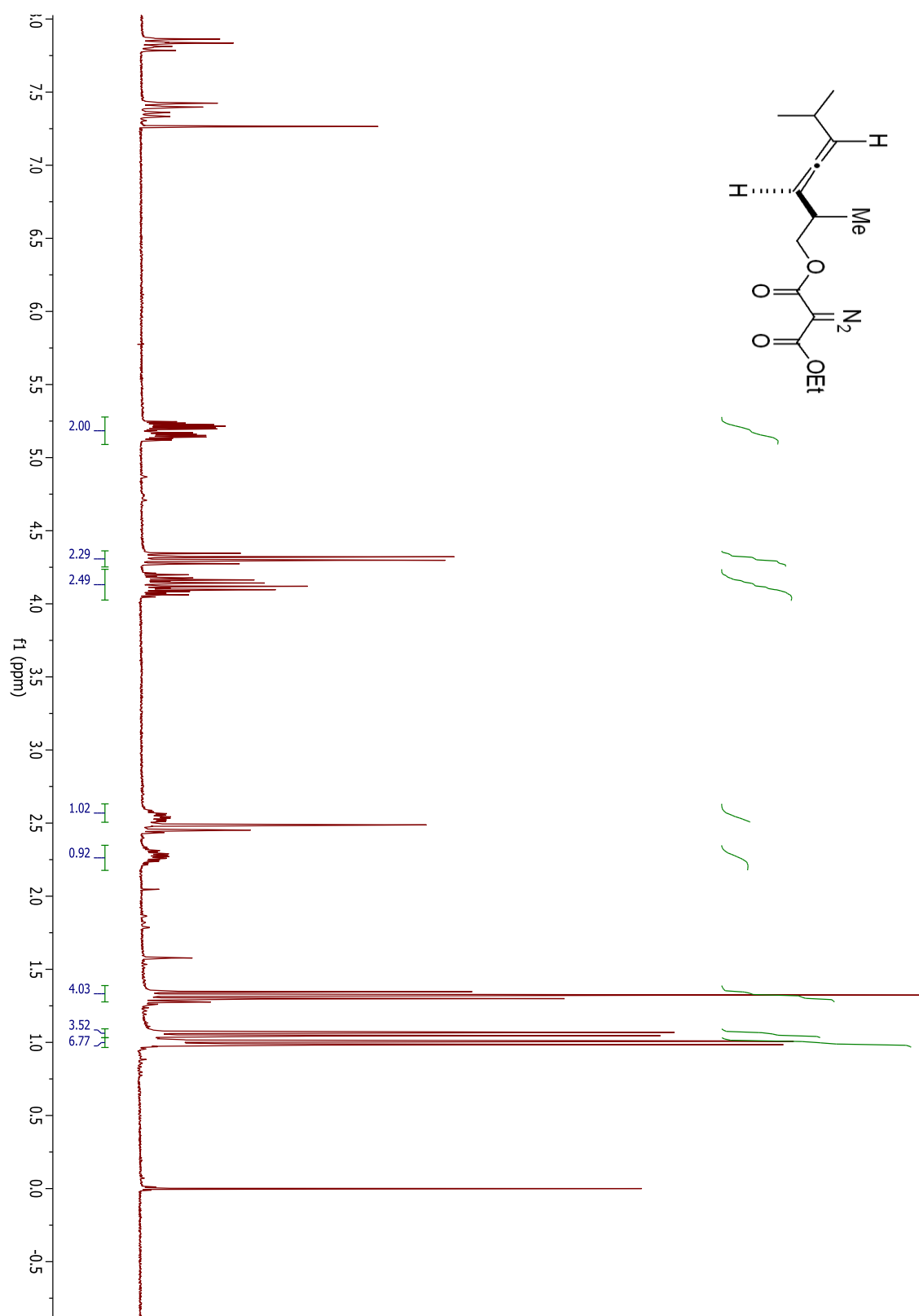




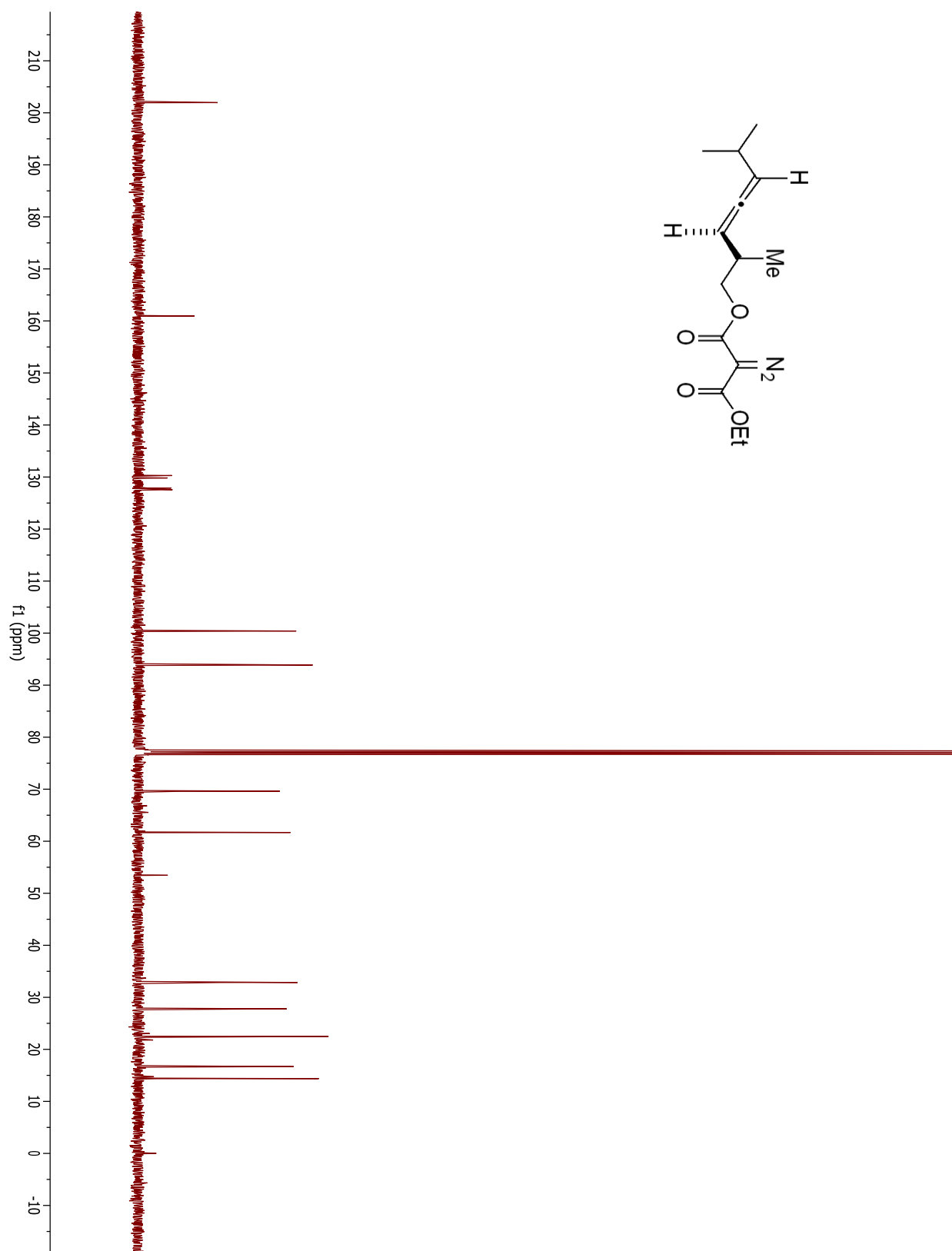
## Compound 1.88



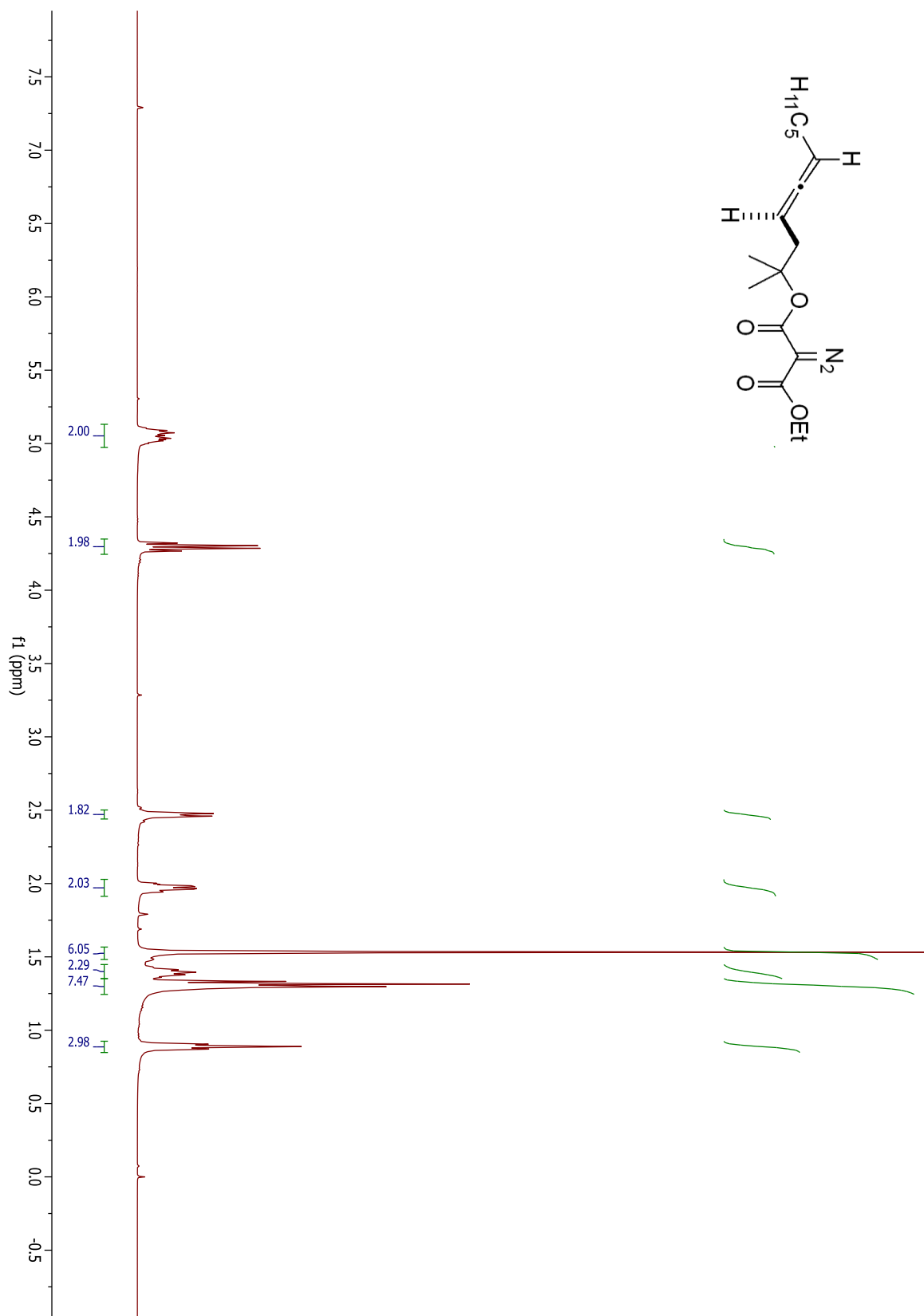
## Compound 1.90



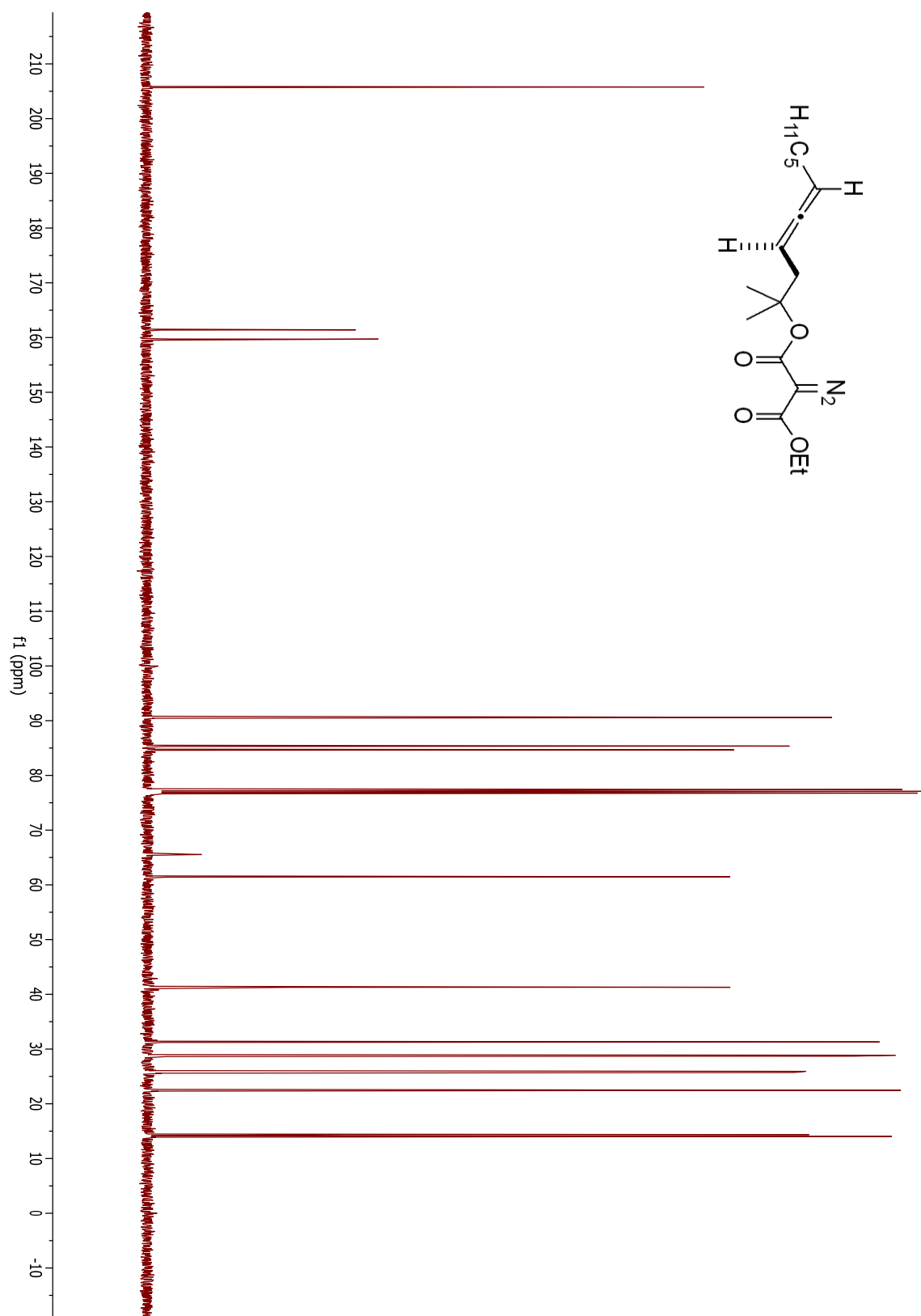
## Compound 1.90



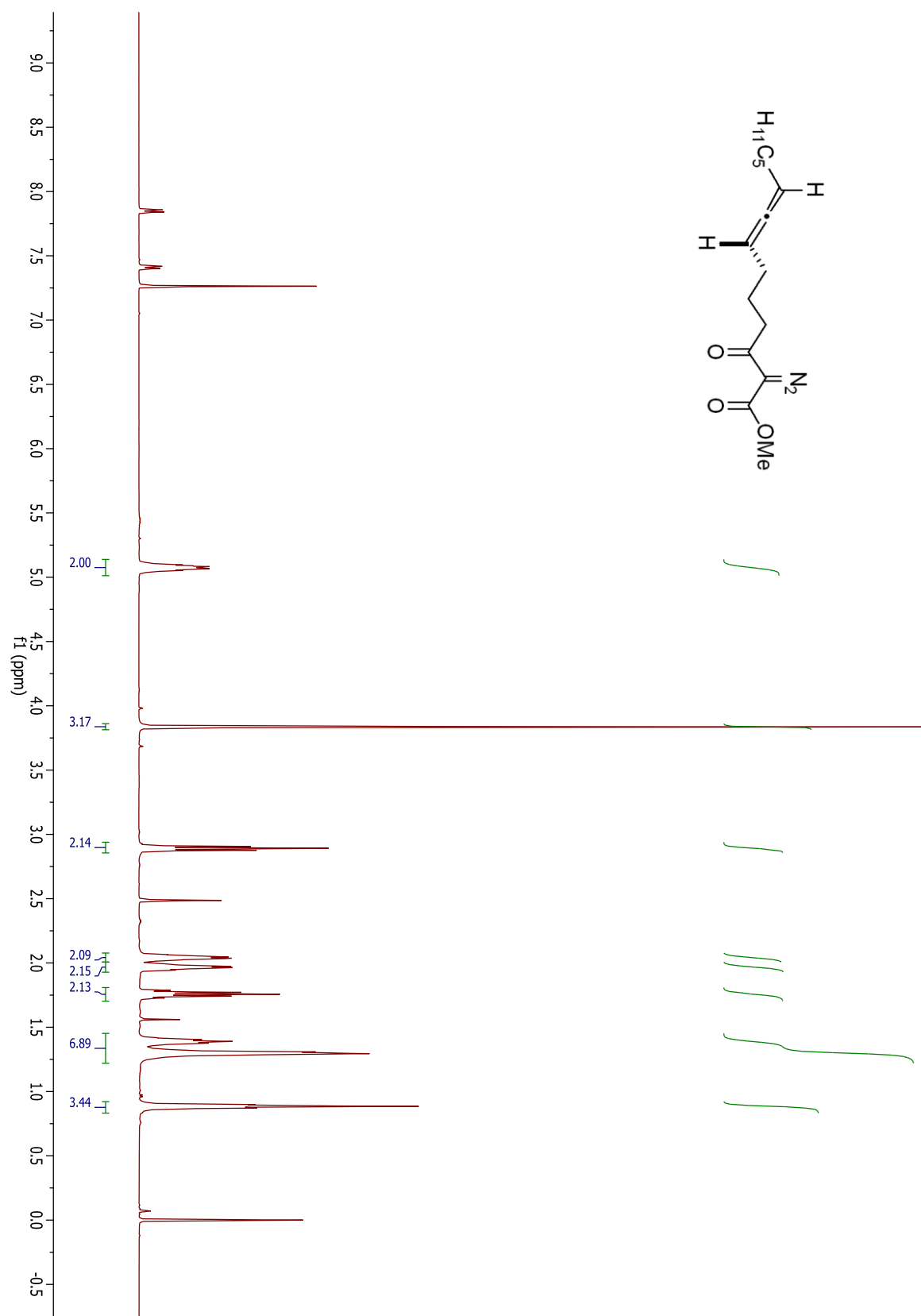
## Compound 1.92



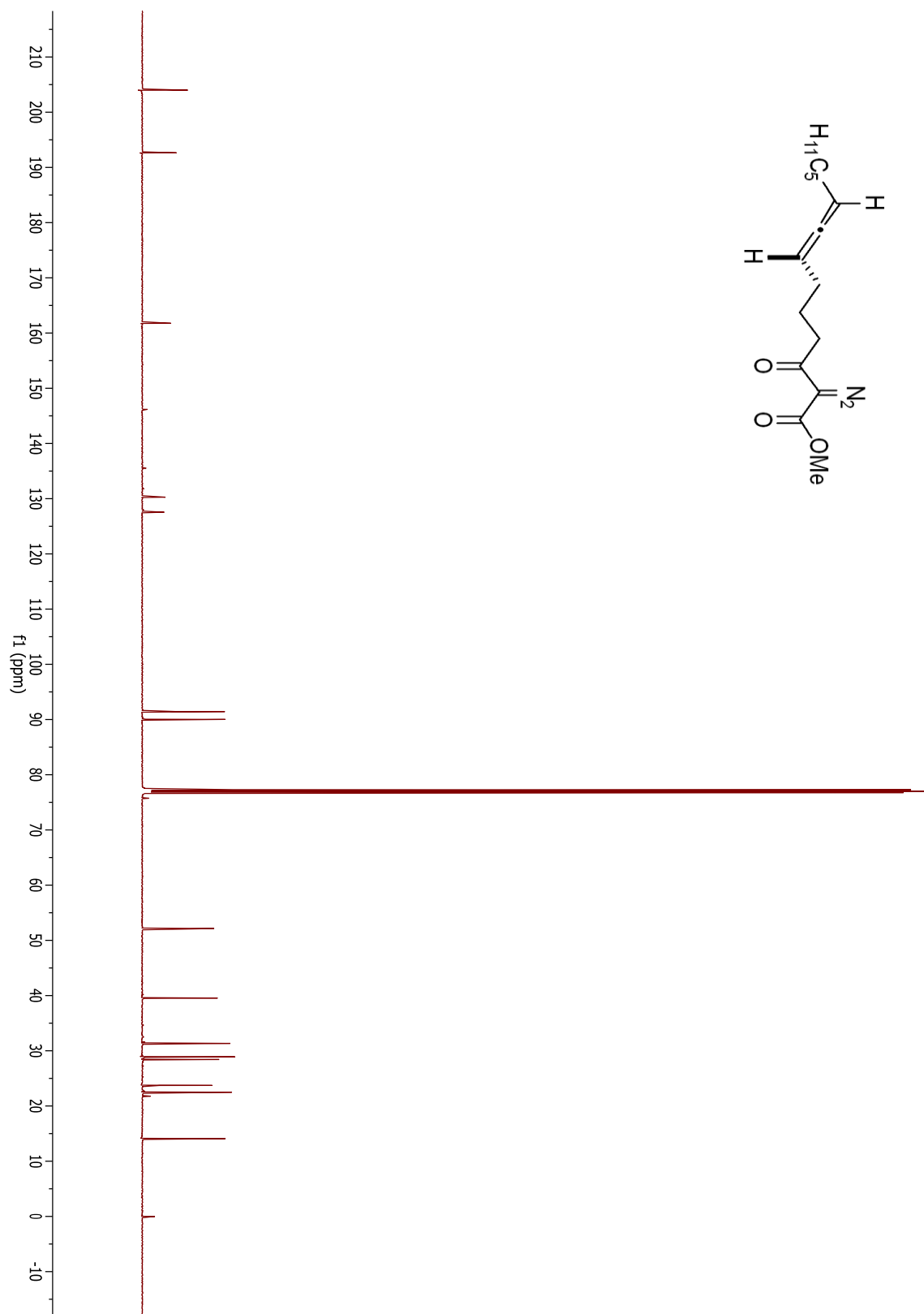
## Compound 1.92



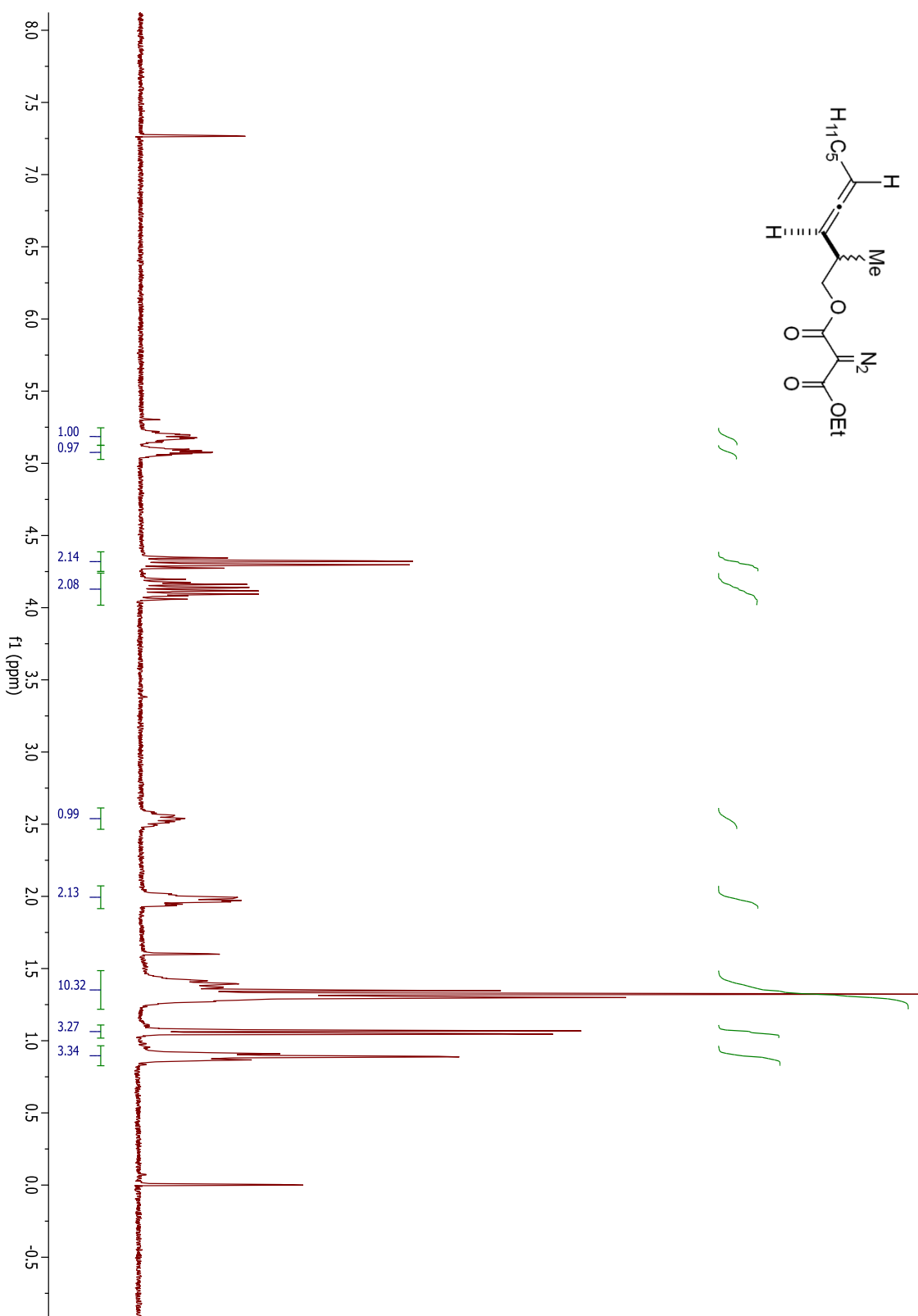
## Compound 1.94



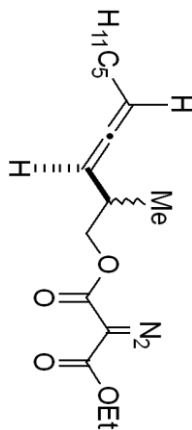
## Compound 1.94



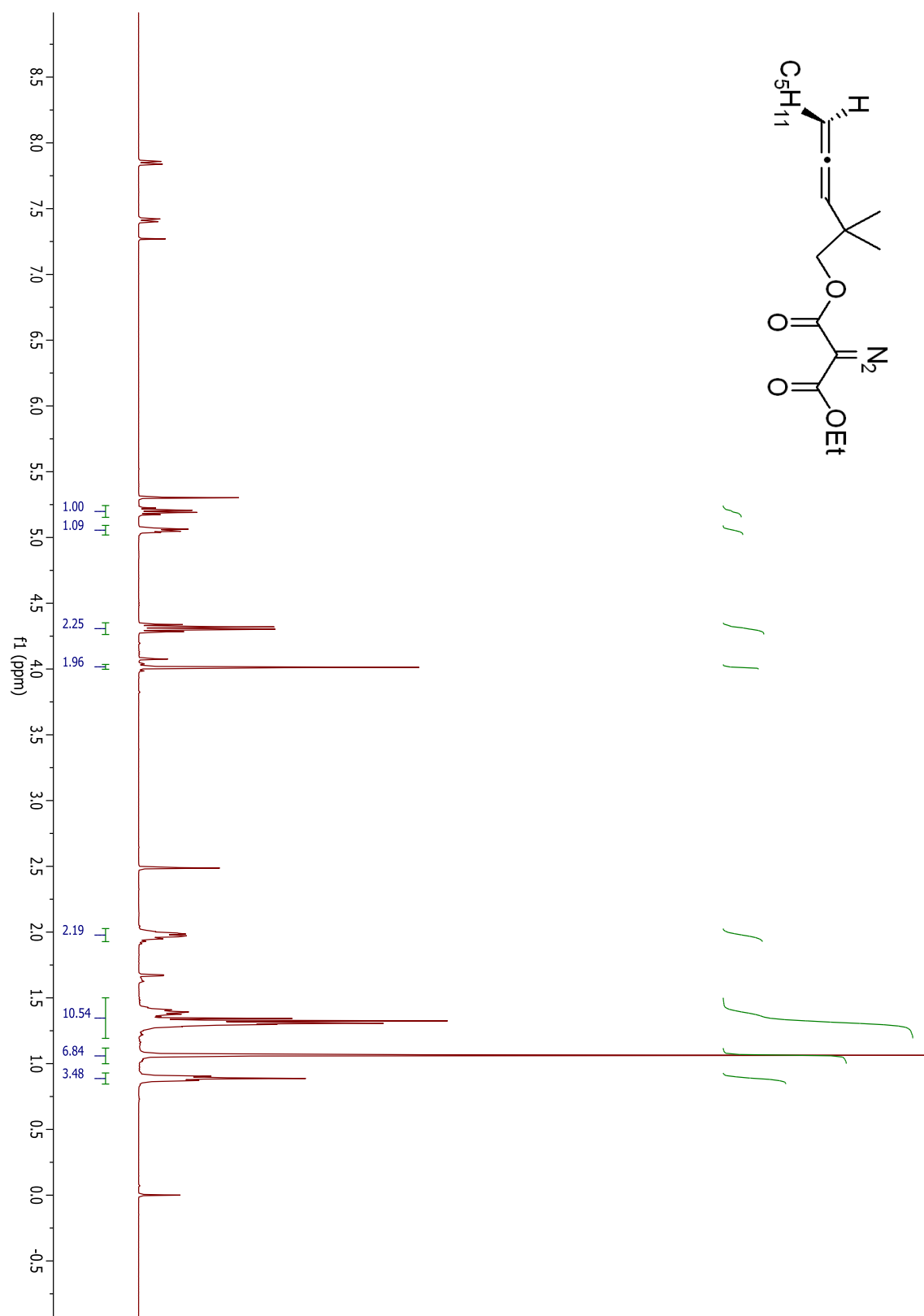
## Compound 1.100

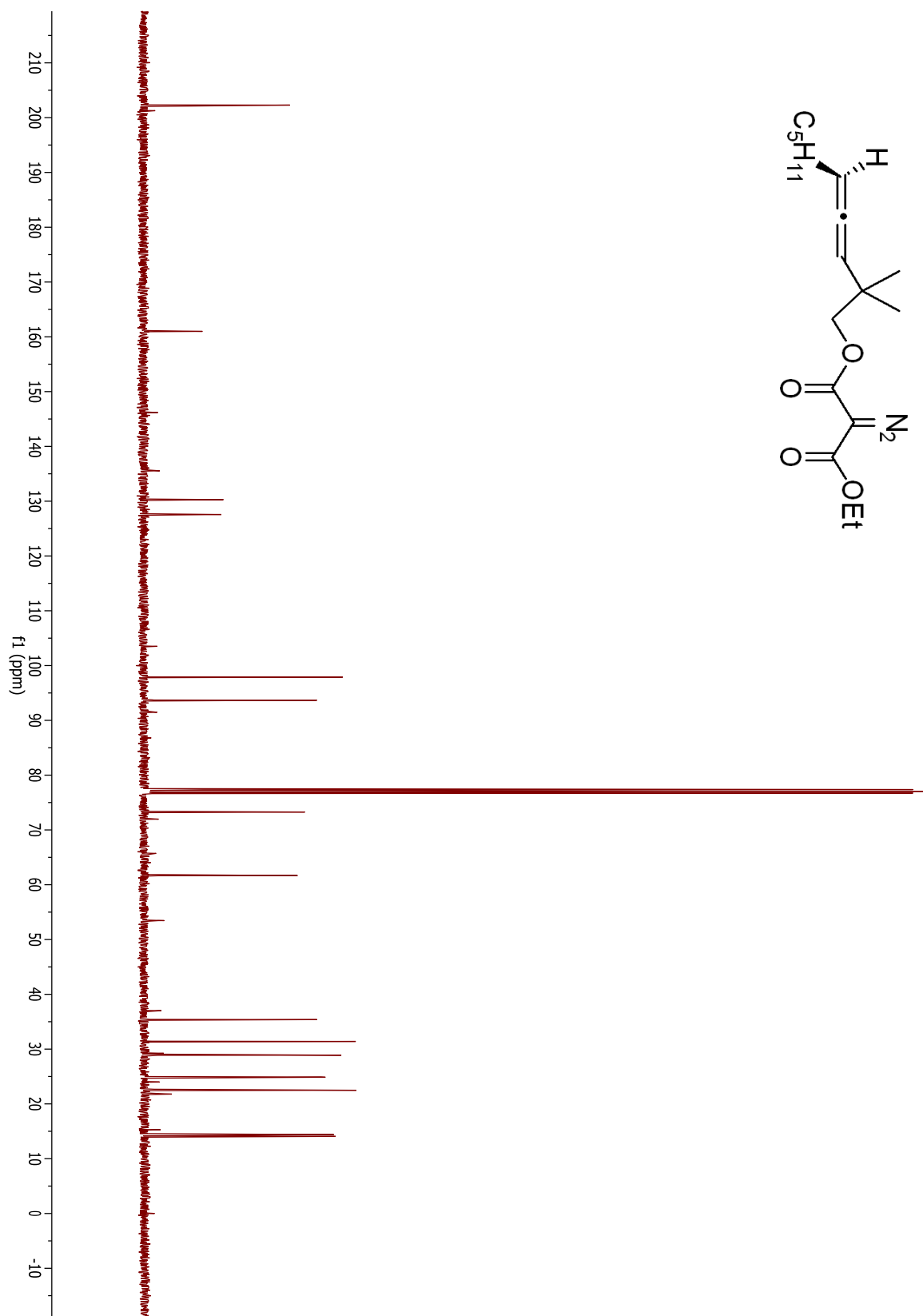




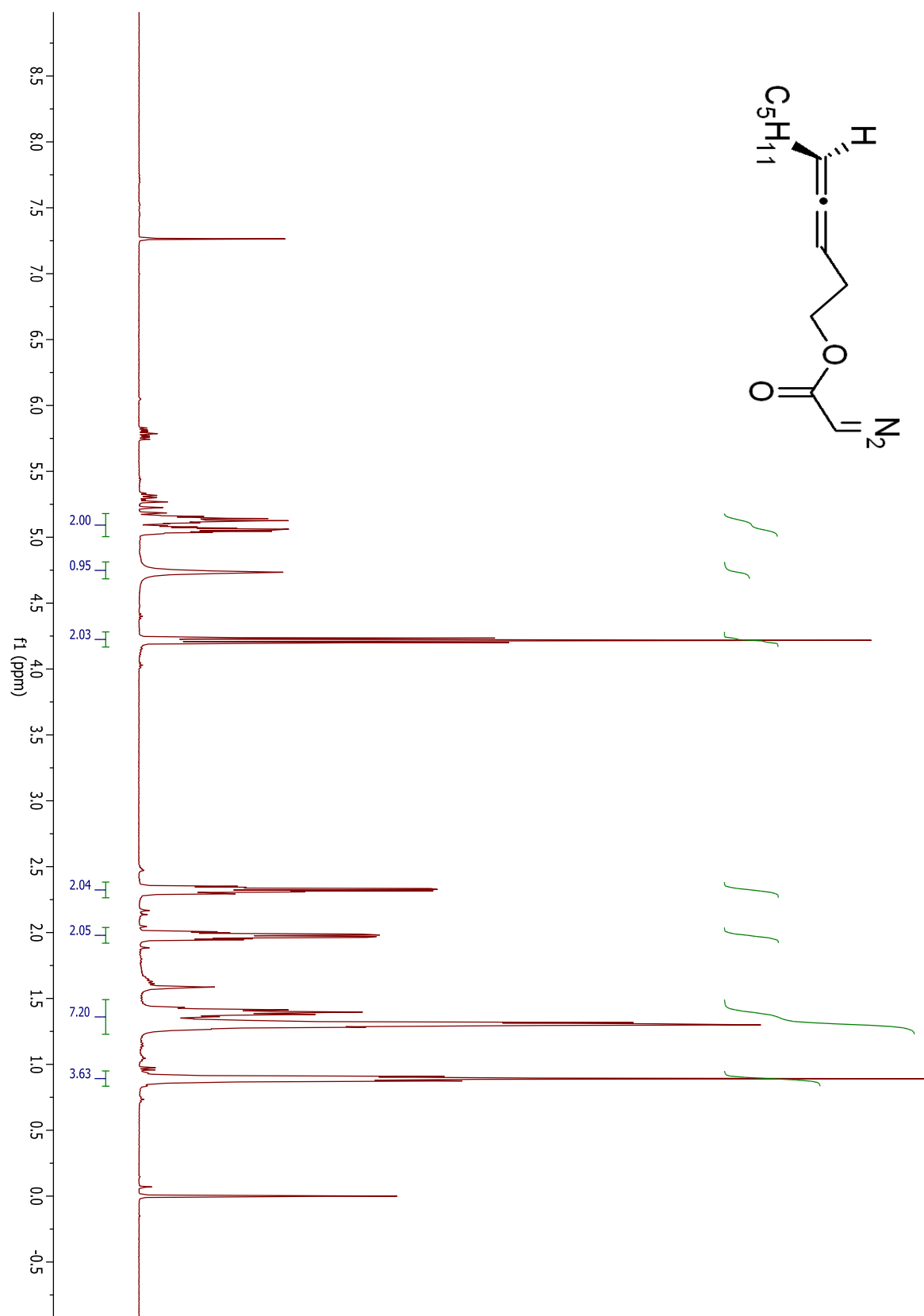


## Compound 1.103

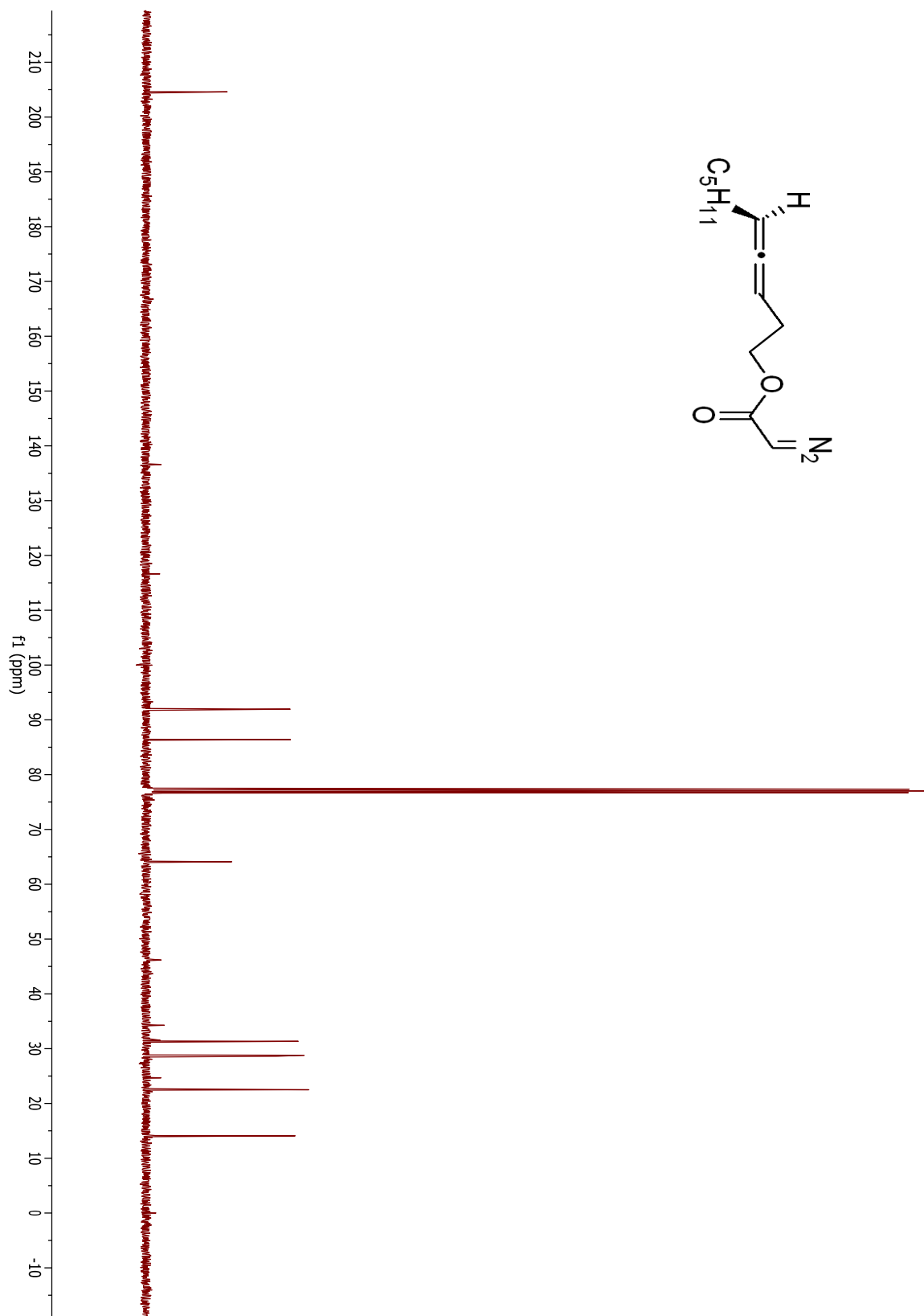




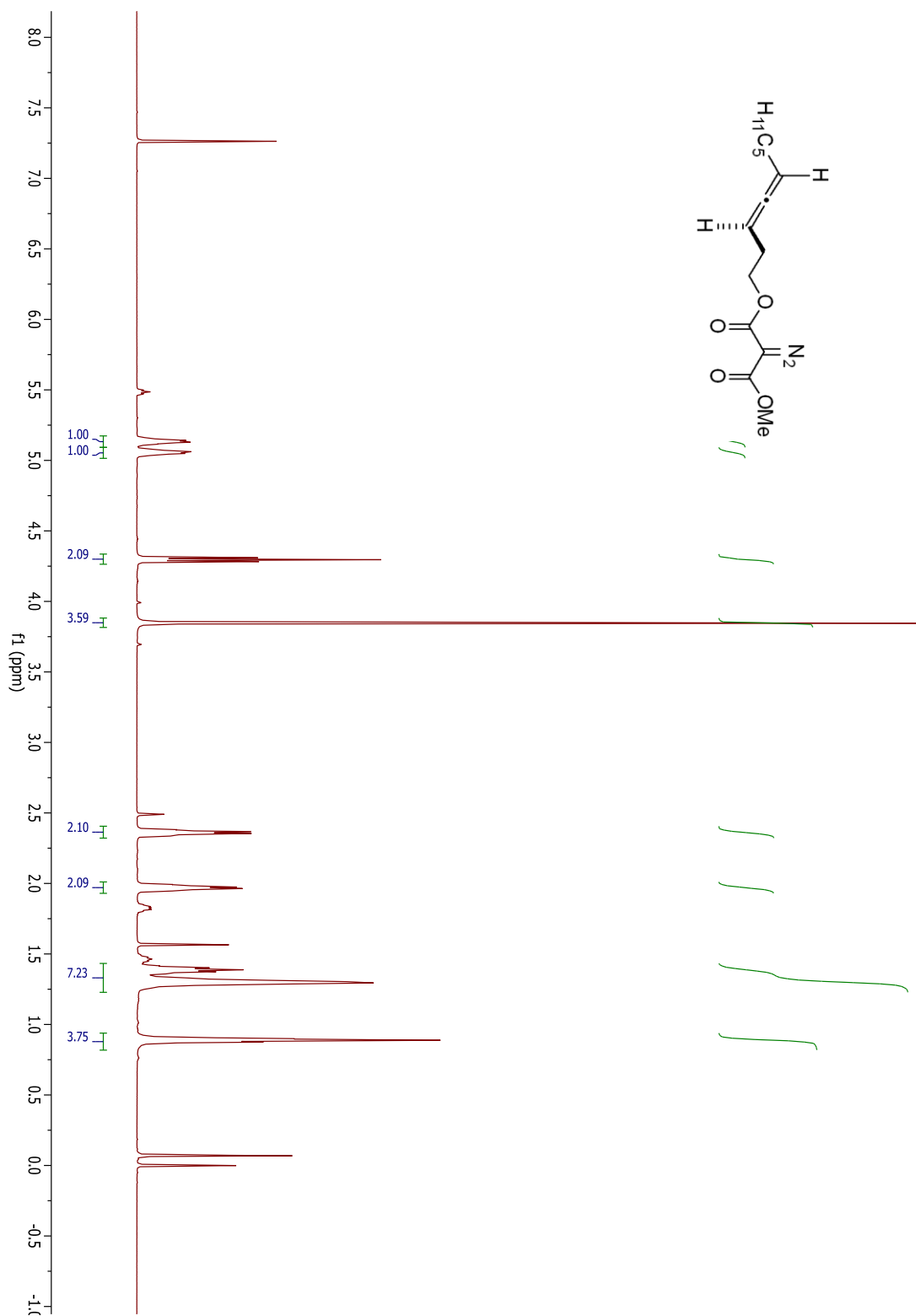
## Compound 1.105



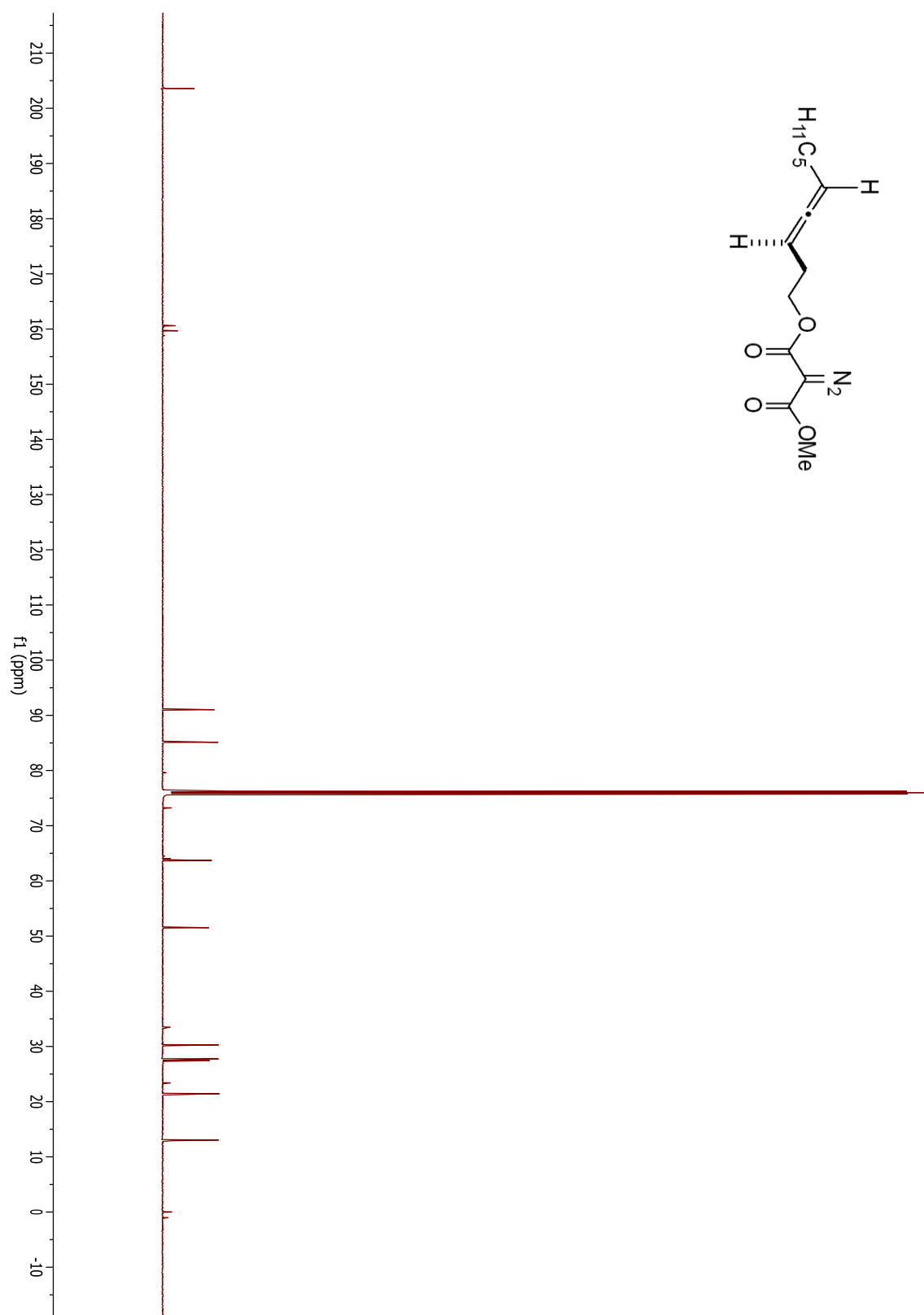
## Compound 1.105



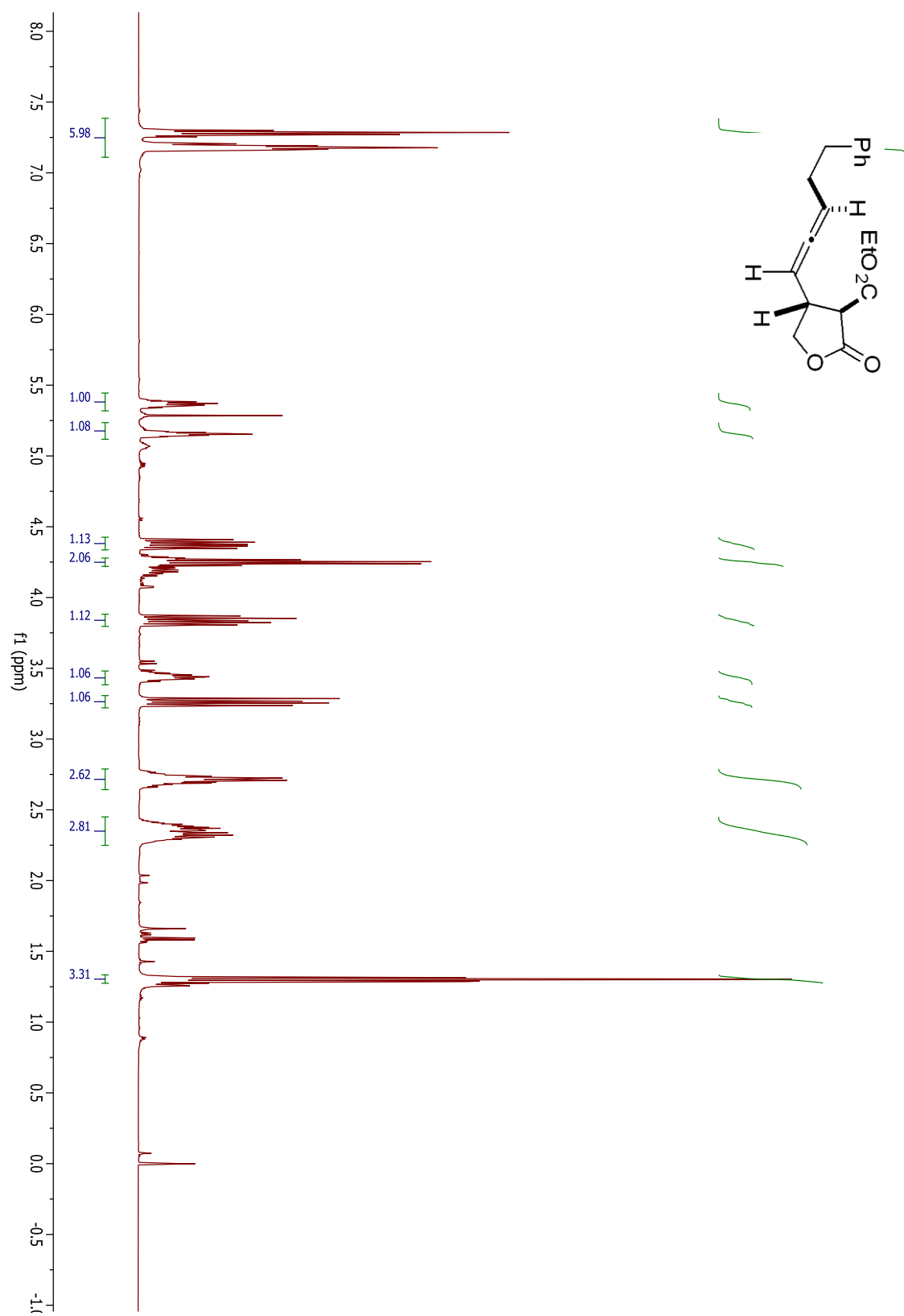
## Compound 1.107



## Compound 1.107

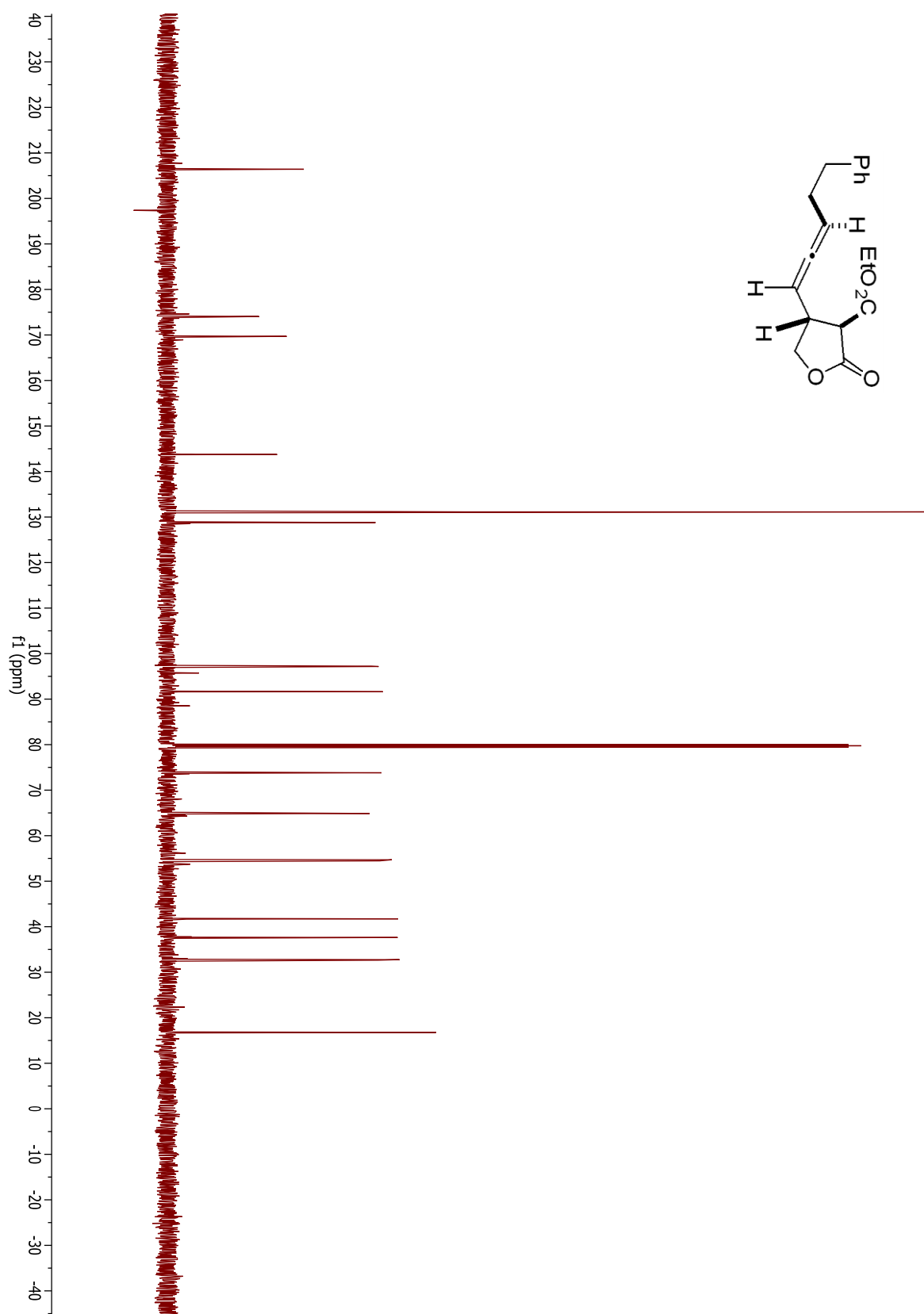


## Compound 1.79

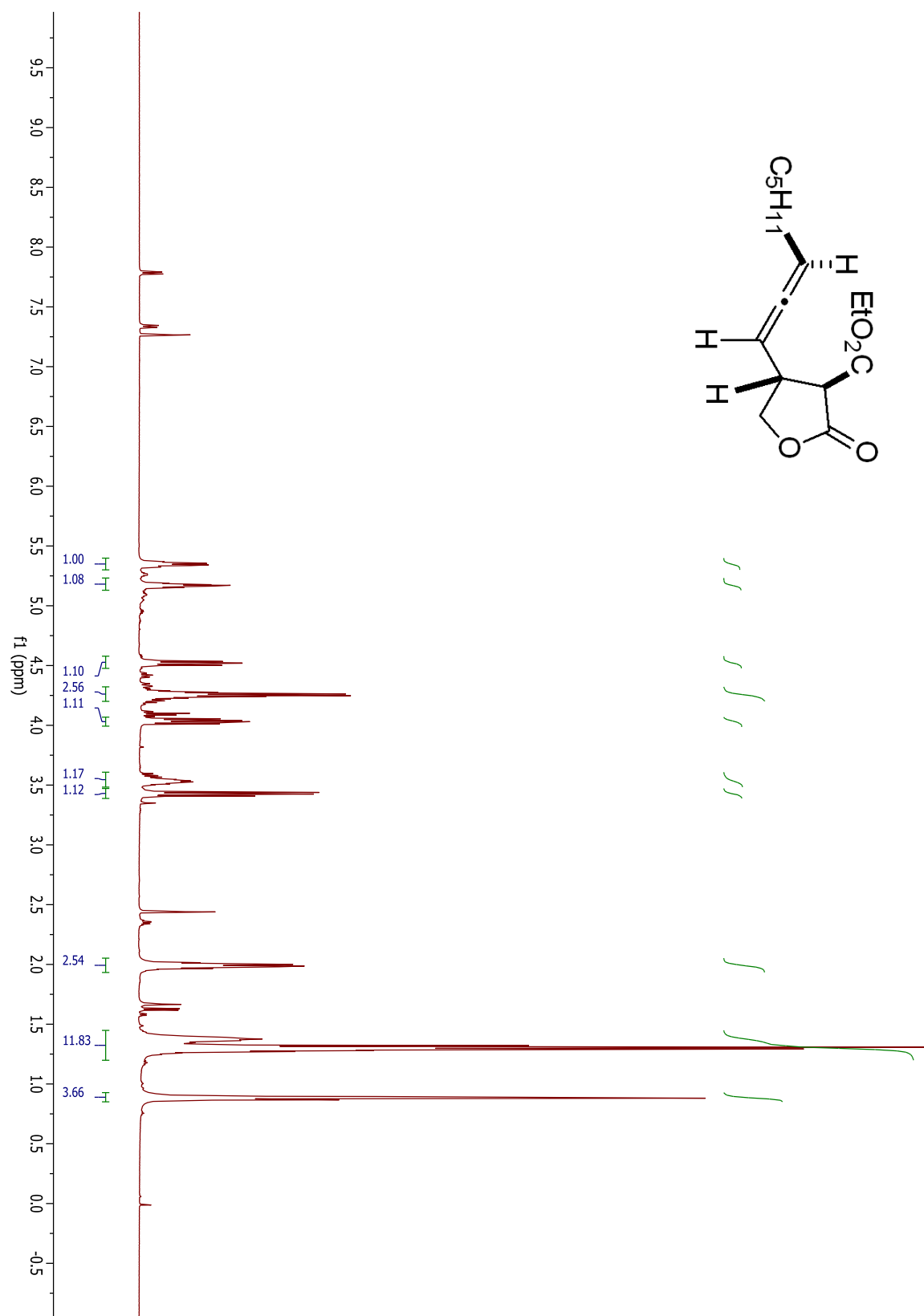




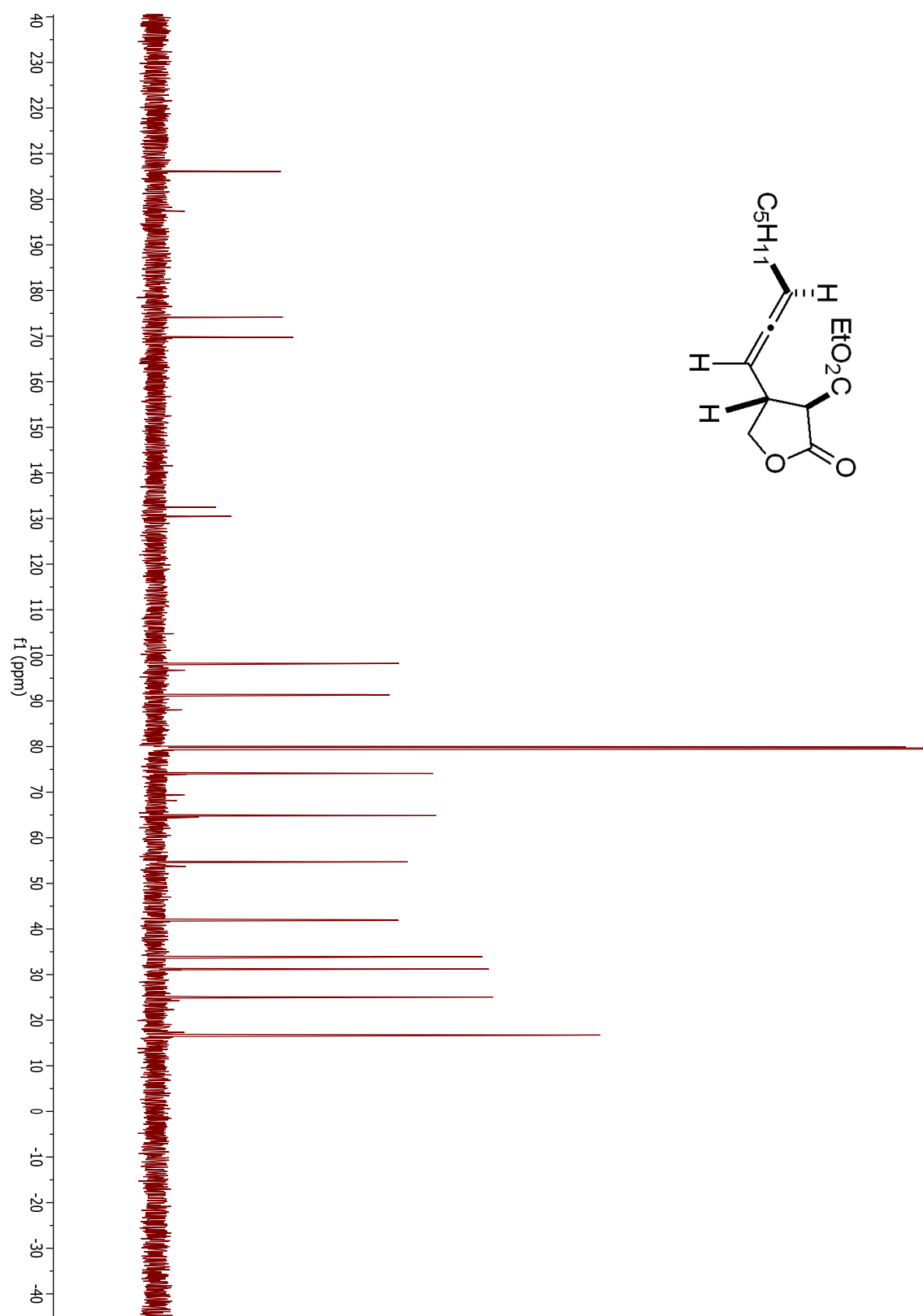
## Compound 1.79



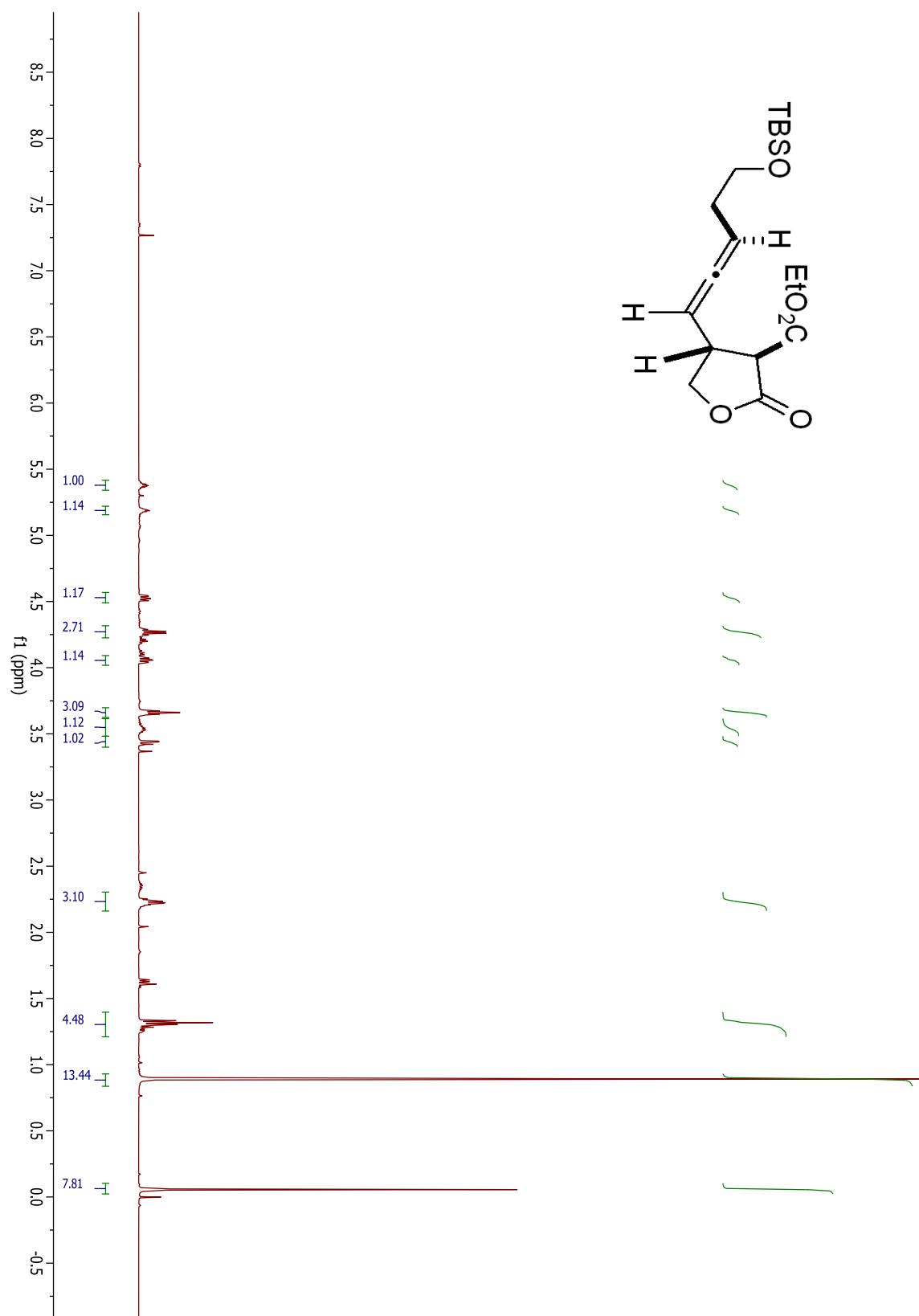
## Compound 1.81



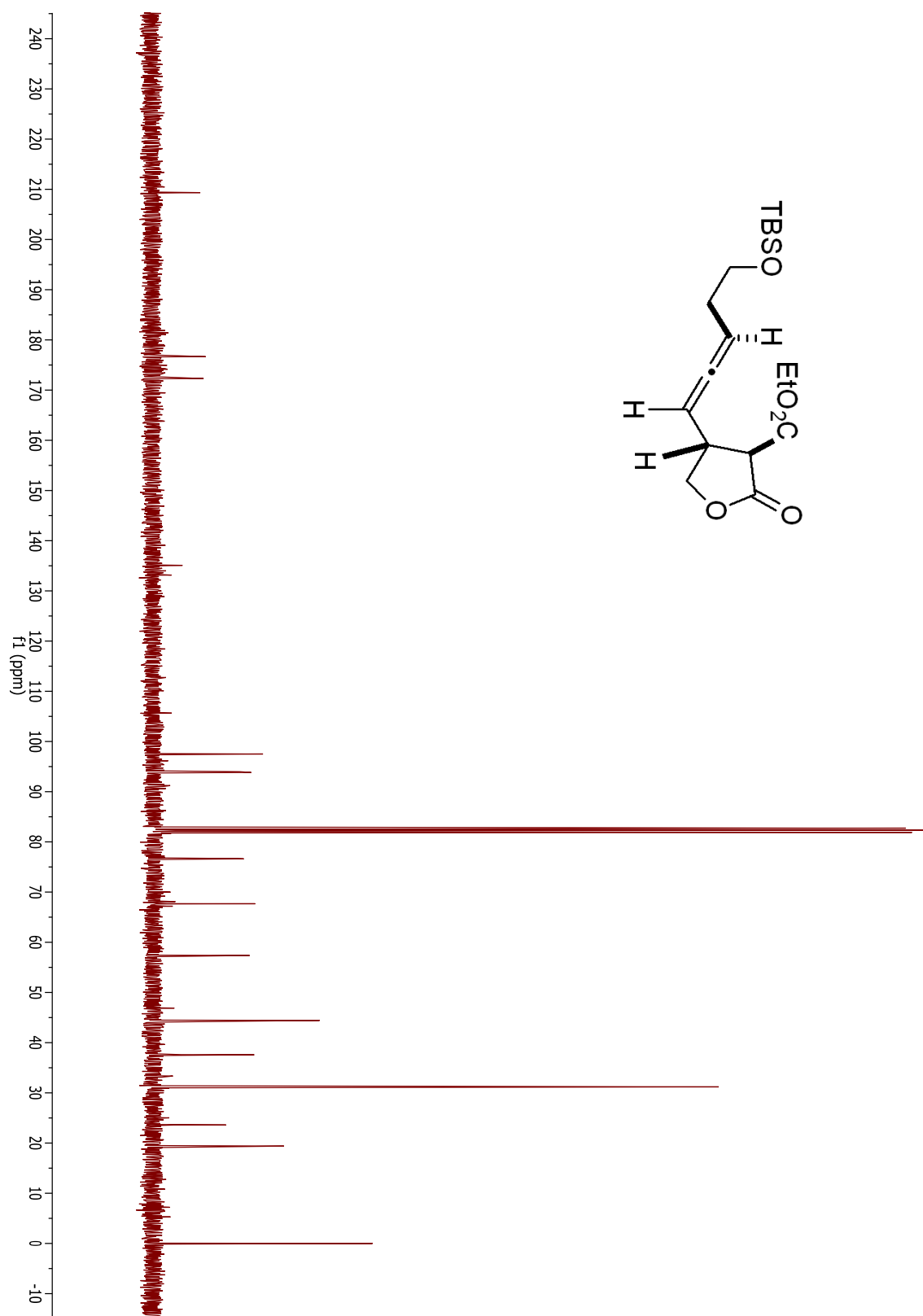
## Compound 1.81



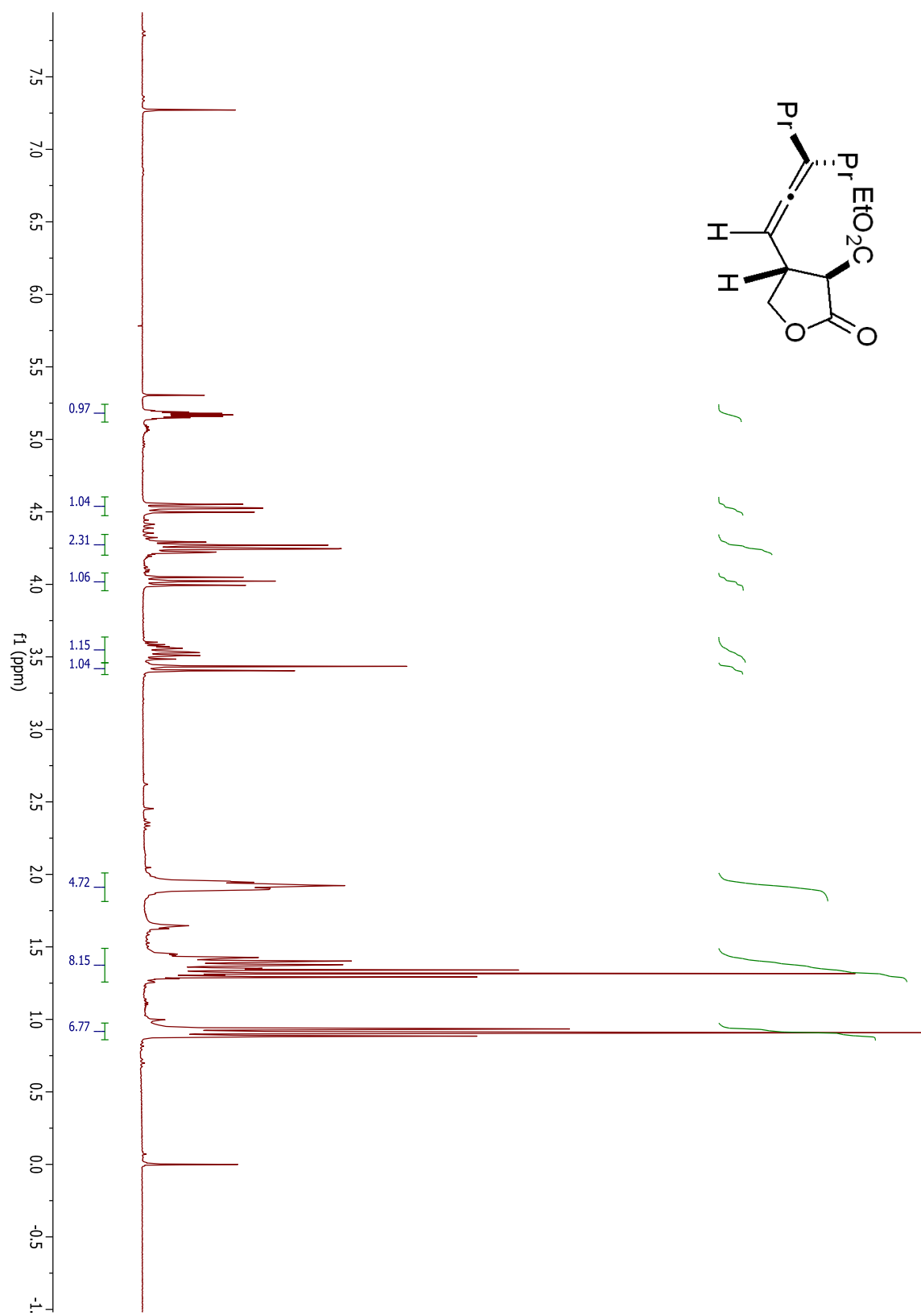
## Compound 1.83



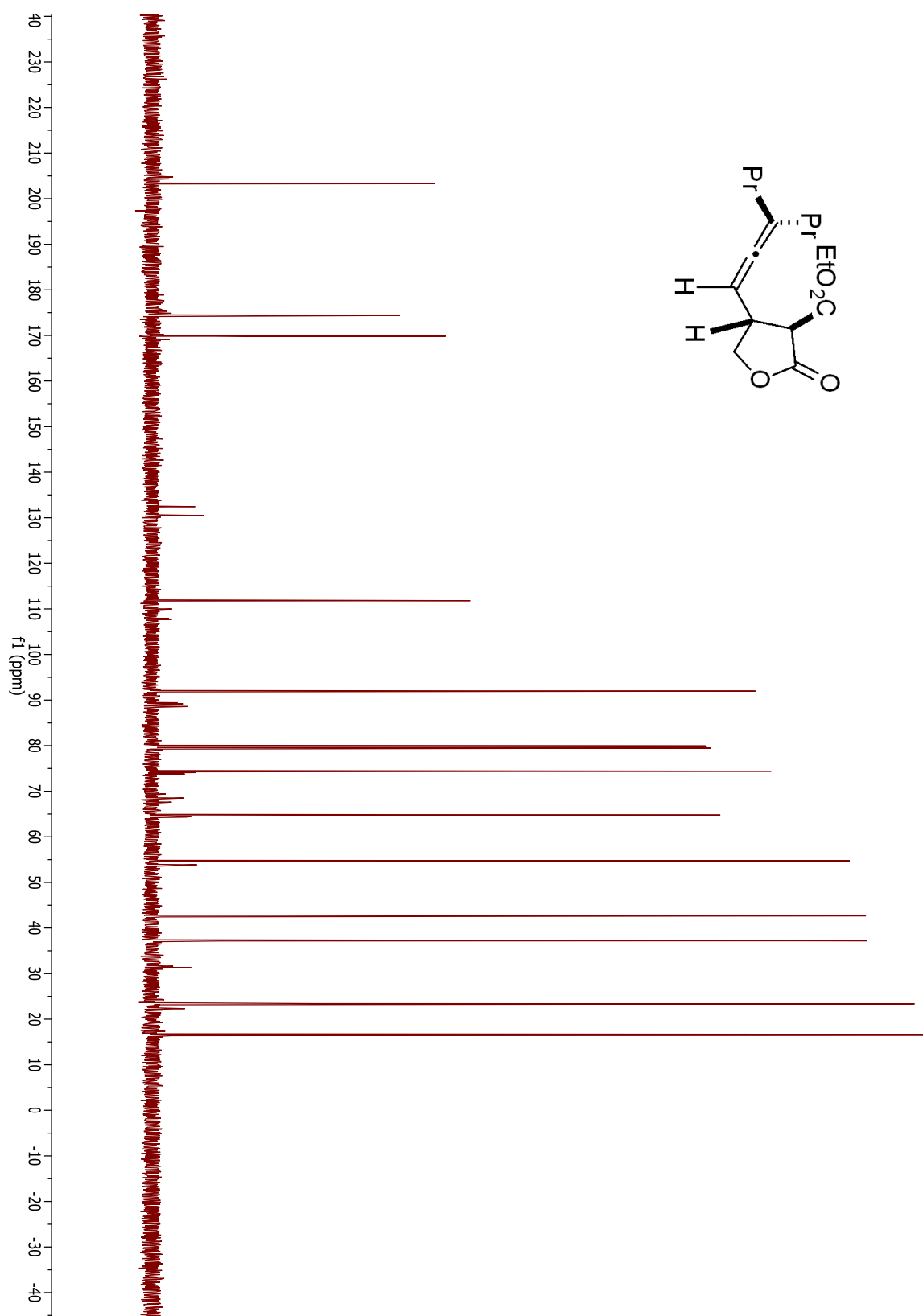
## Compound 1.83



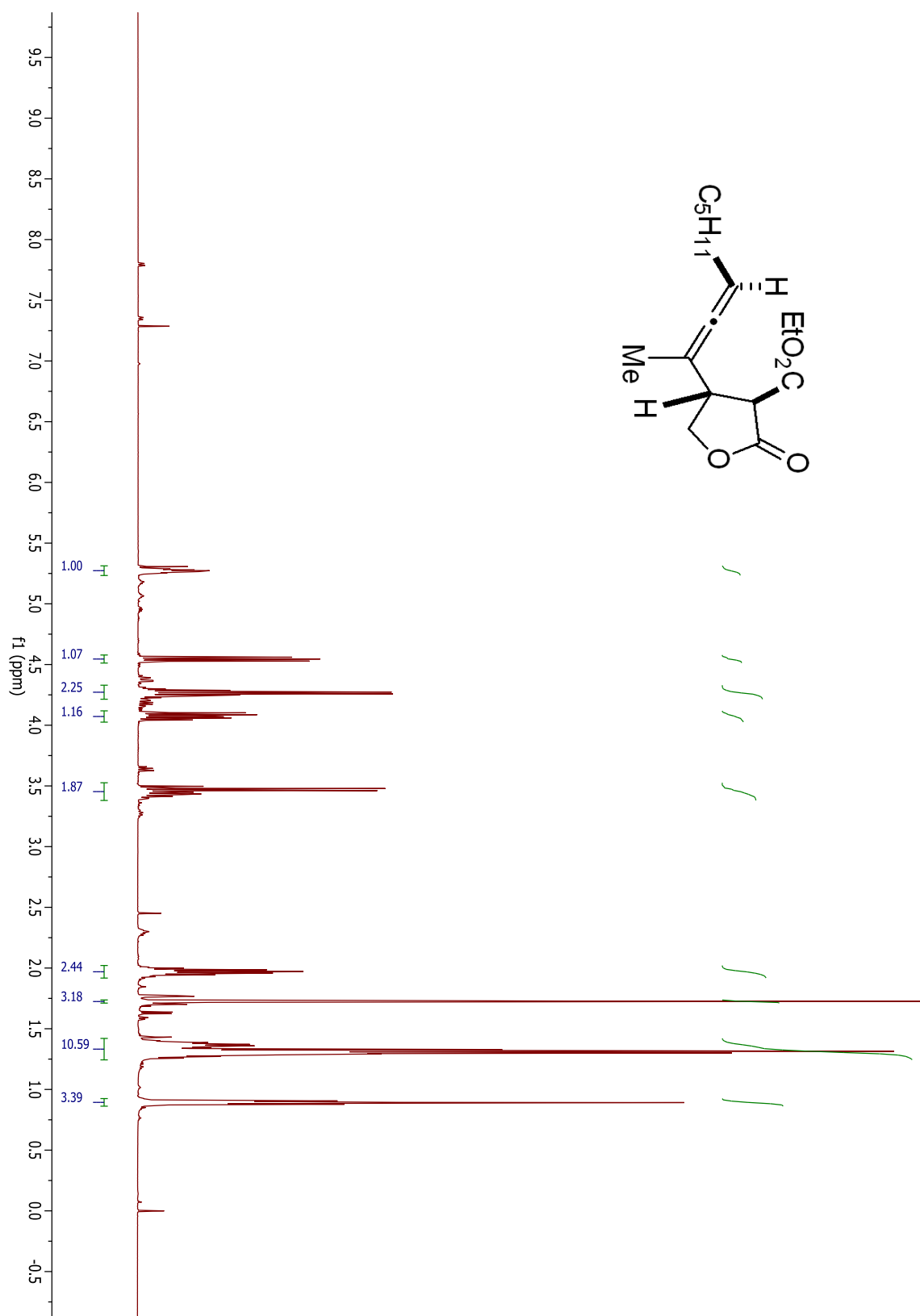
## Compound 1.85



## Compound 1.85

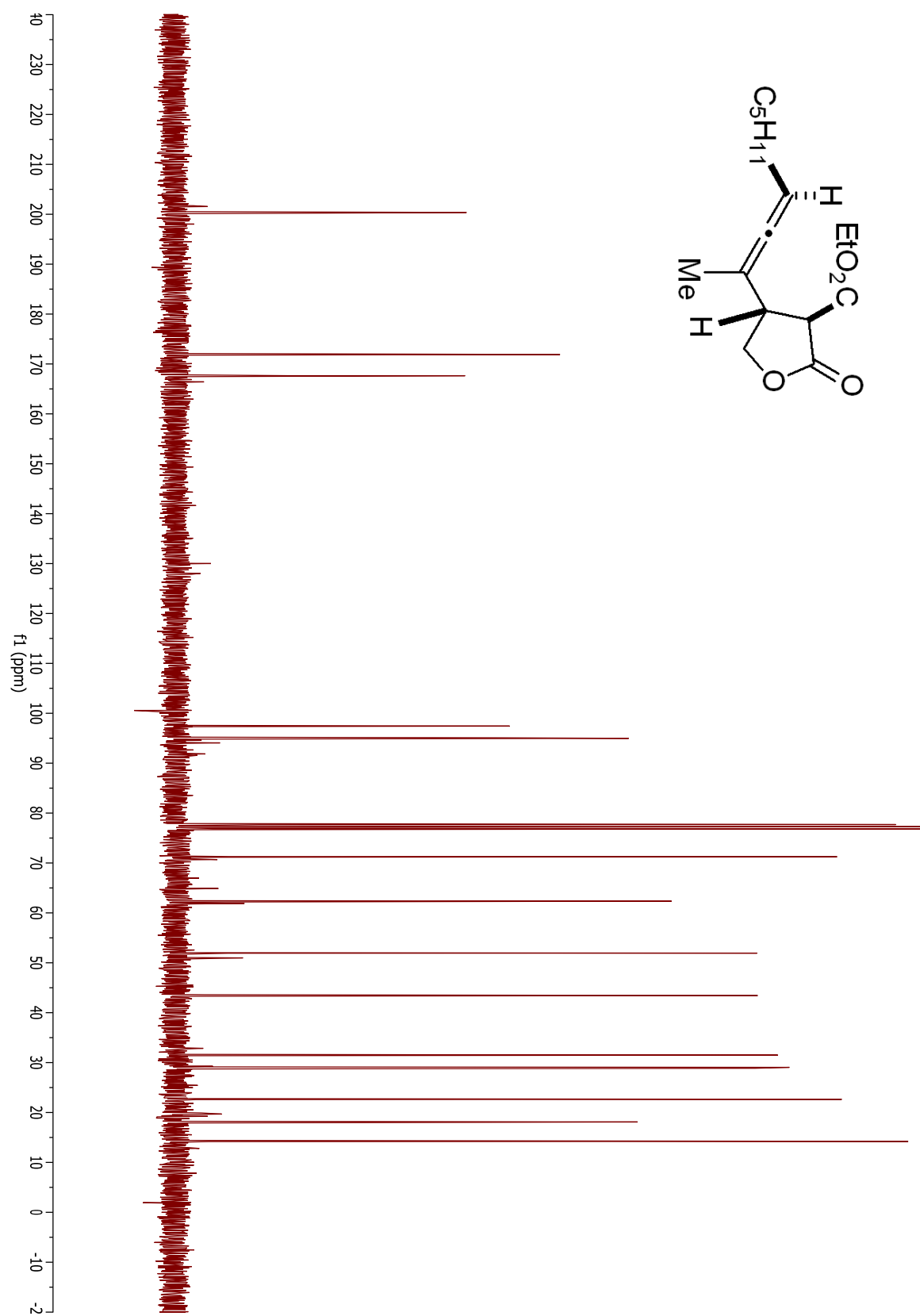


## Compound 1.87

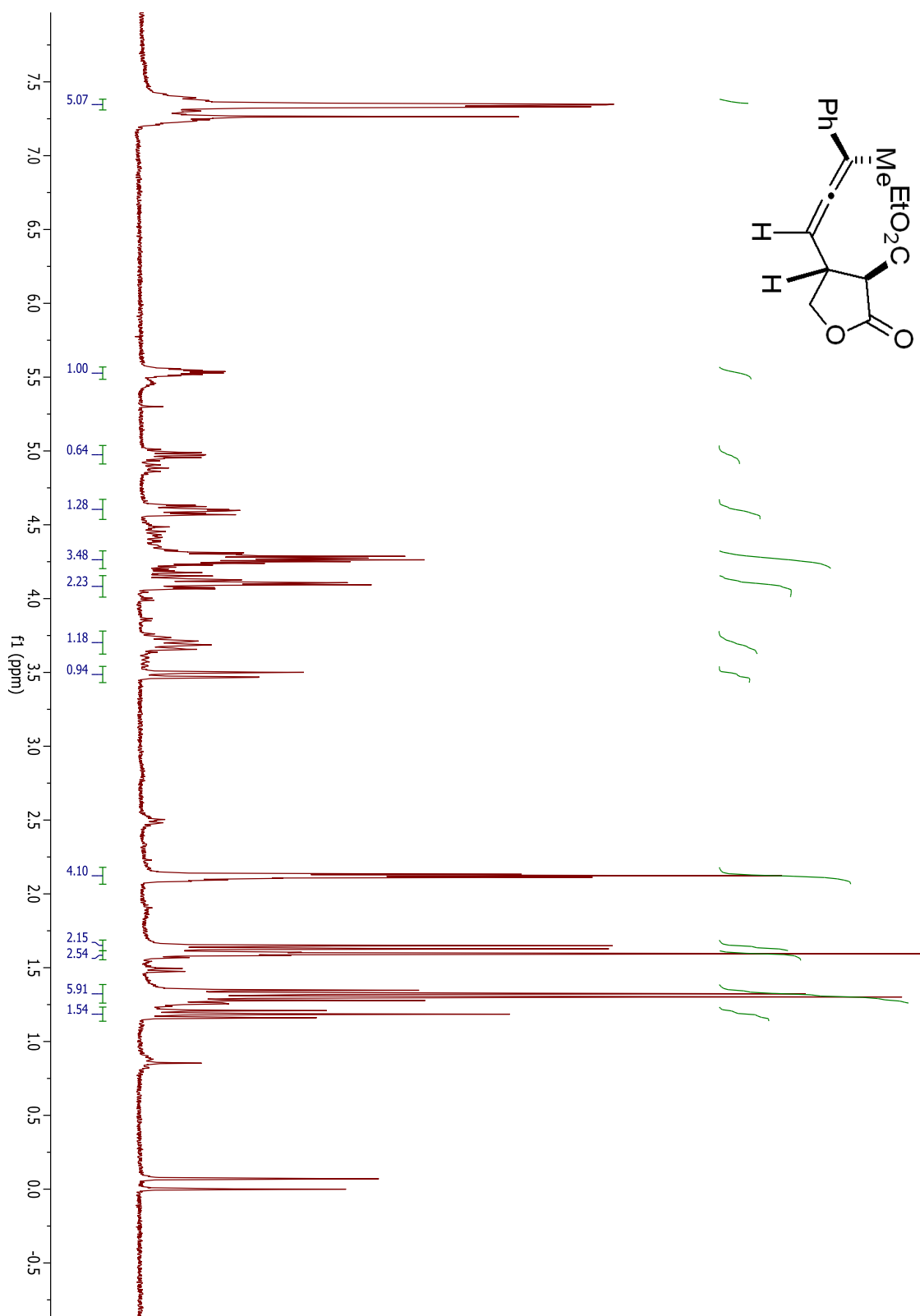




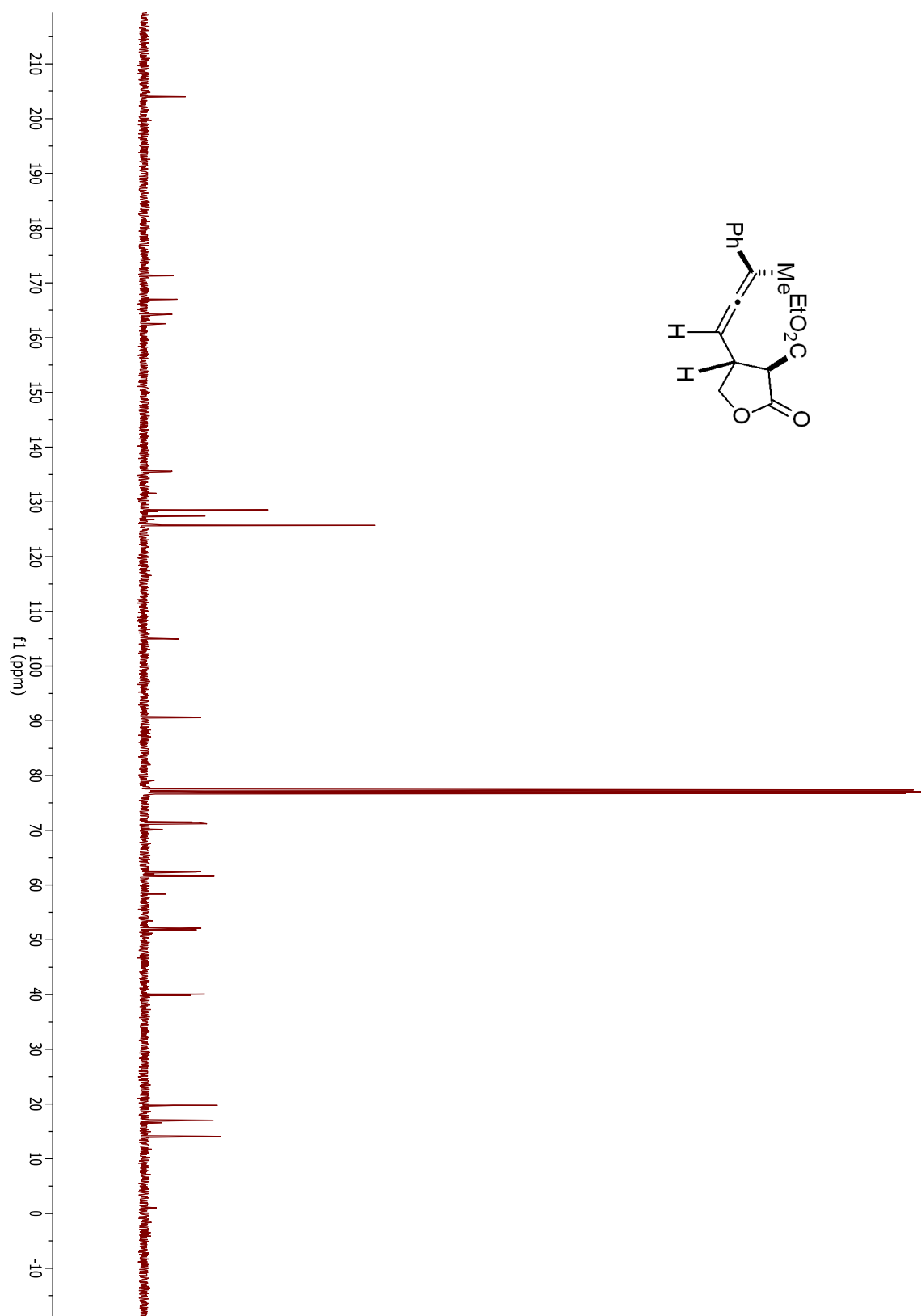
## Compound 1.87



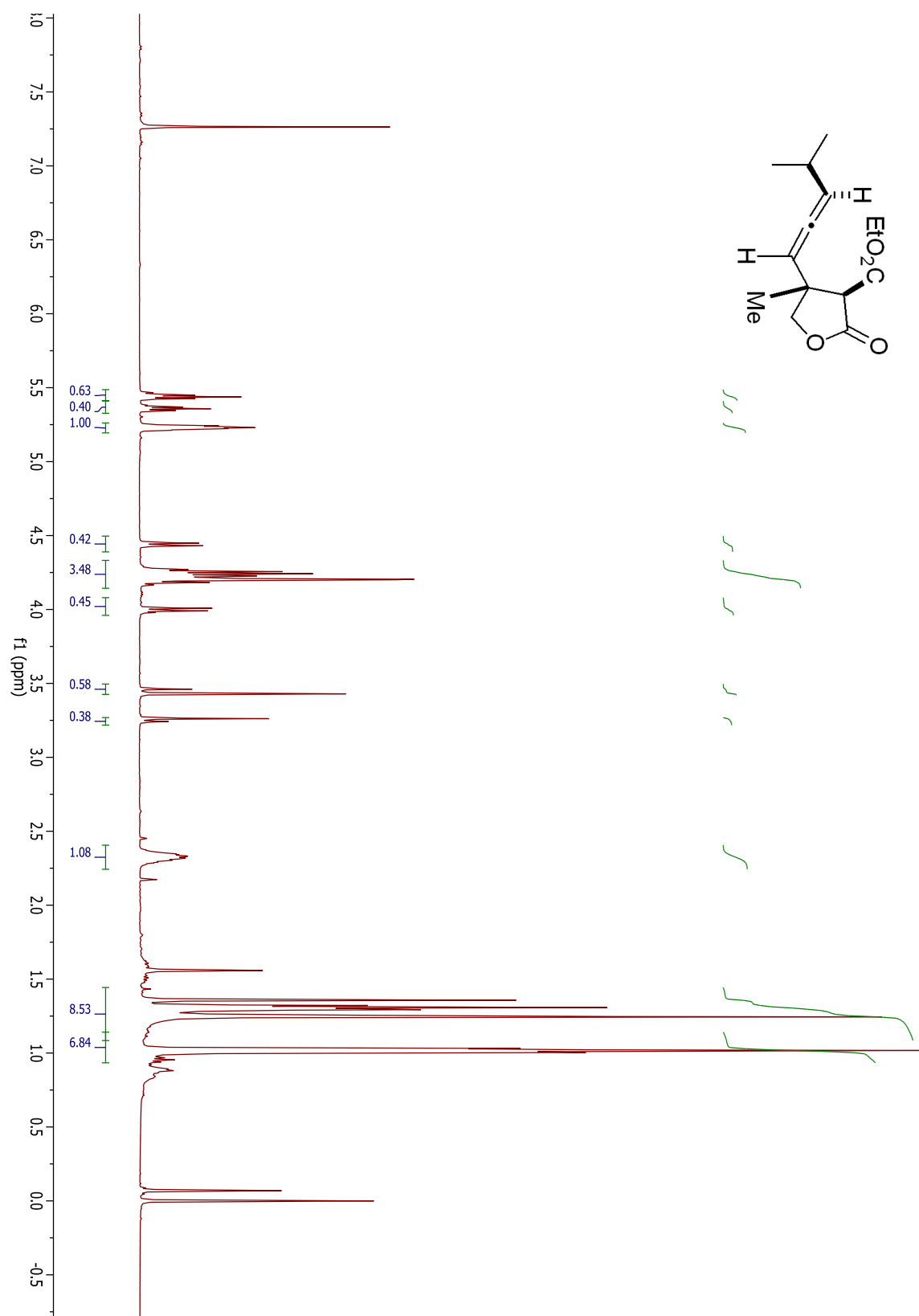
## Compound 1.89



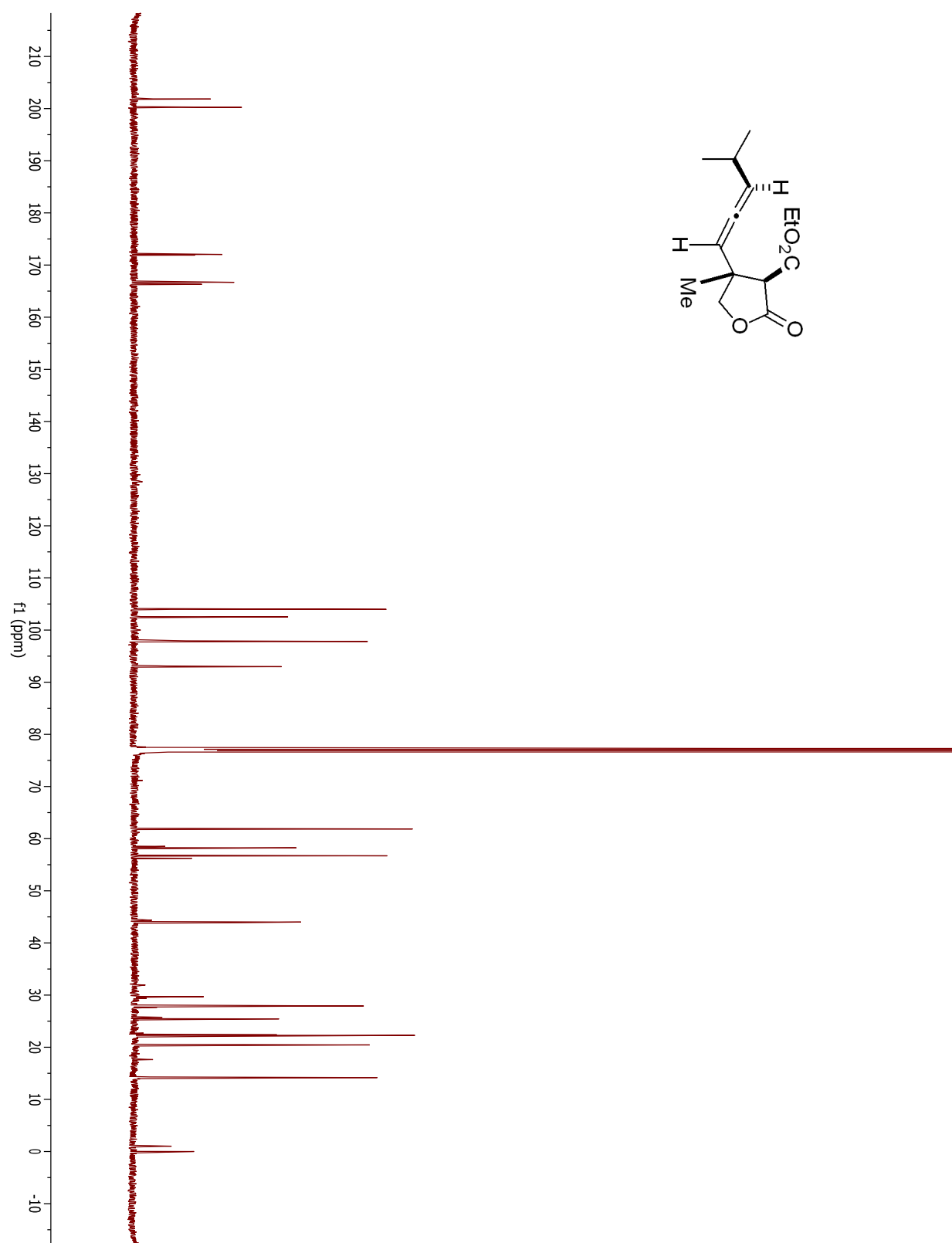
## Compound 1.89



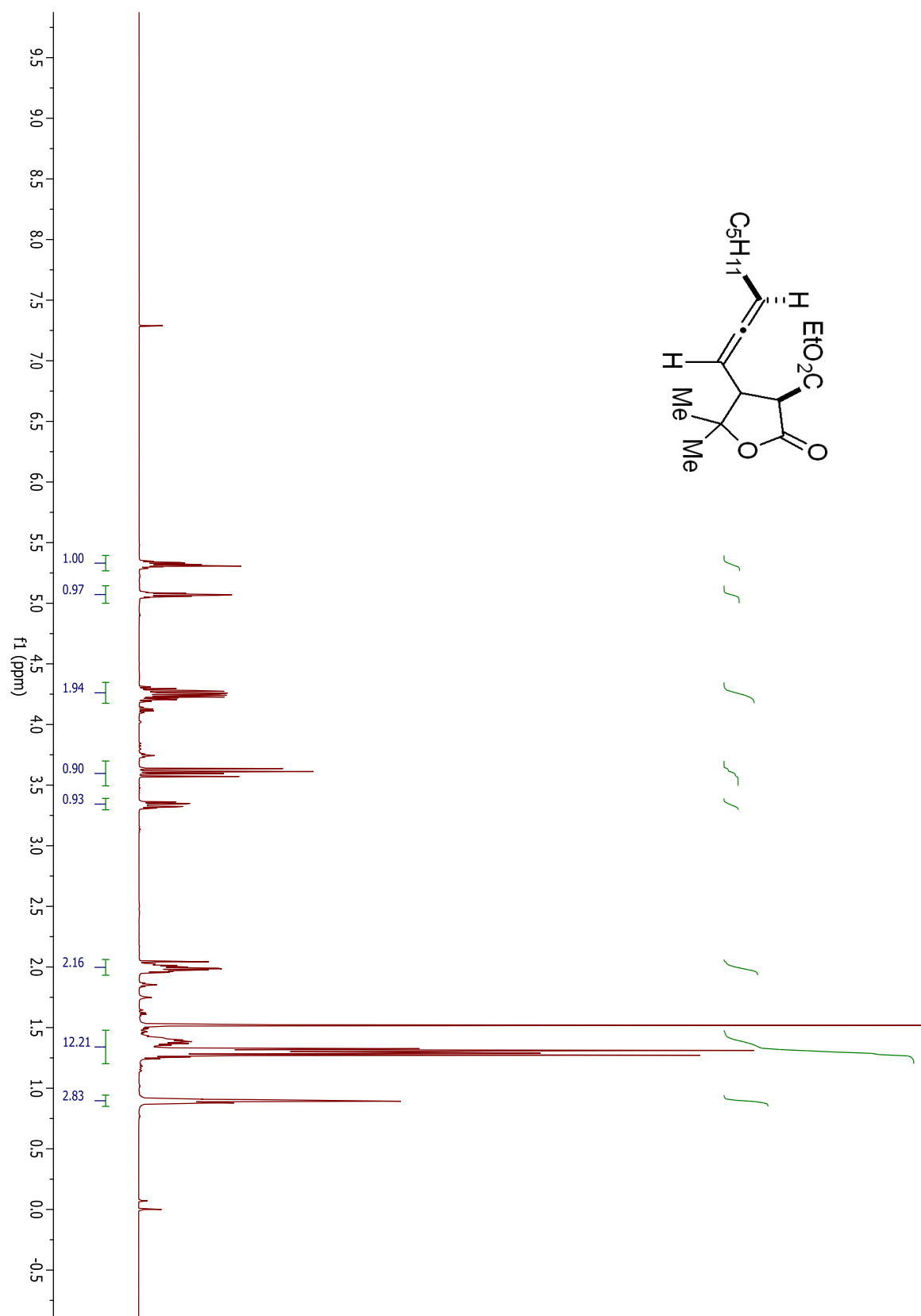
## Compound 1.91



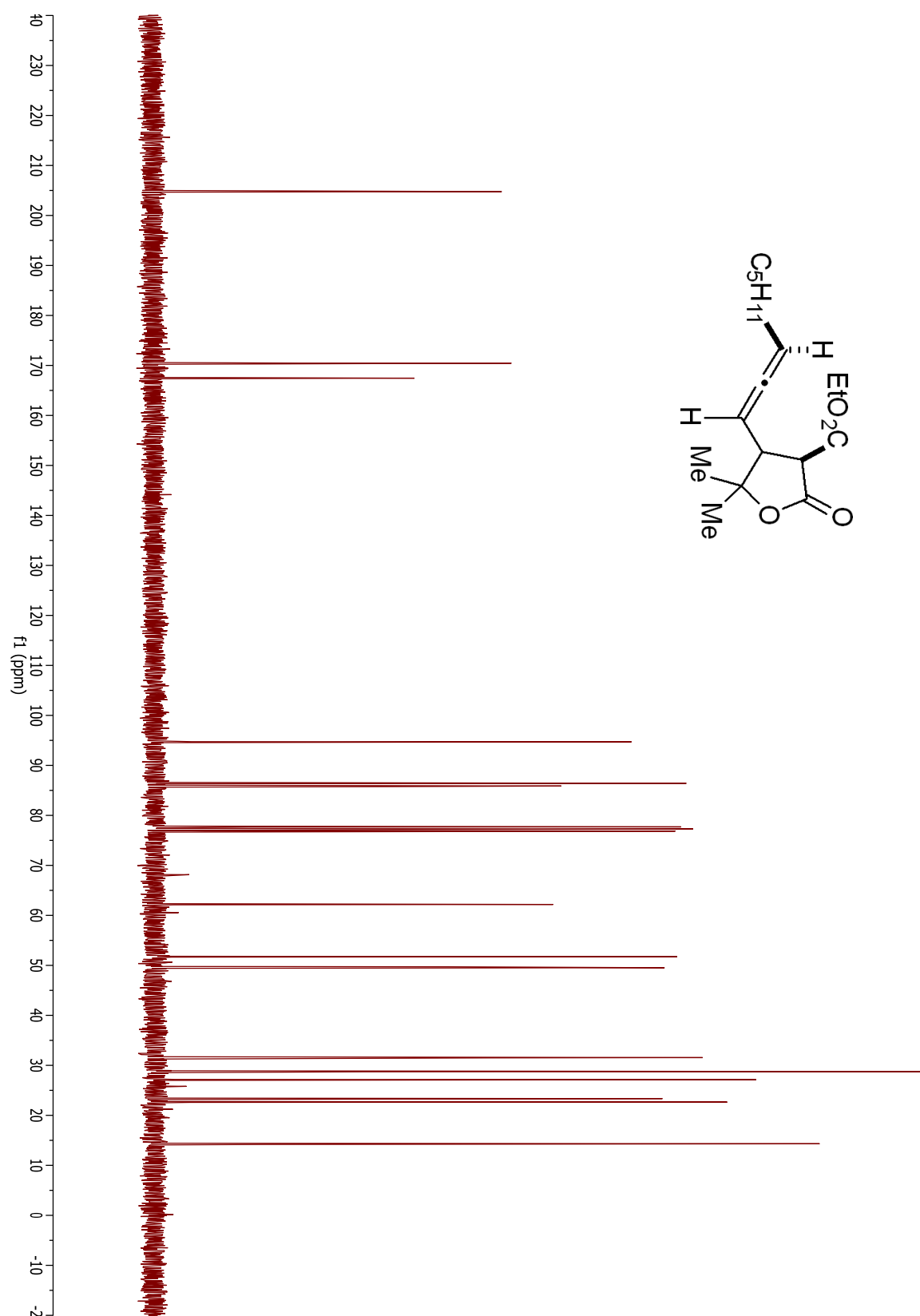
## Compound 1.91



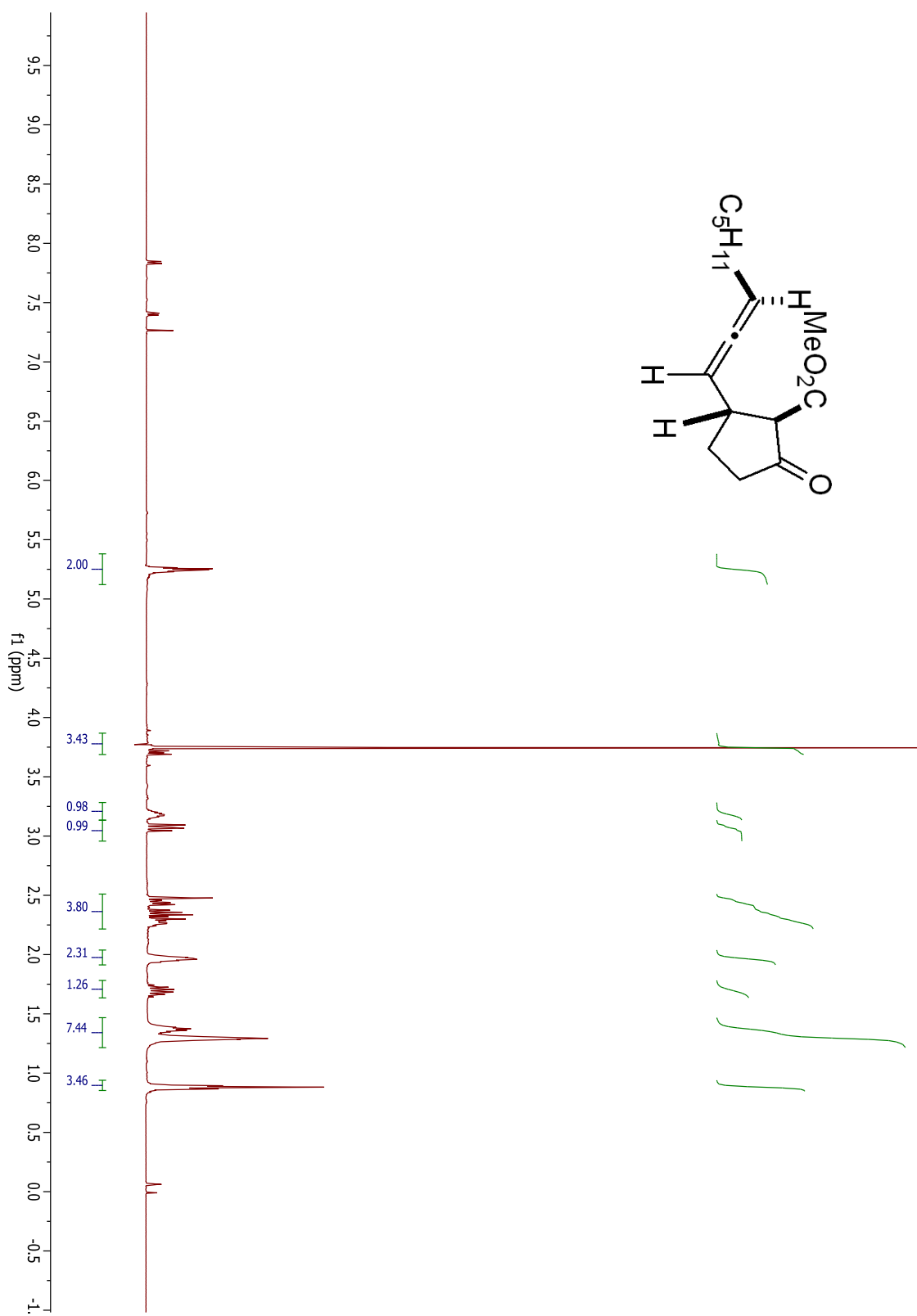
## Compound 1.93



## Compound 1.93

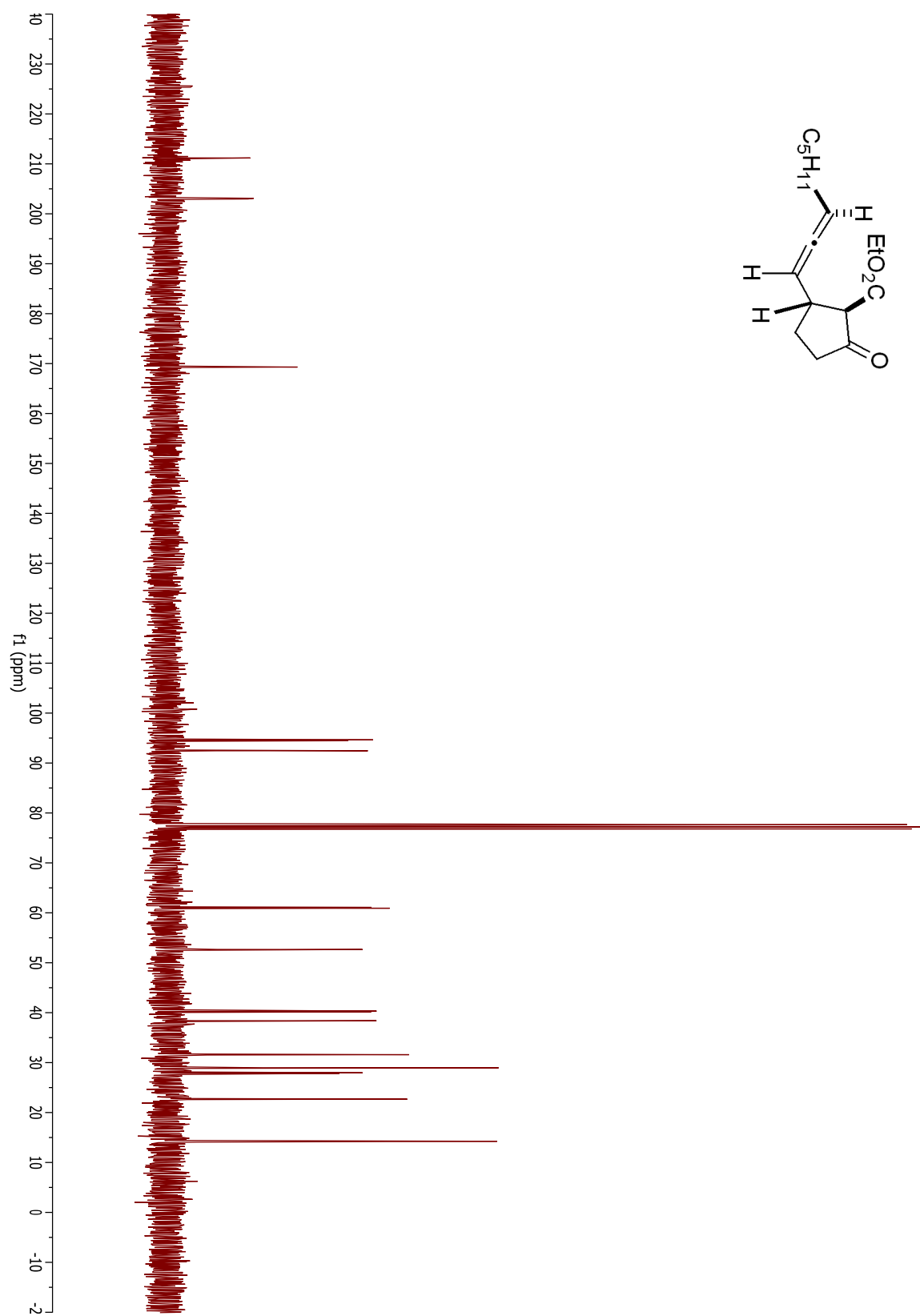


## Compound 1.95

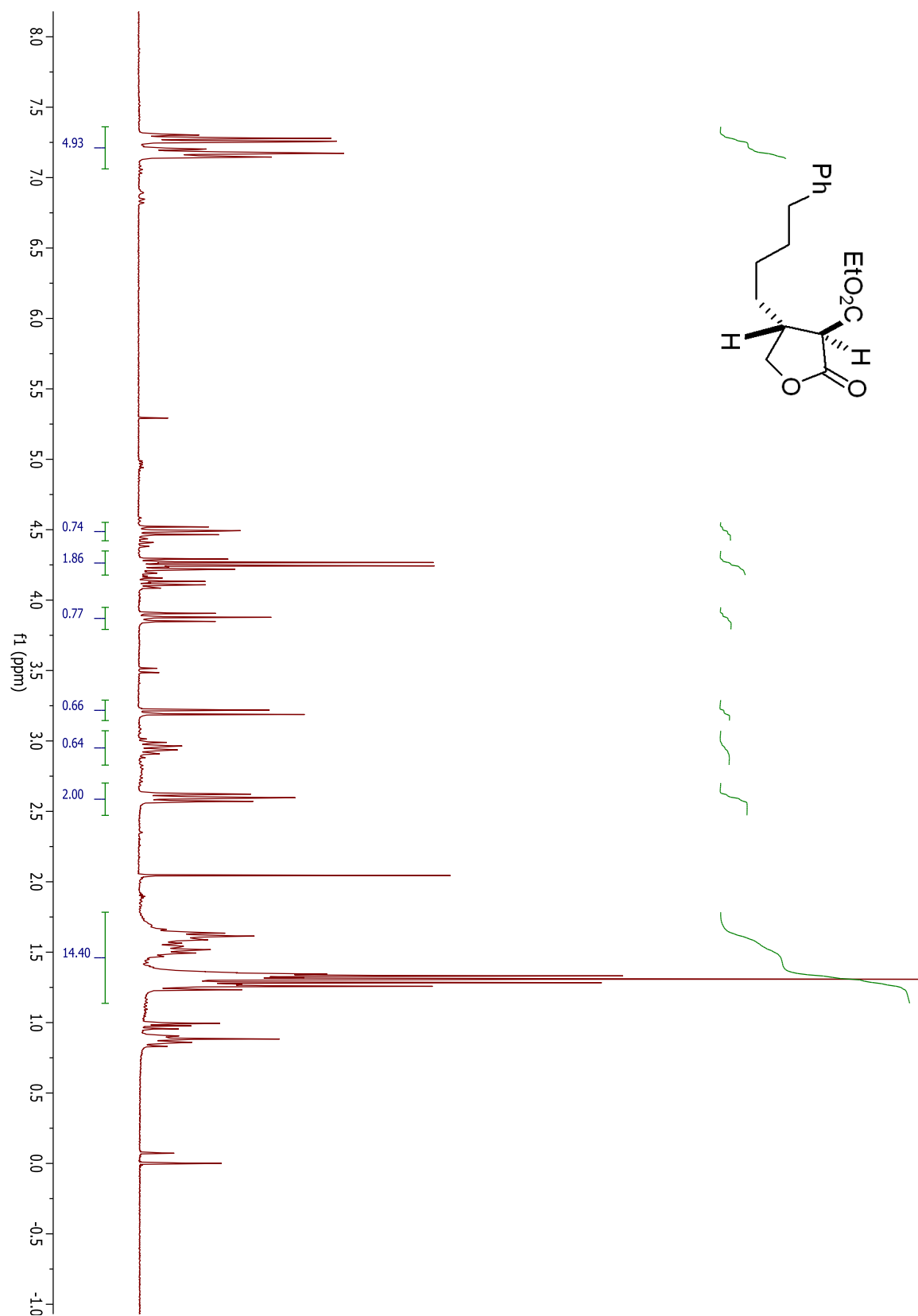




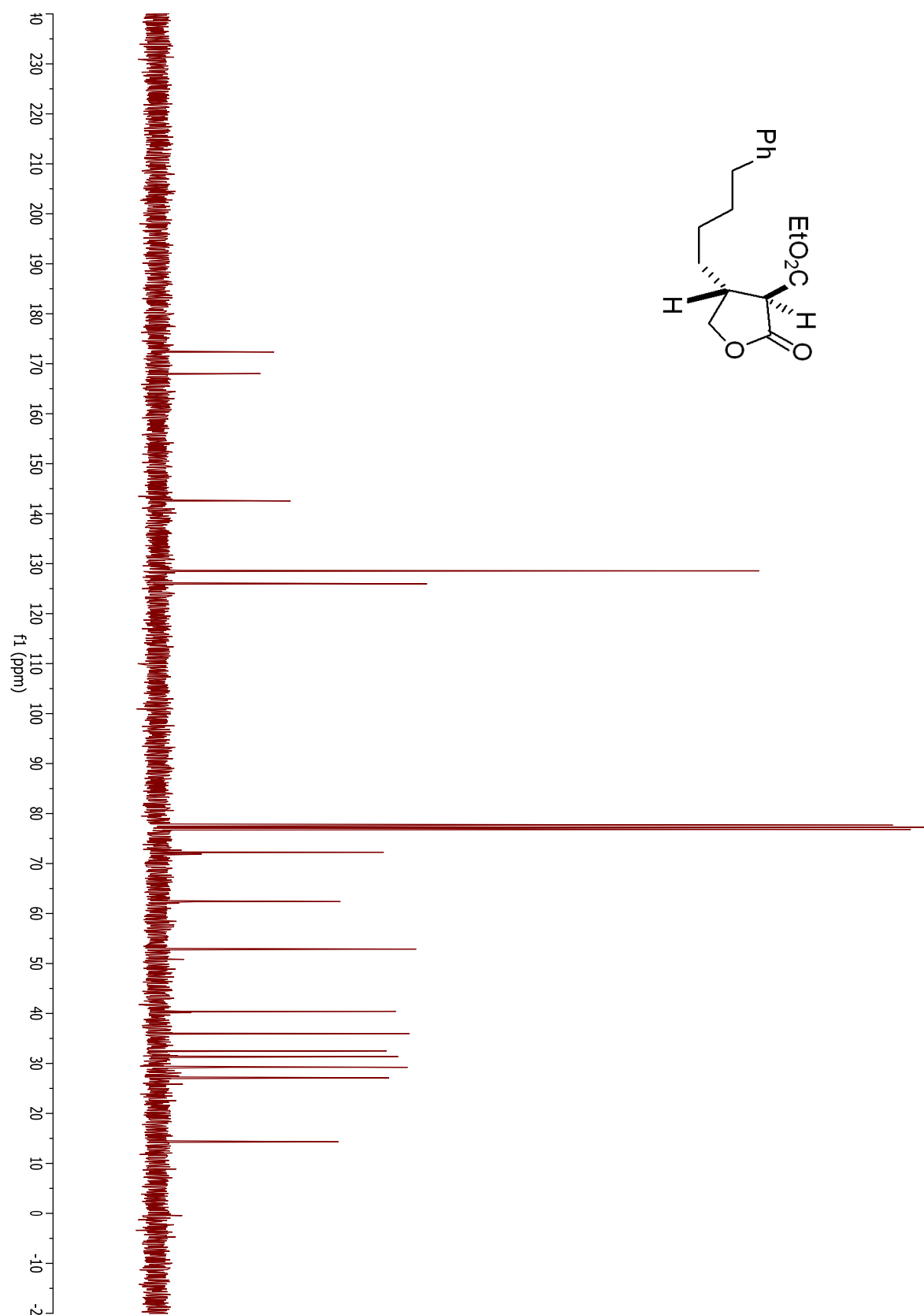
## Compound 1.95



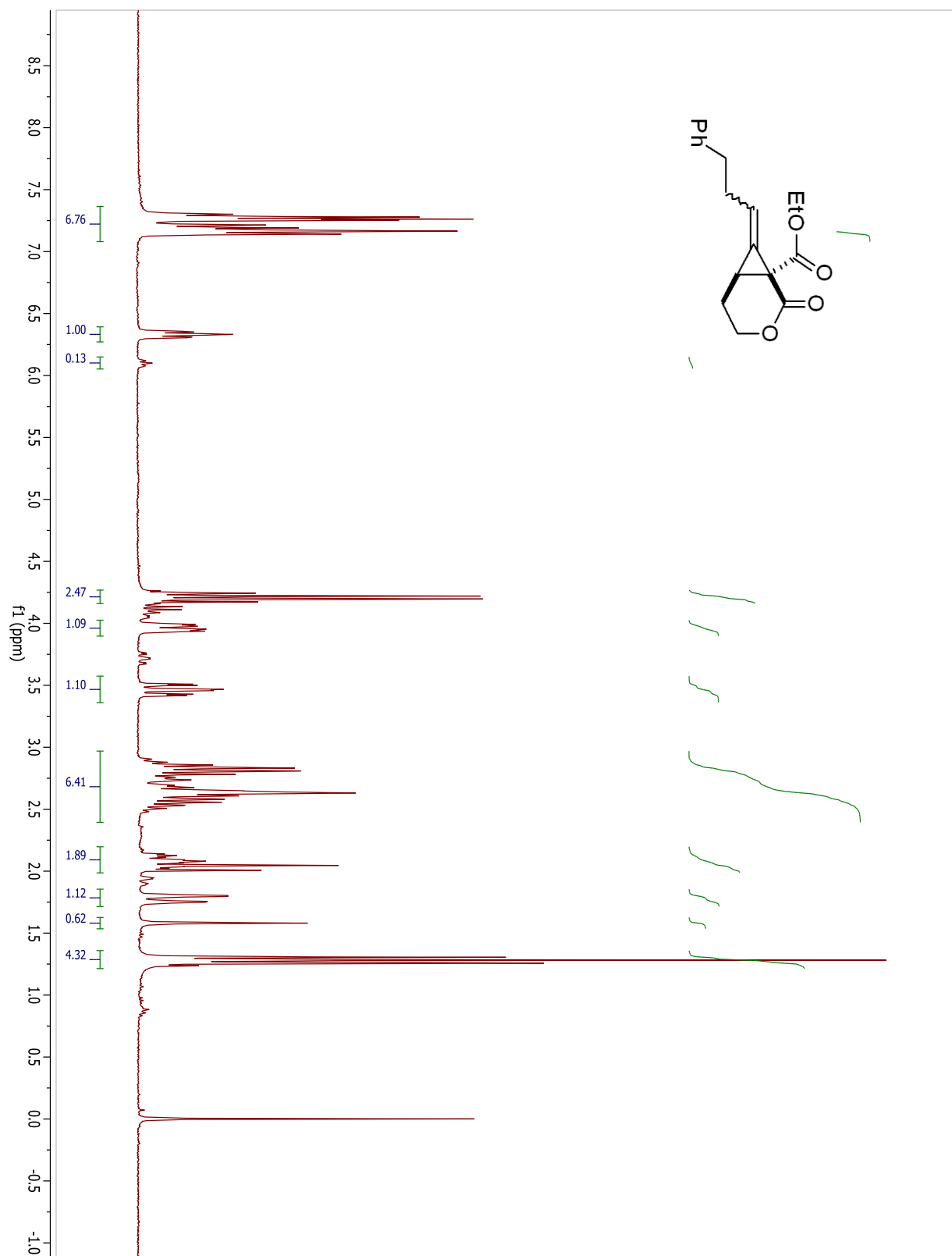
## Compound 1.96



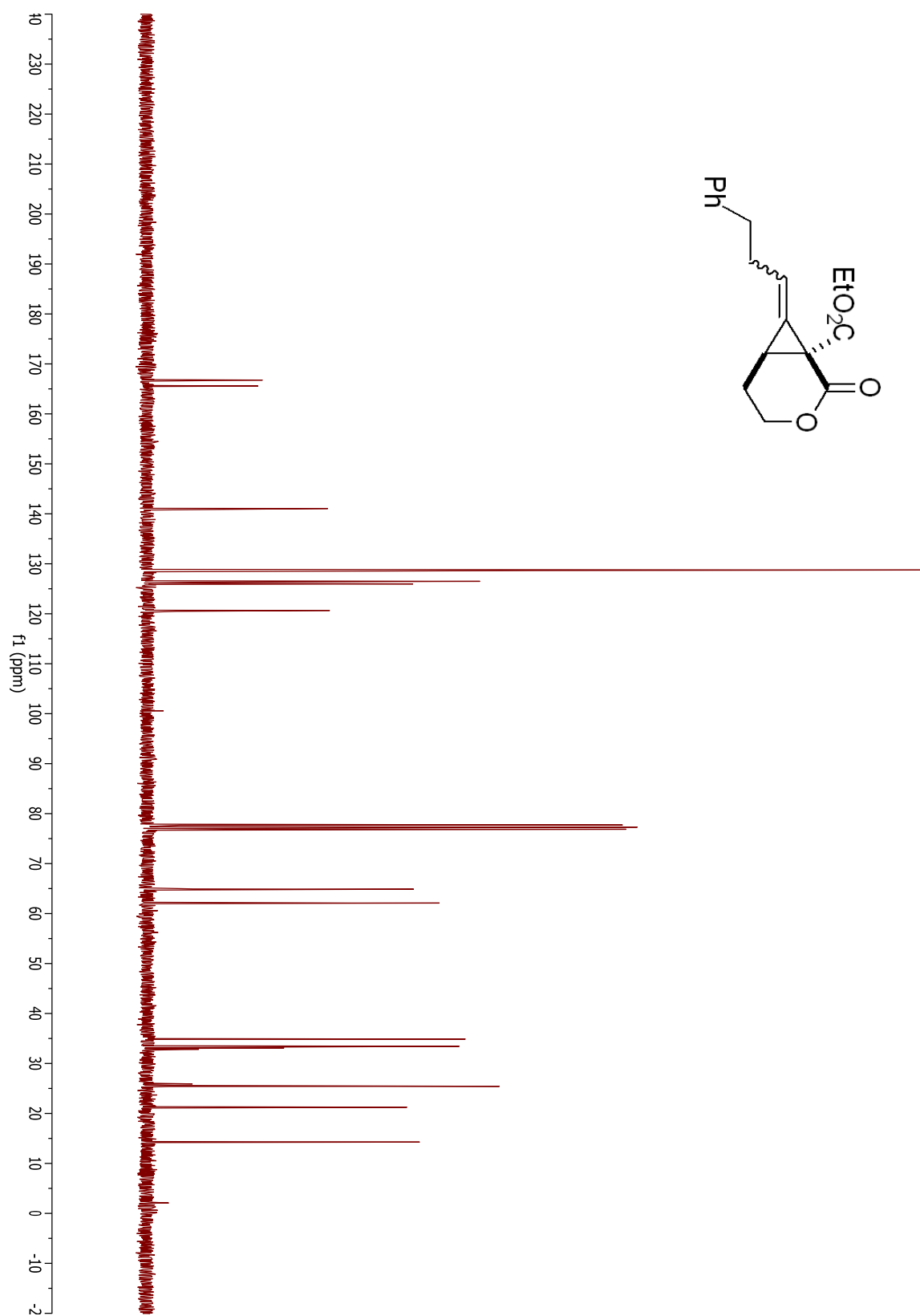
## Compound 1.96



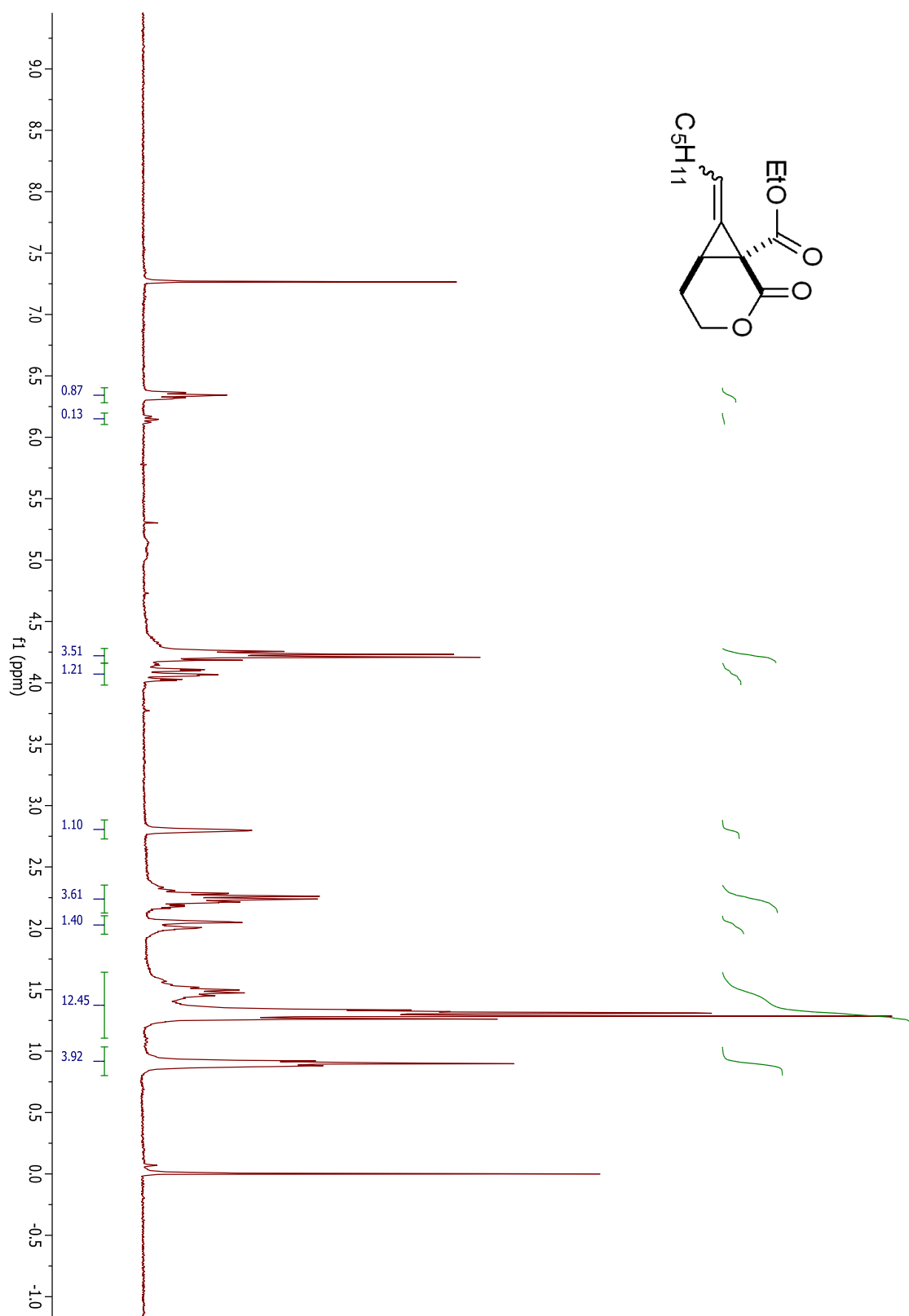
## Compound 1.97



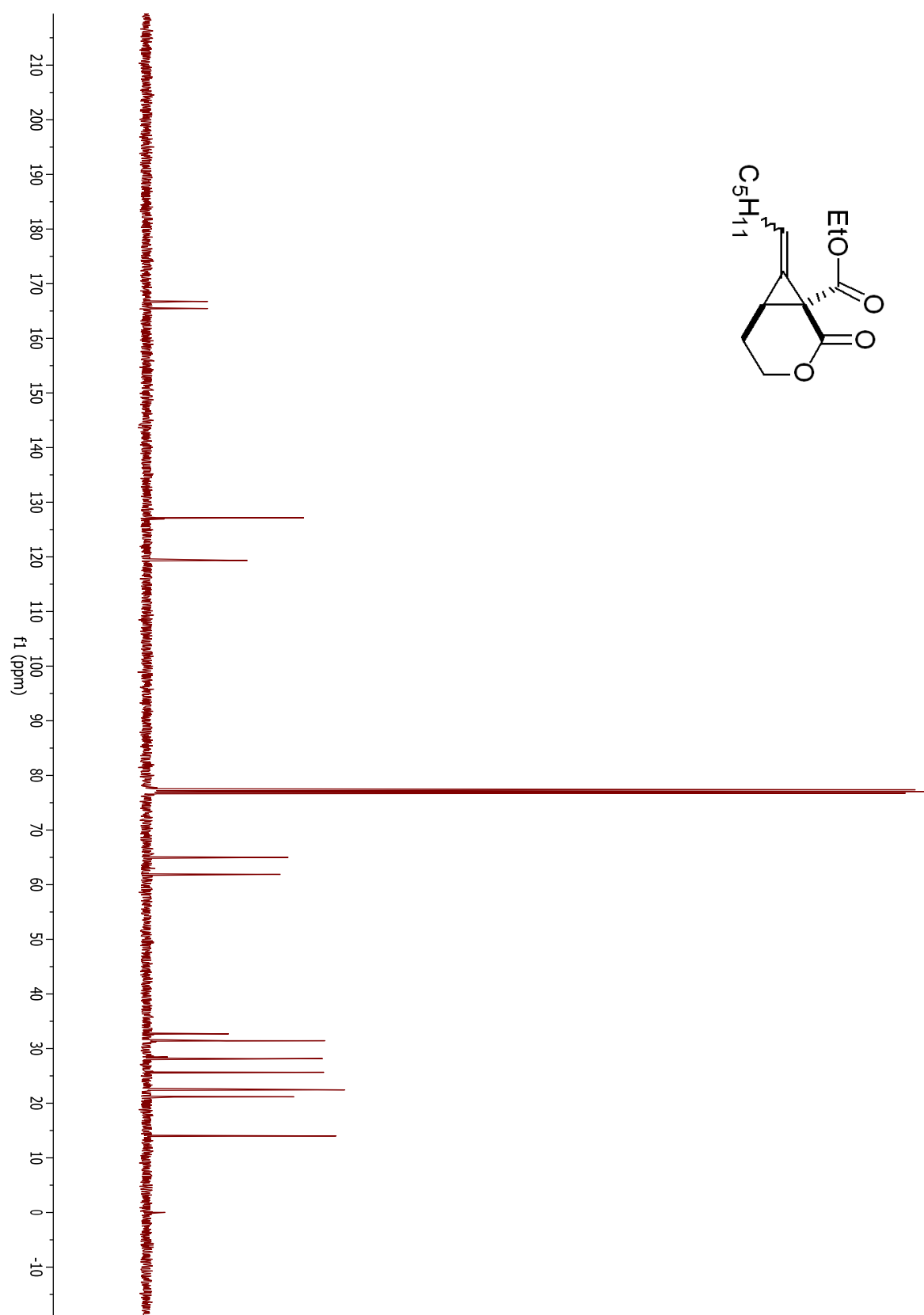
## Compound 1.97



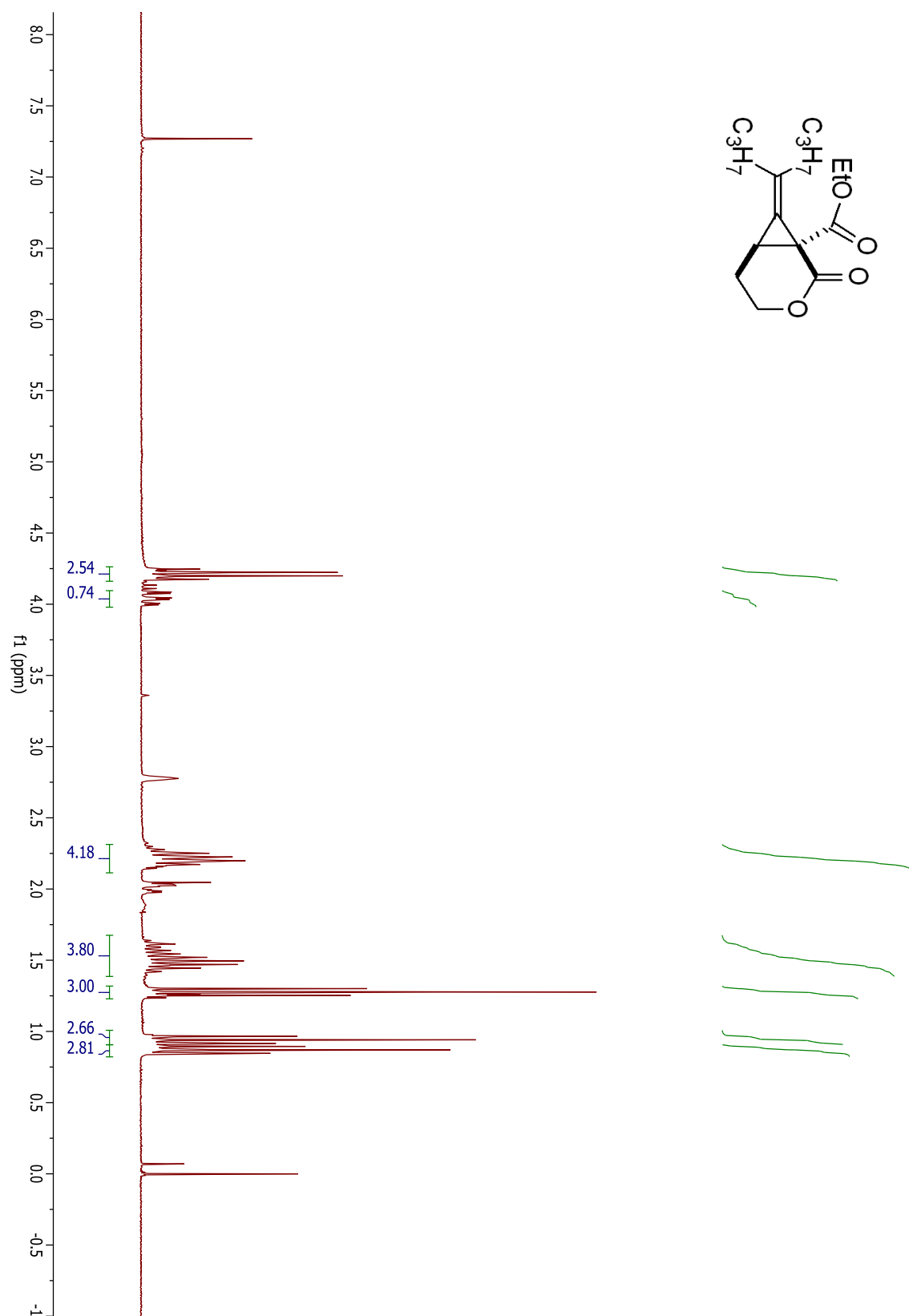
## Compound 1.98



## Compound 1.98

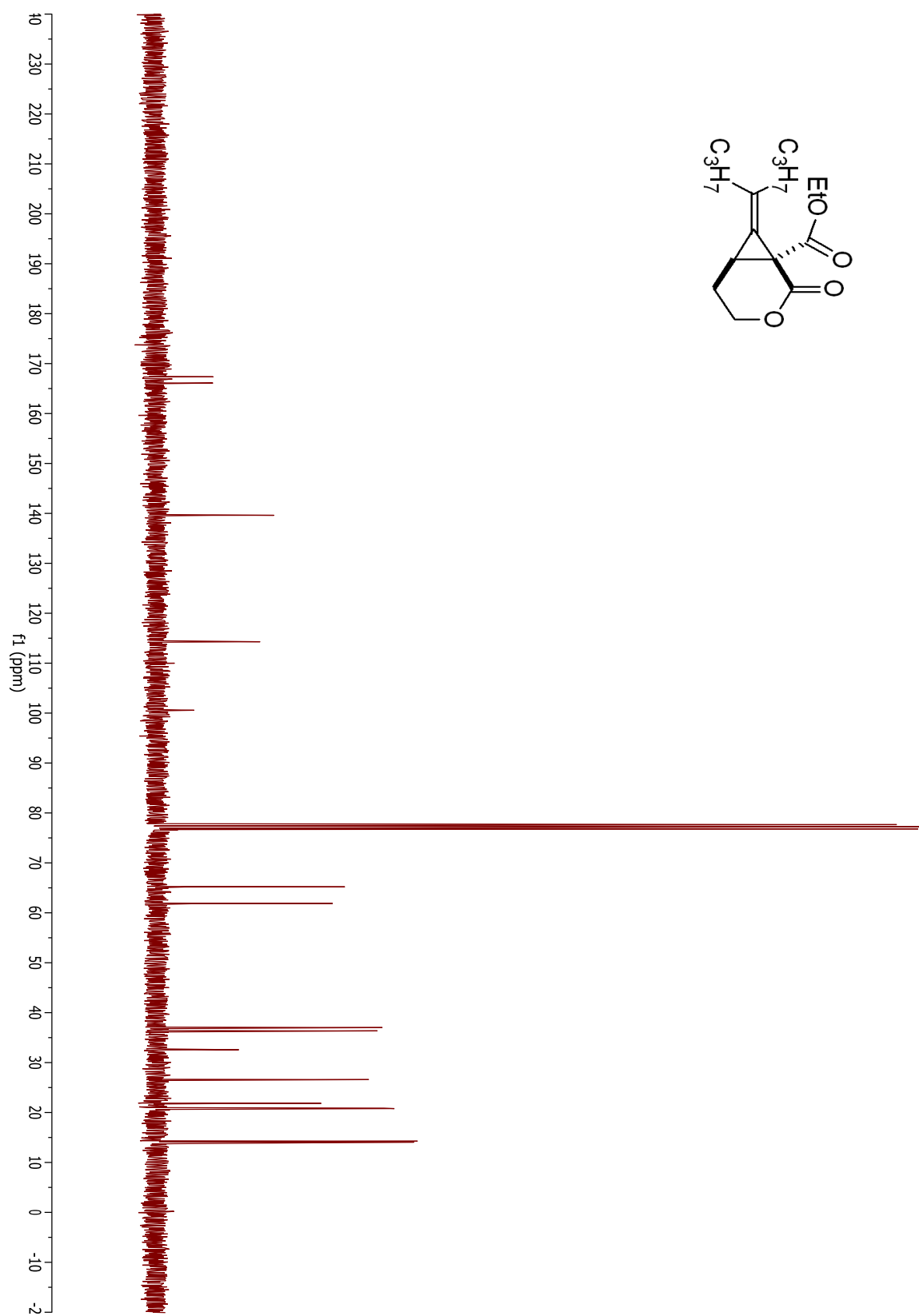


## Compound 1.99

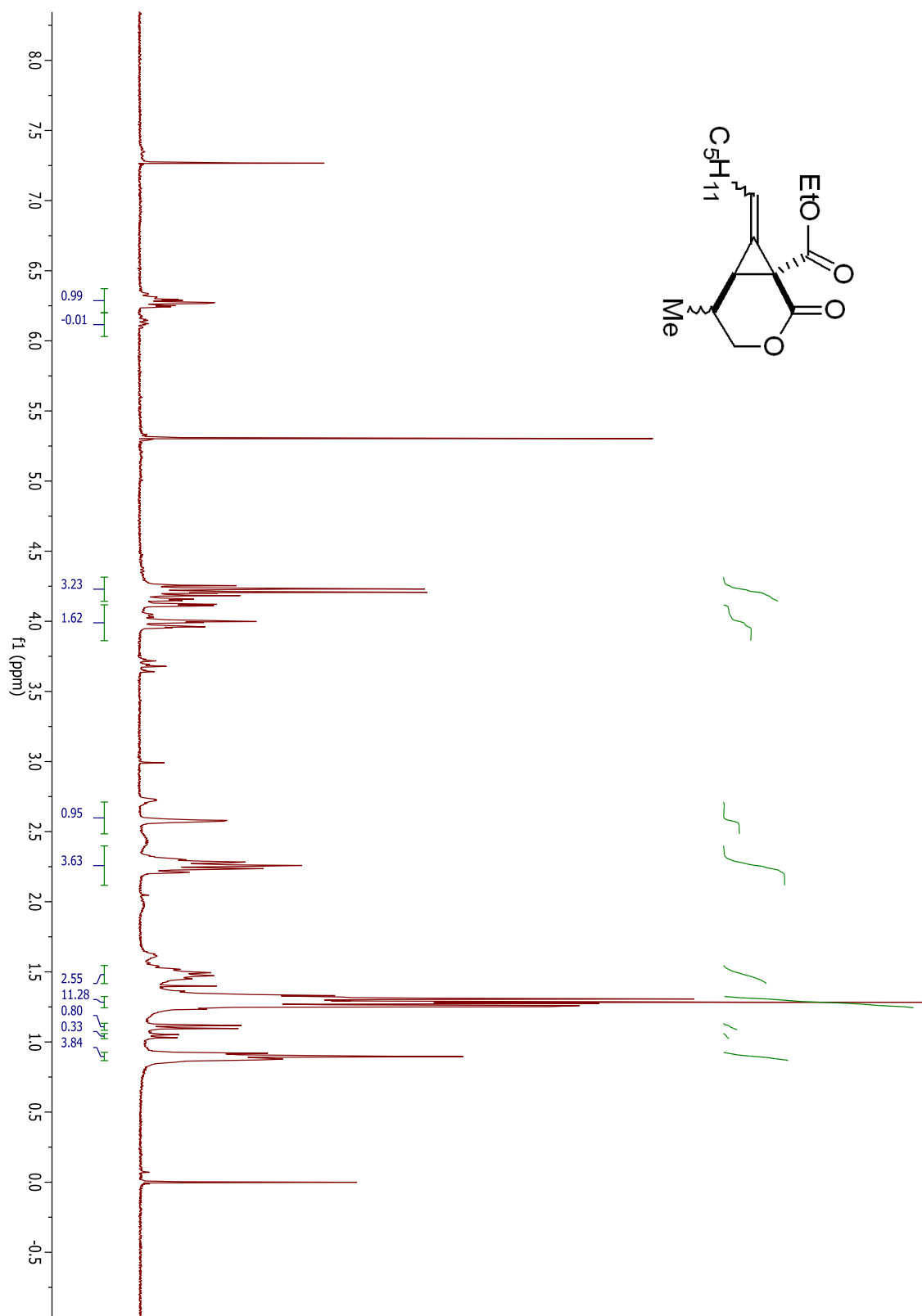




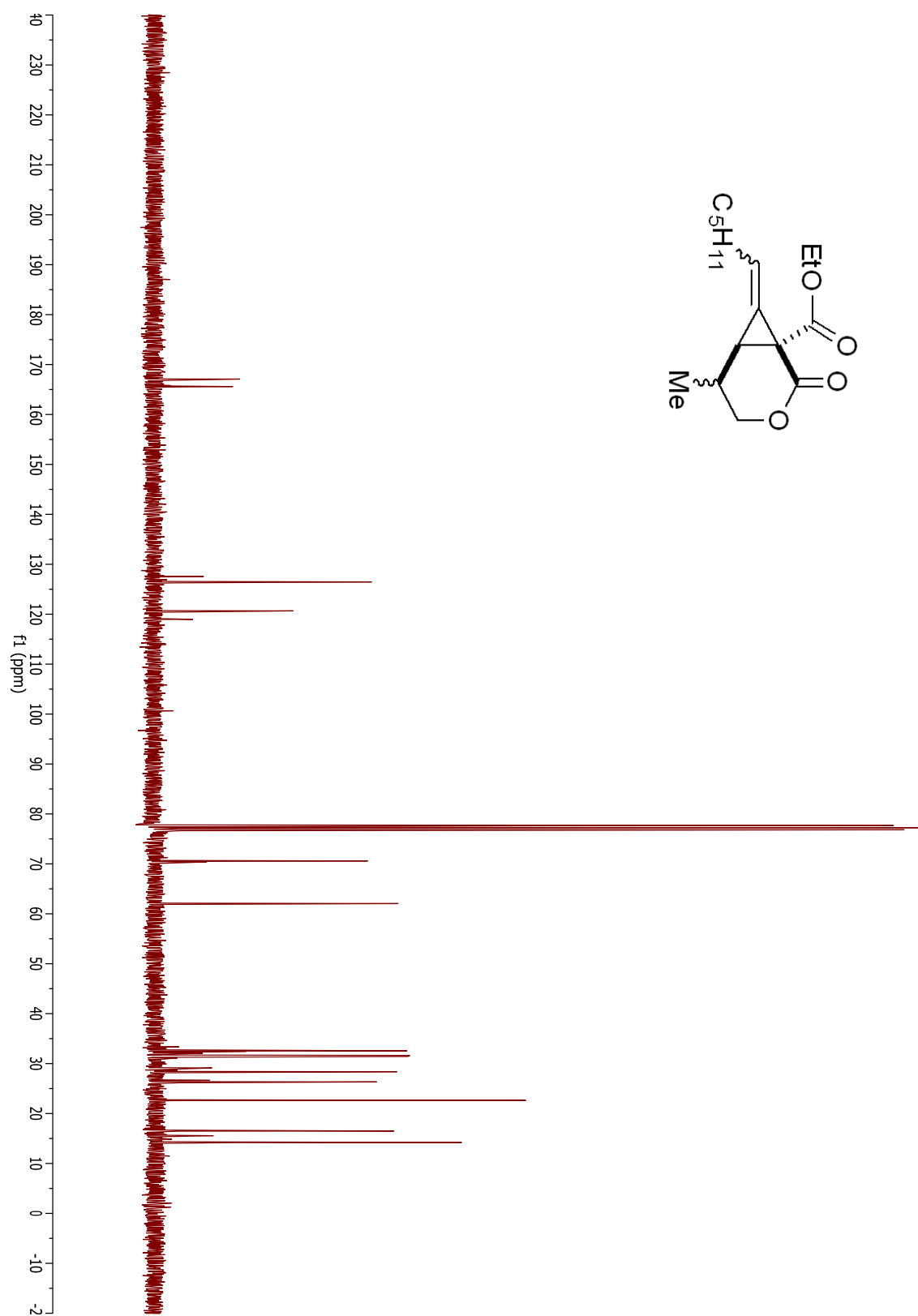
## Compound 1.99



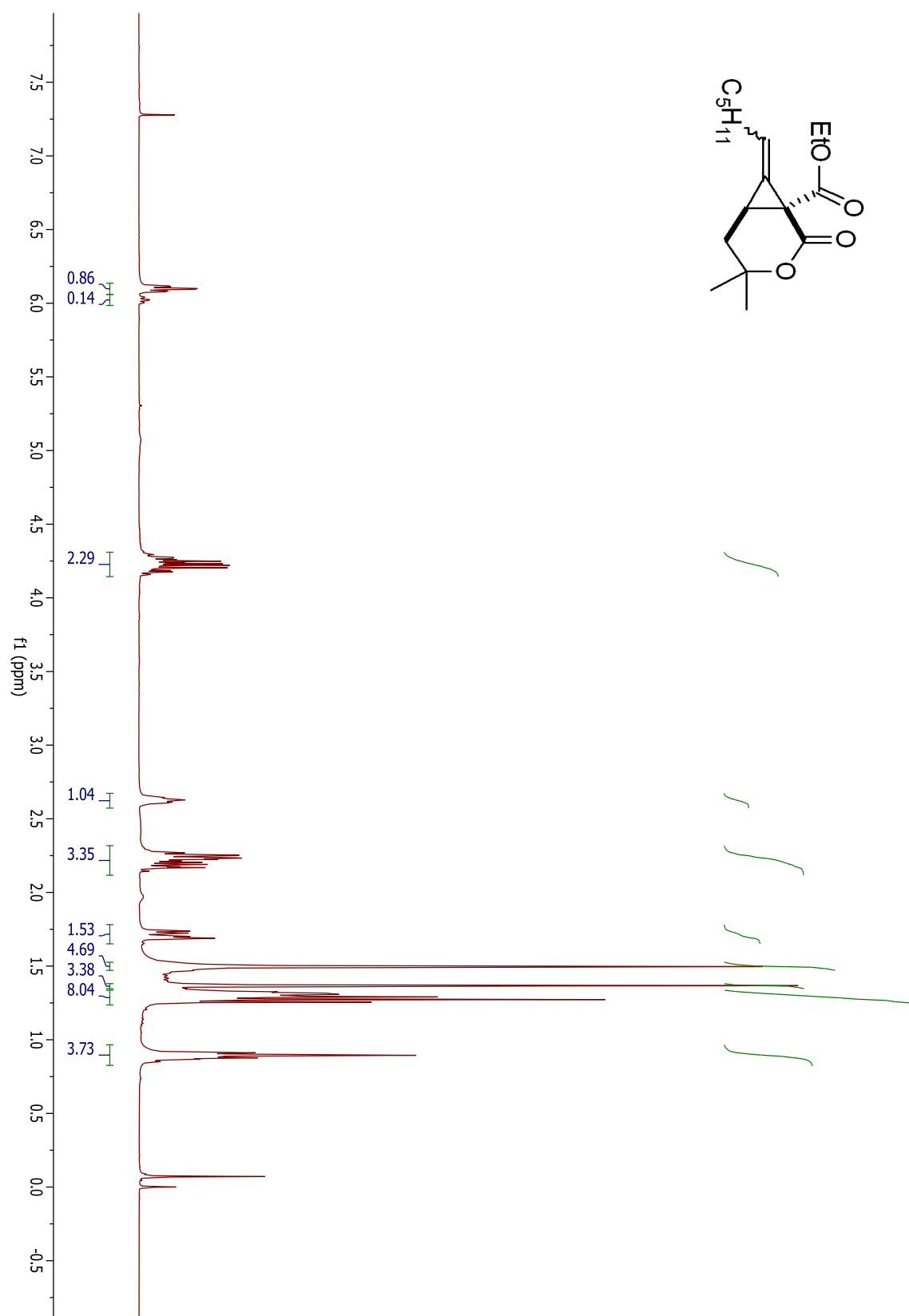
## Compound 1.101



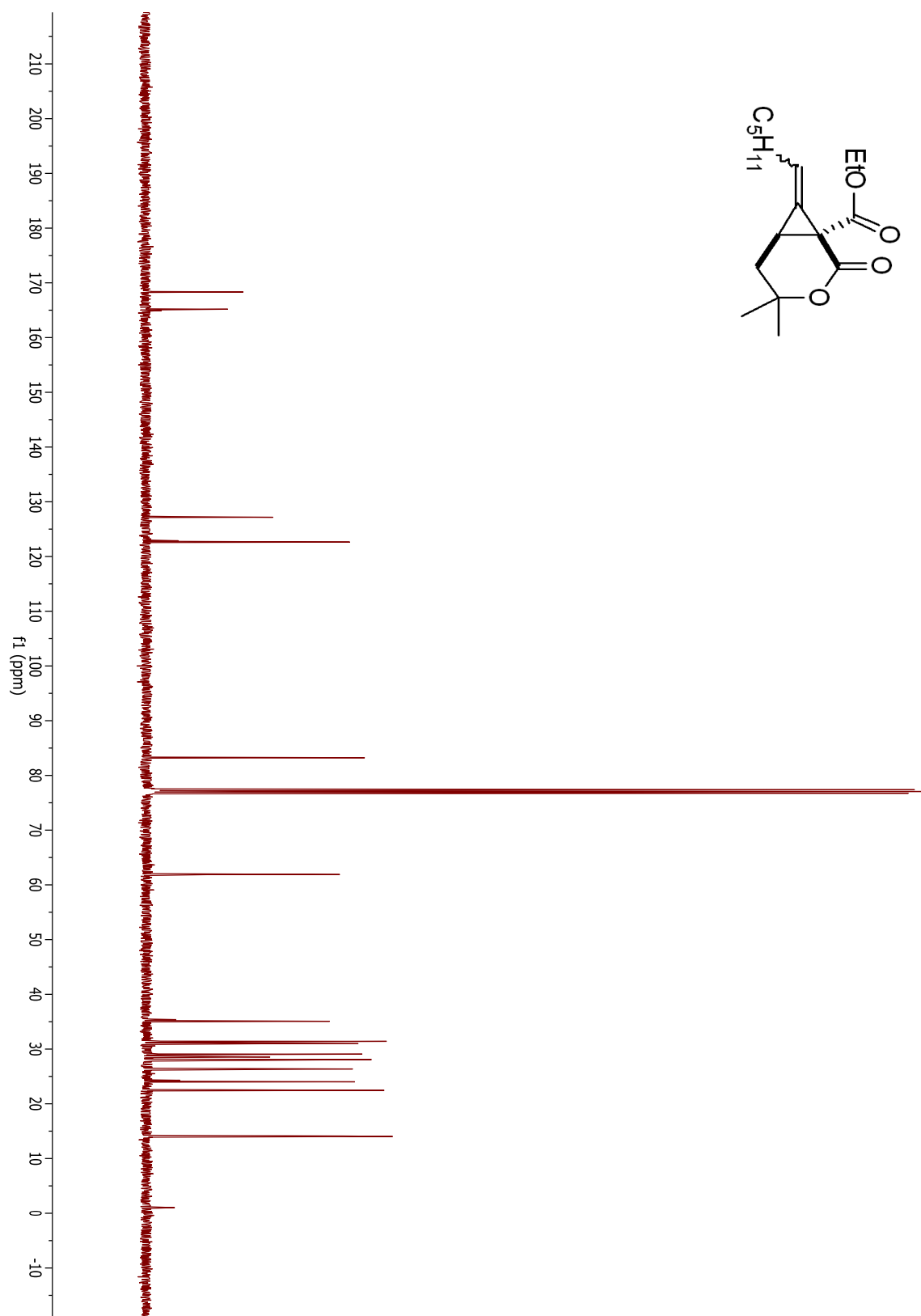
## Compound 1.101



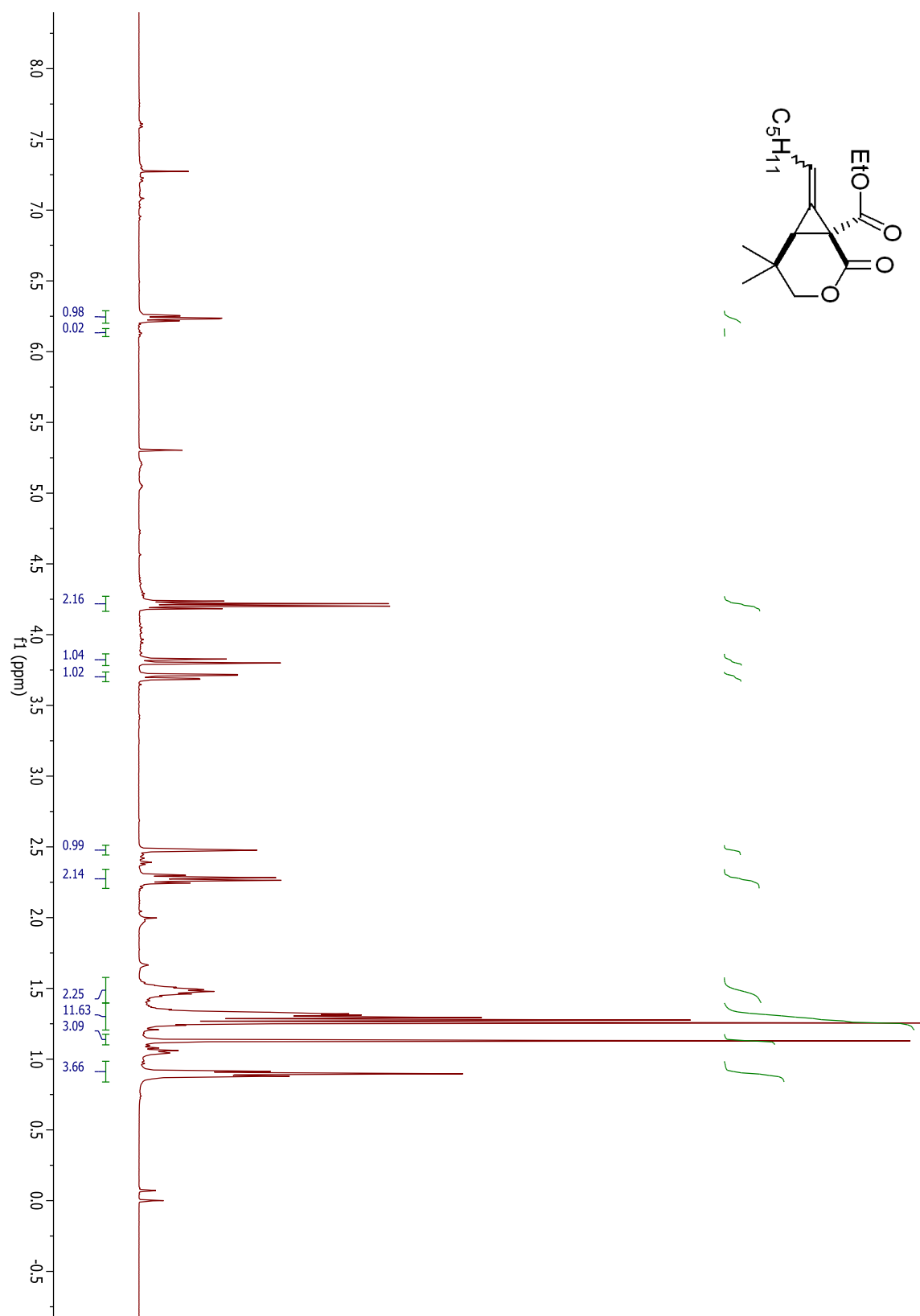
## Compound 1.102



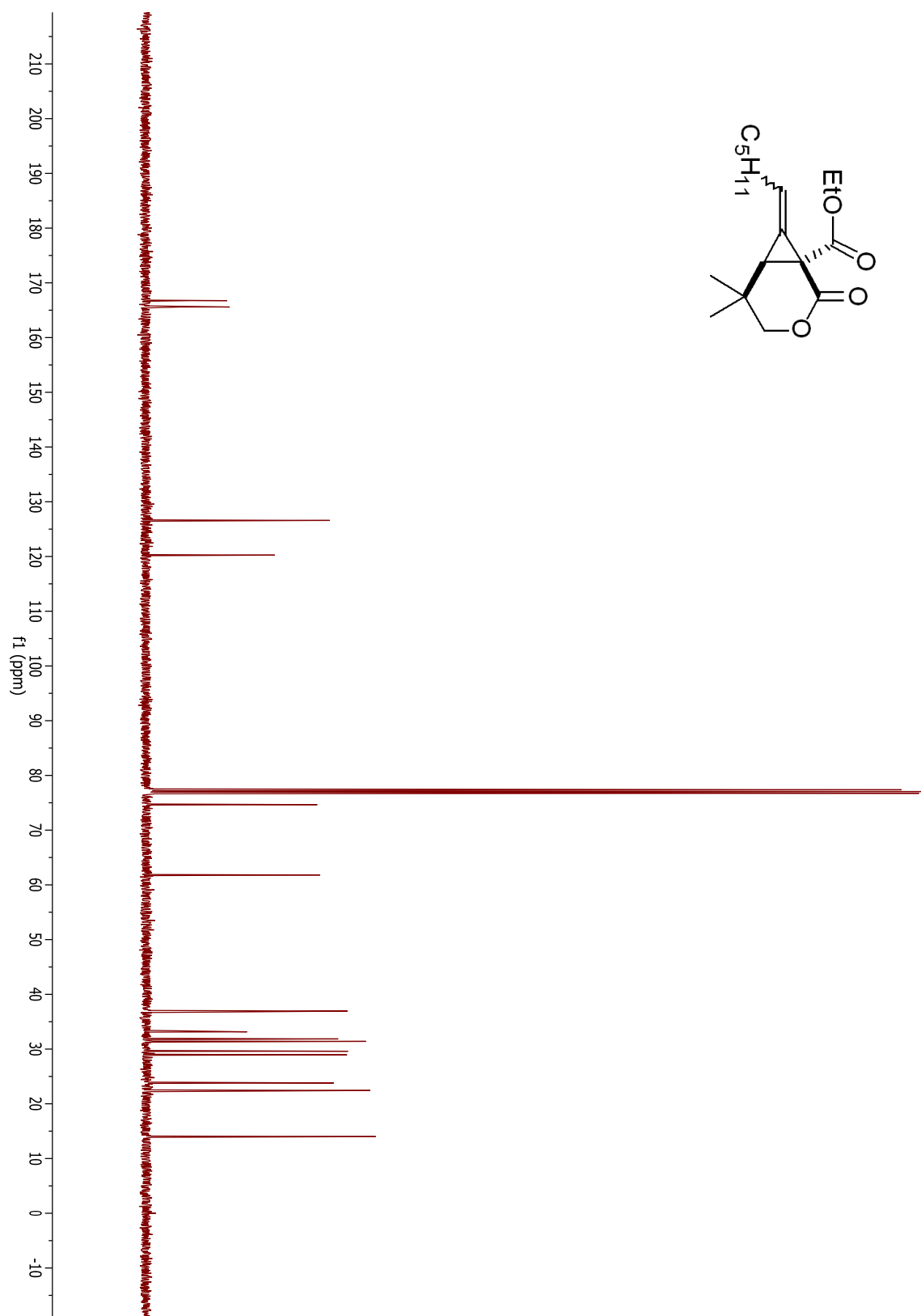
## Compound 1.102



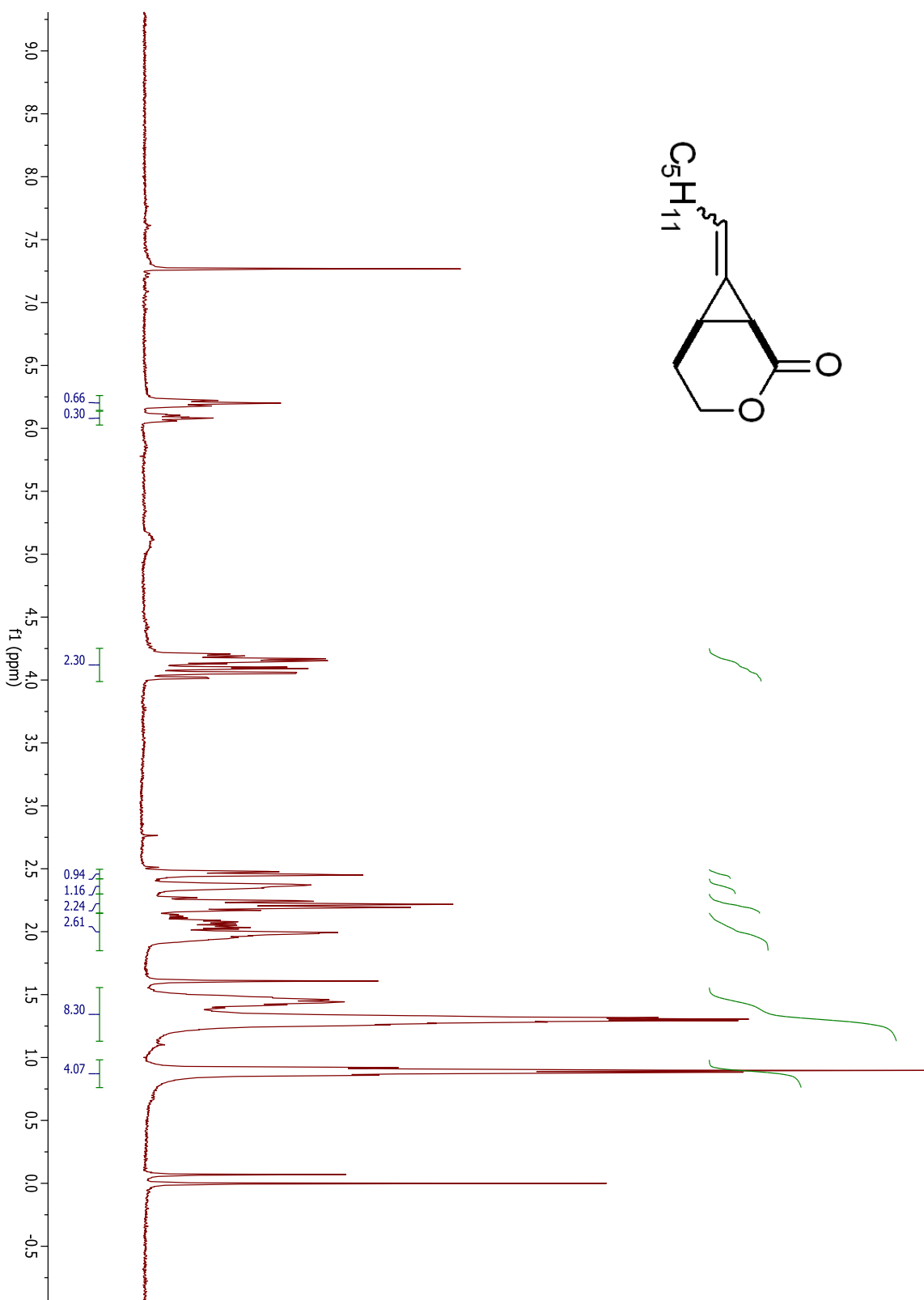
## Compound 1.104



## Compound 1.104

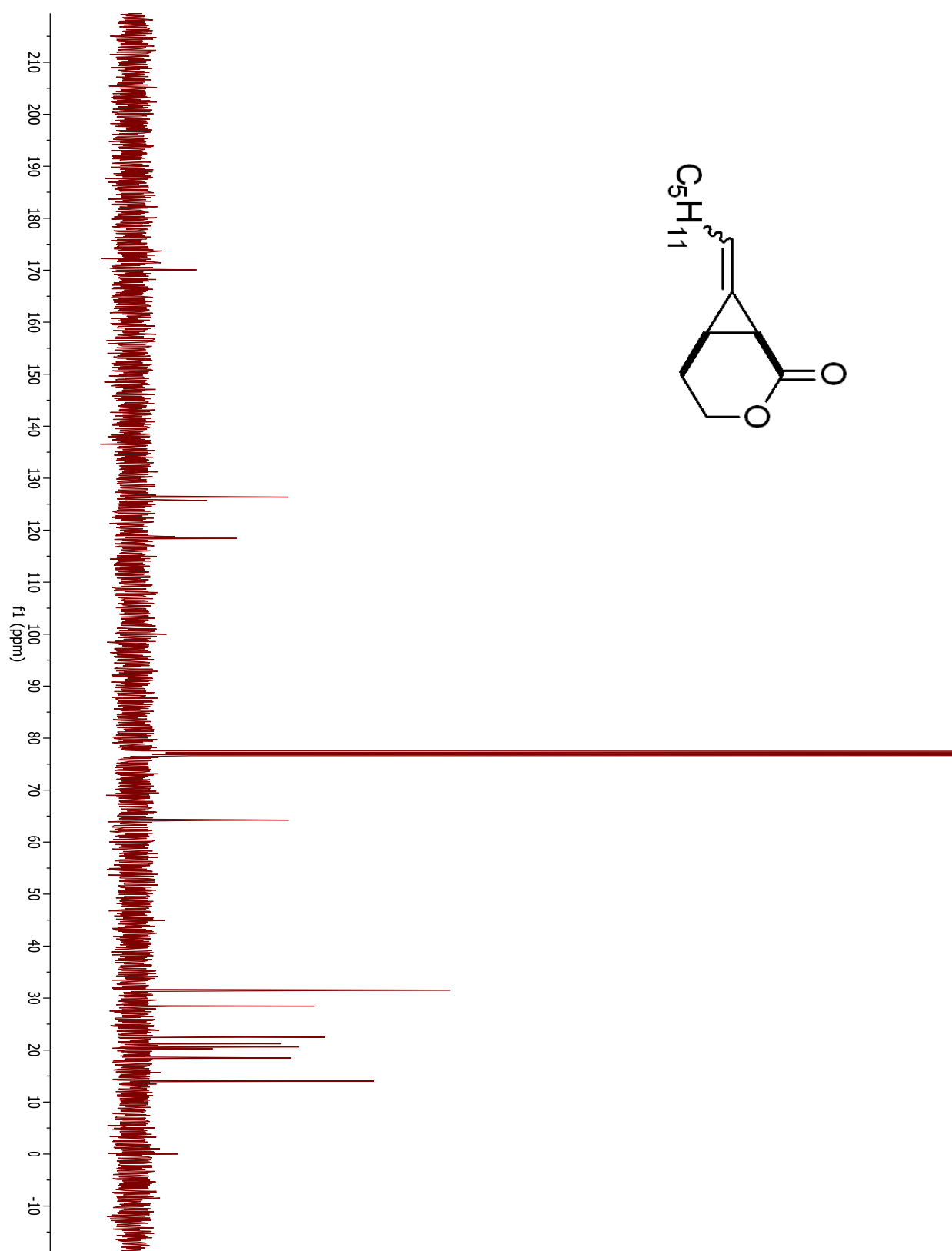


## Compound 1.106

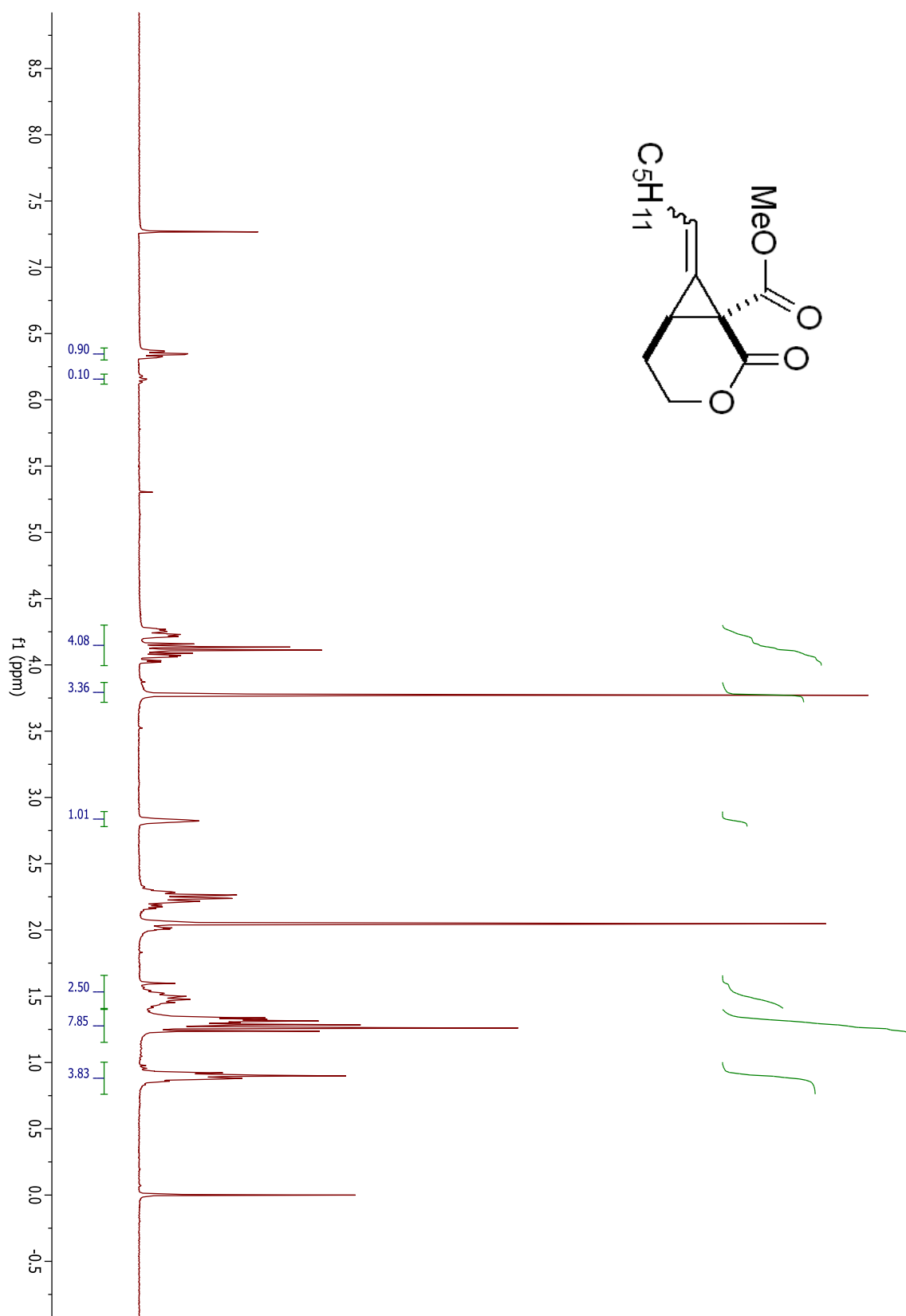




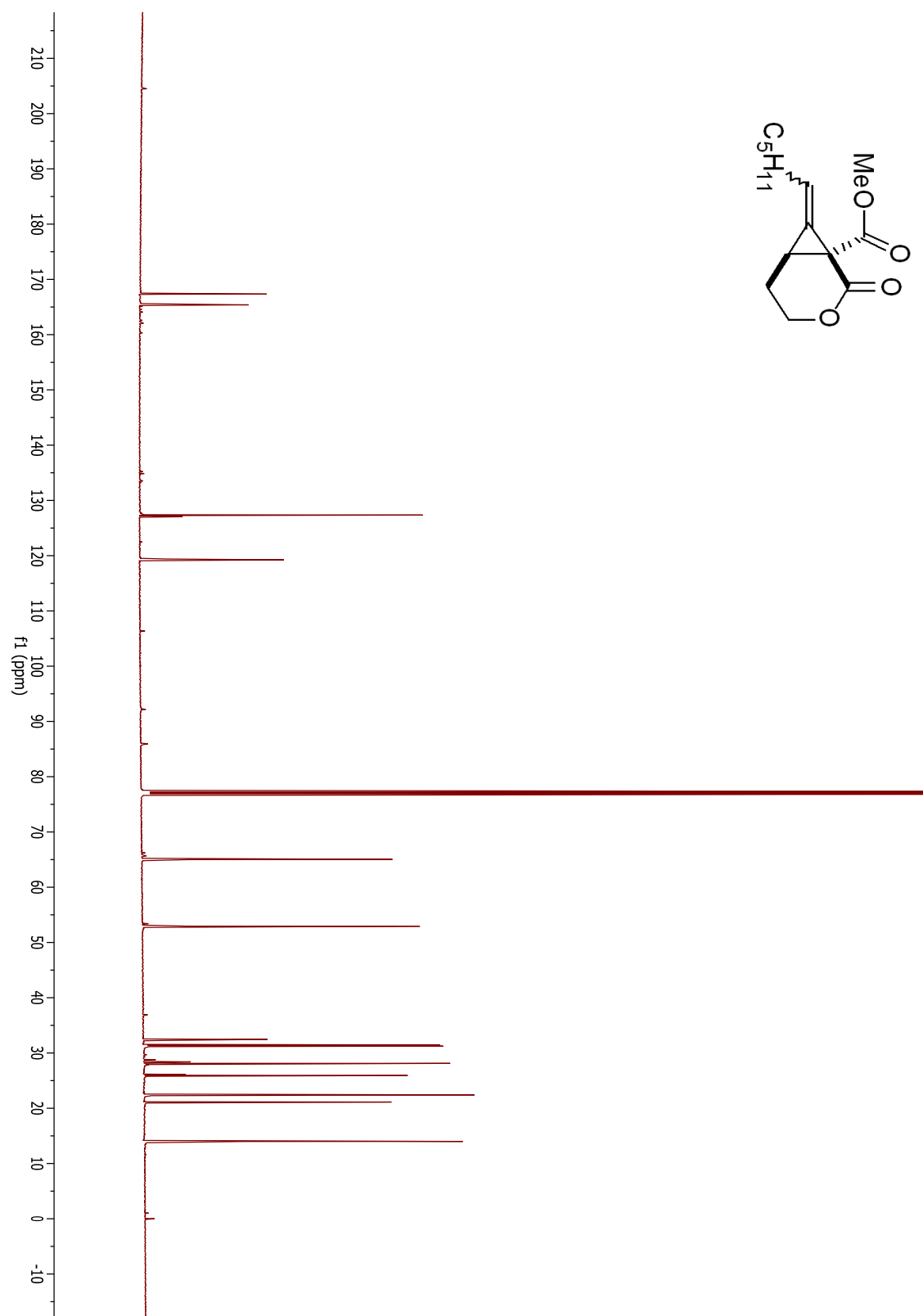
## Compound 1.106



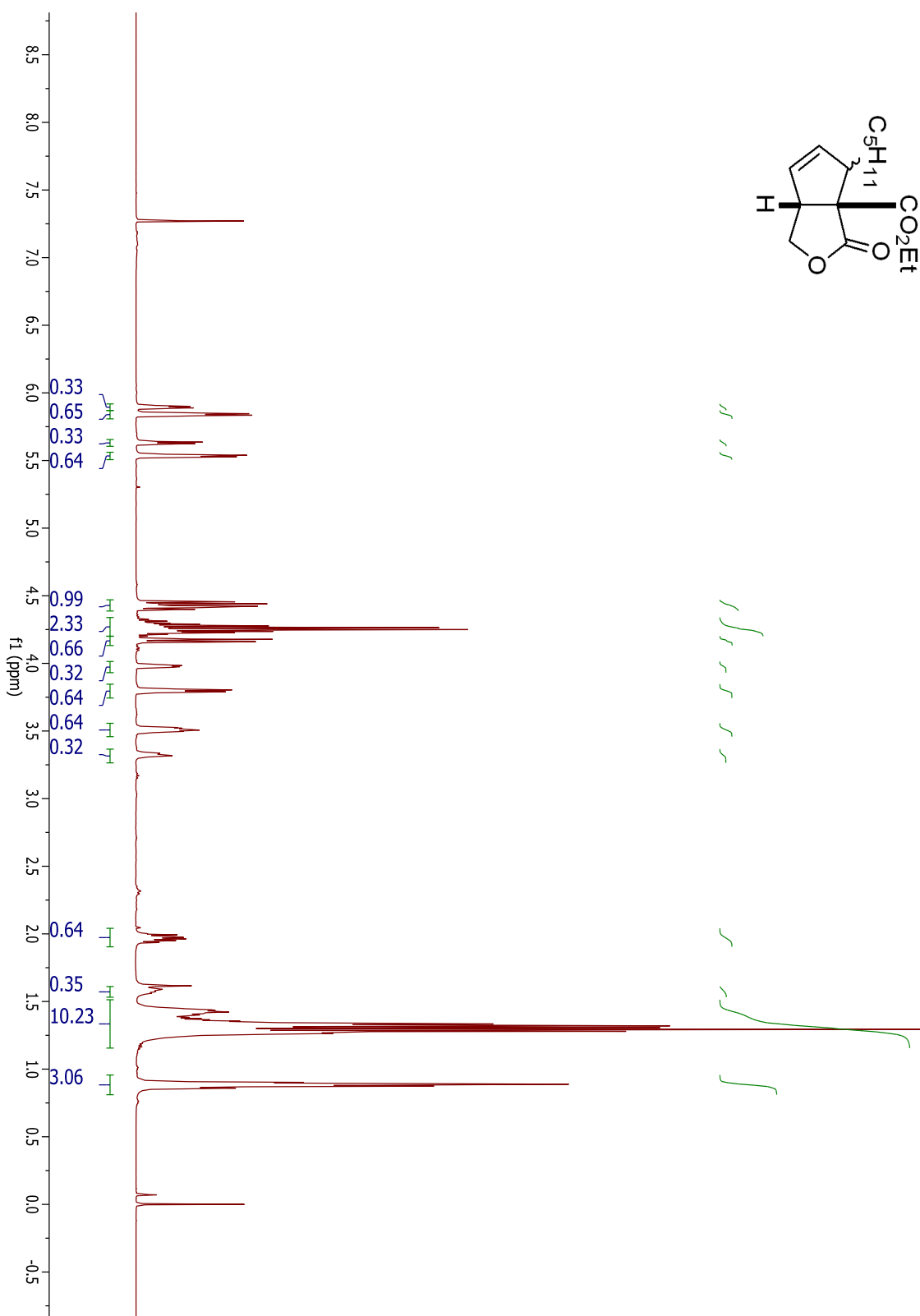
## Compound 1.108



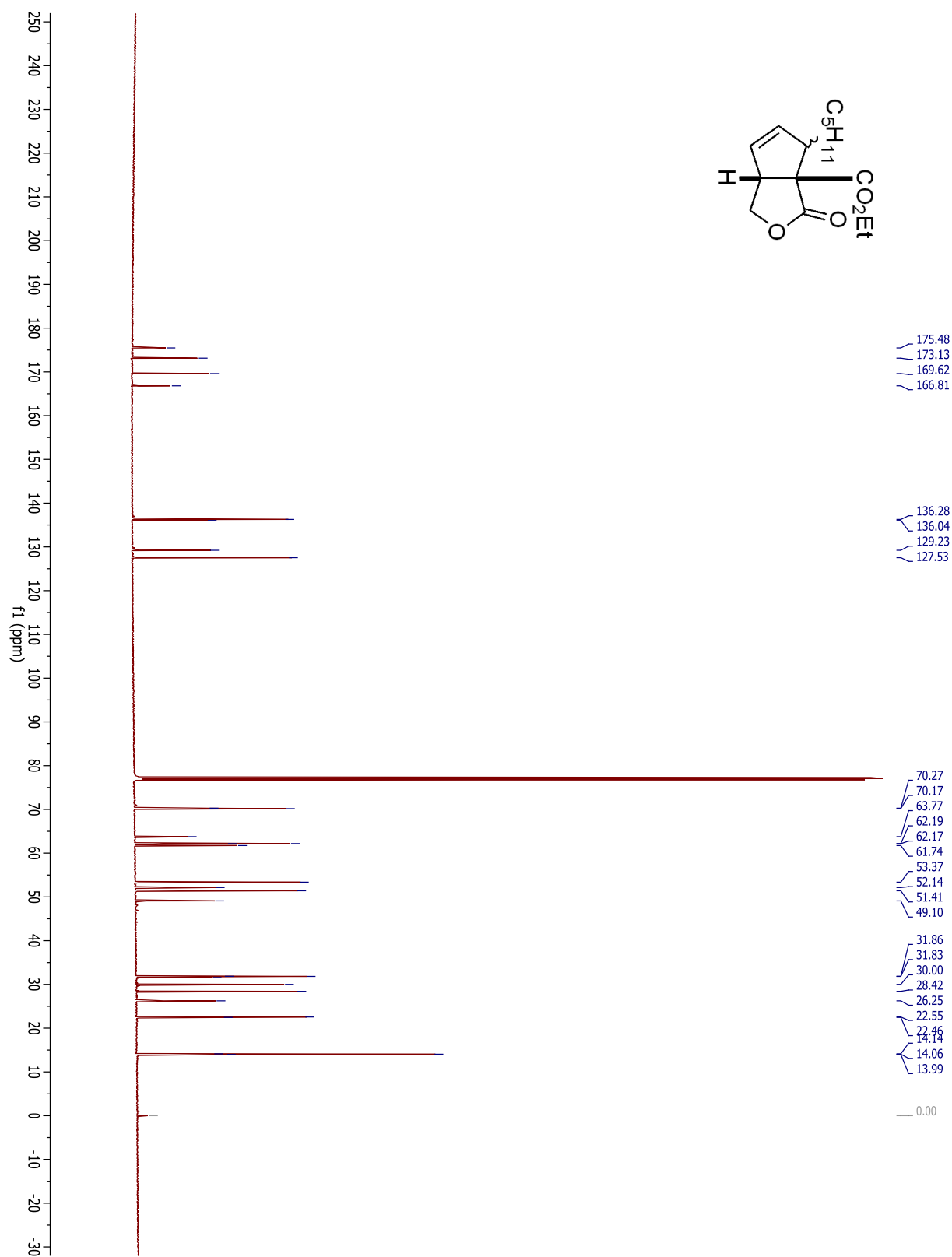
## Compound 1.108



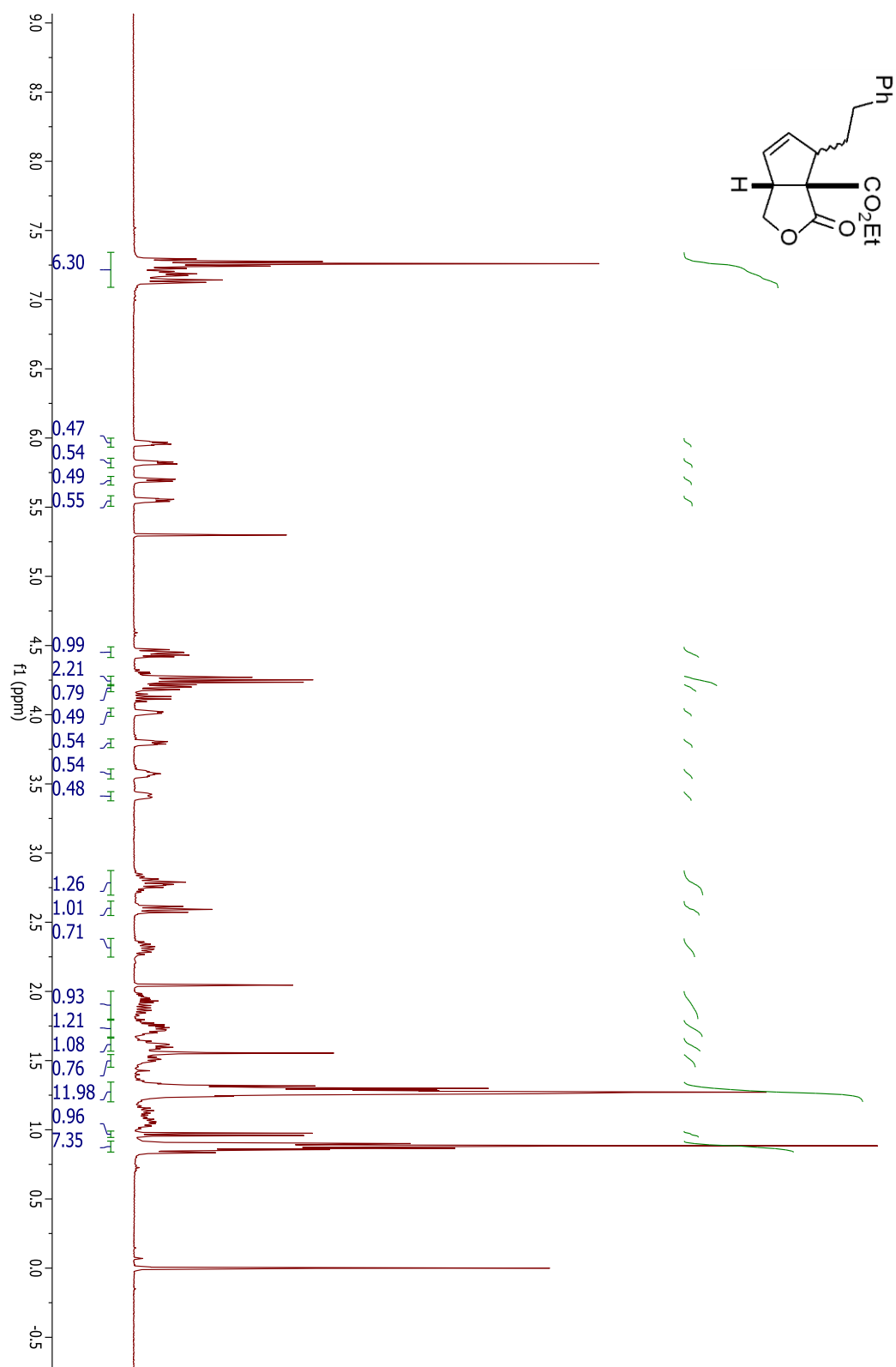
## Compound 2.48



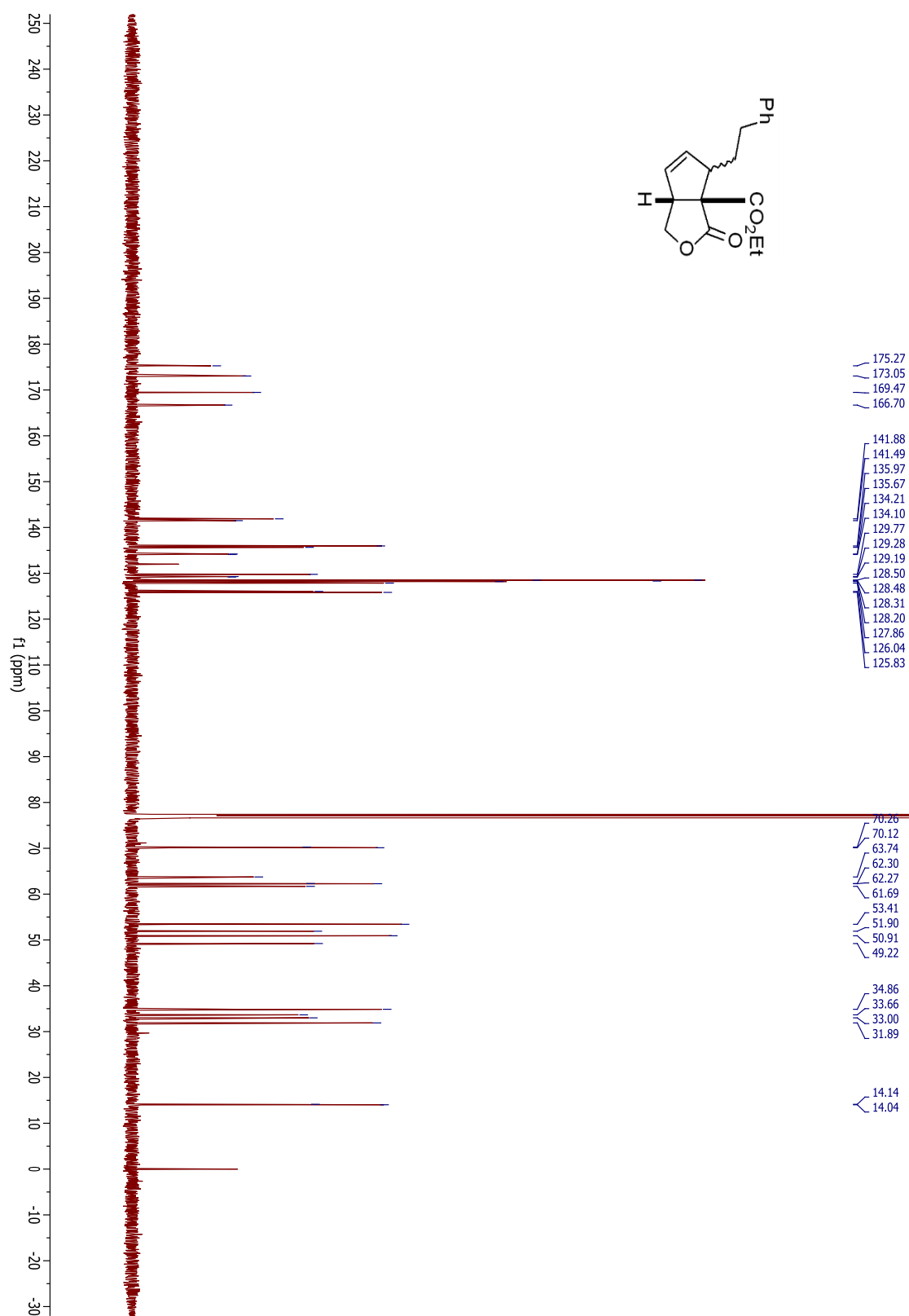
## Compound 2.48



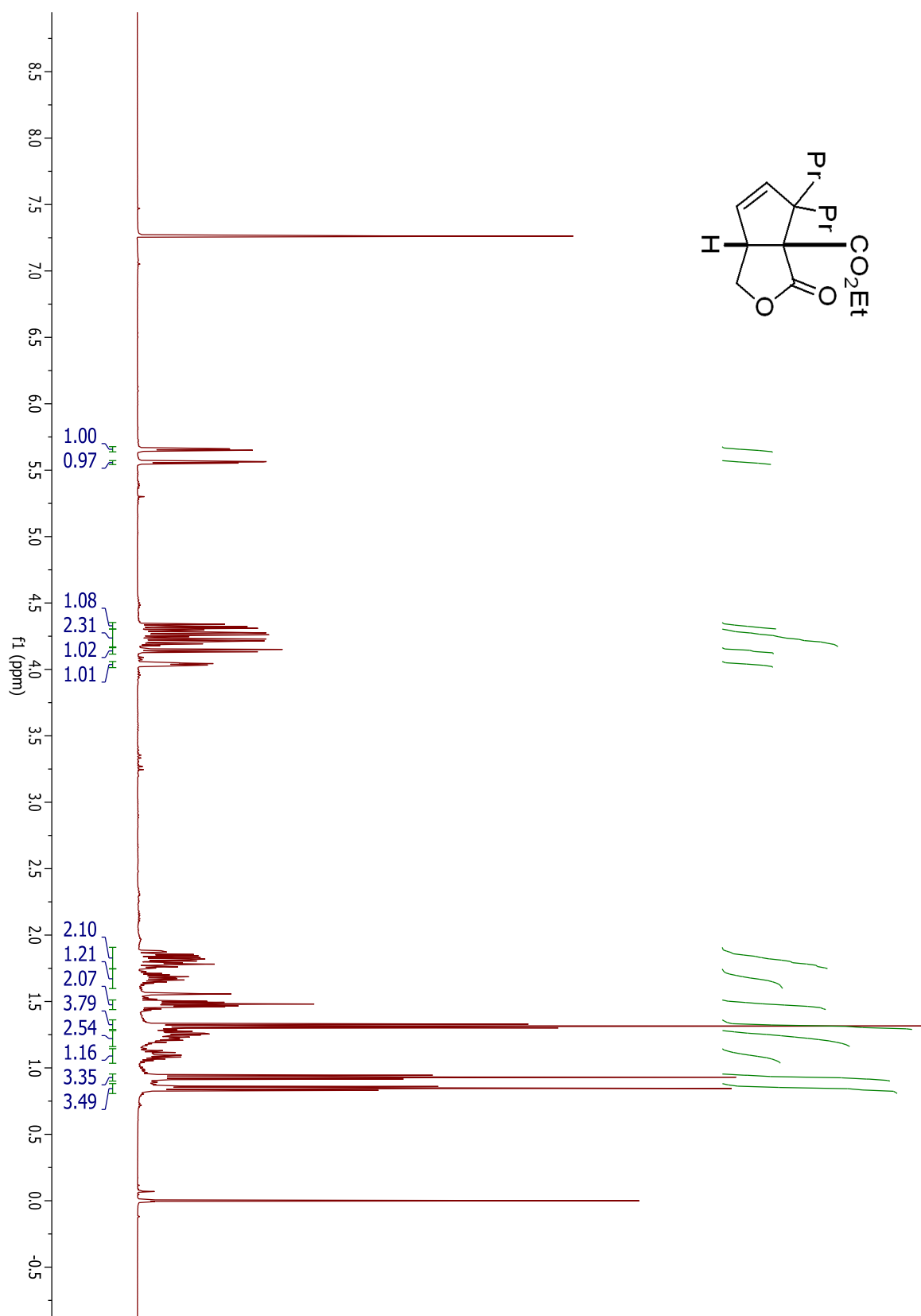
## Compound 2.49



## Compound 2.49

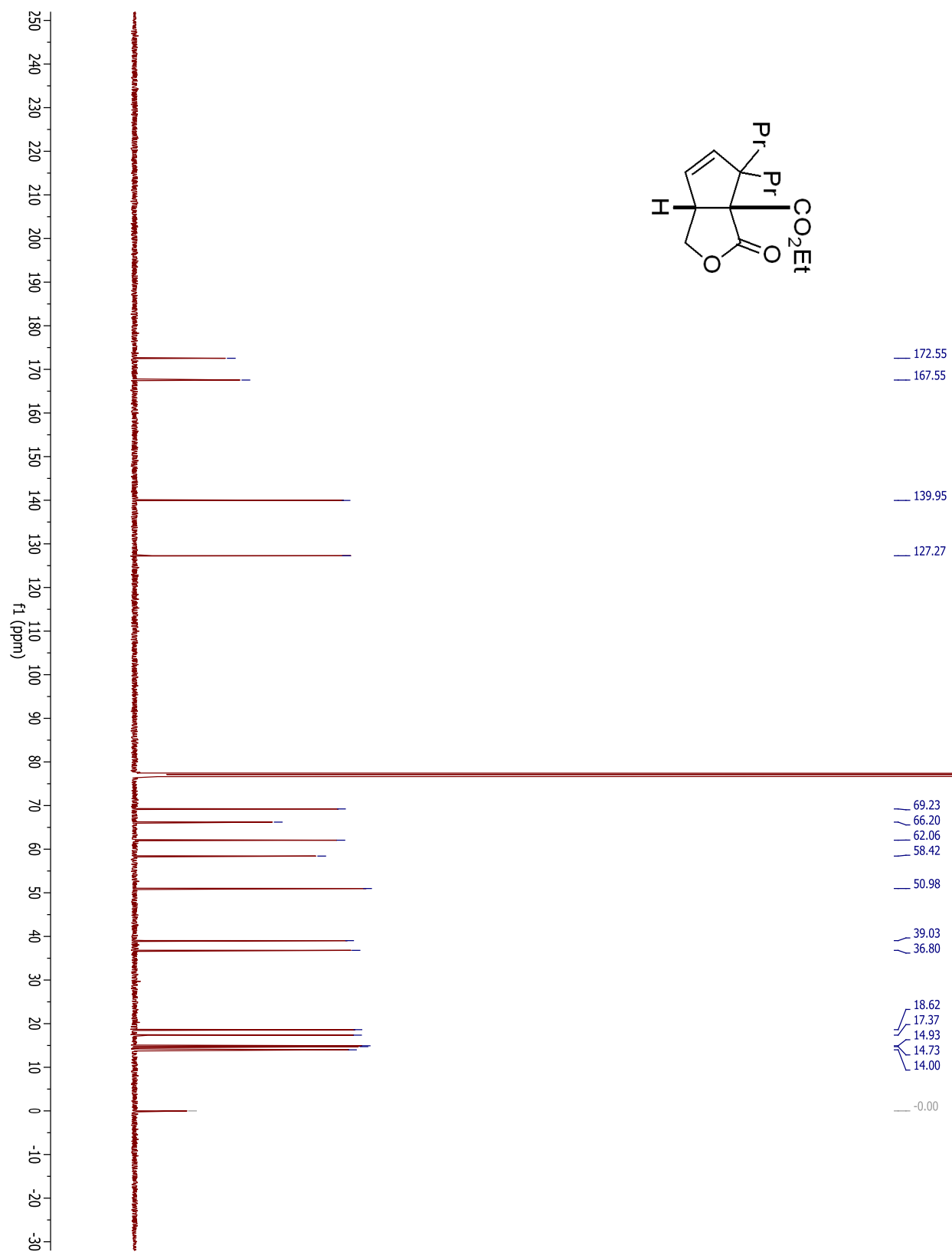


## Compound 2.50

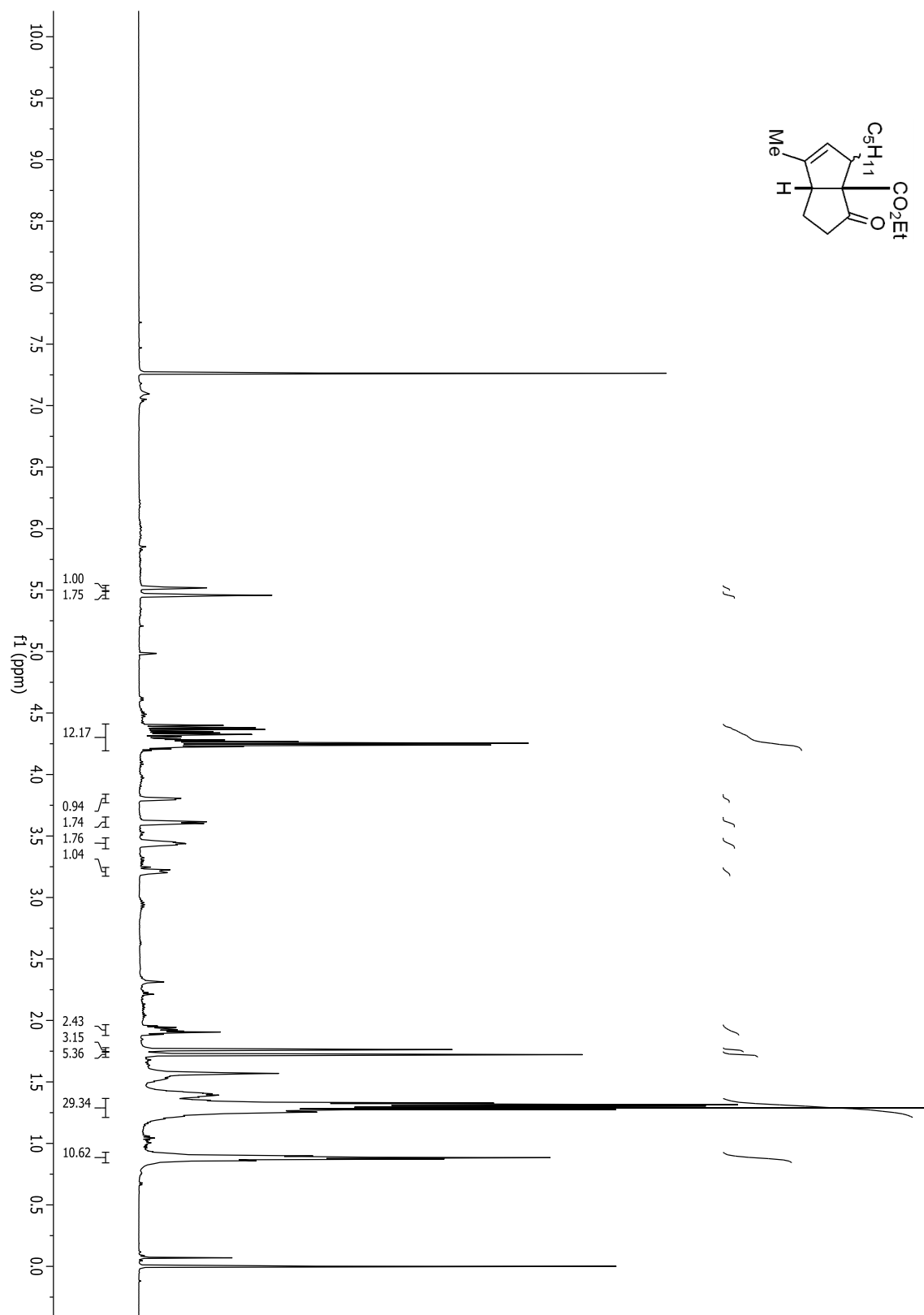




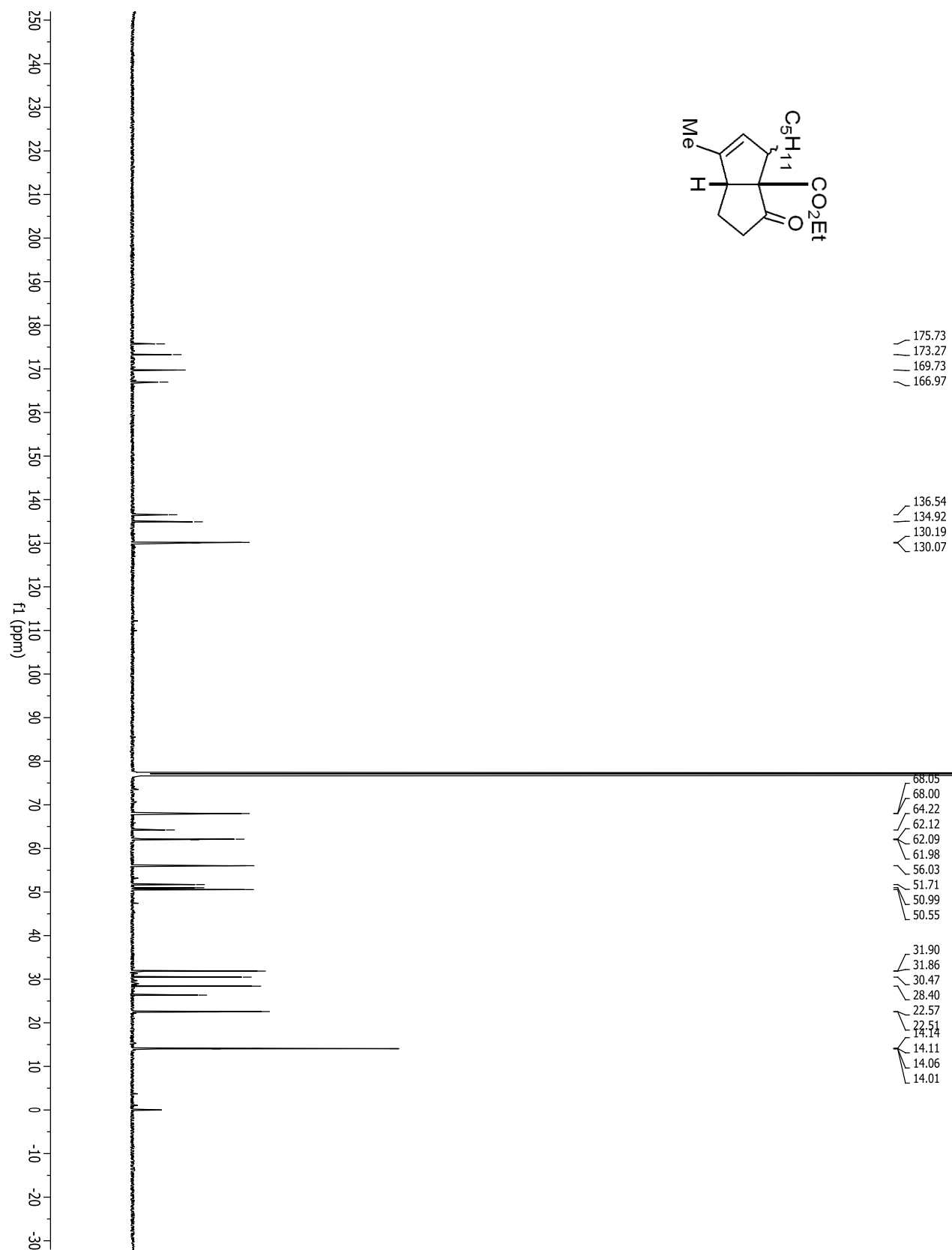
## Compound 2.50



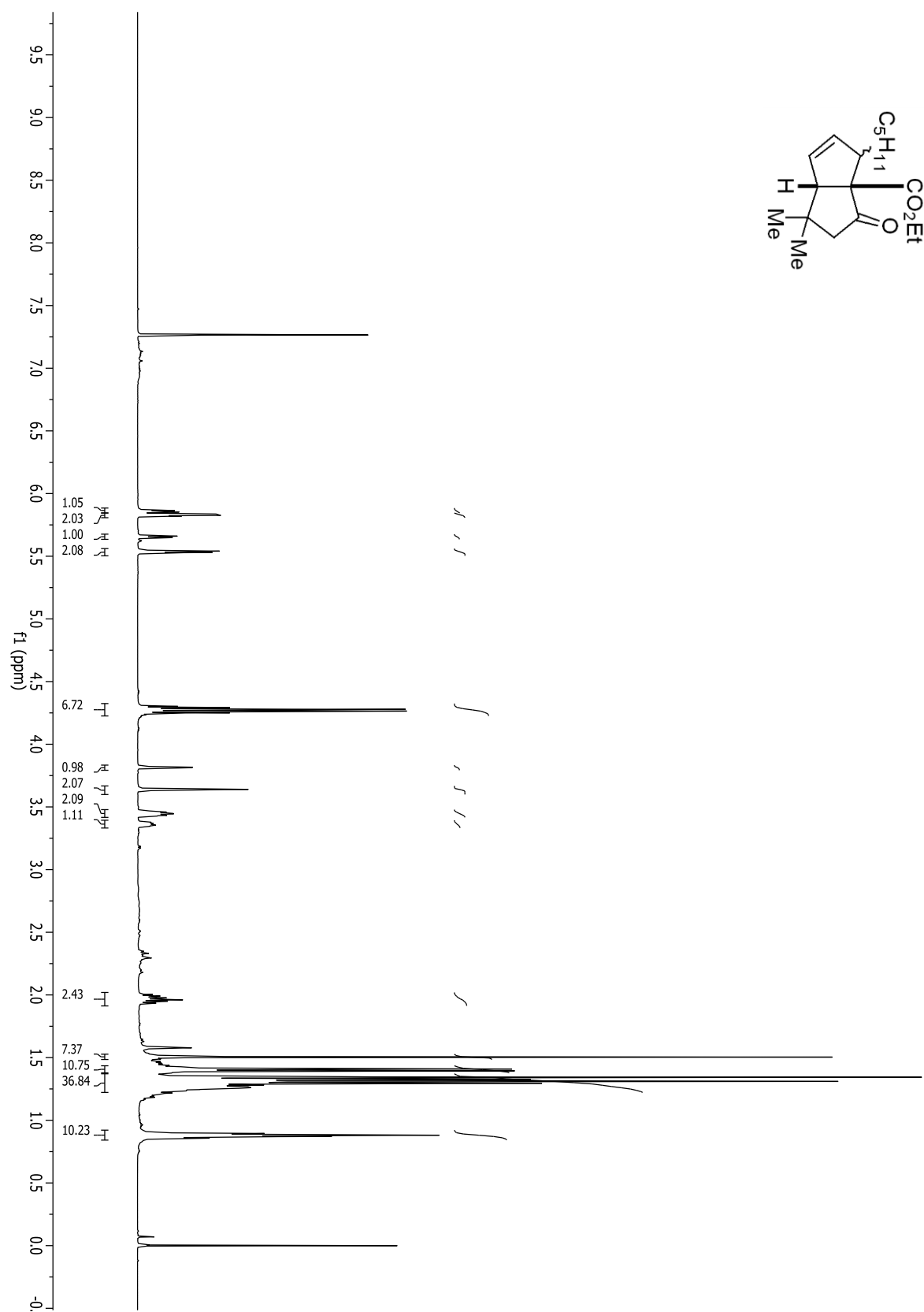
## Compound 2.51



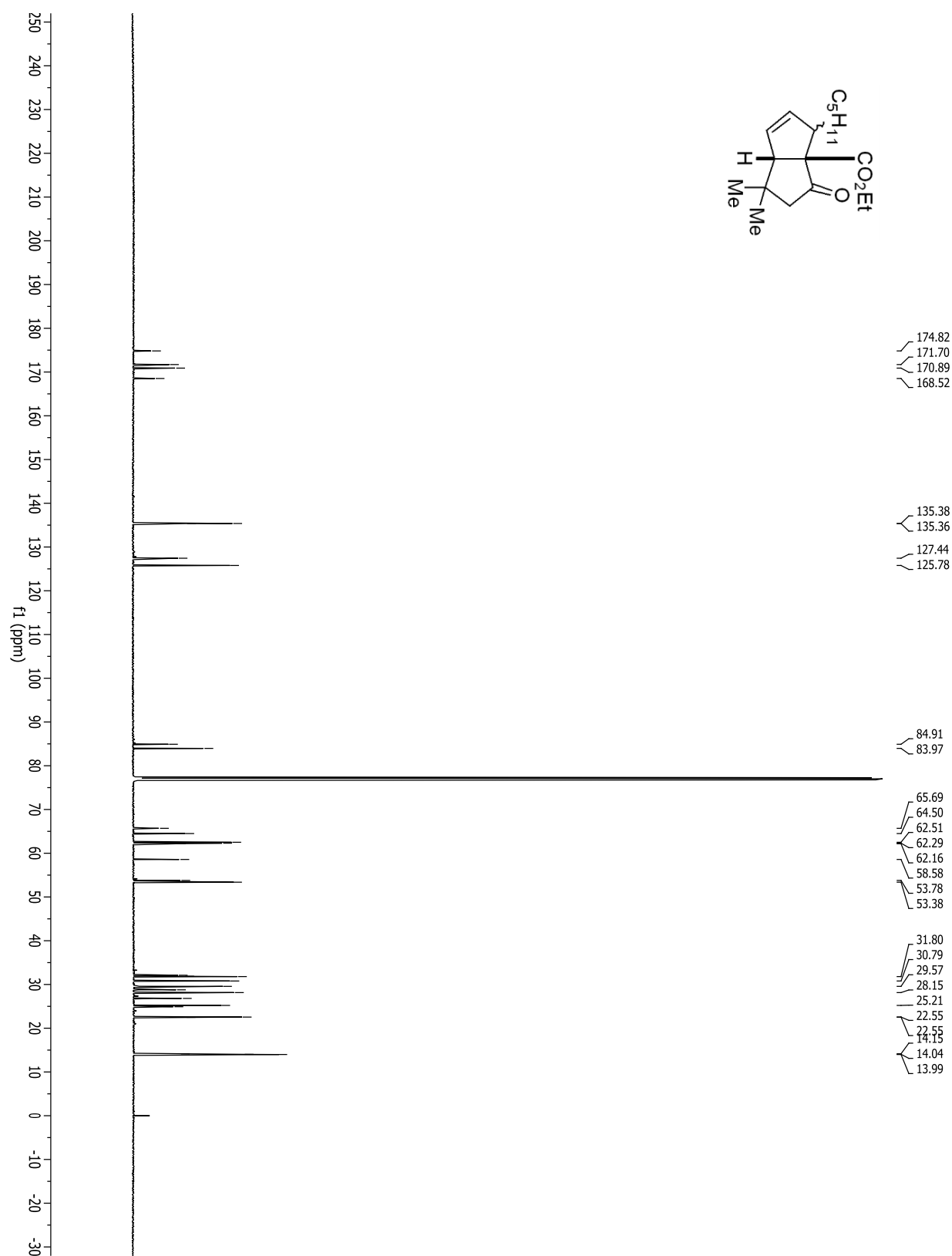
## Compound 2.51



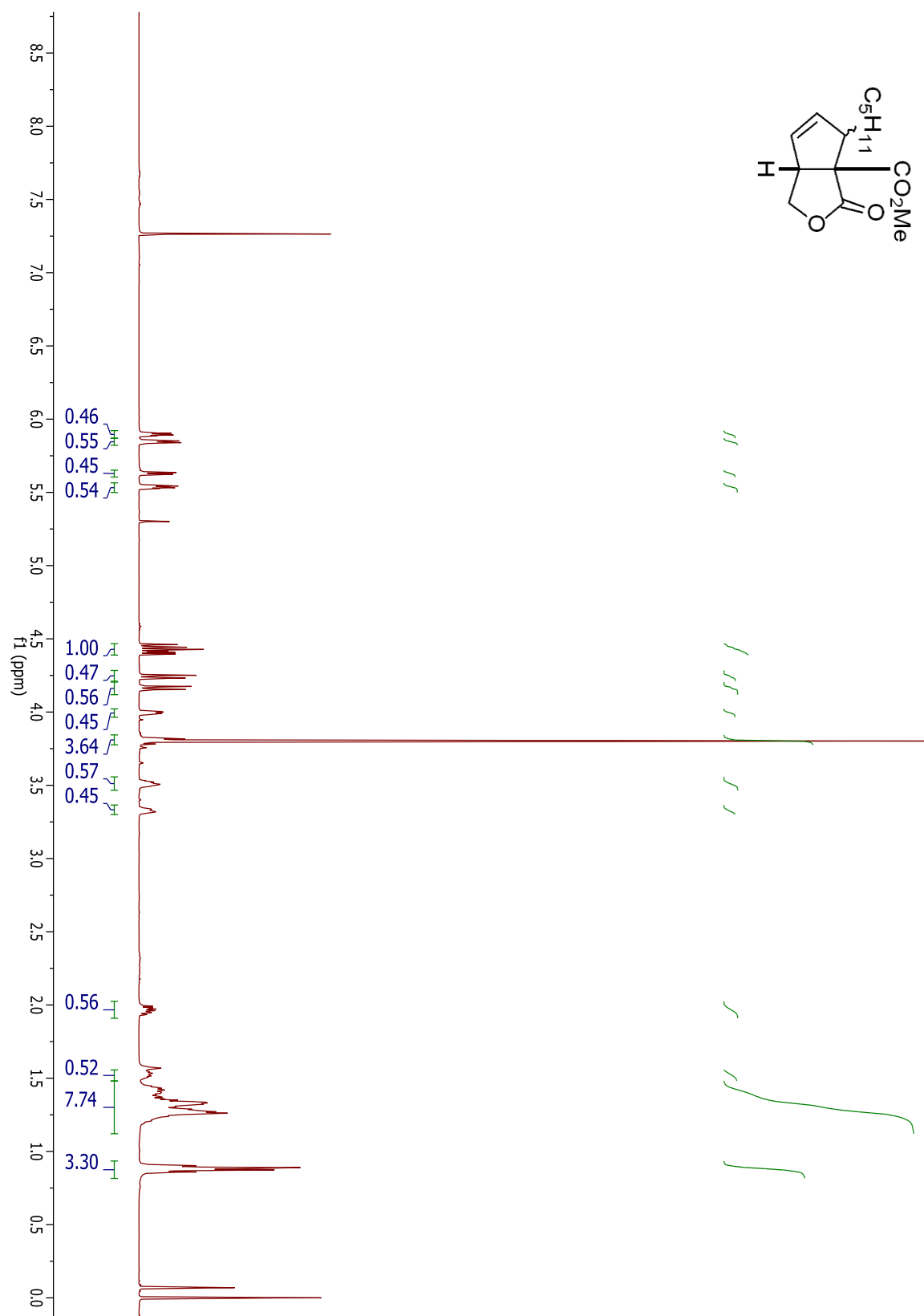
## Compound 2.52



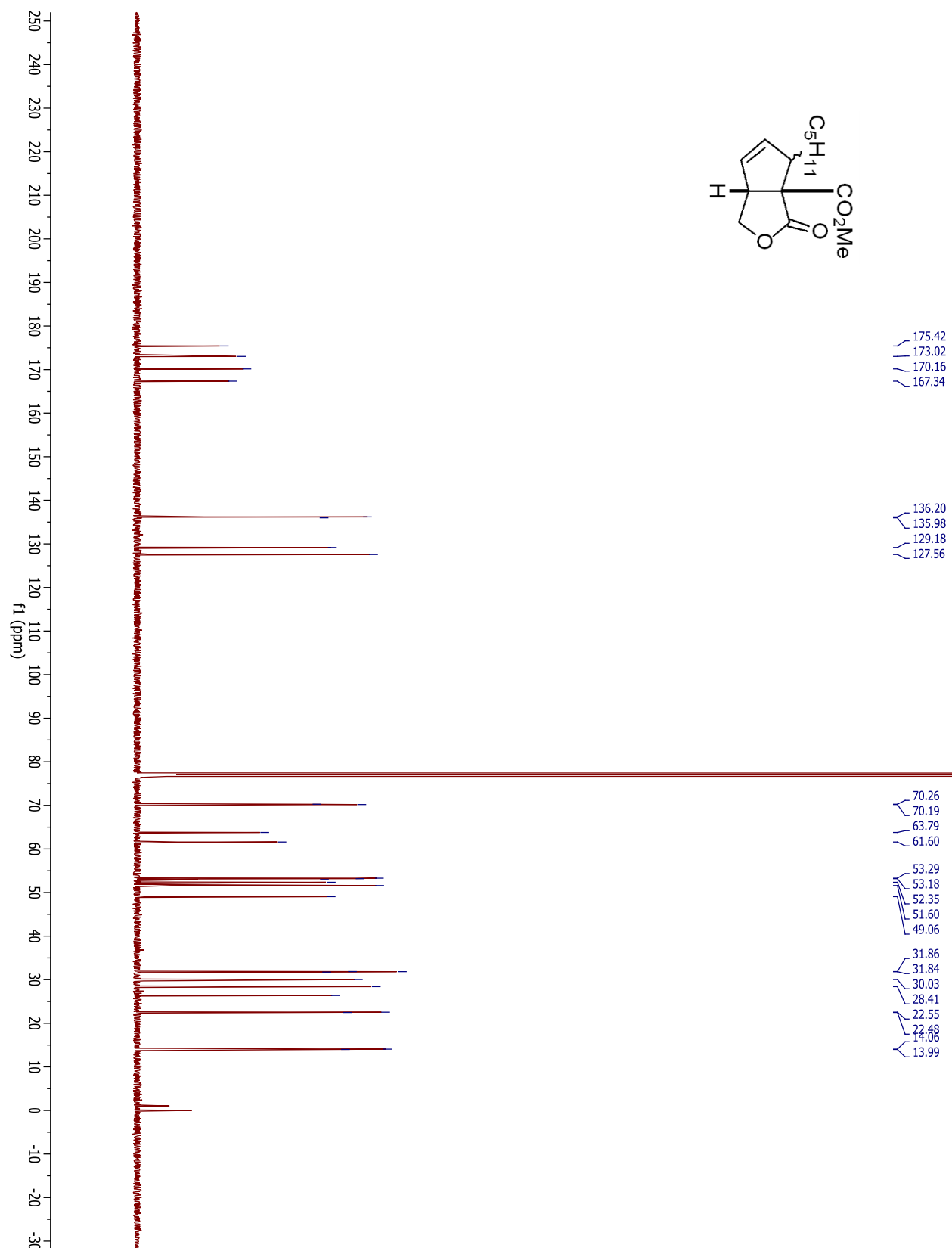
## Compound 2.52



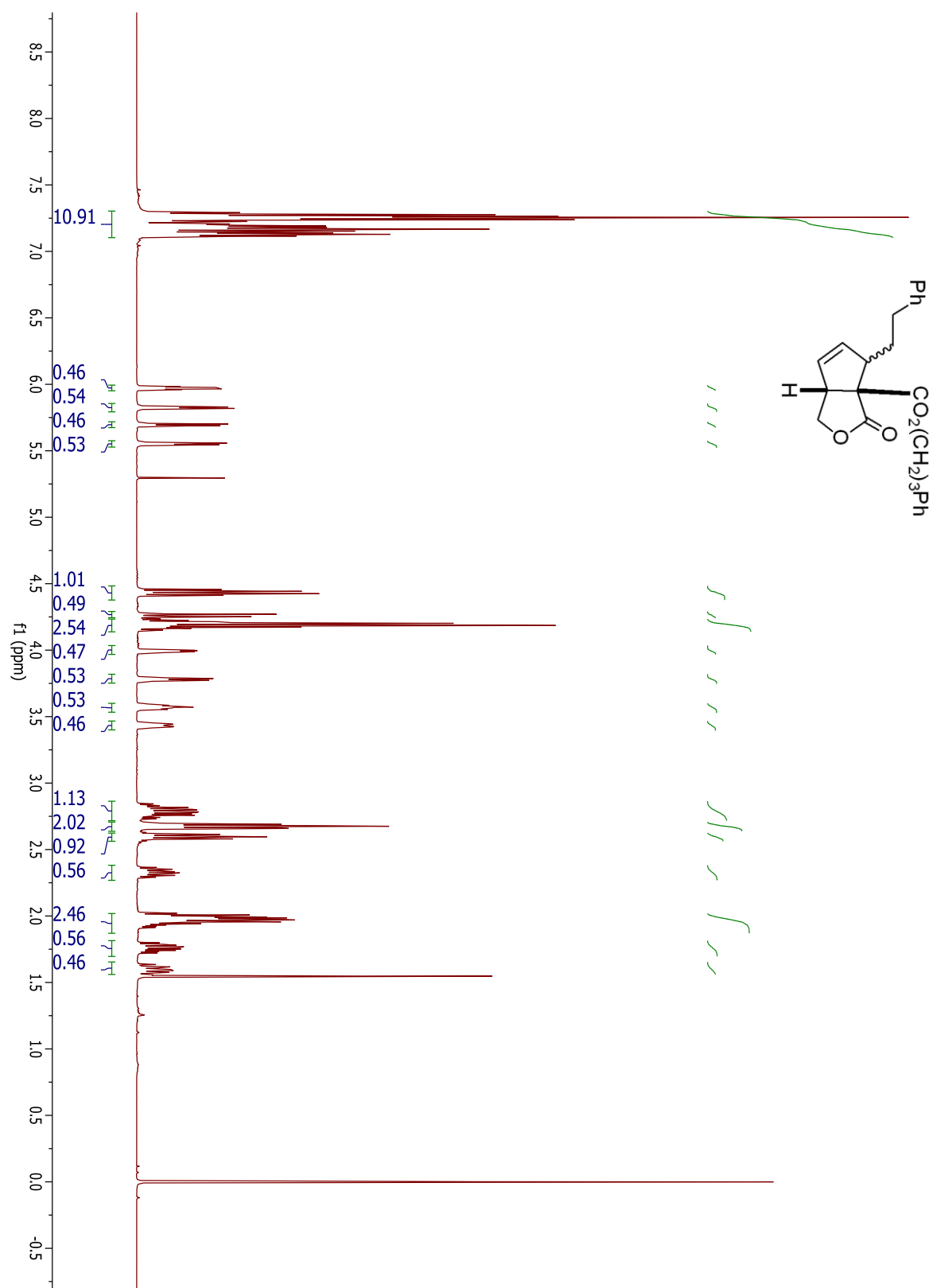
## Compound 2.53



## Compound 2.53

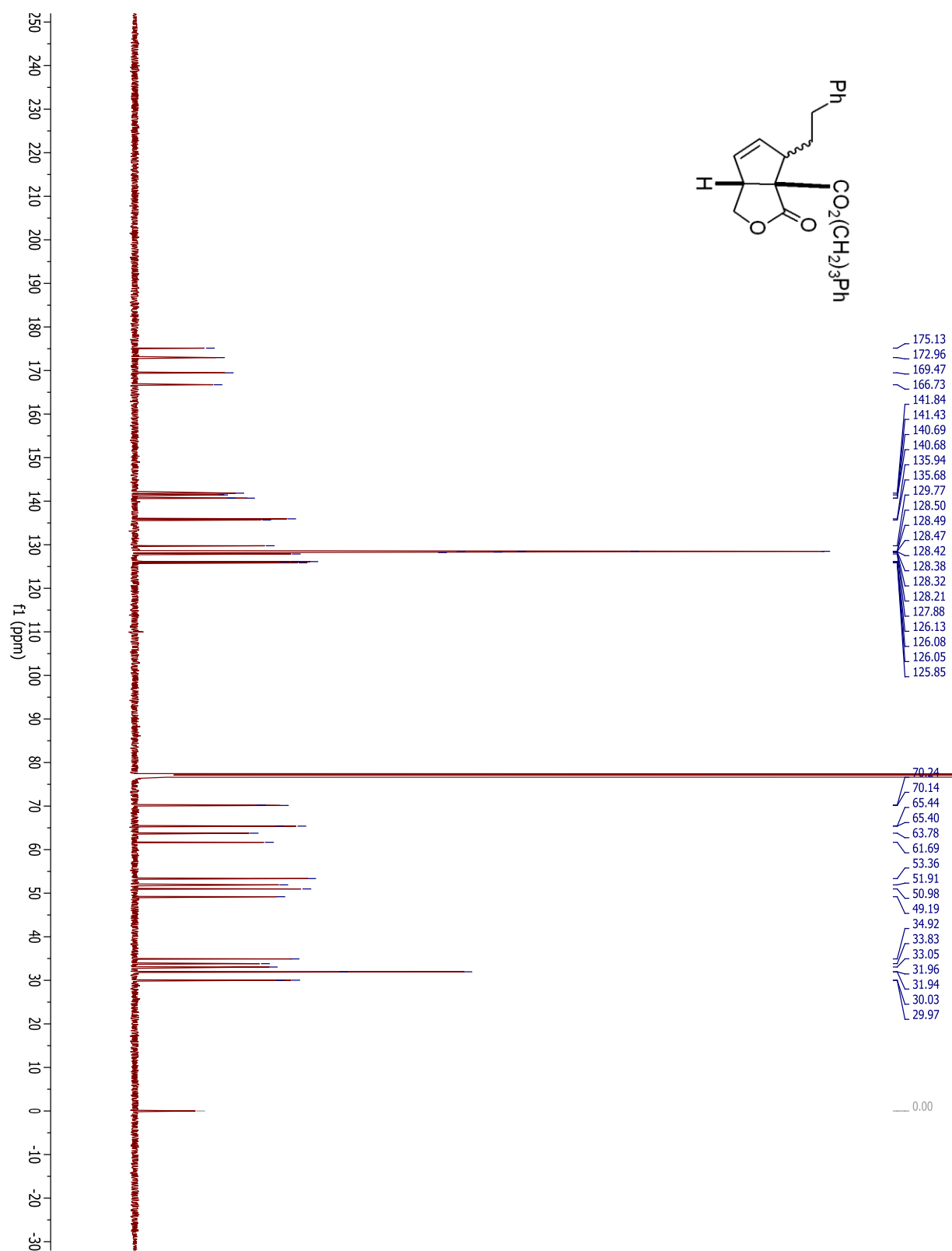


## Compound 2.54

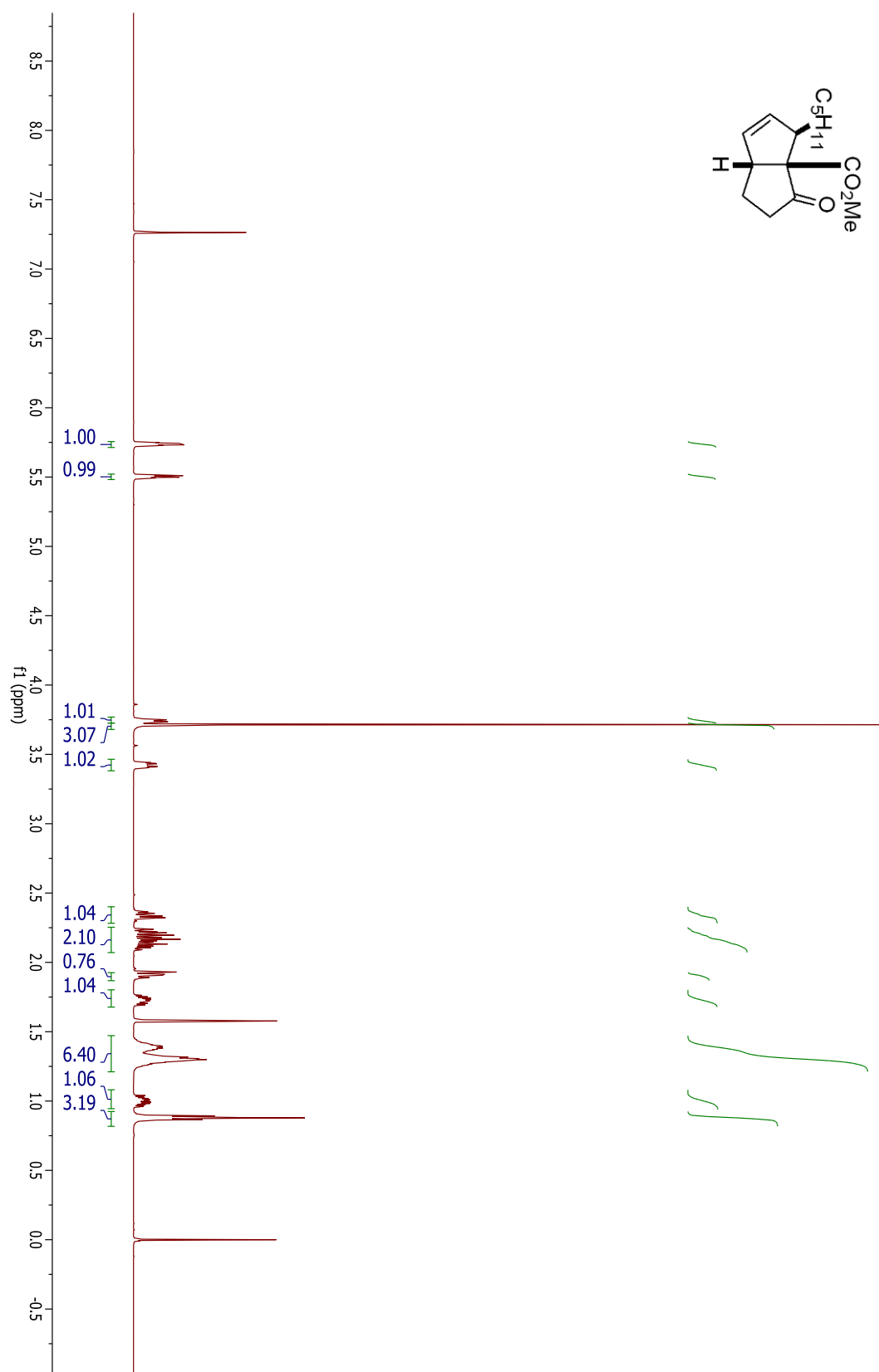




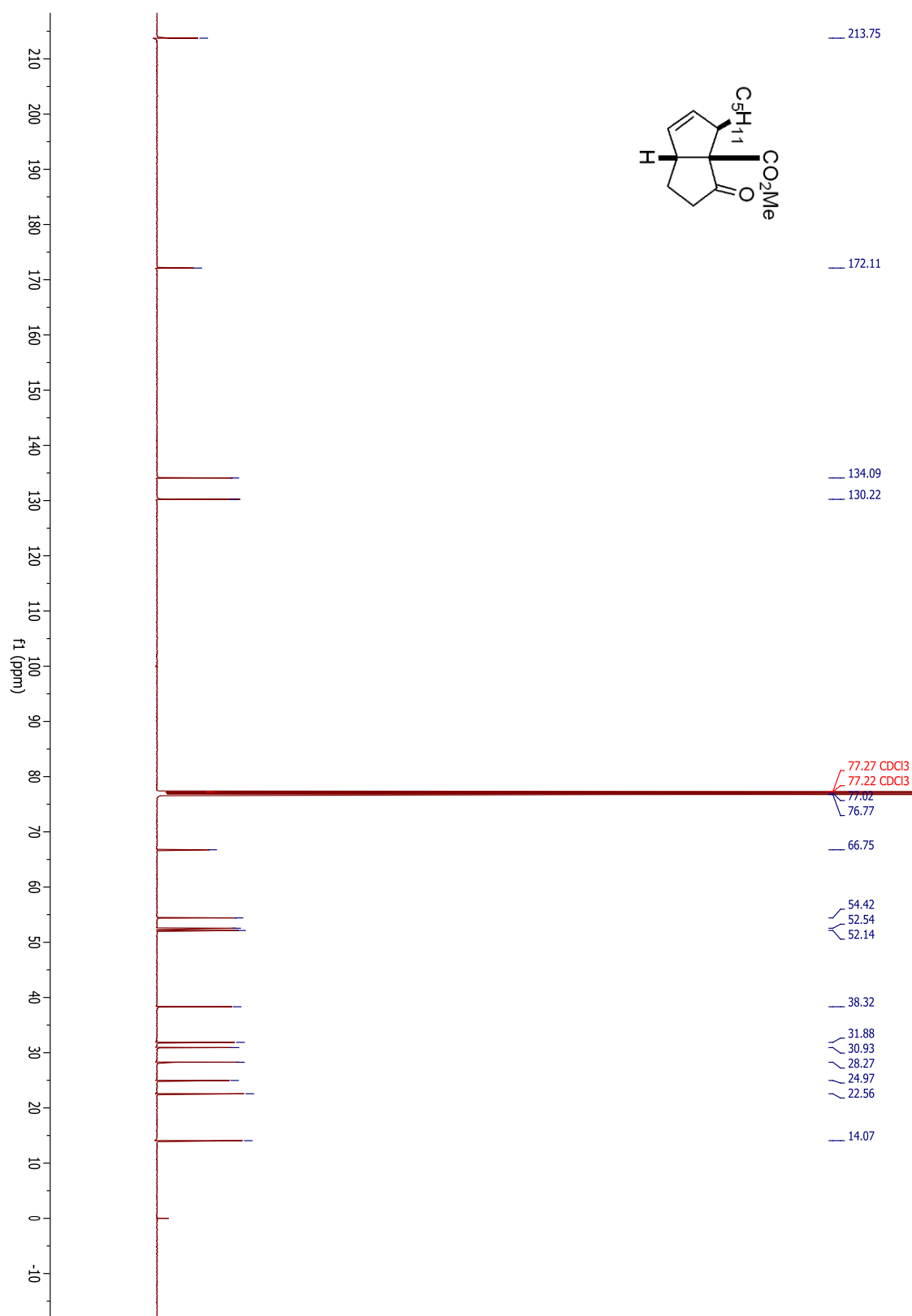
## Compound 2.54



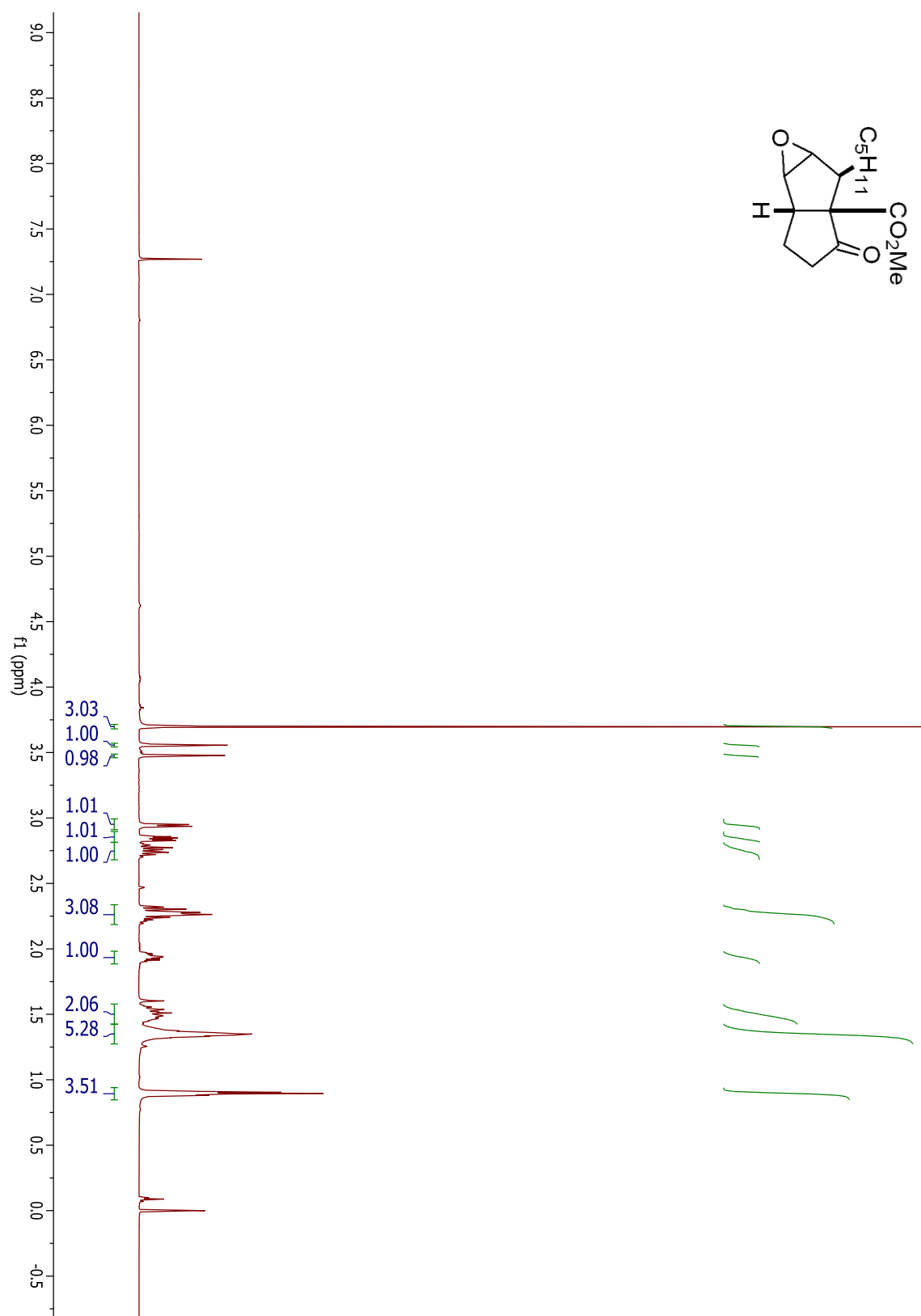
## Compound 2.55



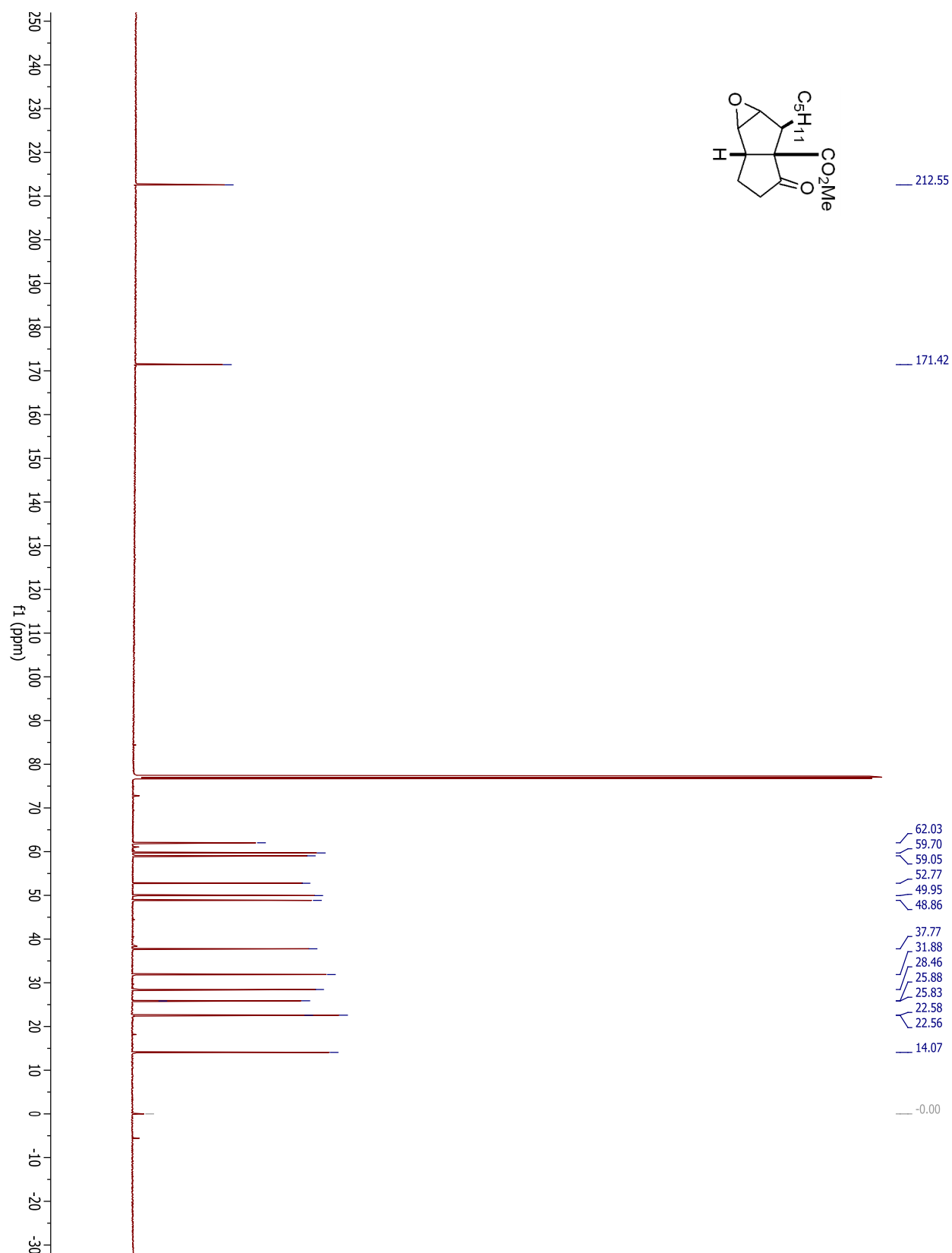
## Compound 2.55



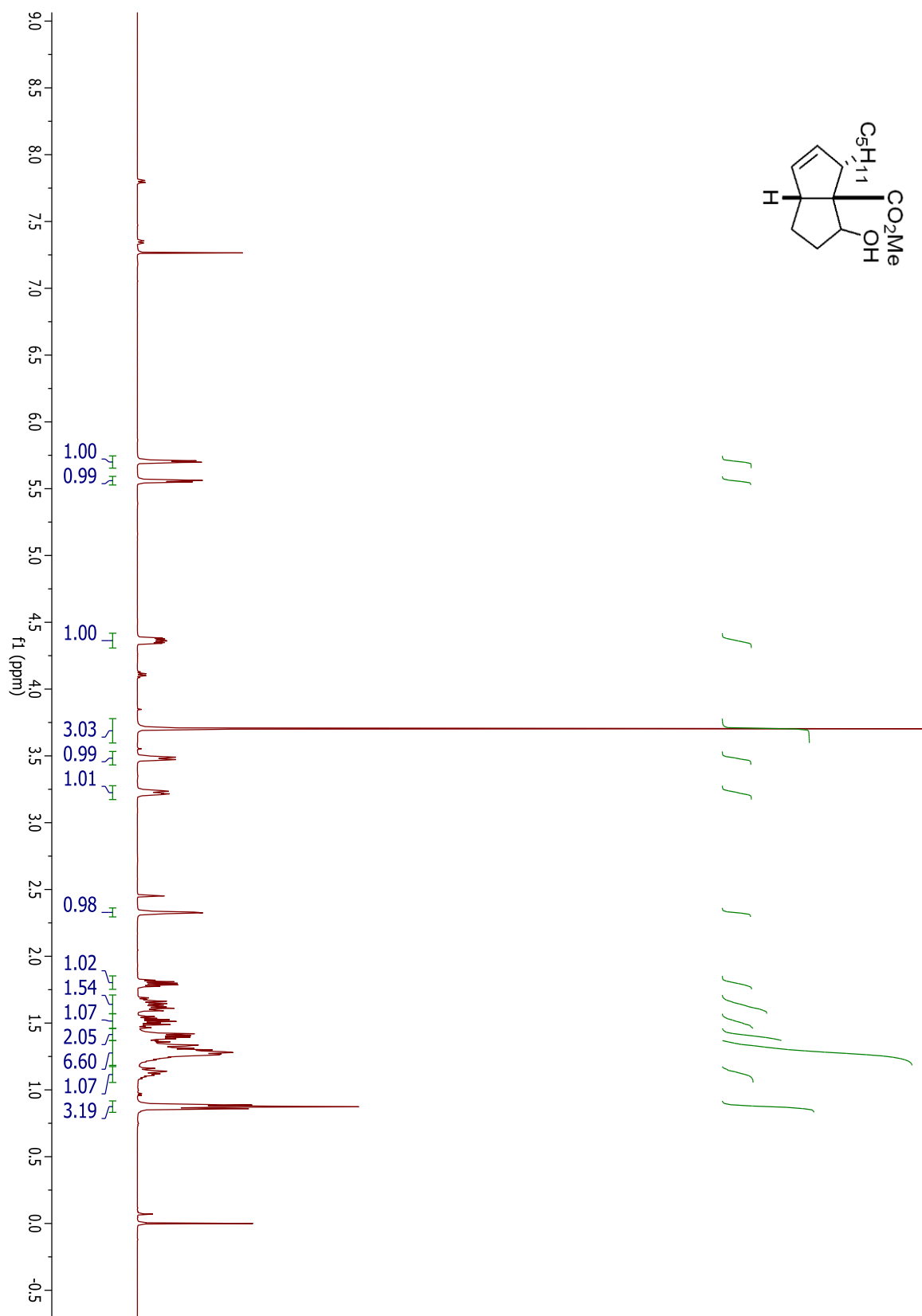
## Compound 2.56



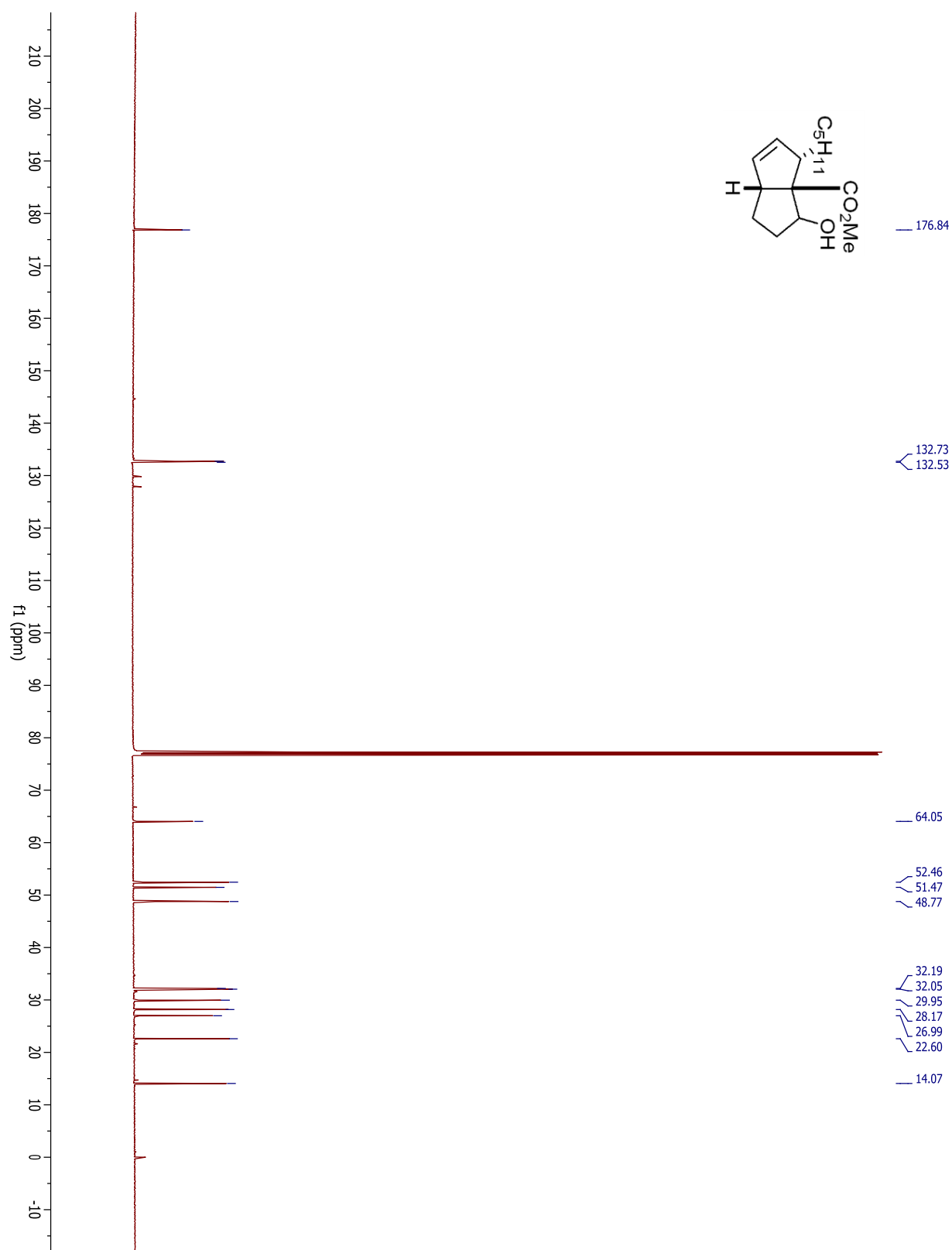
## Compound 2.56



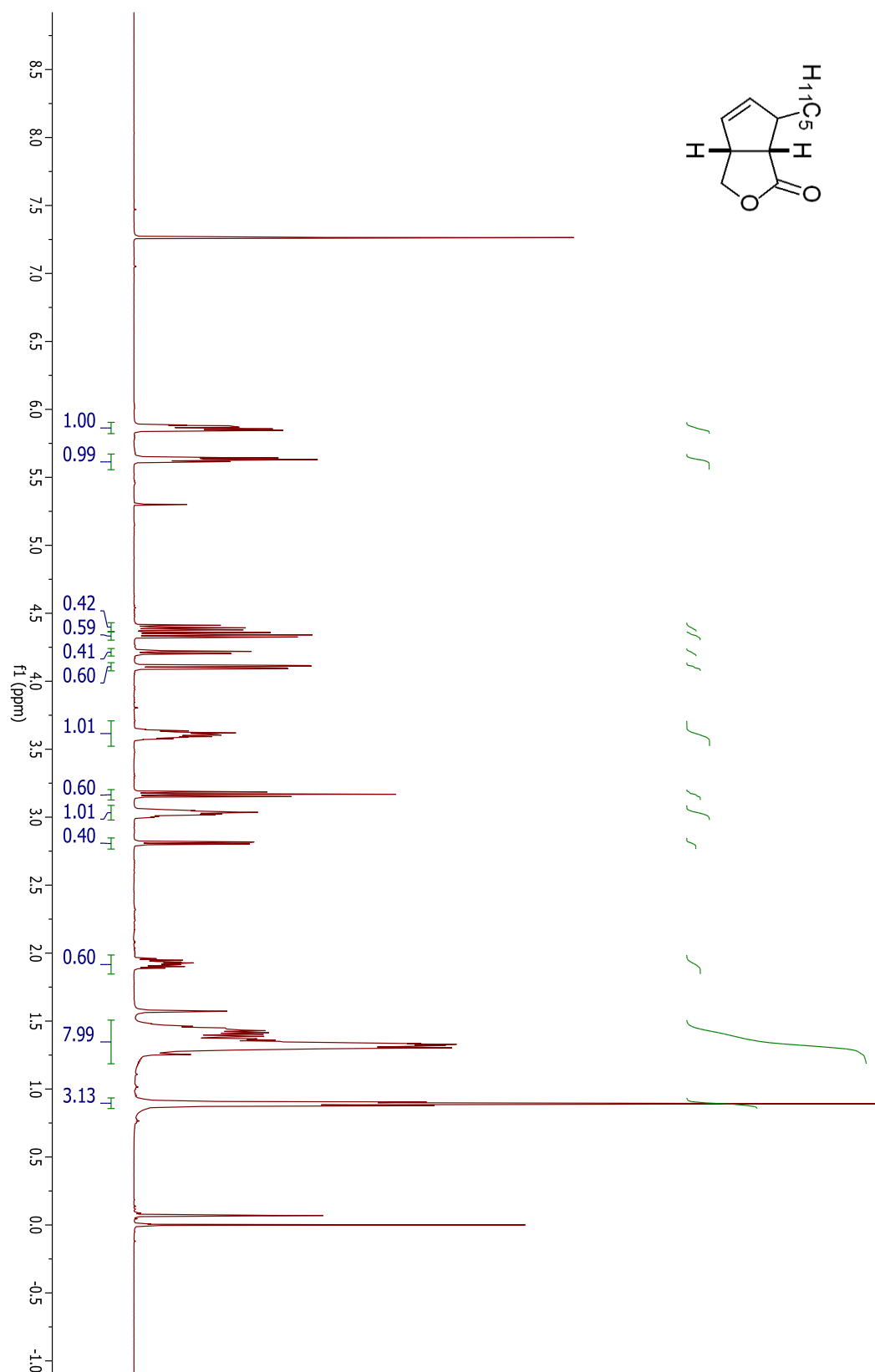
## Compound 2.57



## Compound 2.57

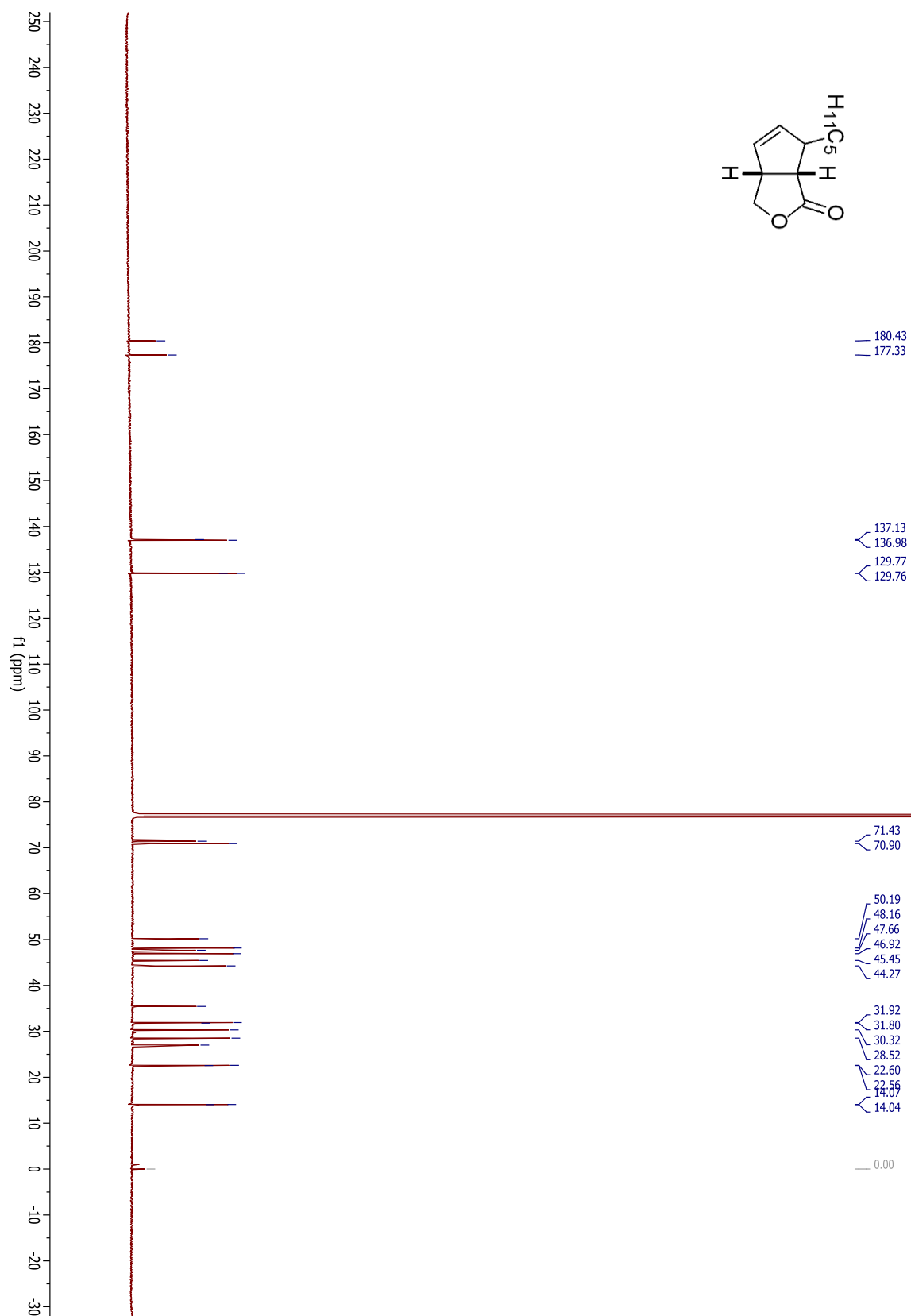


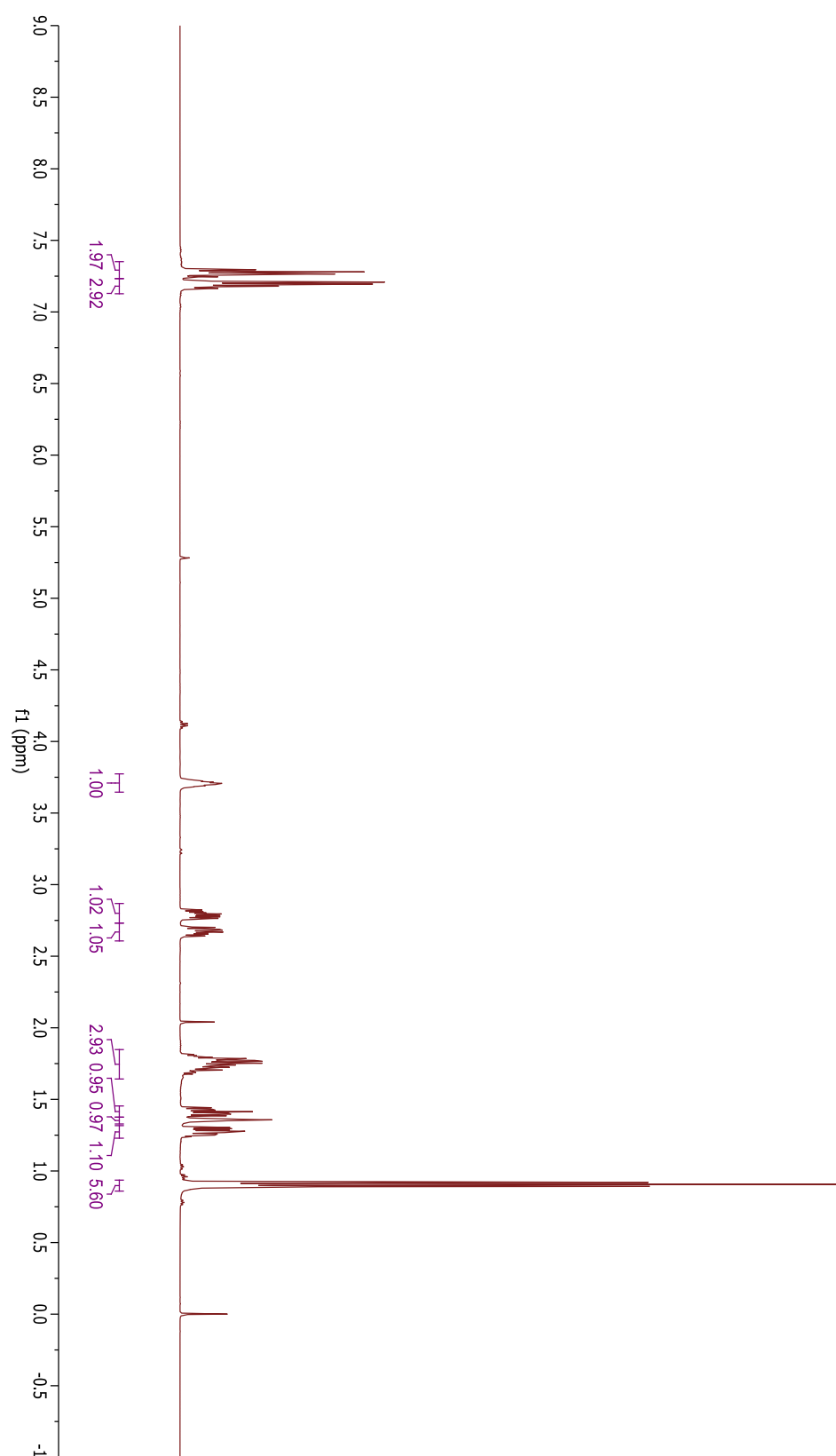
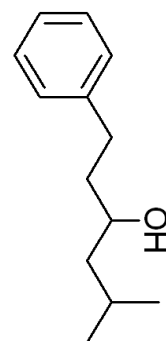
## Compound 2.58

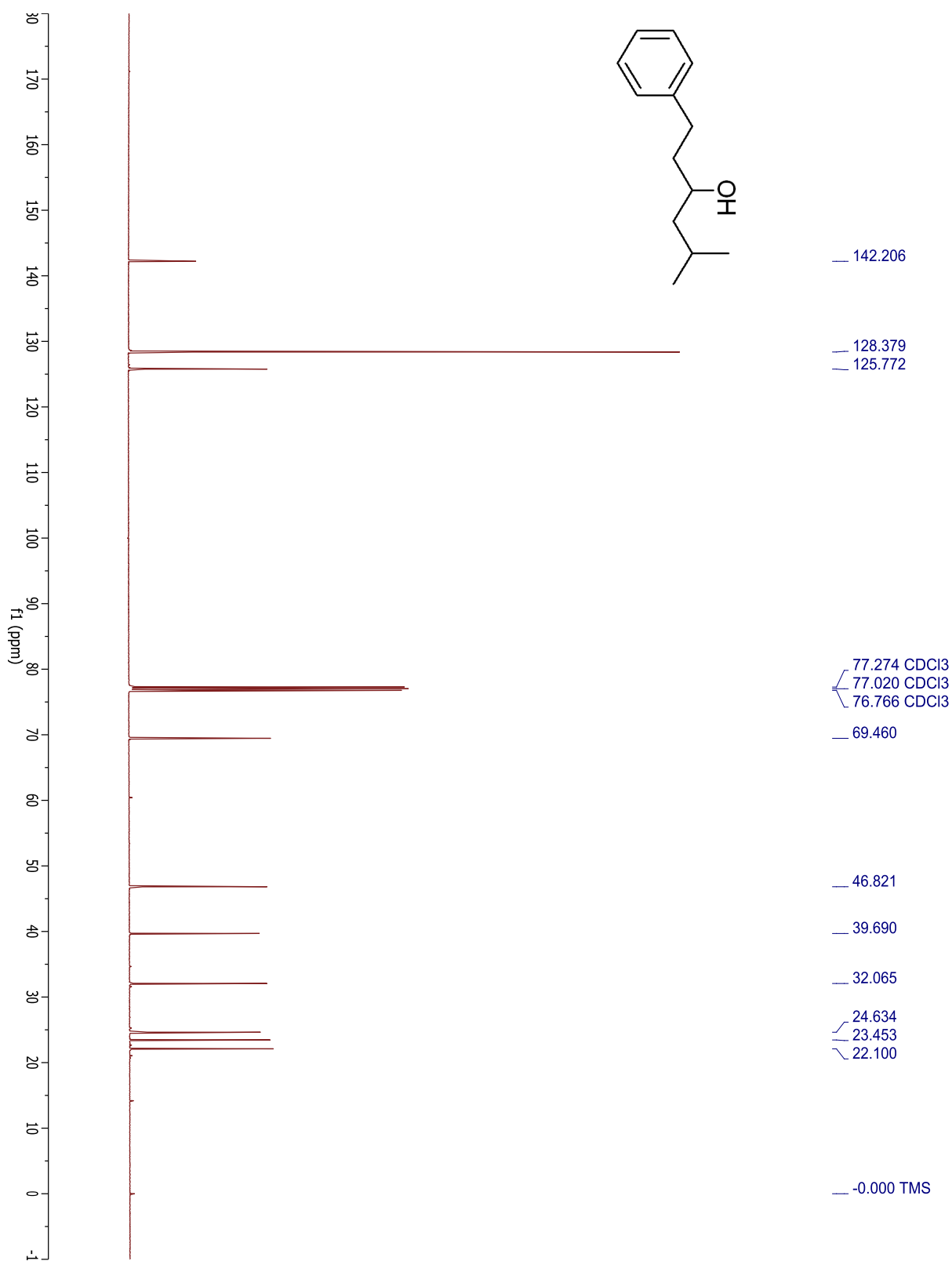




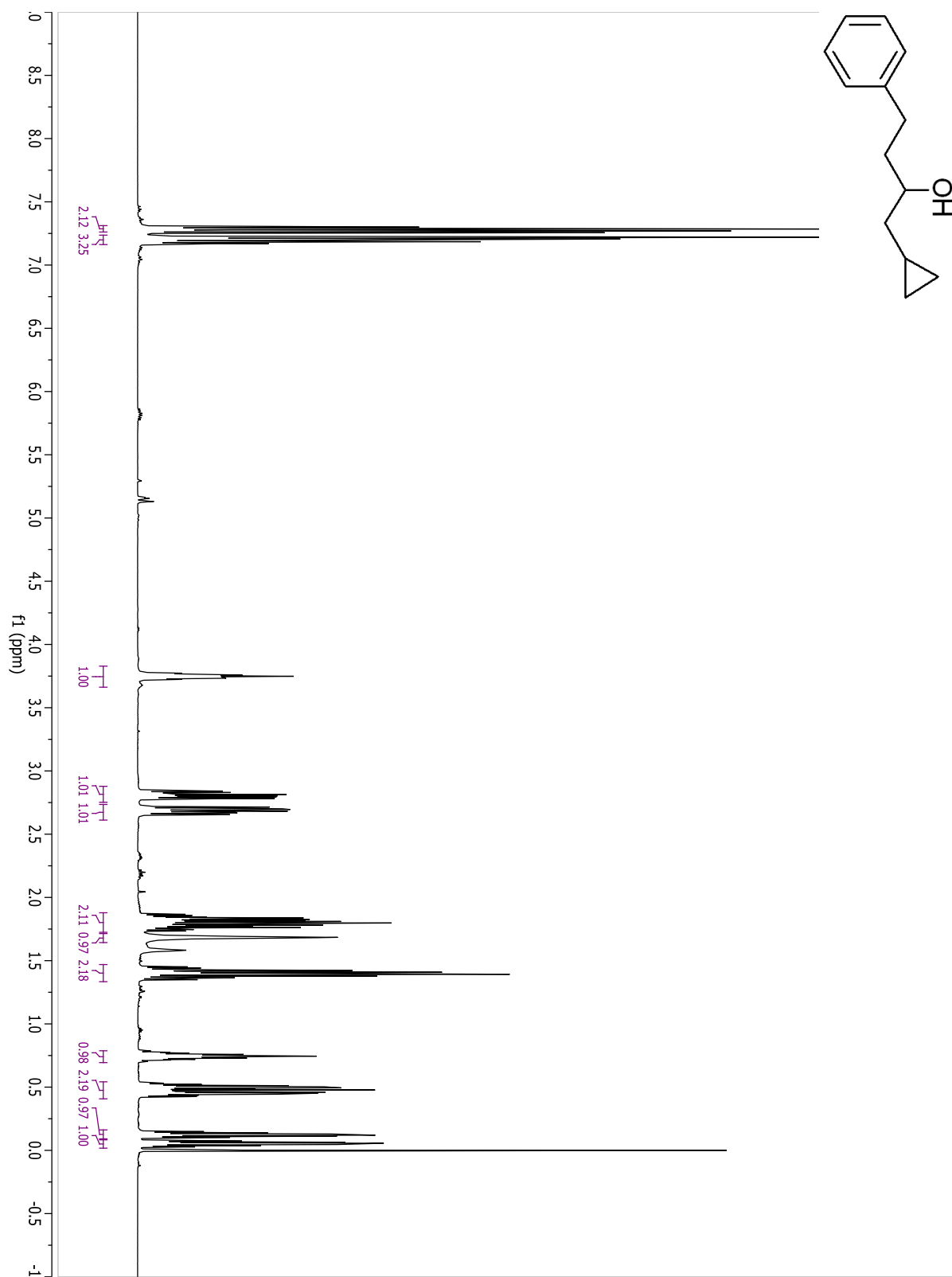
## Compound 2.58

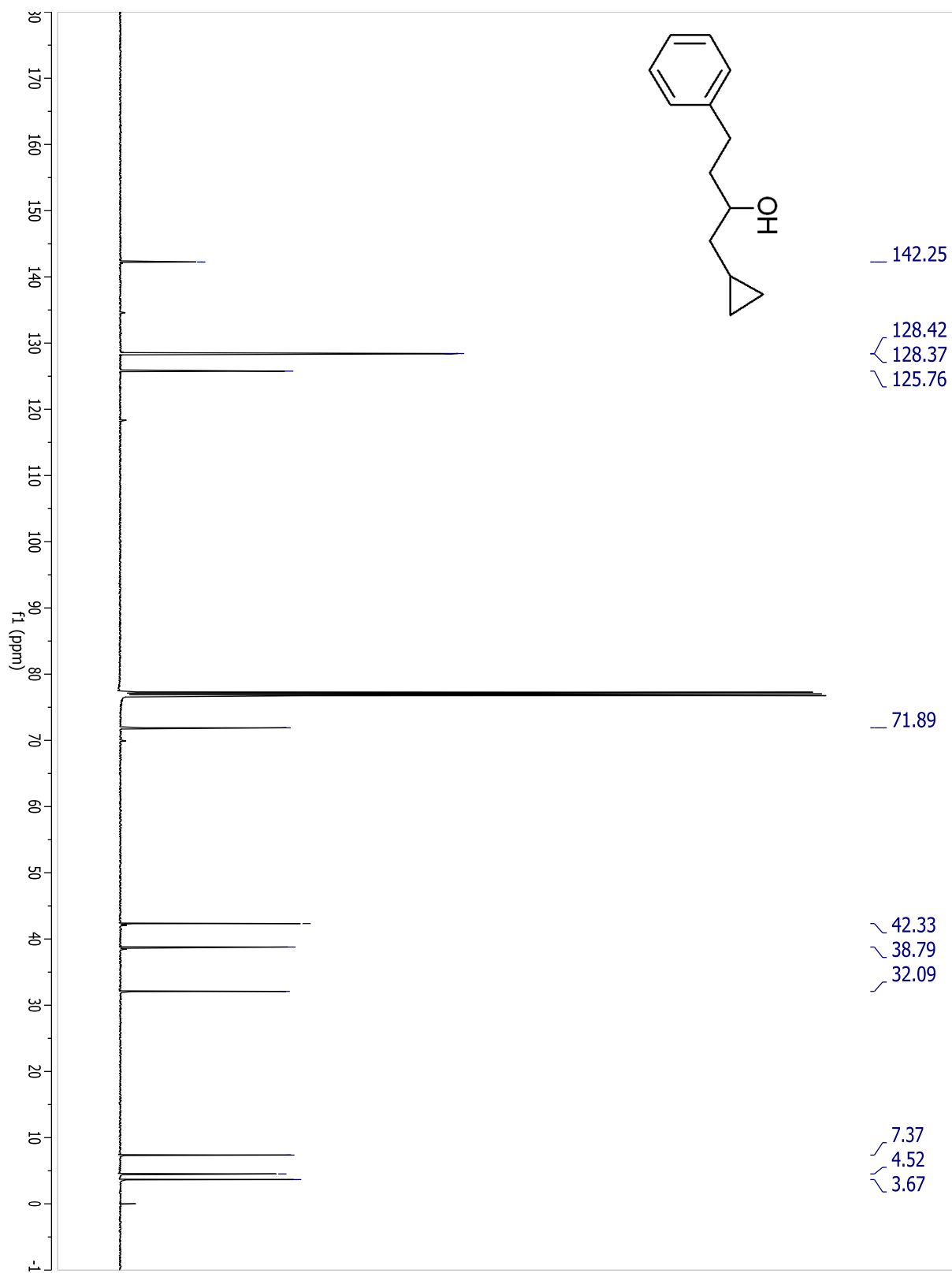


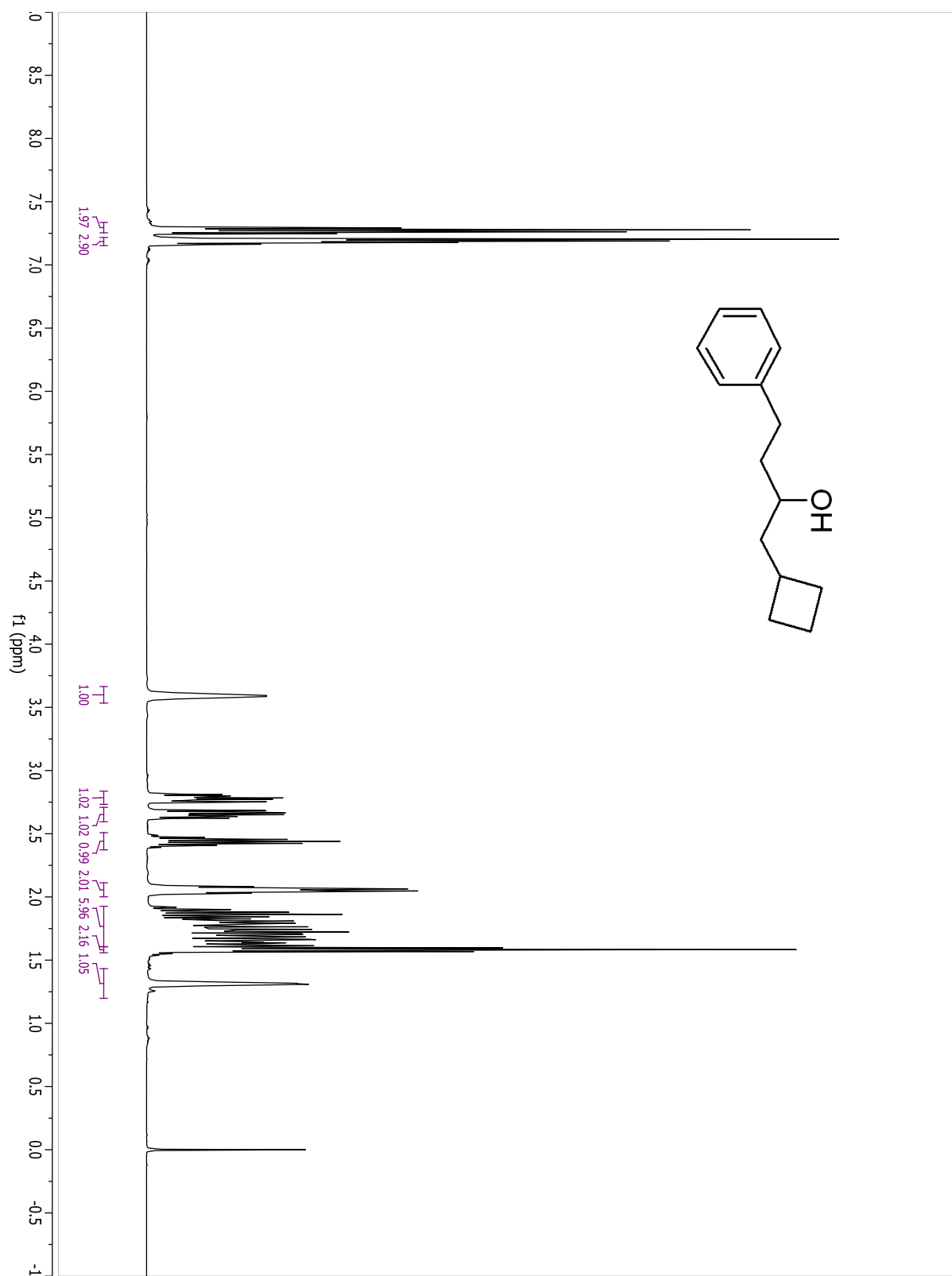
**5-methyl-1-phenylhexan-3-ol**

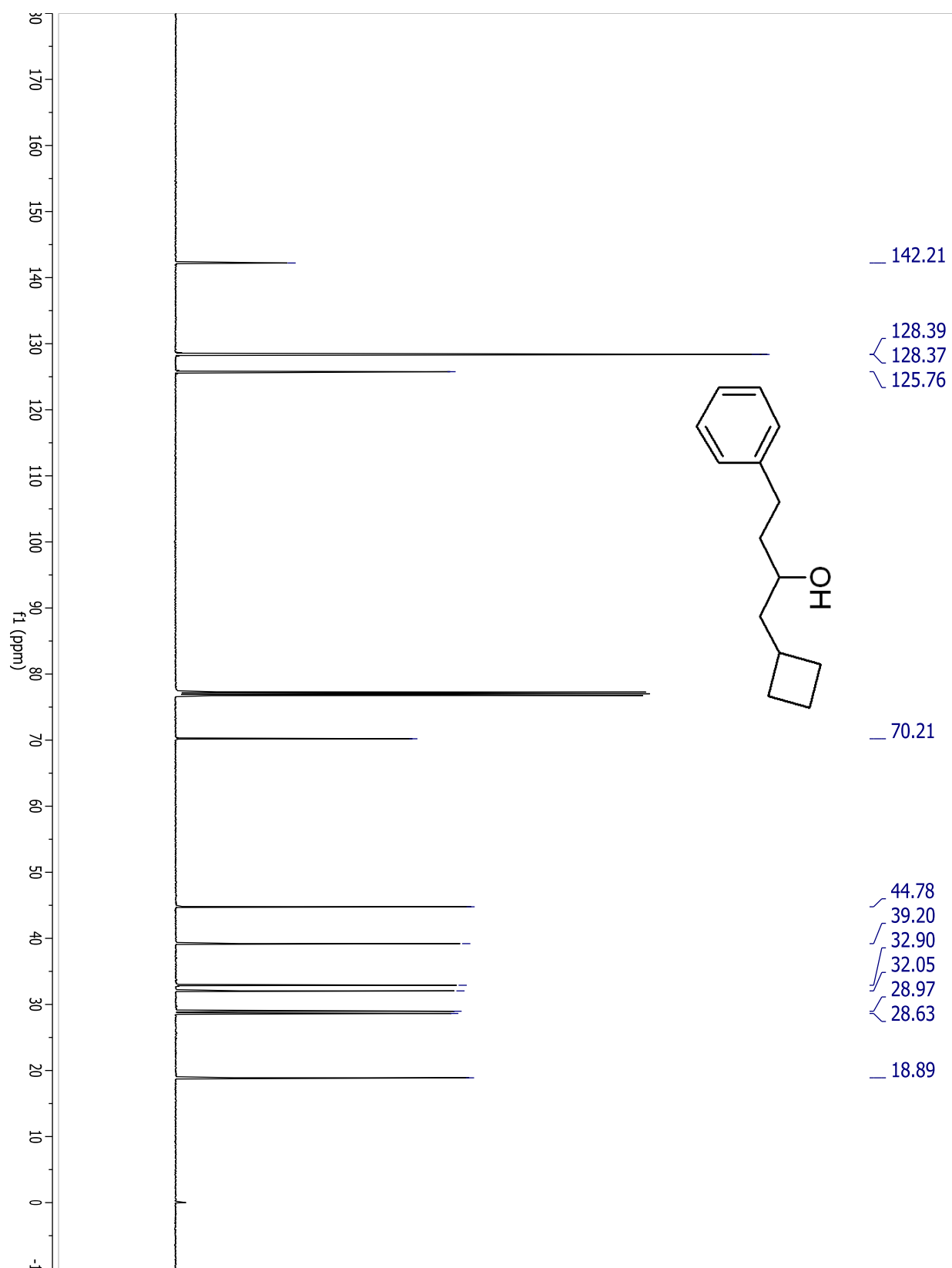
**5-methyl-1-phenylhexan-3-ol**

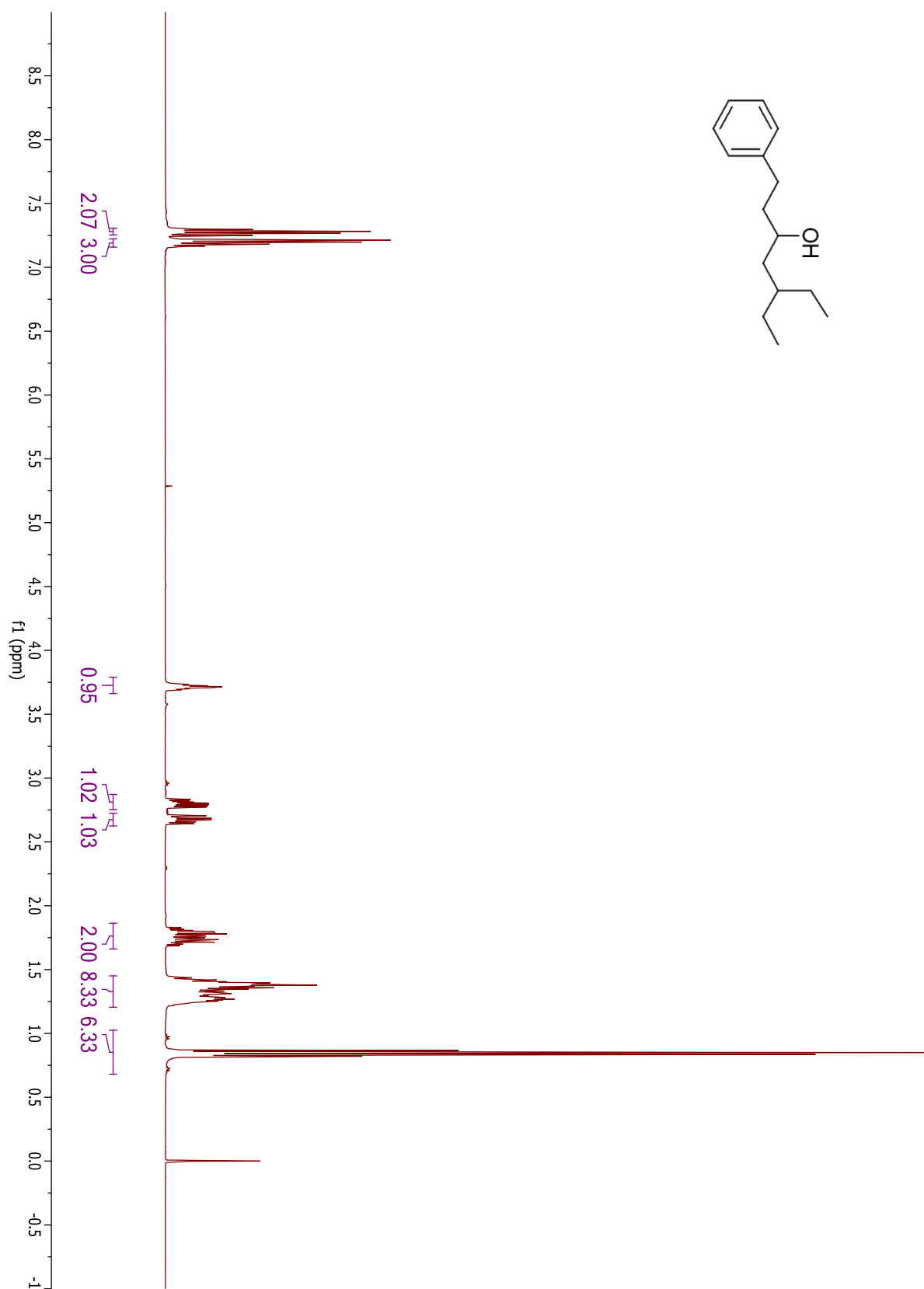
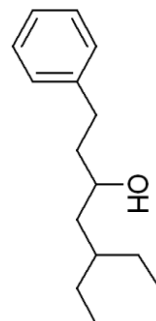
## 1-cyclopropyl-4-phenylbutan-2-ol



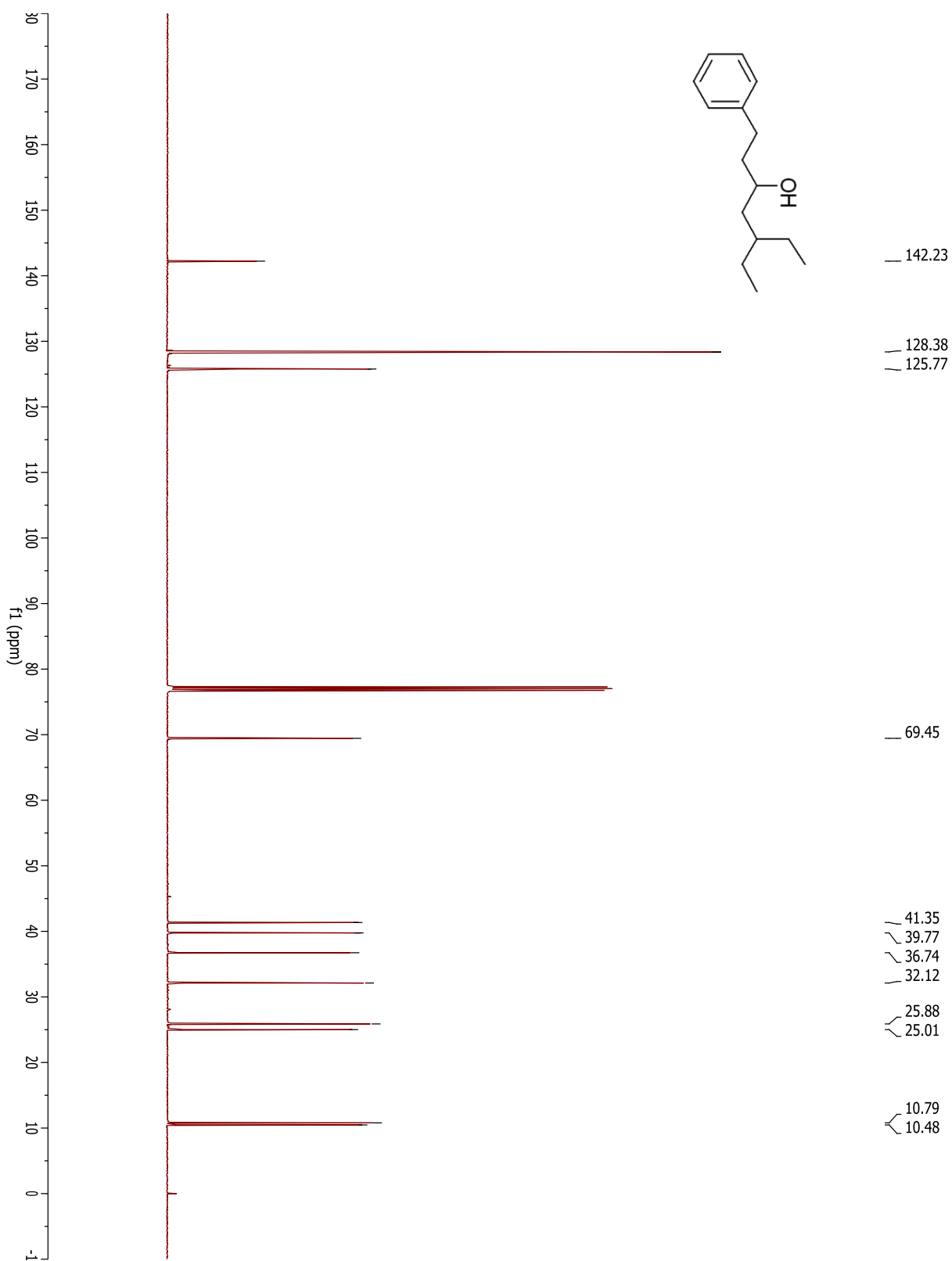
**1-cyclopropyl-4-phenylbutan-2-ol**

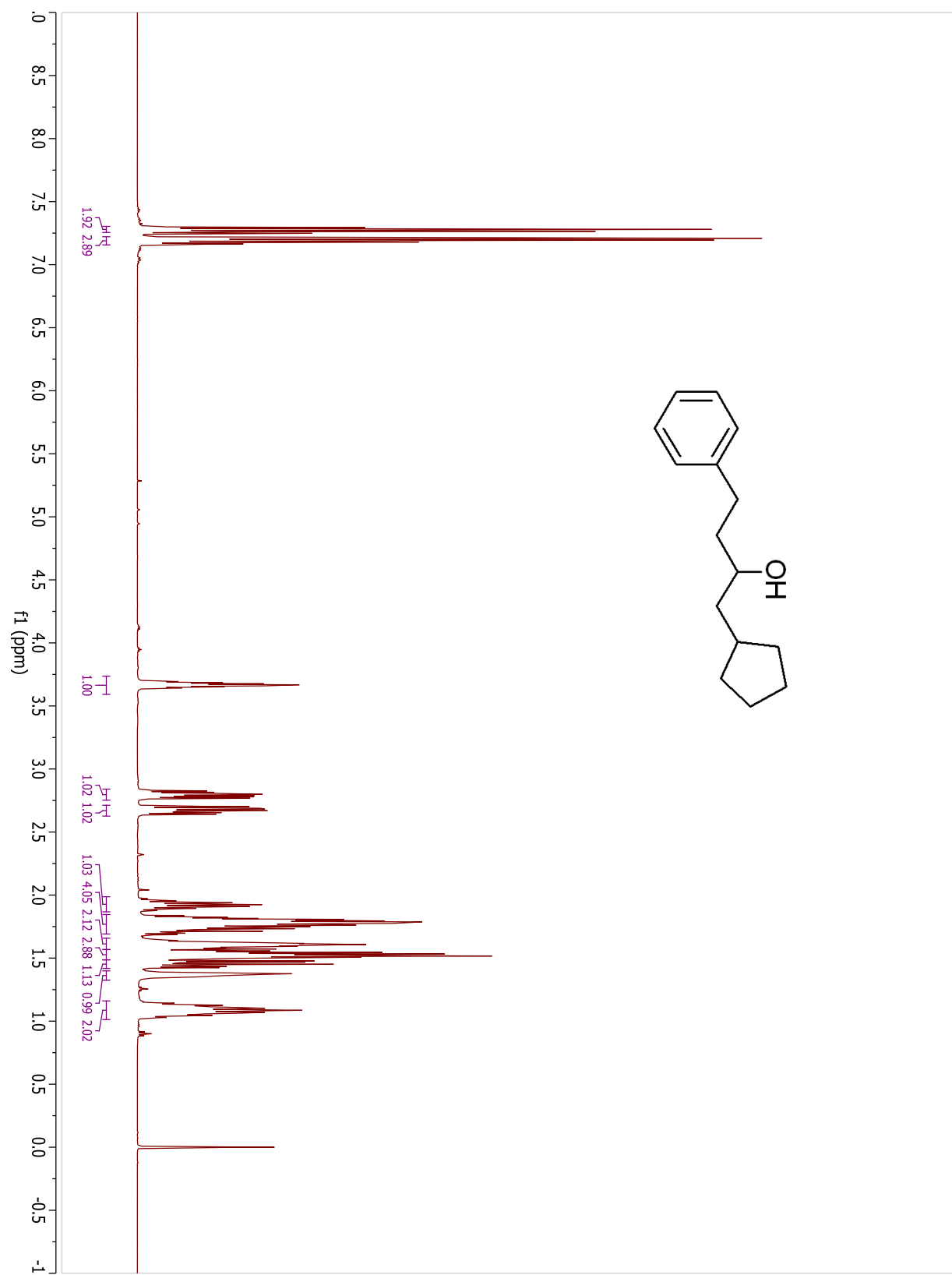
**1-cyclobutyl-4-phenylbutan-2-ol**

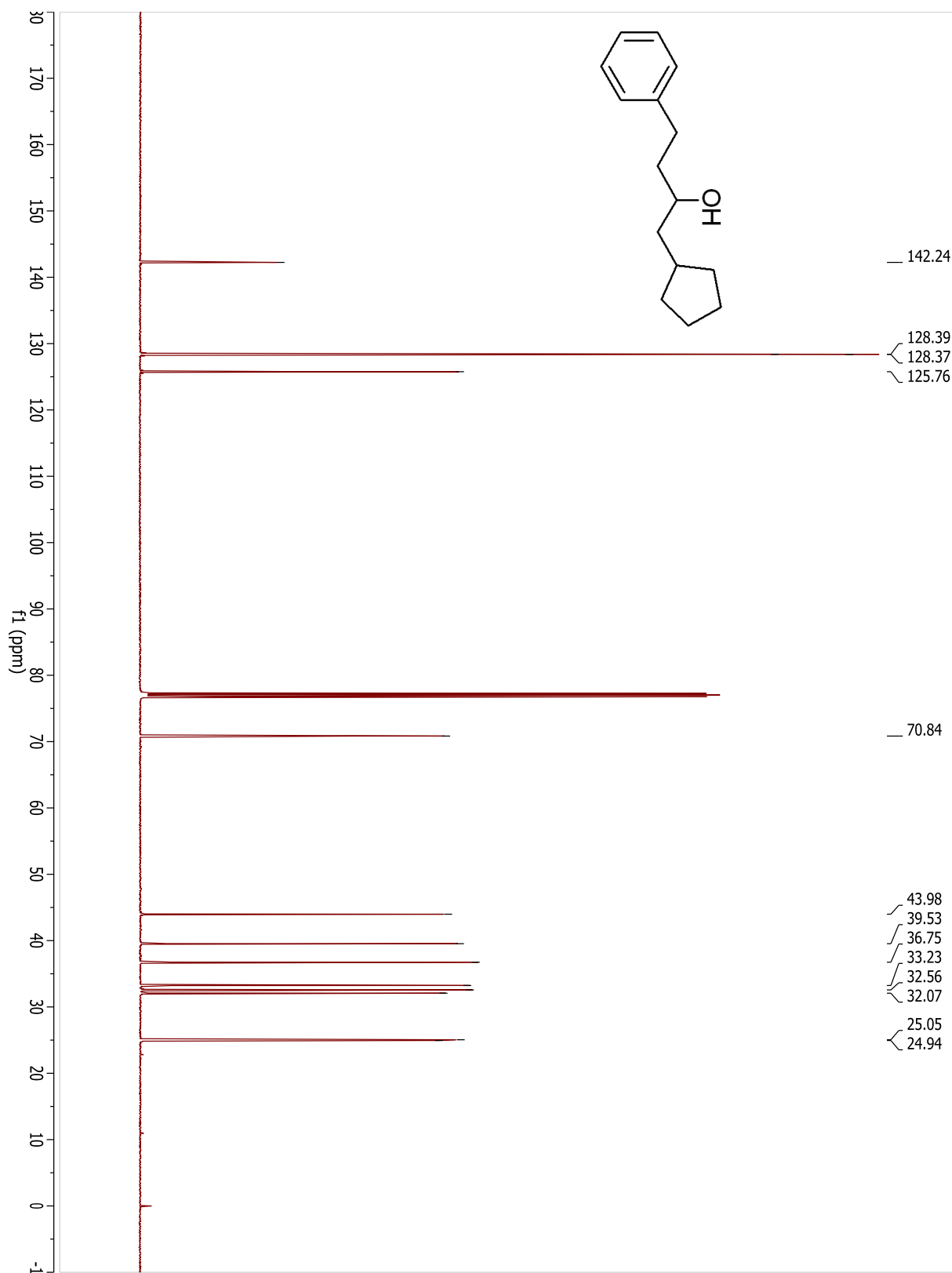
**1-cyclobutyl-4-phenylbutan-2-ol**

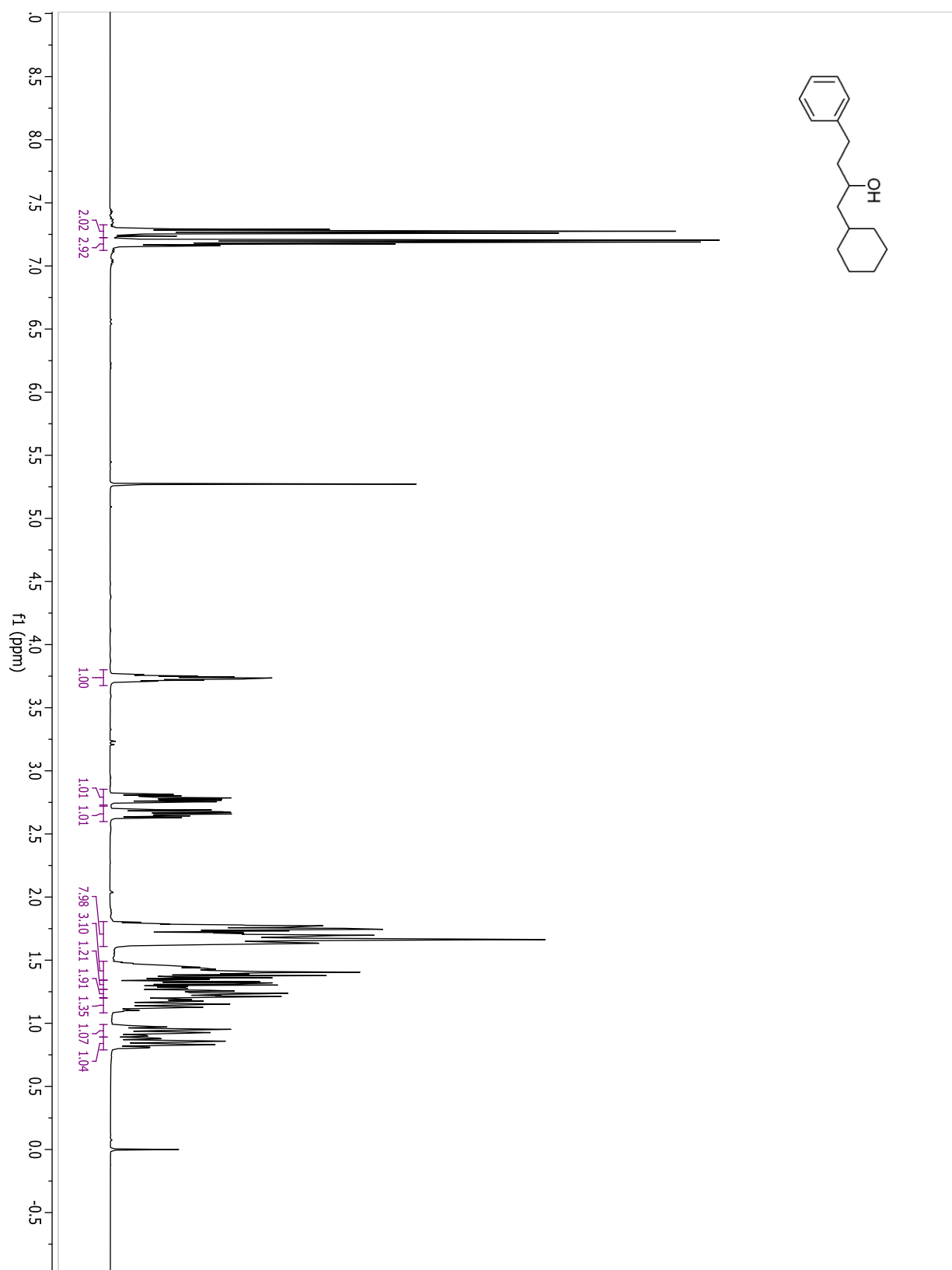
**5-ethyl-1-phenylheptan-3-ol**

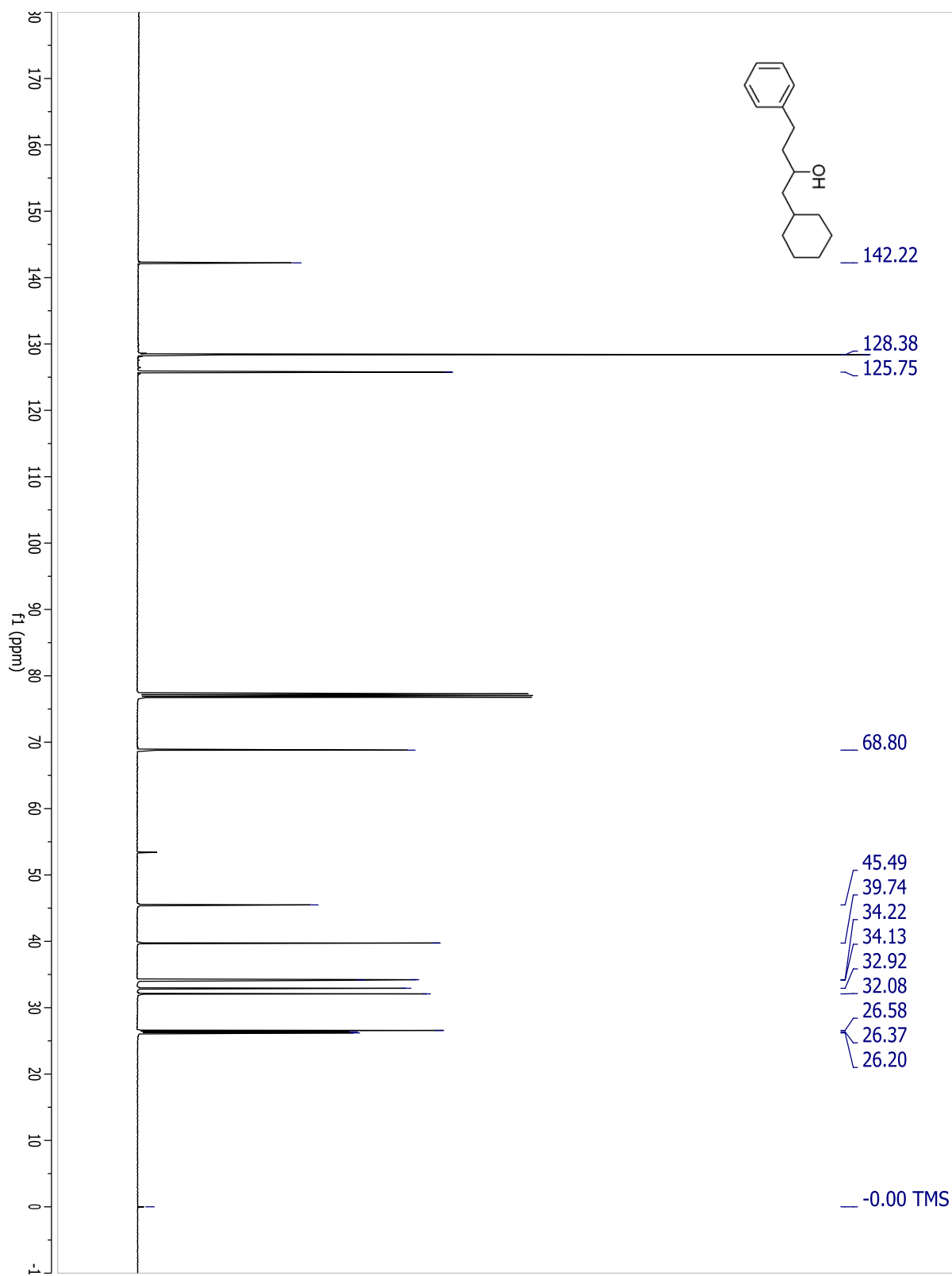


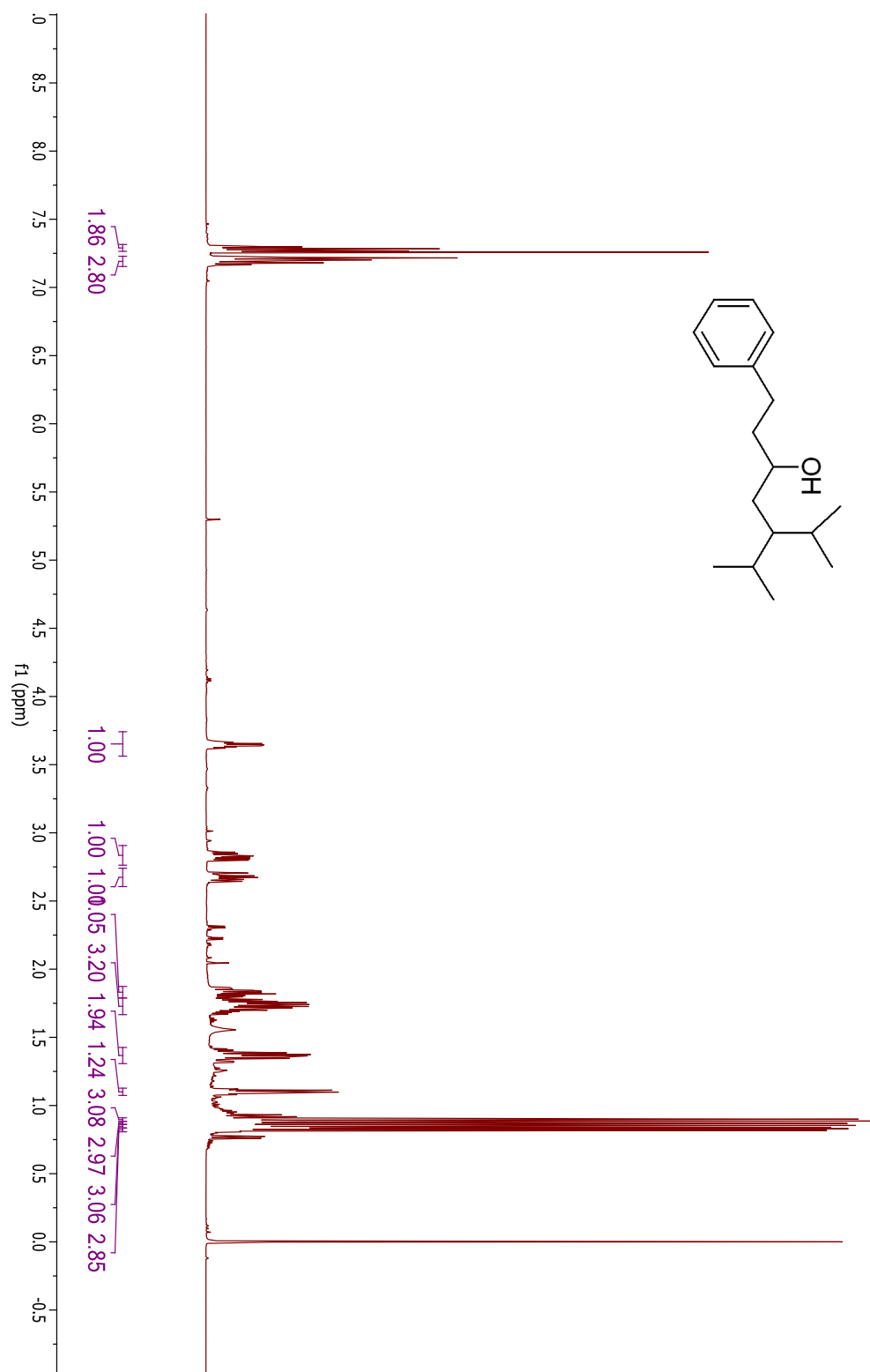
**5-ethyl-1-phenylheptan-3-ol**

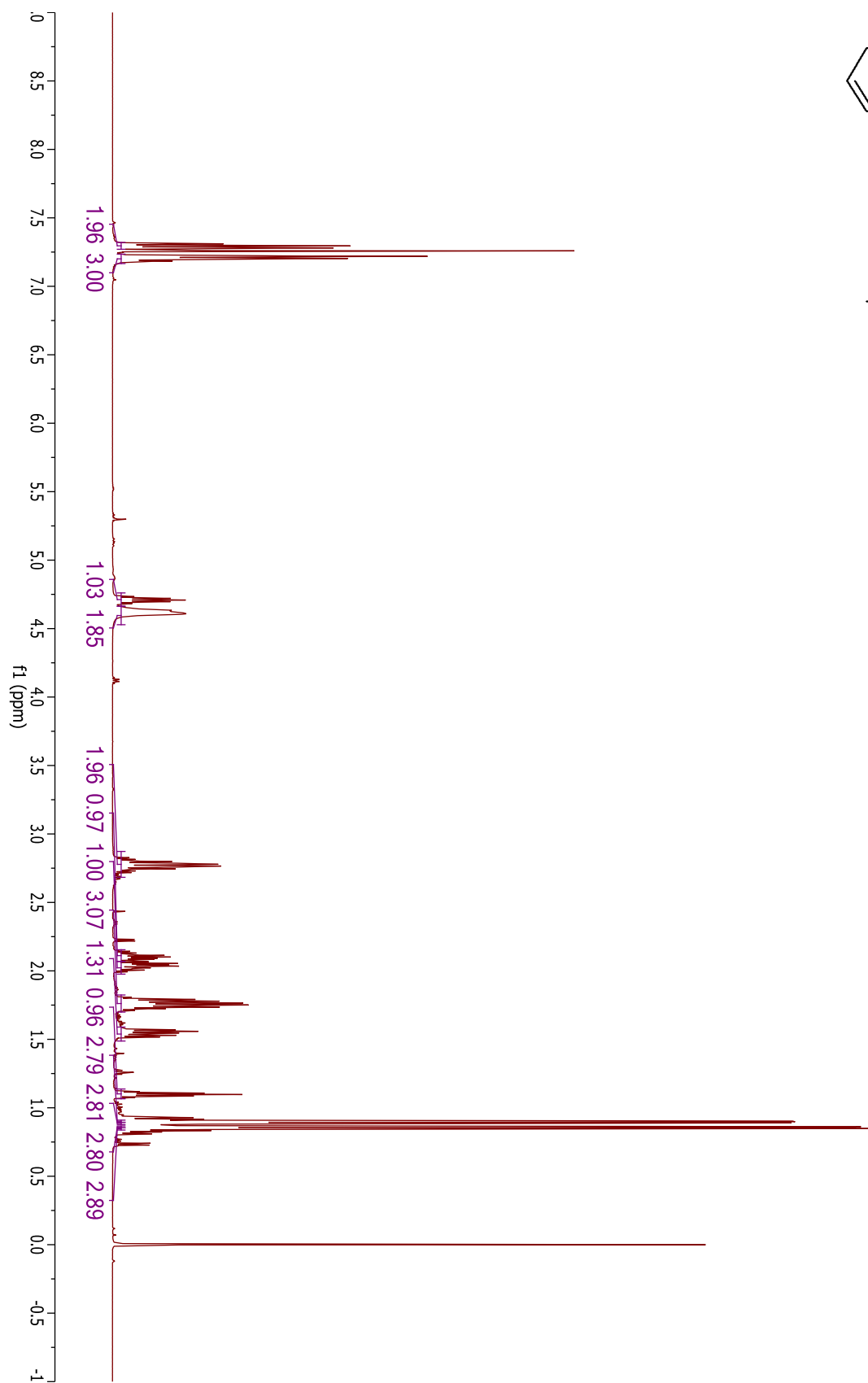
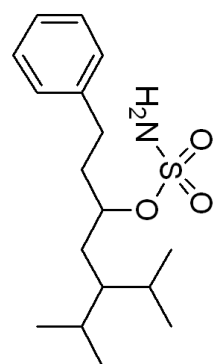
**1-cyclopentyl-4-phenylbutan-2-ol**

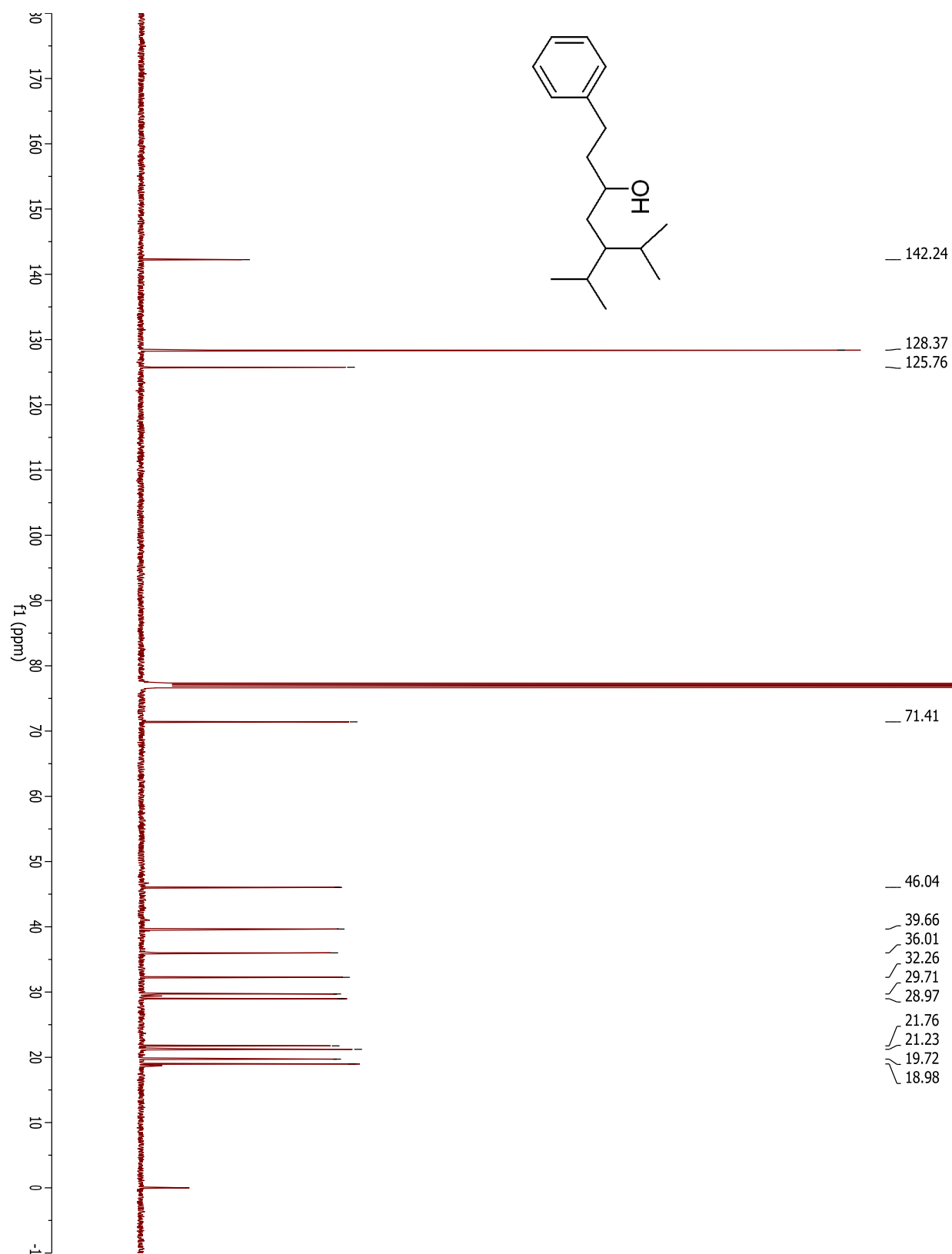
**1-cyclopentyl-4-phenylbutan-2-ol**

**1-cyclohexyl-4-phenylbutan-2-ol**

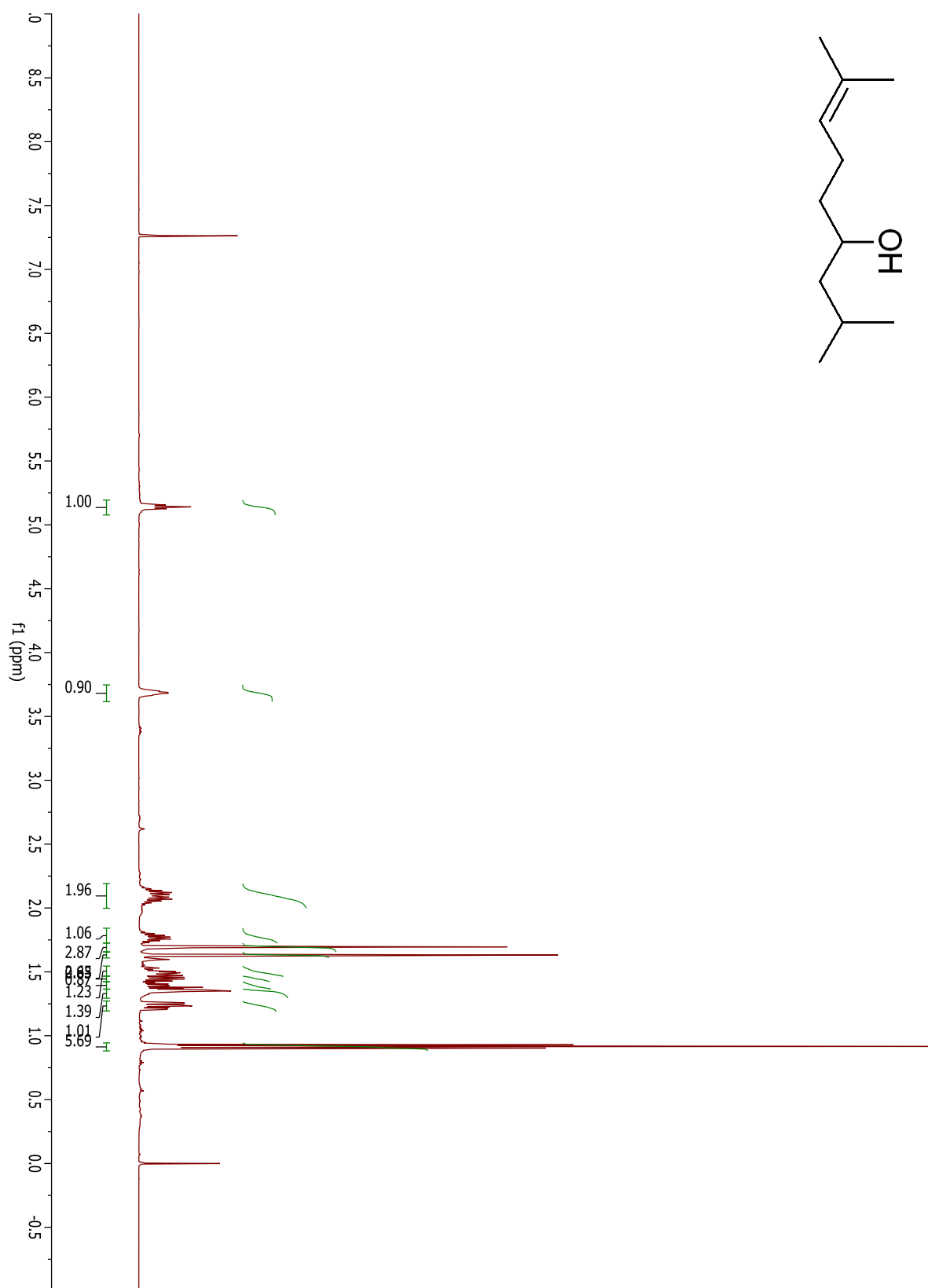
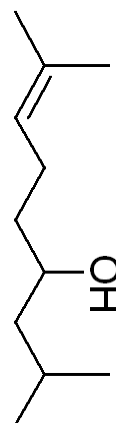
**1-cyclohexyl-4-phenylbutan-2-ol**

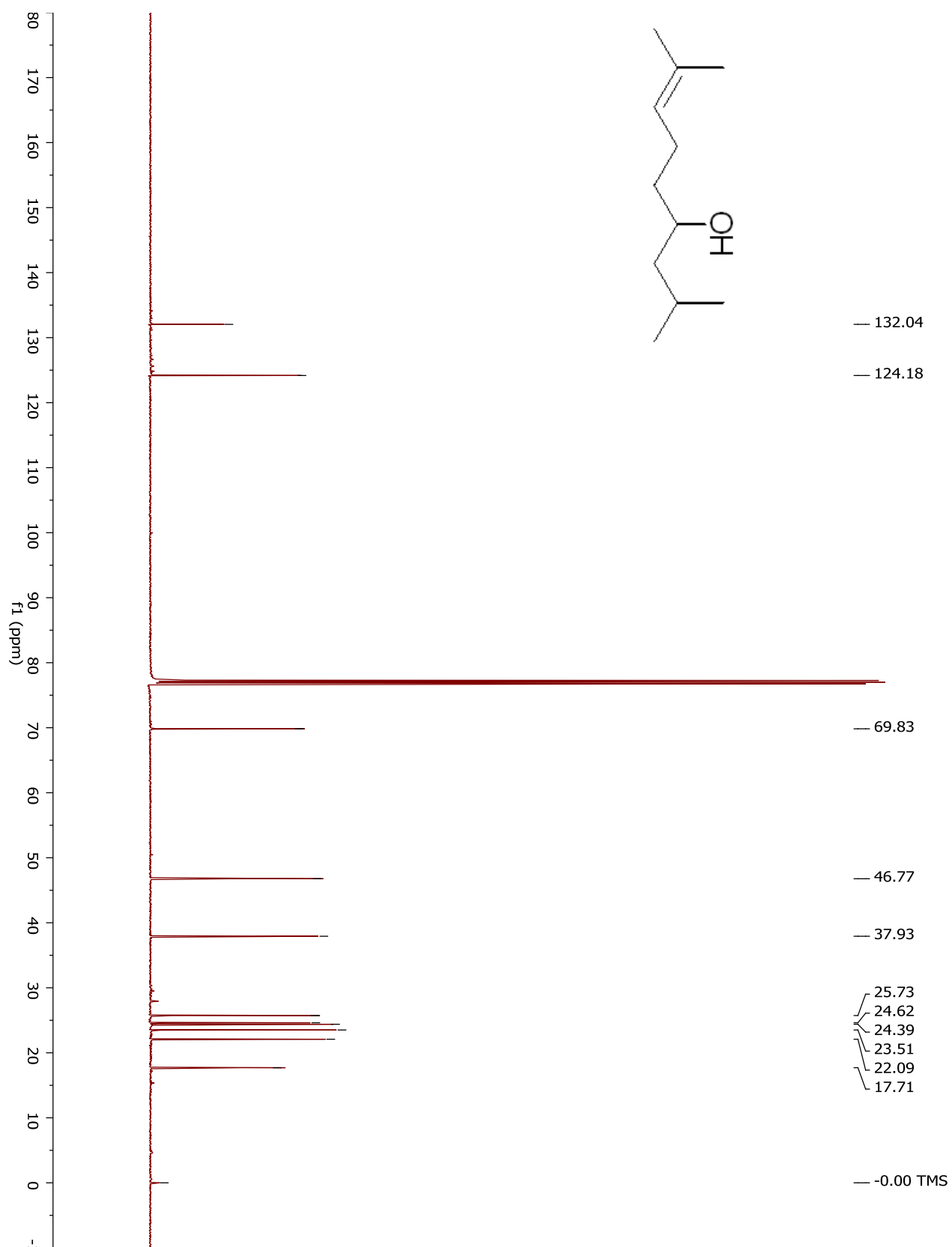
**6-methyl-1-phenyl-5-(propan-2-yl)heptan-3-ol**

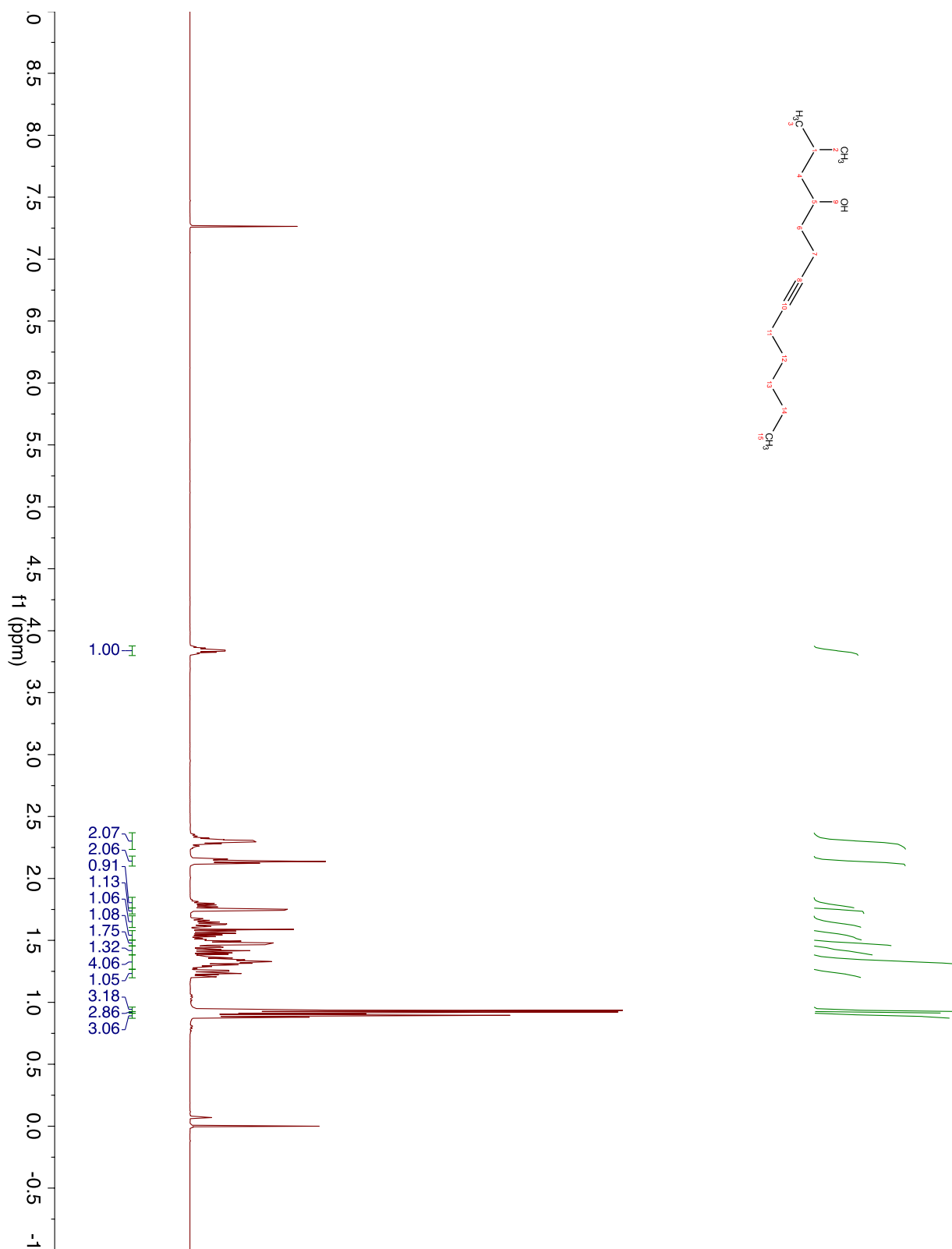


**6-methyl-1-phenyl-5-(propan-2-yl)heptan-3-ol**

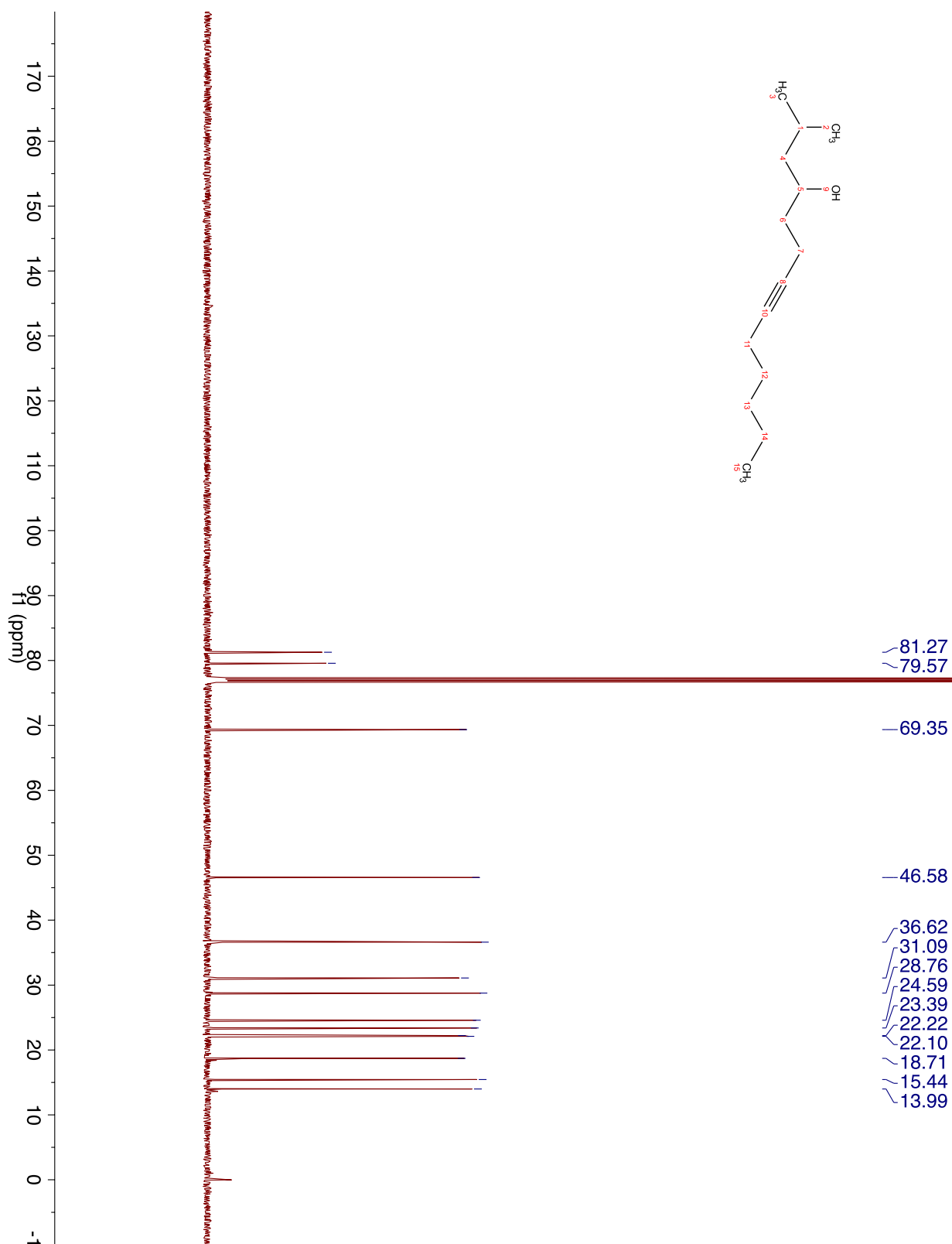


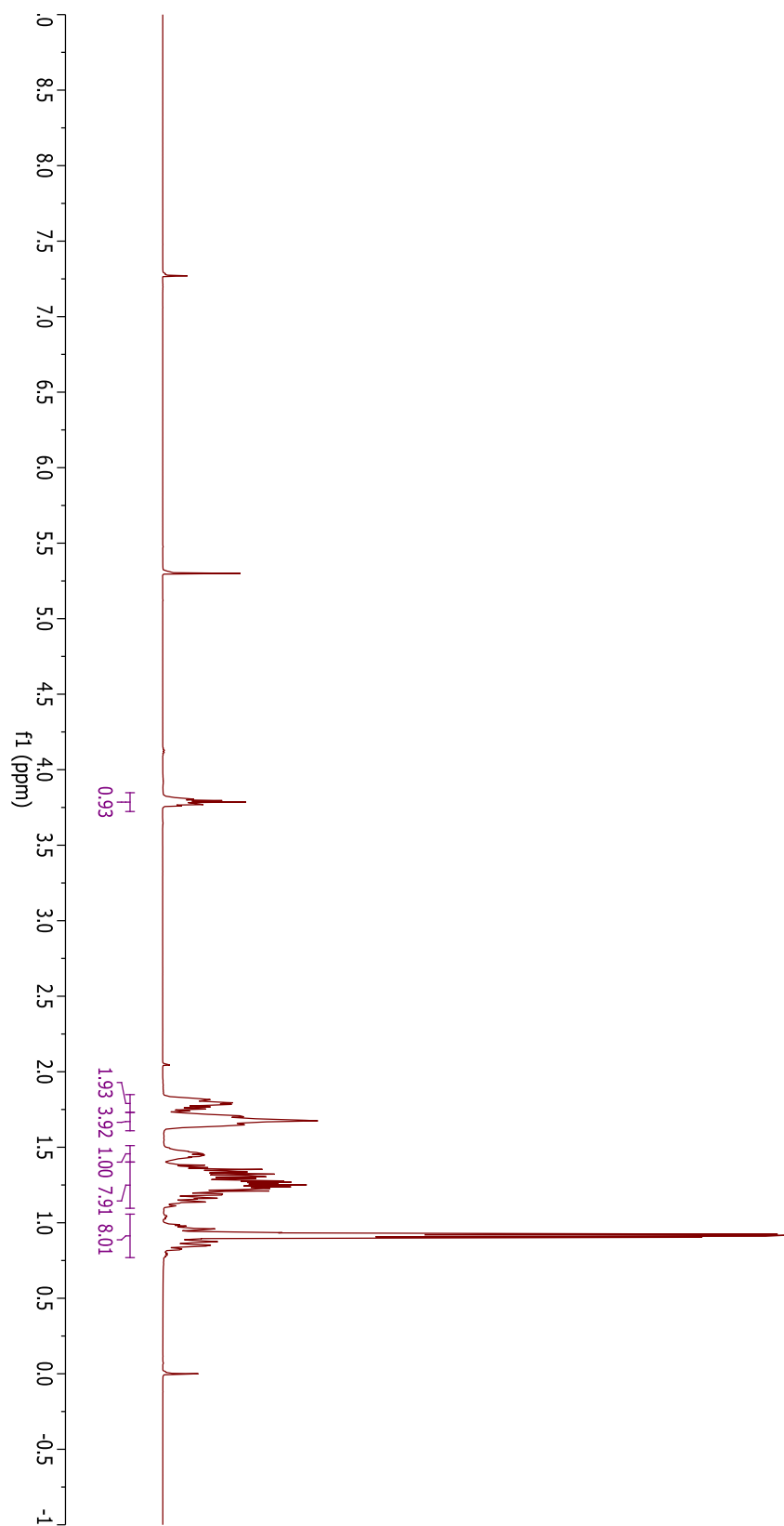
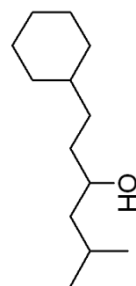
**2,8-dimethylnon-7-en-4-ol**

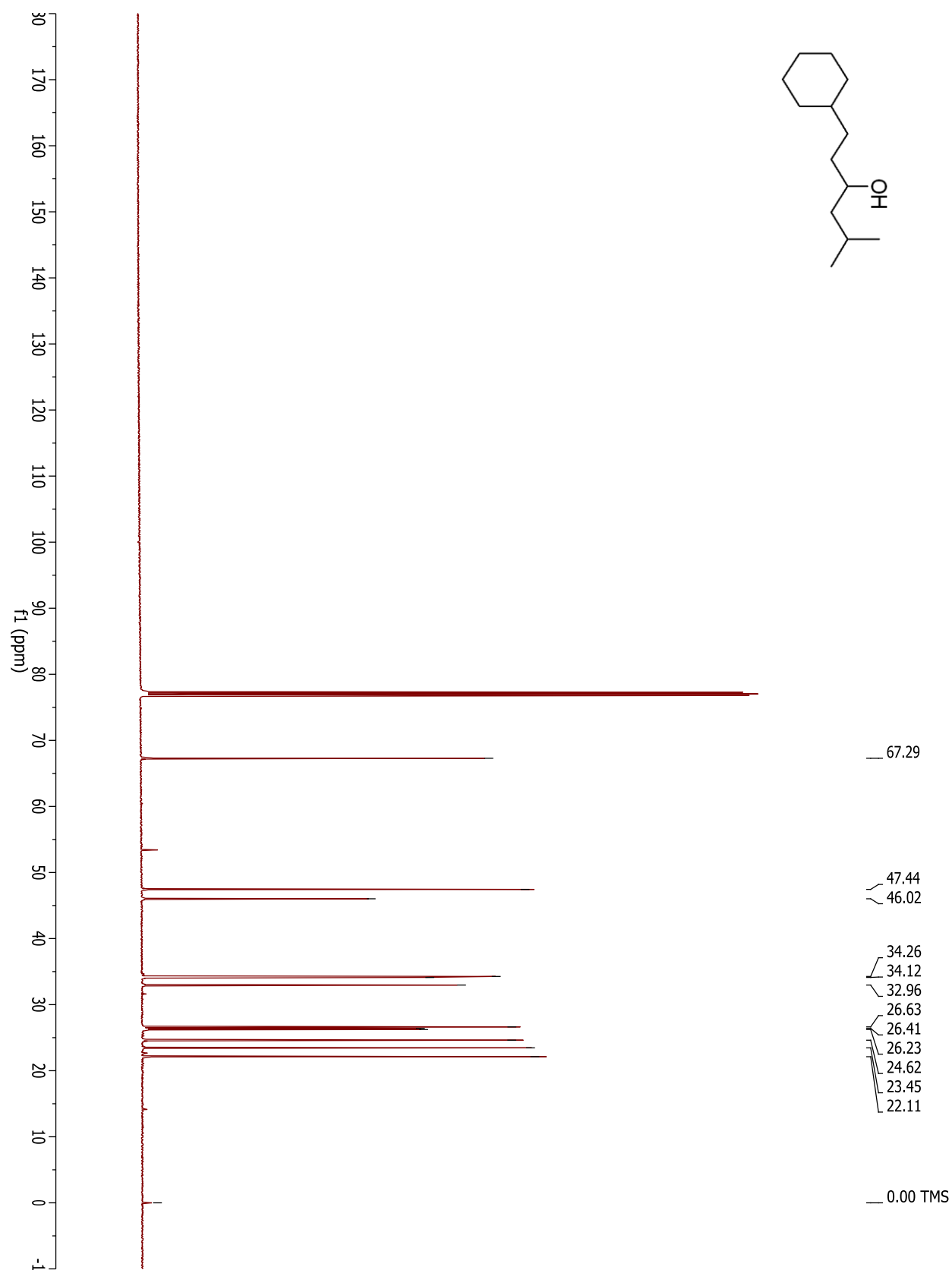
**2,8-dimethylnon-7-en-4-ol**

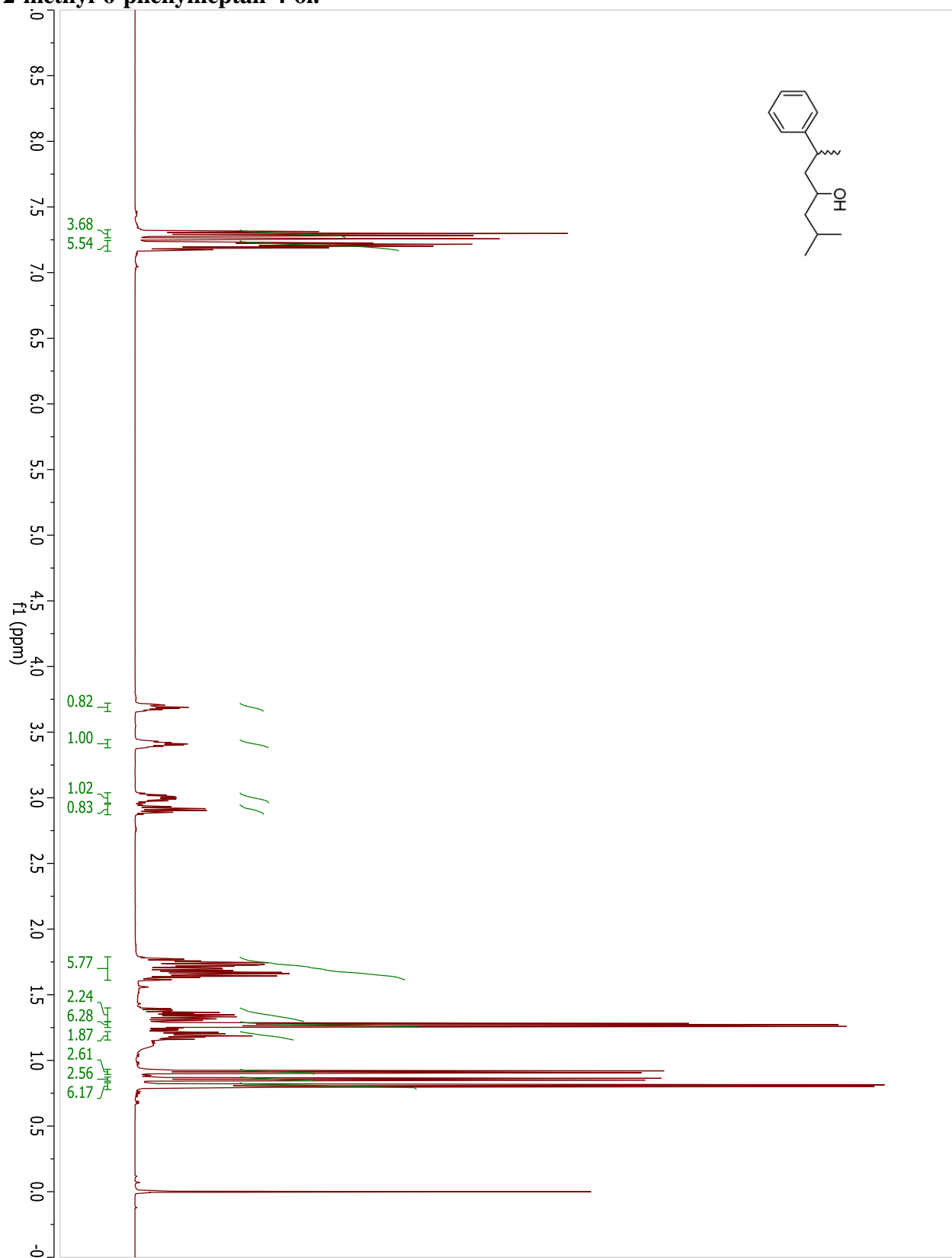
**2-methyltridec-7-yn-4-ol**

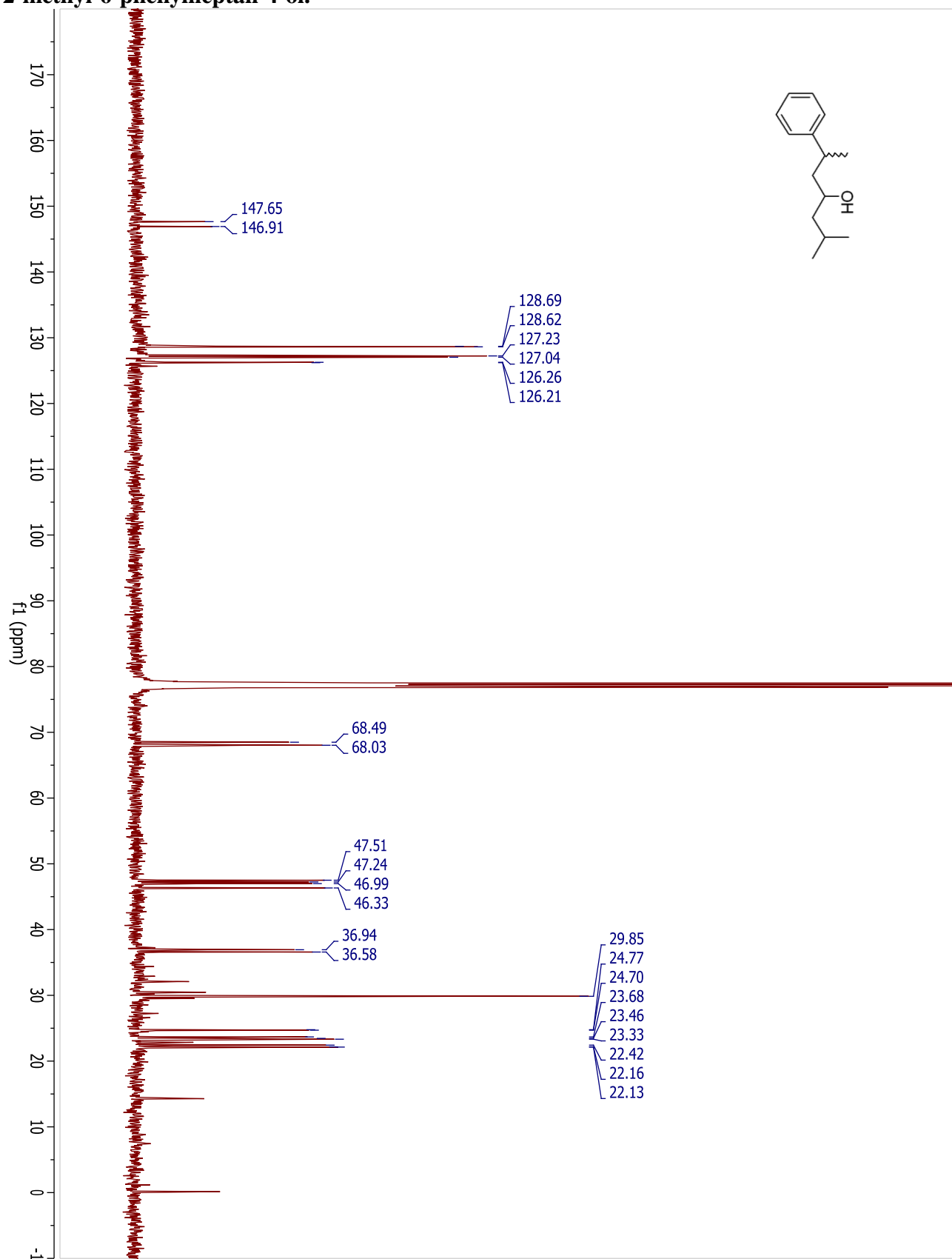
## 2-methyltridec-7-yn-4-ol



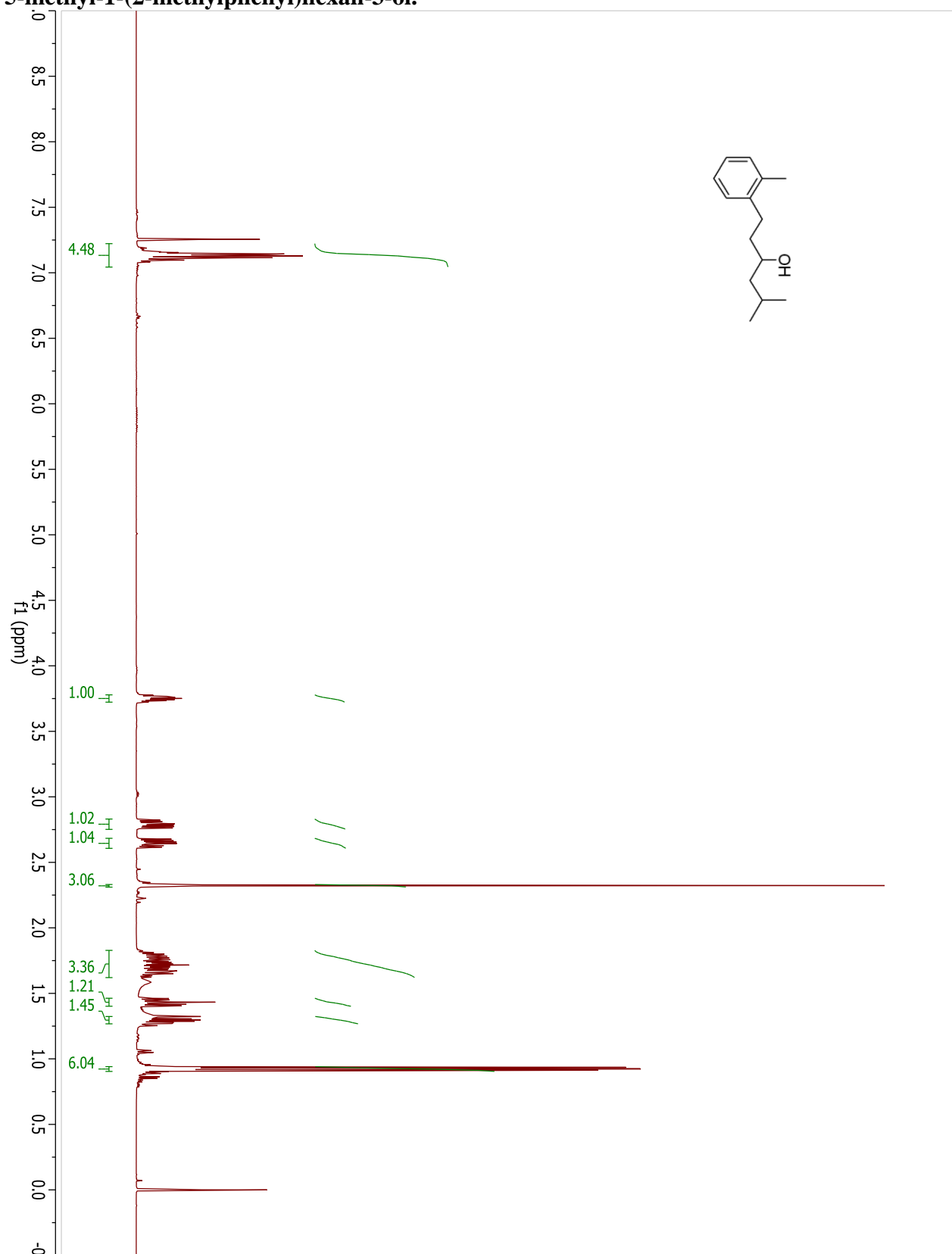
**1-cyclohexyl-4-methylpentan-2-ol**

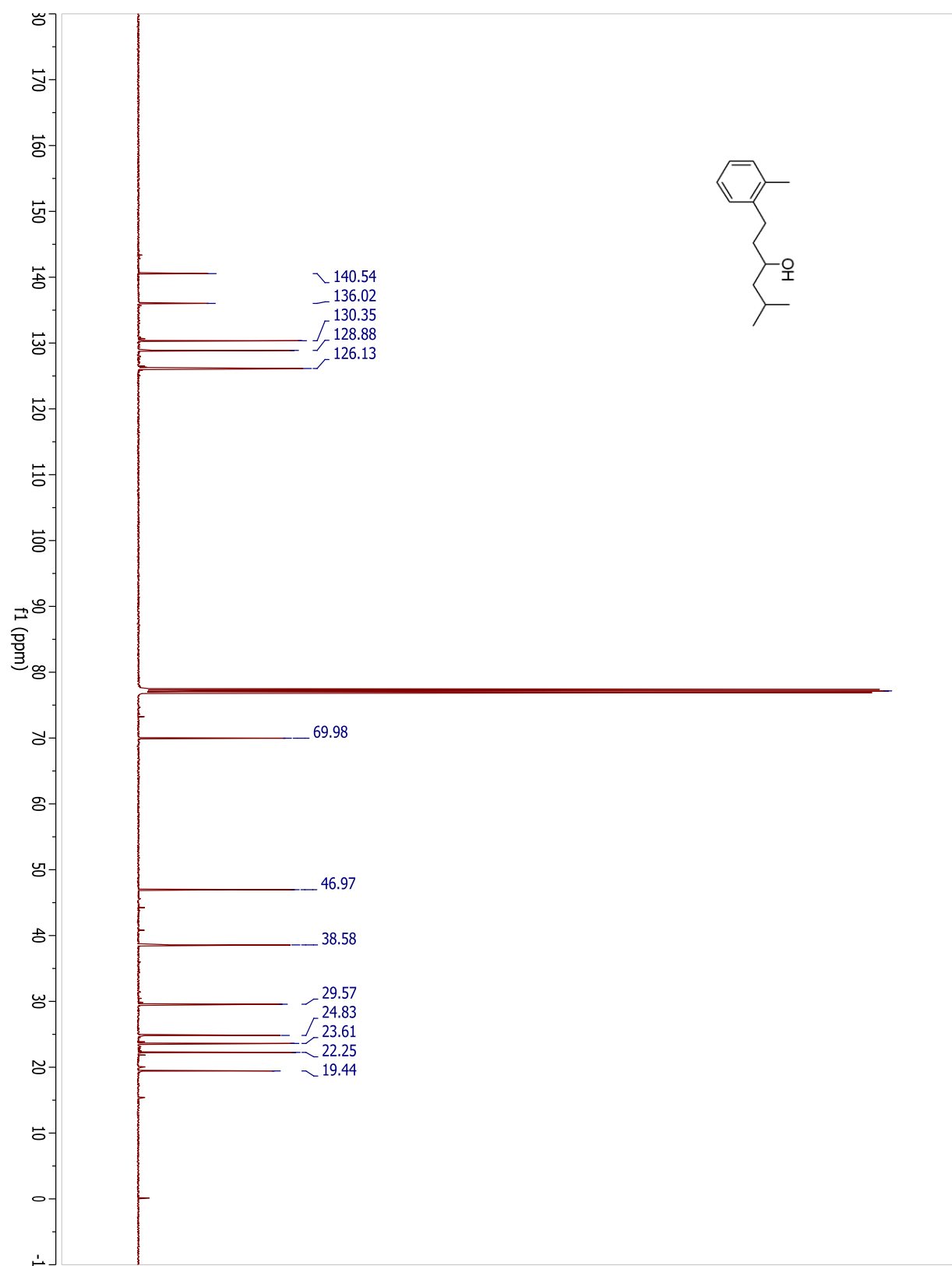
**1-cyclohexyl-4-methylpentan-2-ol**

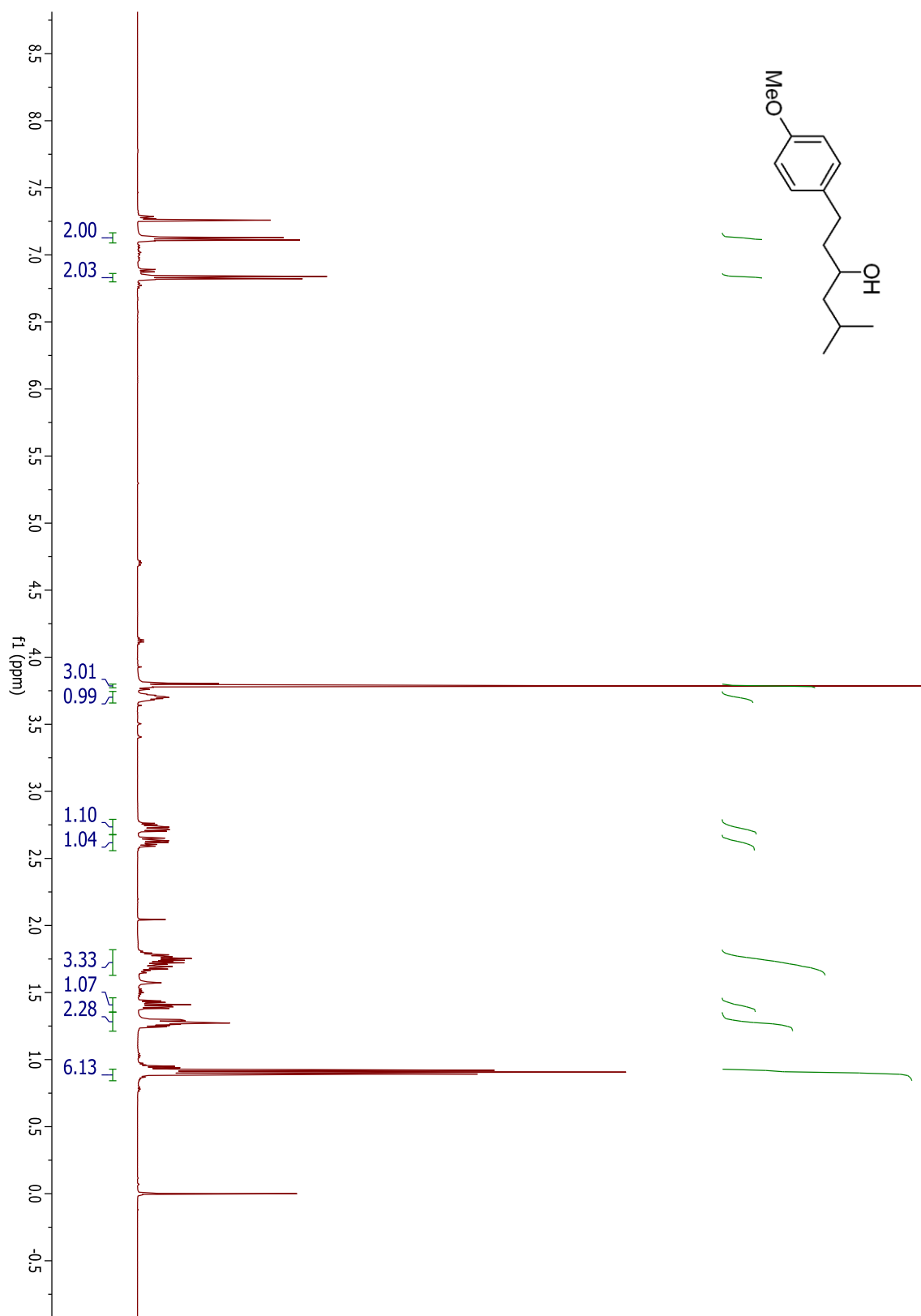
**2-methyl-6-phenylheptan-4-ol.**

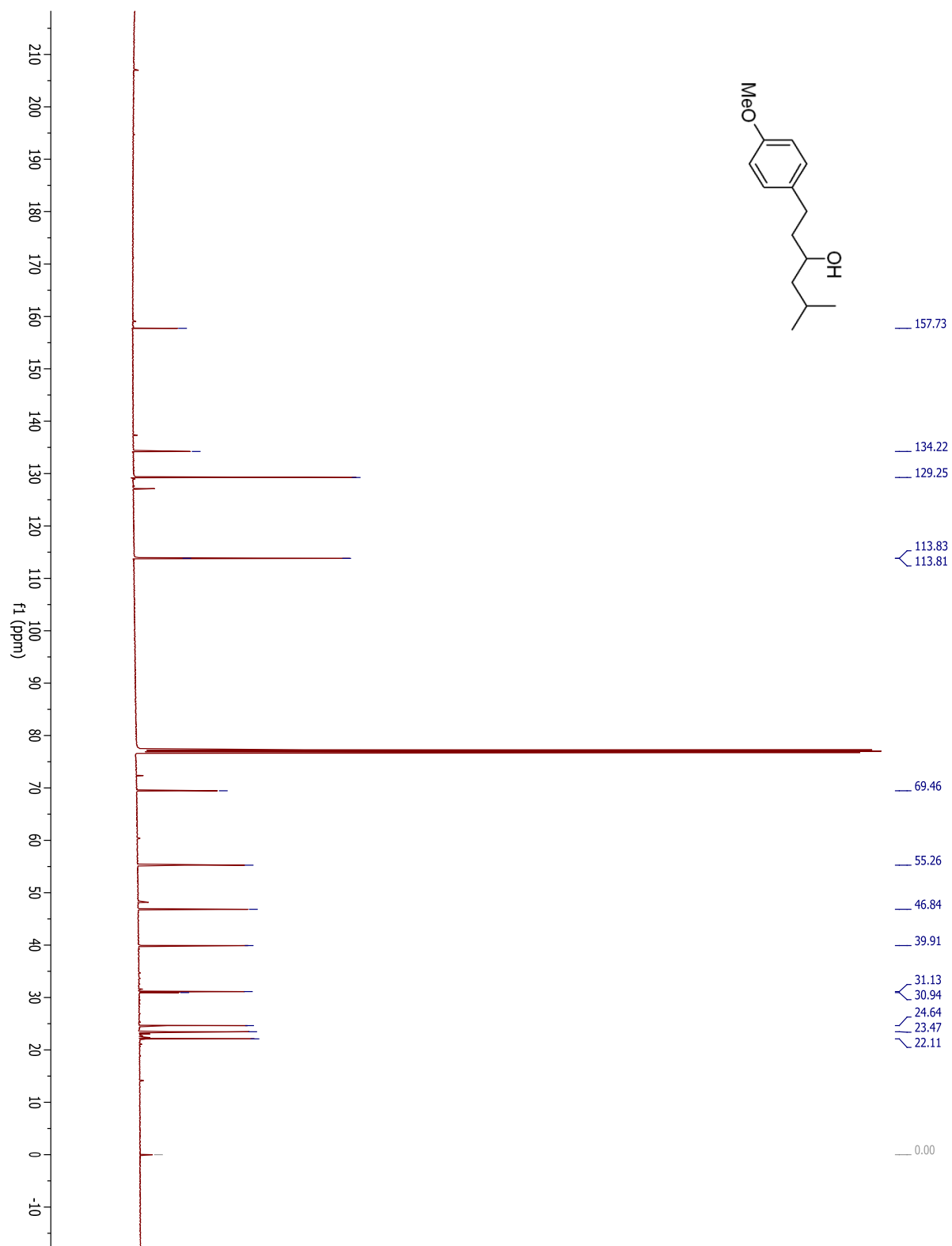
**2-methyl-6-phenylheptan-4-ol.**

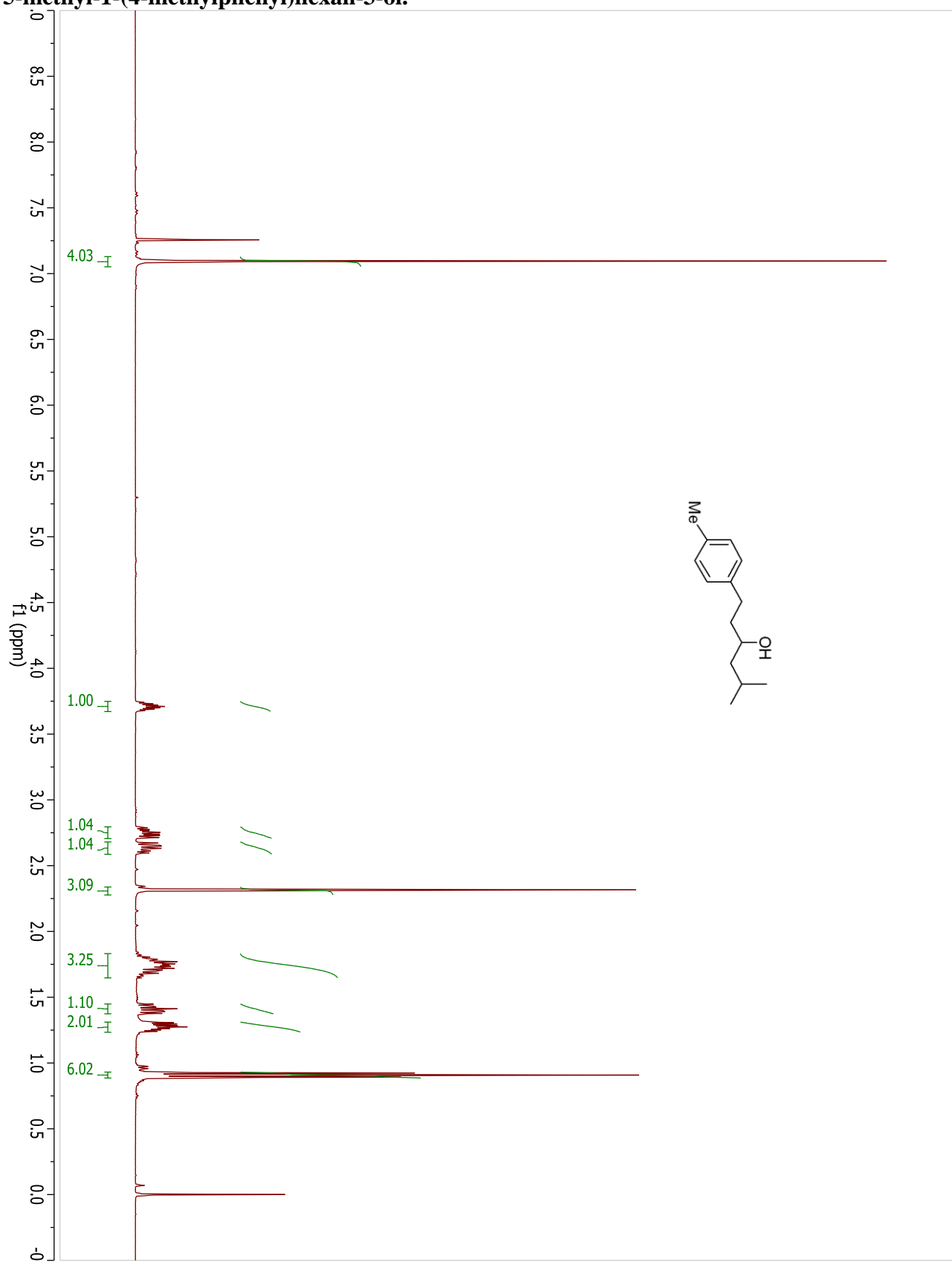


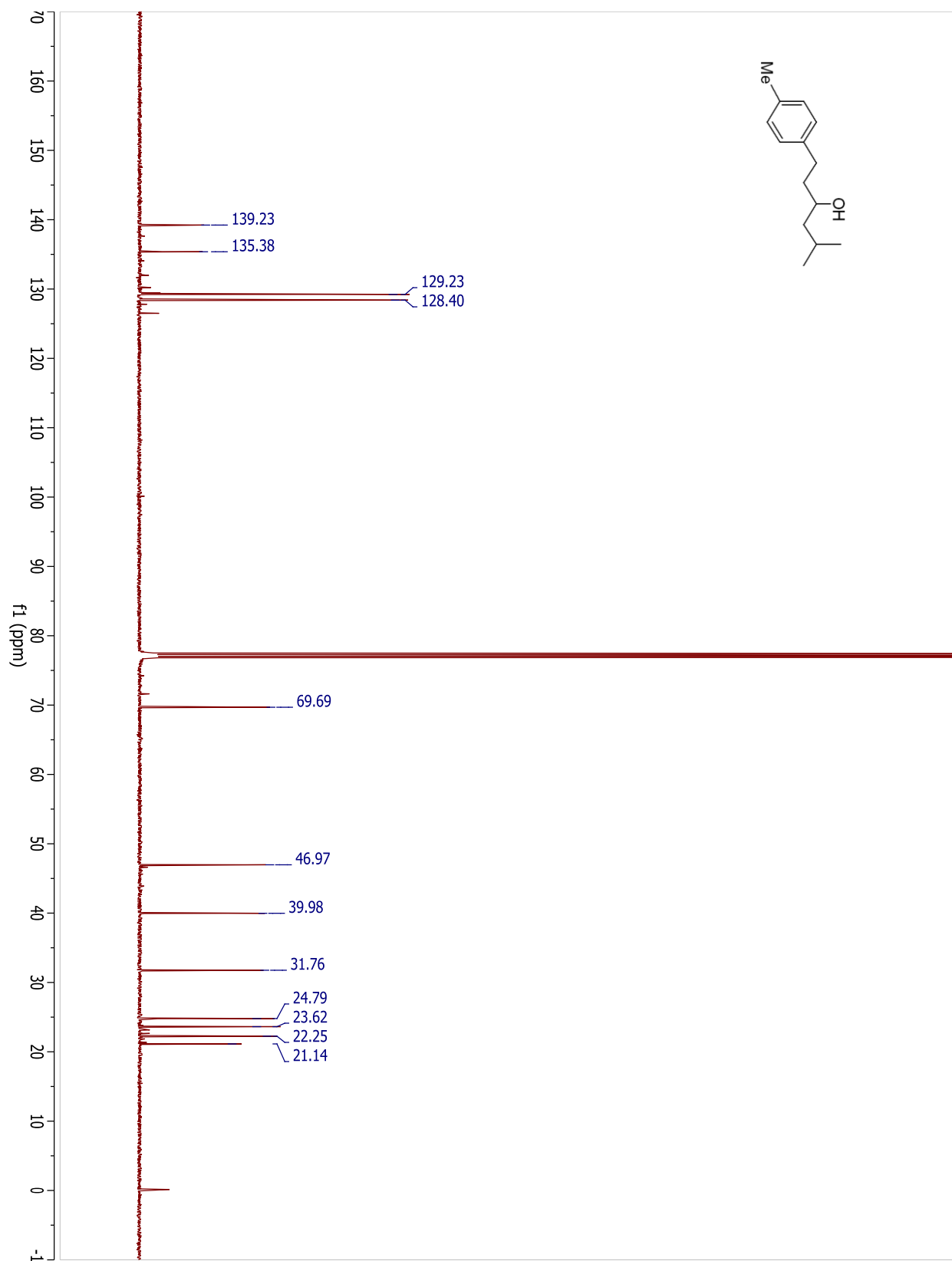
**5-methyl-1-(2-methylphenyl)hexan-3-ol.**

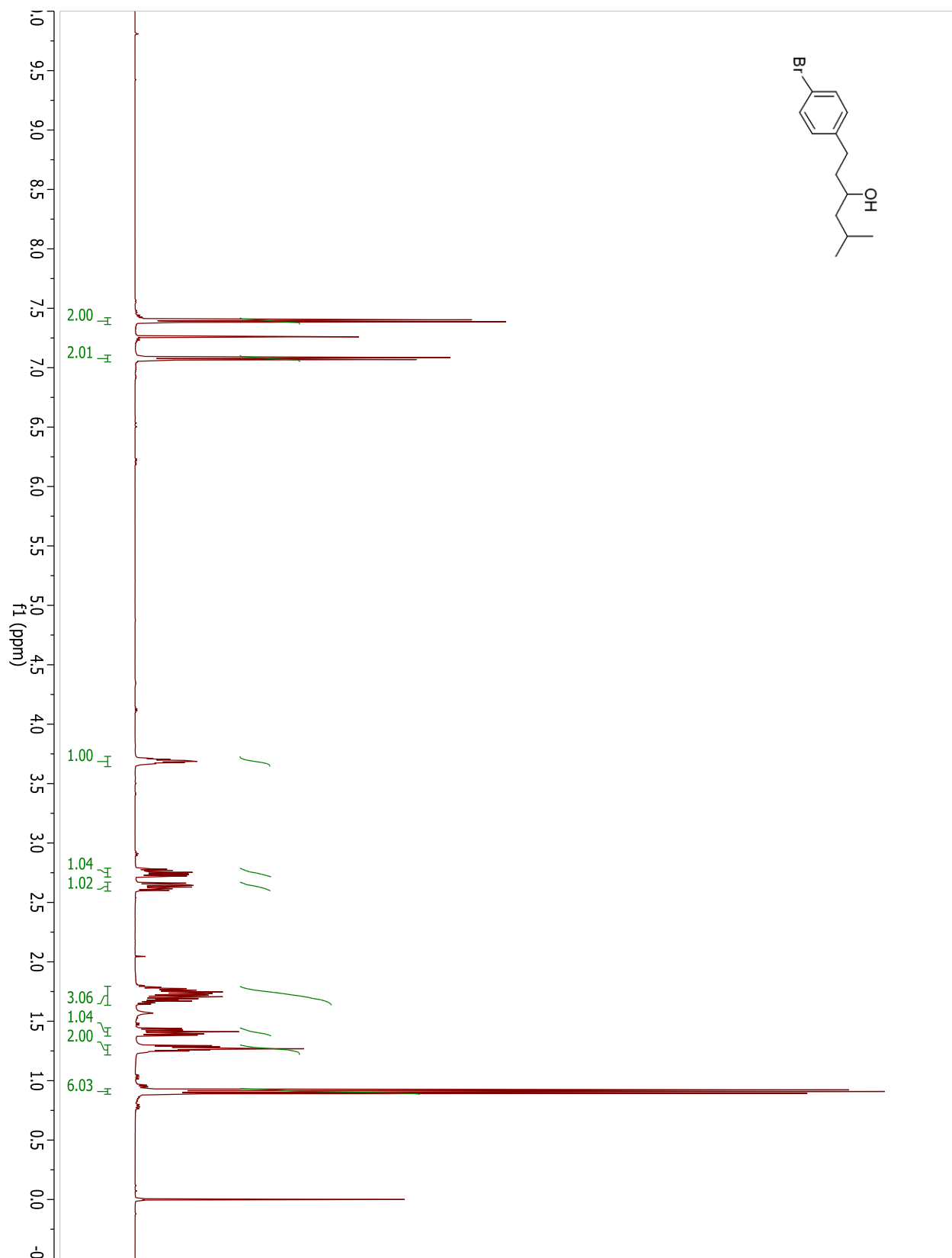
**5-methyl-1-(2-methylphenyl)hexan-3-ol.**

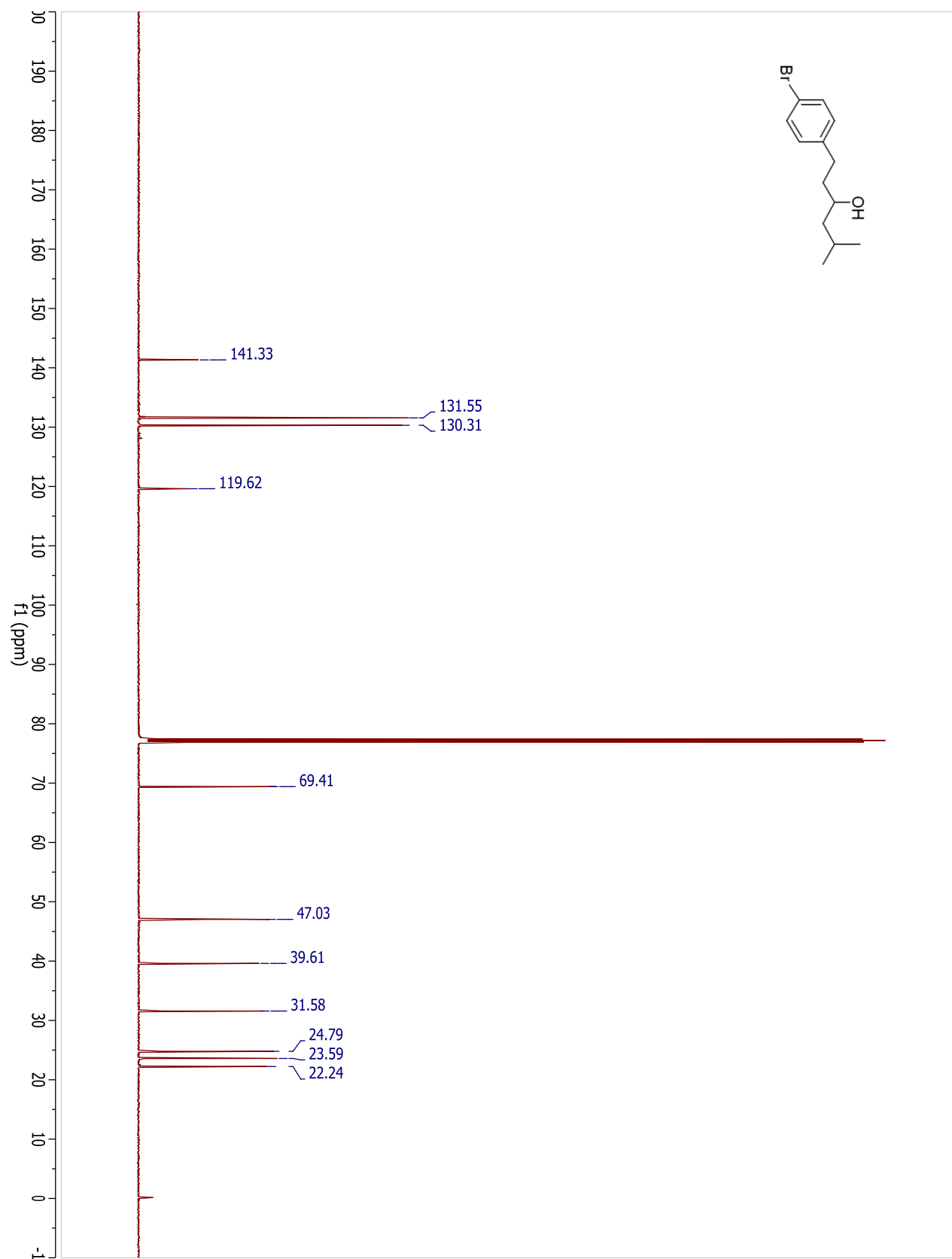
**1-(4-methoxyphenyl)-5-methylhexan-3-ol.**

**1-(4-methoxyphenyl)-5-methylhexan-3-ol.**

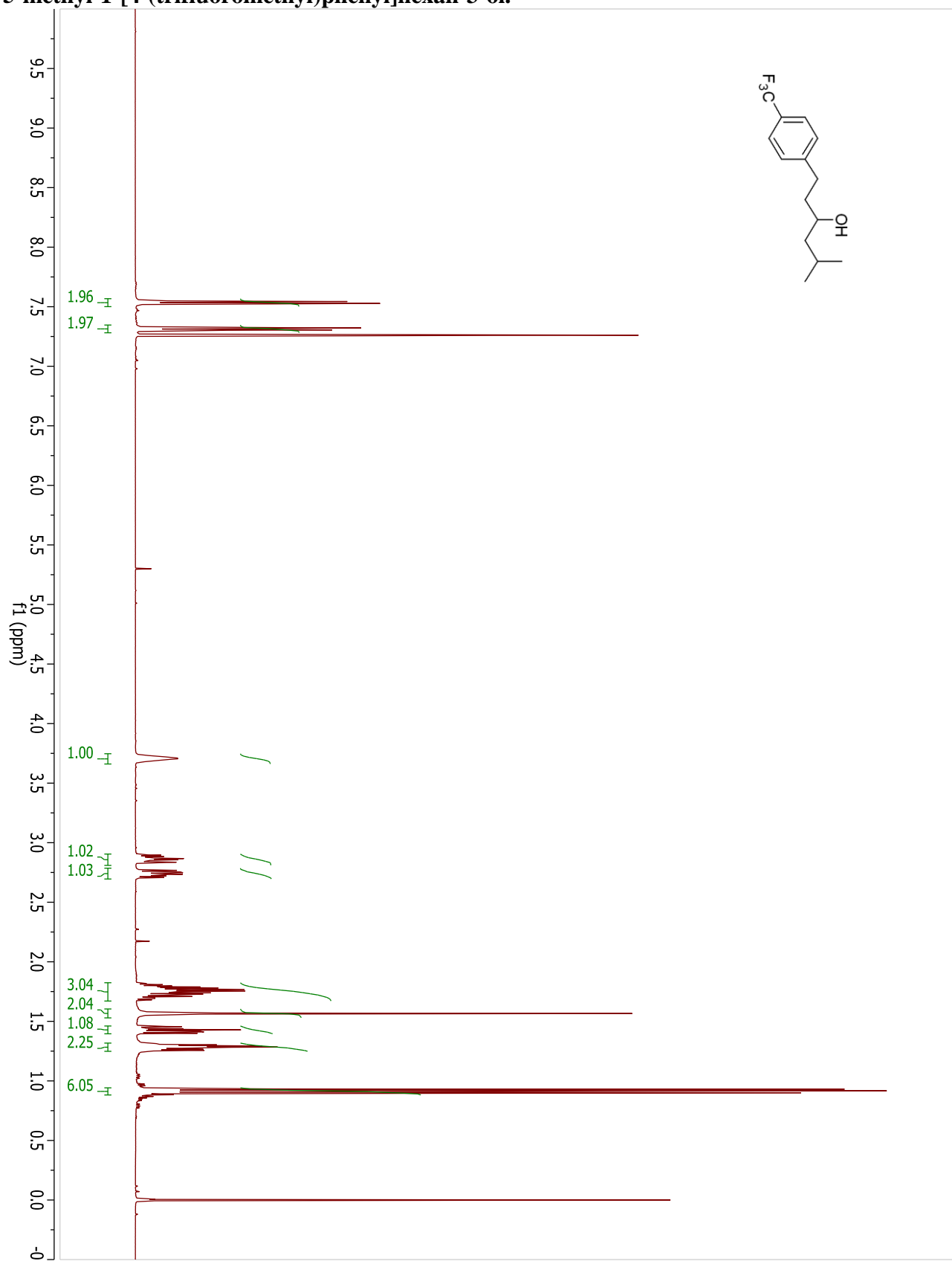
**5-methyl-1-(4-methylphenyl)hexan-3-ol.**

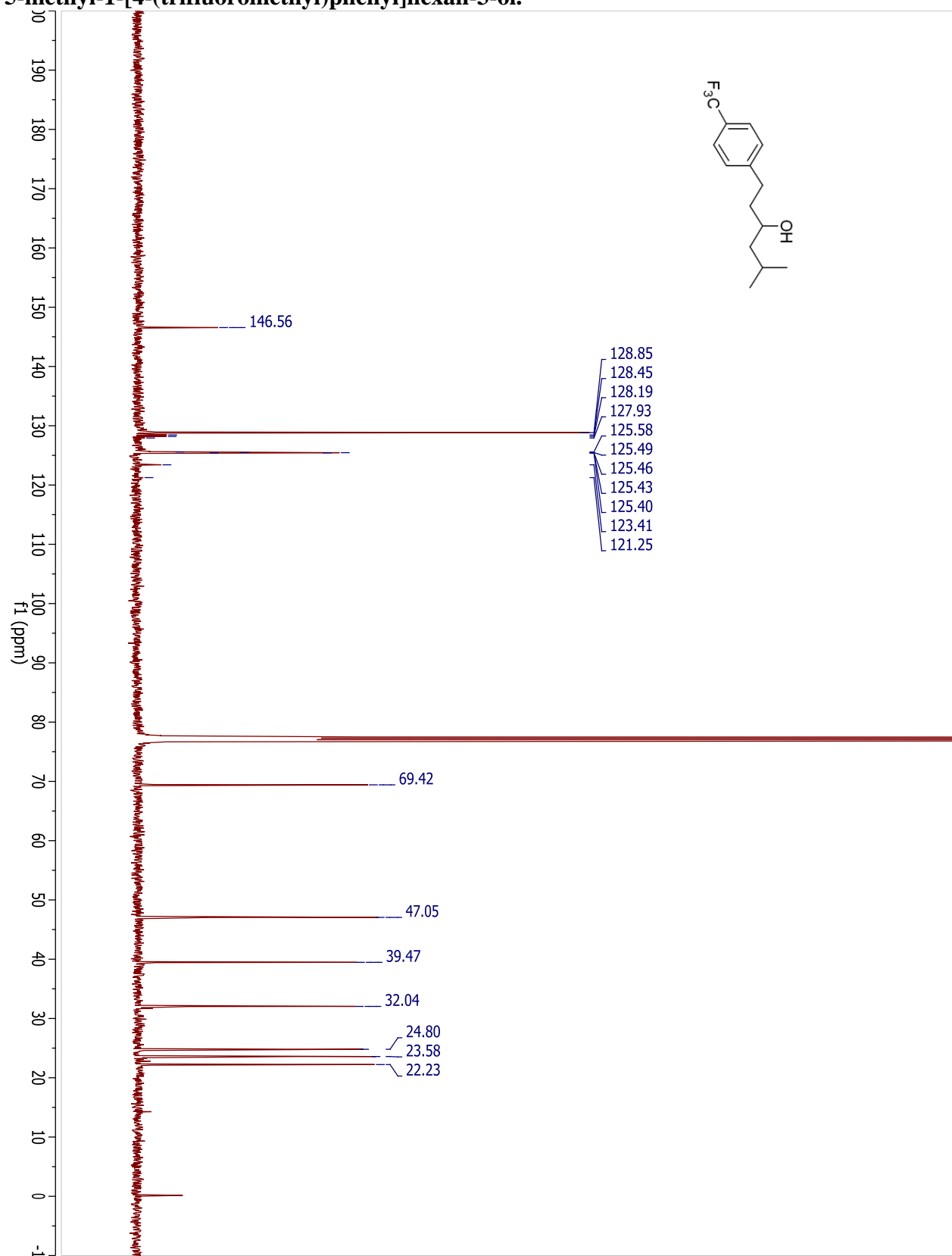
**5-methyl-1-(4-methylphenyl)hexan-3-ol.**

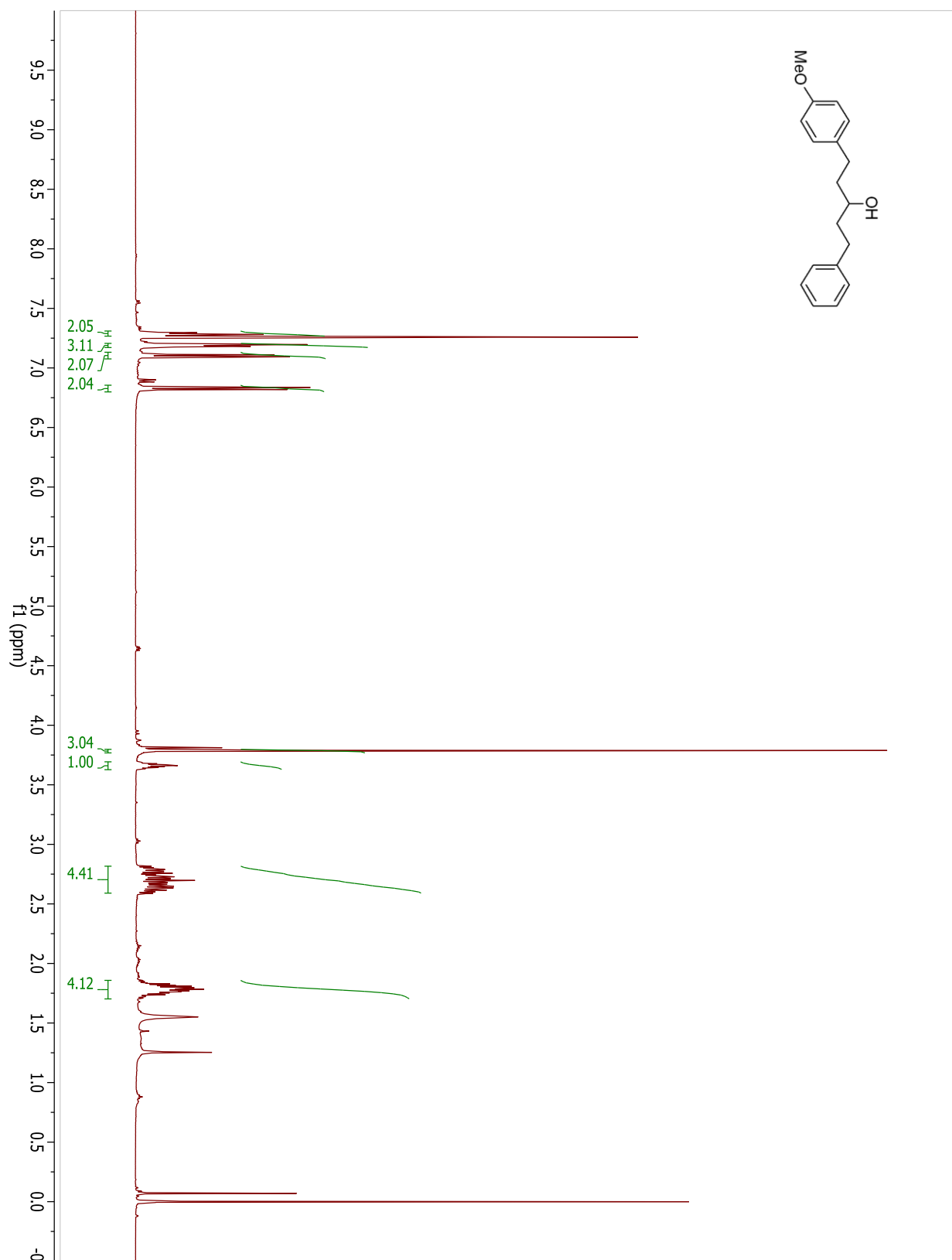
**1-(4-bromophenyl)-5-methylhexan-3-ol.**

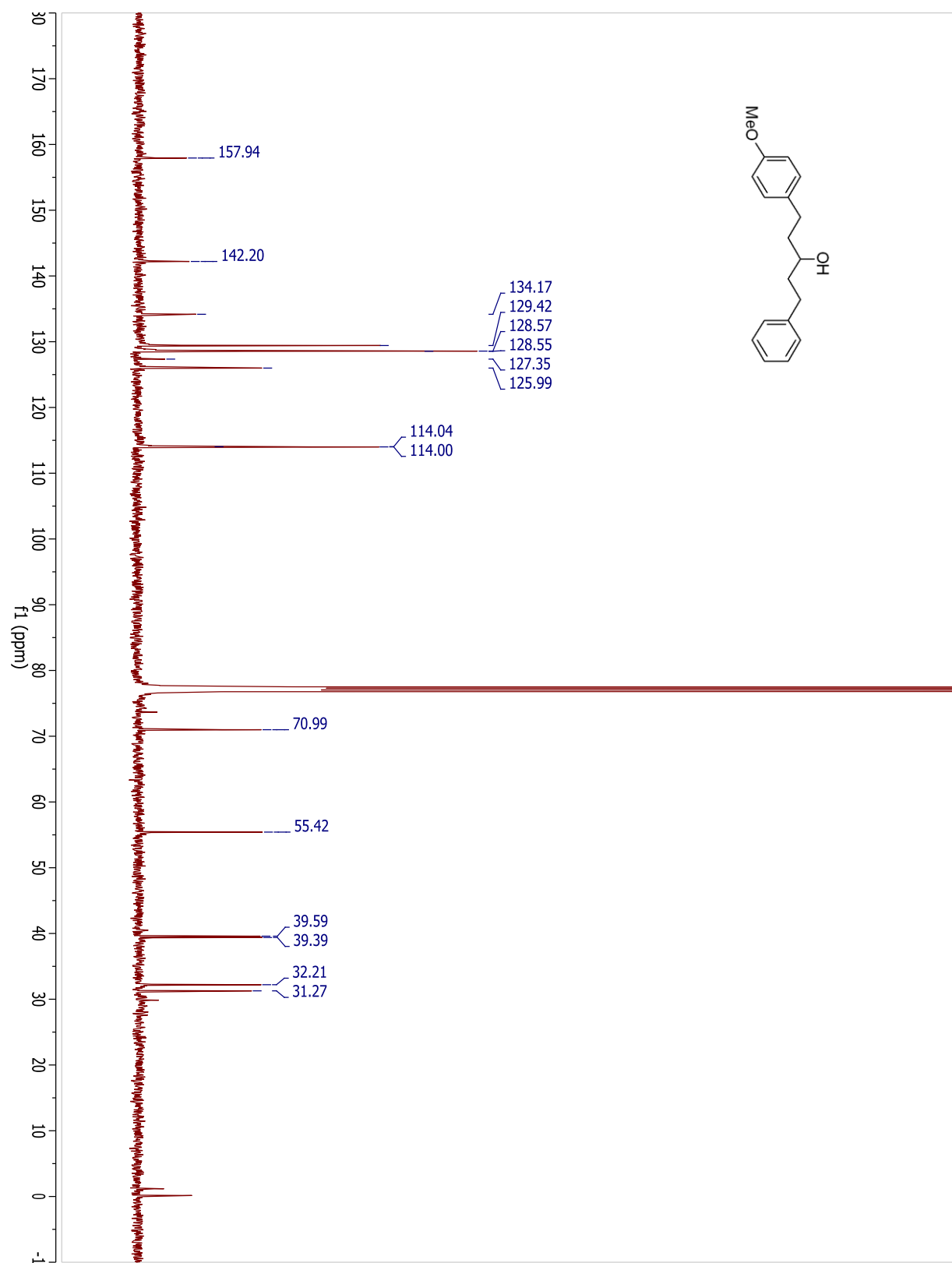
**1-(4-bromophenyl)-5-methylhexan-3-ol.**

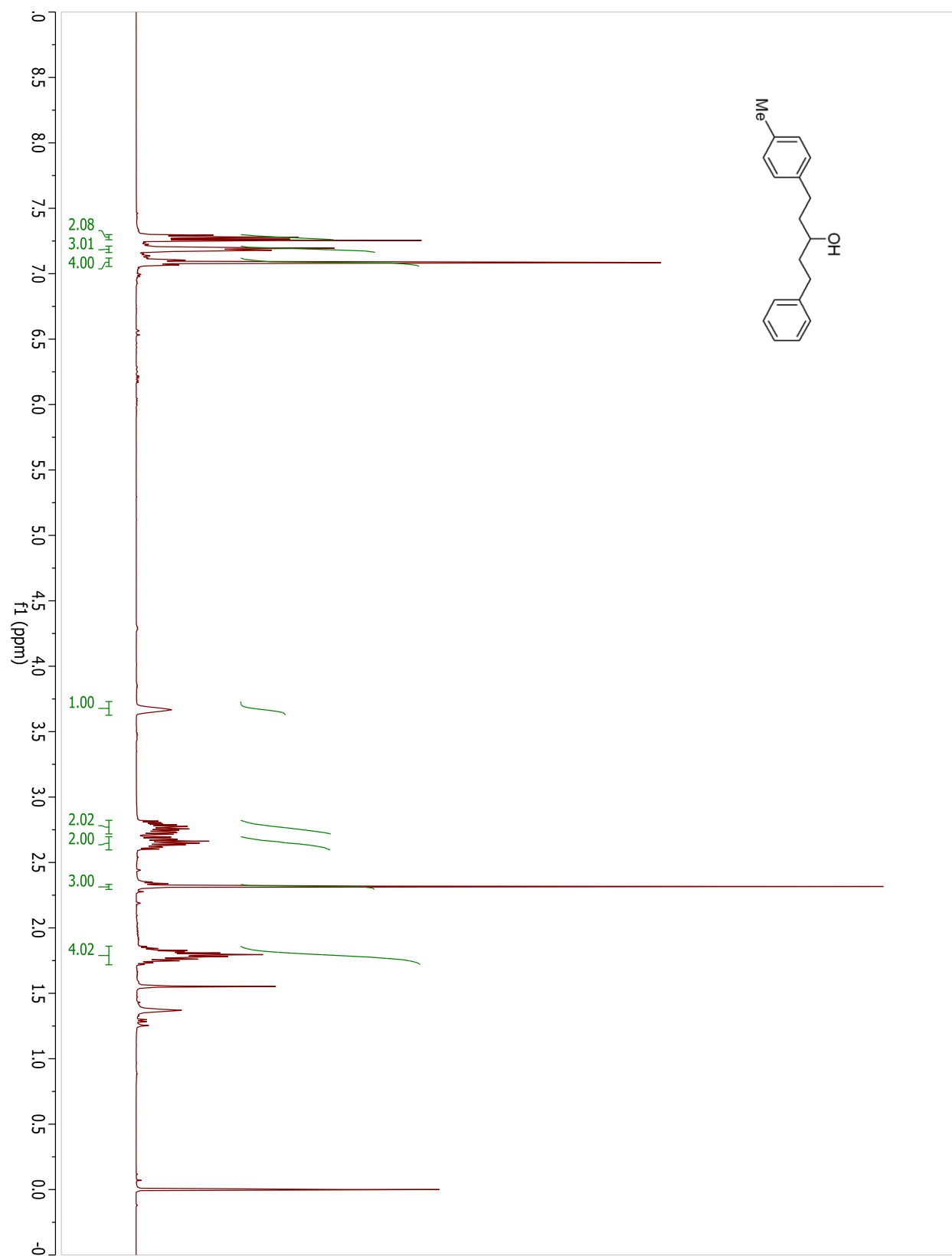


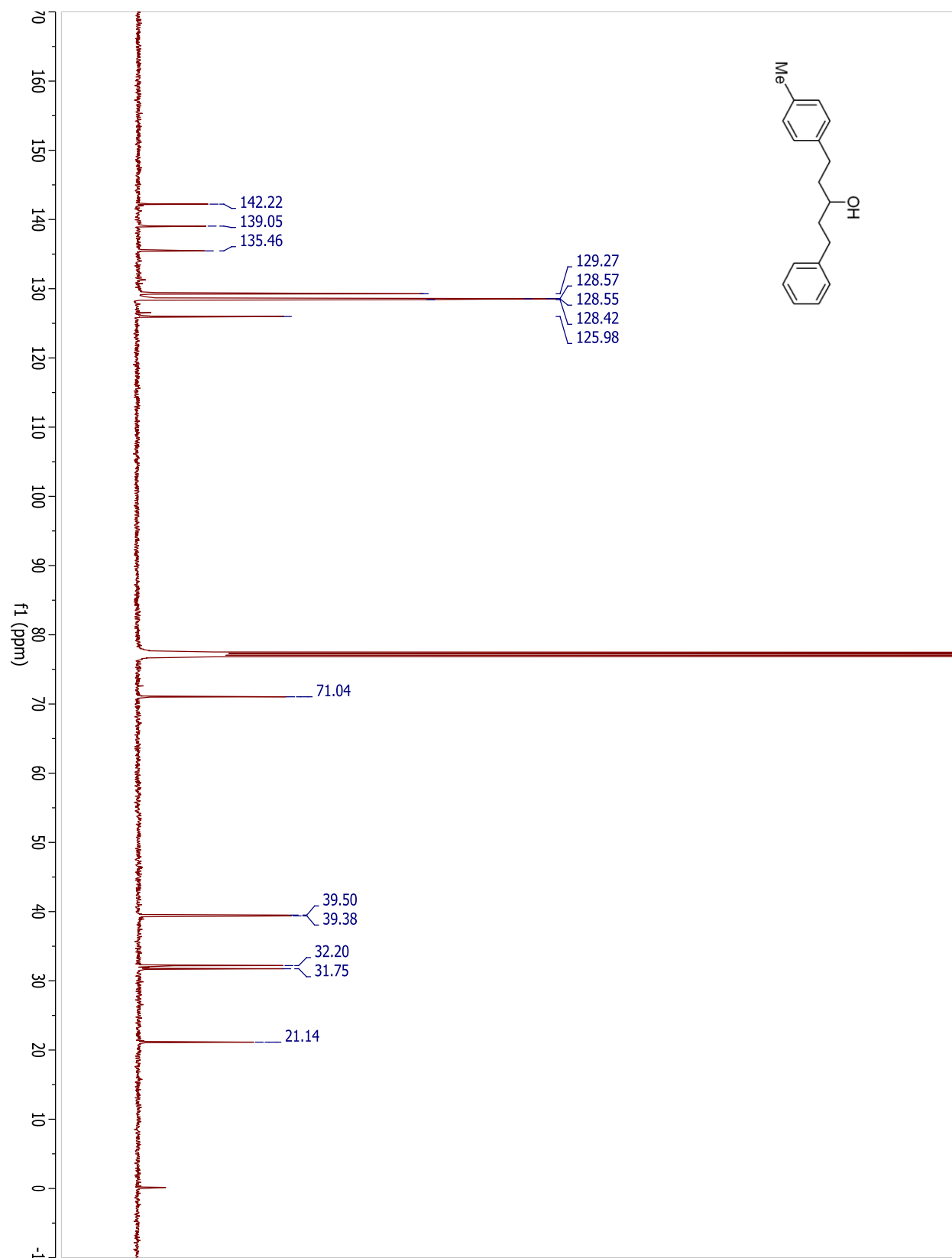
**5-methyl-1-[4-(trifluoromethyl)phenyl]hexan-3-ol.**

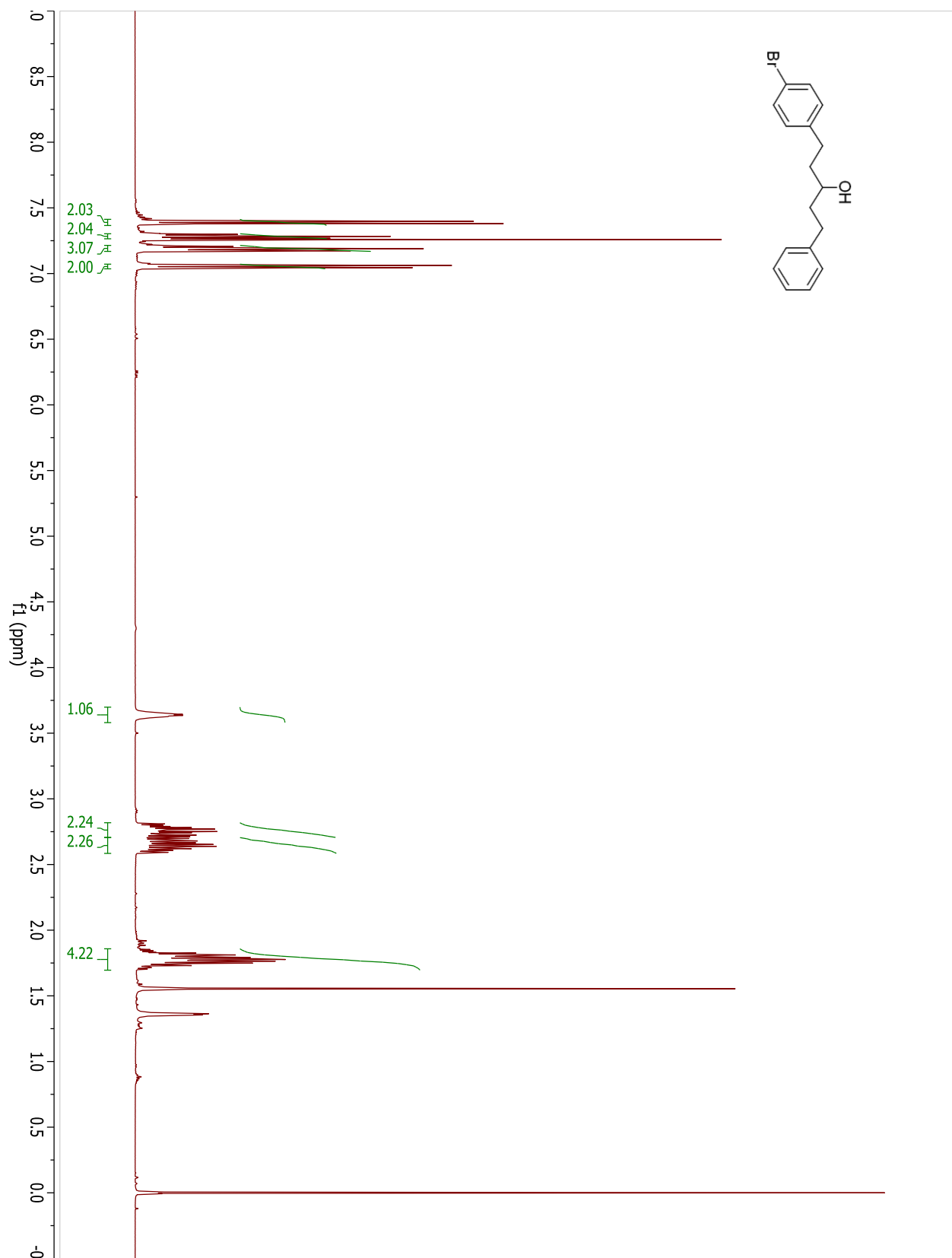
**5-methyl-1-[4-(trifluoromethyl)phenyl]hexan-3-ol.**

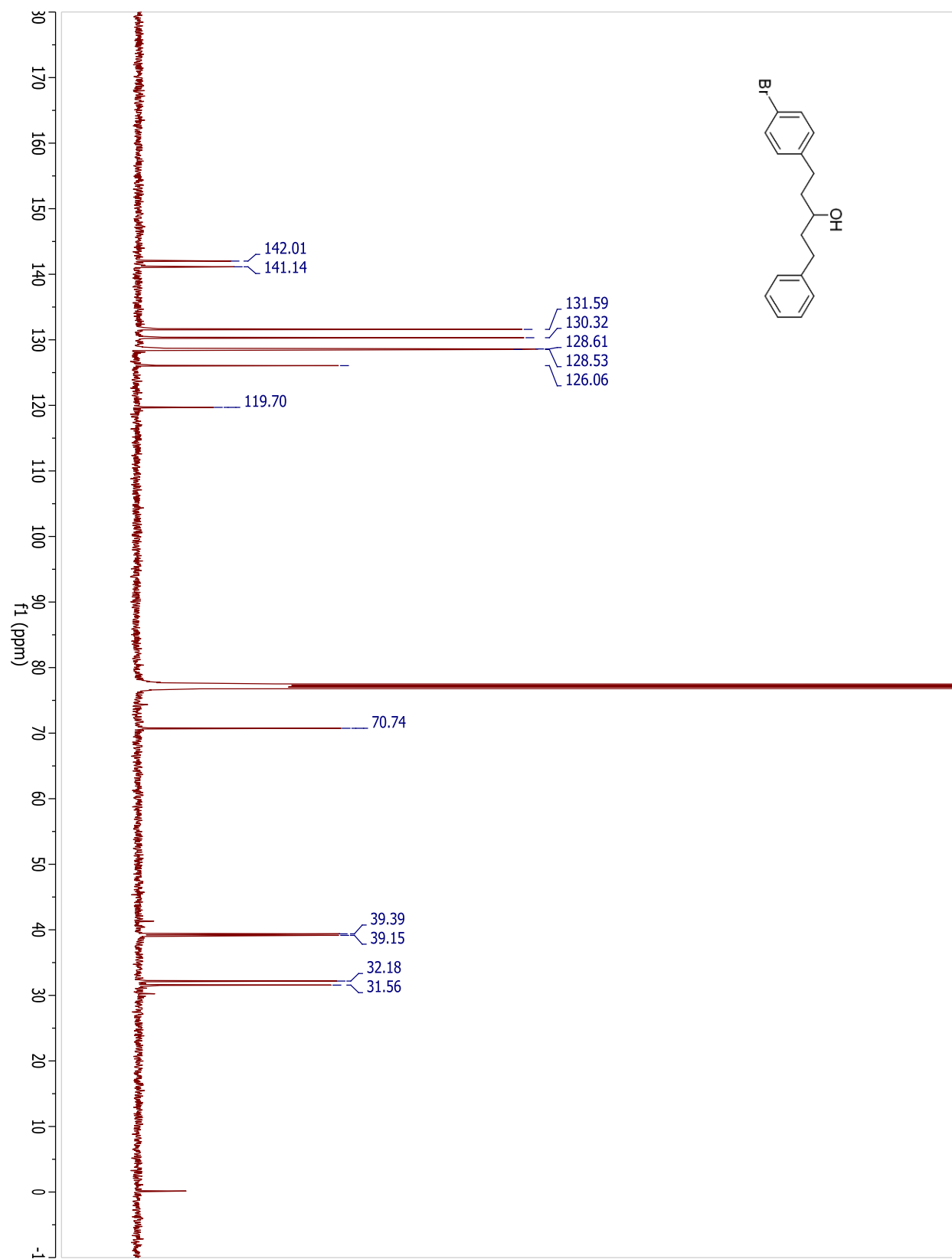
**1-(4-methoxyphenyl)-5-phenylpentan-3-ol.**

**1-(4-methoxyphenyl)-5-phenylpentan-3-ol.**

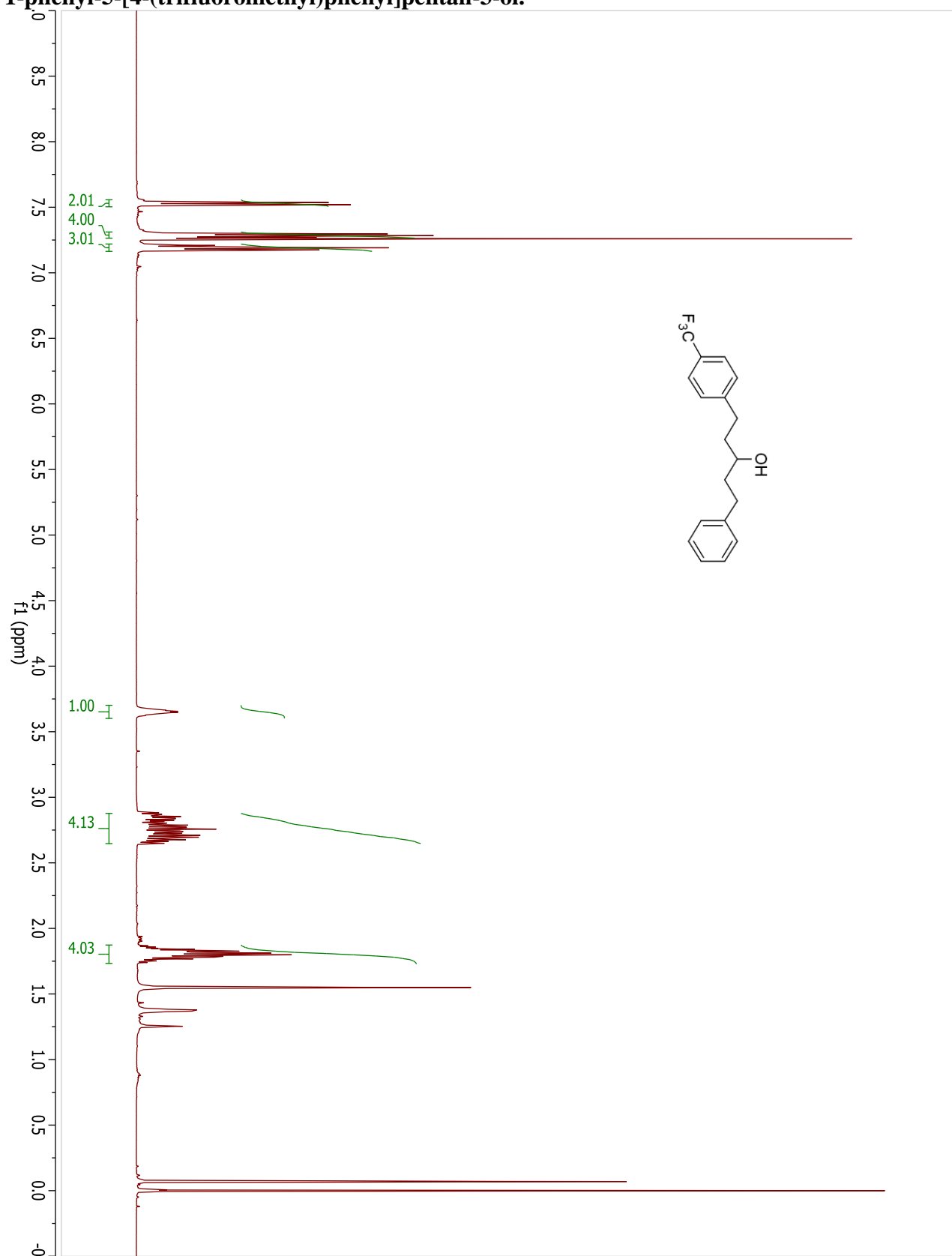
**1-(4-methylphenyl)-5-phenylpentan-3-ol.**

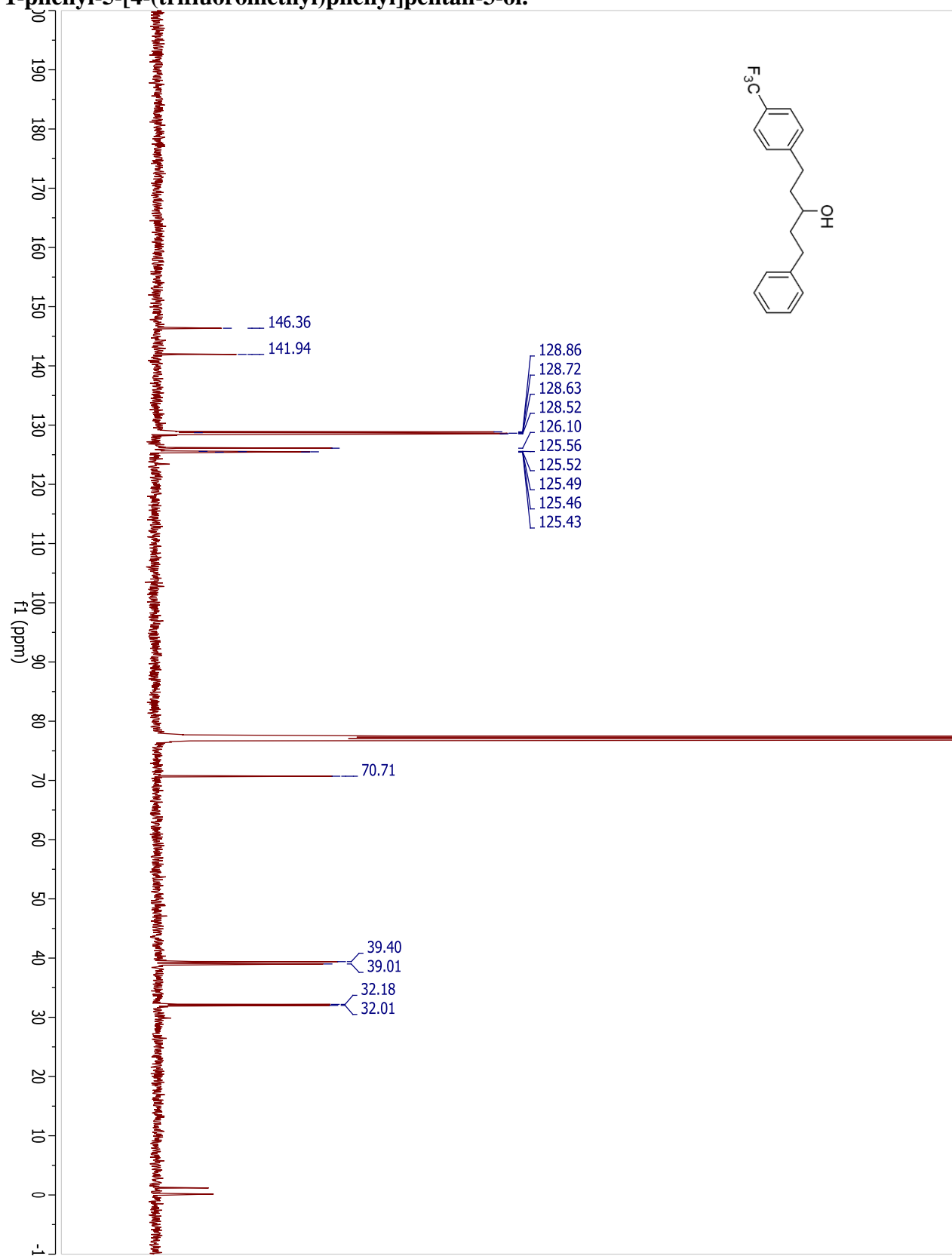
**1-(4-methylphenyl)-5-phenylpentan-3-ol.**

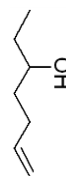
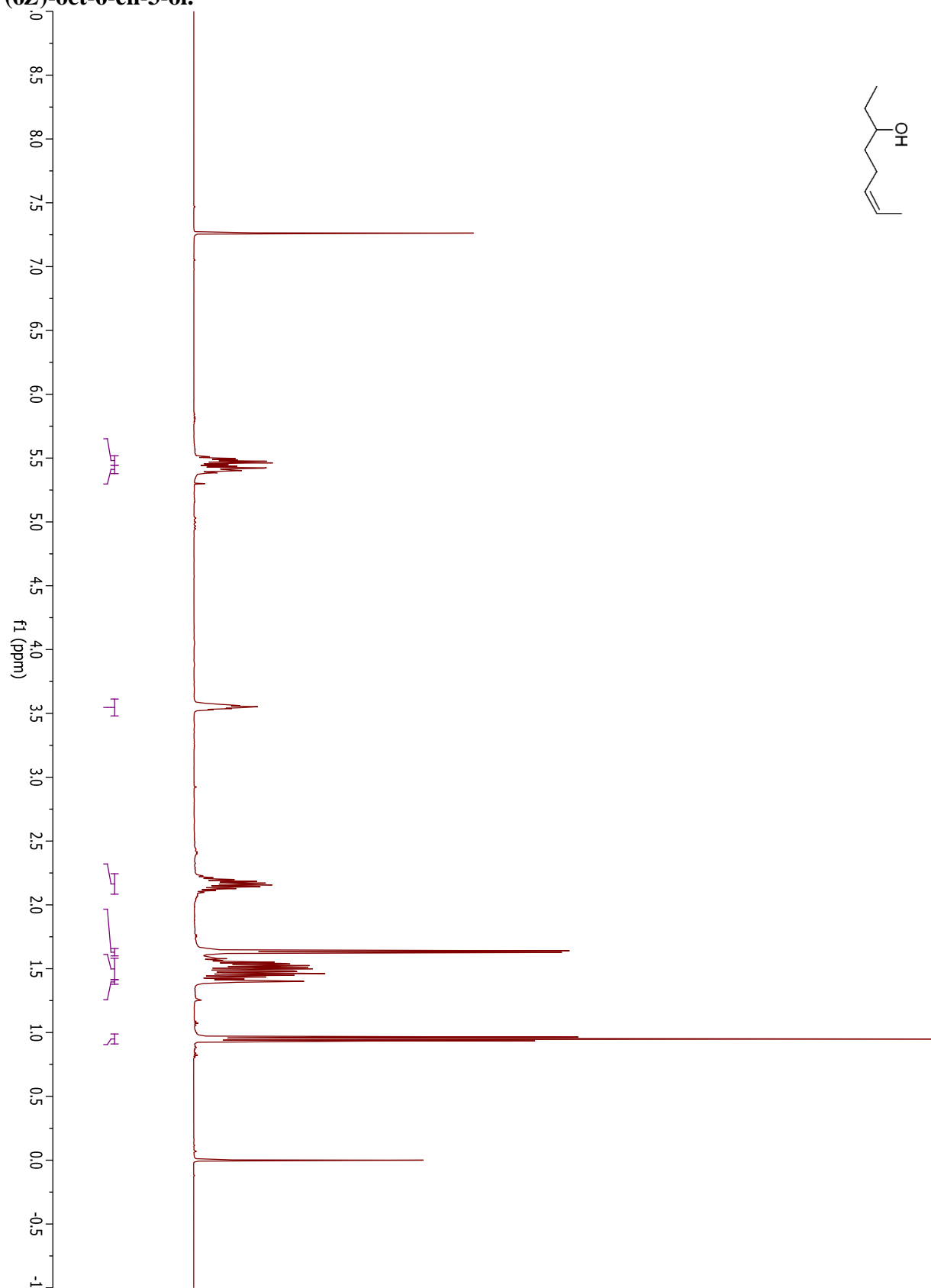
**1-(4-bromophenyl)-5-phenylpentan-3-ol.**

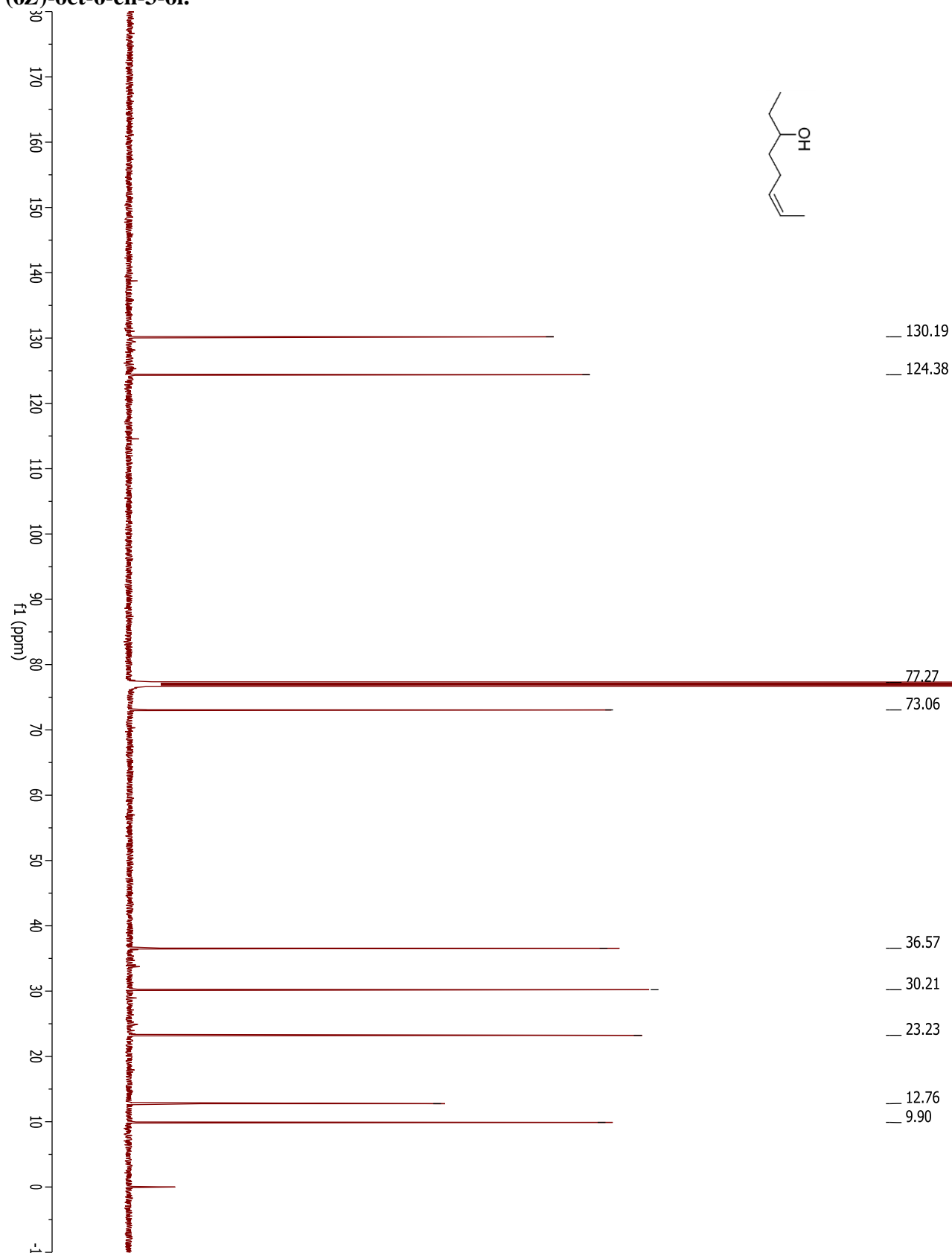
**1-(4-bromophenyl)-5-phenylpentan-3-ol.**

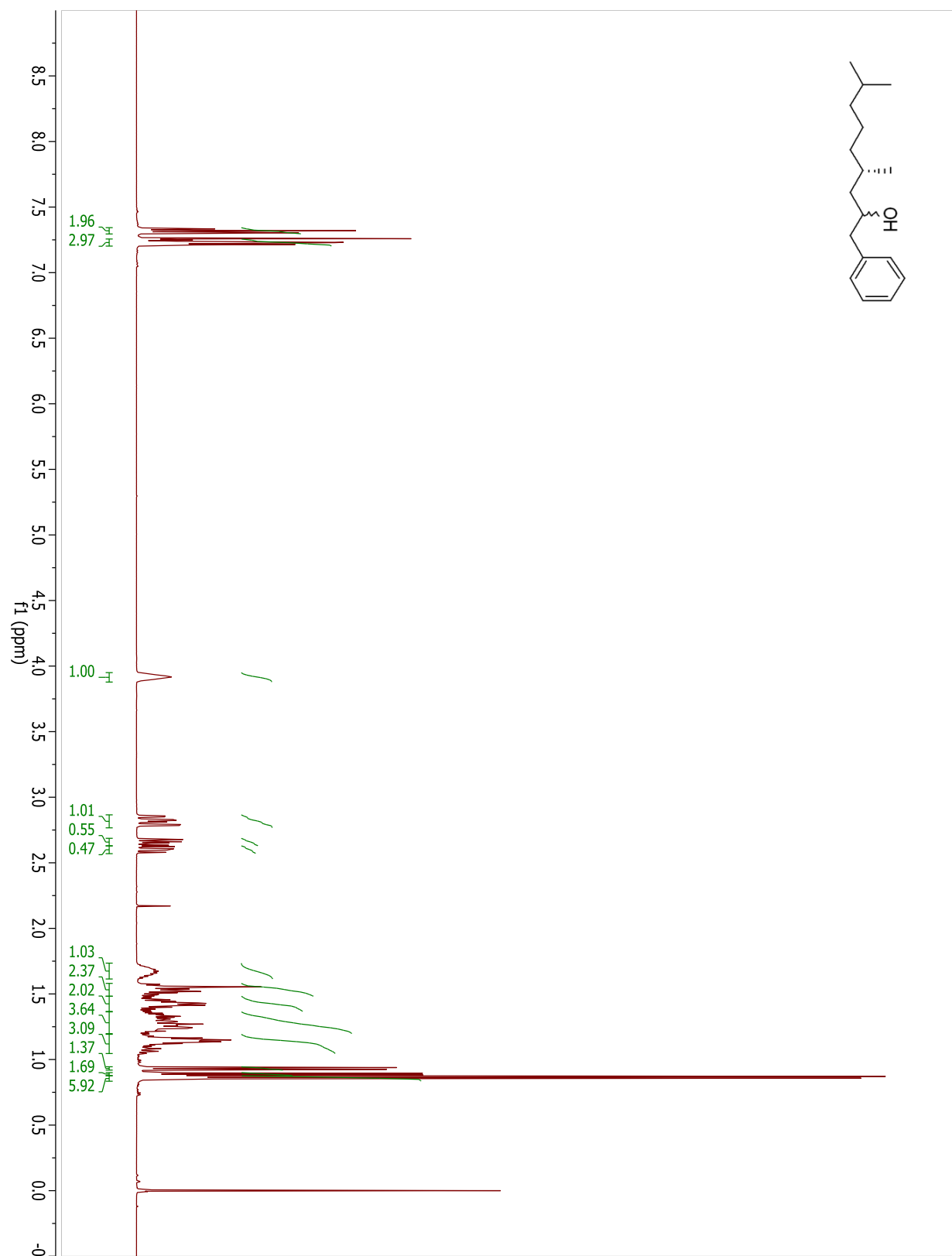


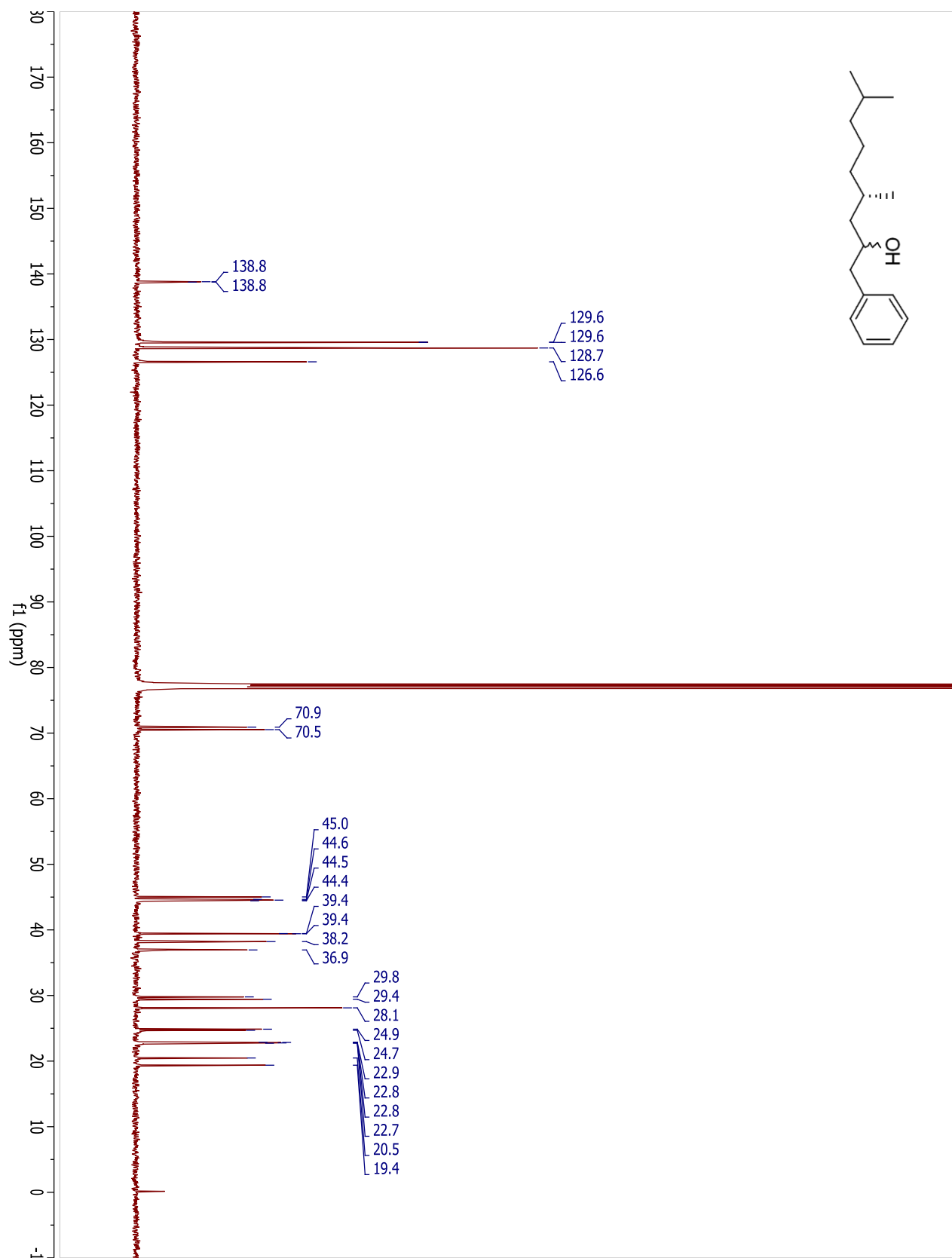
**1-phenyl-5-[4-(trifluoromethyl)phenyl]pentan-3-ol.**

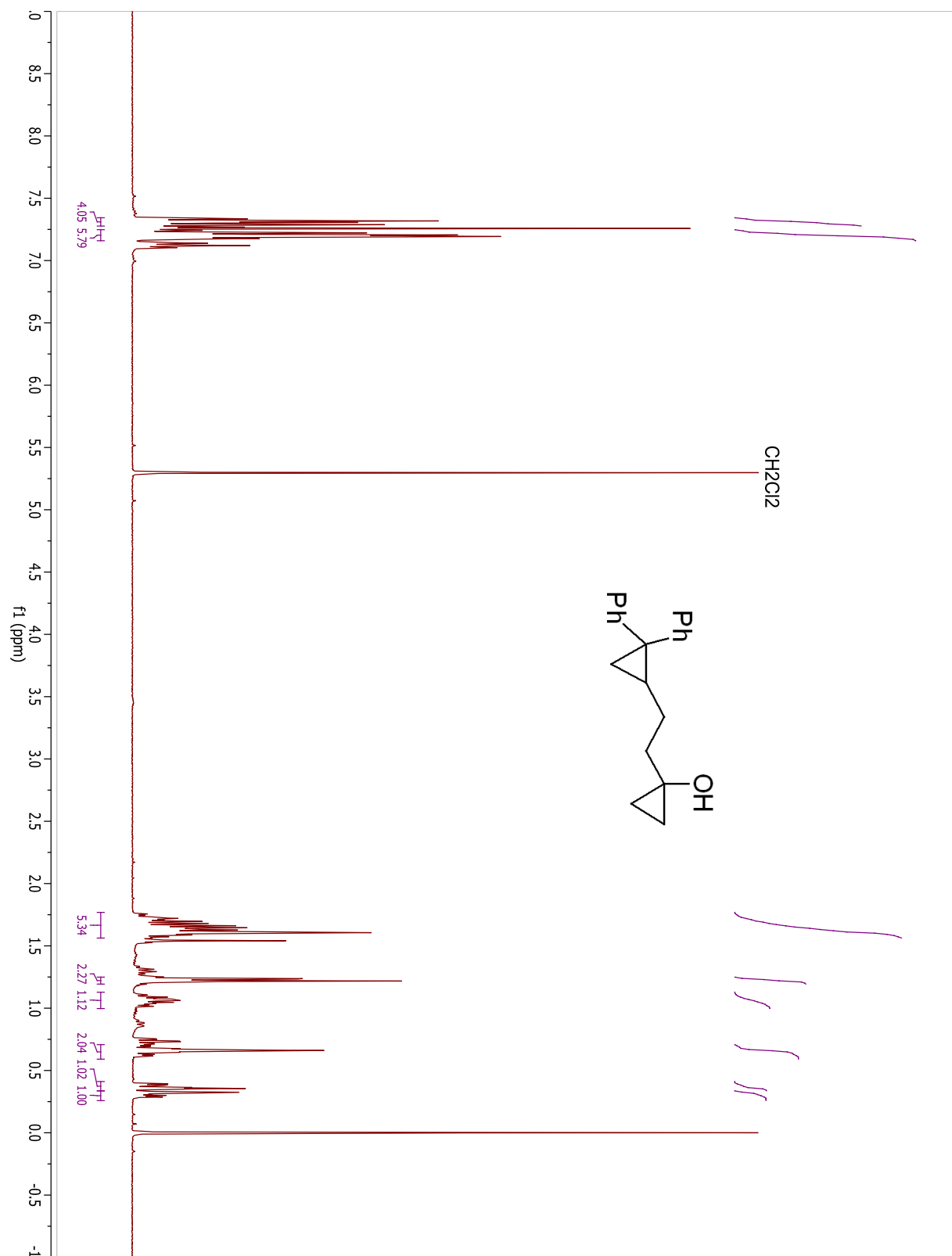
**1-phenyl-5-[4-(trifluoromethyl)phenyl]pentan-3-ol.**

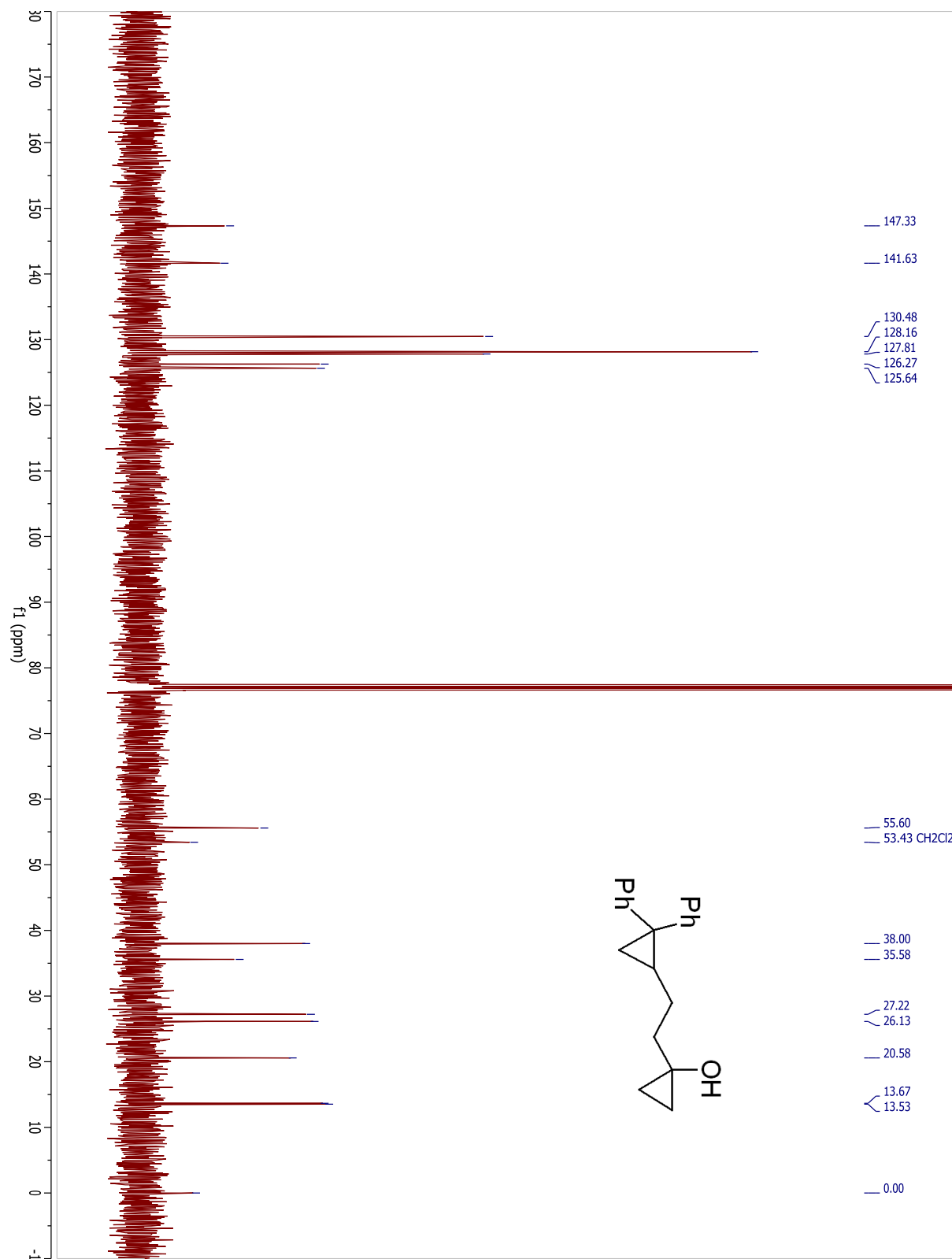
**(6Z)-oct-6-en-3-ol.**

**(6Z)-oct-6-en-3-ol.**

**(4S)-4,8-dimethyl-1-phenylnonan-2-ol.**

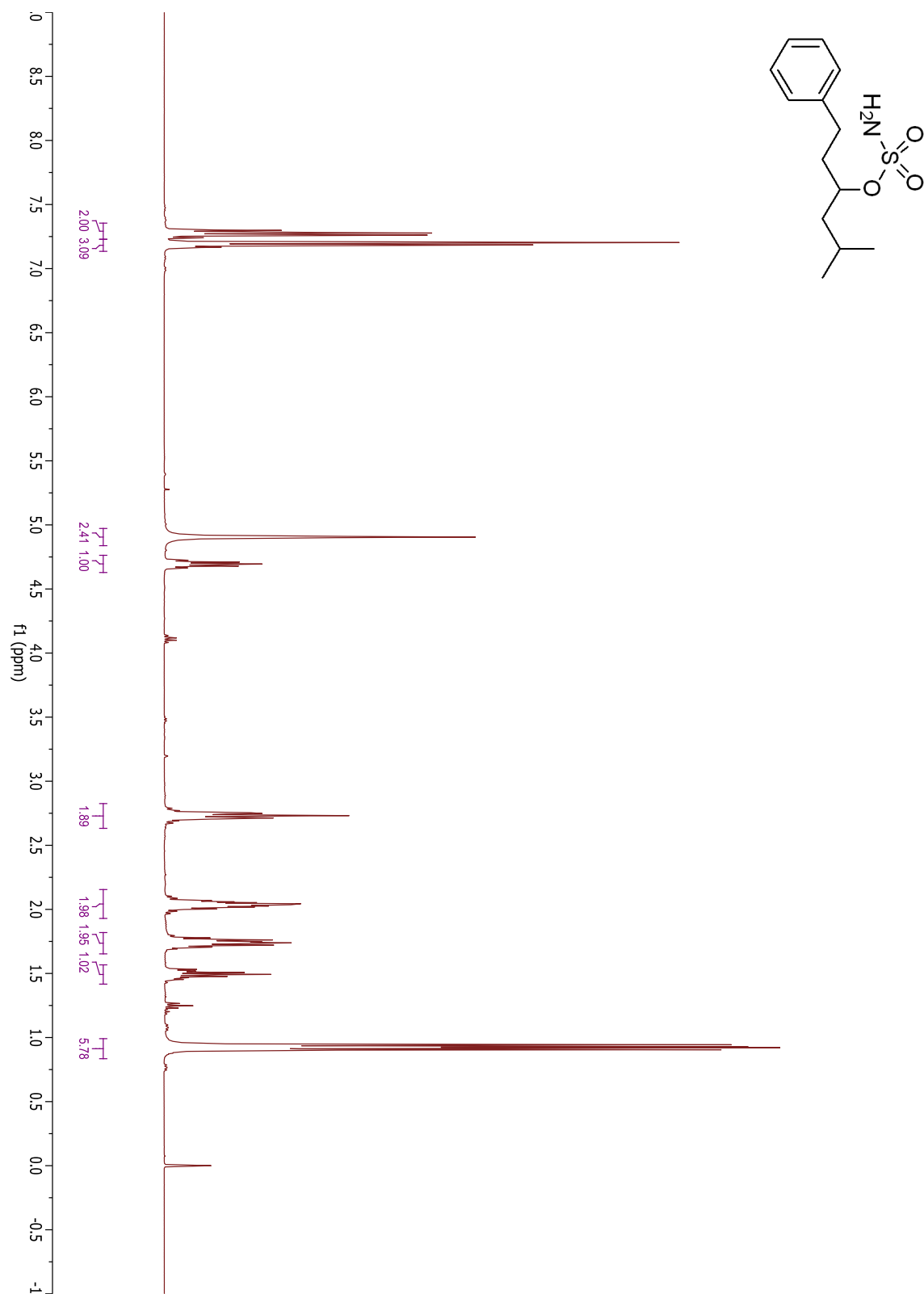
**(4S)-4,8-dimethyl-1-phenylnonan-2-ol.**

**1-(1-Hydroxycyclopropyl)-2-(2,2-diphenylcyclopropyl)ethane.**

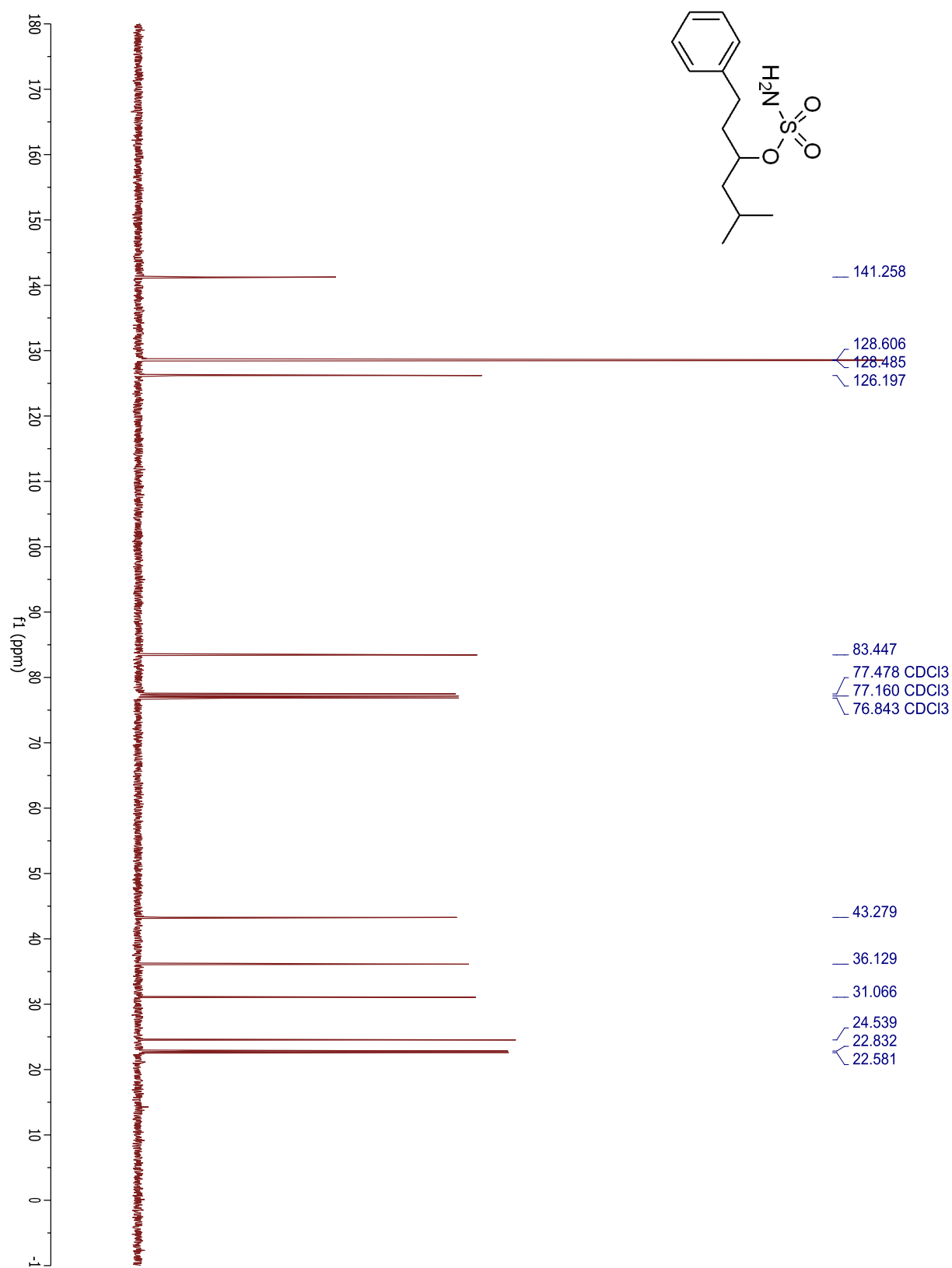
**1-(1-Hydroxycyclopropyl)-2-(2,2-diphenylcyclopropyl)ethane.**



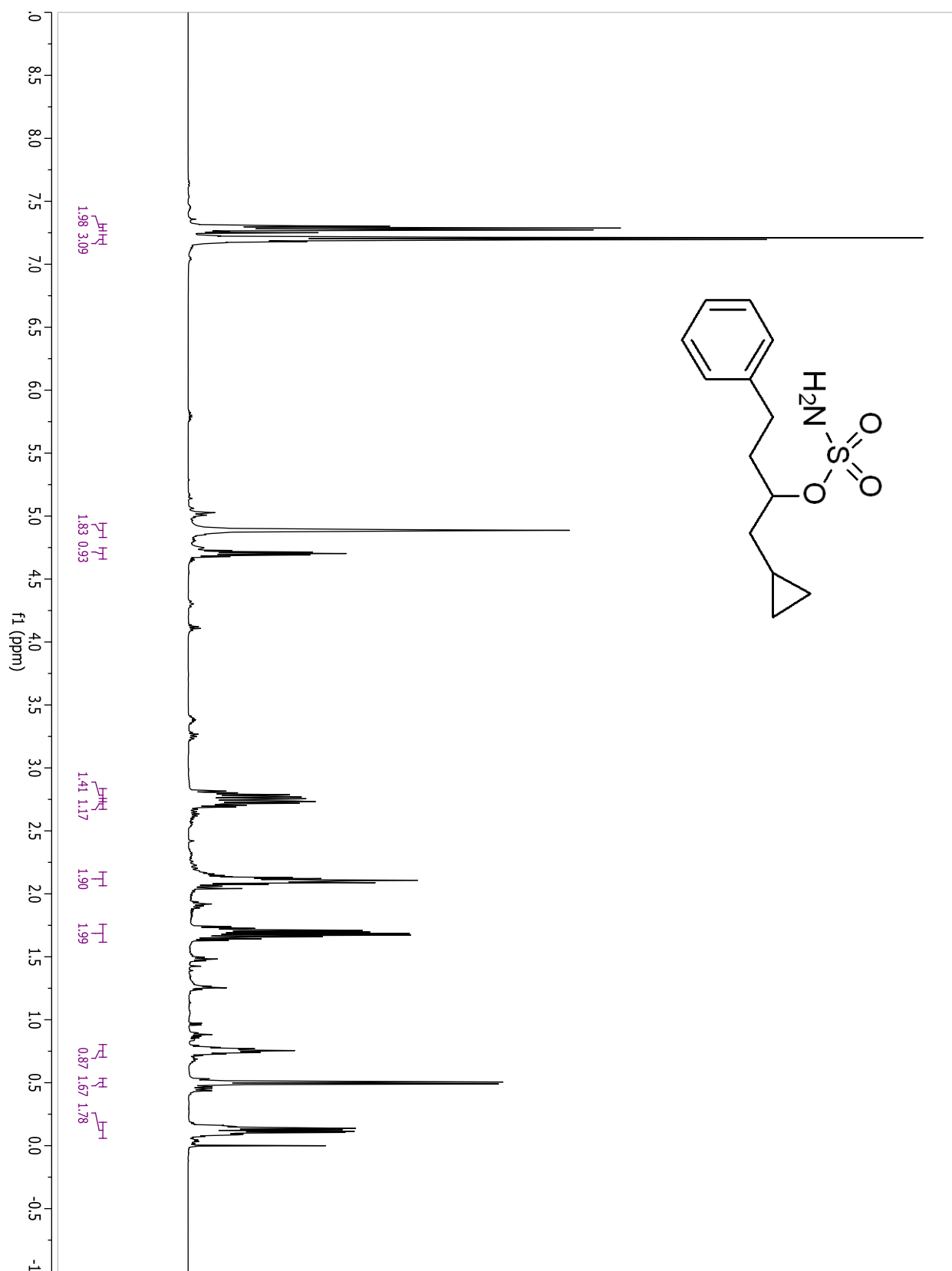
## Compound 3.2



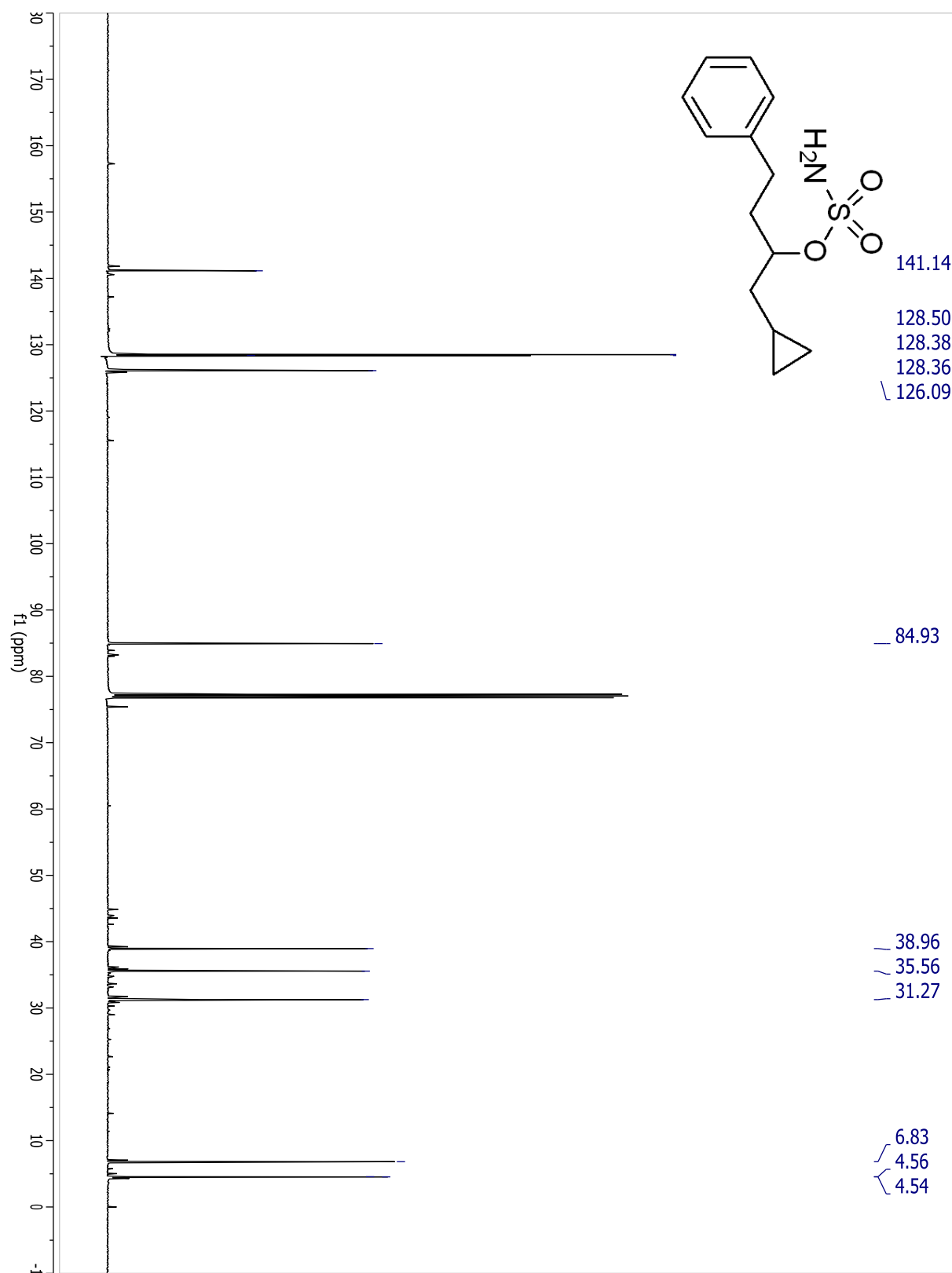
## Compound 3.2



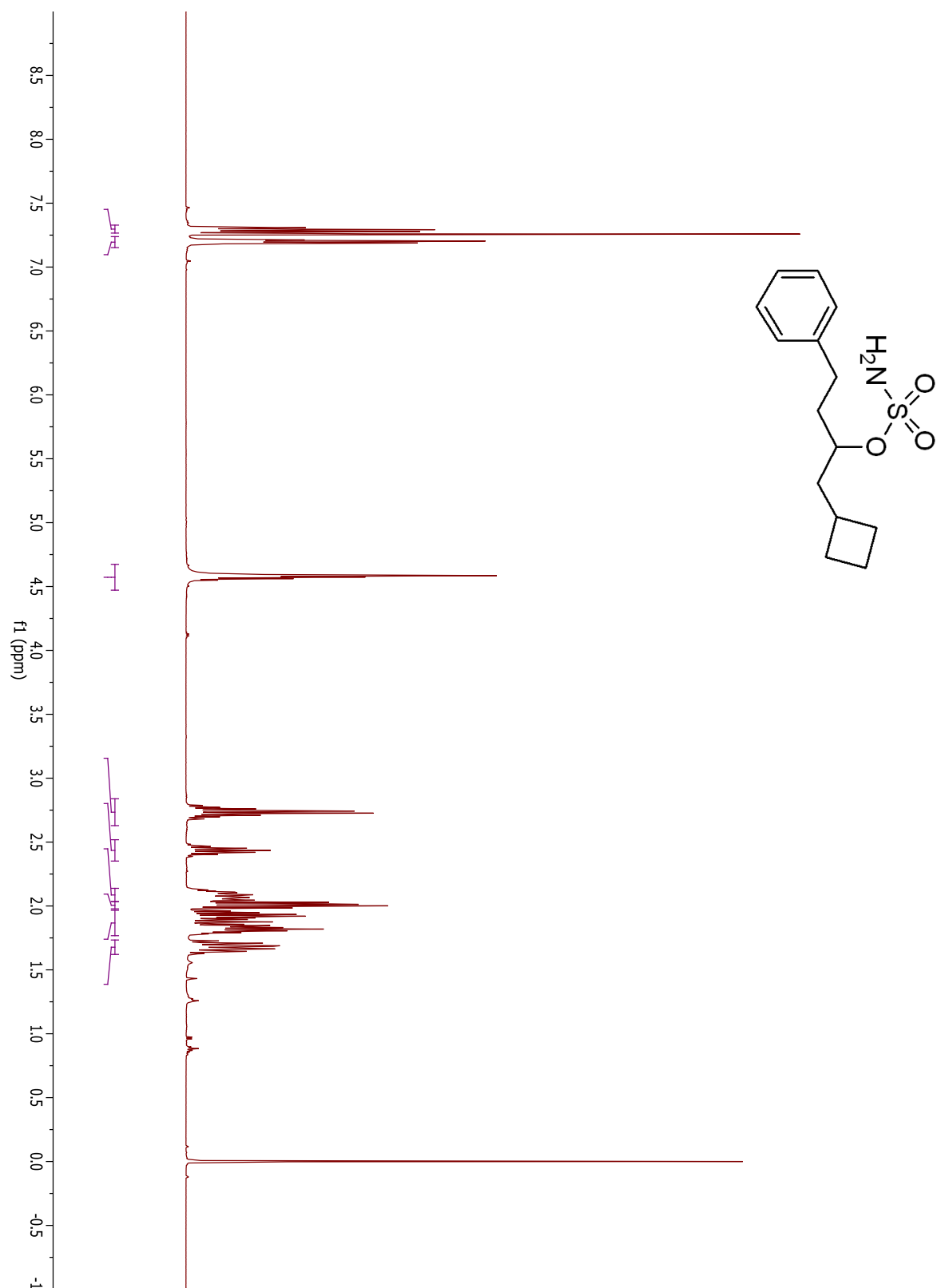
## Compound 3.47



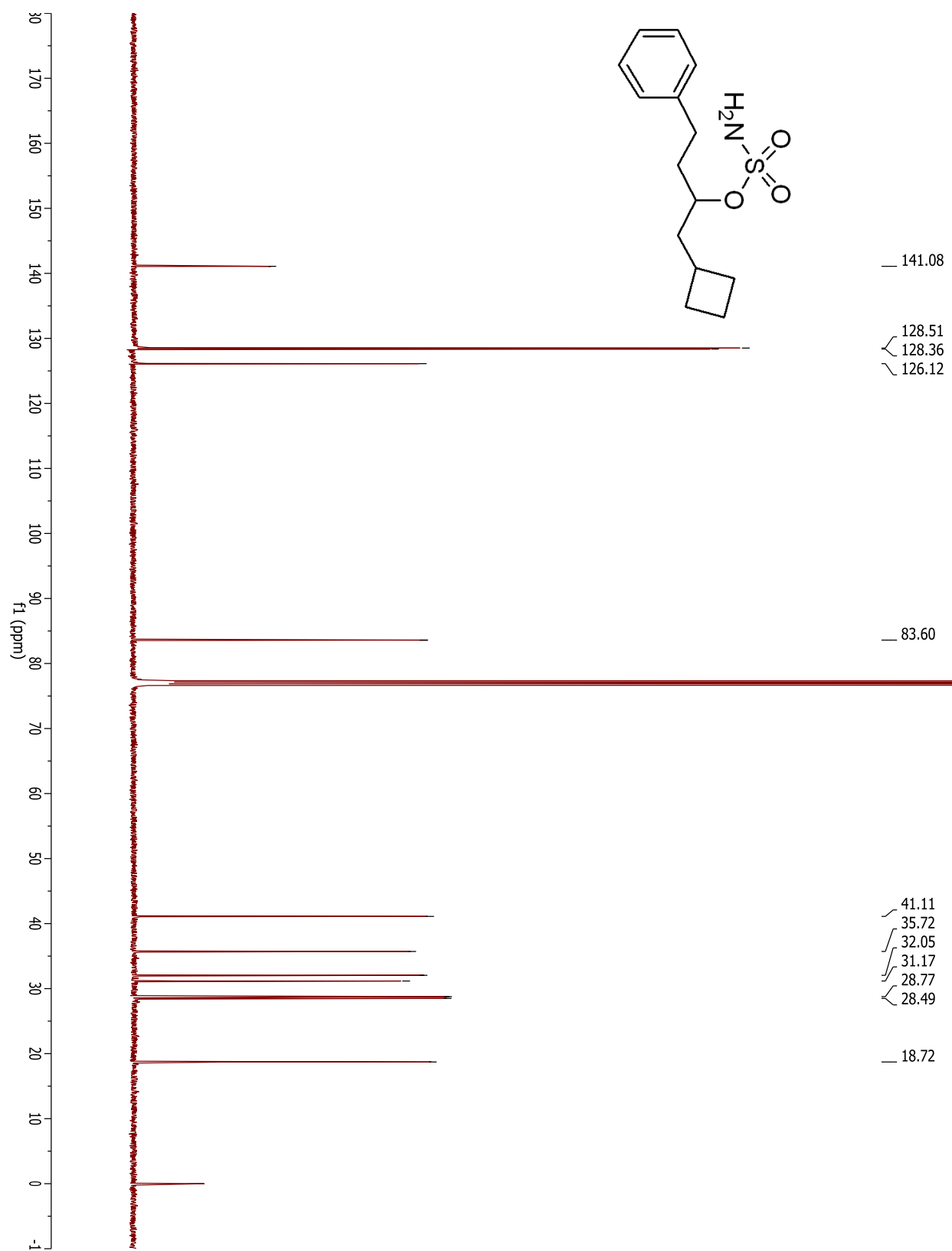
## Compound 3.47



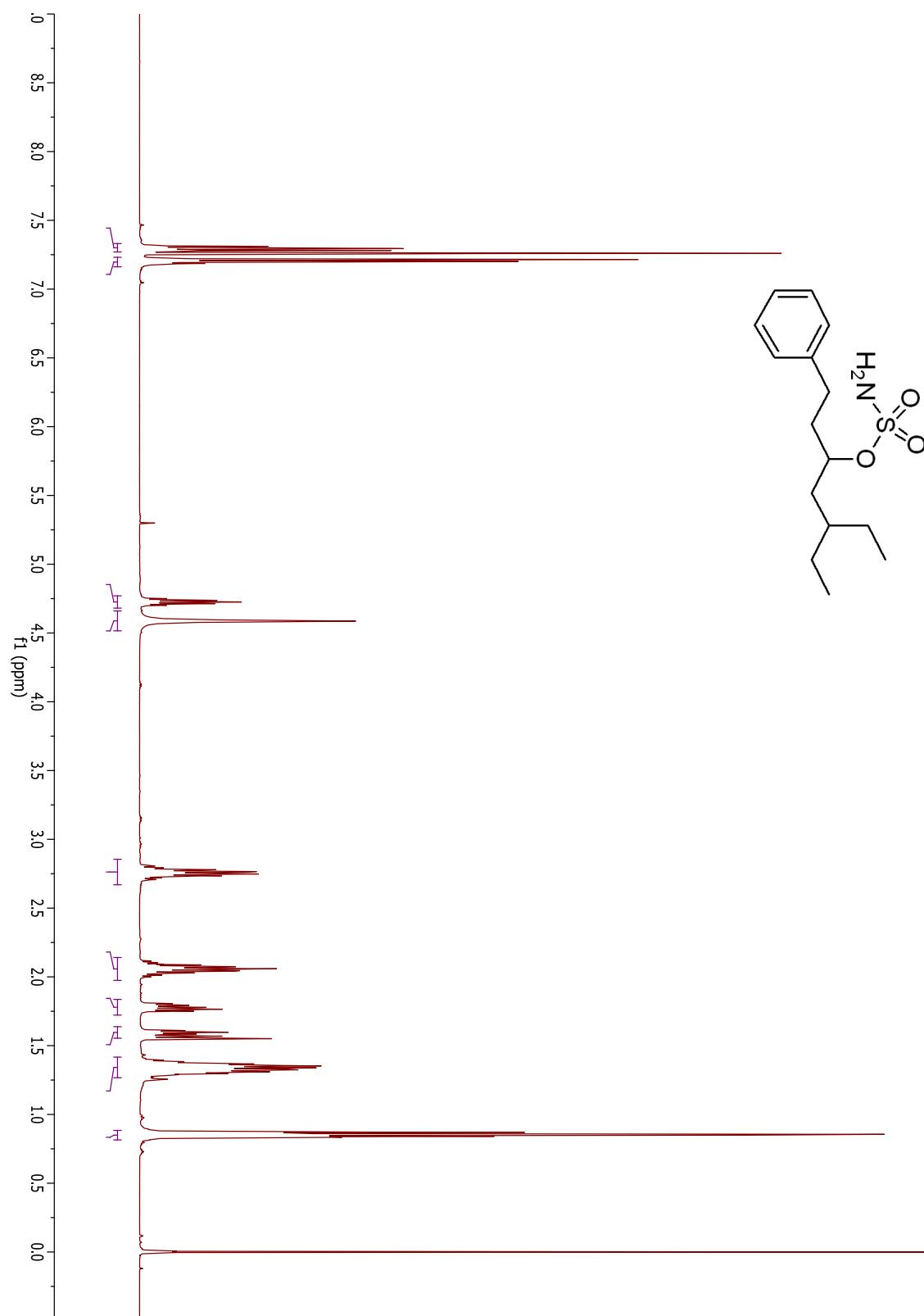
## Compound 3.48



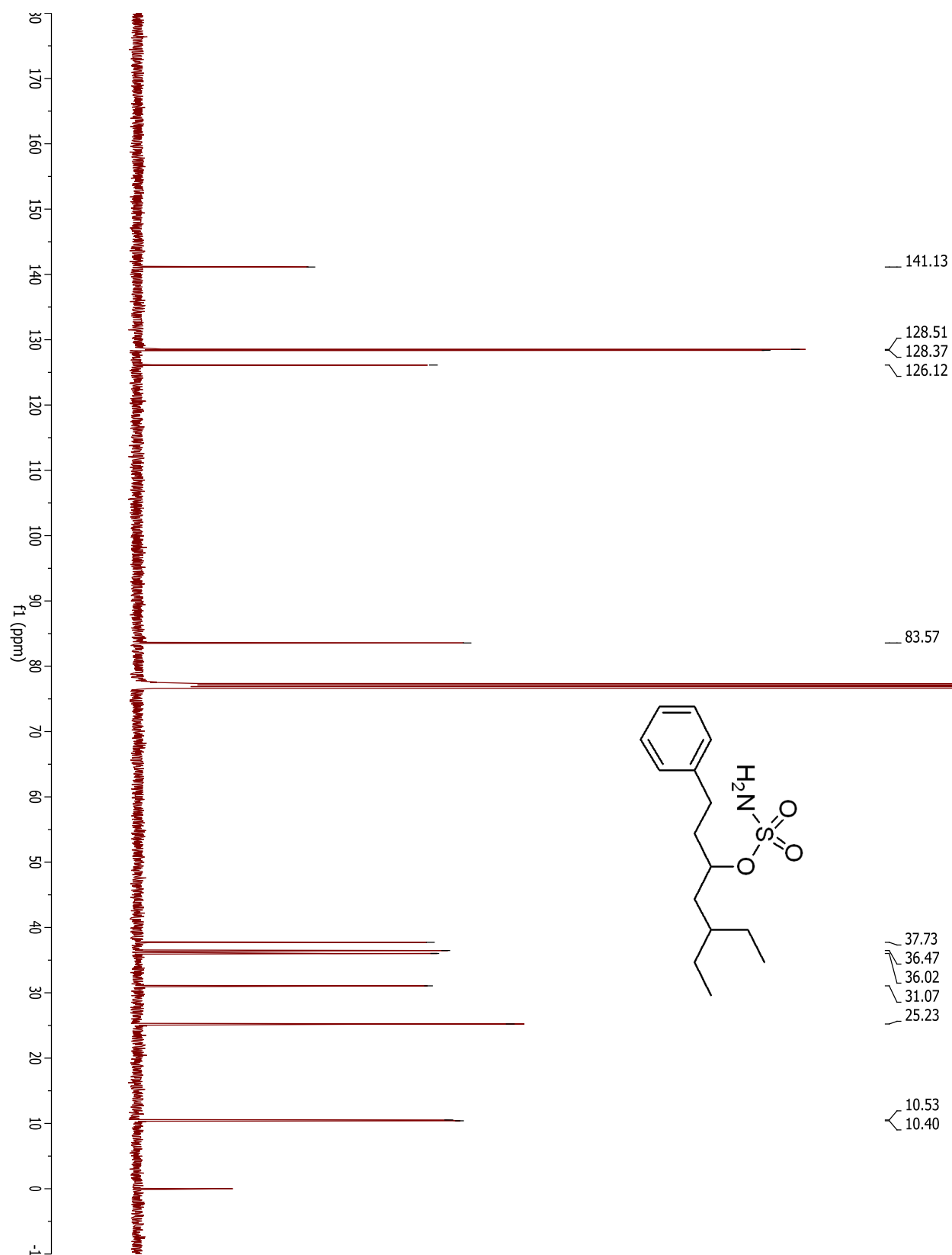
## Compound 3.48



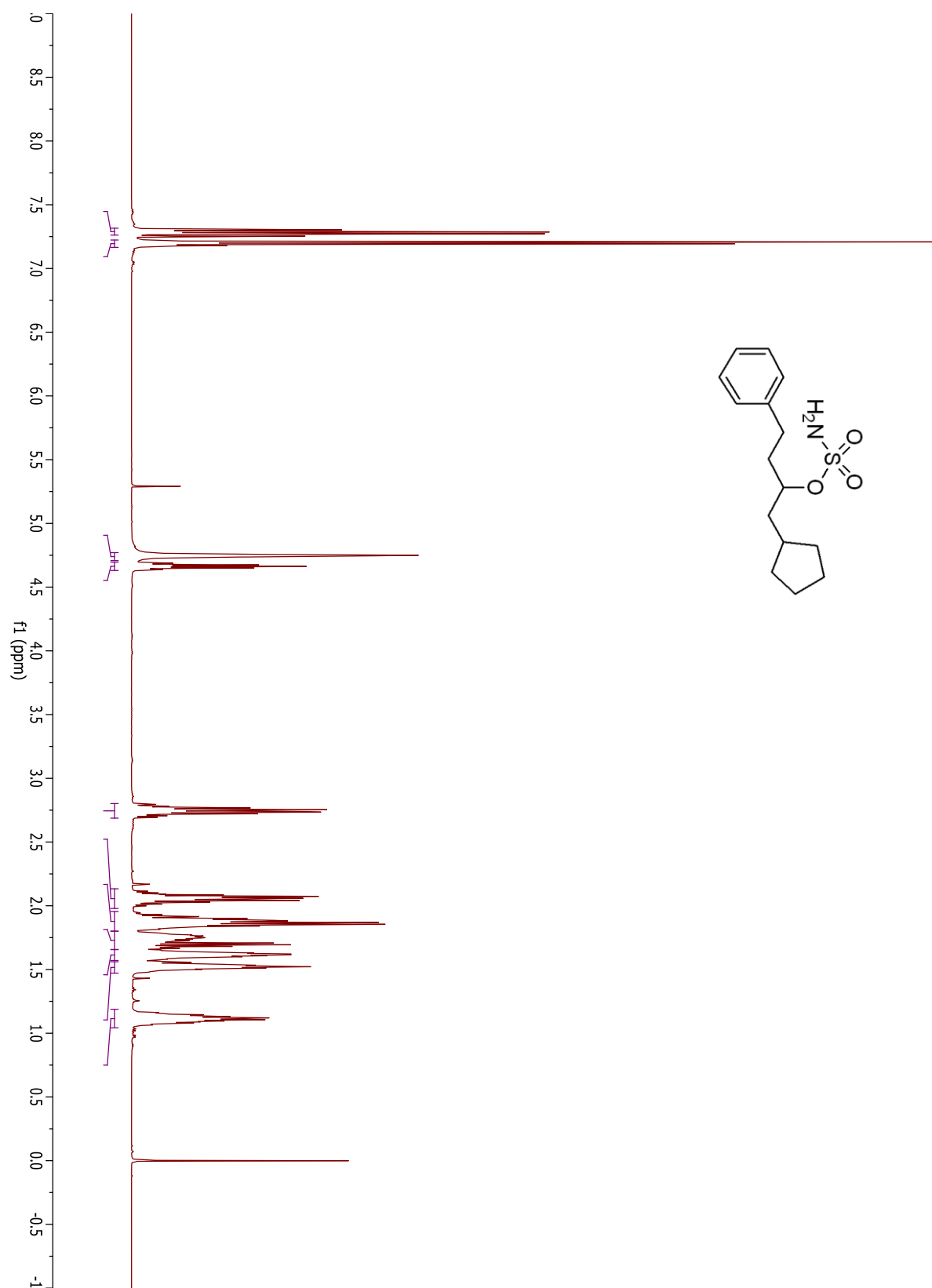
## Compound 3.49



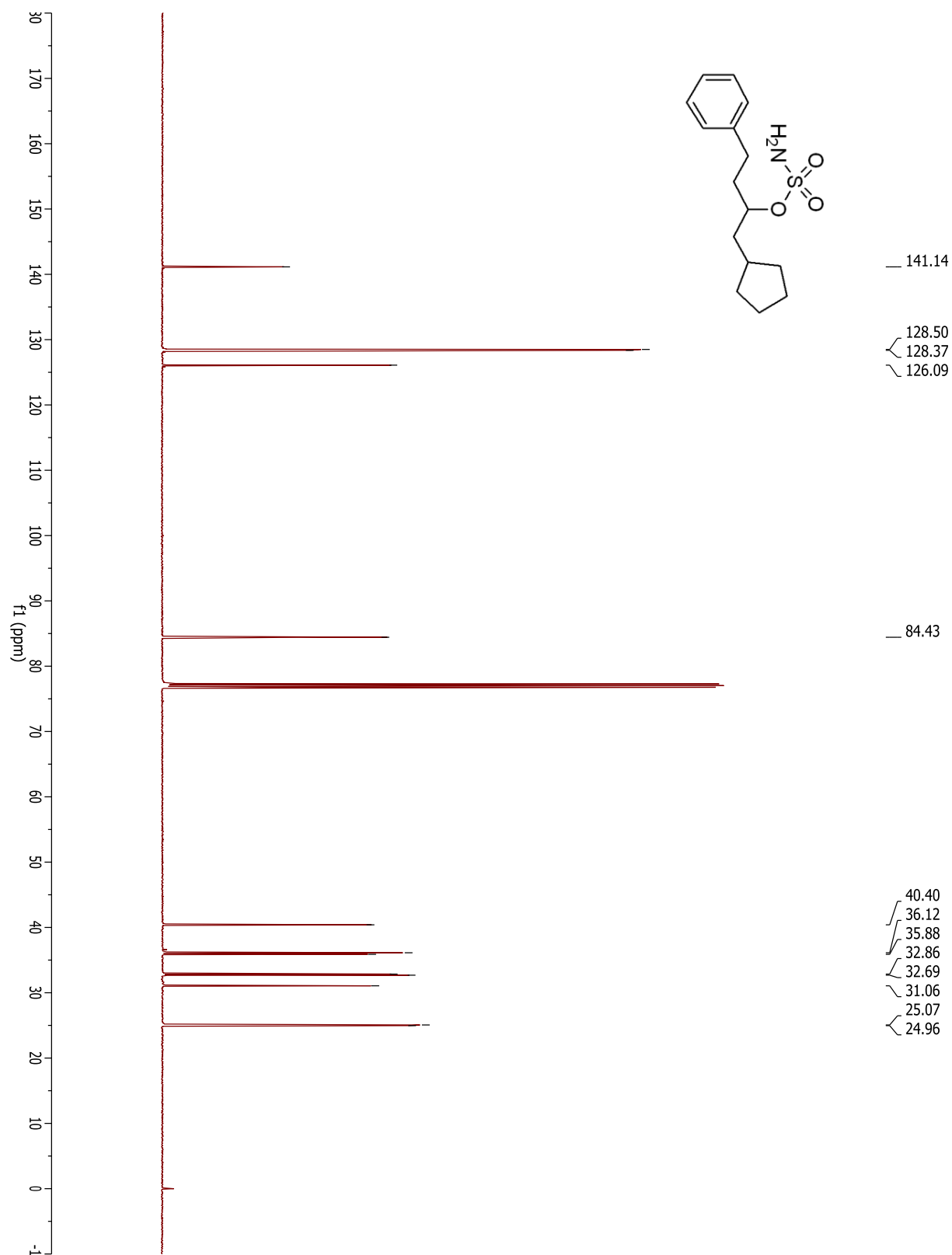
## Compound 3.49



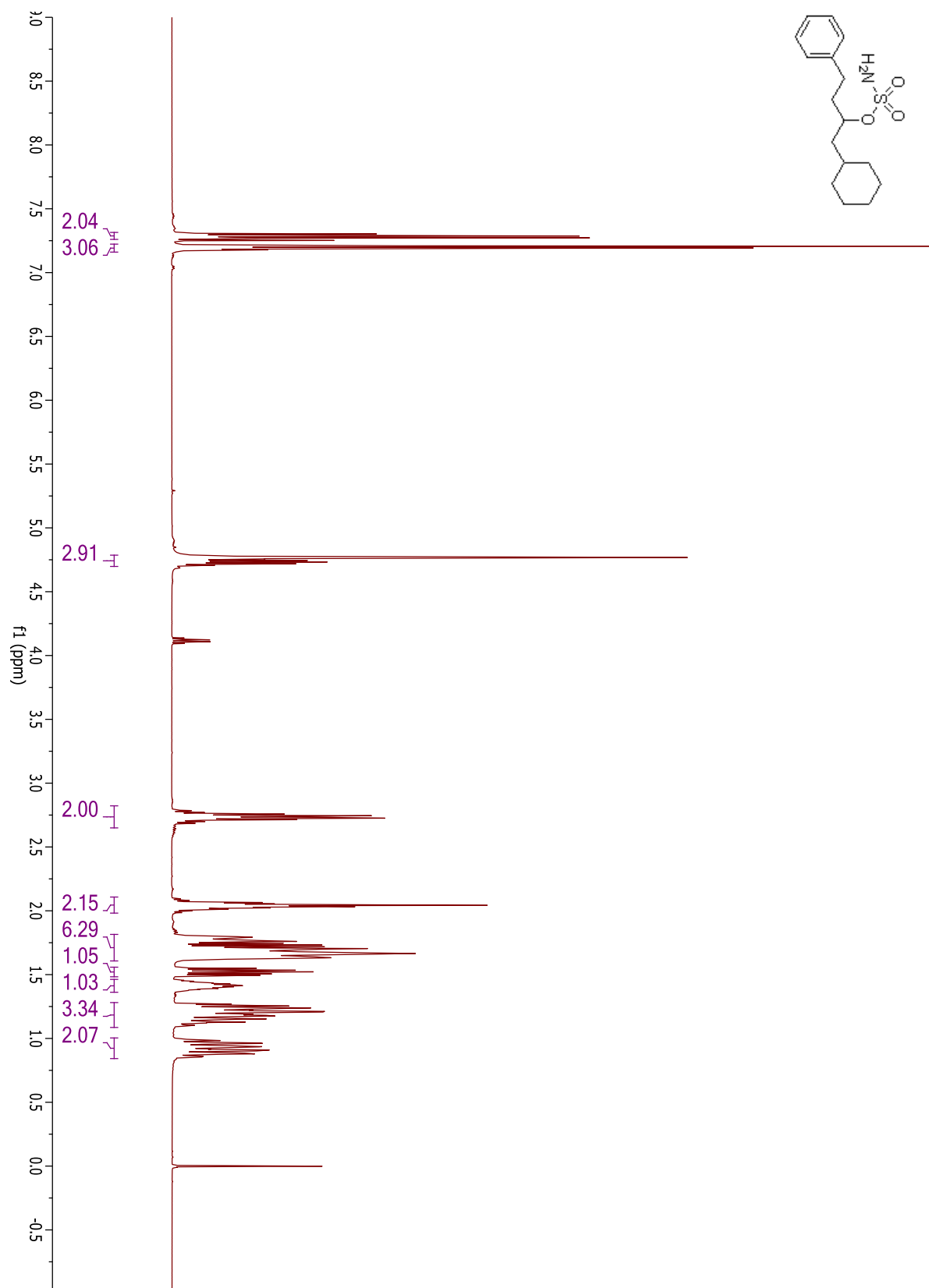


**Compound 3.50**

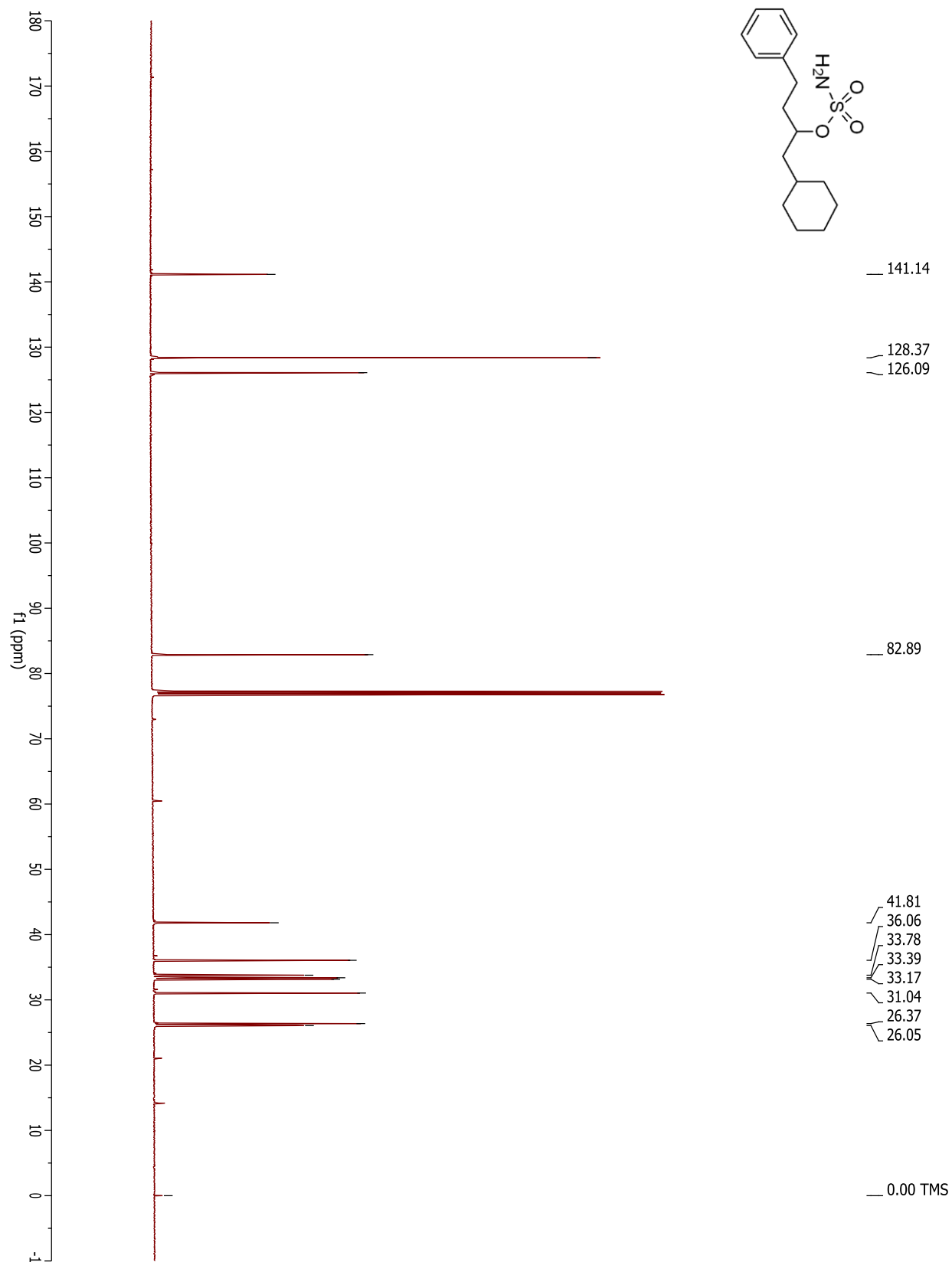
## Compound 3.50

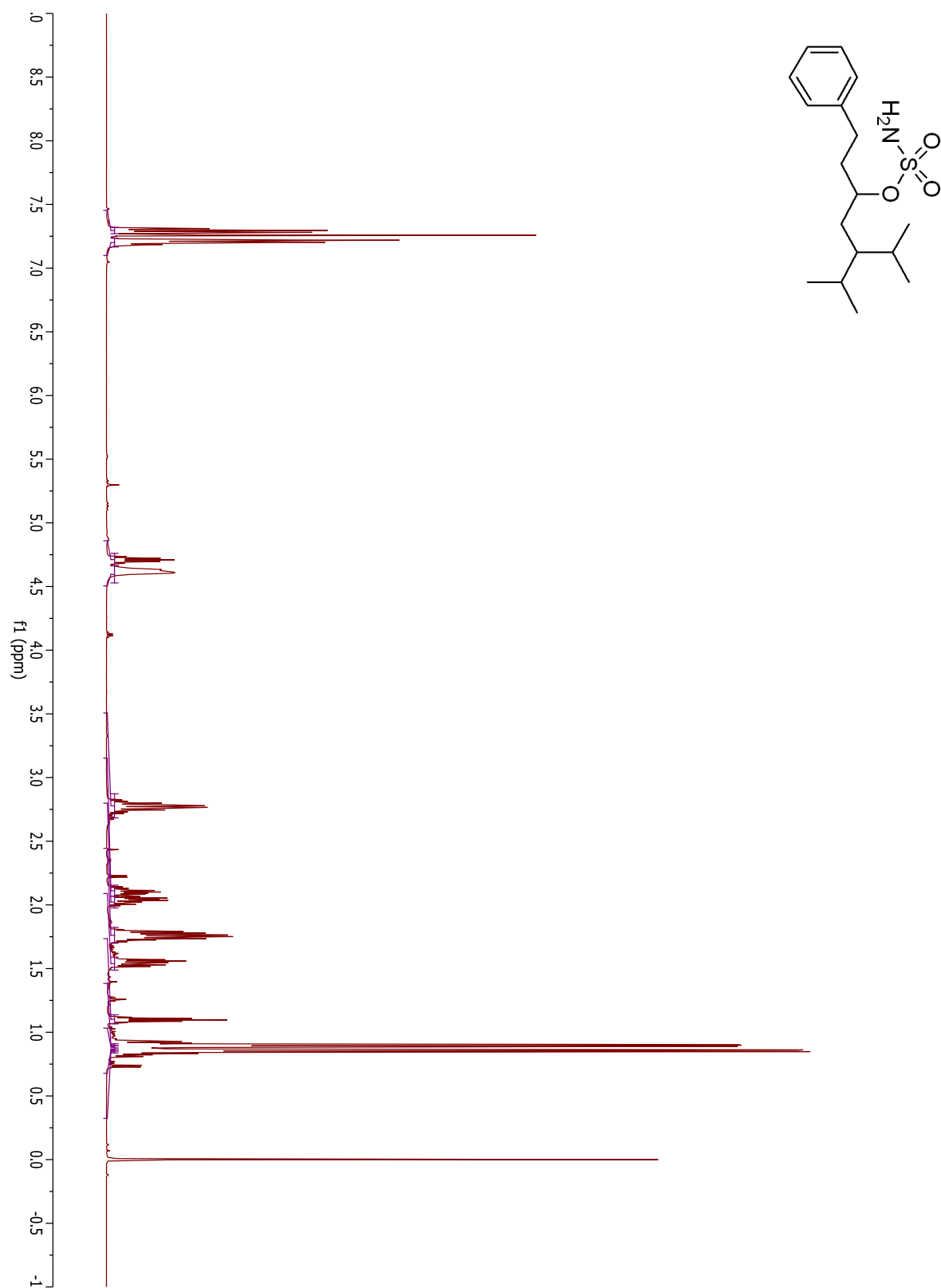


## Compound 3.51

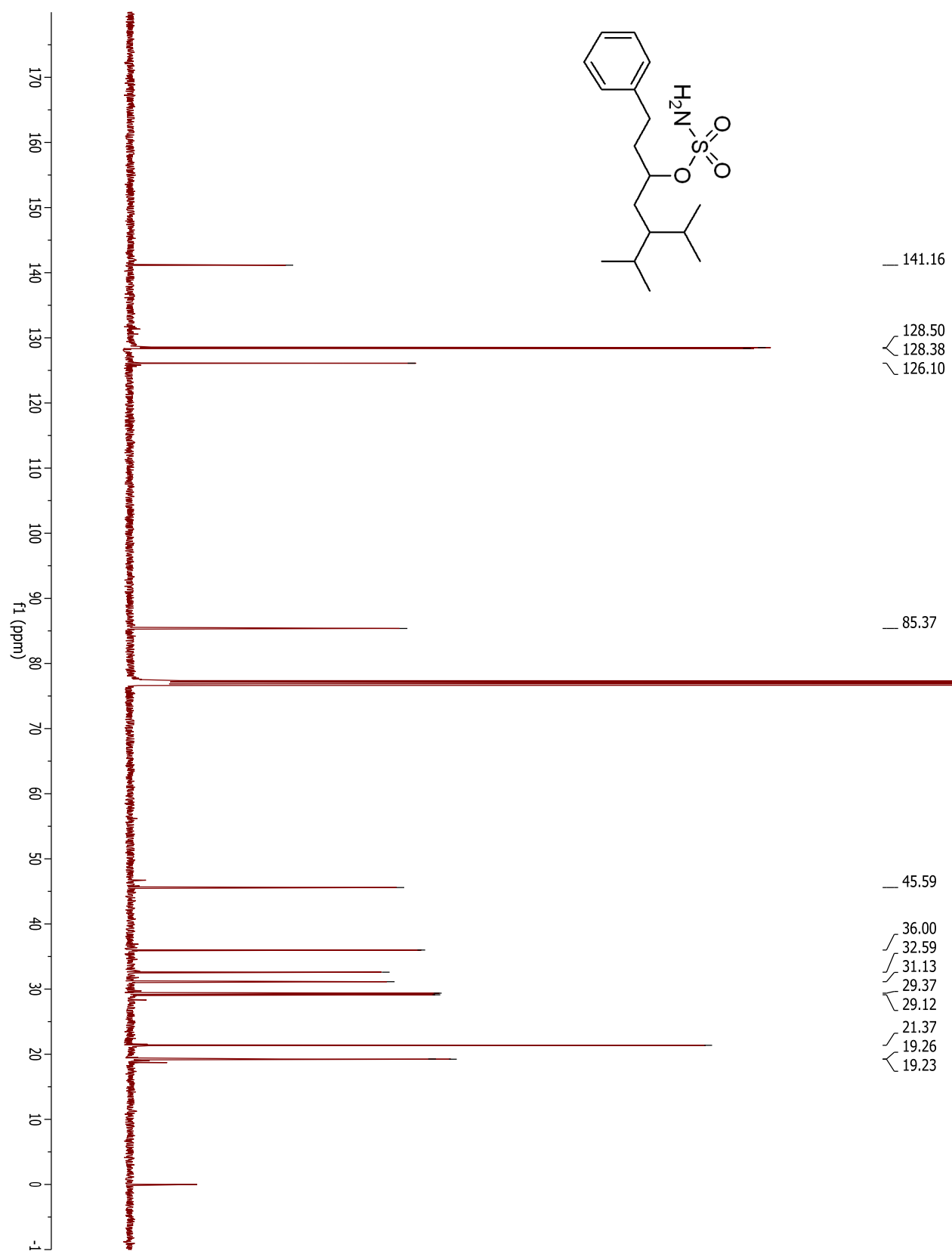


## Compound 3.51

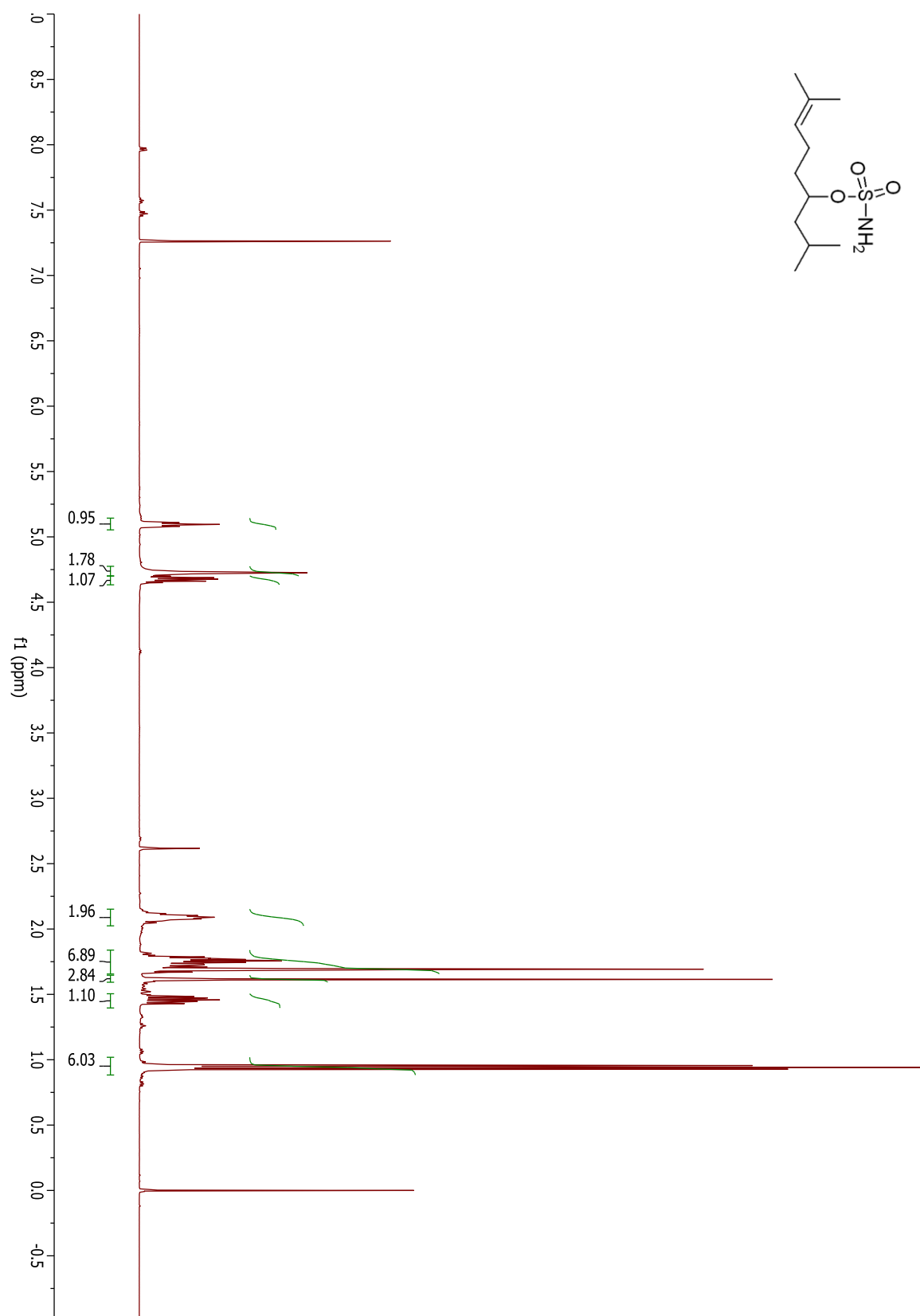


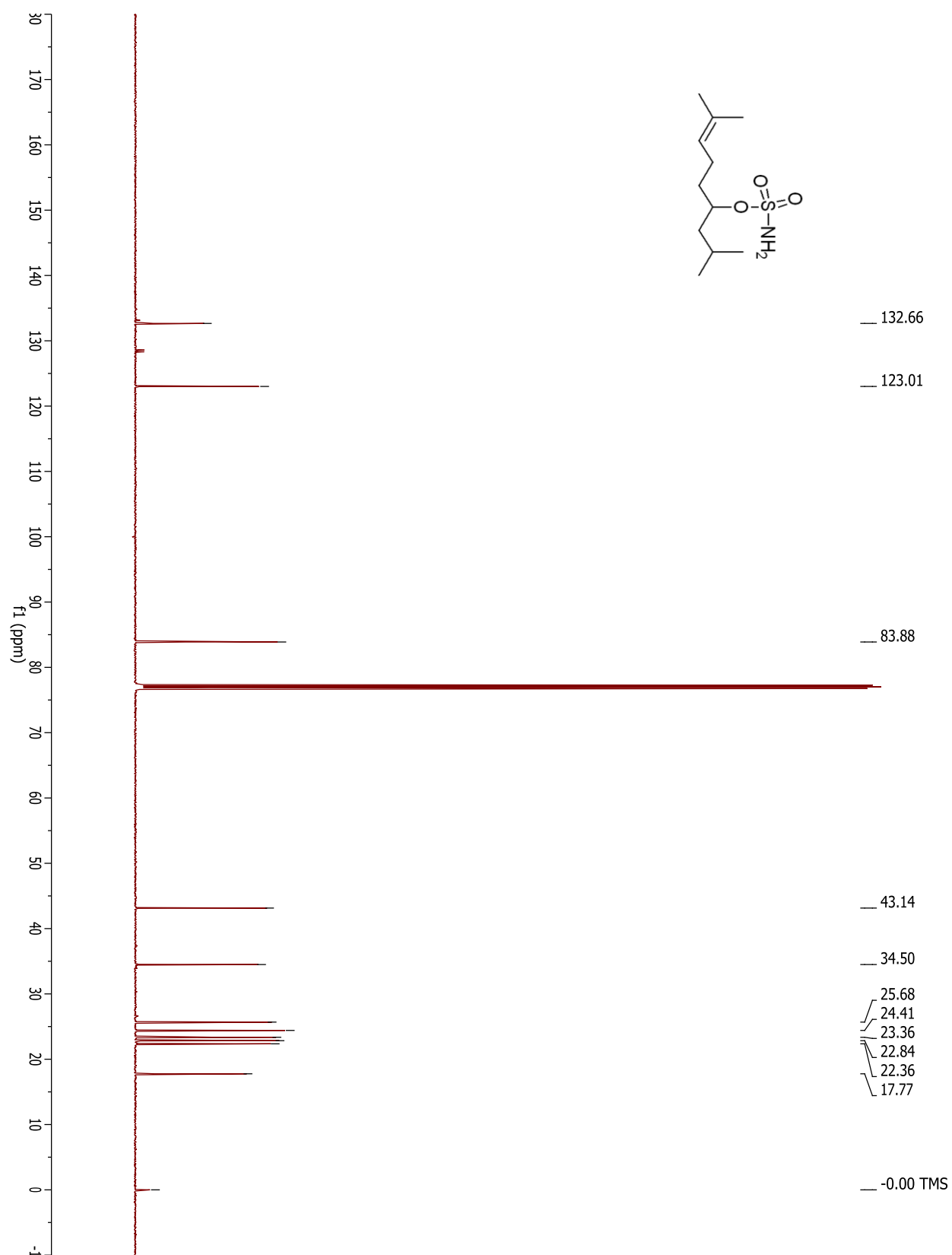


## Compound 3.52



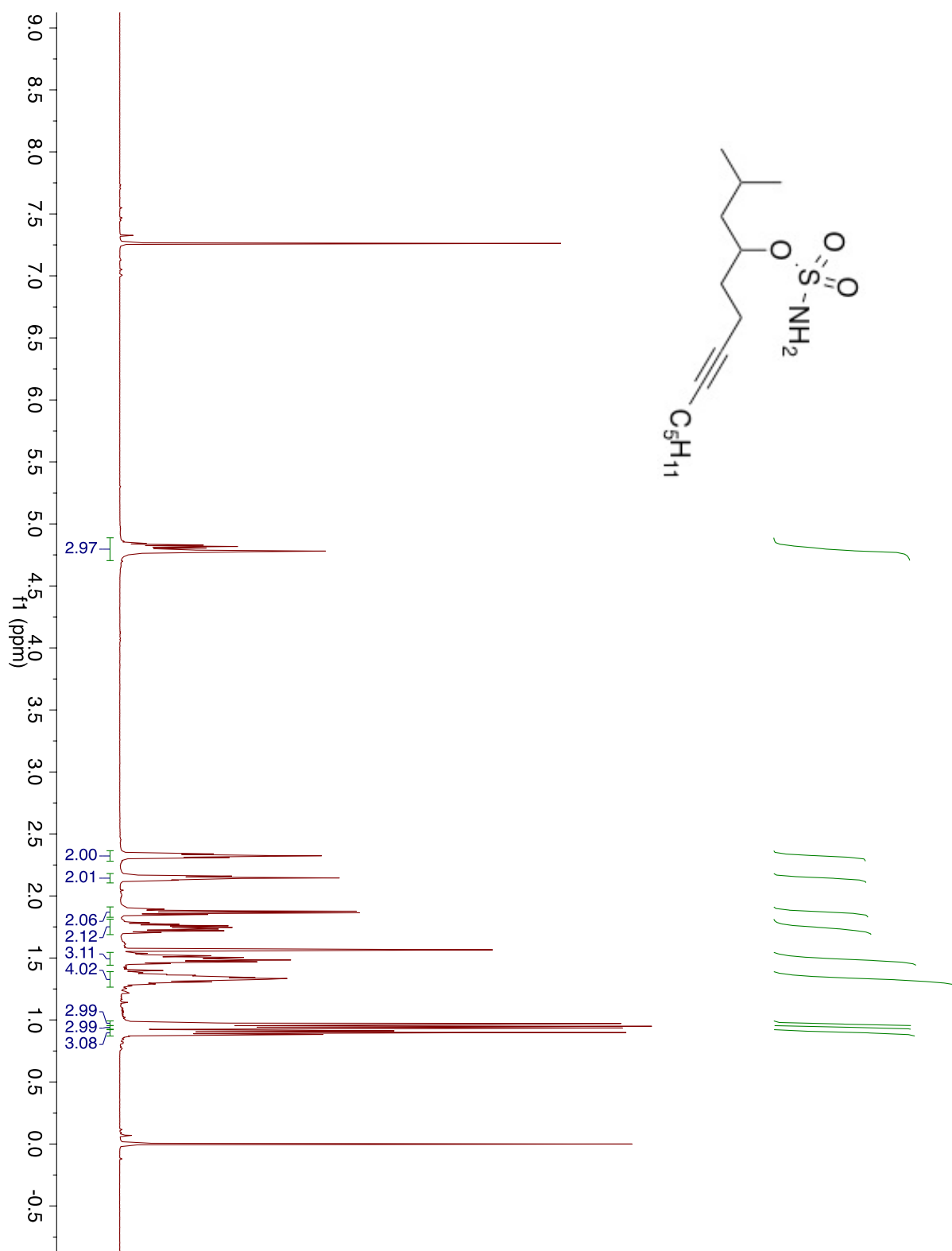
## Compound 3.53



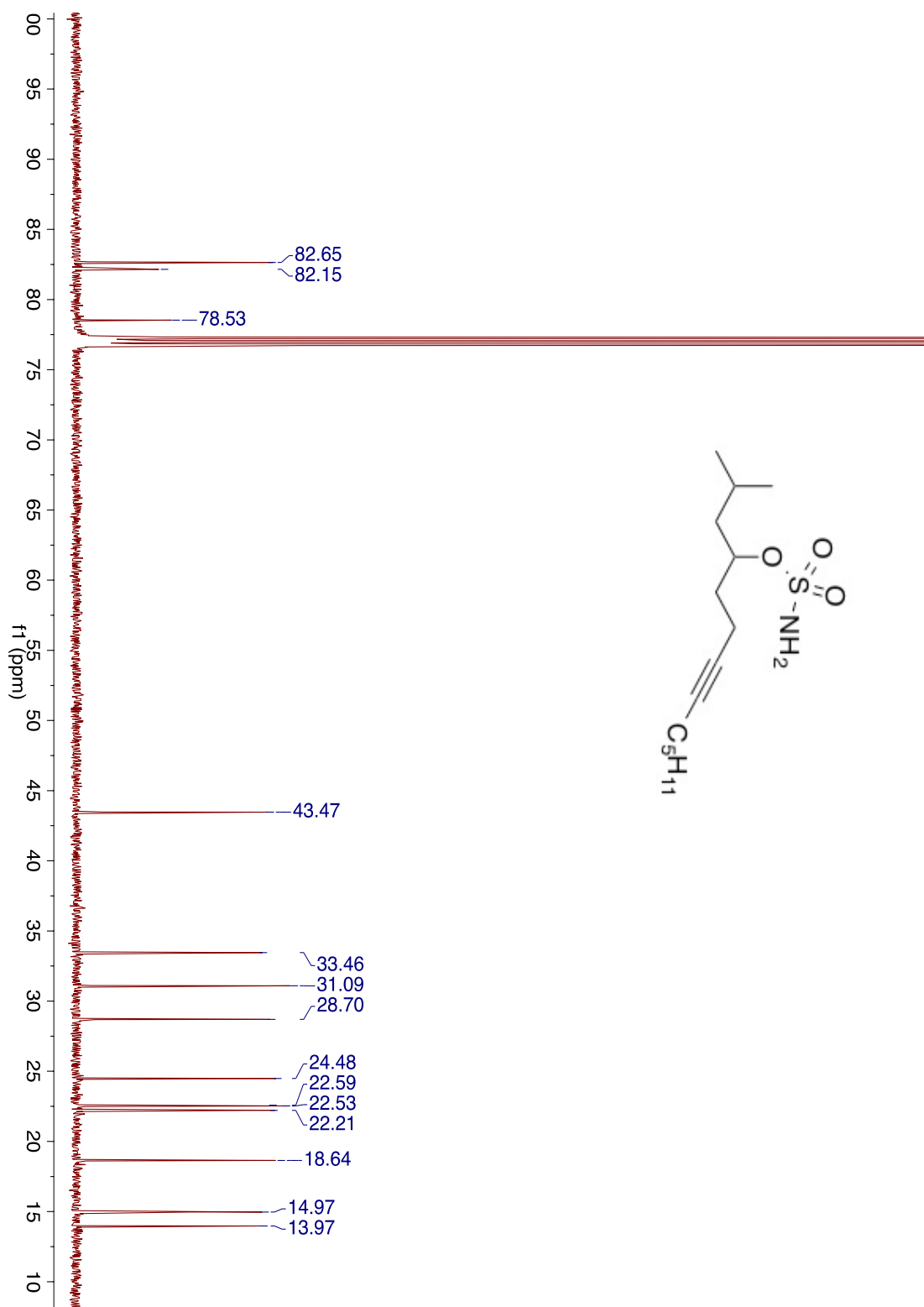




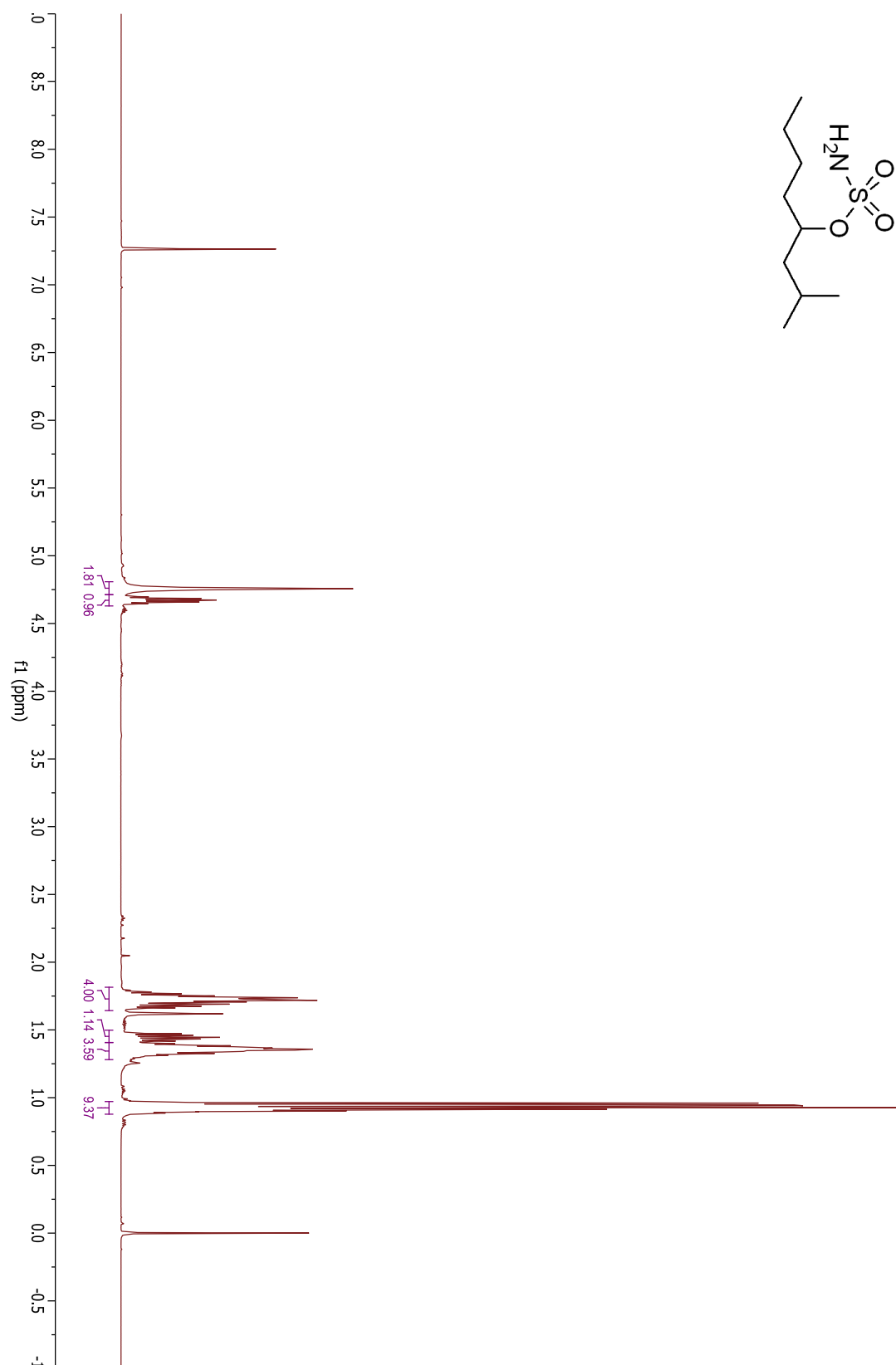
## Compound 3.54



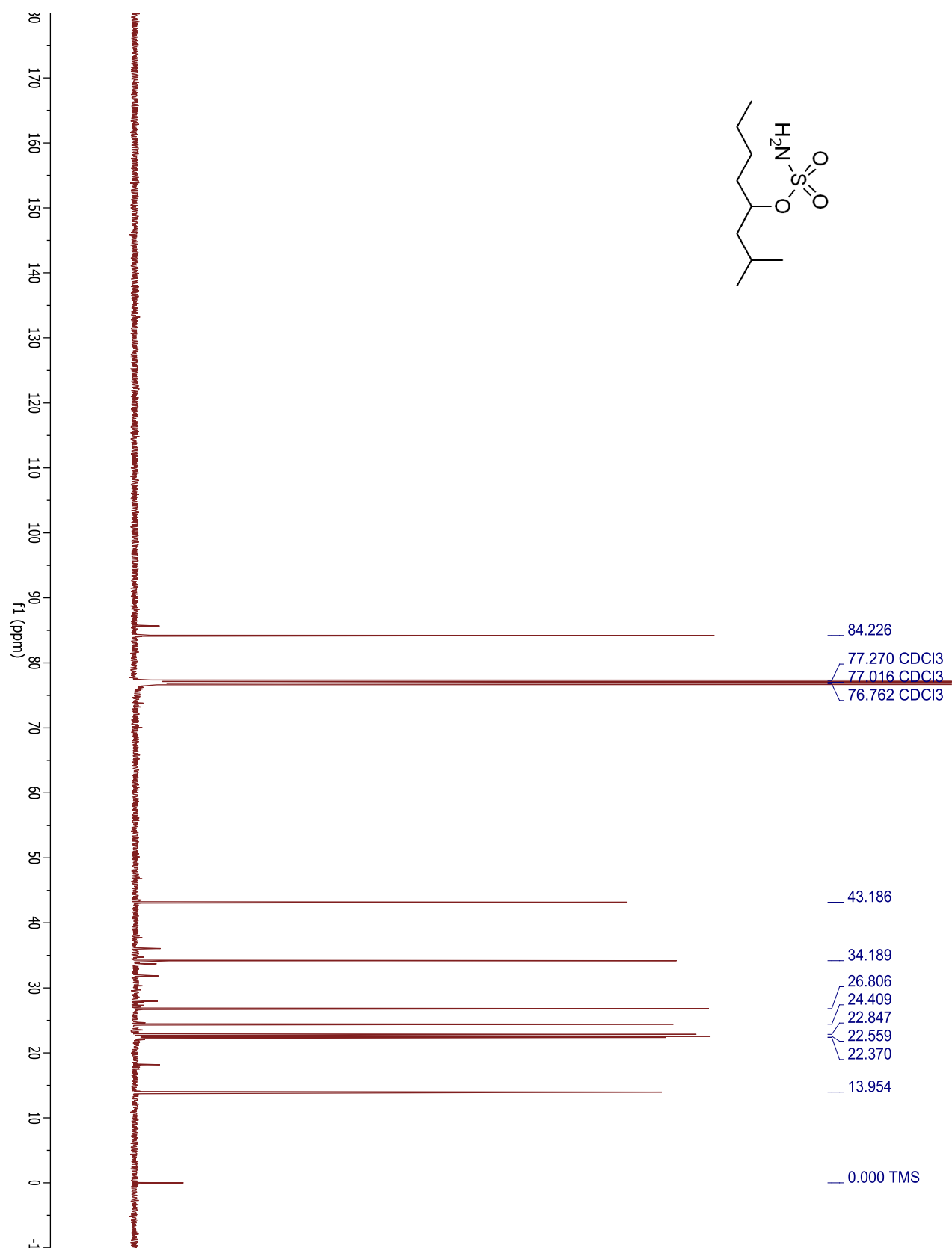
## Compound 3.54

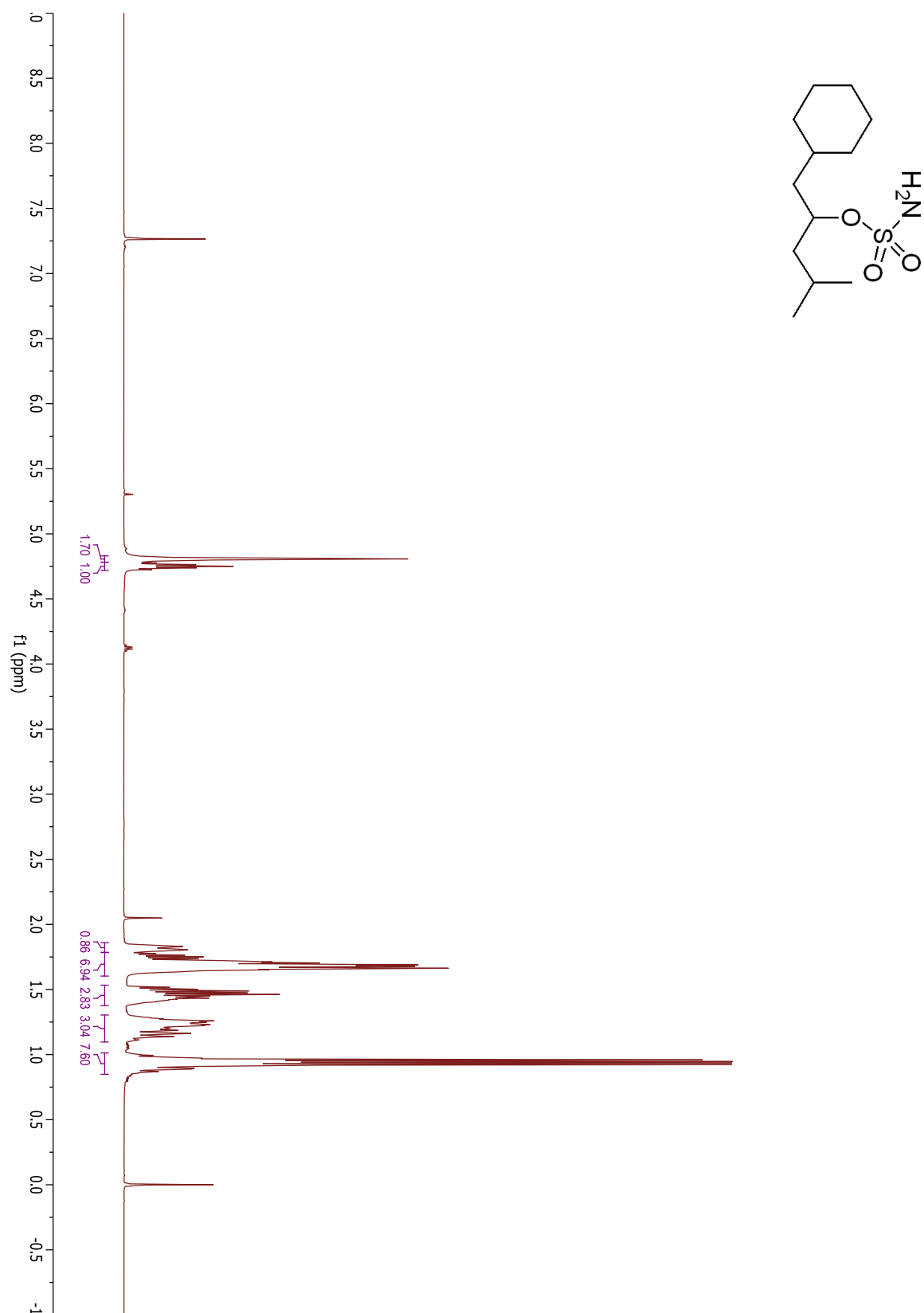


## Compound 3.23

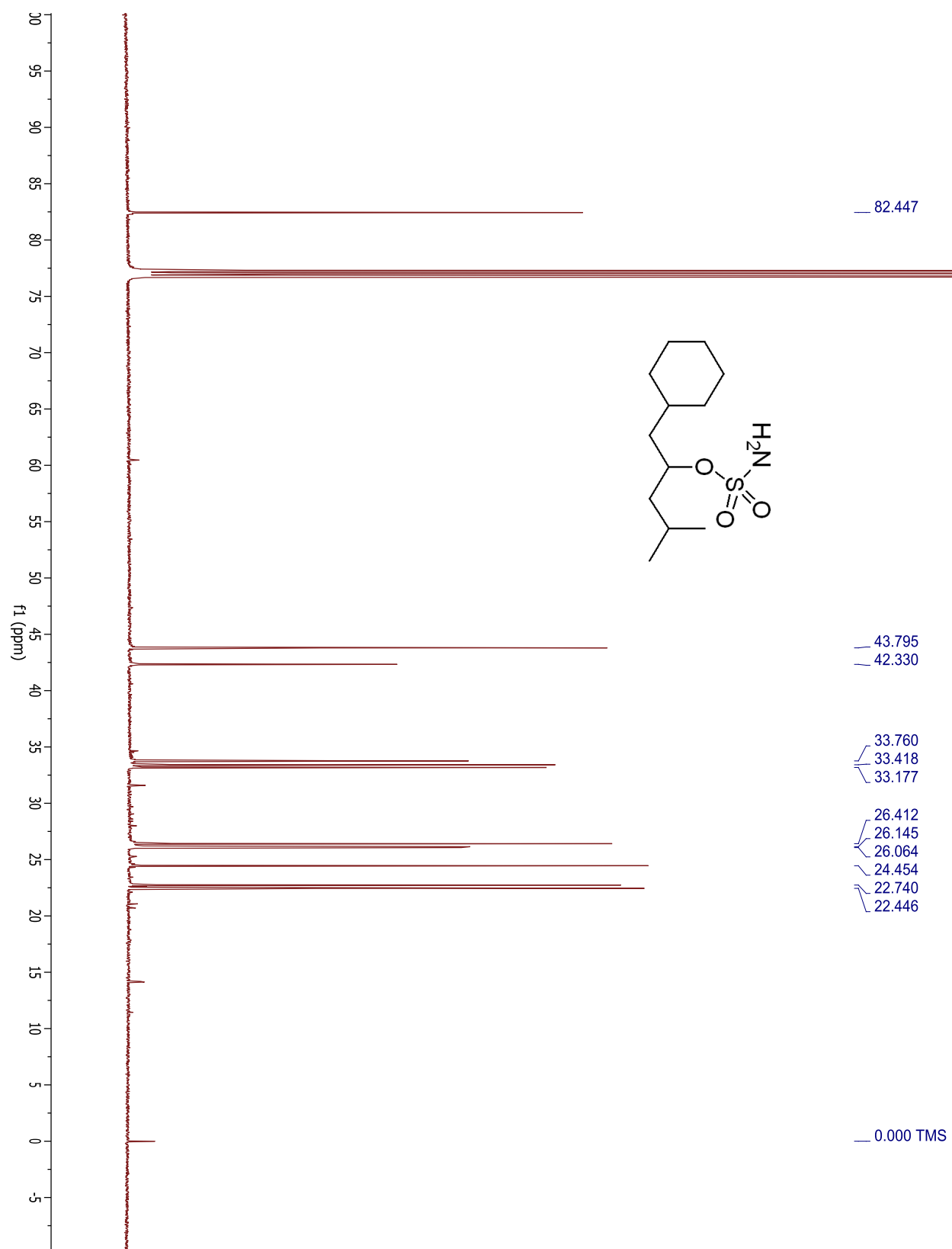


## Compound 3.23

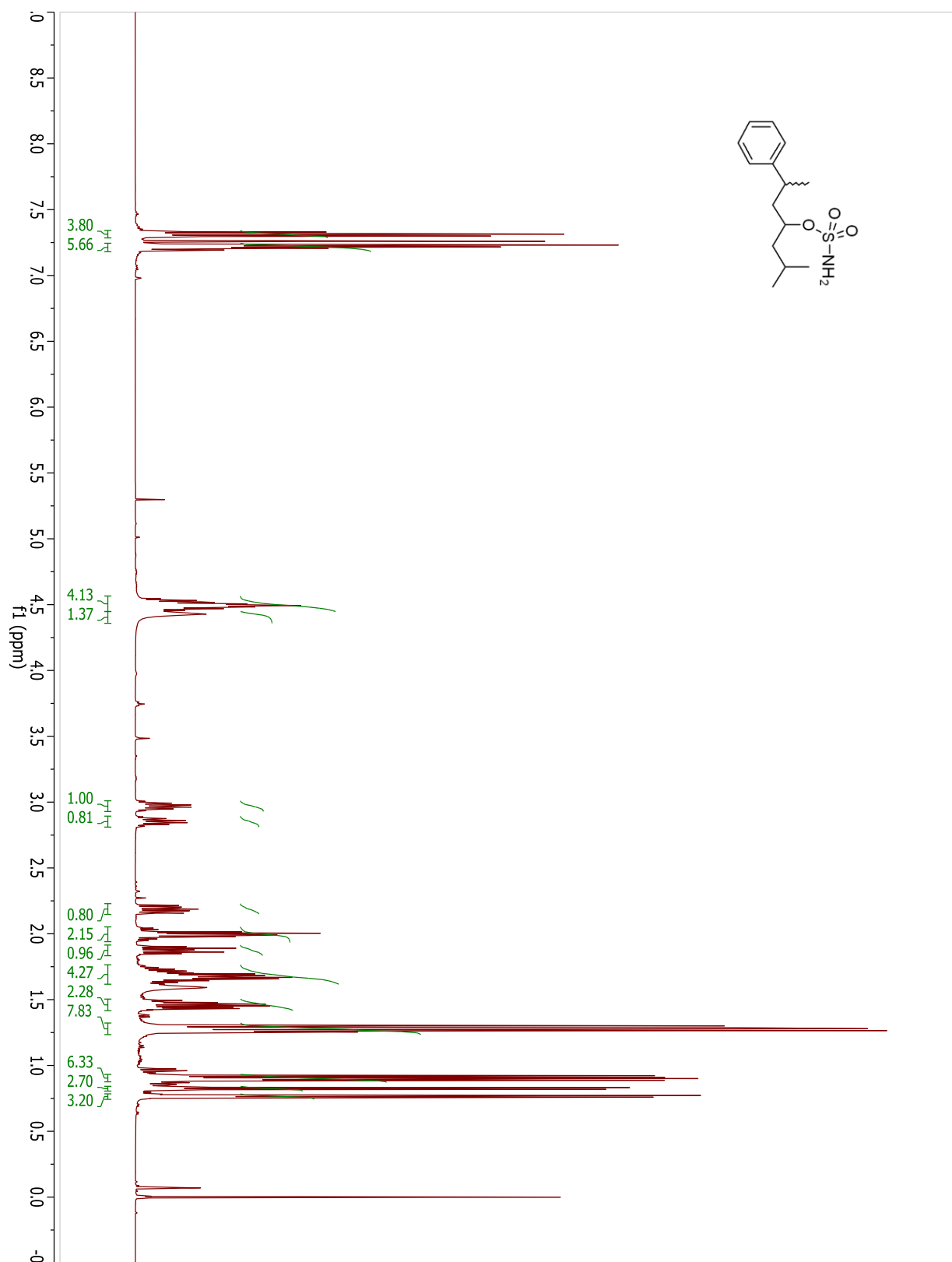


**Compound 3.7**

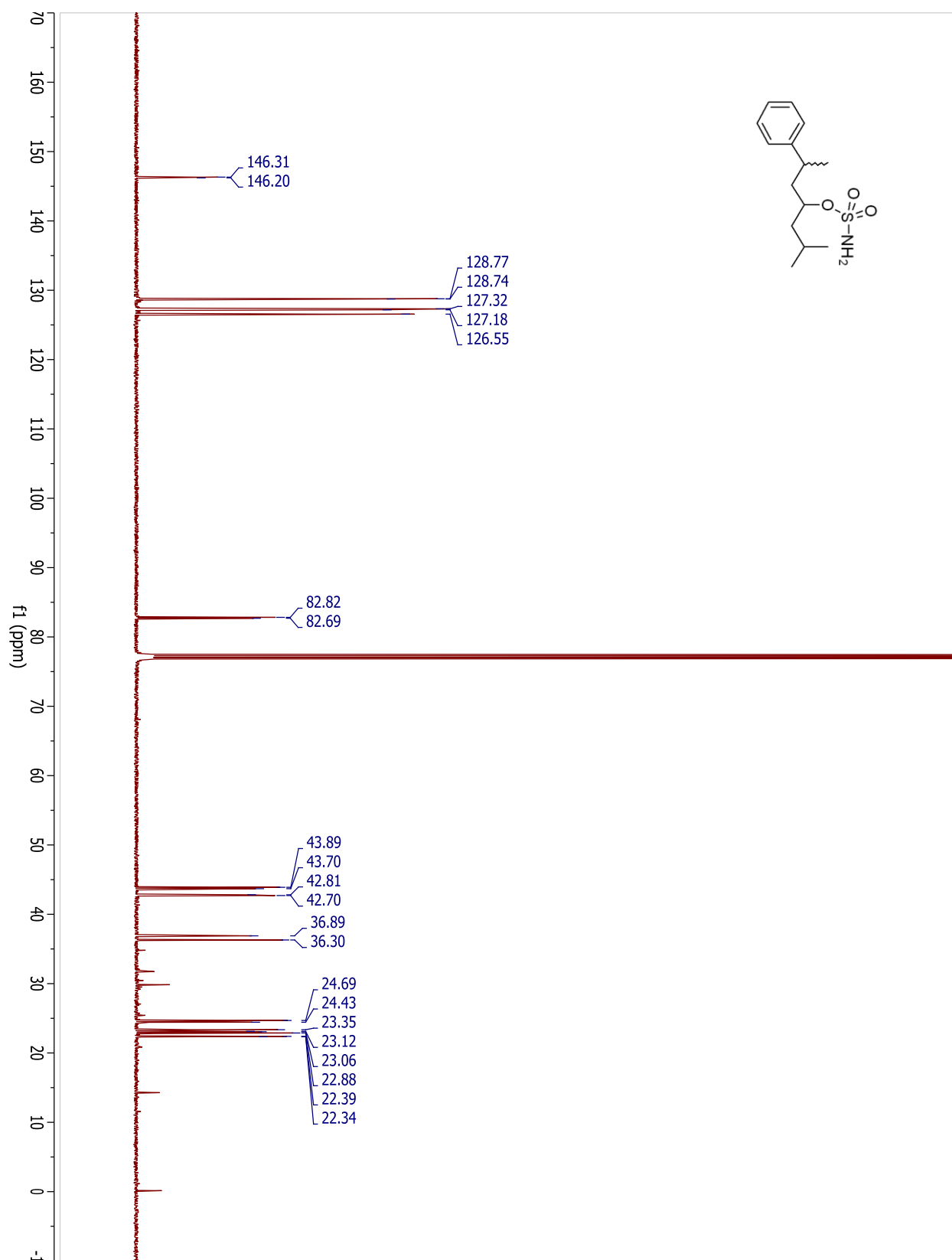
## Compound 3.7



## Compound 3.55

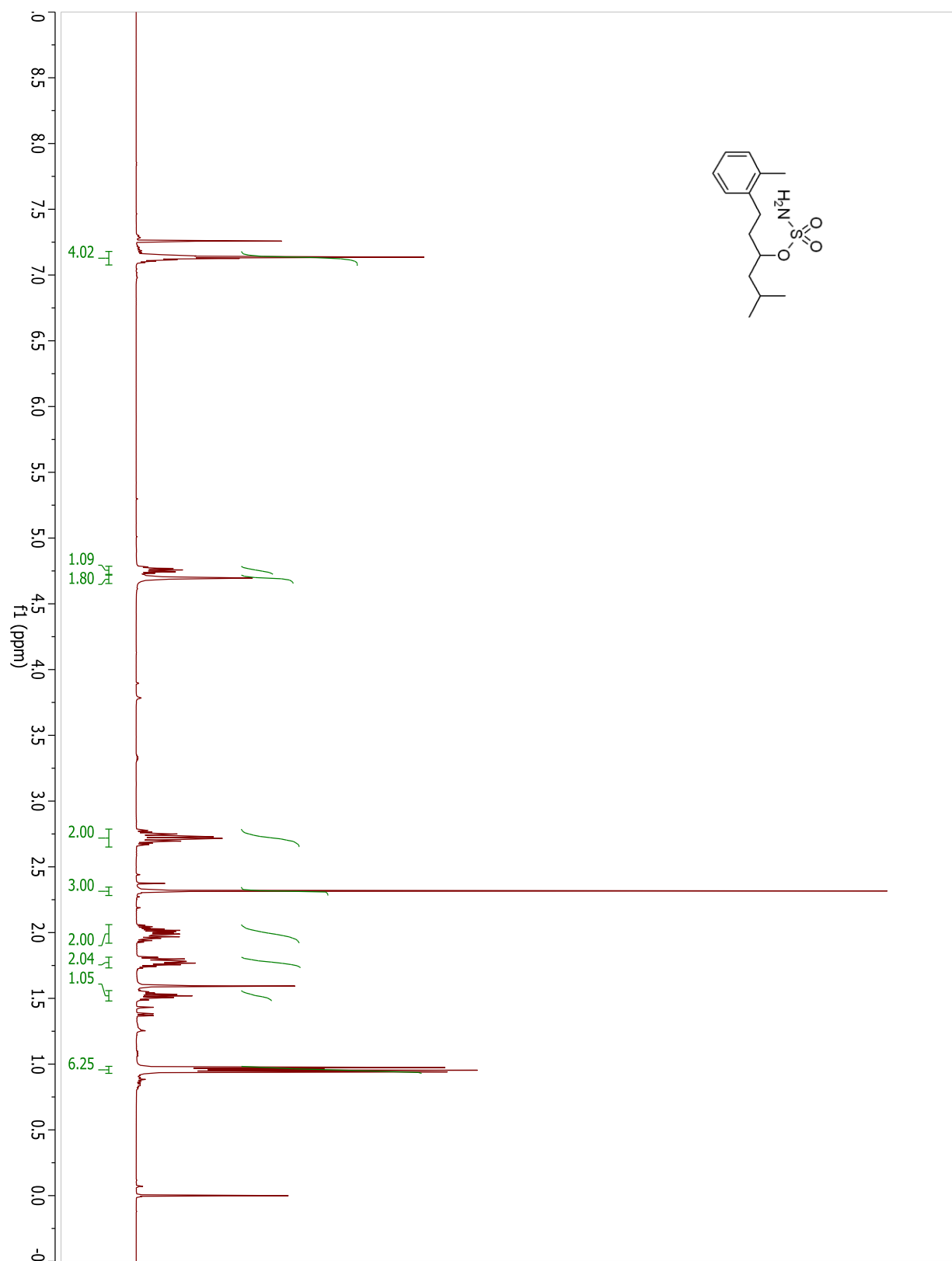


## Compound 3.55

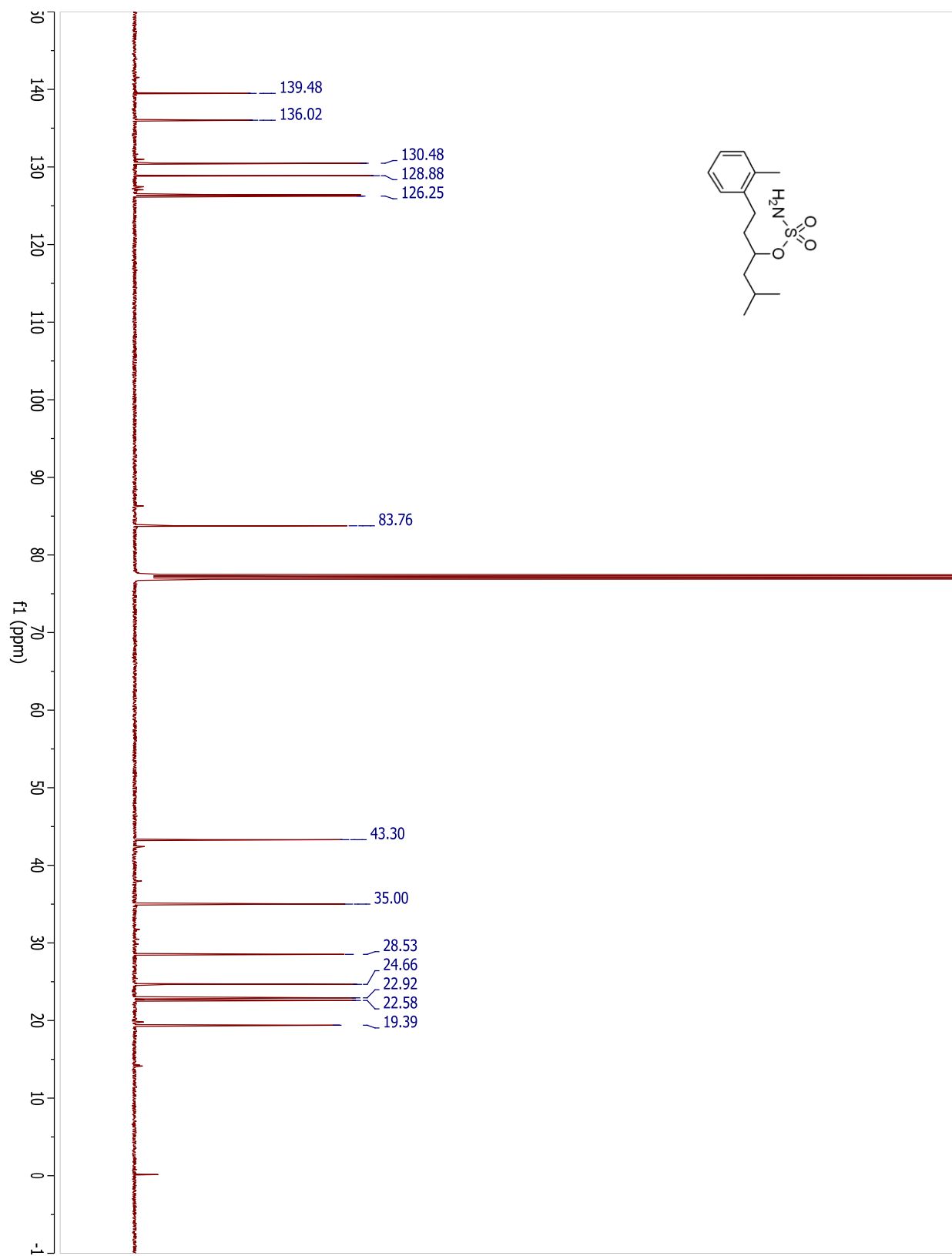


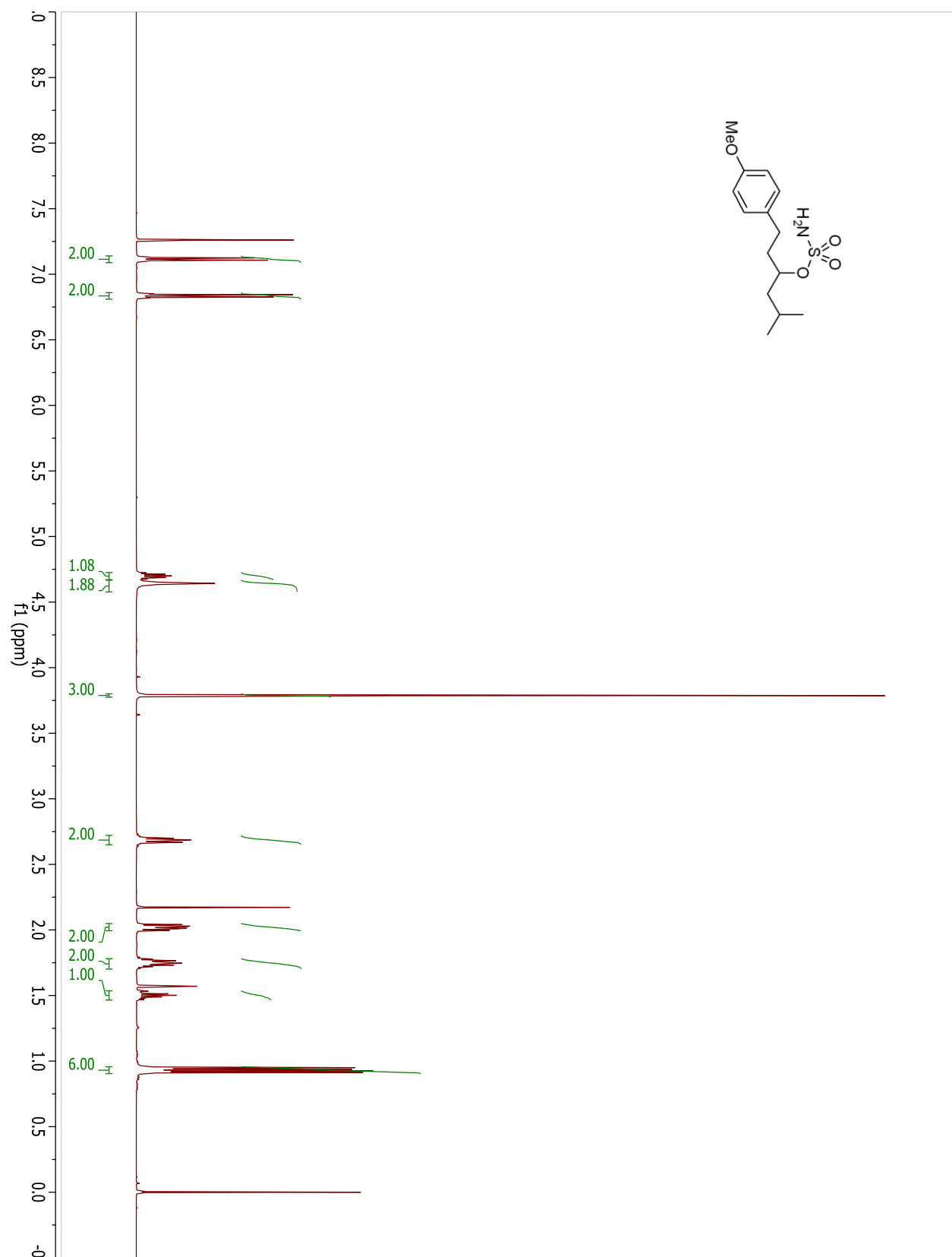


## Compound 3.56

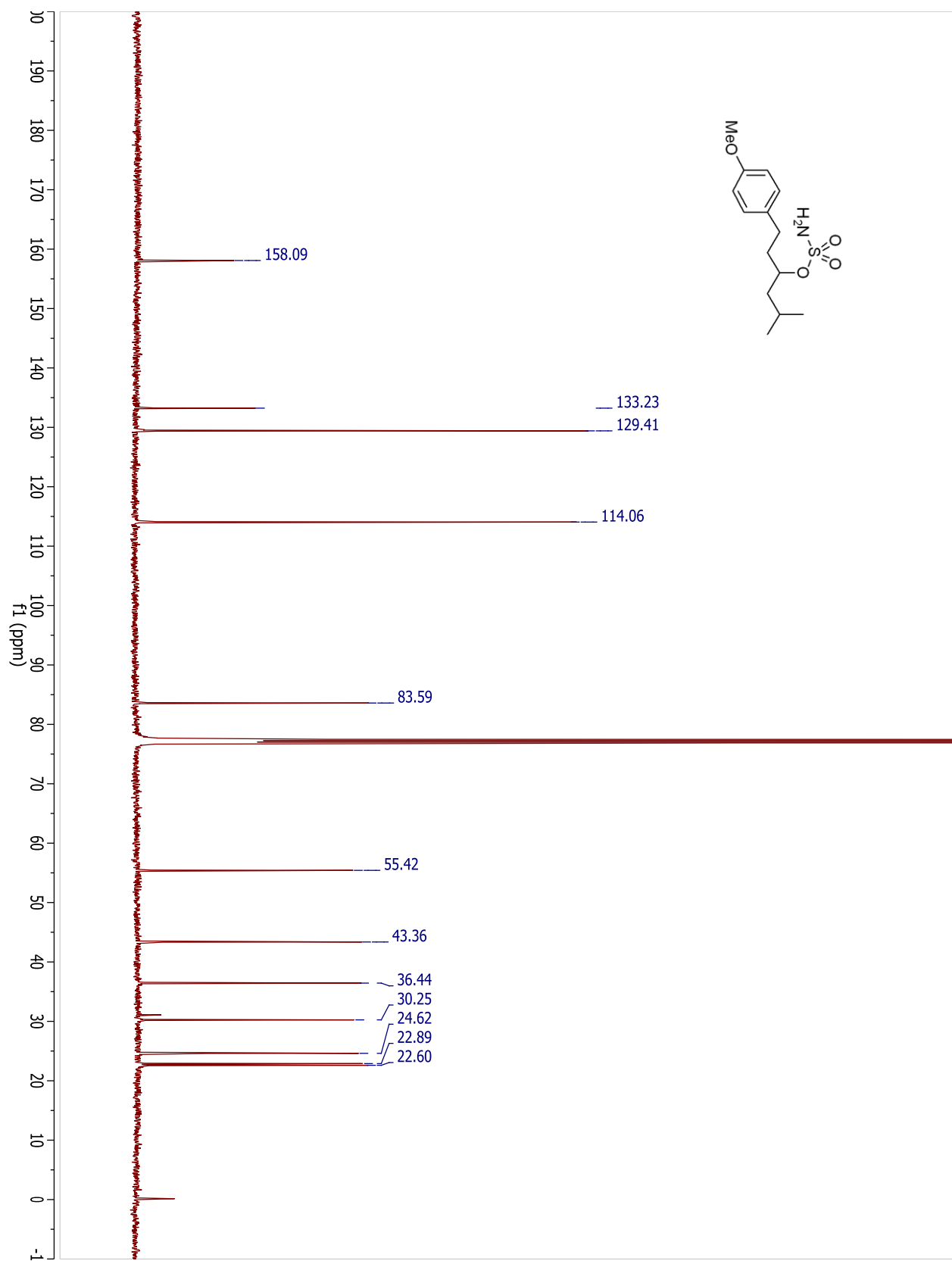


## Compound 3.56

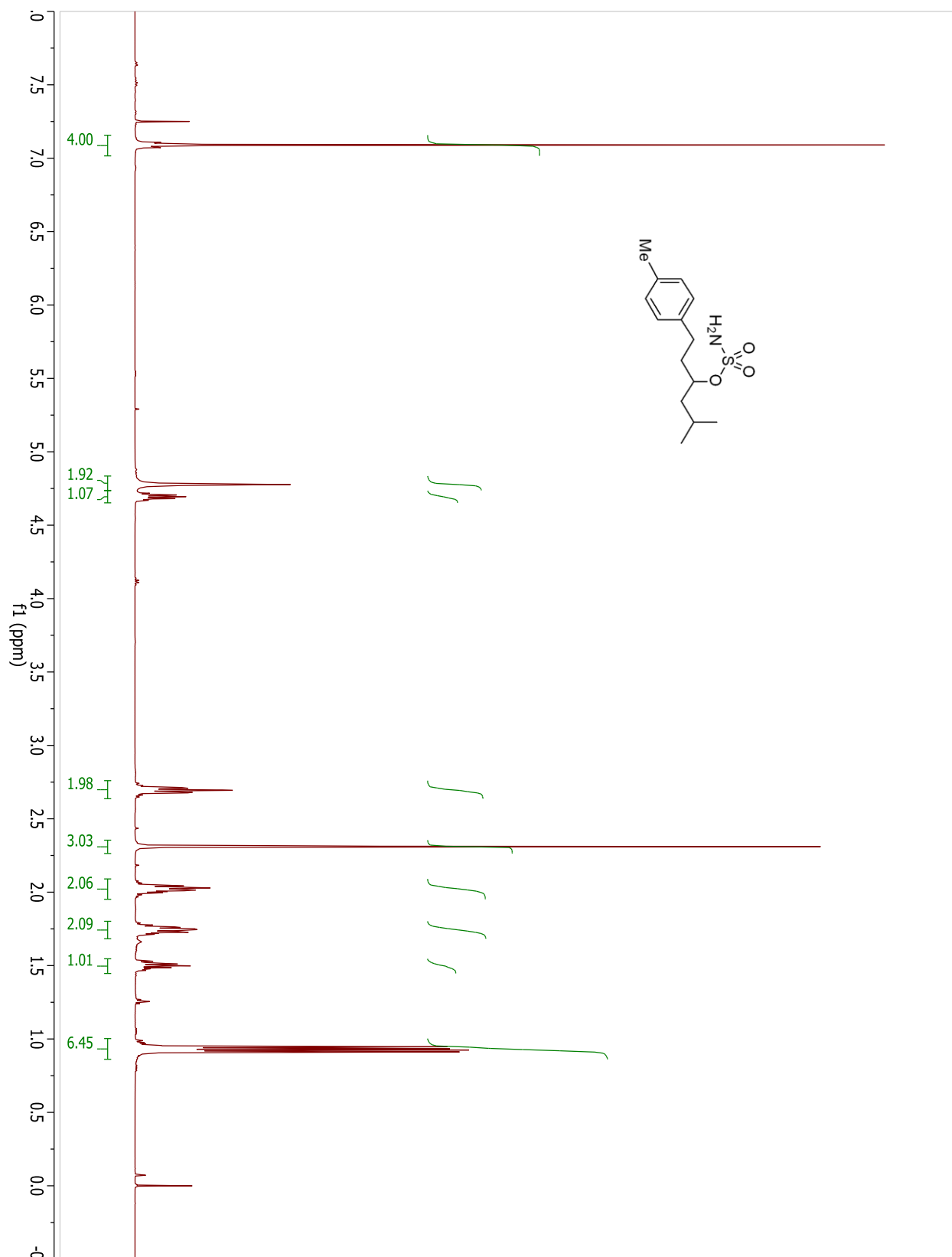


**Compound 3.57**

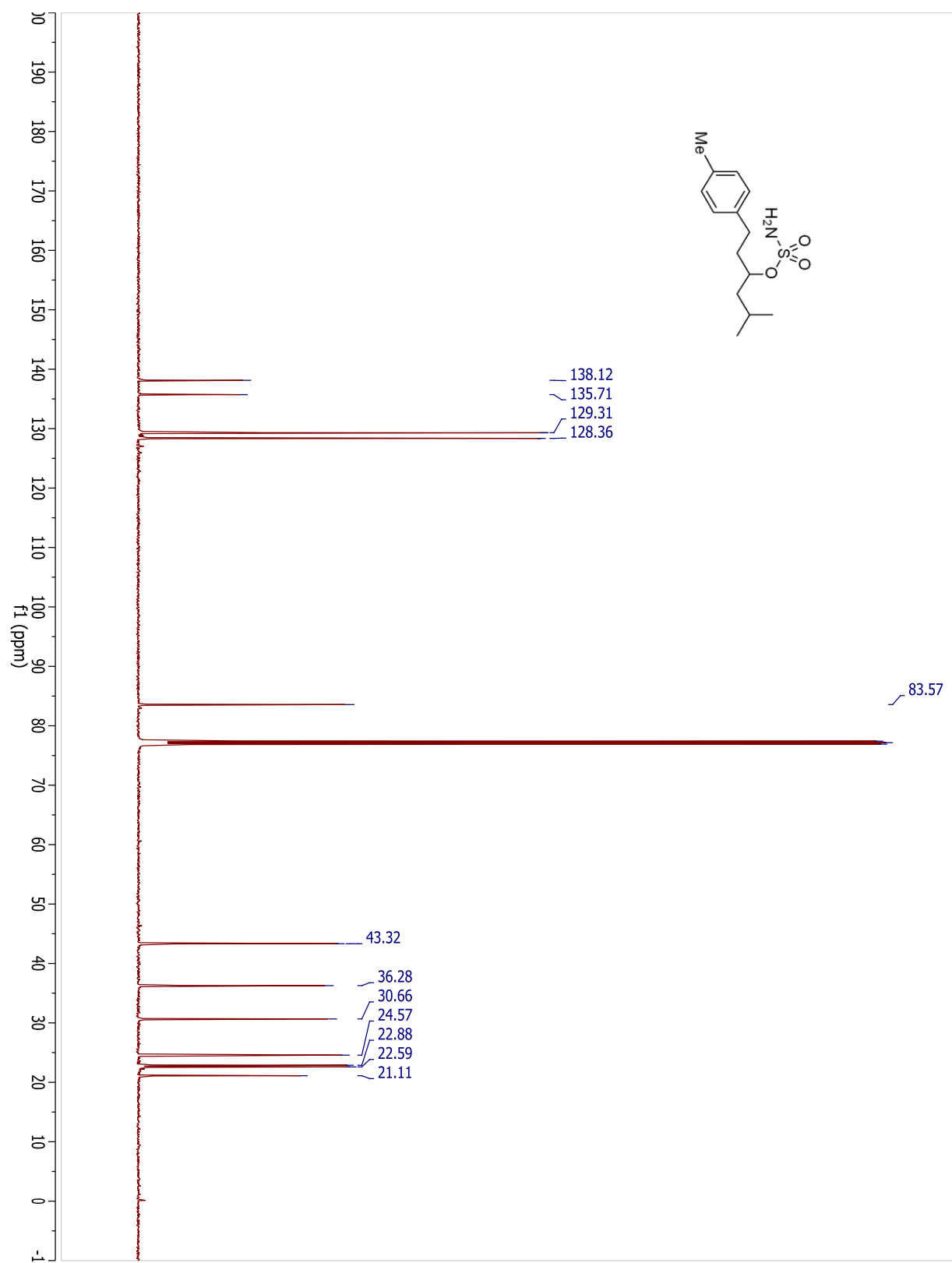
## Compound 3.57

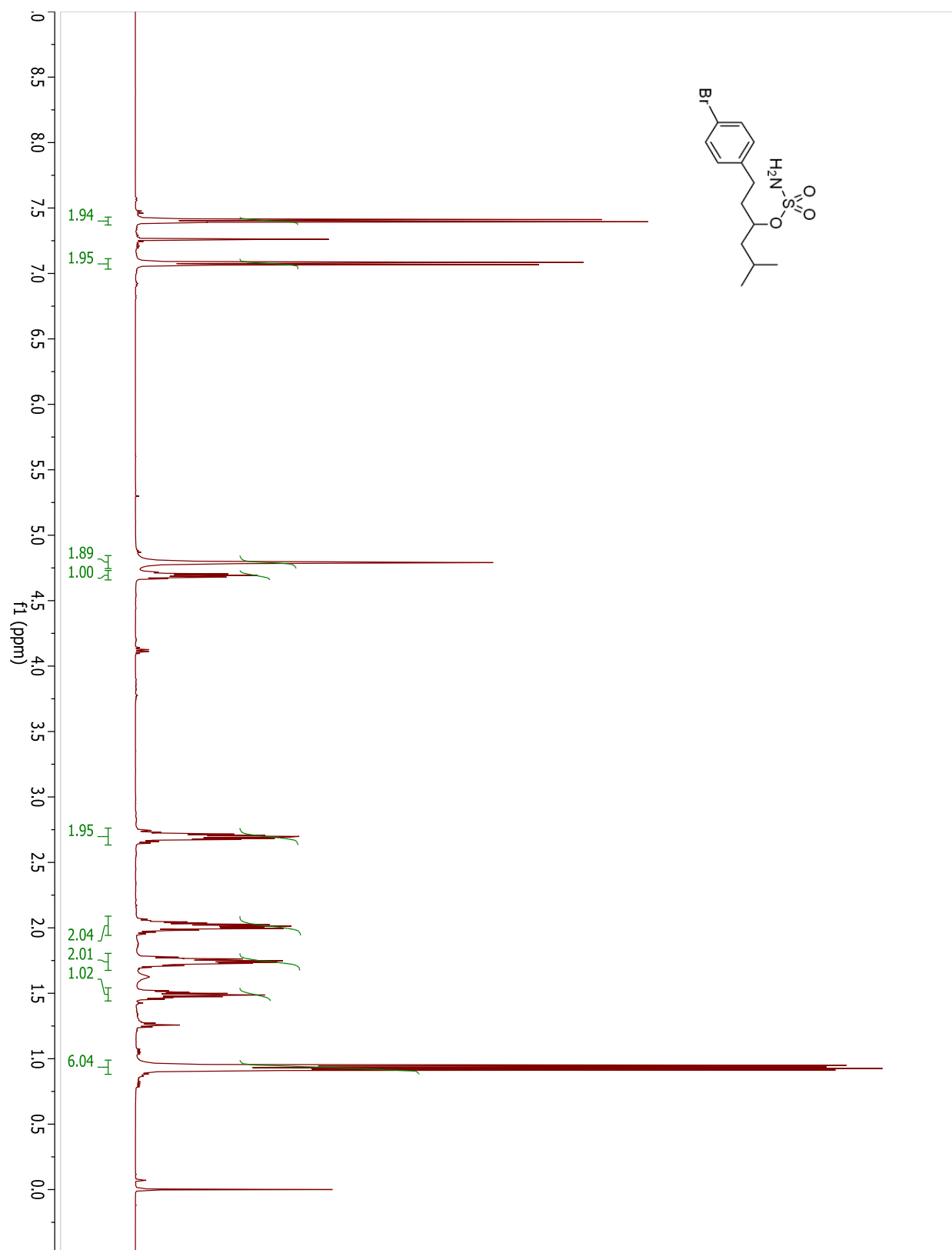


## Compound 3.58

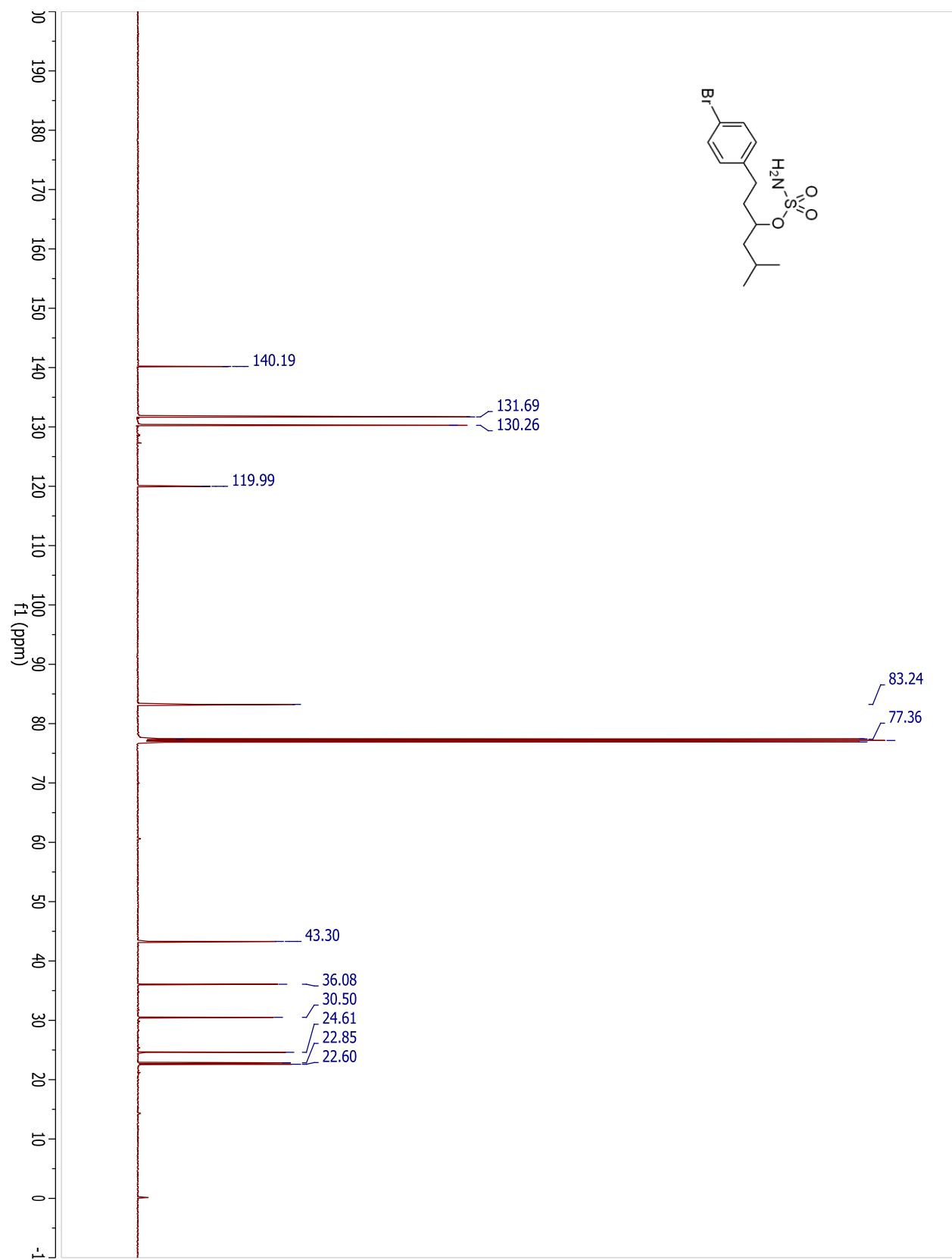


## Compound 3.58

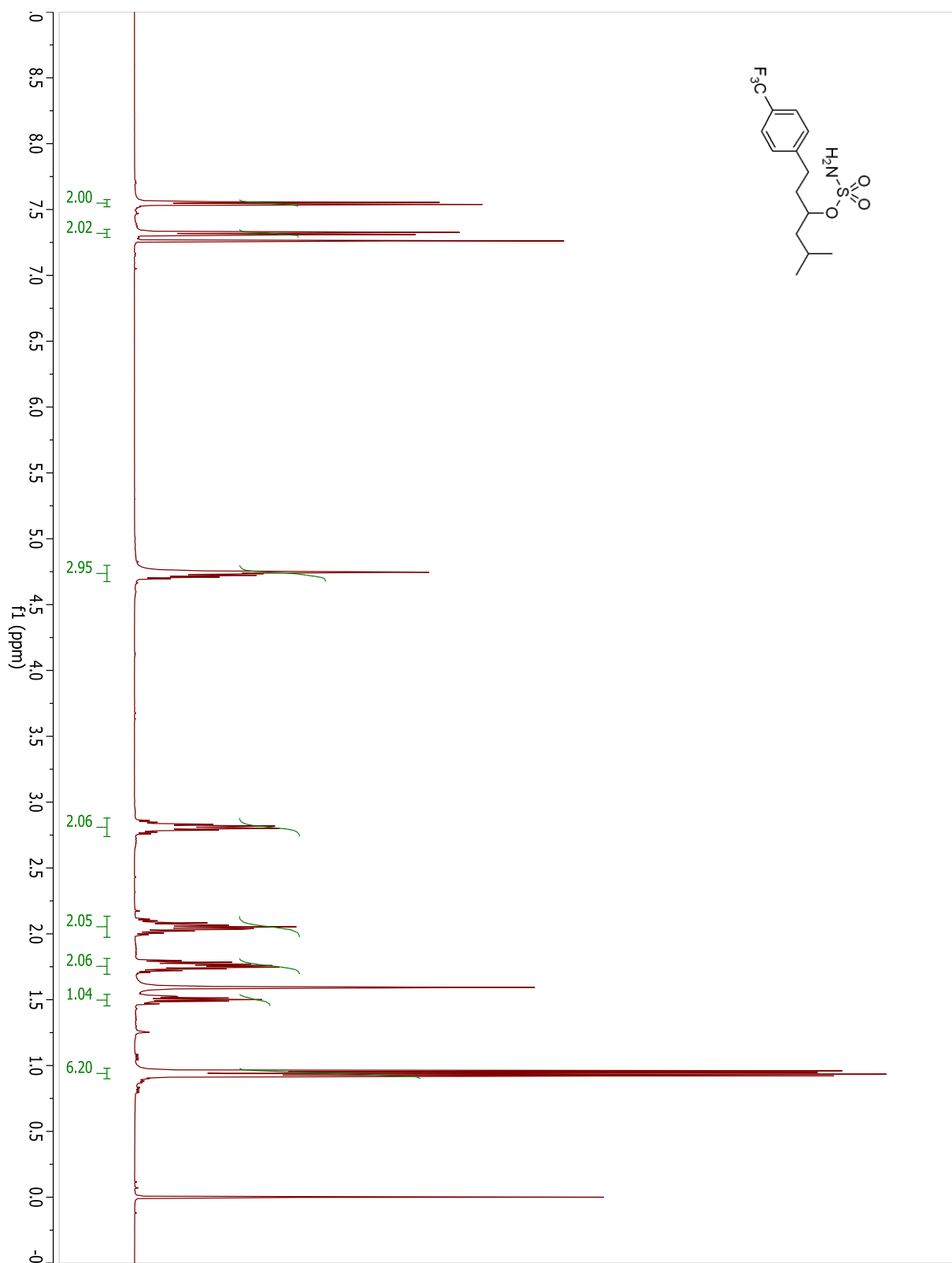


**Compound 3.59**

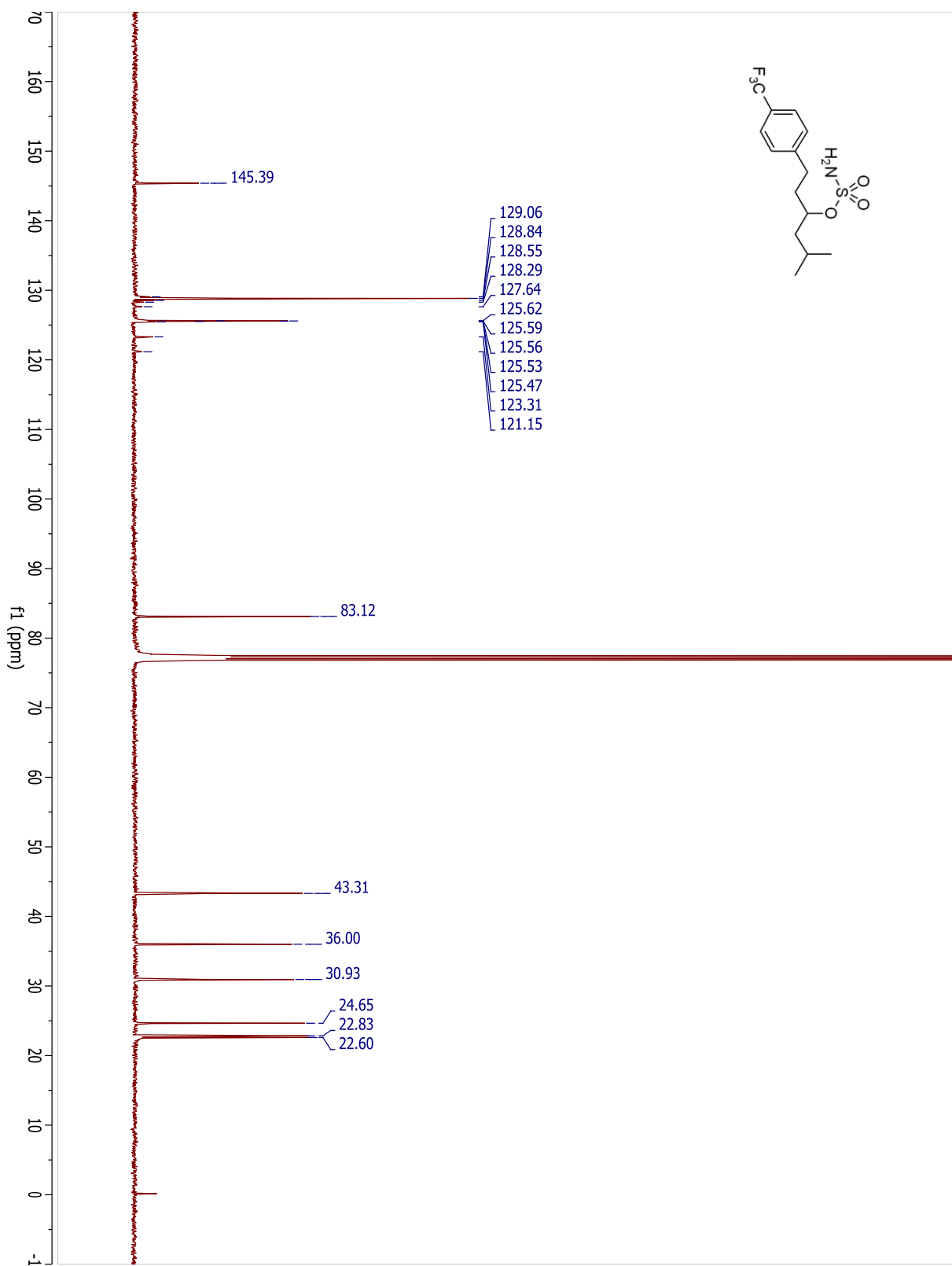
## Compound 3.59



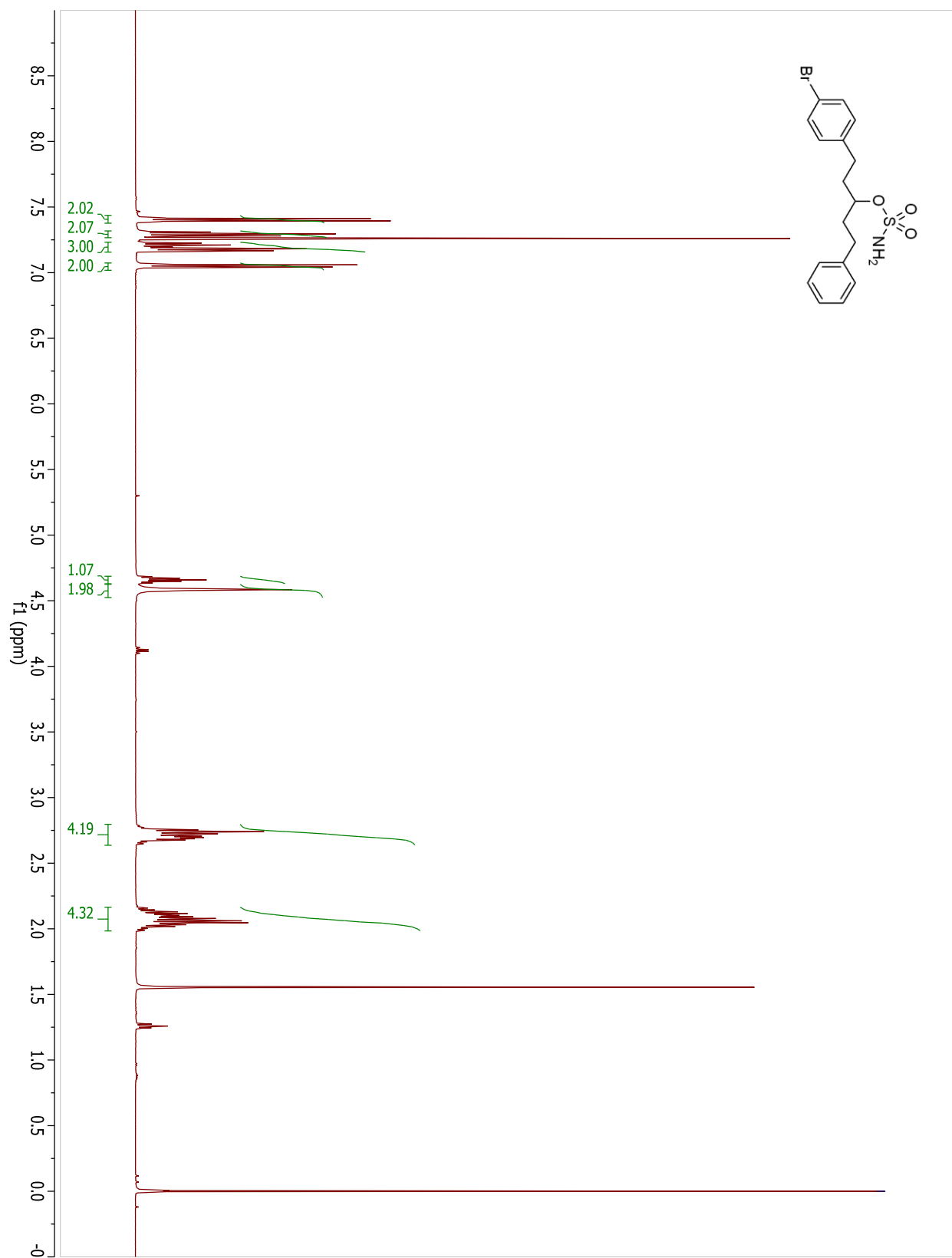


**Compound 3.60**

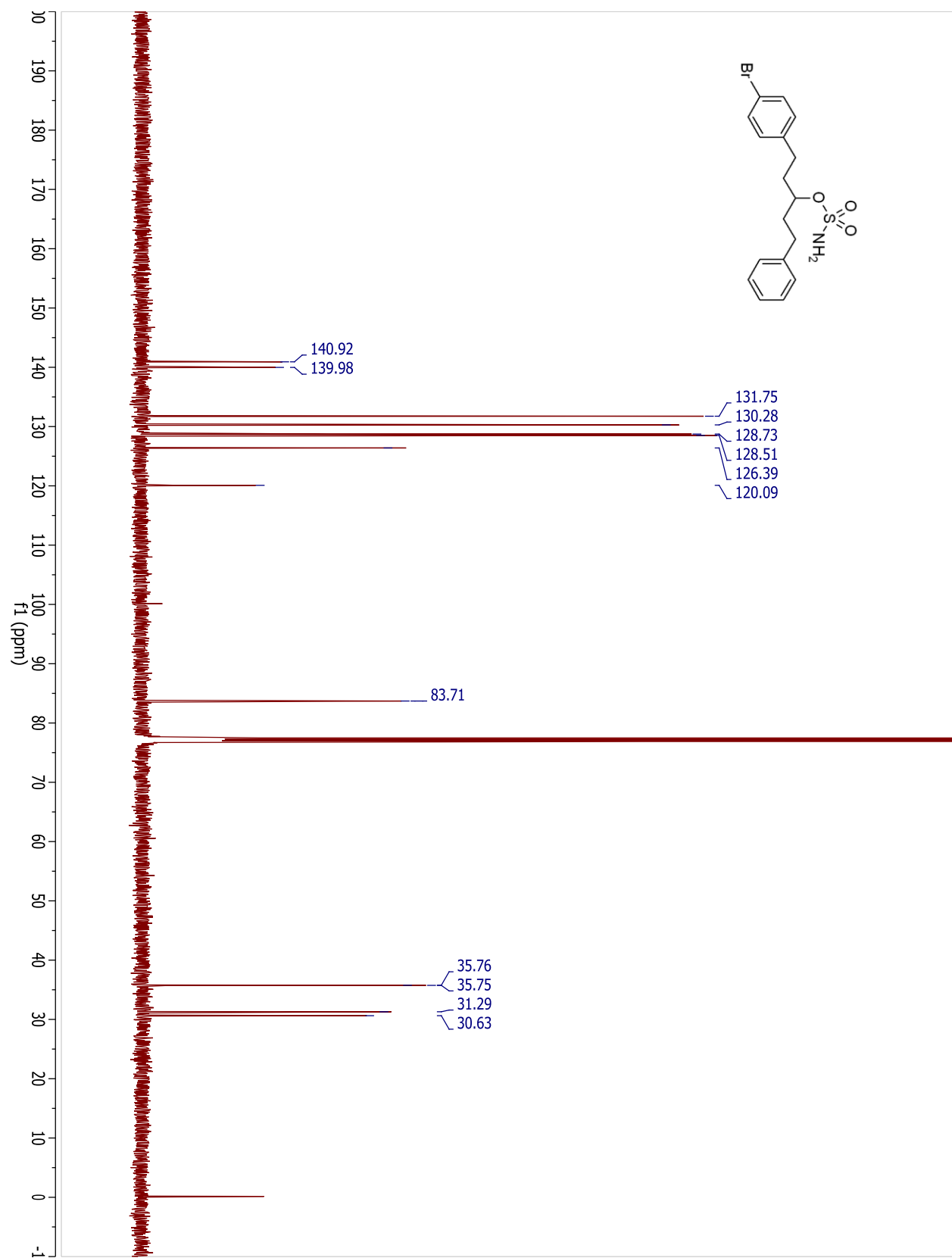
## Compound 3.60



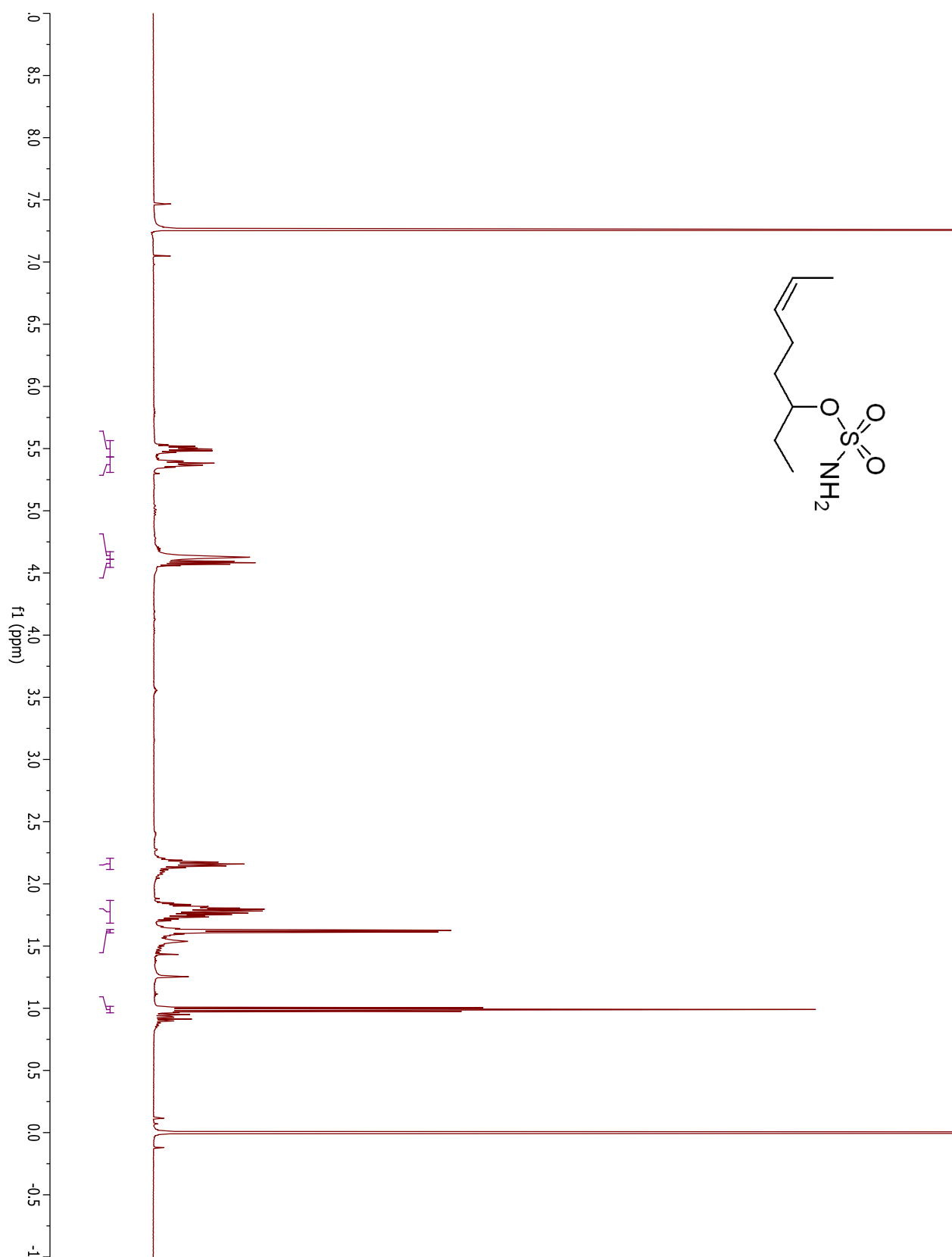
## Compound 3.62



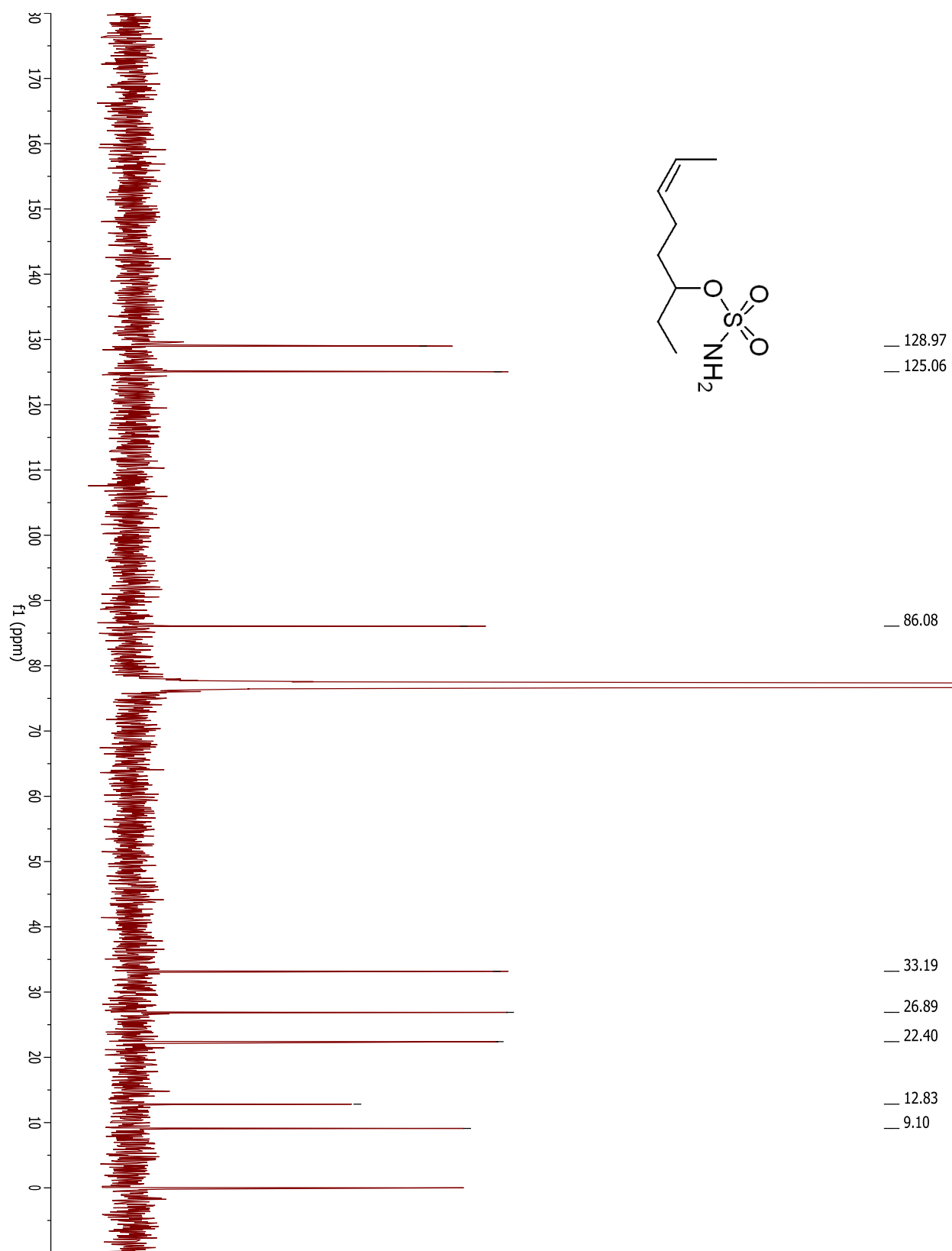
## Compound 3.62



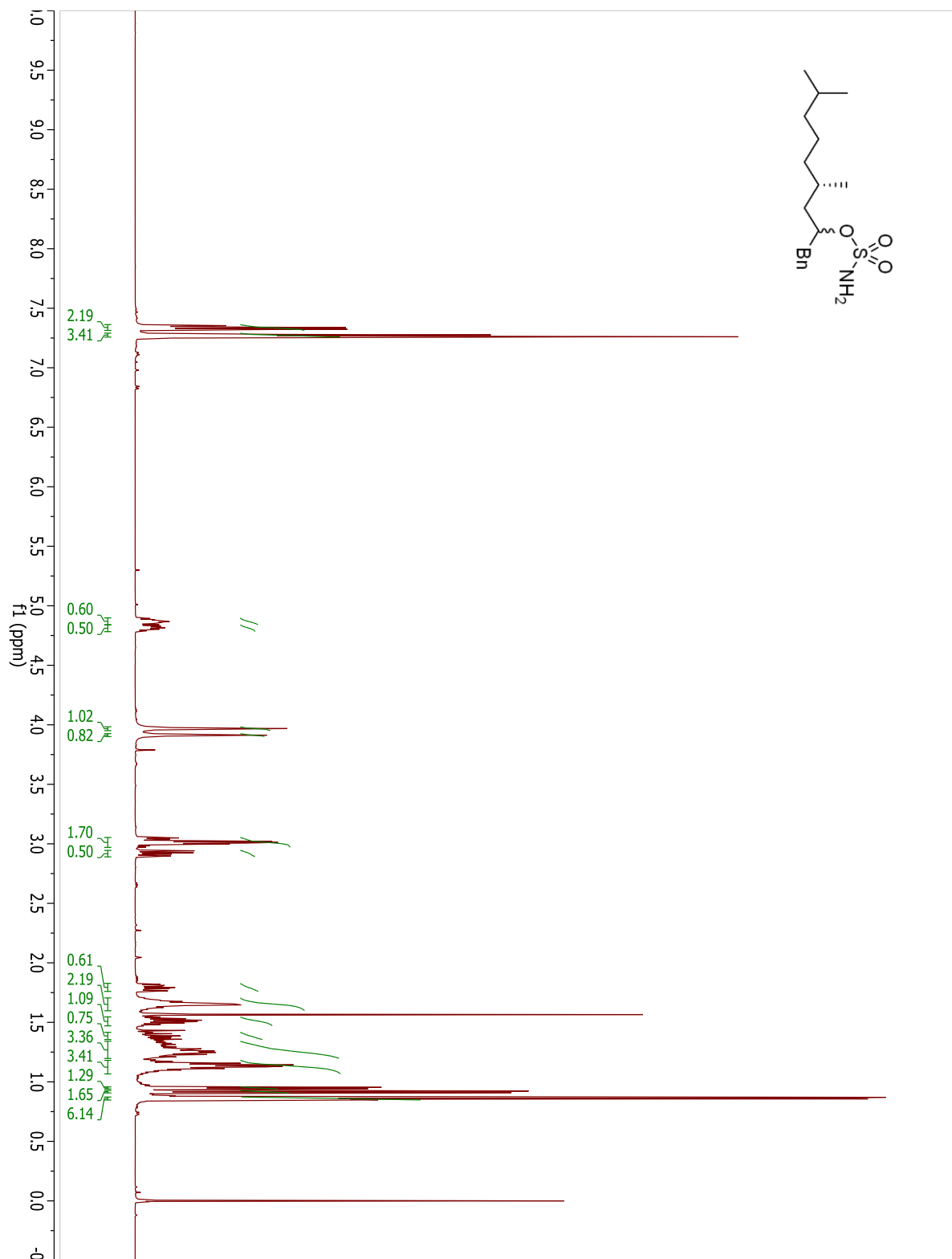
## Compound 3.65



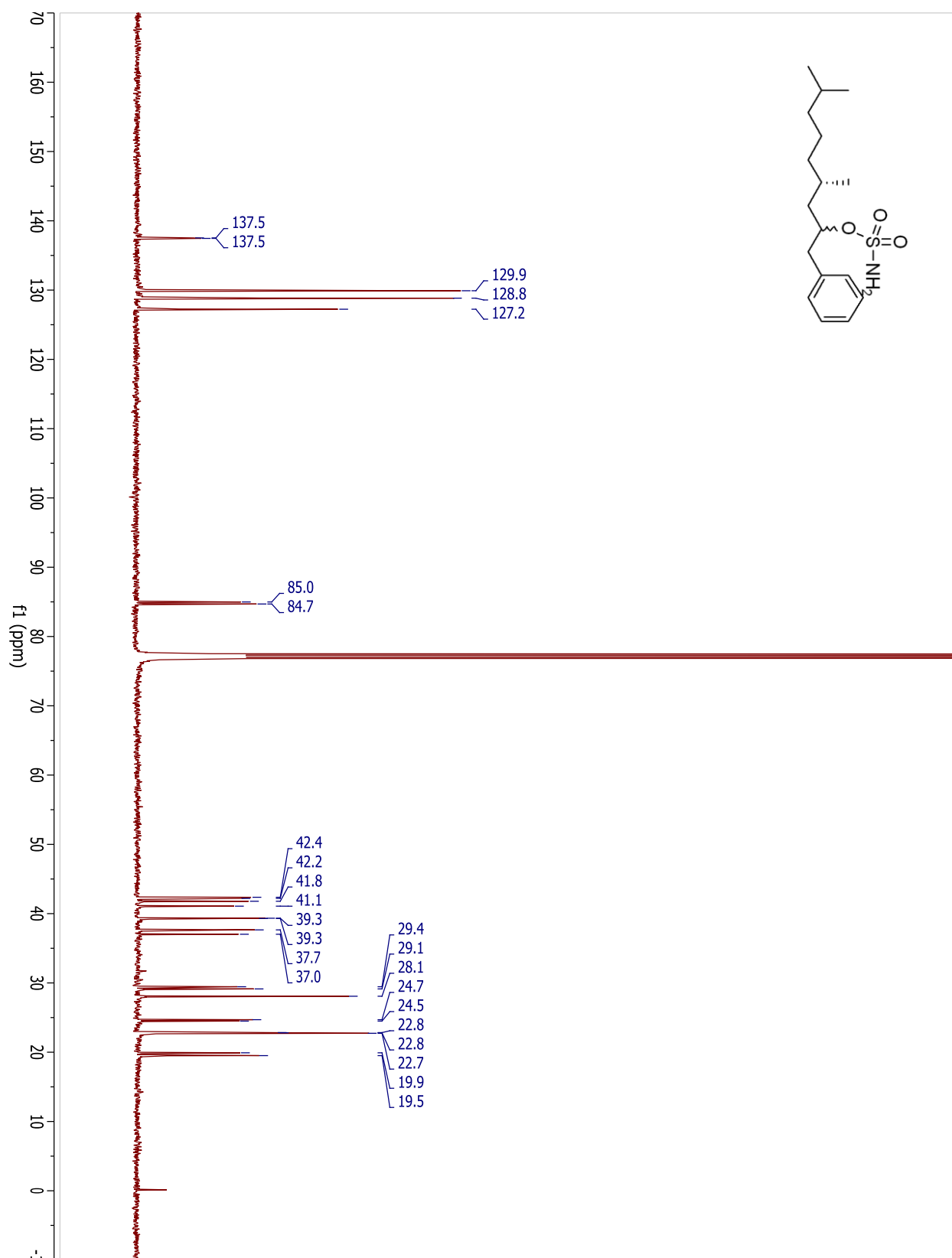
## Compound 3.65



## Compound 3.66

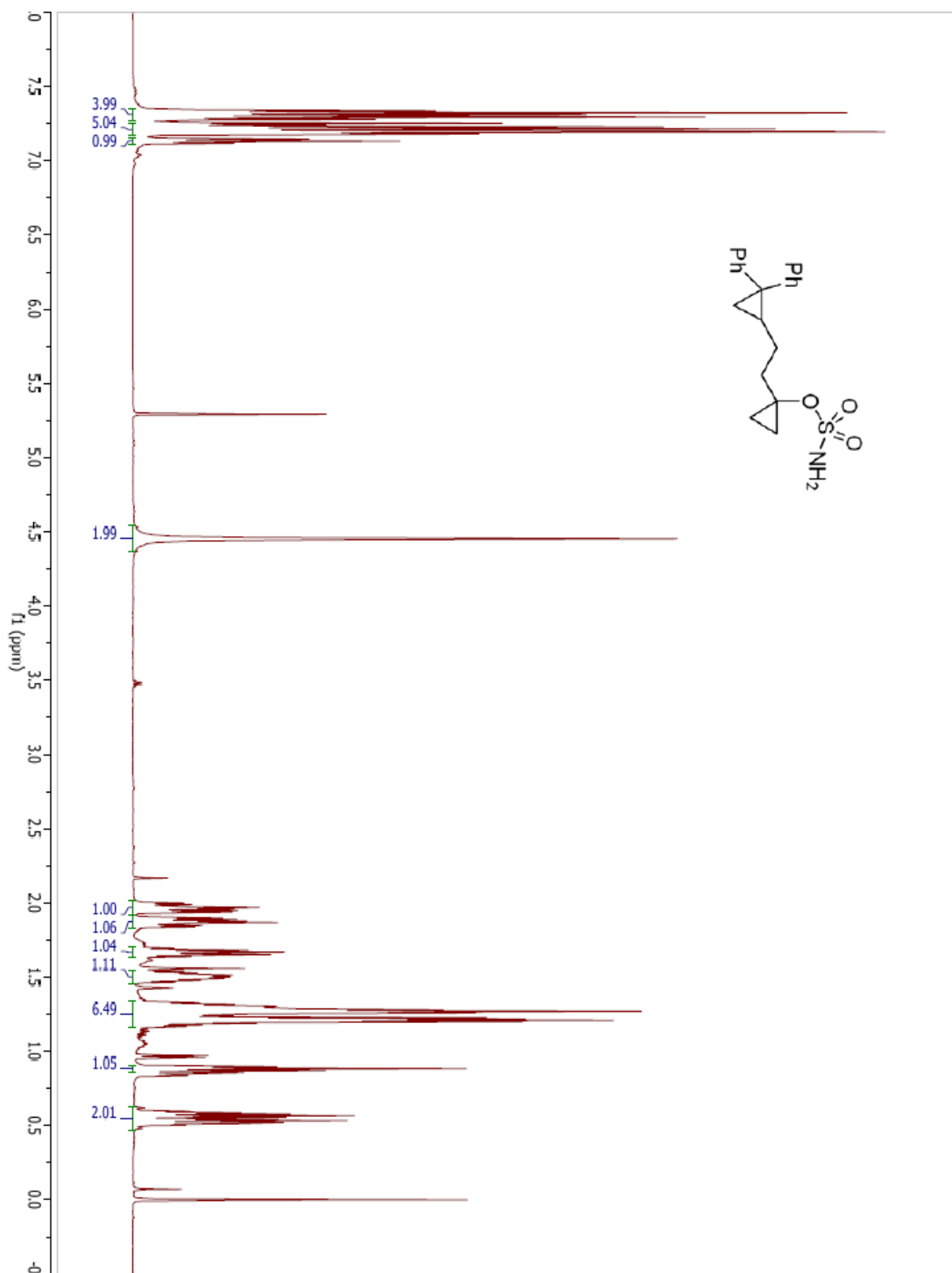


## Compound 3.66

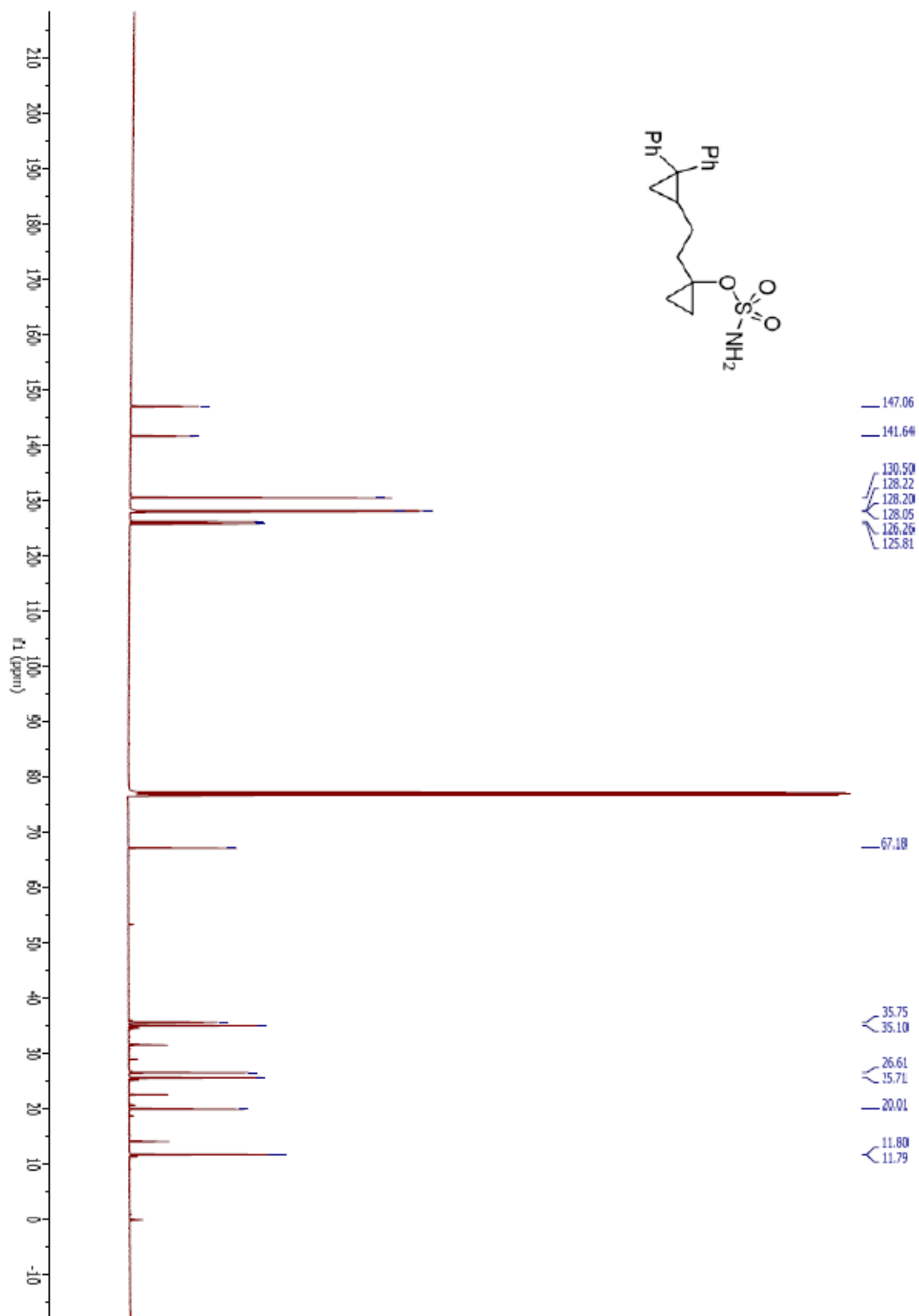




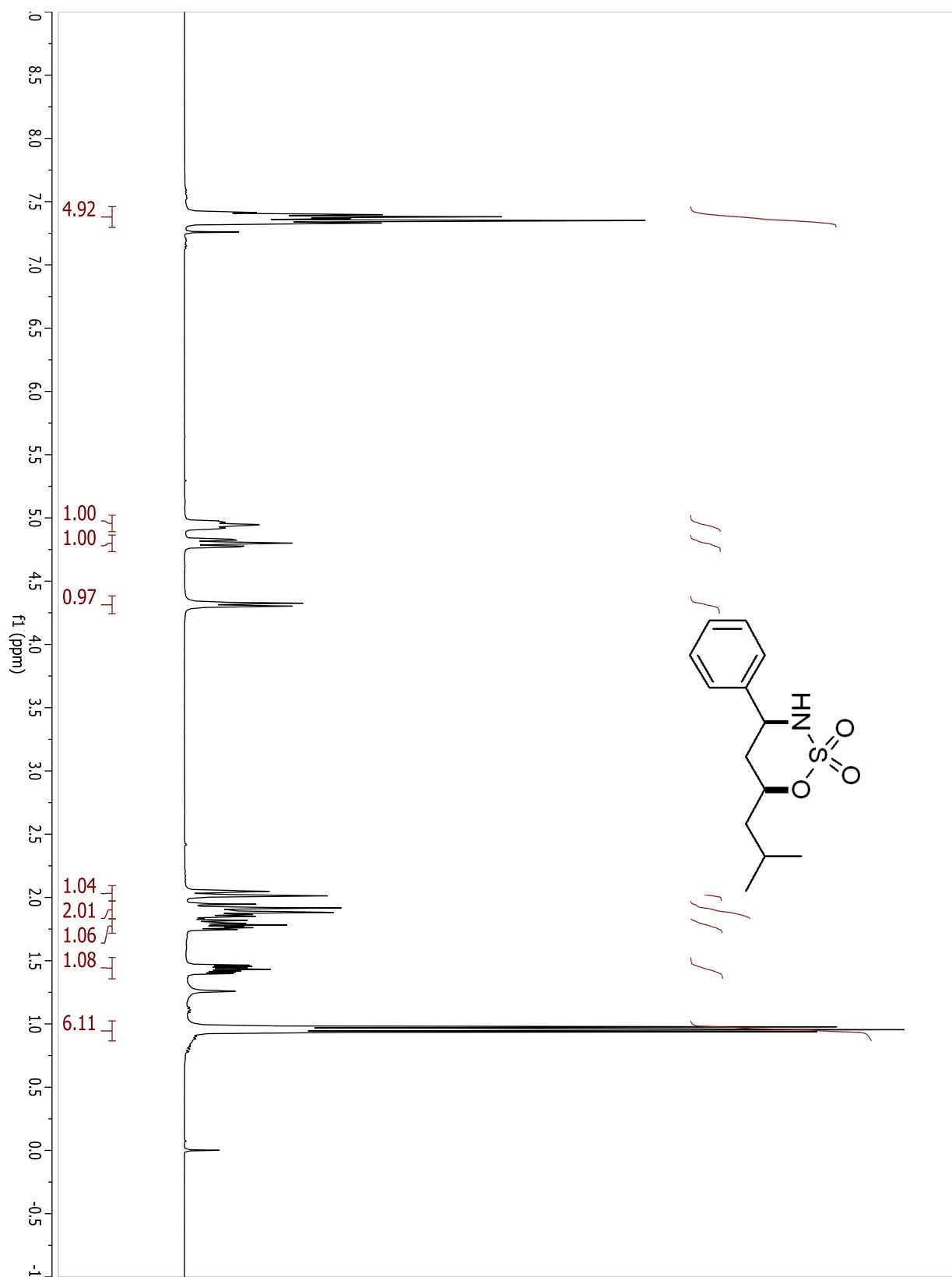
## Compound 3.67



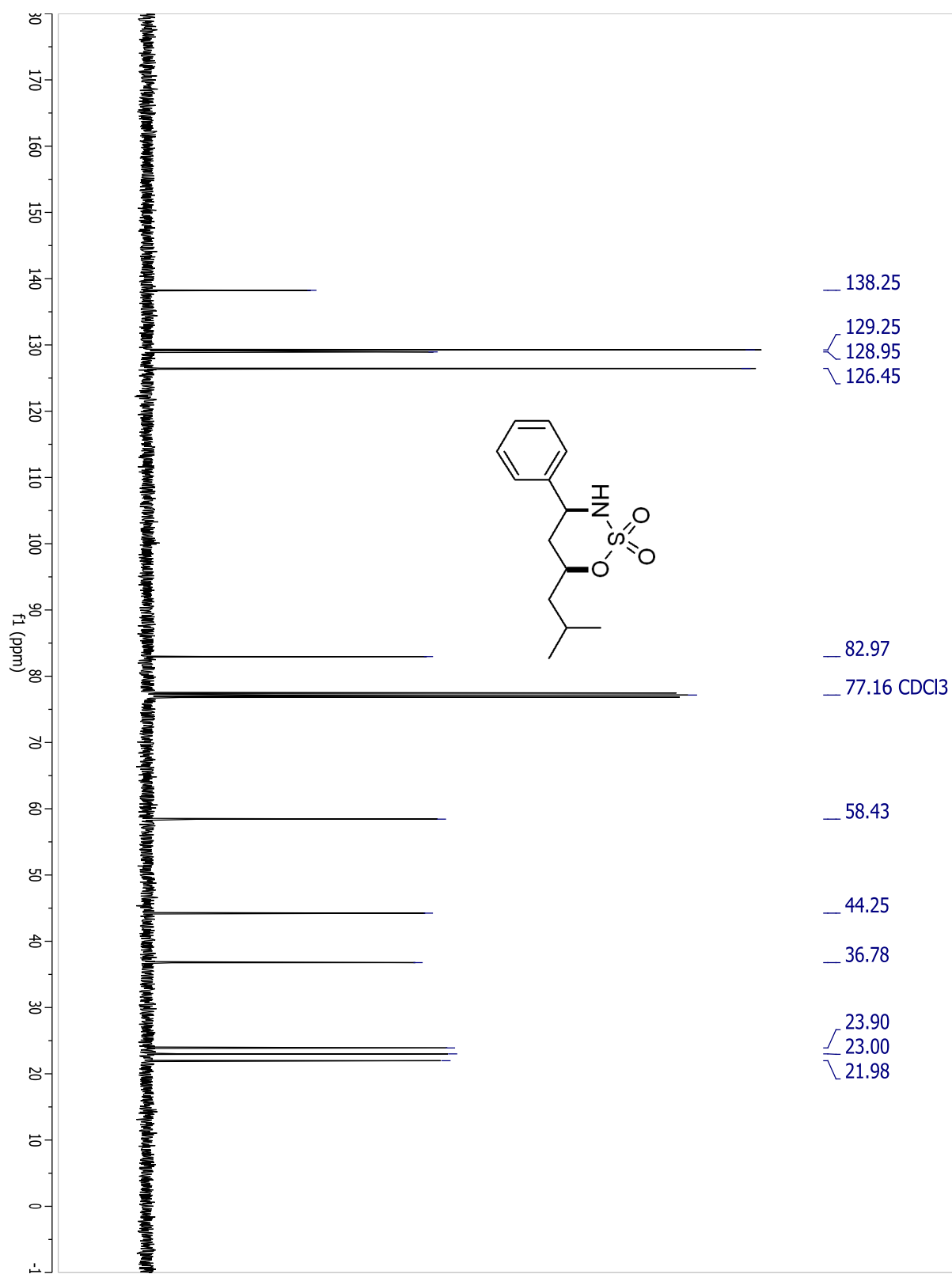
## Compound 3.67



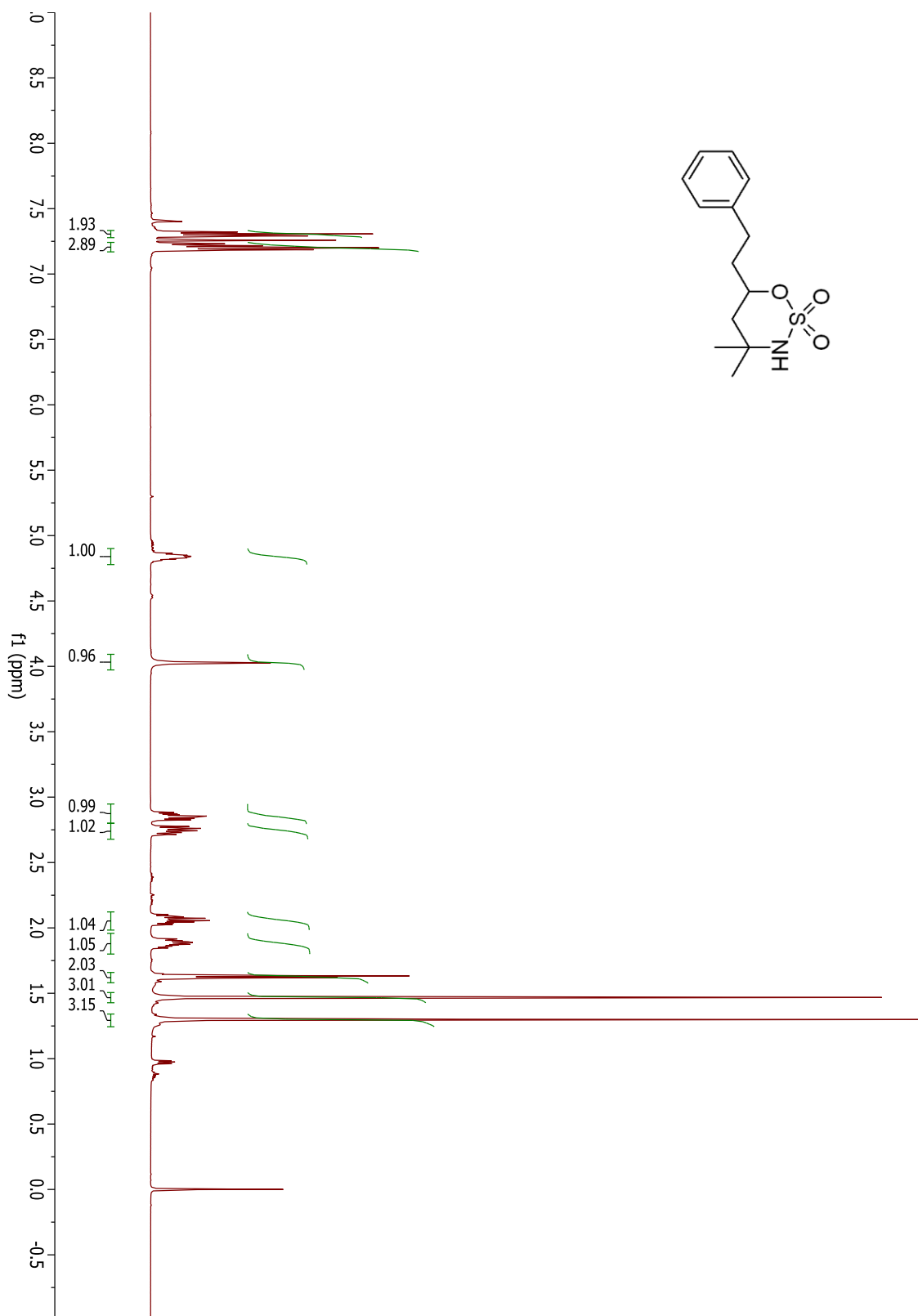
## Compound 3.2a



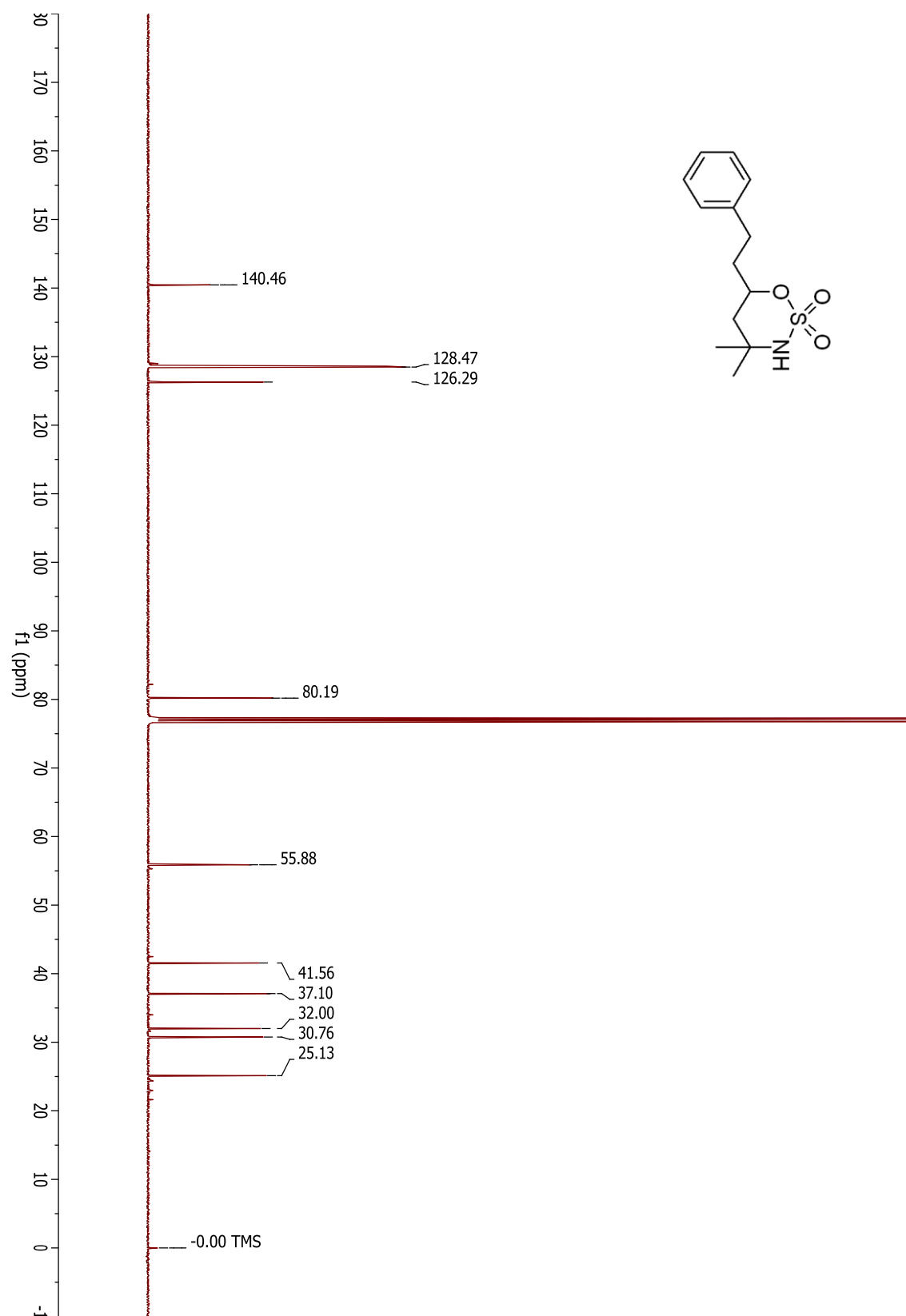
## Compound 3.2a



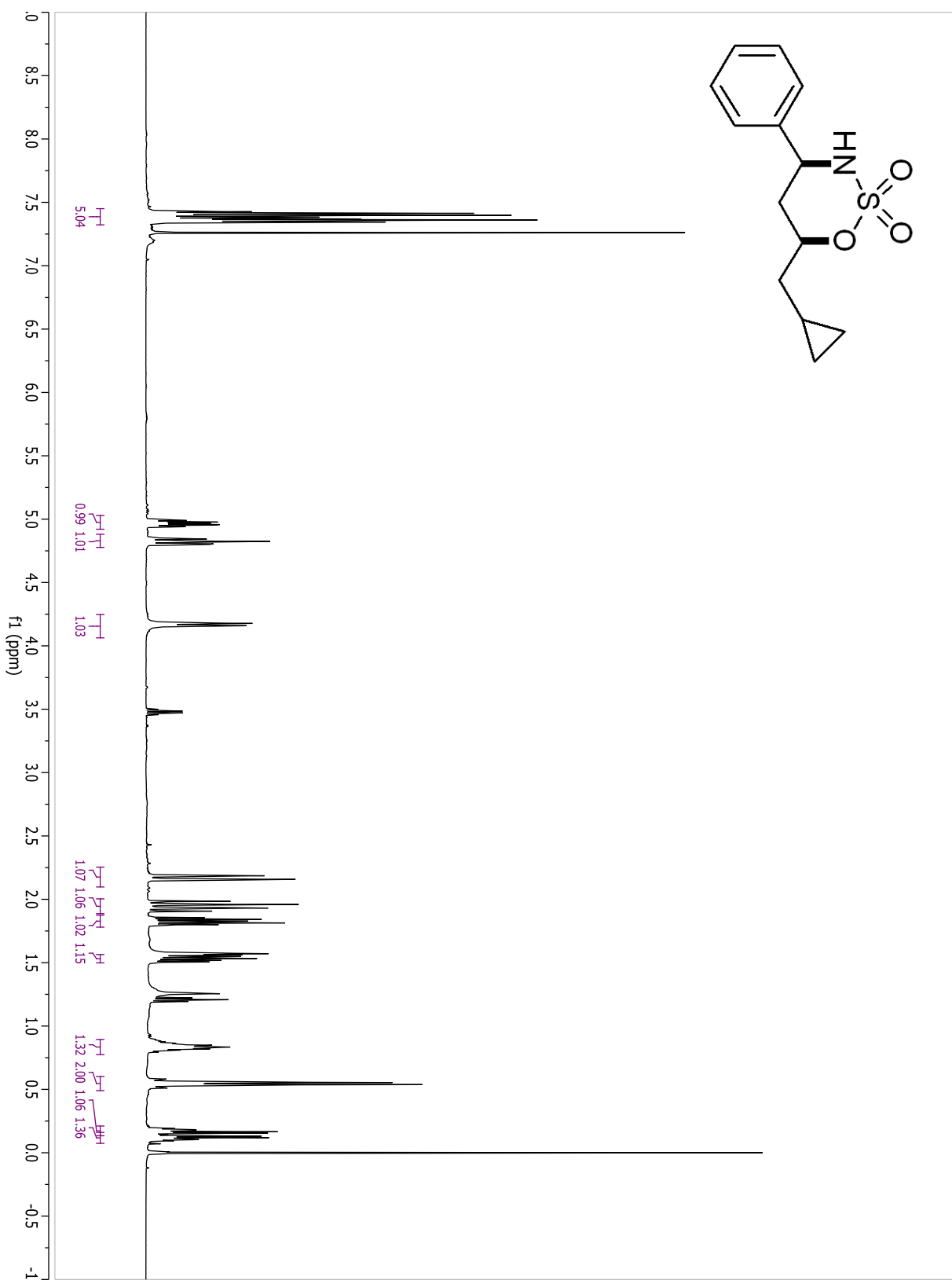
## Compound 3.2b



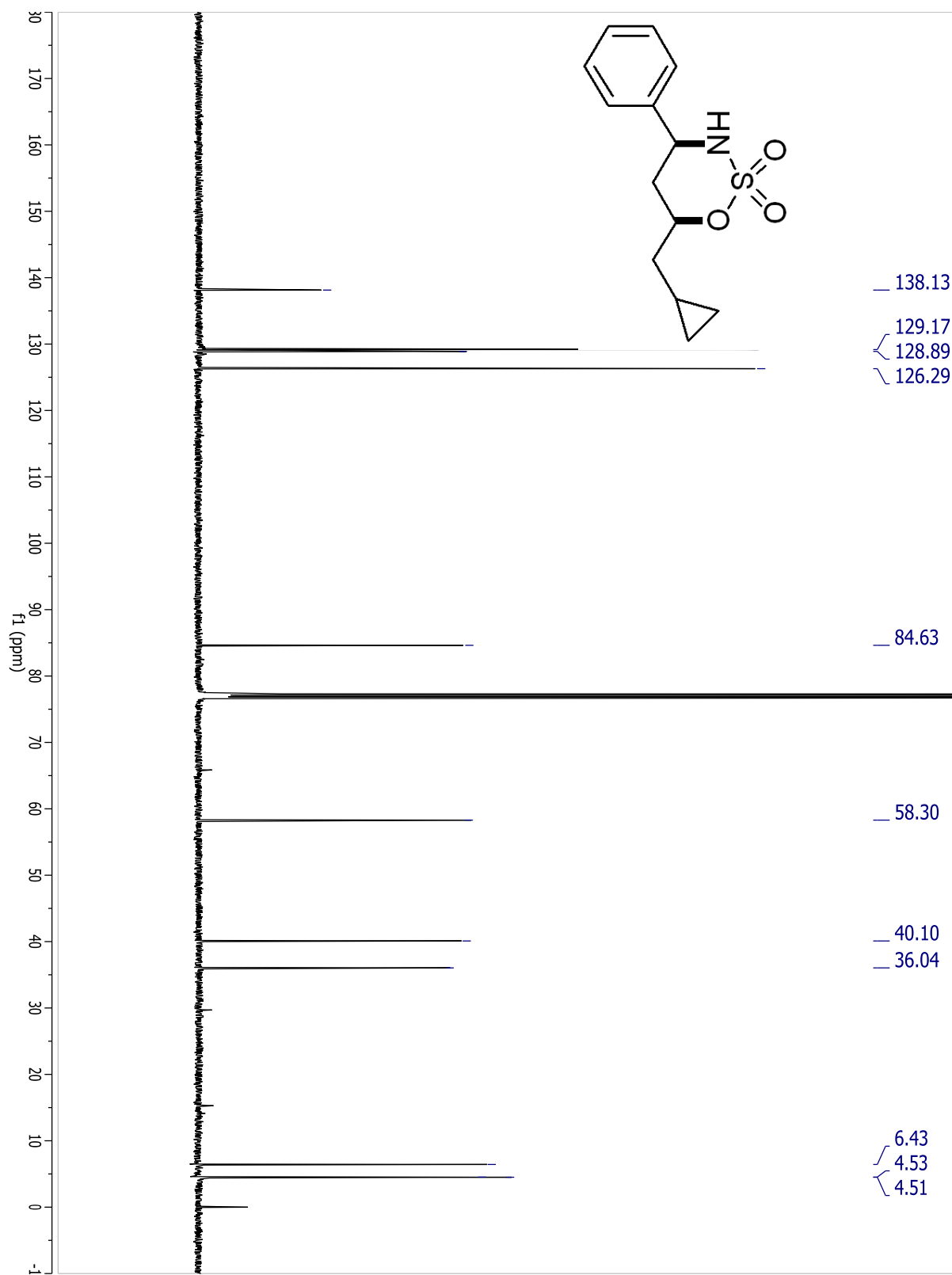
## Compound 3.2b



Compound 3.47a

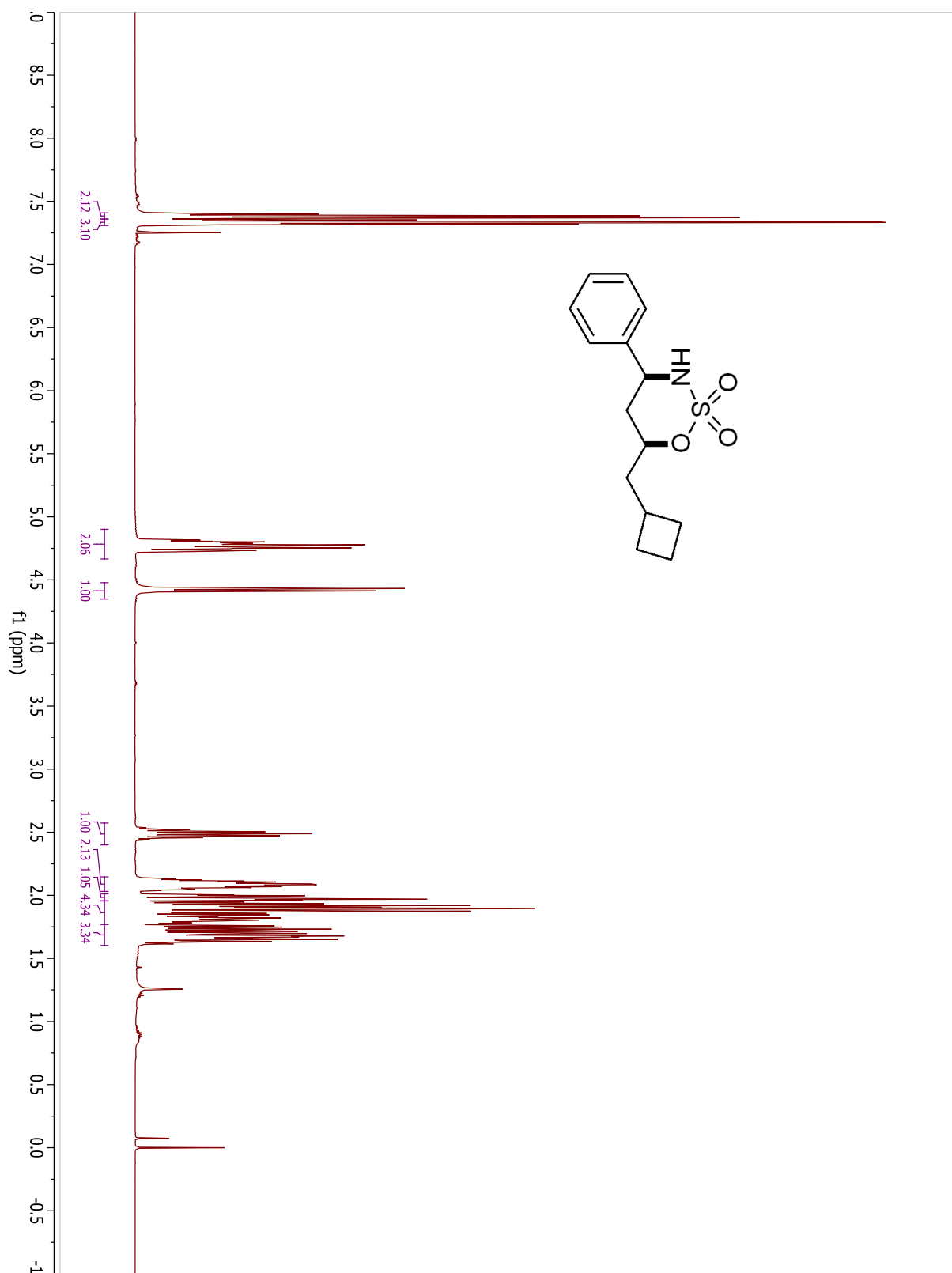


## Compound 3.47a

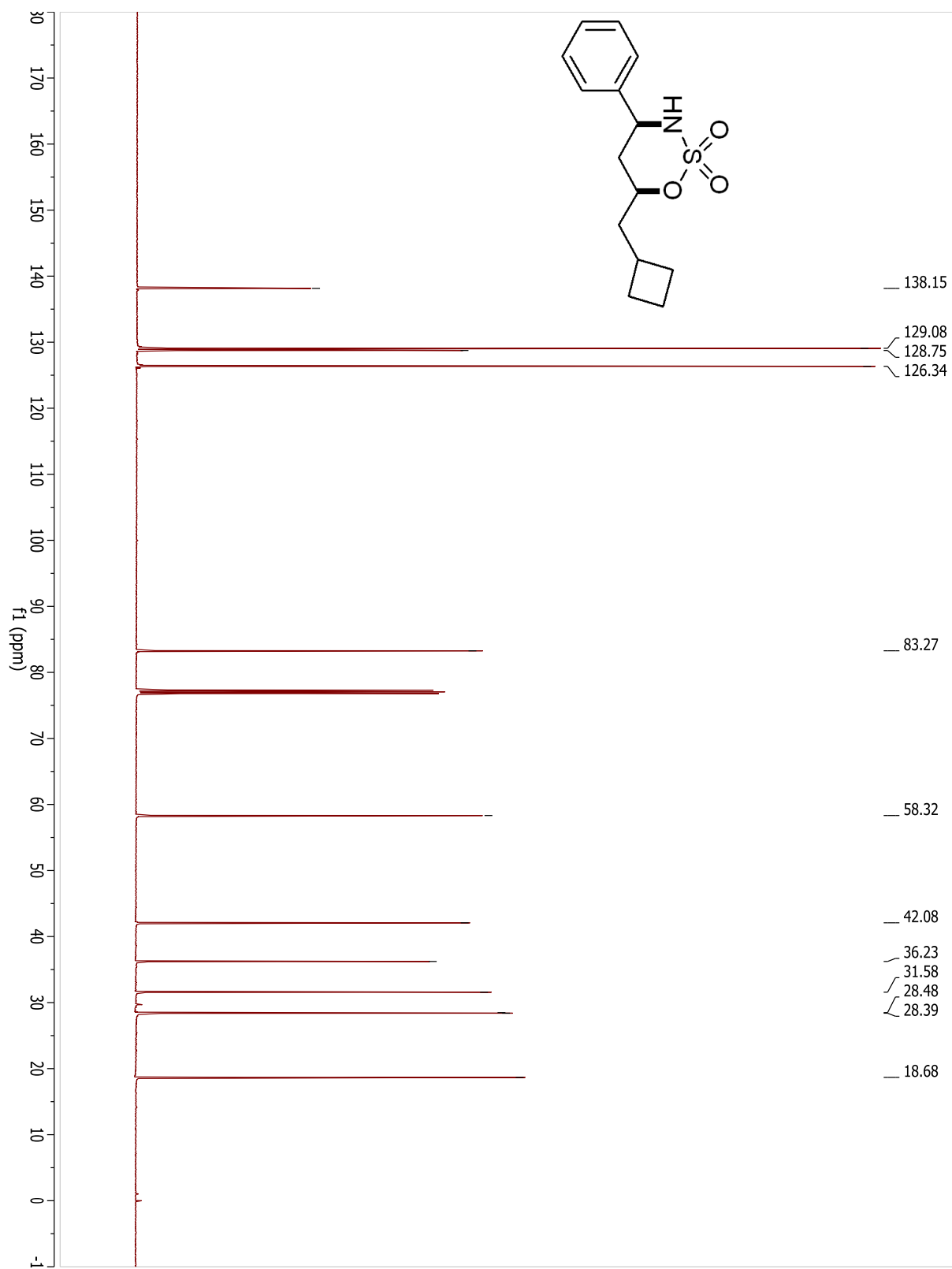




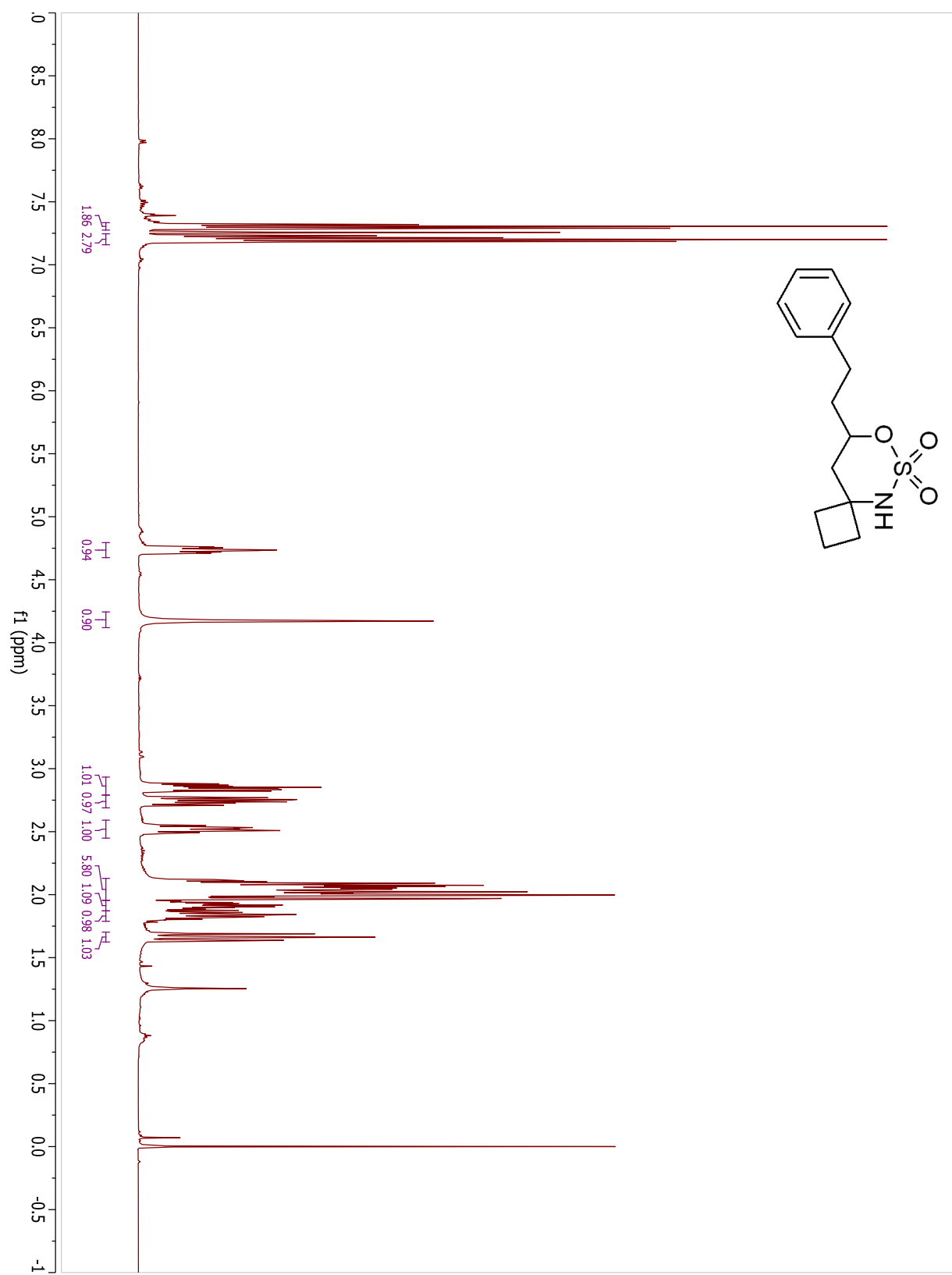
## Compound 3.48a



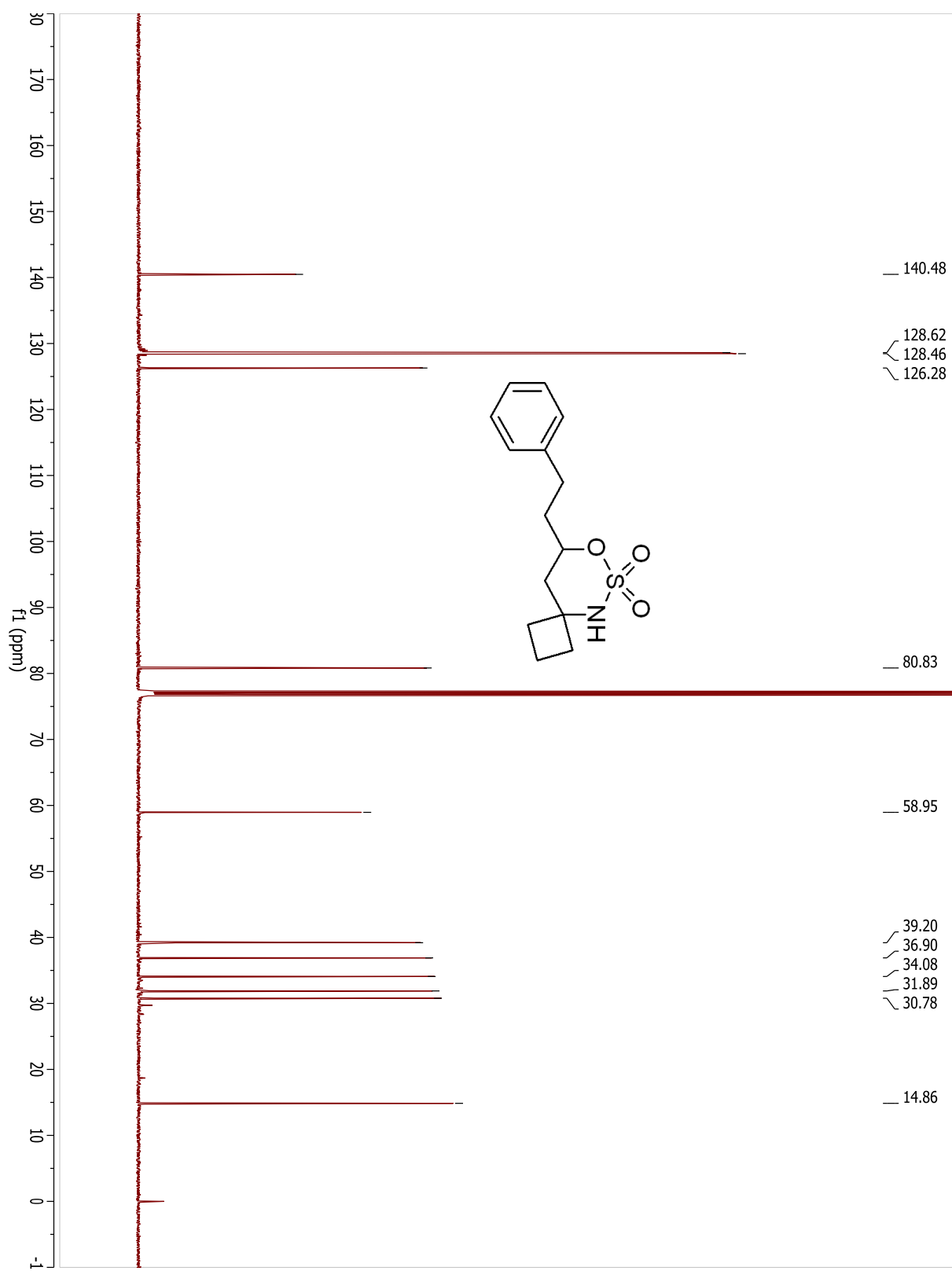
## Compound 3.48a



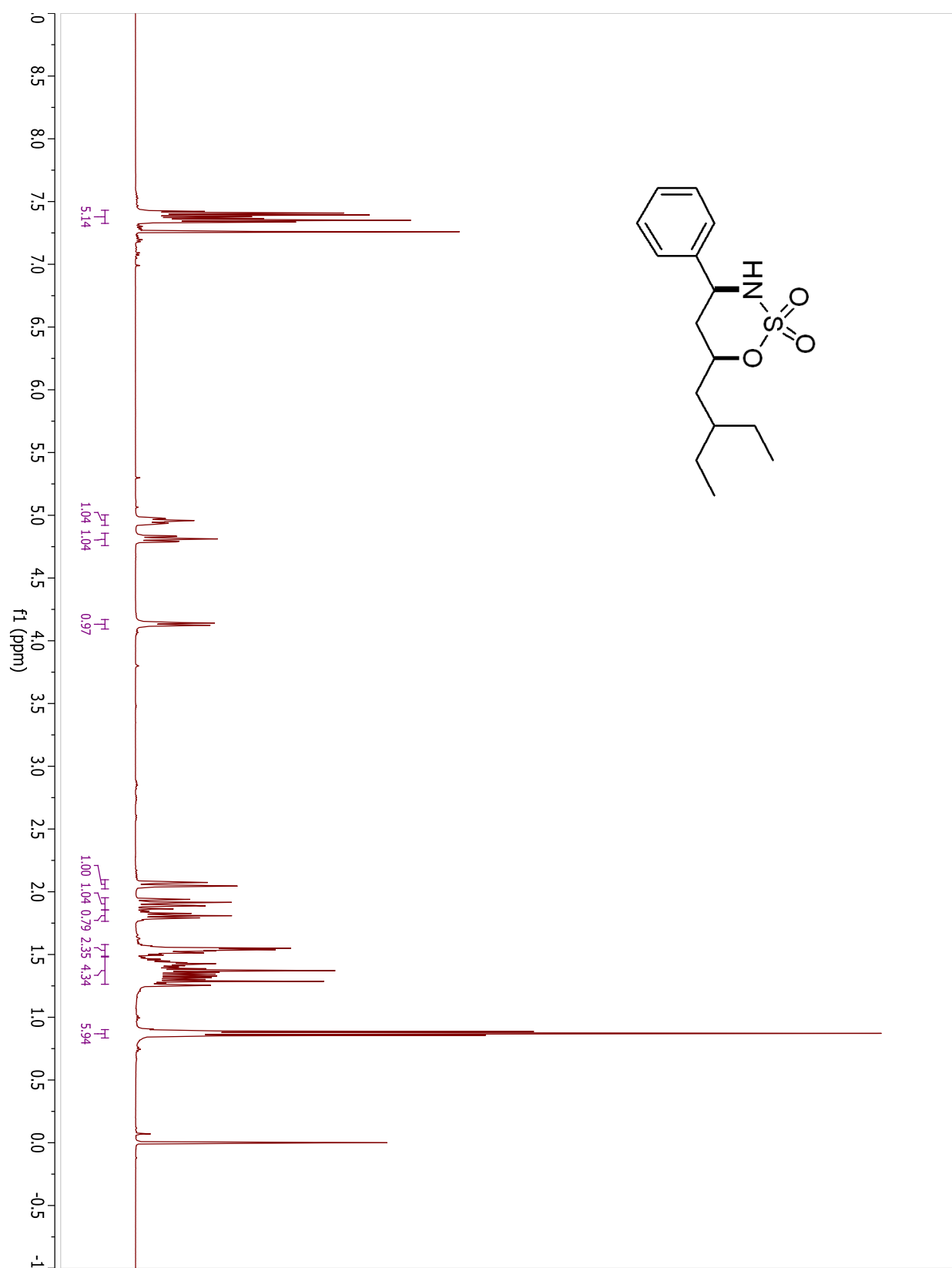
## Compound 3.48b



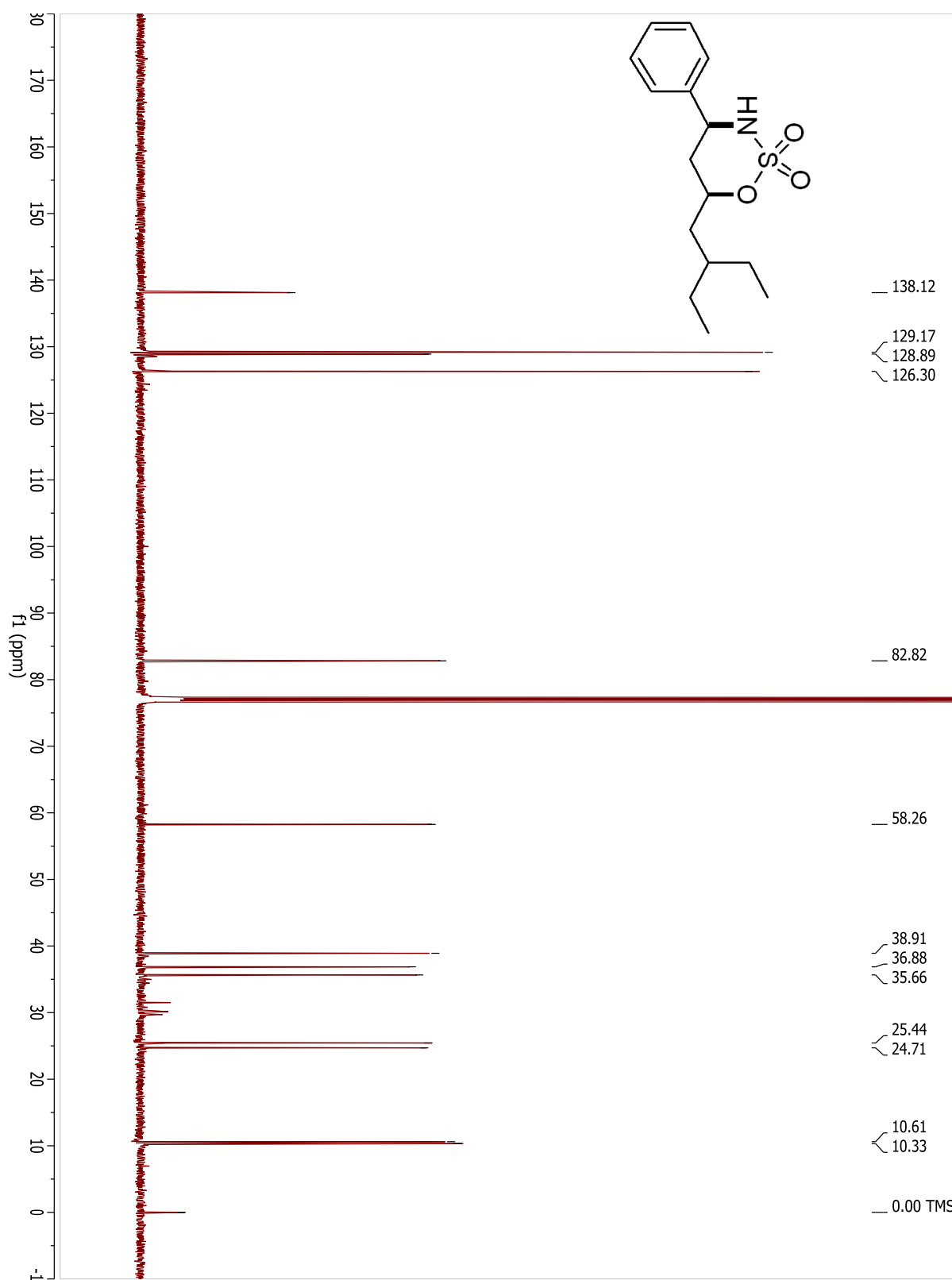
## Compound 3.48b



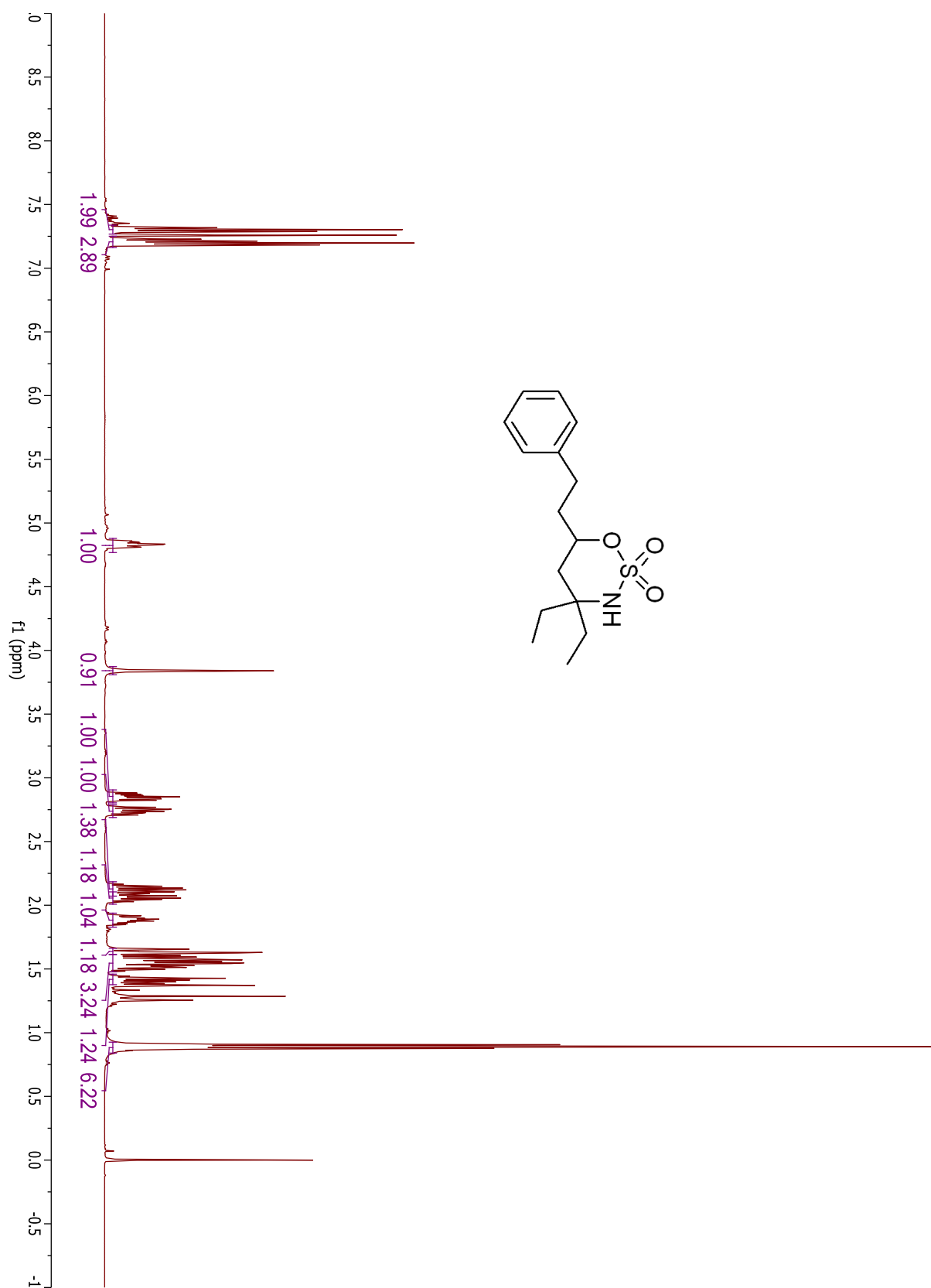
## Compound 3.49a



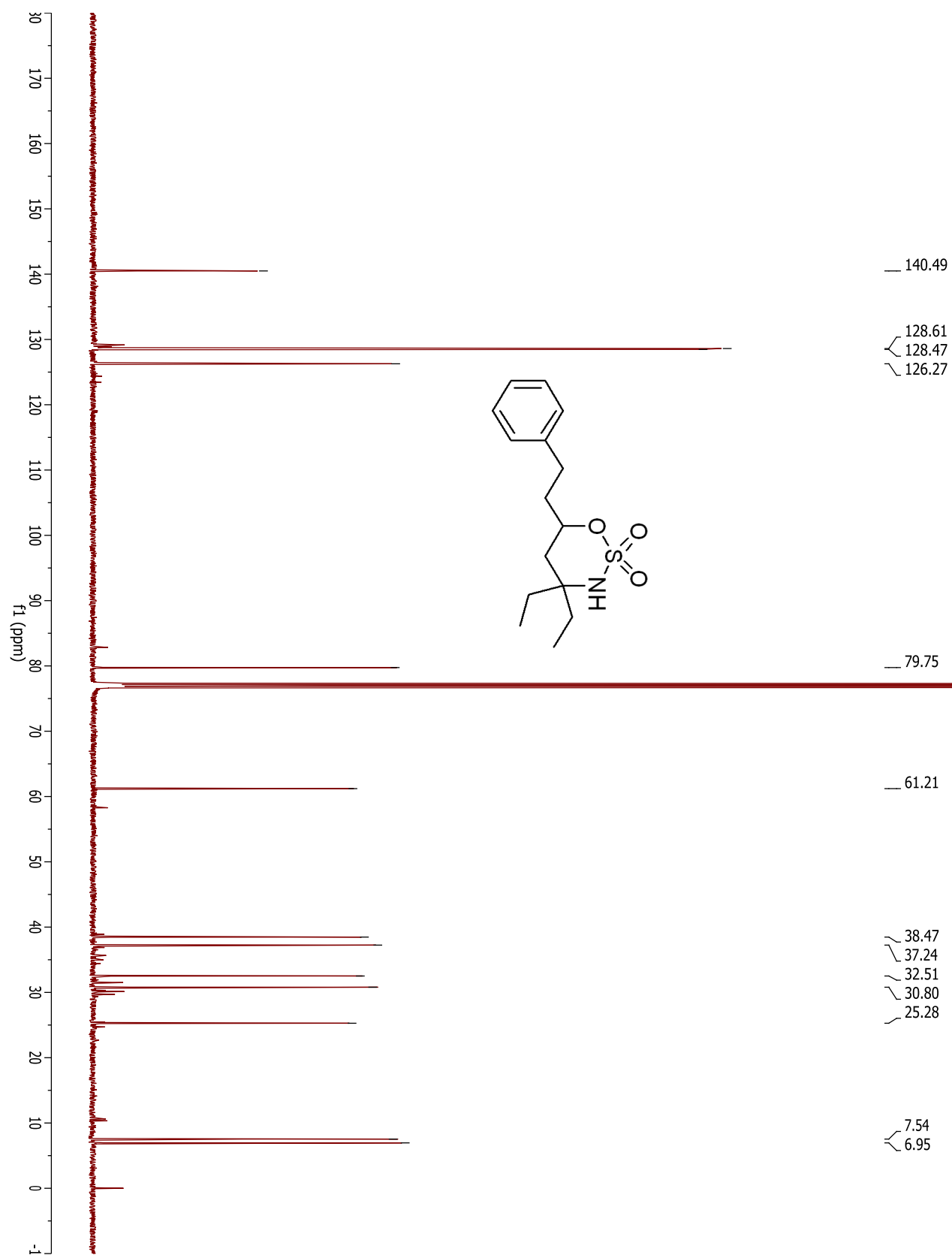
## Compound 3.49a



## Compound 3.49b



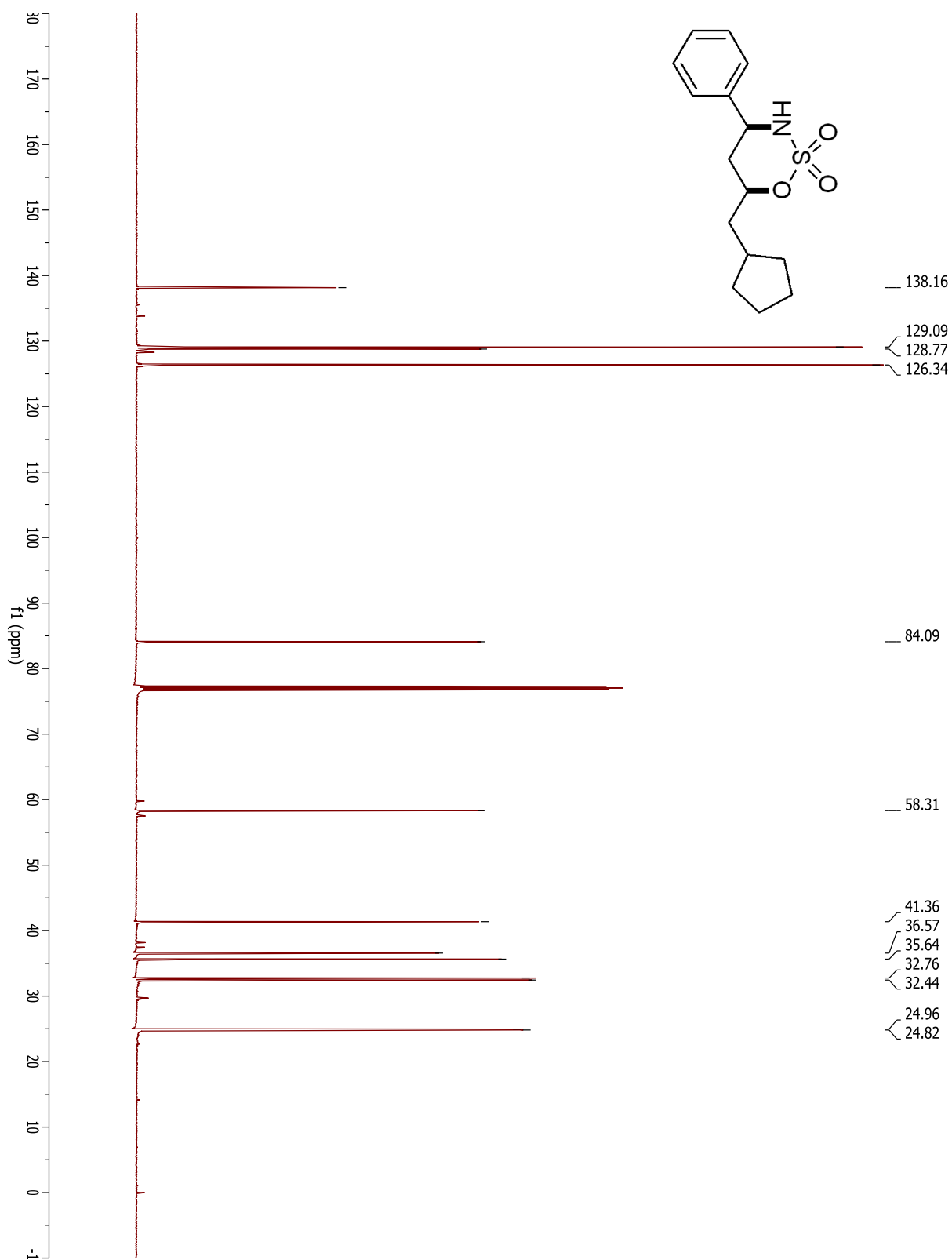
## Compound 3.49b



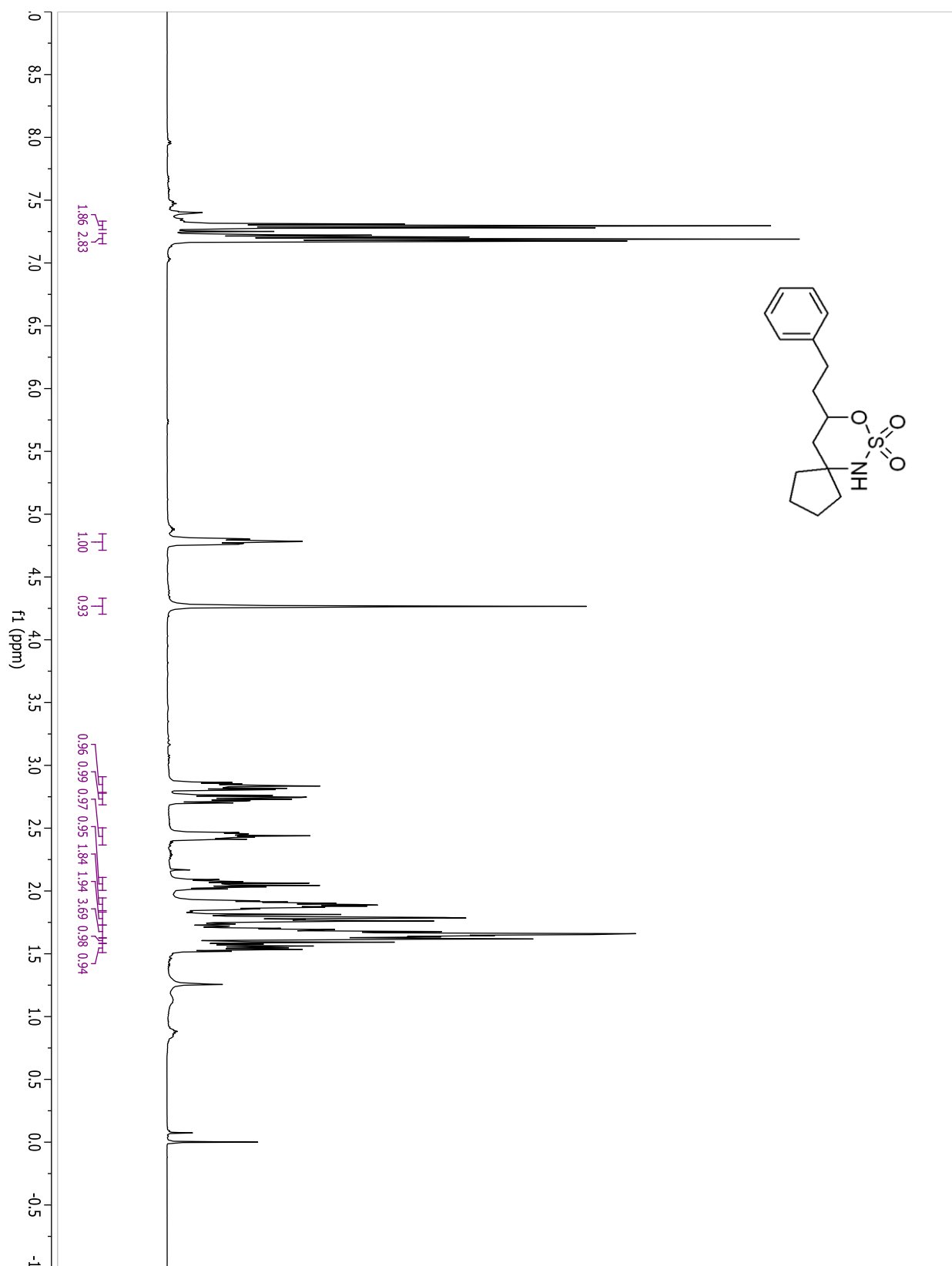




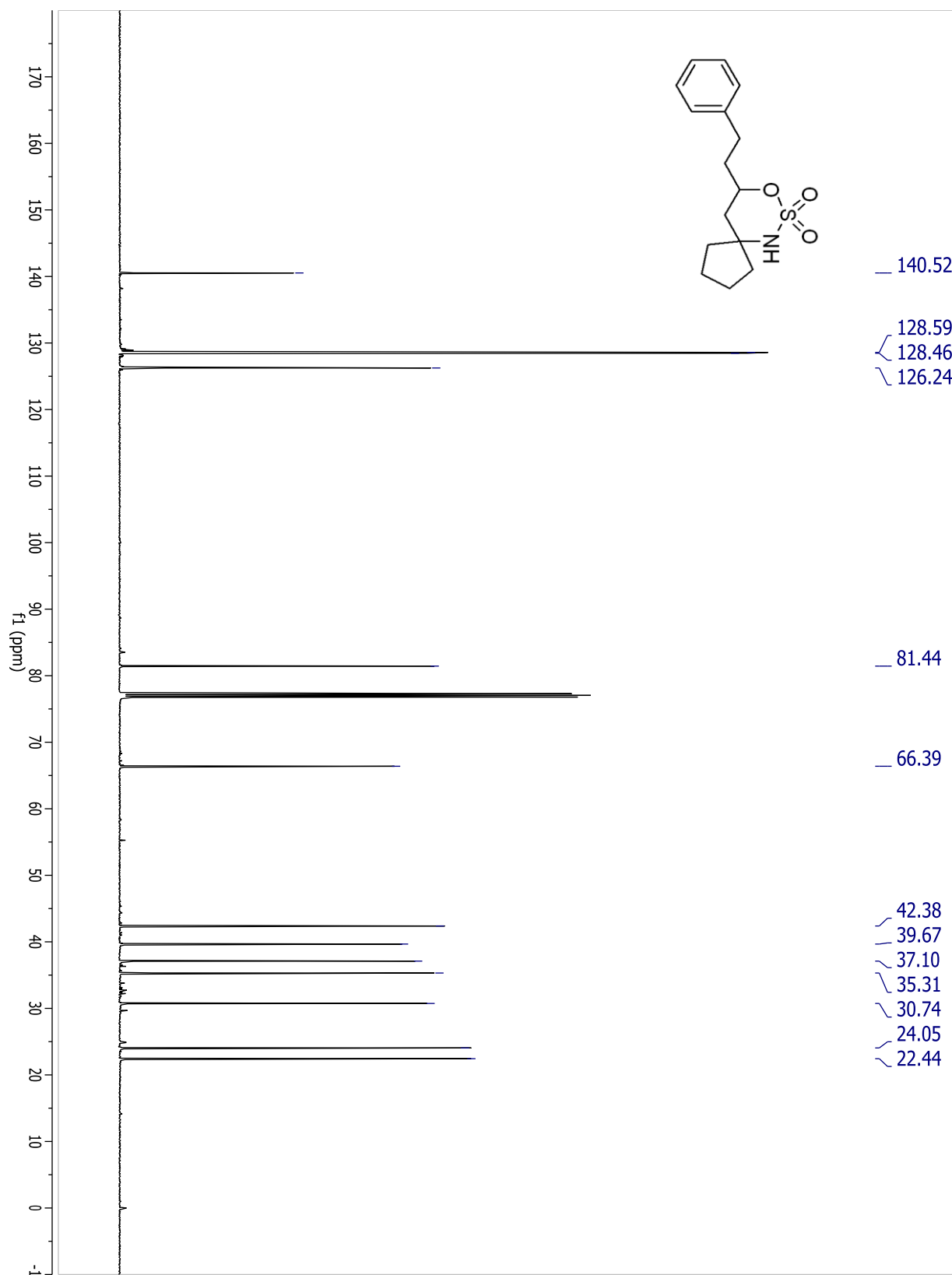
## Compound 3.50a



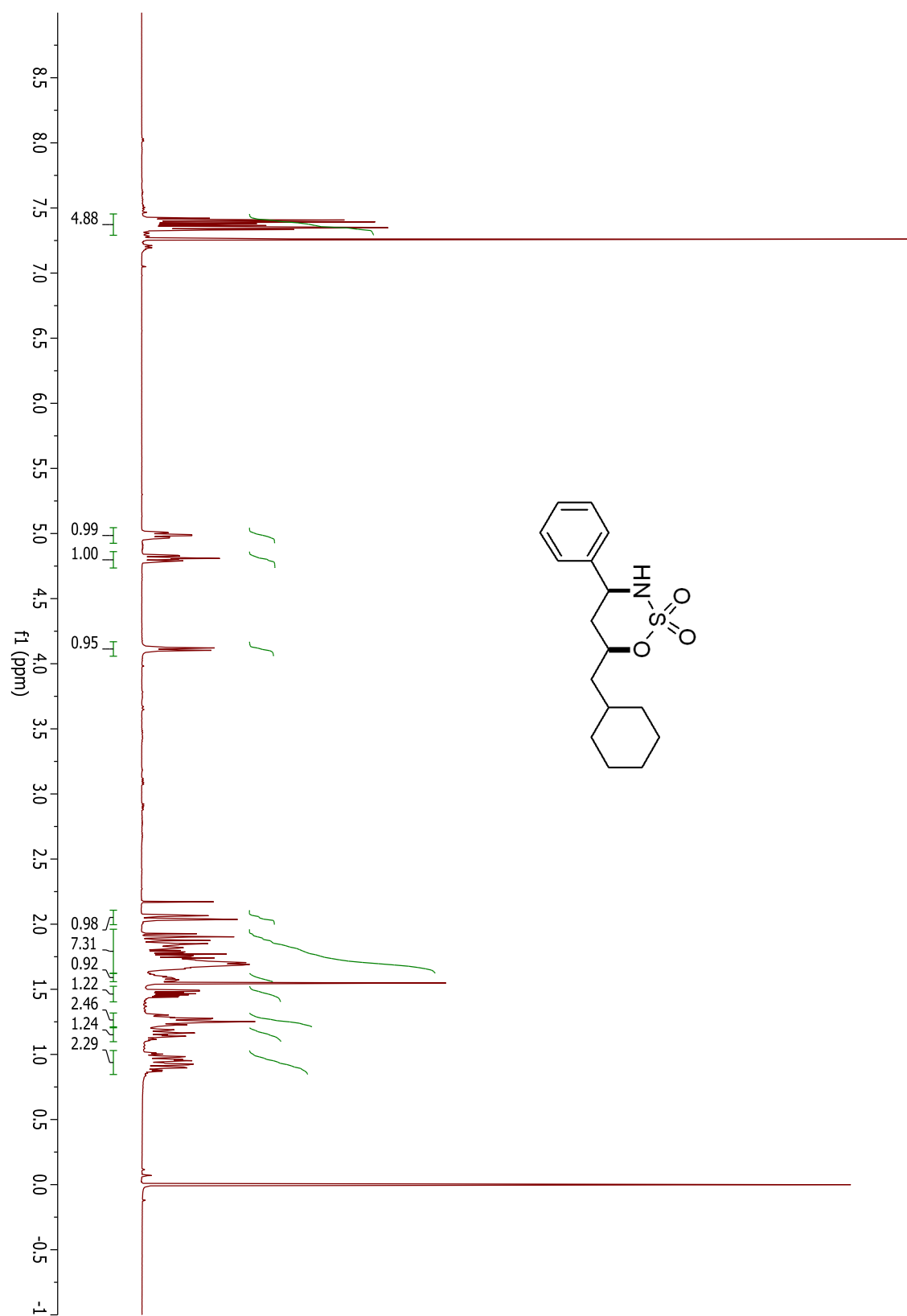
## Compound 3.50b



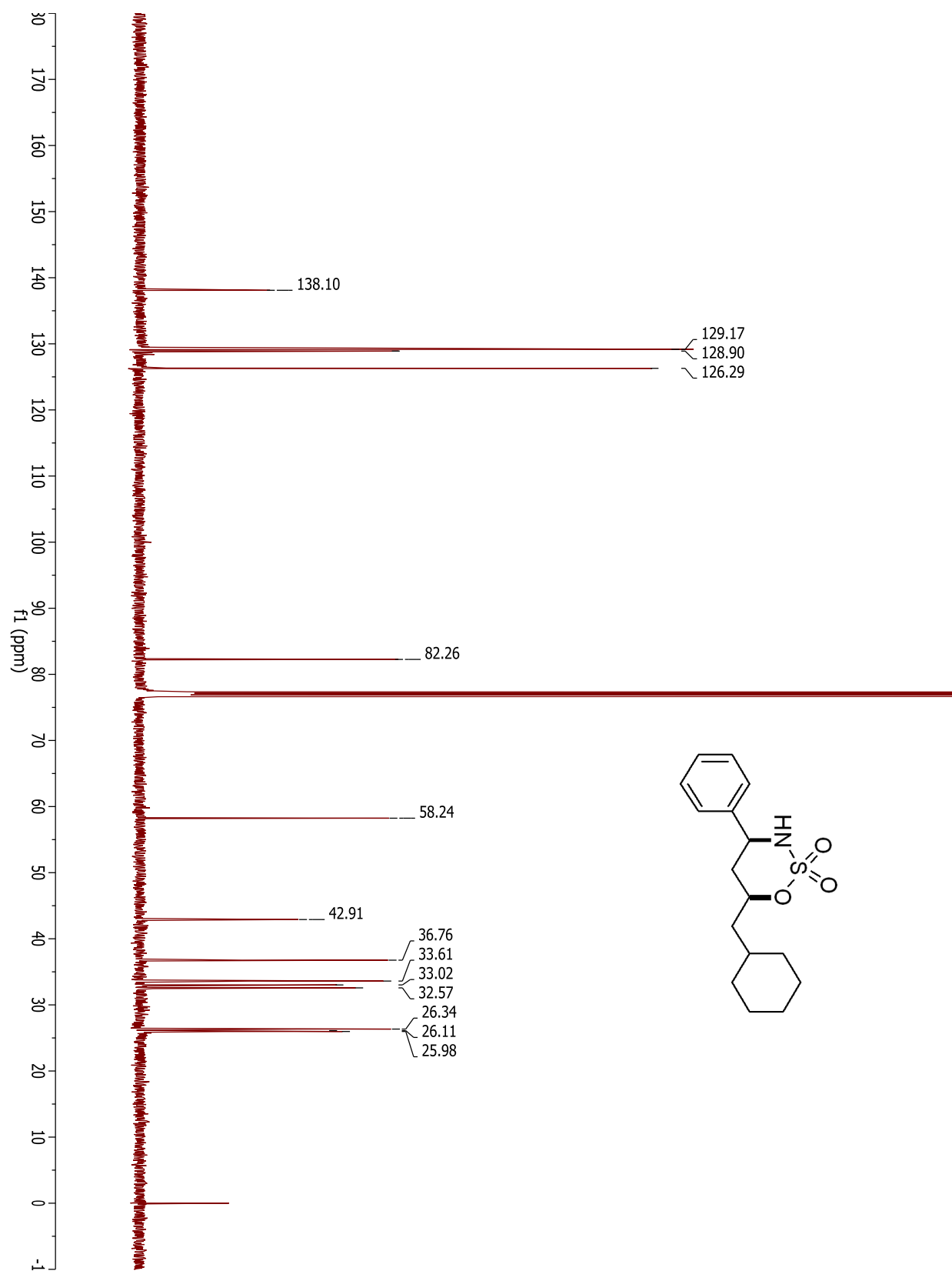
## Compound 3.50b



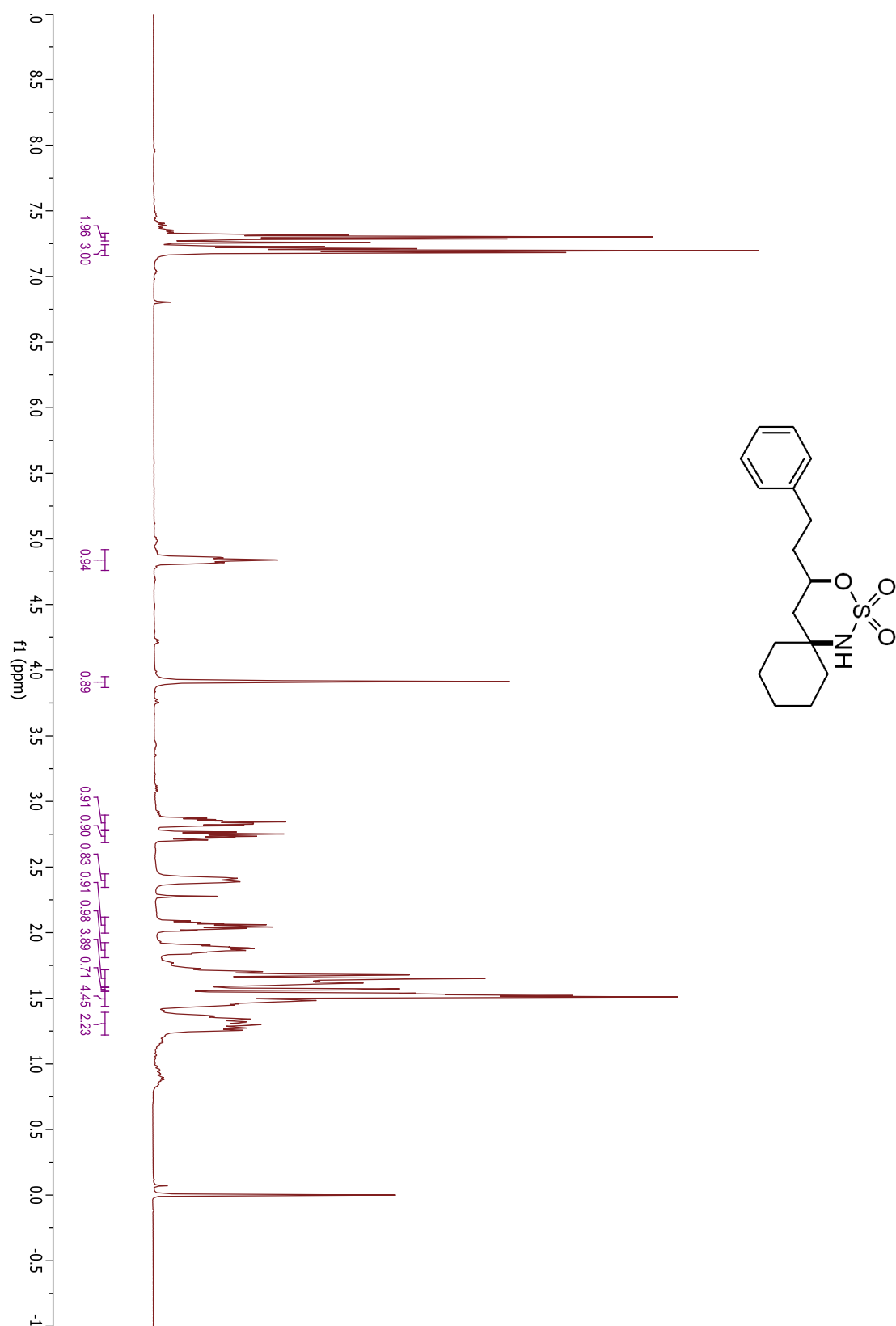
## Compound 3.51a



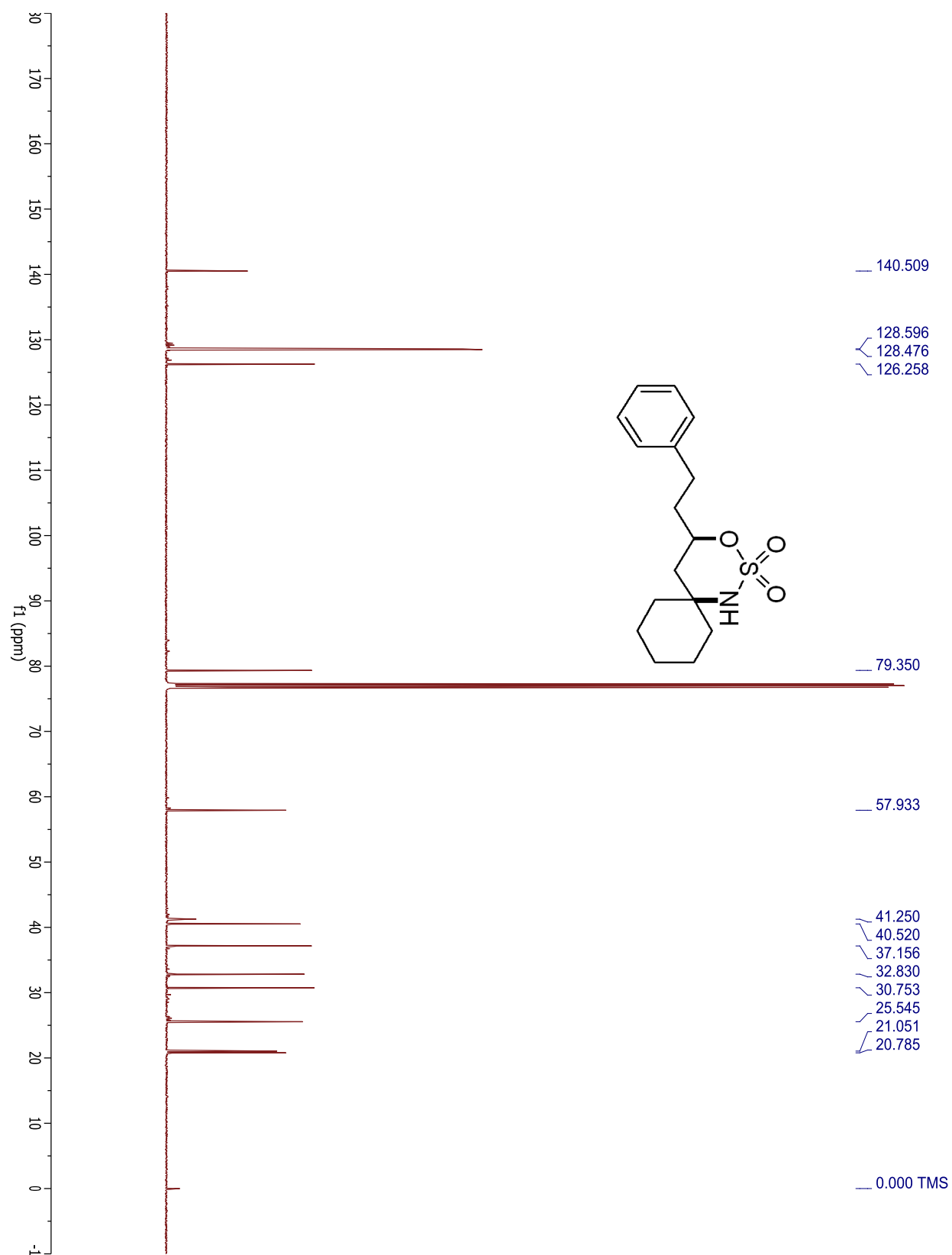
## Compound 3.51a



## Compound 3.51b

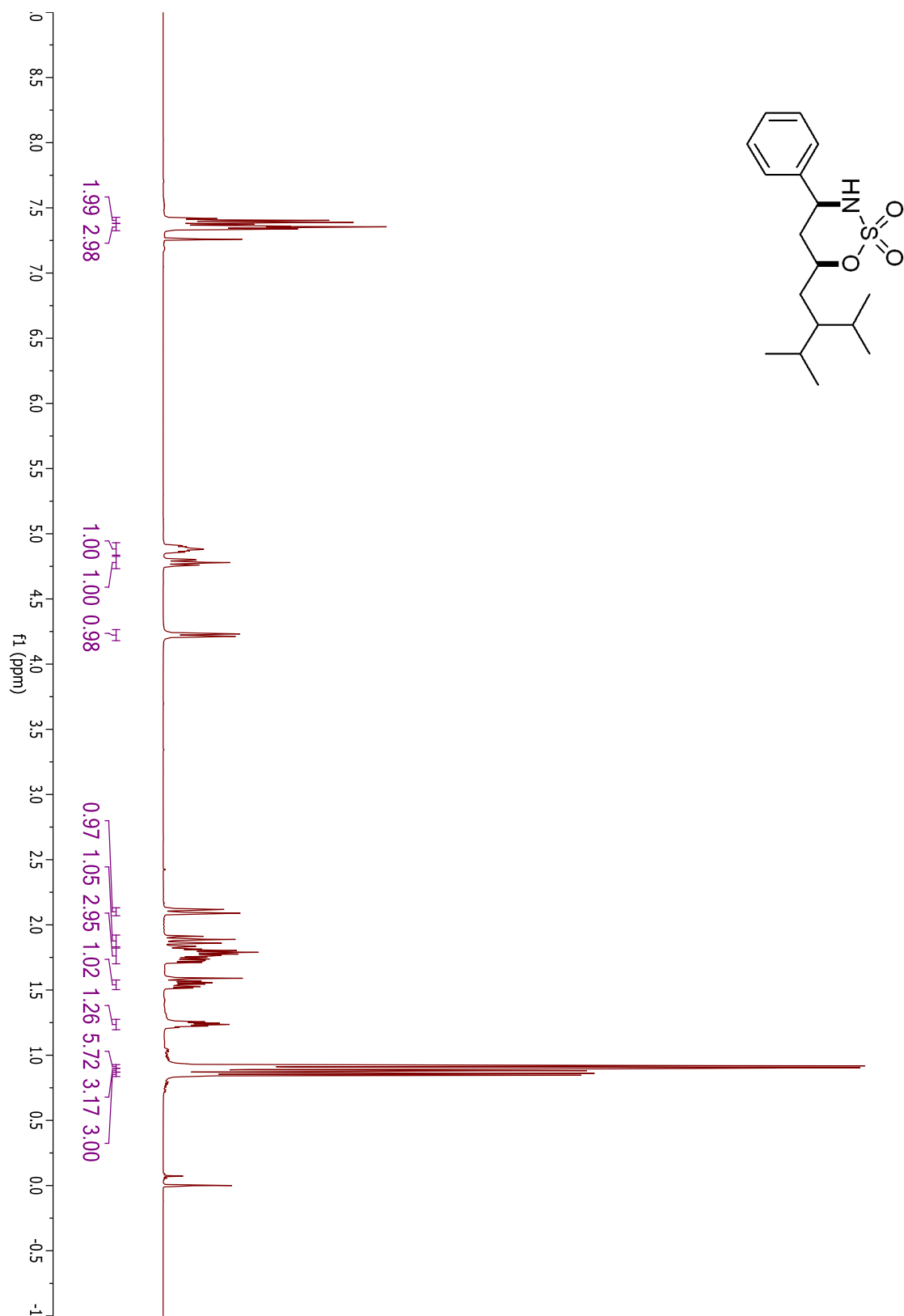


## Compound 3.51b

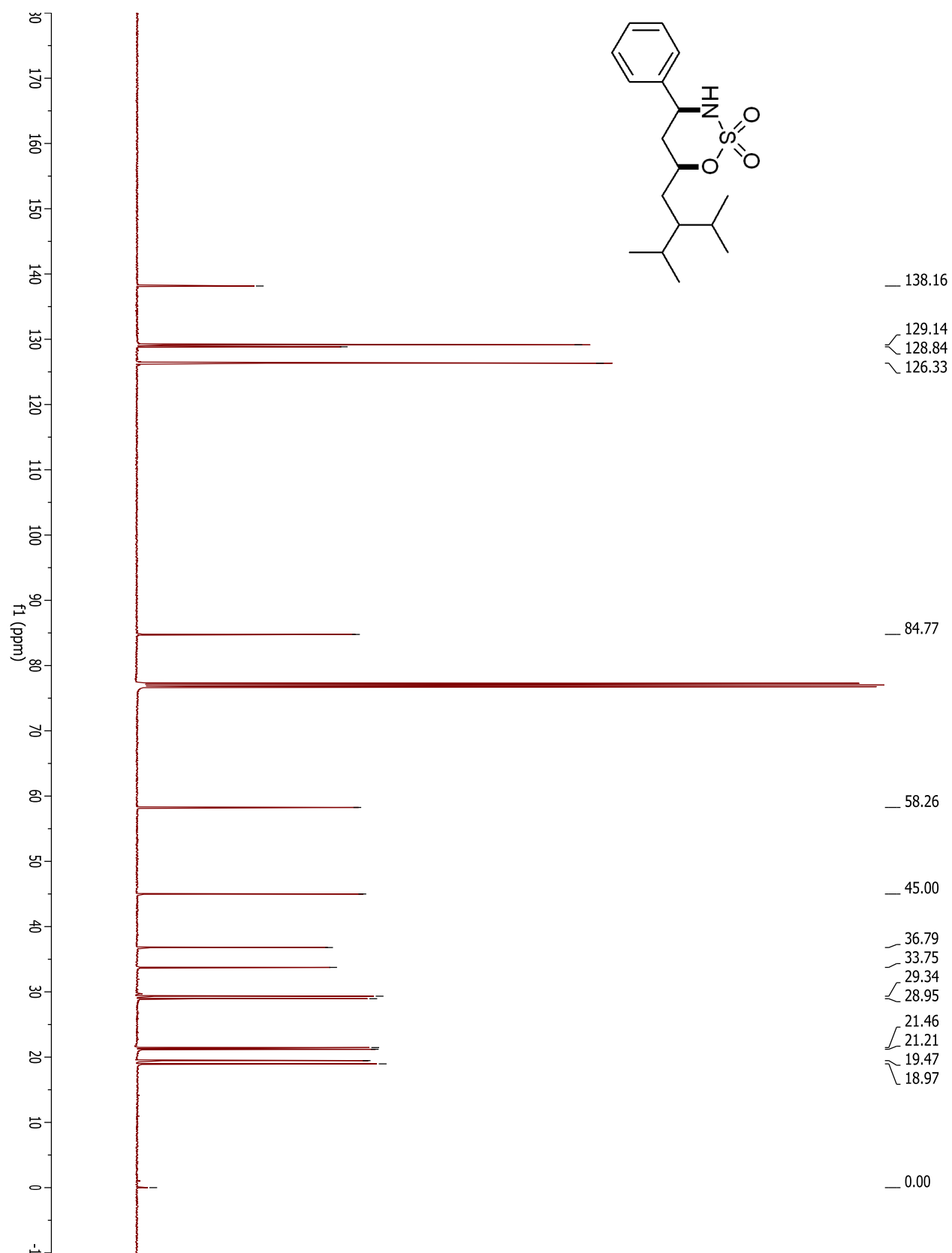


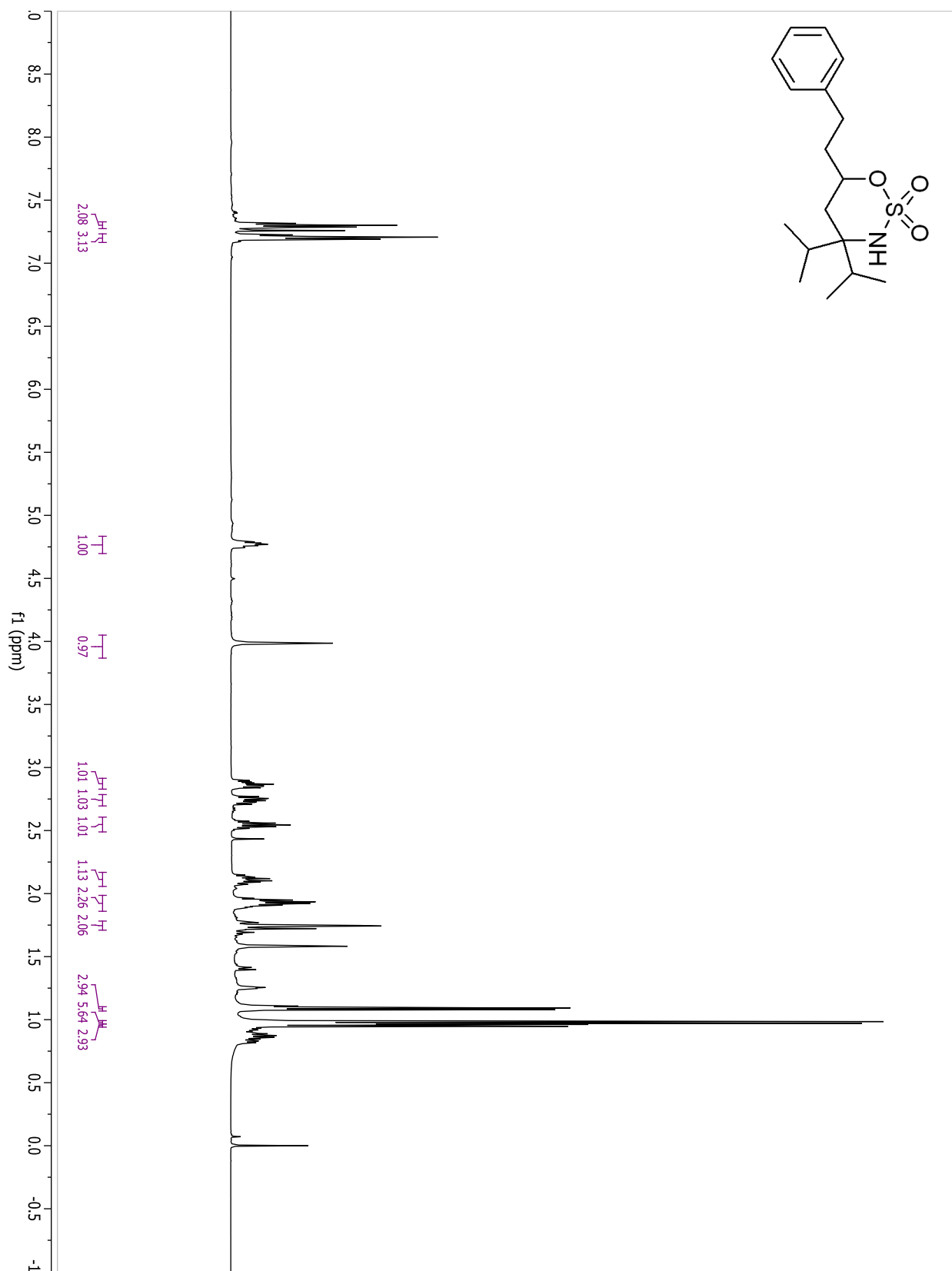


## Compound 3.52a

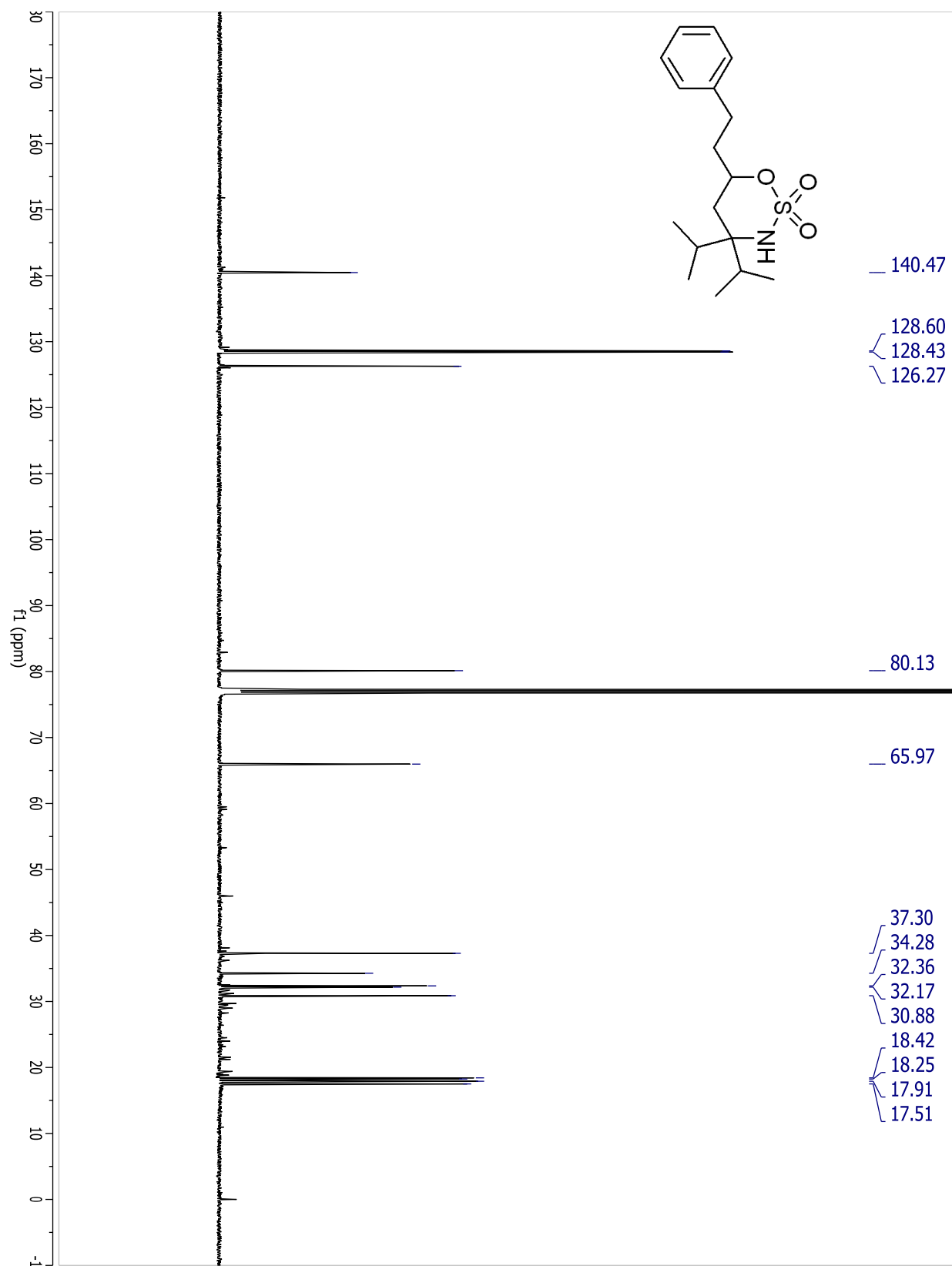


## Compound 3.52a

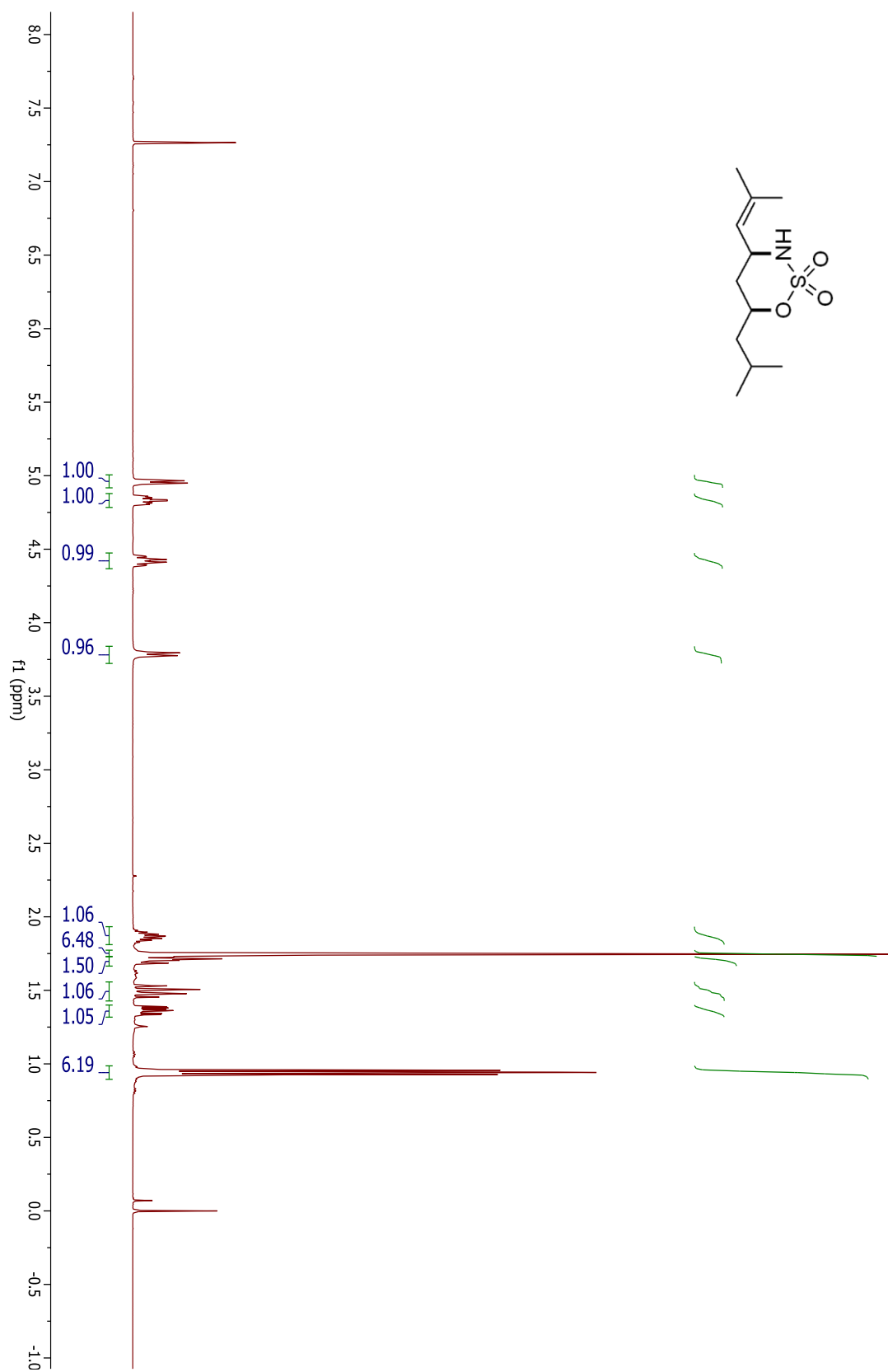




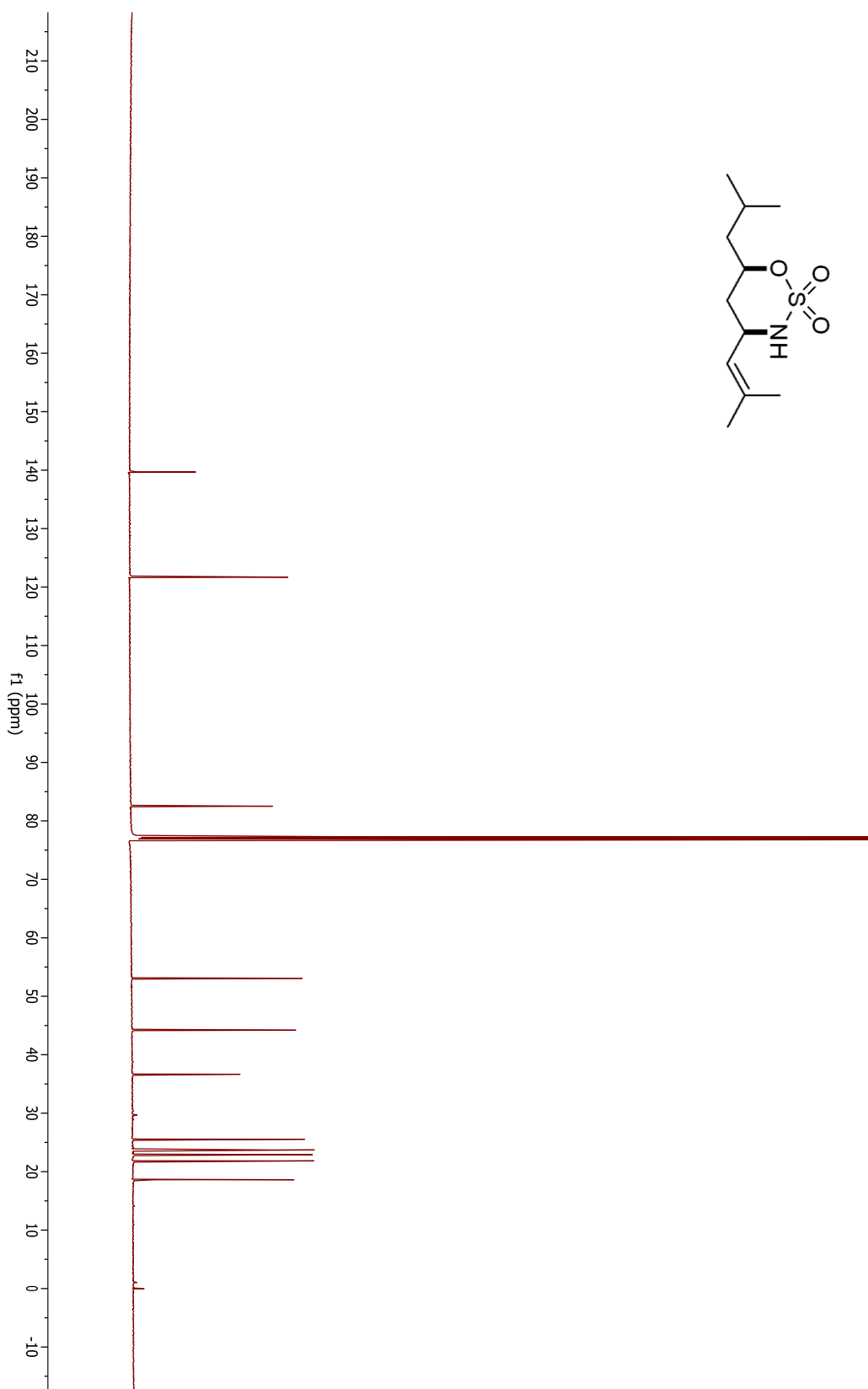
## Compound 3.52b



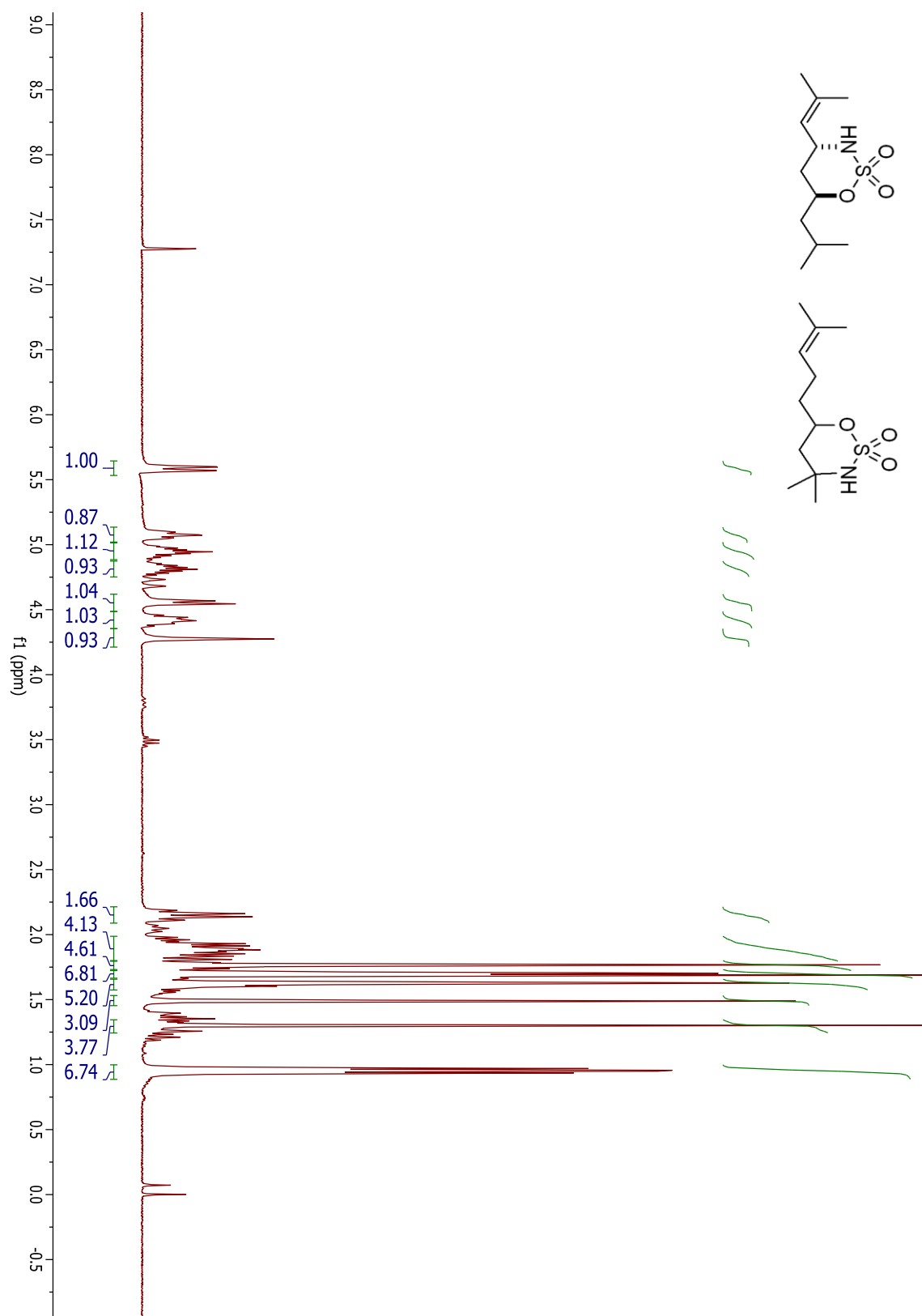
## Compound 3.53a



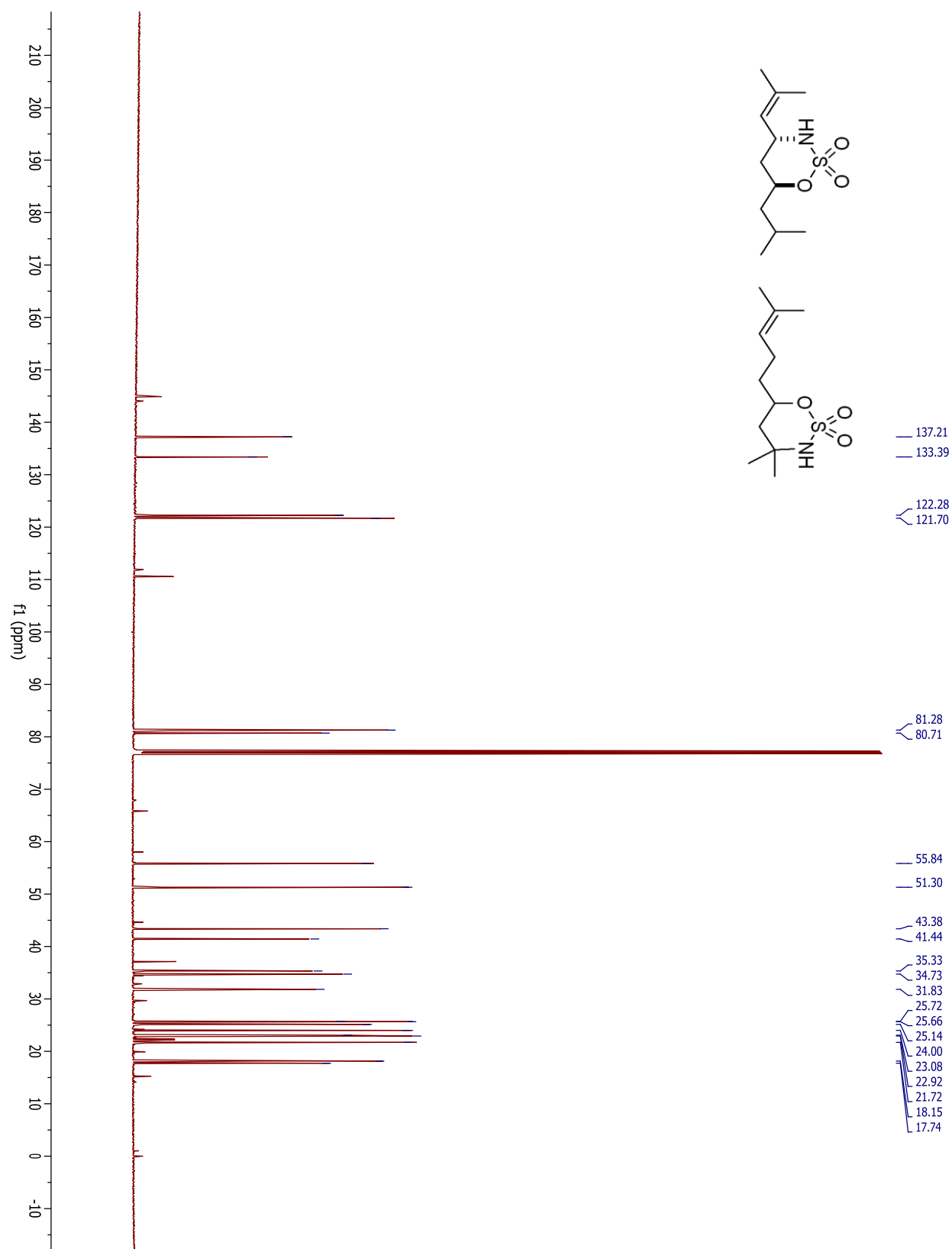
## Compound 3.53a



## Compound 3.53b



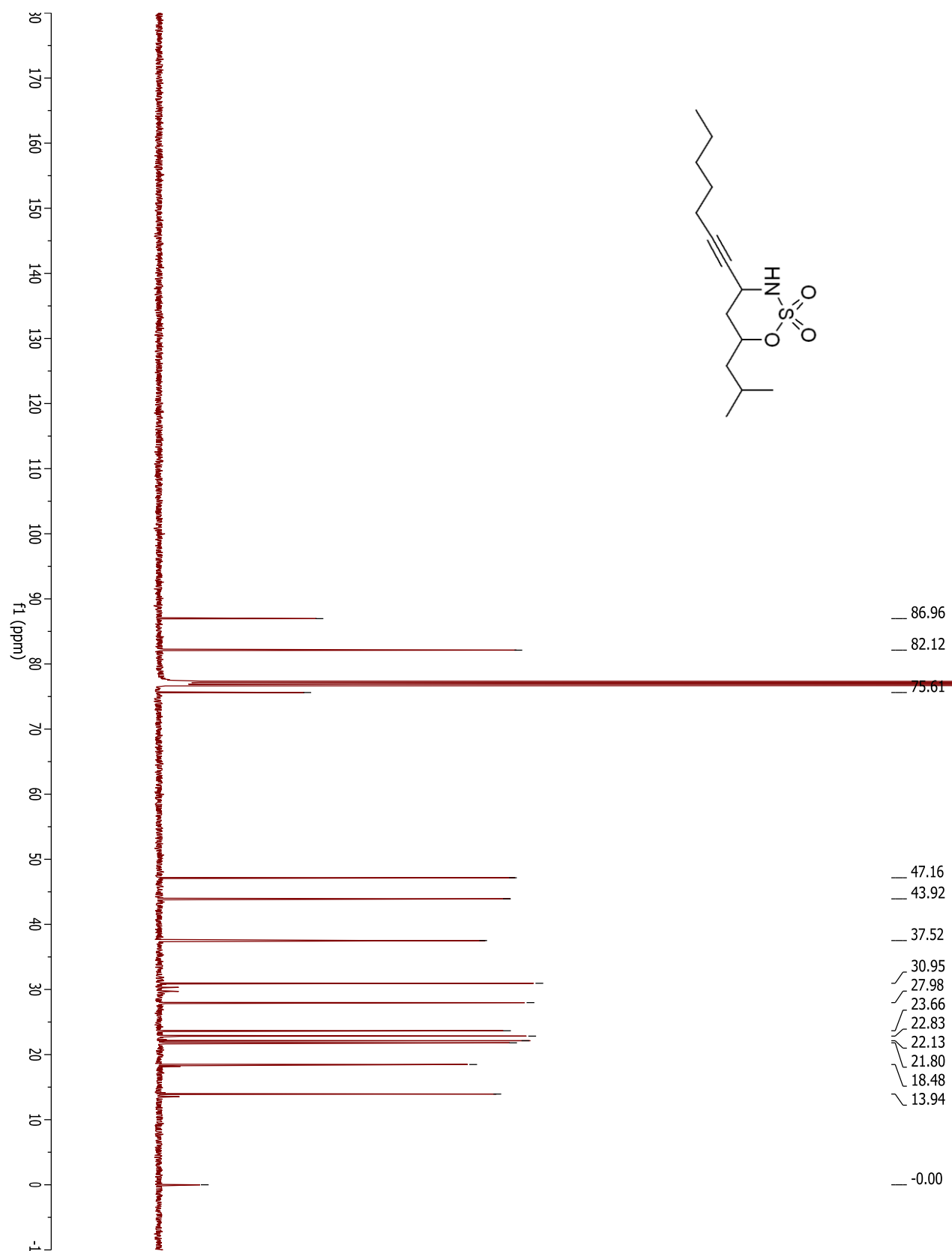
## Compound 3.53b



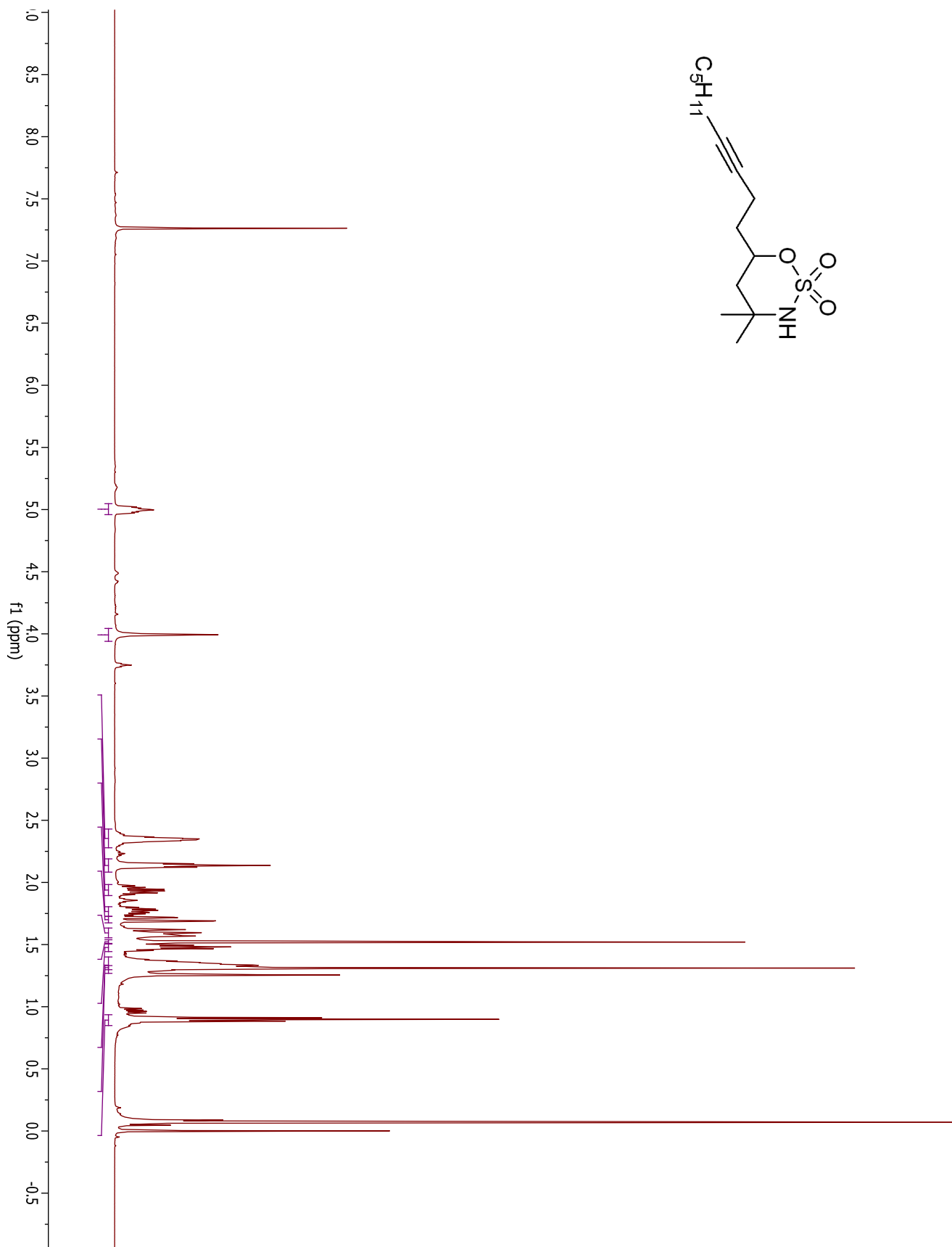
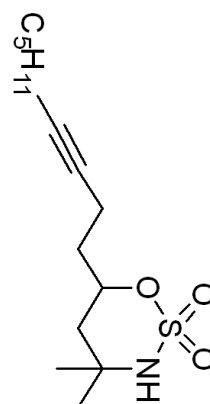




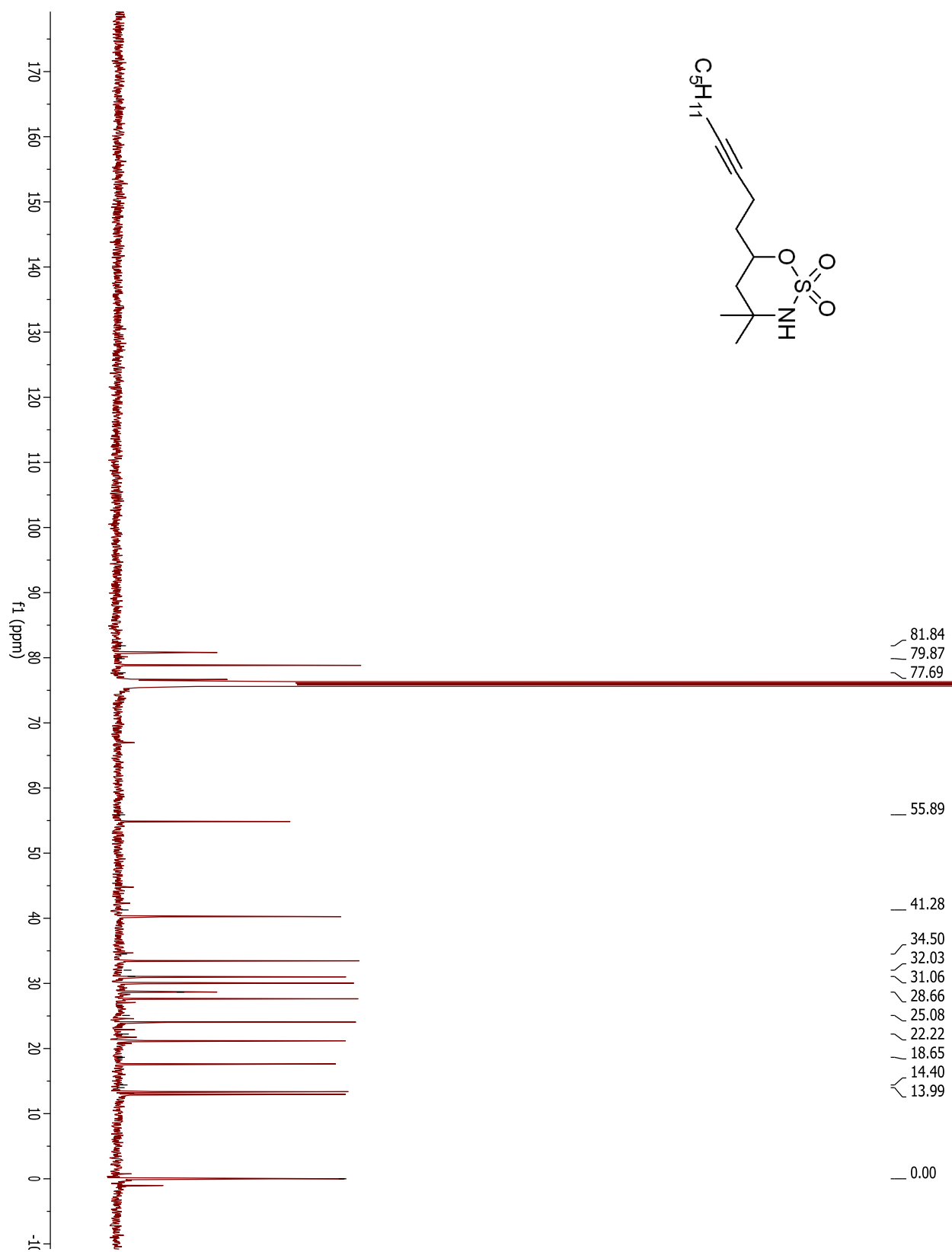
## Compound 3.54a



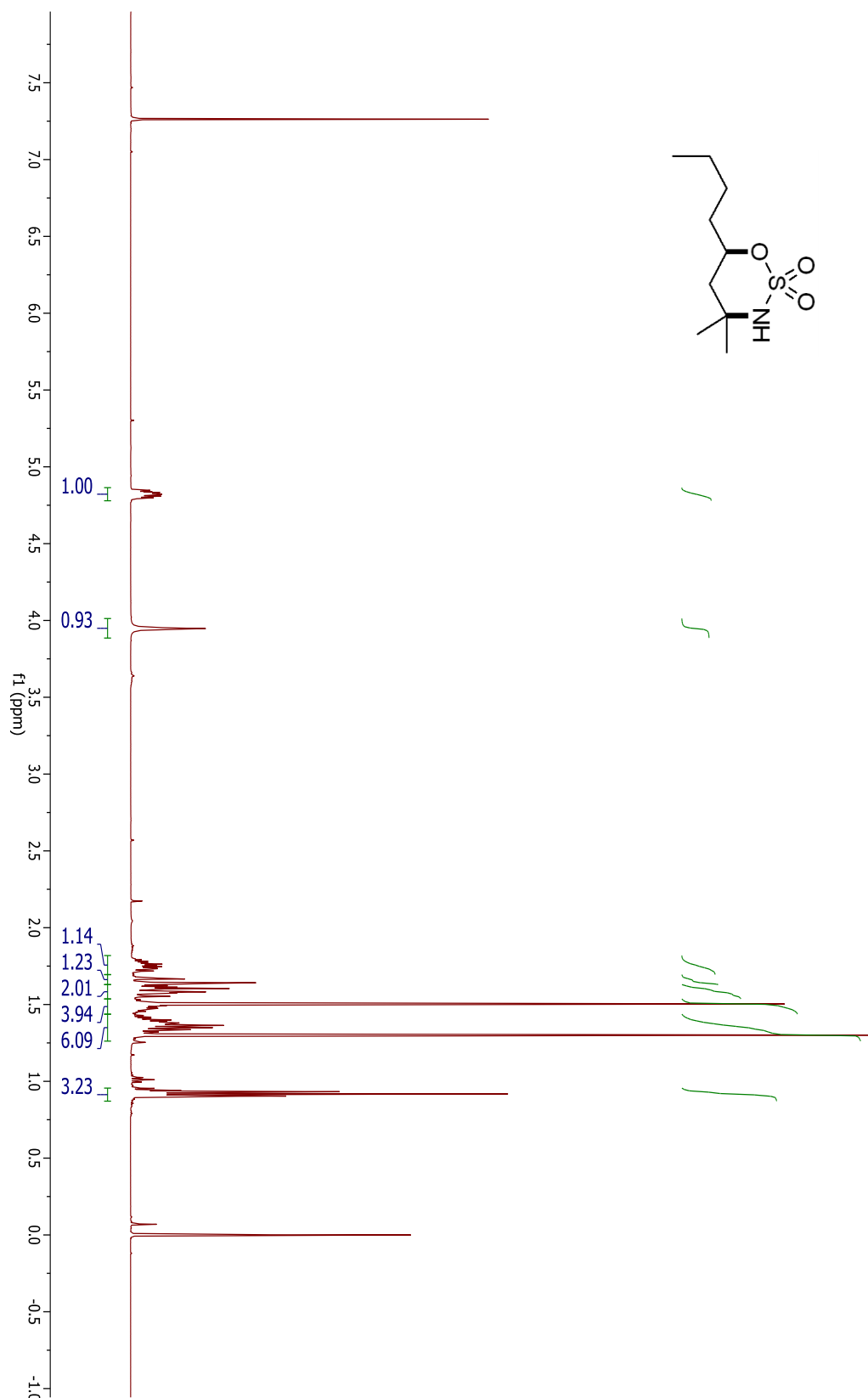
**Compound 3.54b**



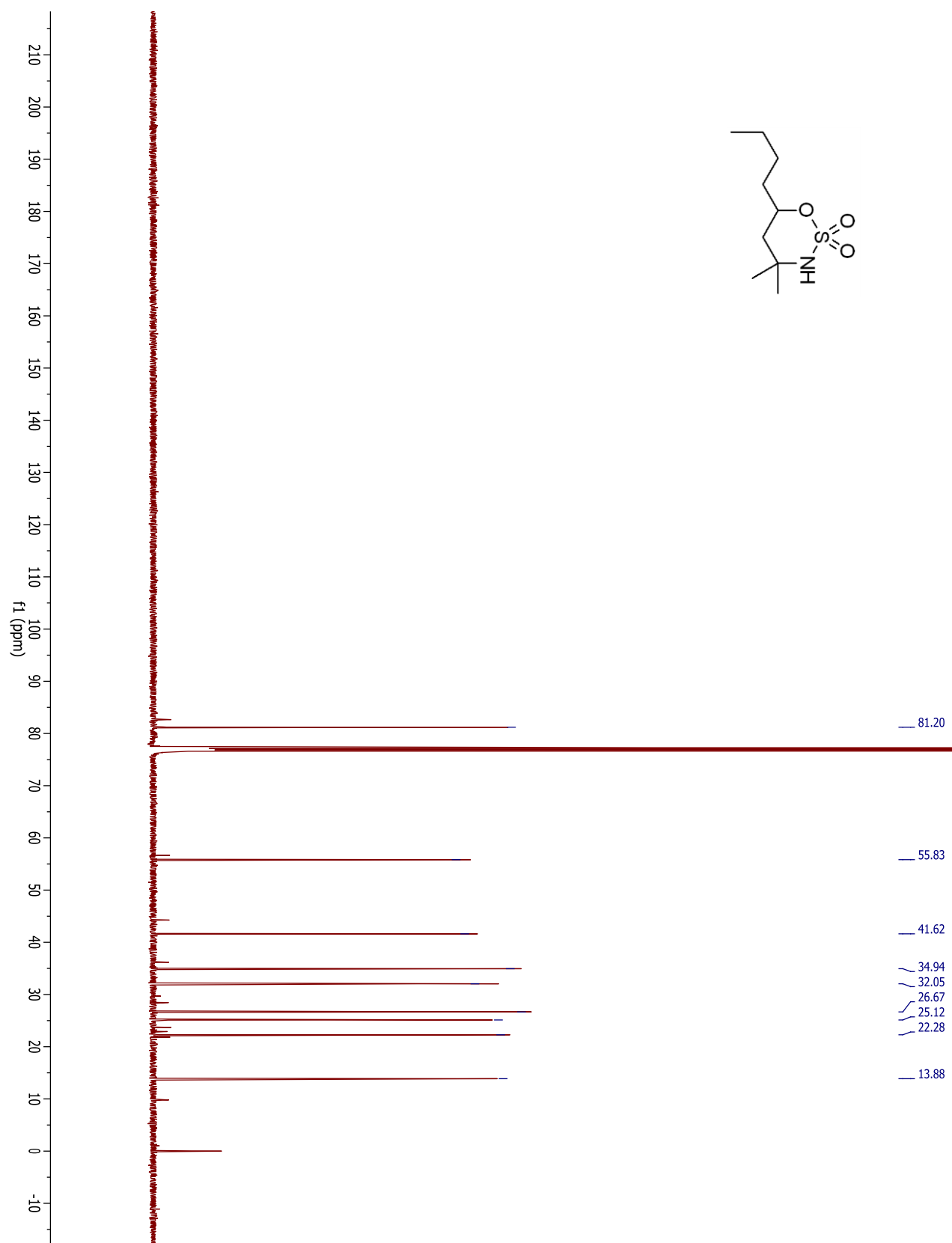
## Compound 3.54b



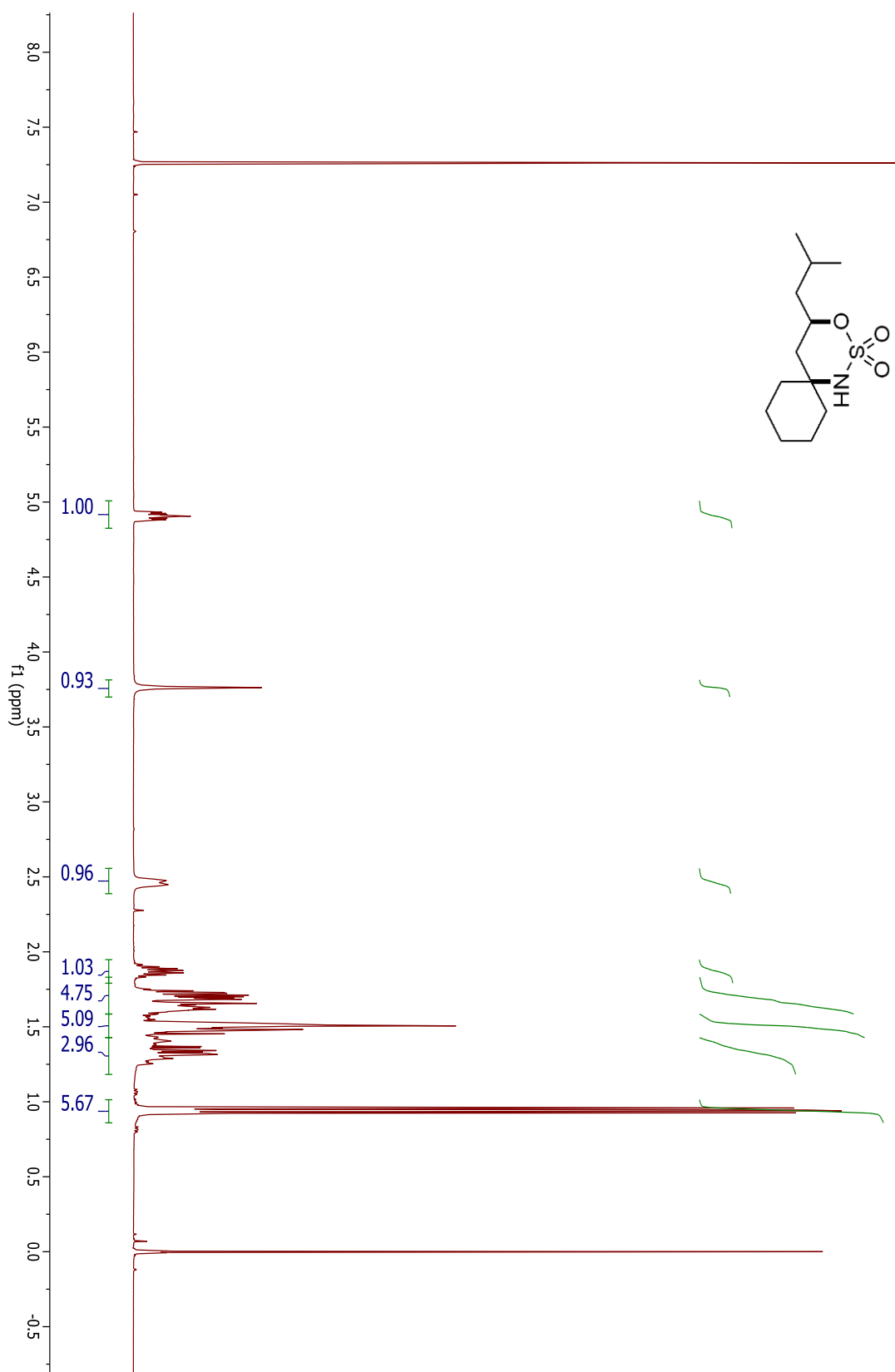
## Compound 3.23a



## Compound 3.23a

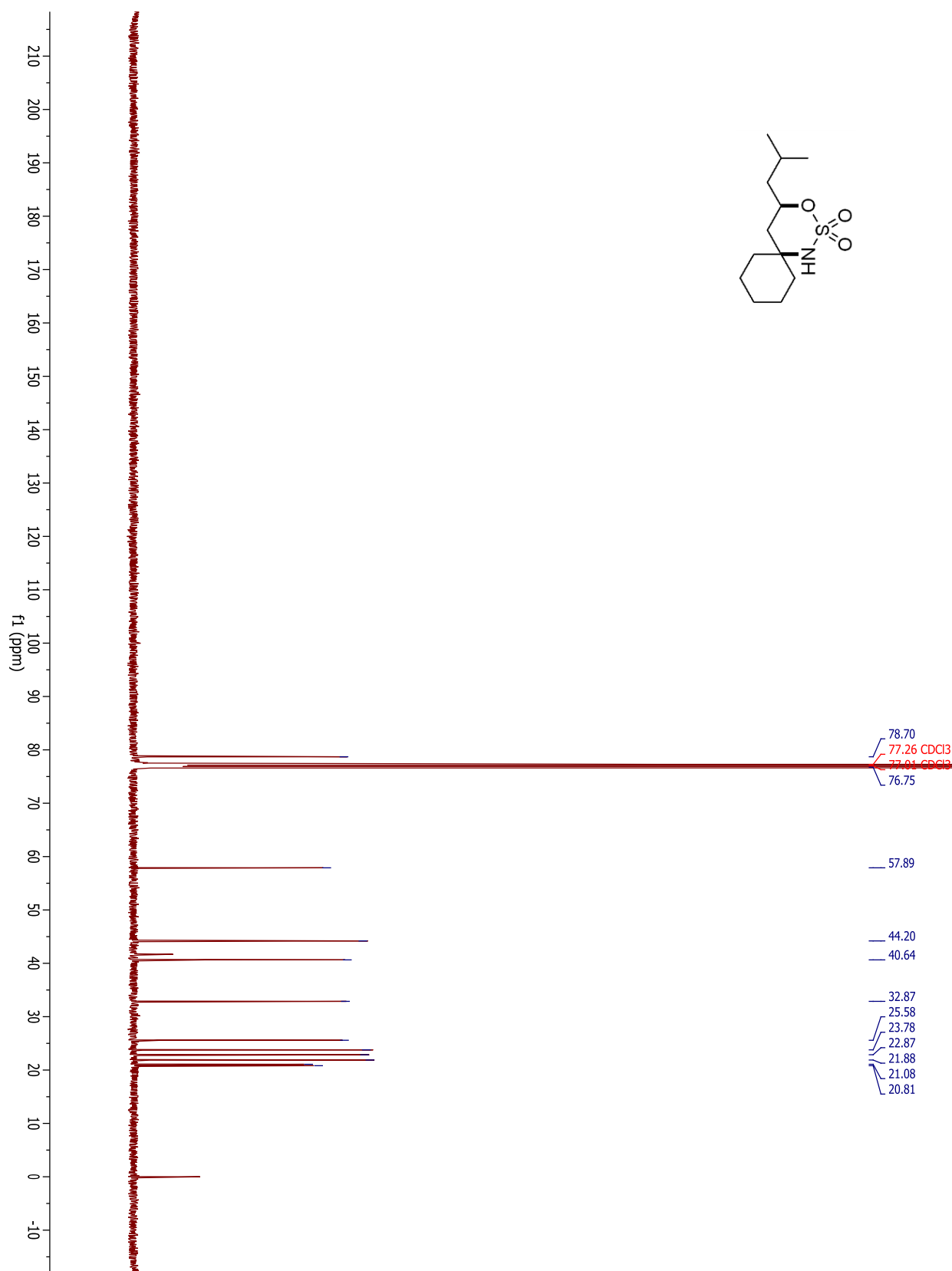


## Compound 3.7a

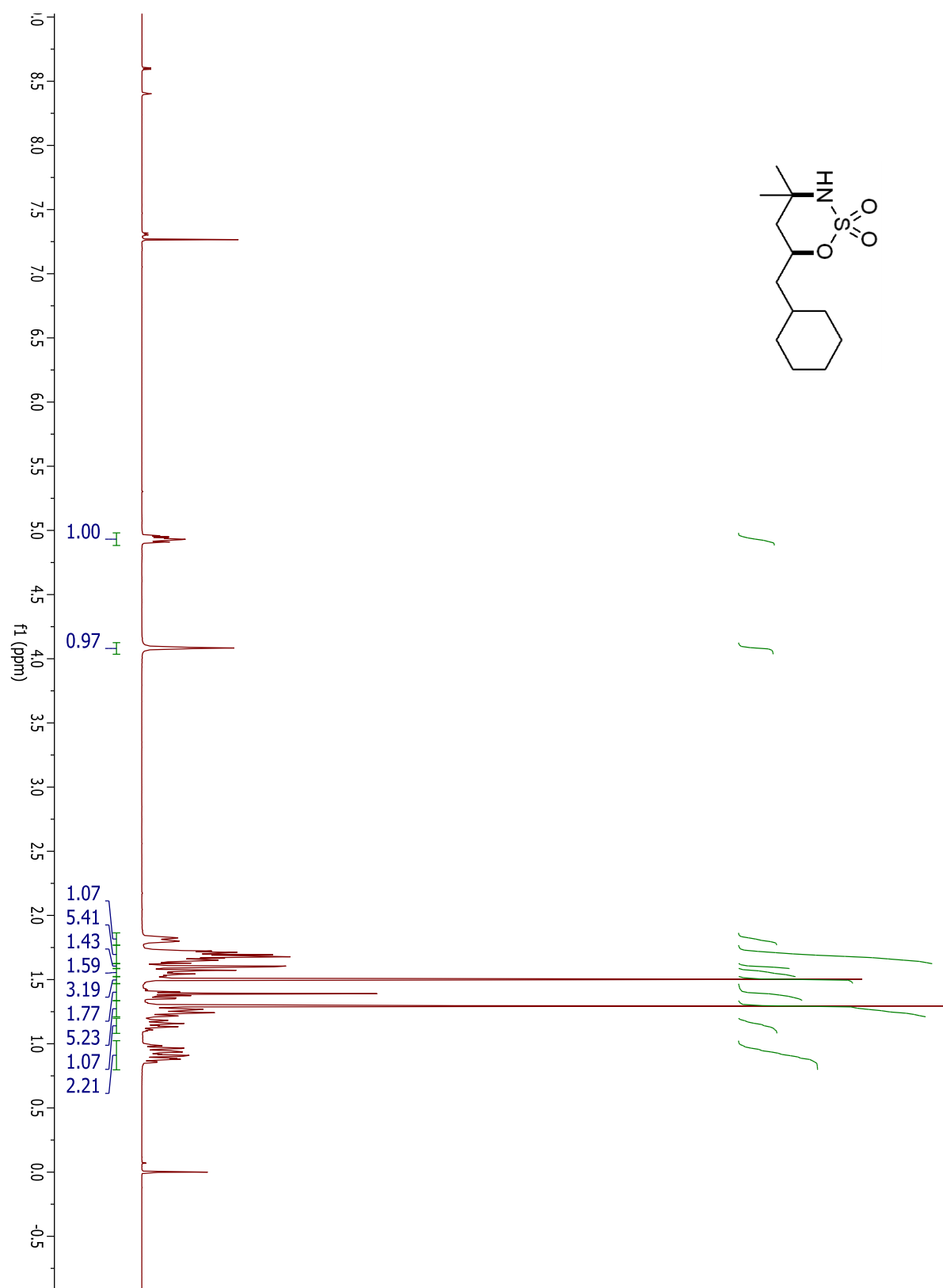




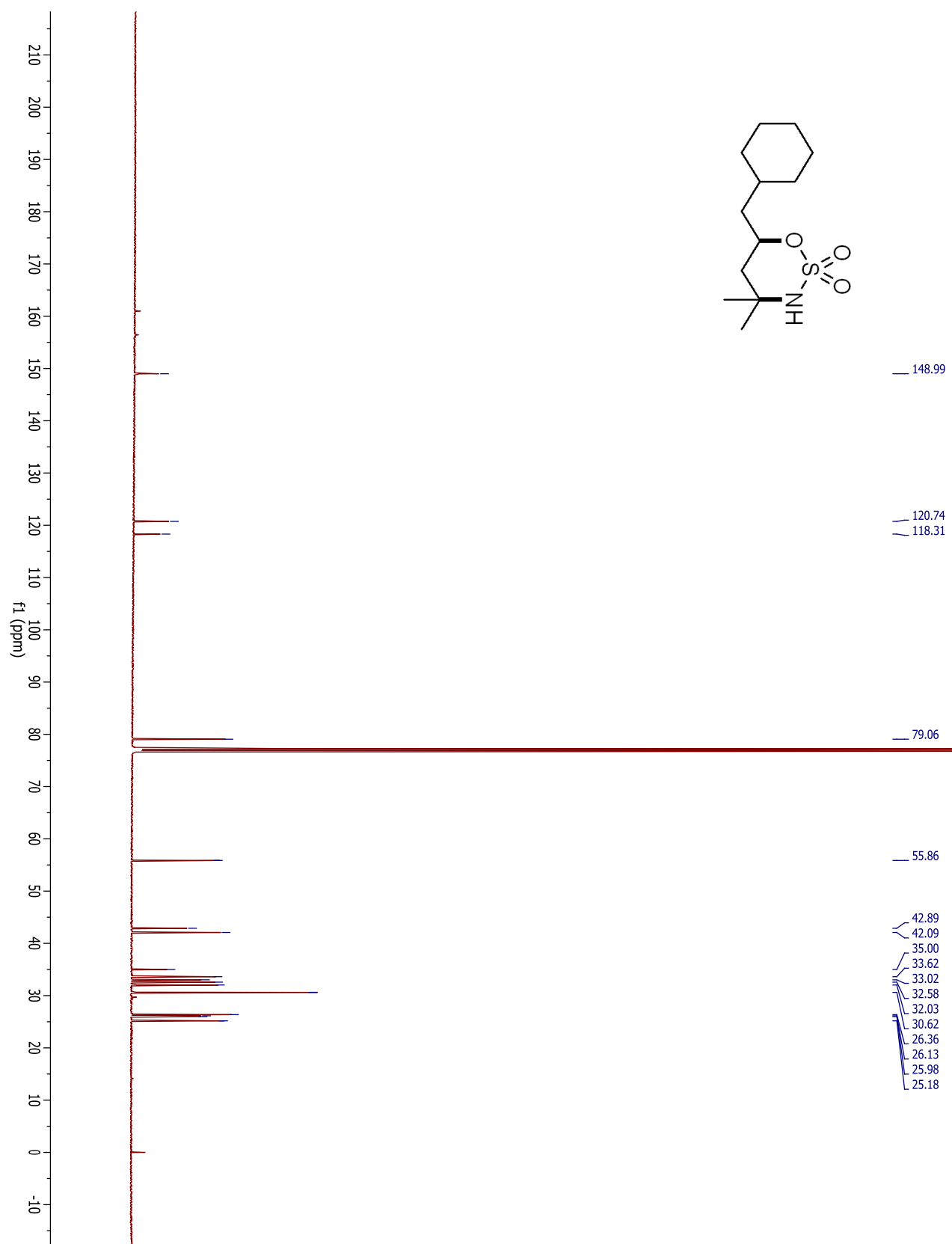
## Compound 3.7a



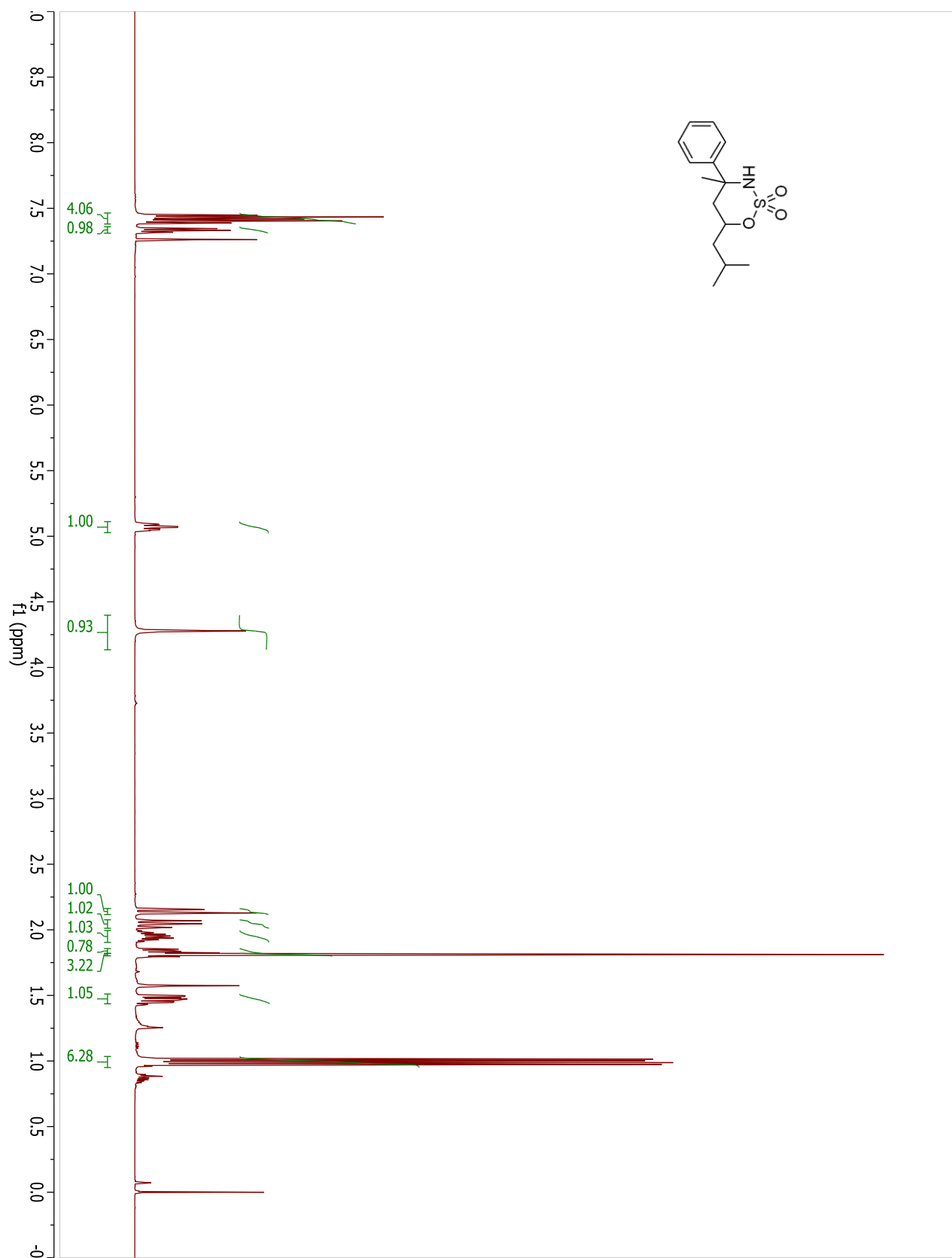
## Compound 3.7b



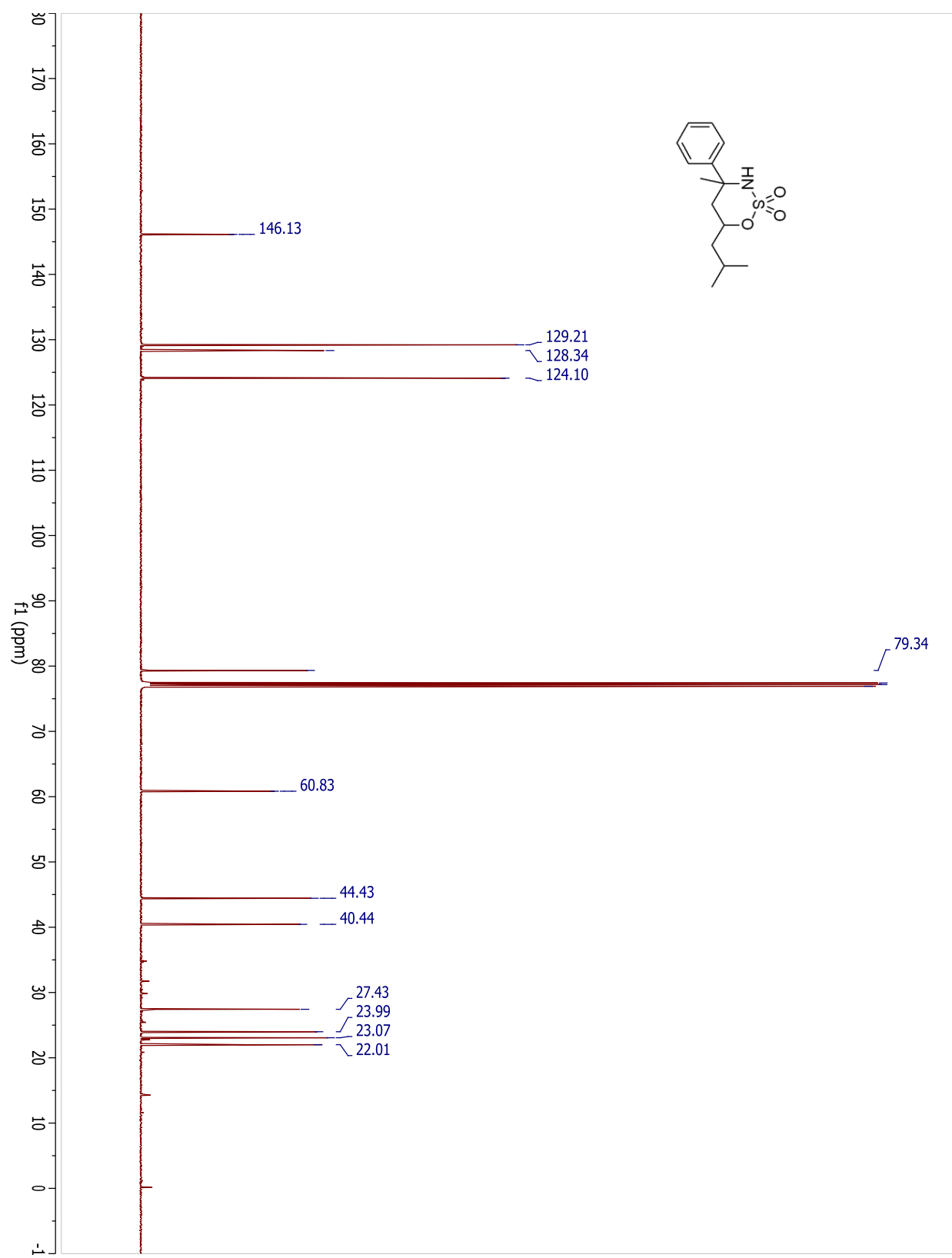
## Compound 3.7b



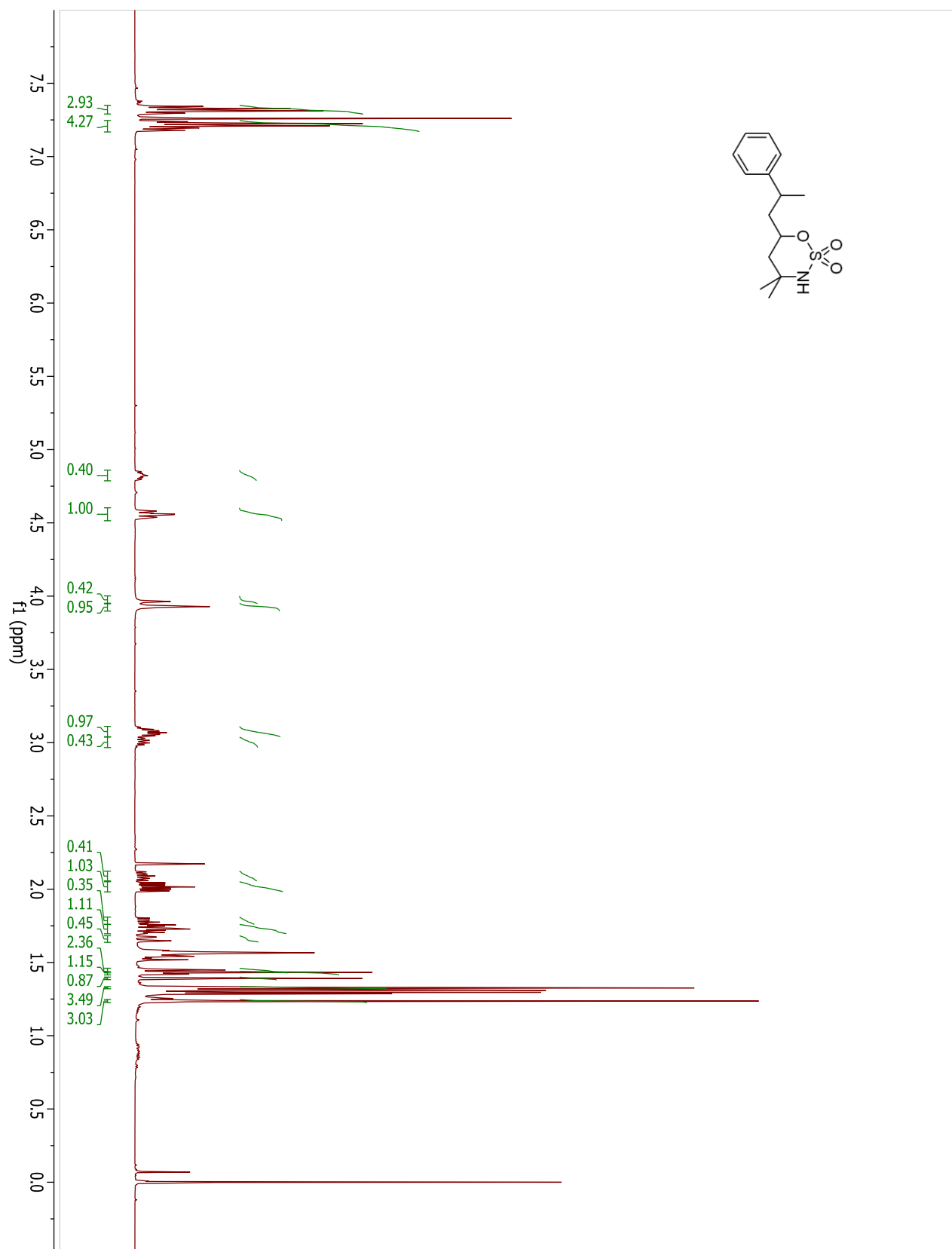
## Compound 3.55a



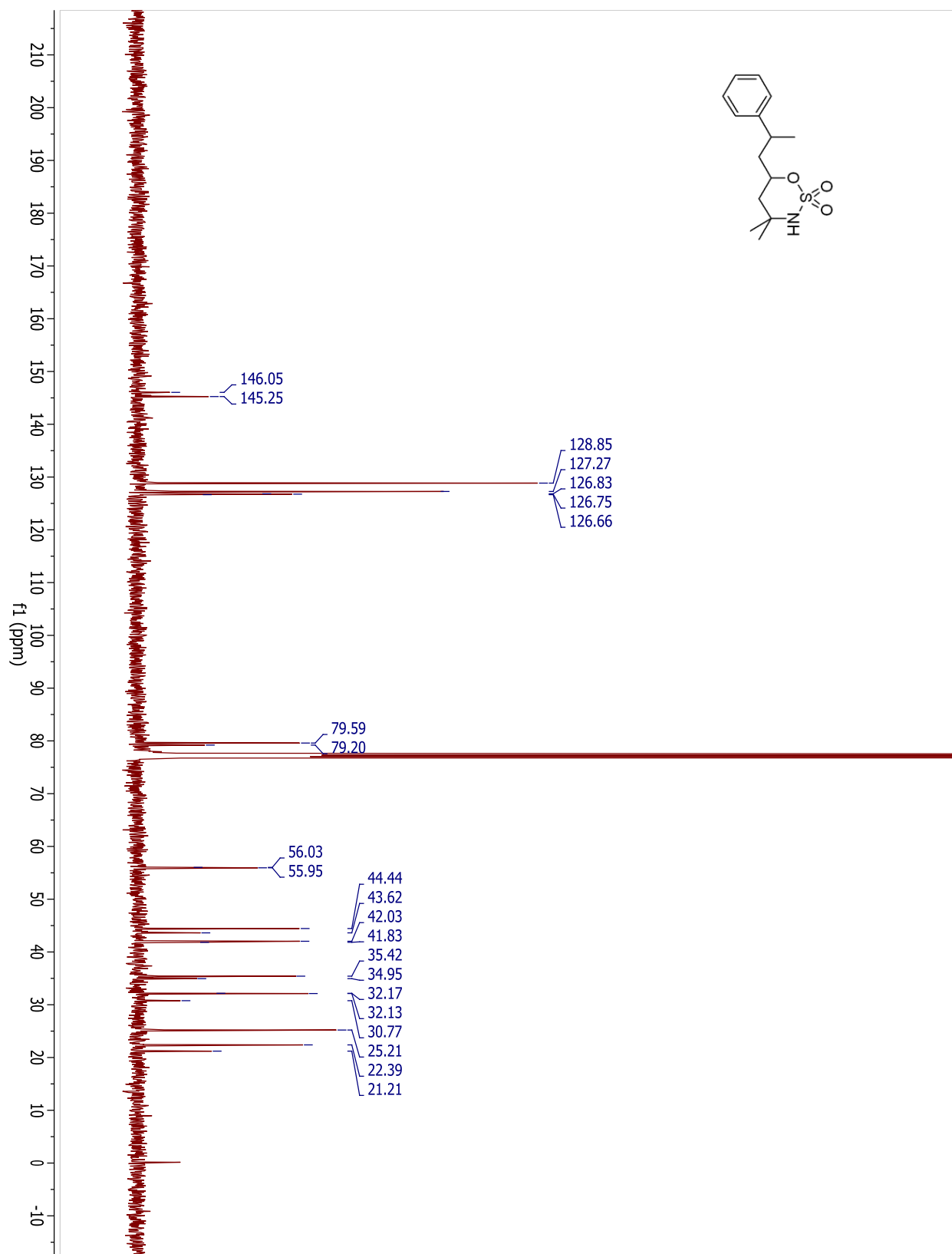
## Compound 3.55a



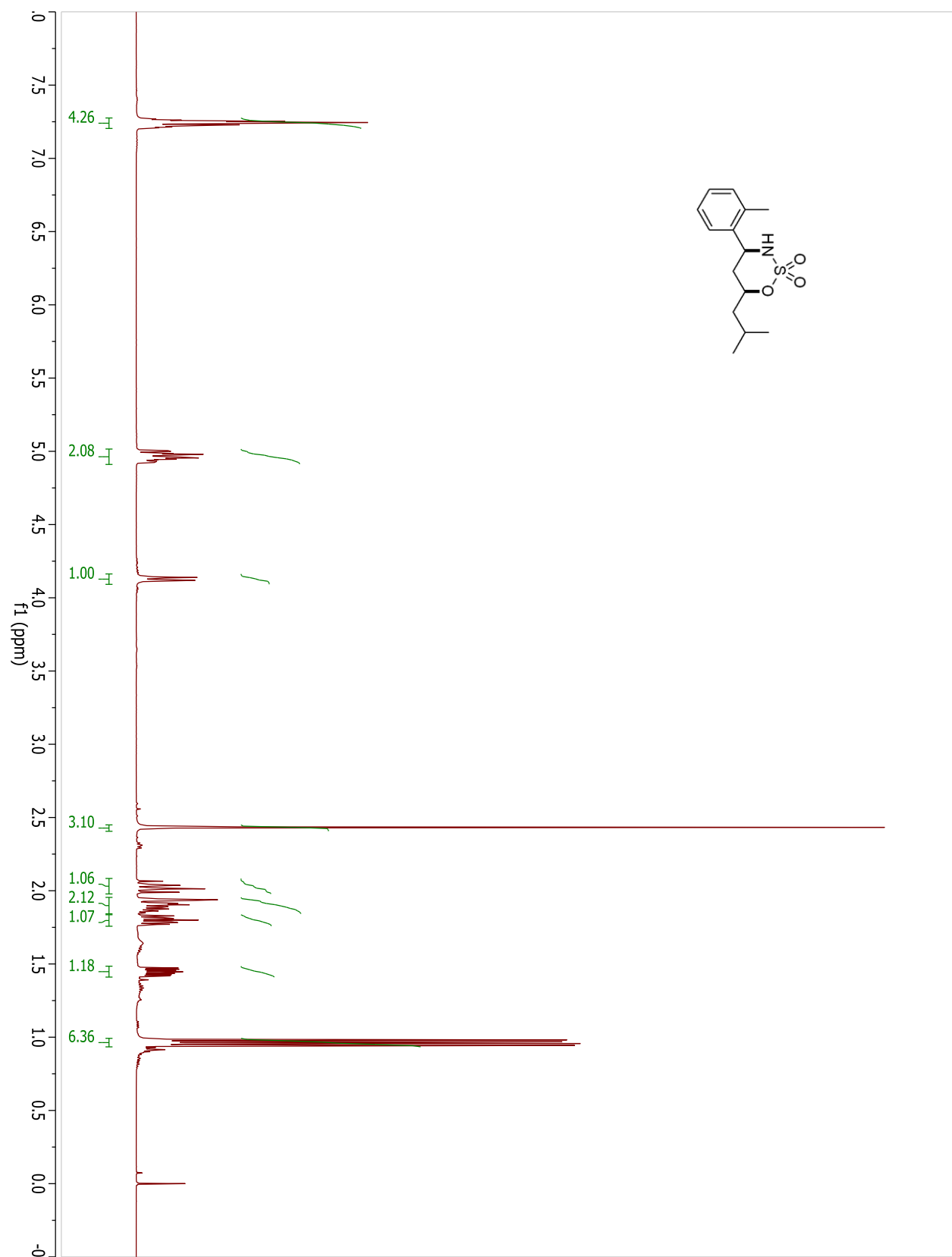
## Compound 3.55b



## Compound 3.55b

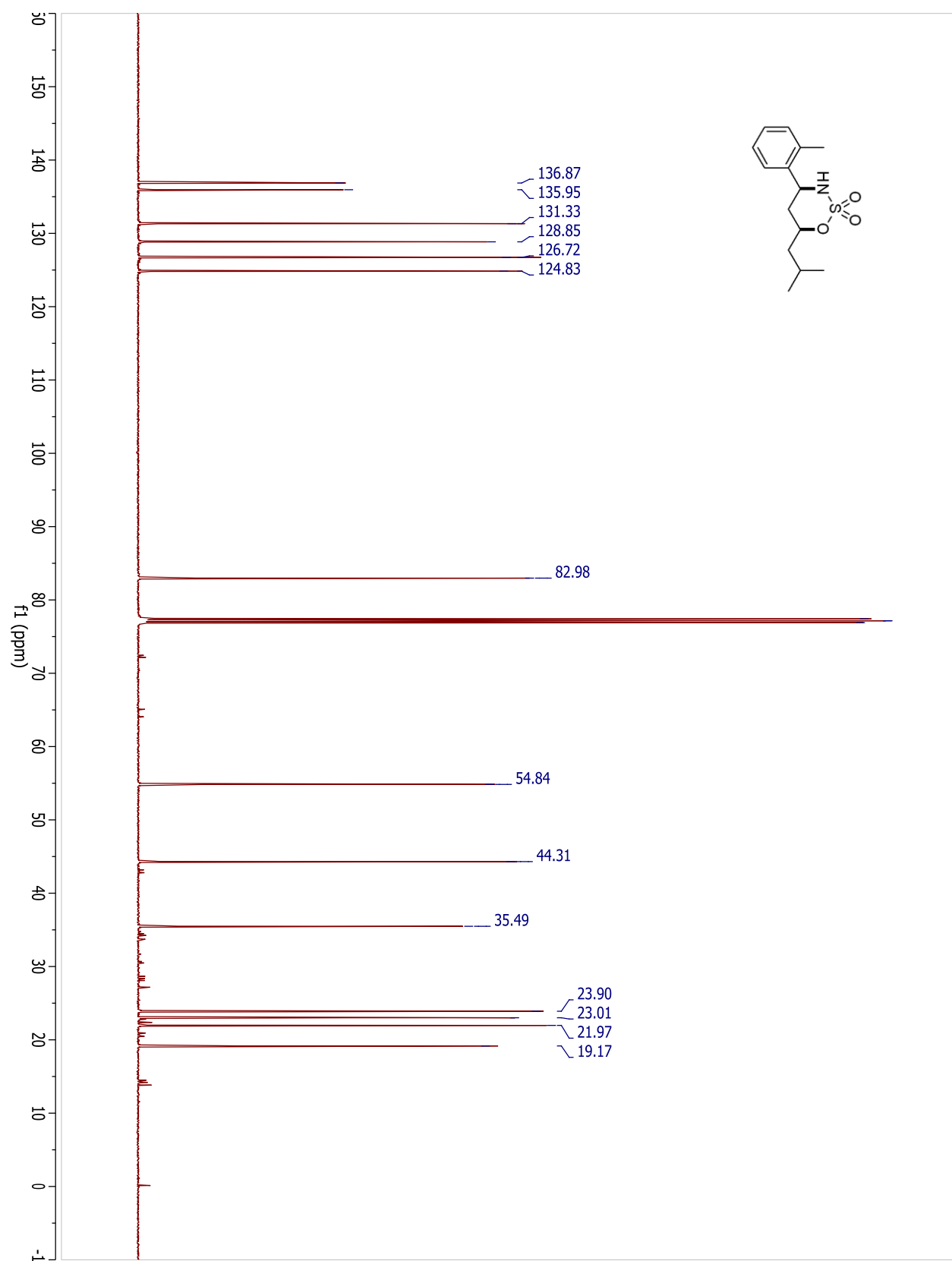


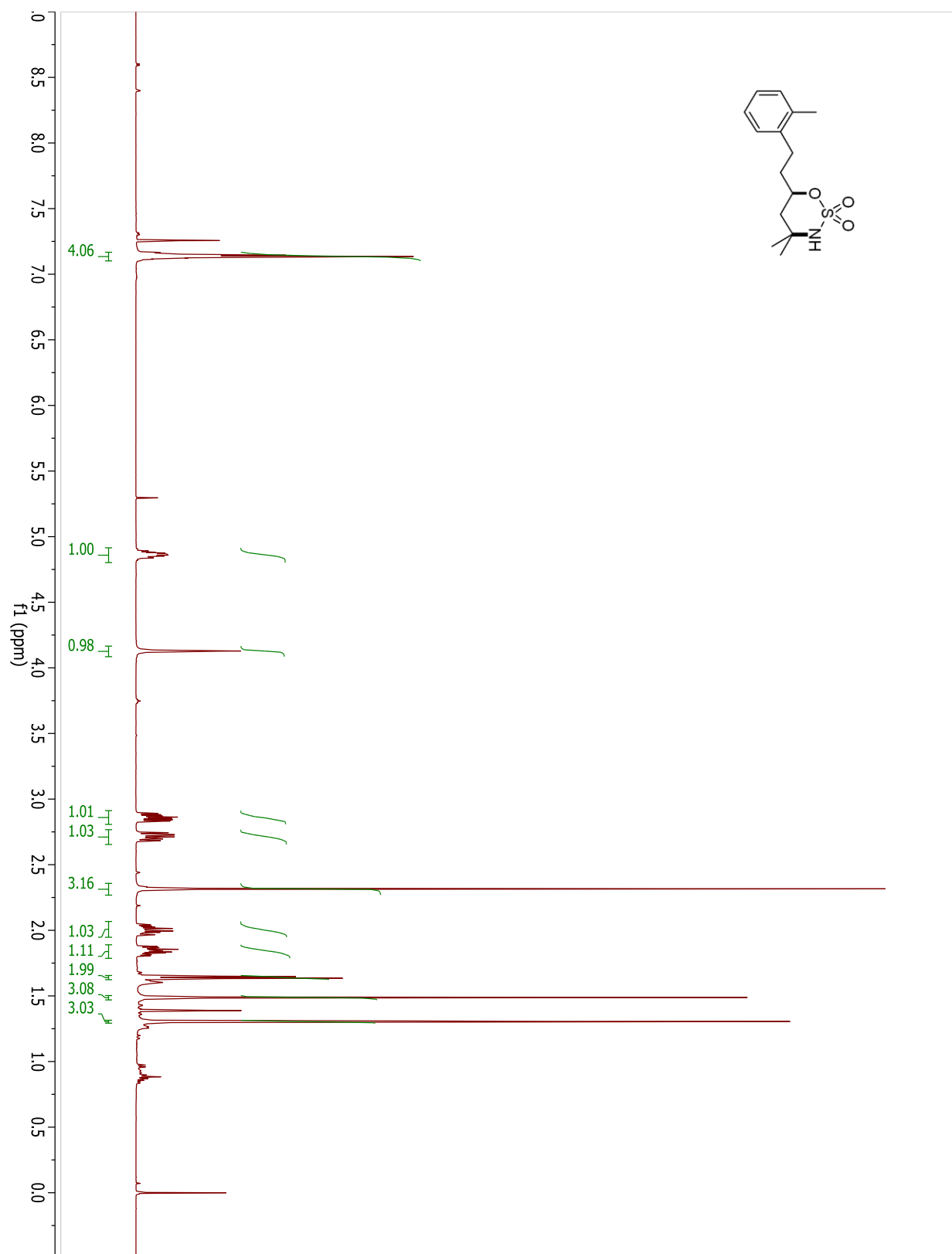
## Compound 3.56a



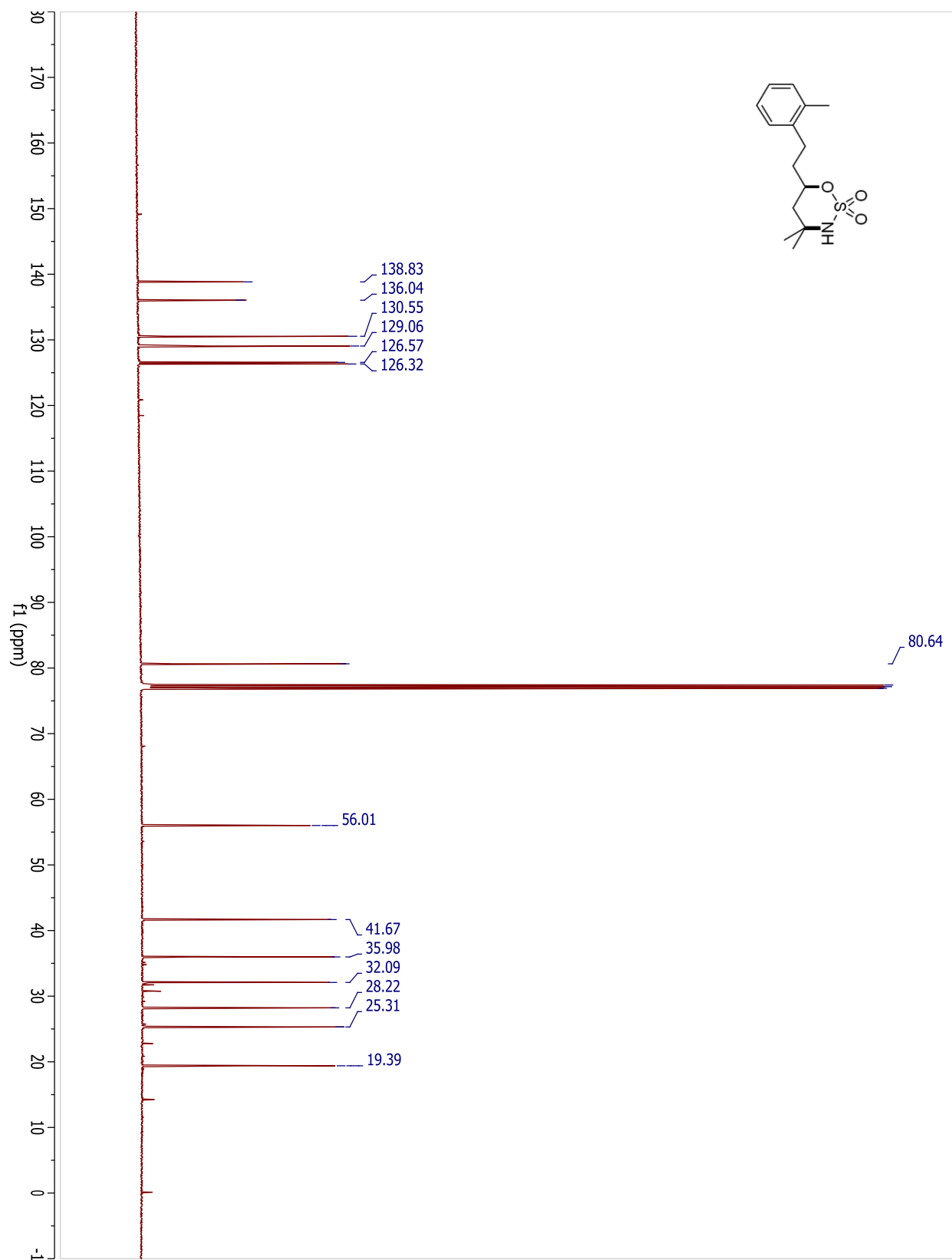


## Compound 3.56a

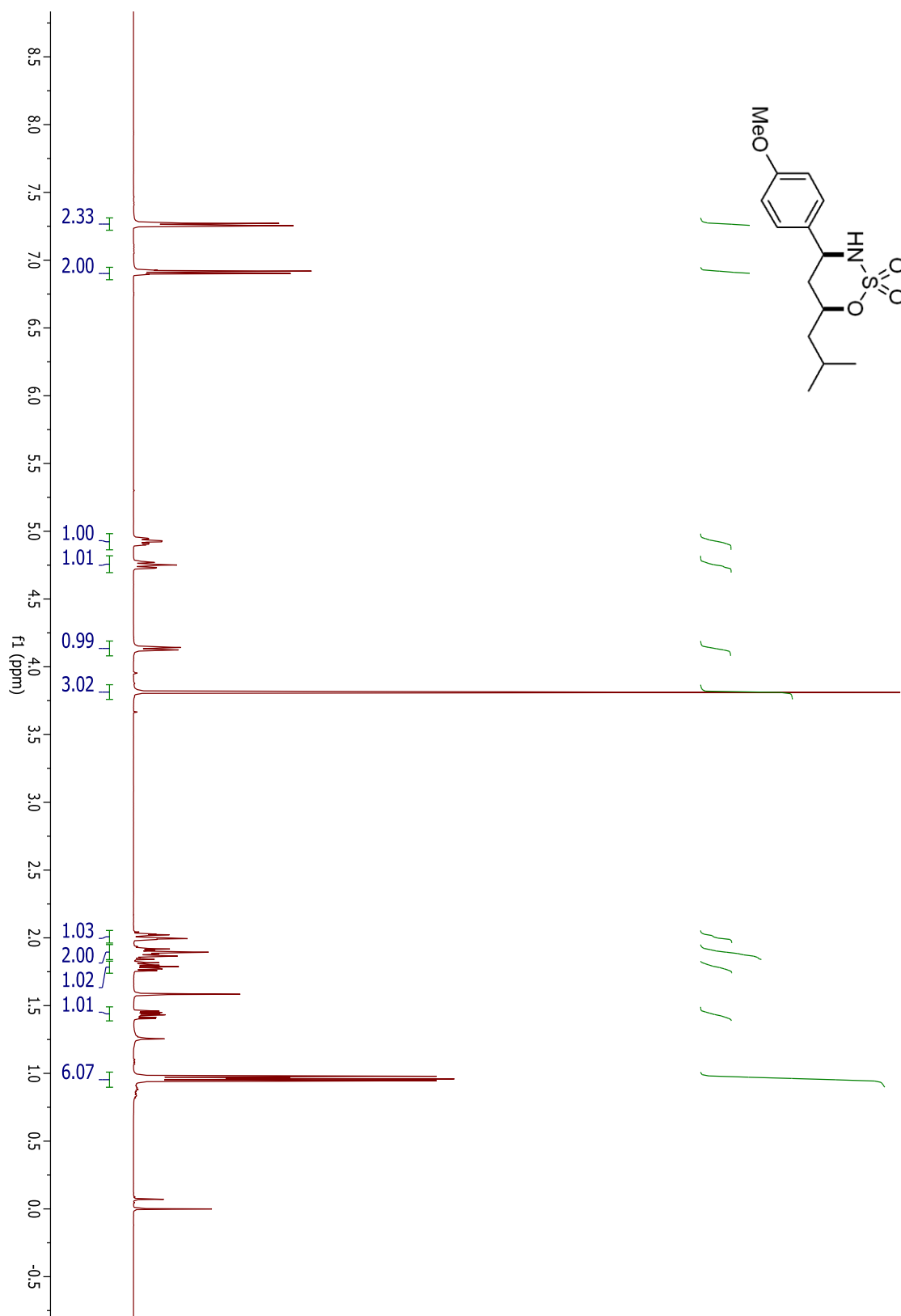


**Compound 3.56b**

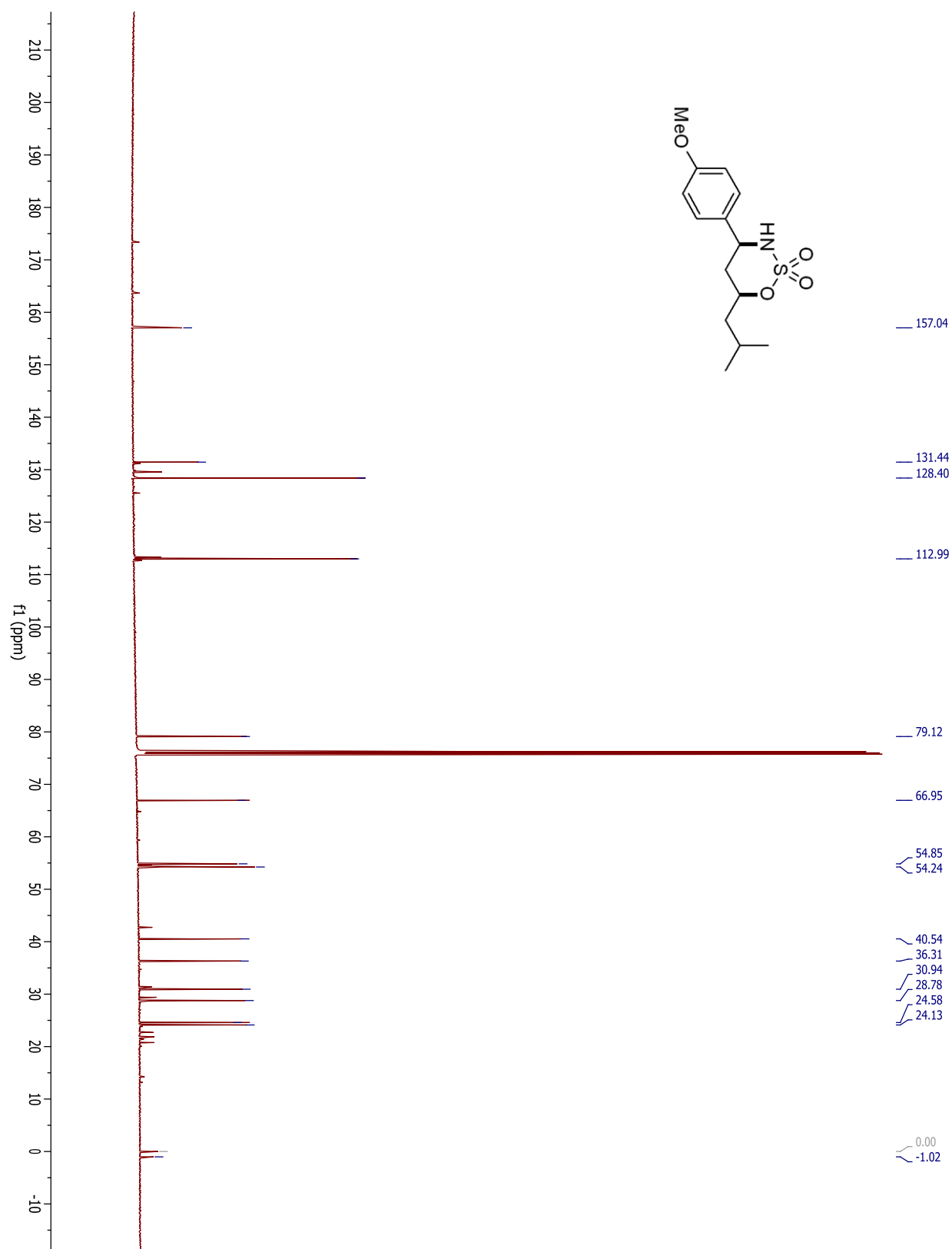
## Compound 3.56b



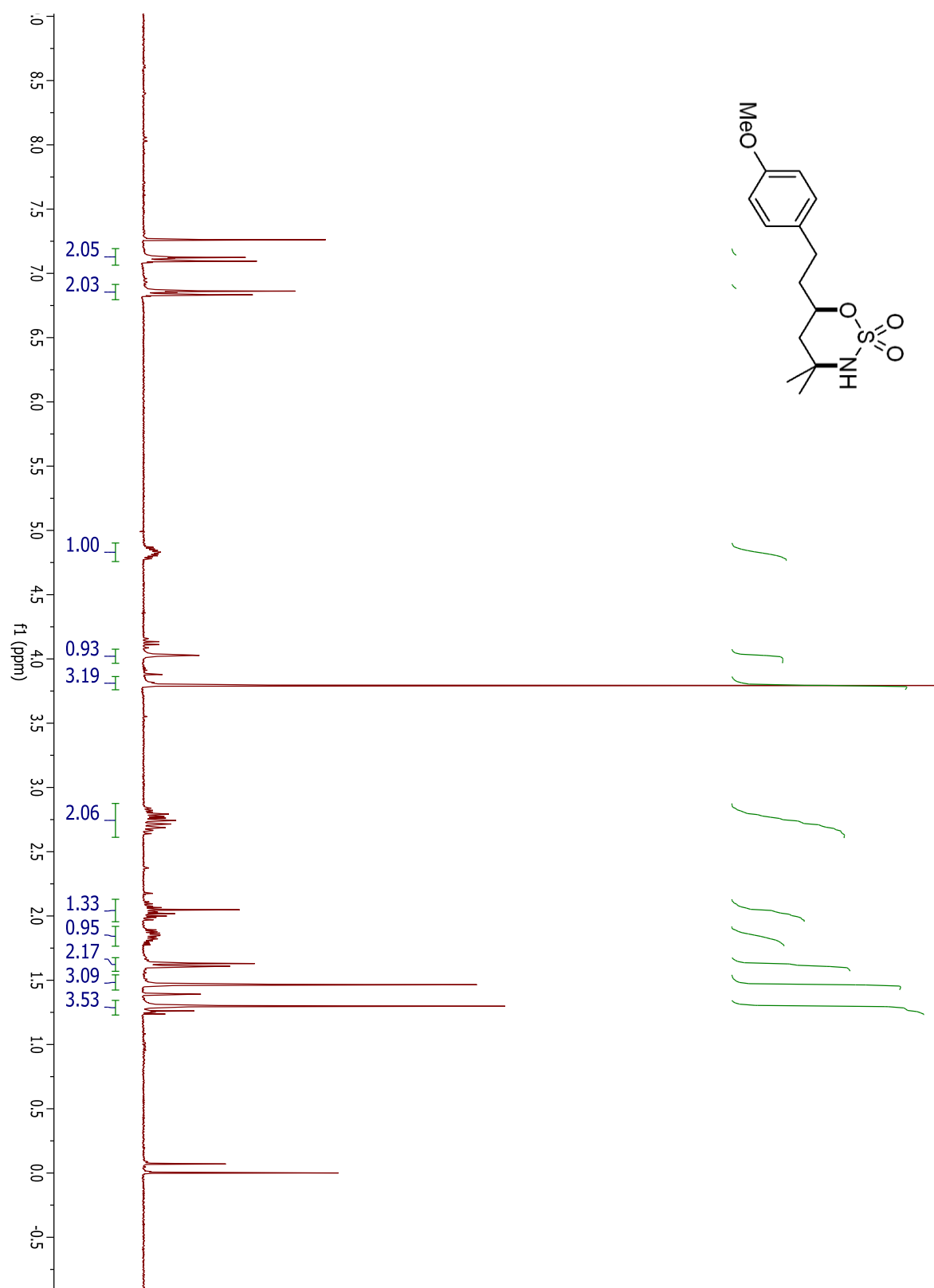
## Compound 3.57a



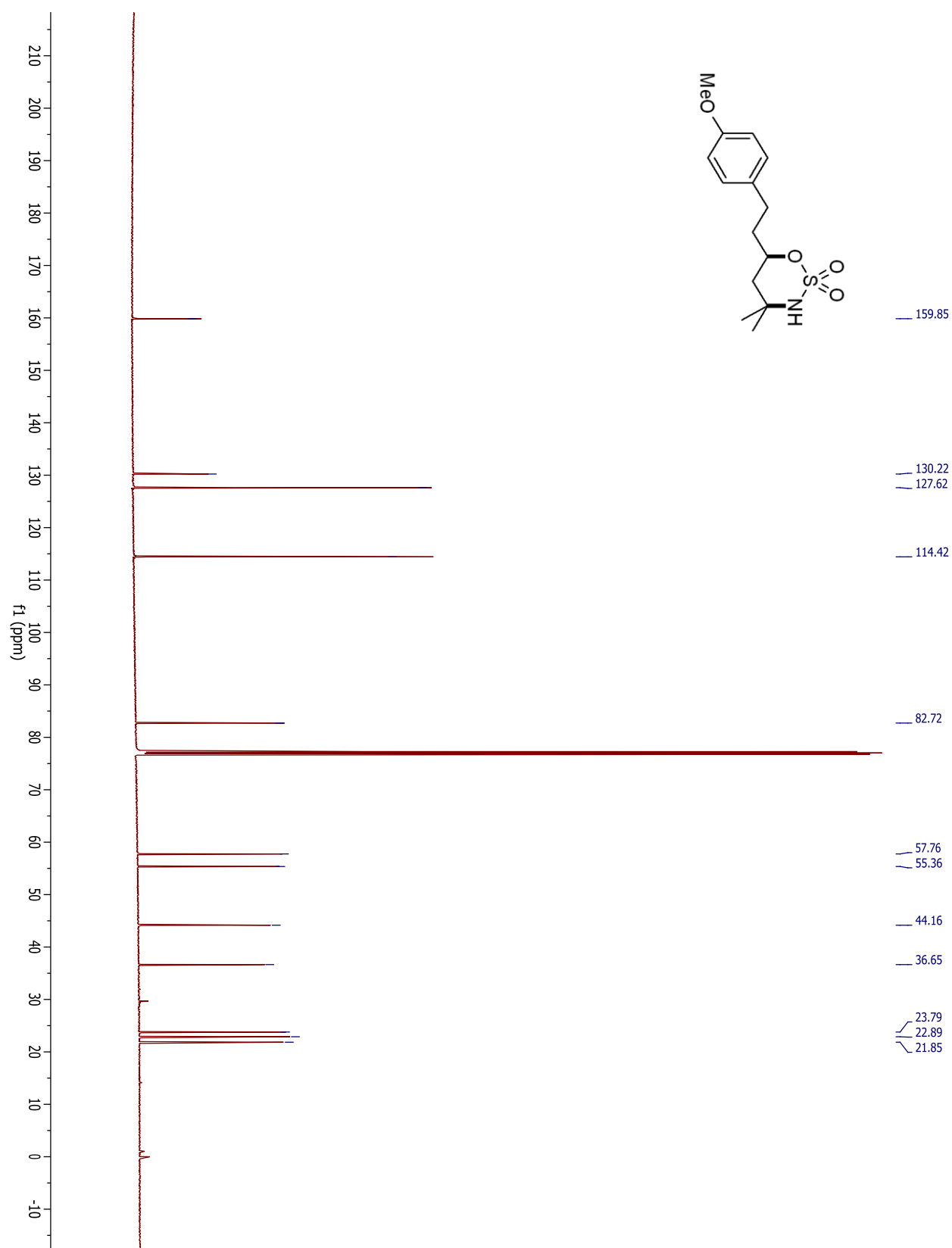
## Compound 3.57a



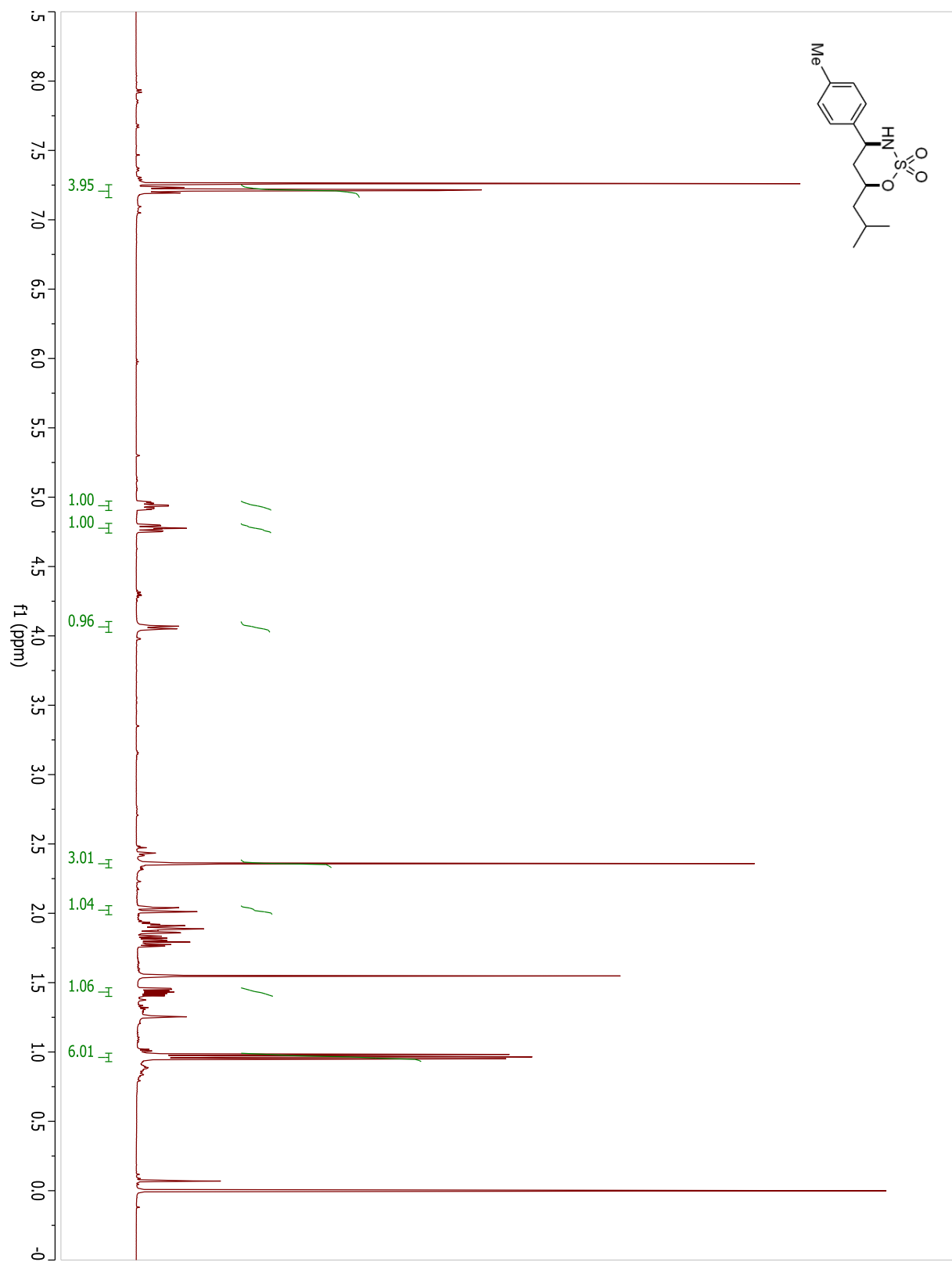
## Compound 3.57b



## Compound 3.57b

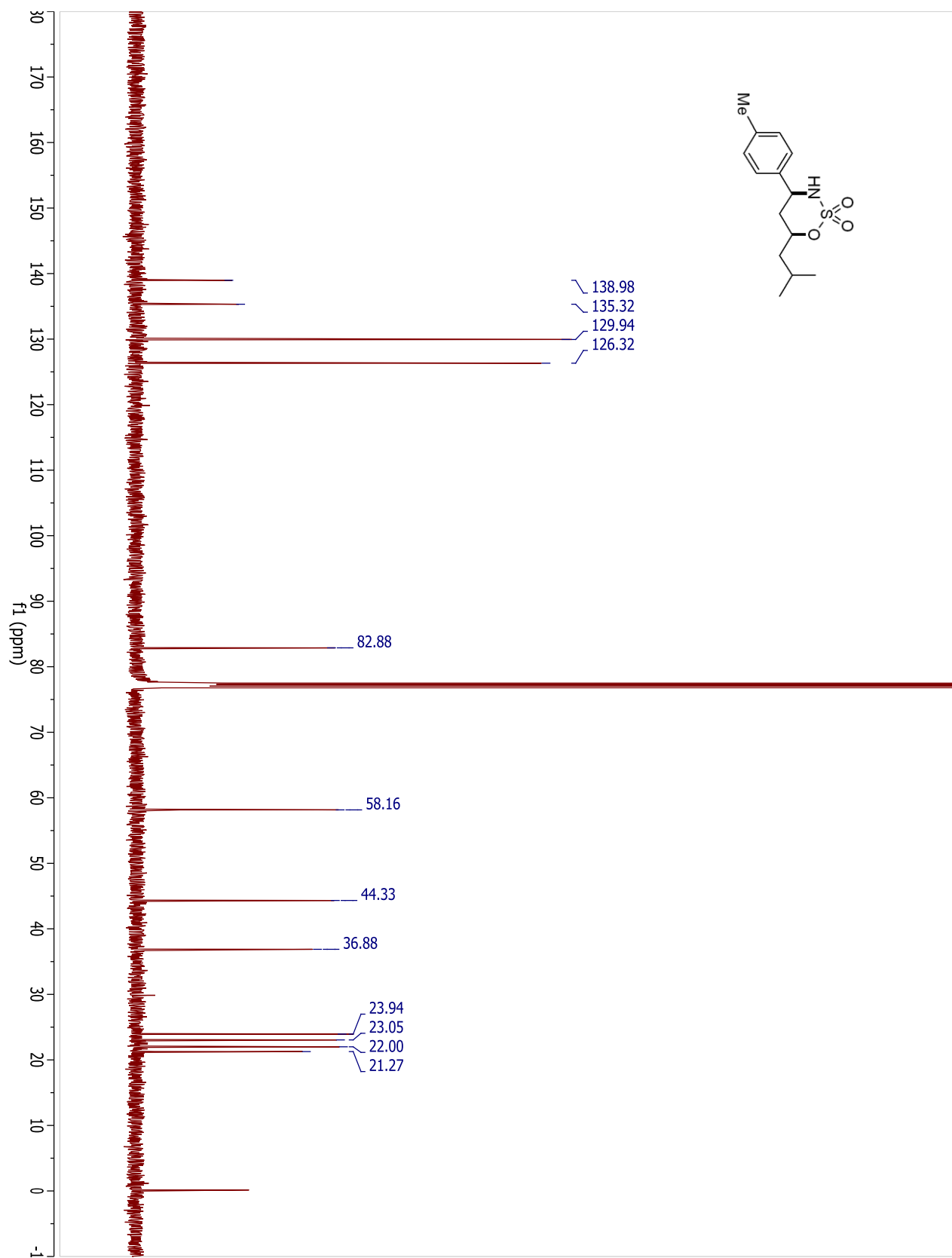


## Compound 3.58a

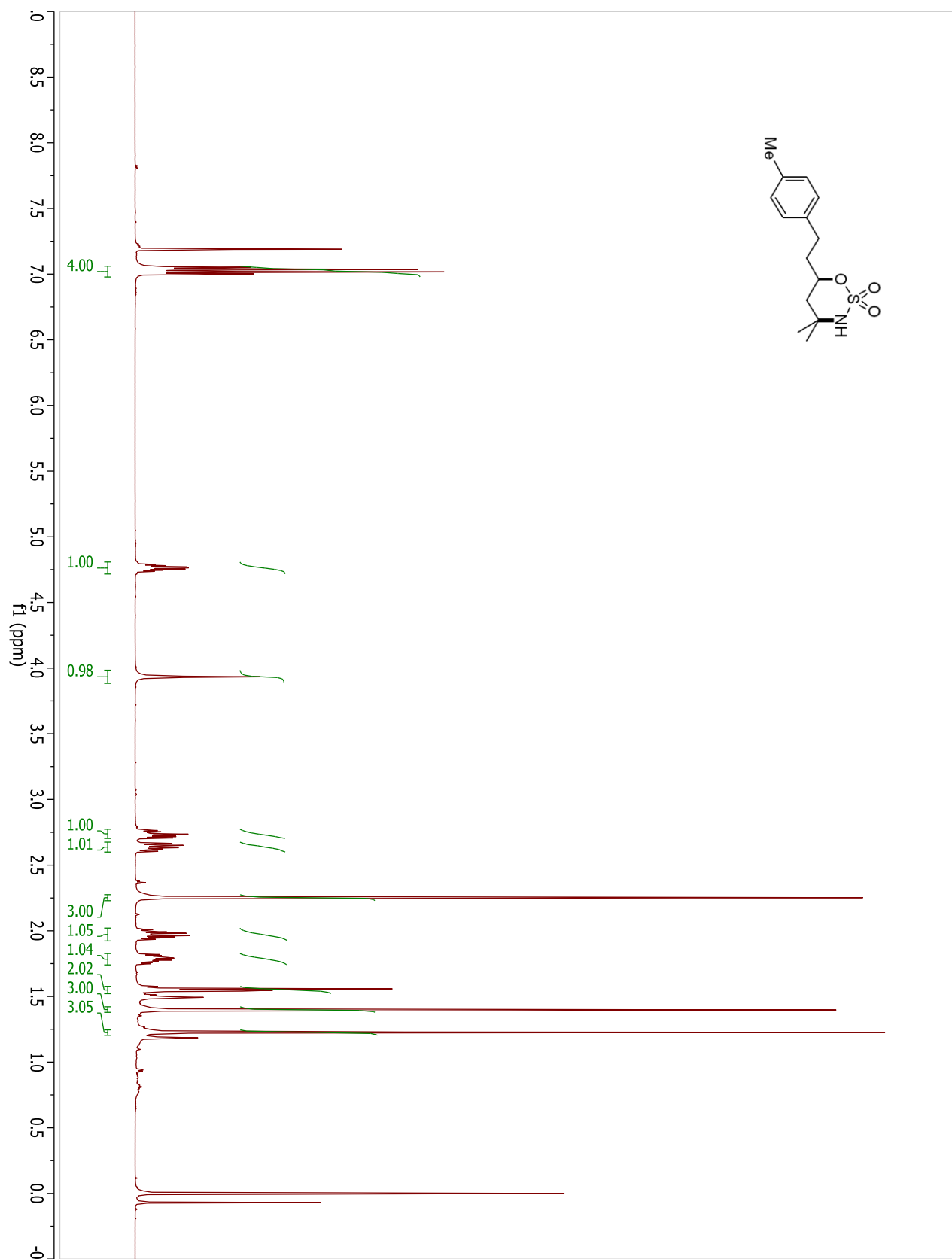




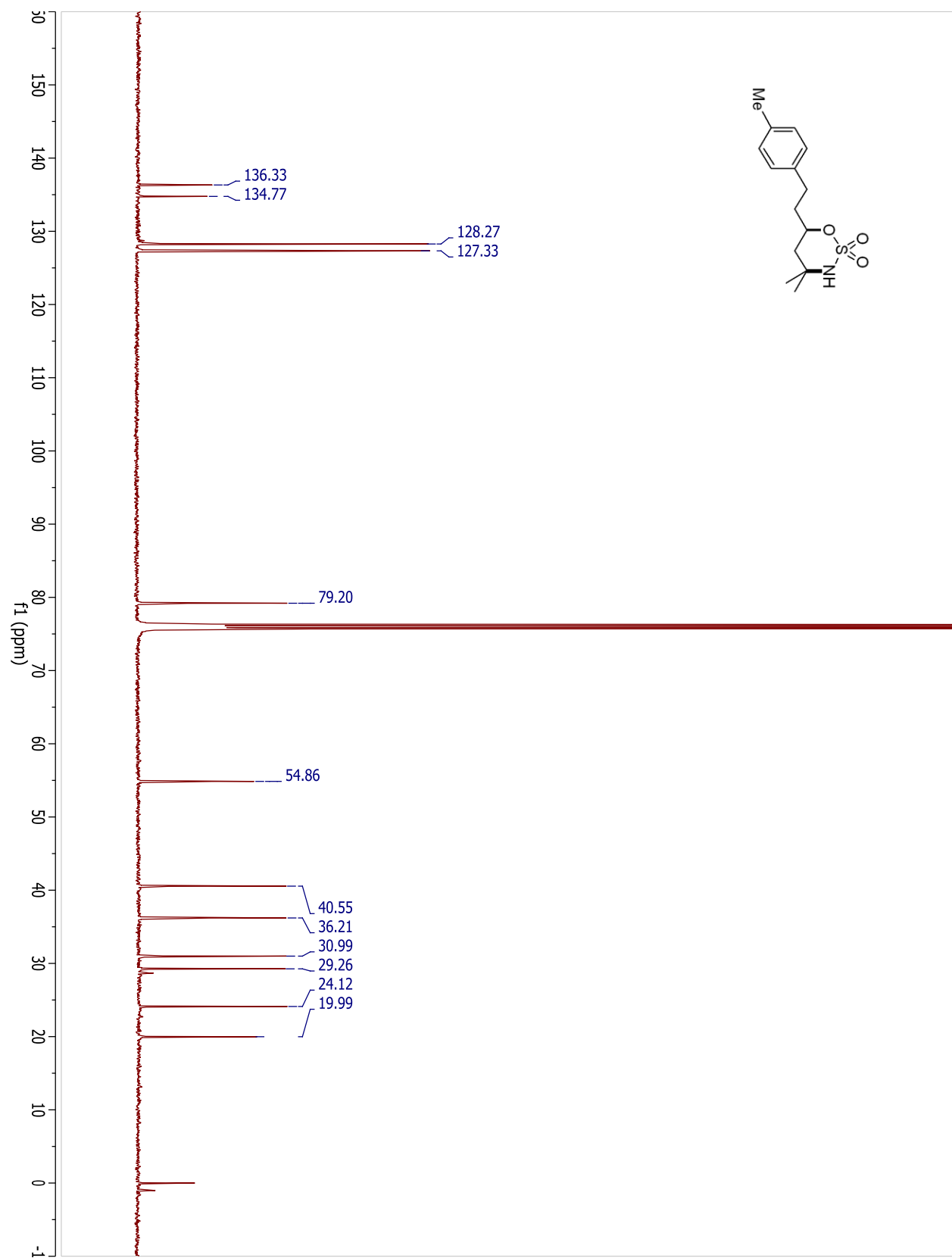
## Compound 3.58a



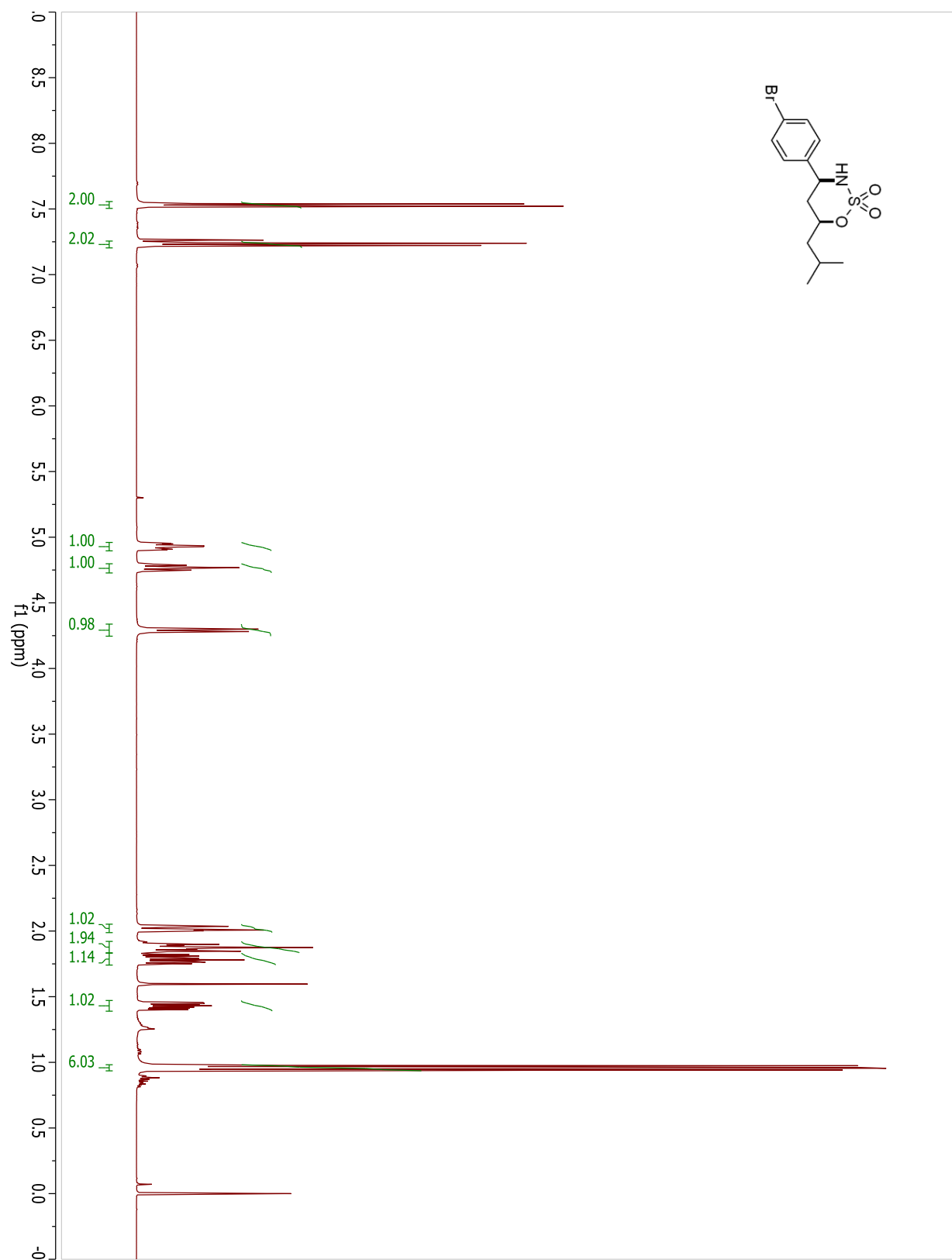
## Compound 3.58b



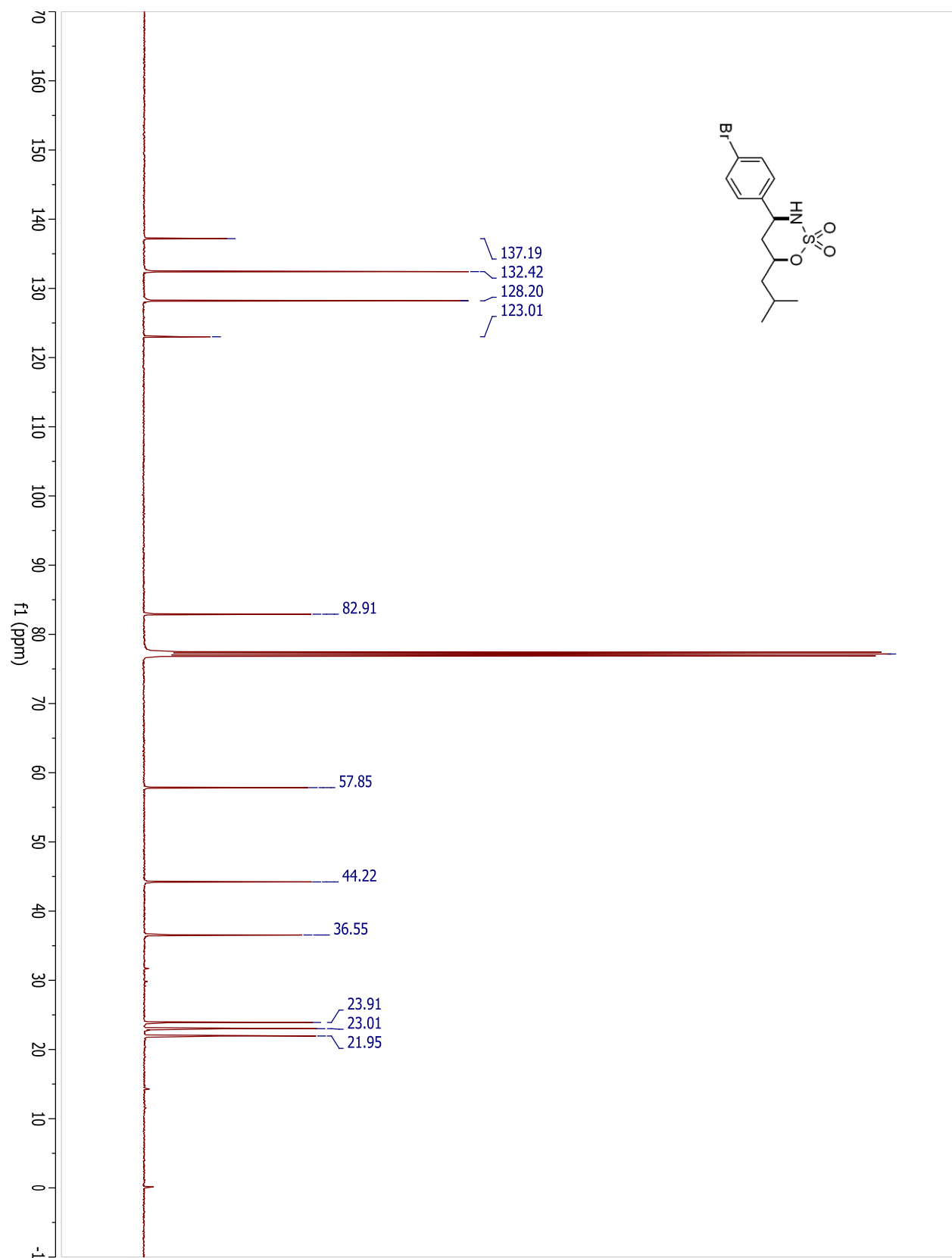
## Compound 3.58b



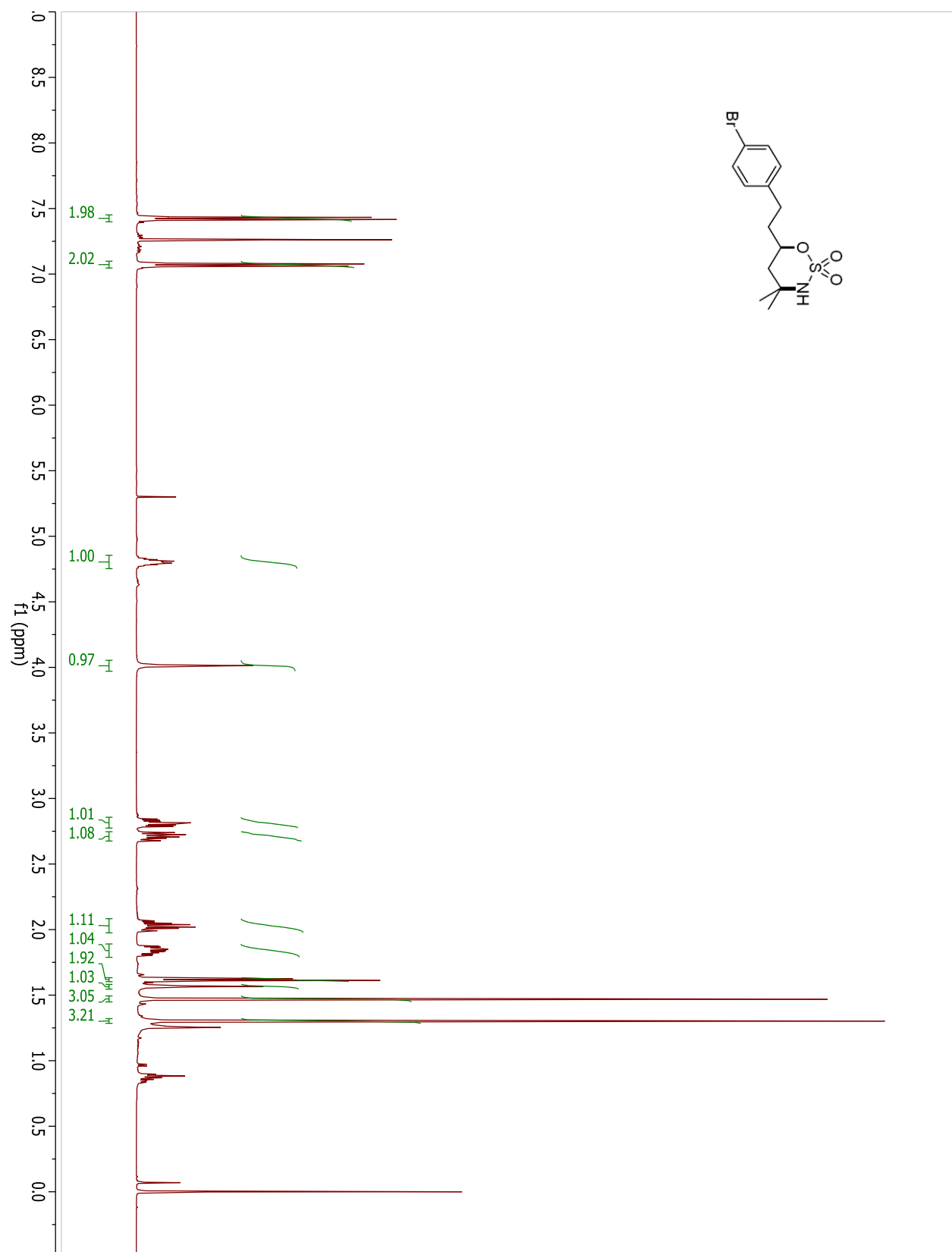
## Compound 3.59a



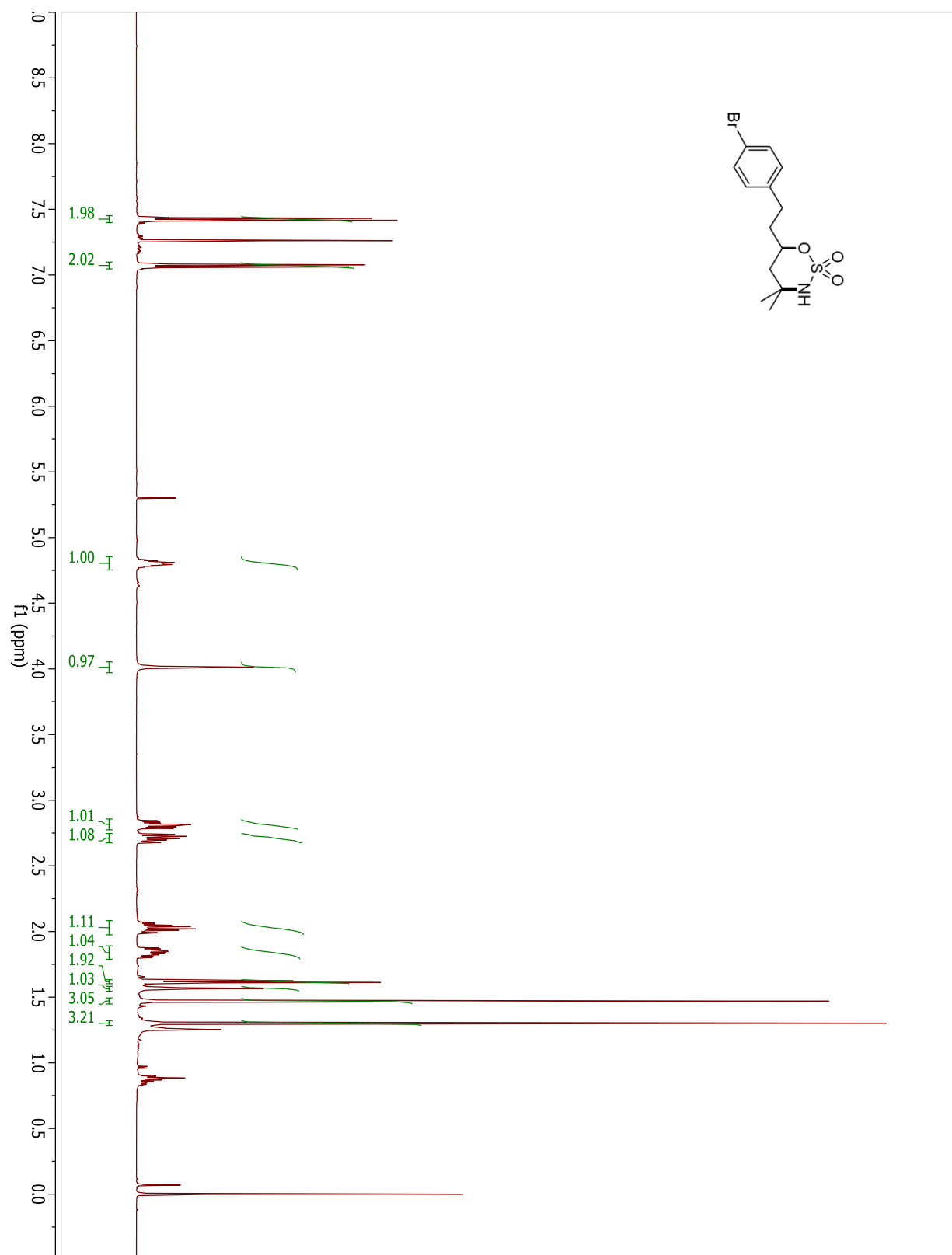
## Compound 3.59a



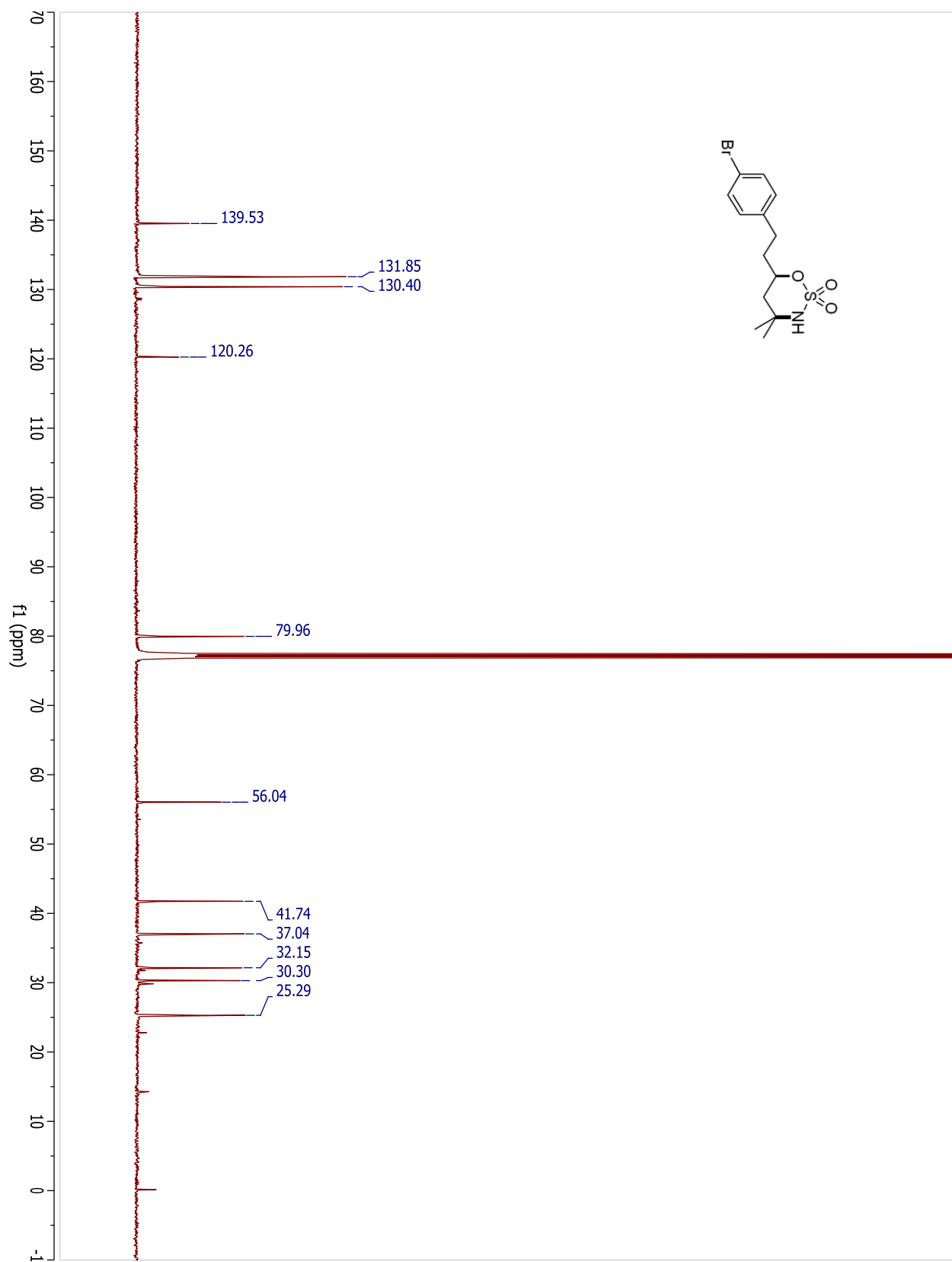
## Compound 3.59b



## Compound 3.59b

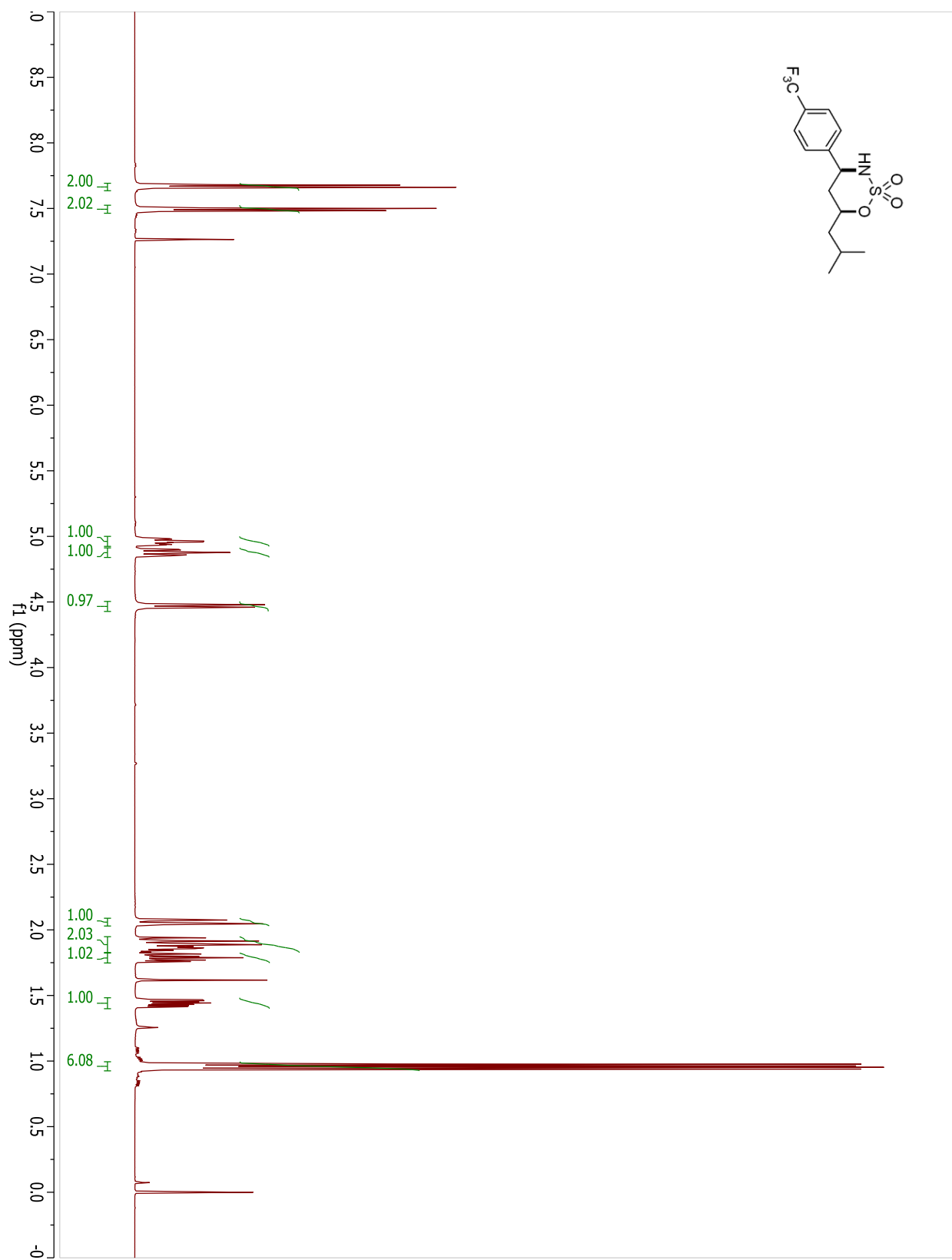


## Compound 3.59b

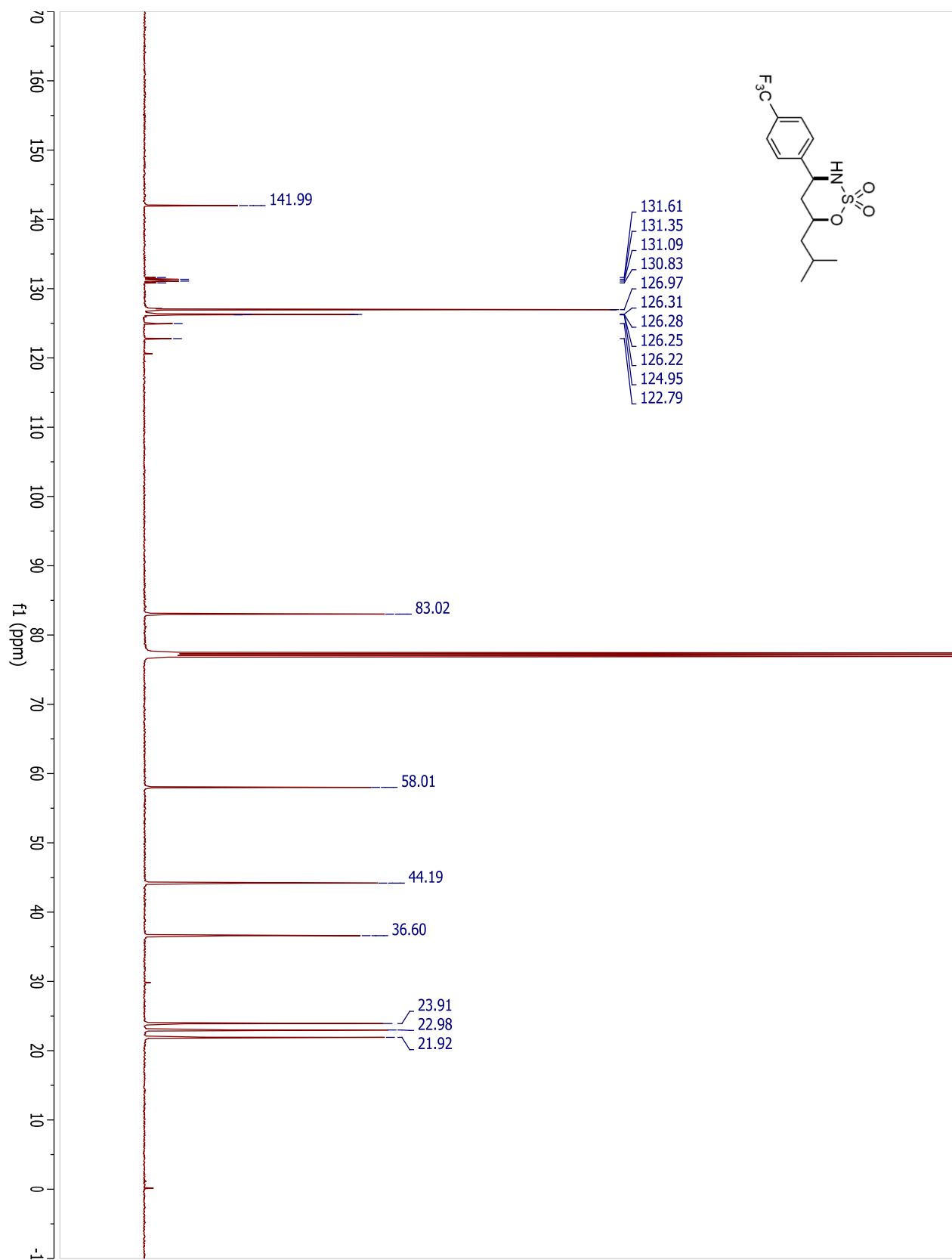


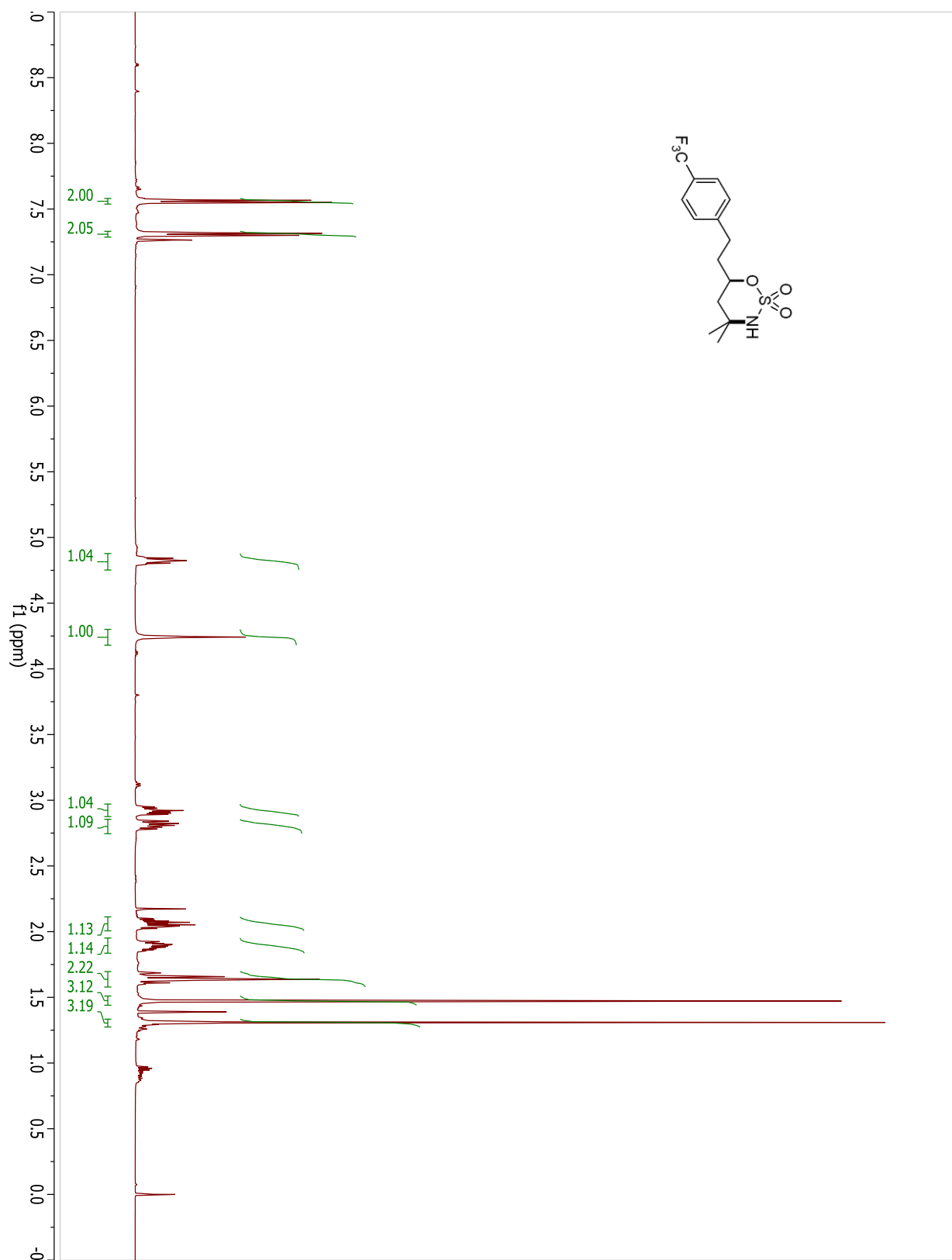


## Compound 3.60a

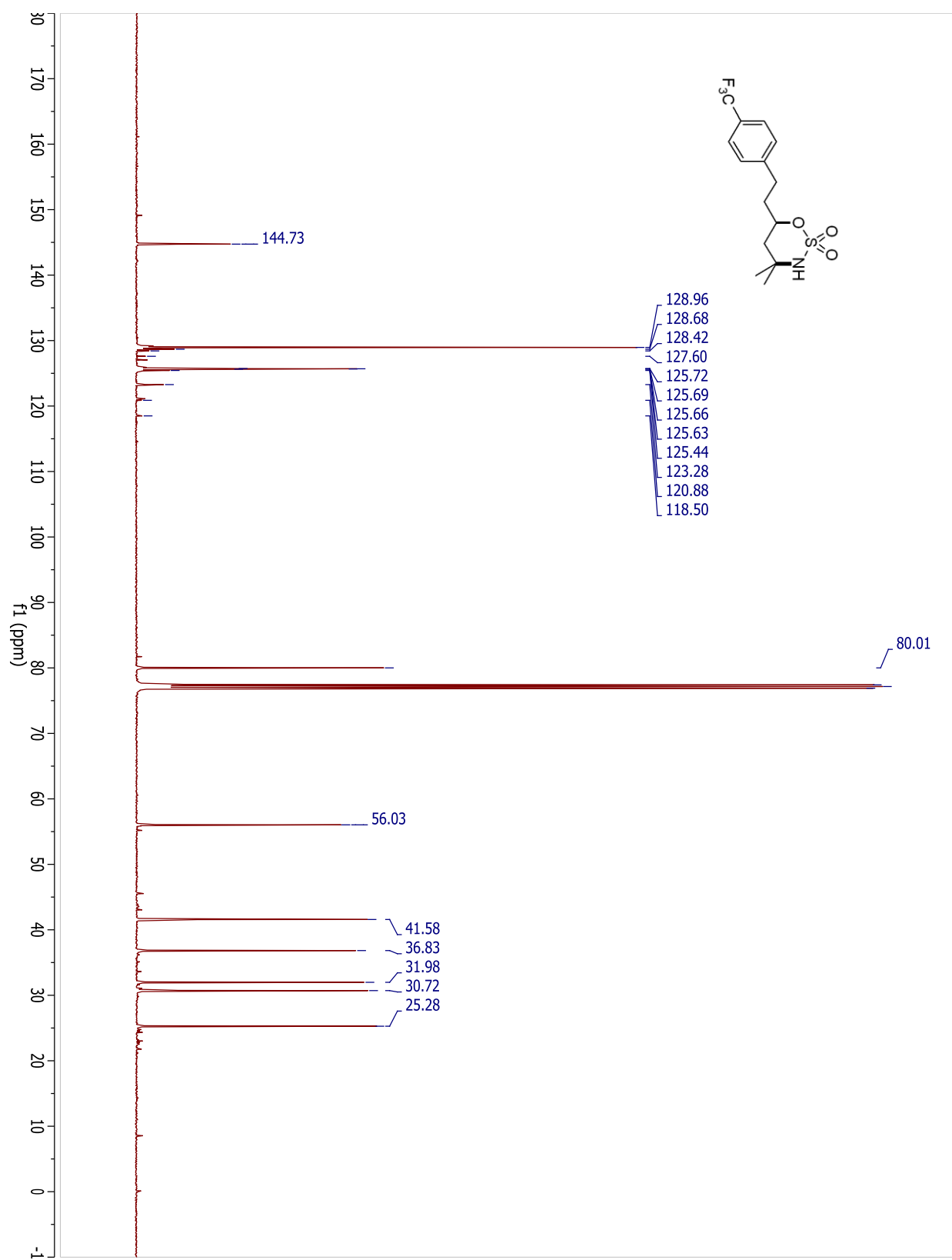


## Compound 3.60a

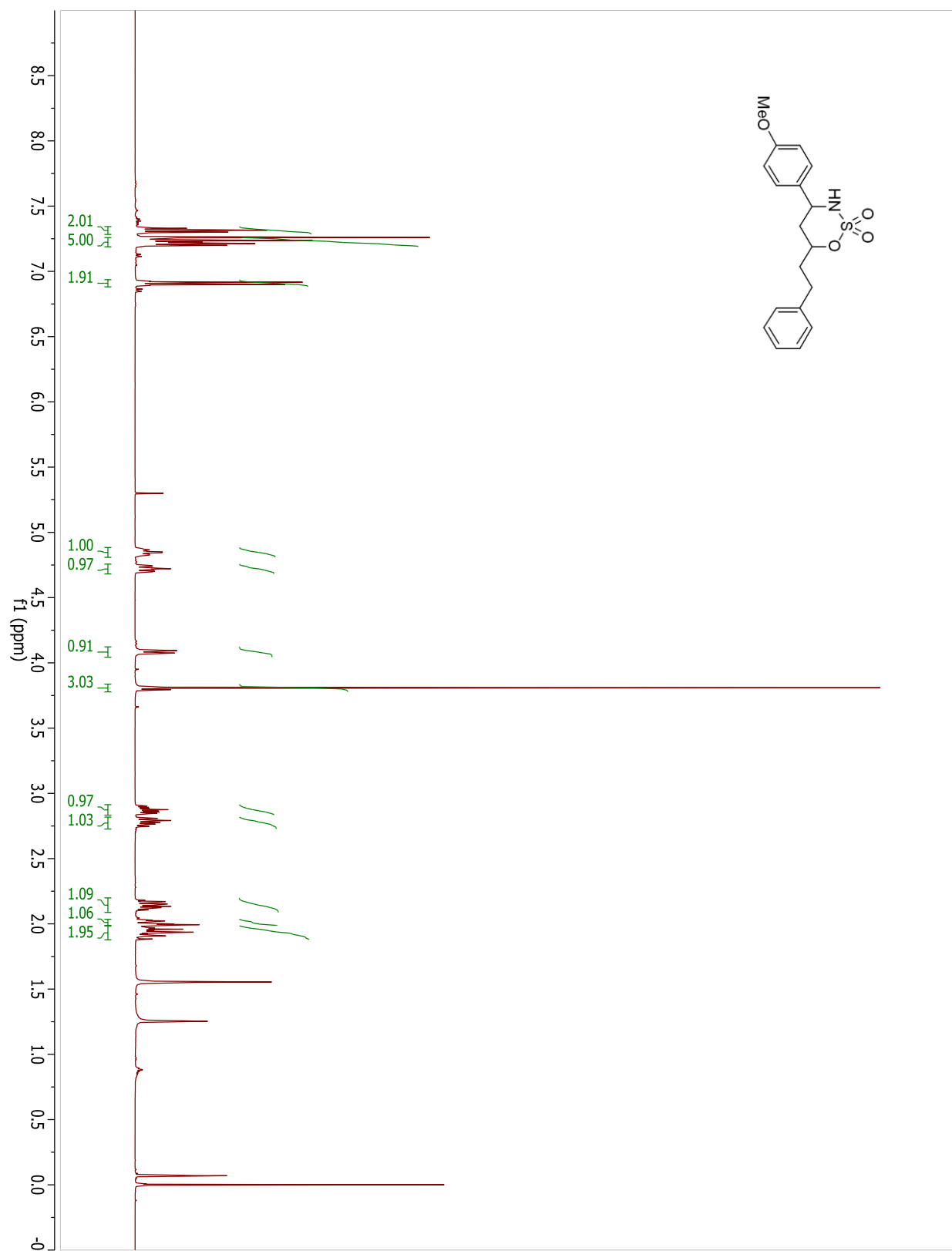


**Compound 3.60b**

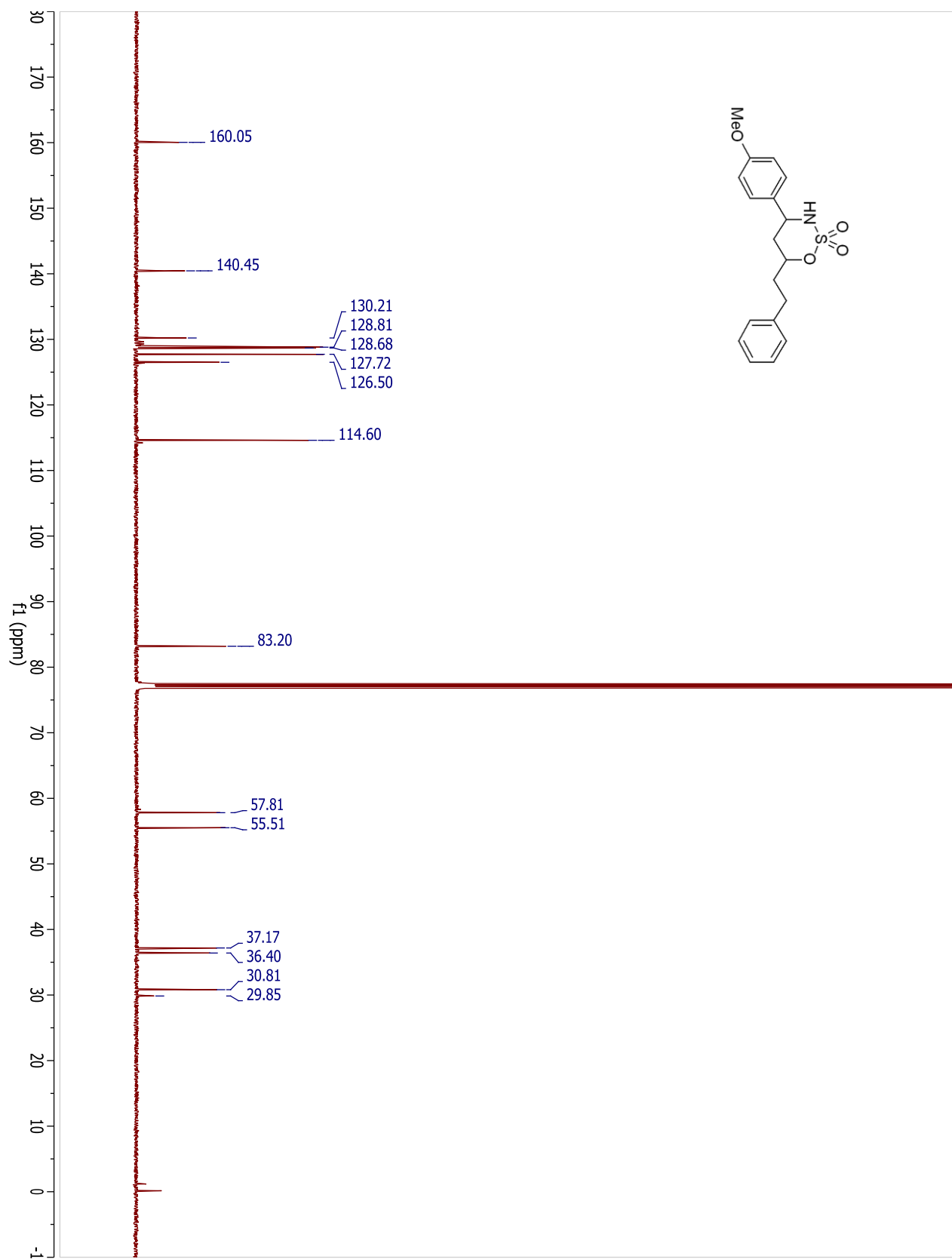
## Compound 3.60b



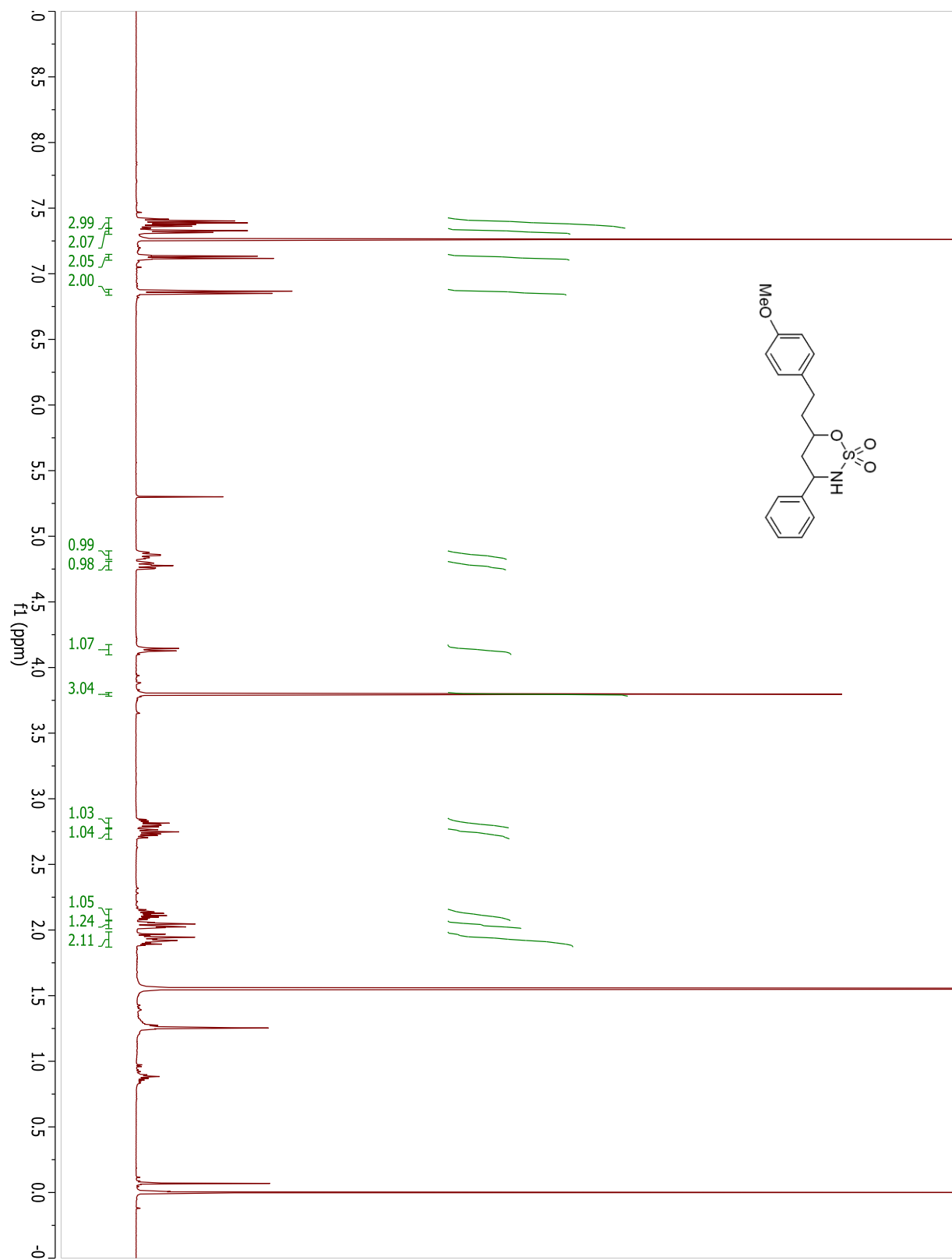
## Compound 3.61a



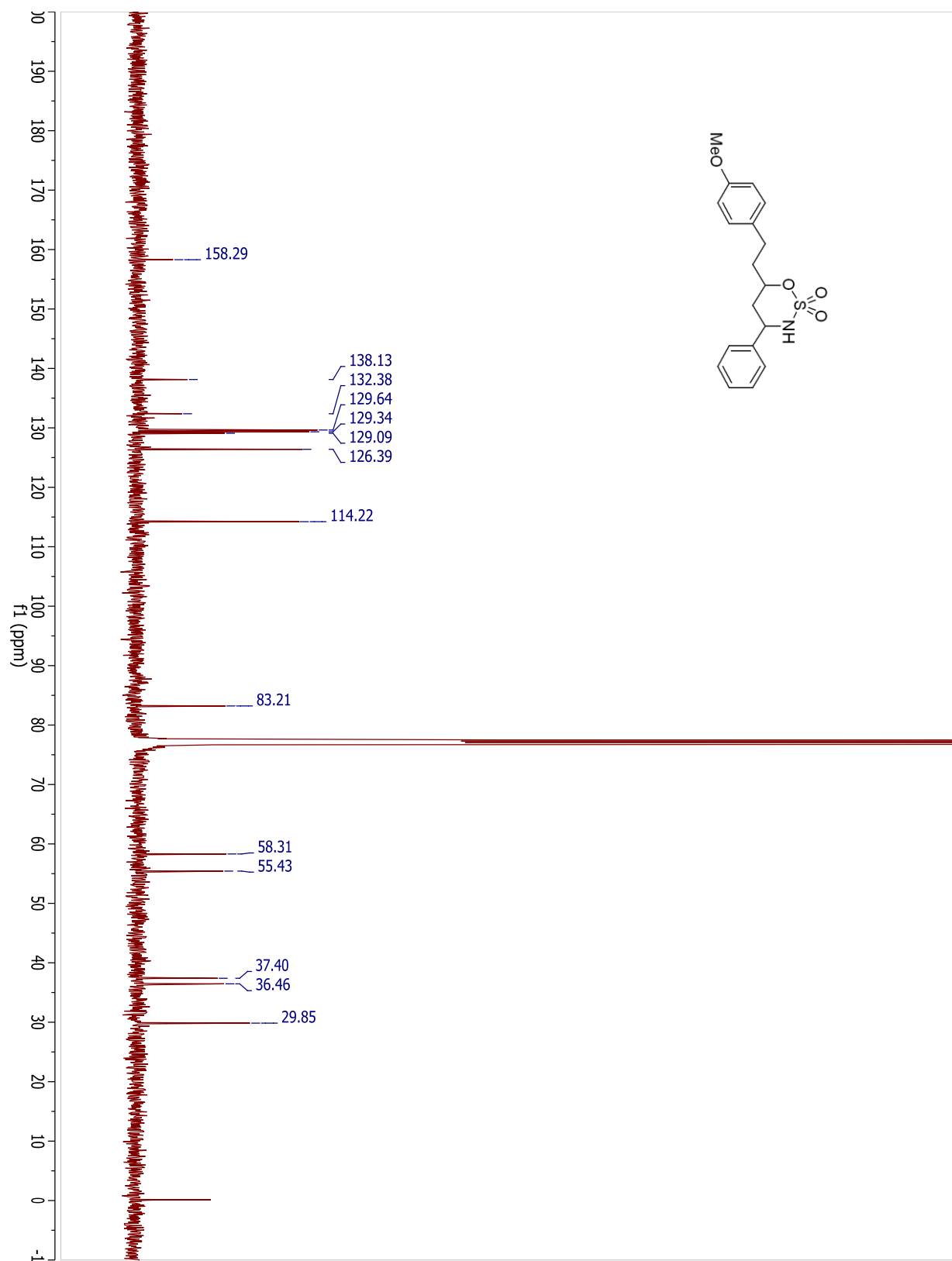
## Compound 3.61a



## Compound 3.61b

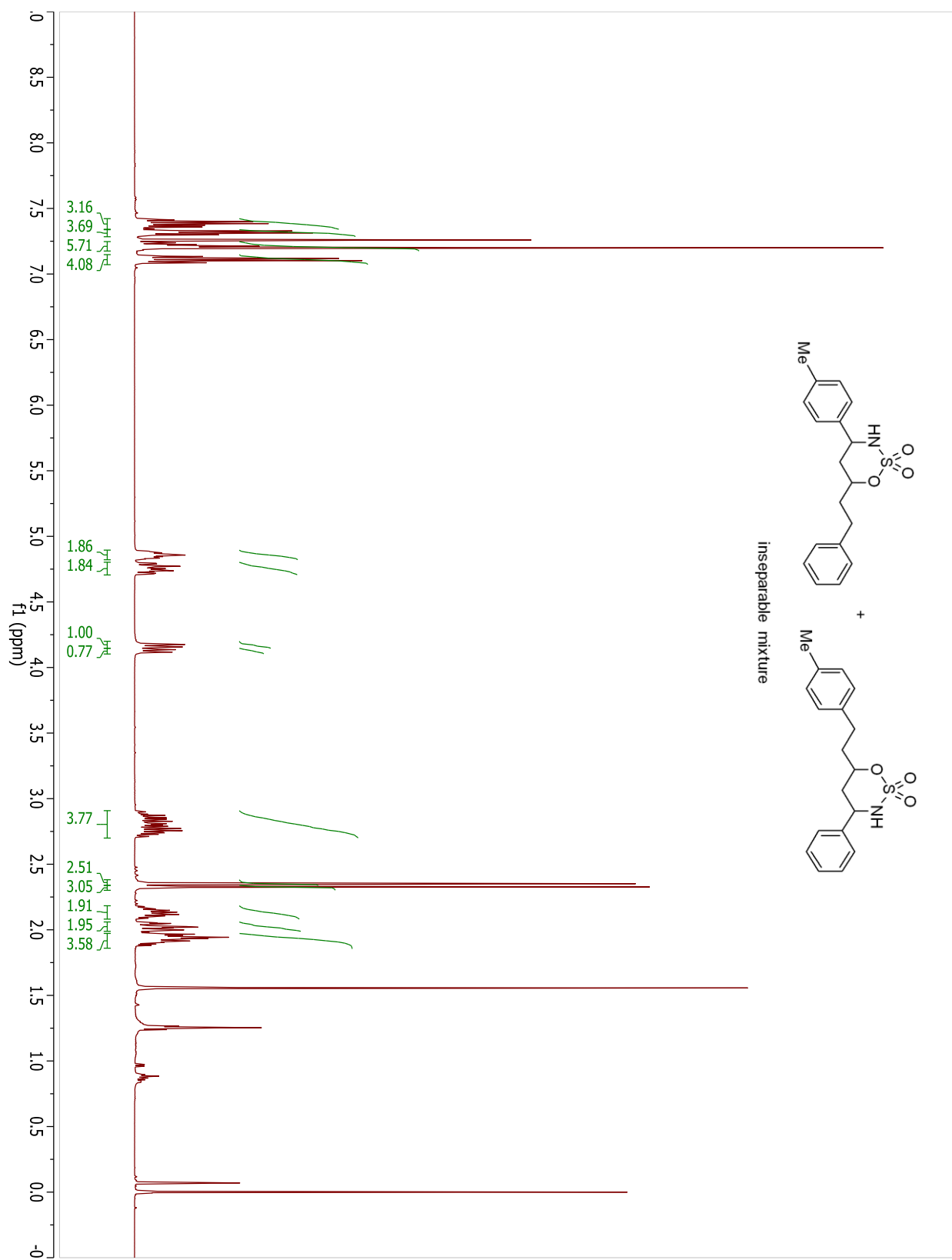


## Compound 3.61b

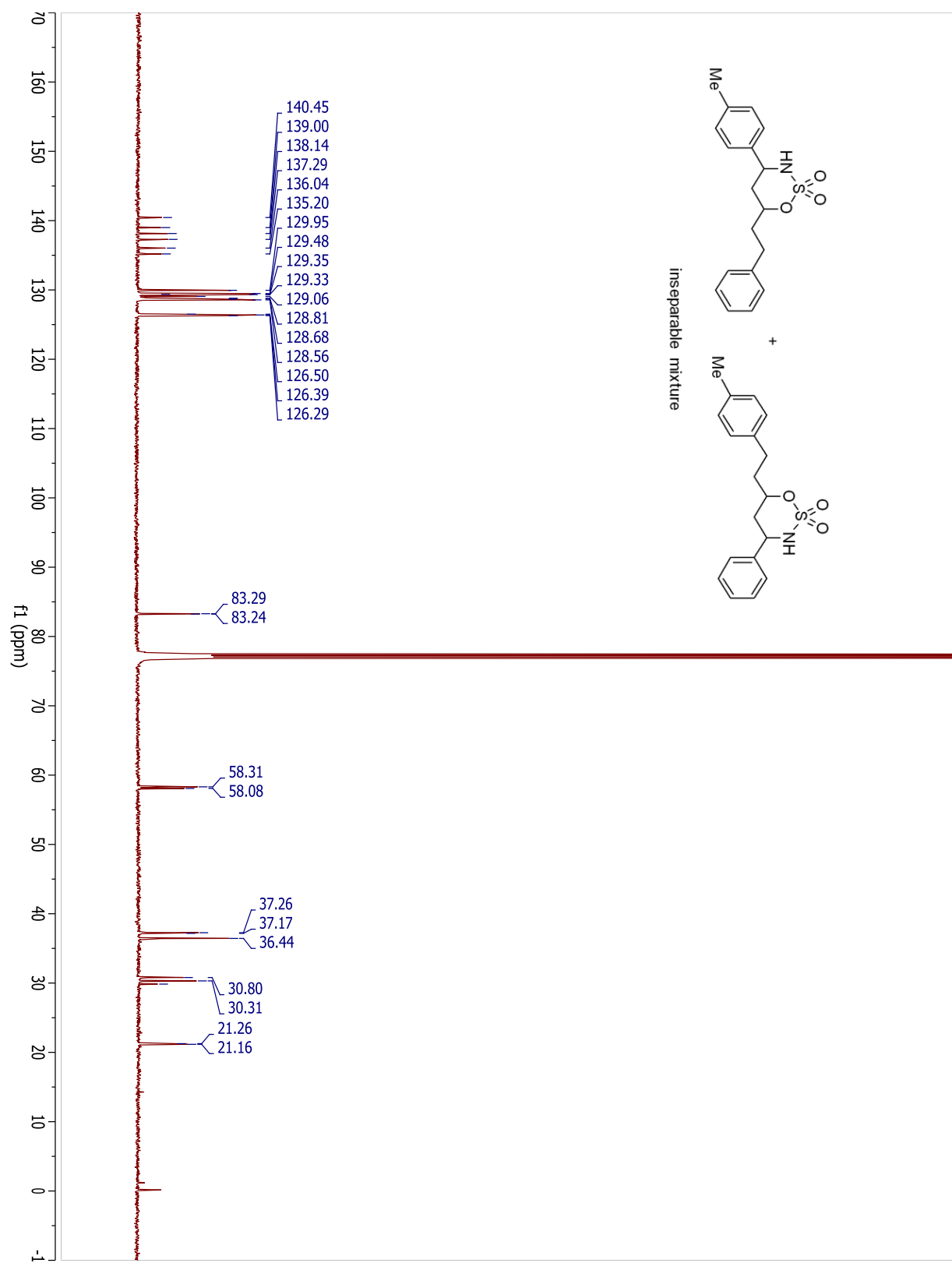




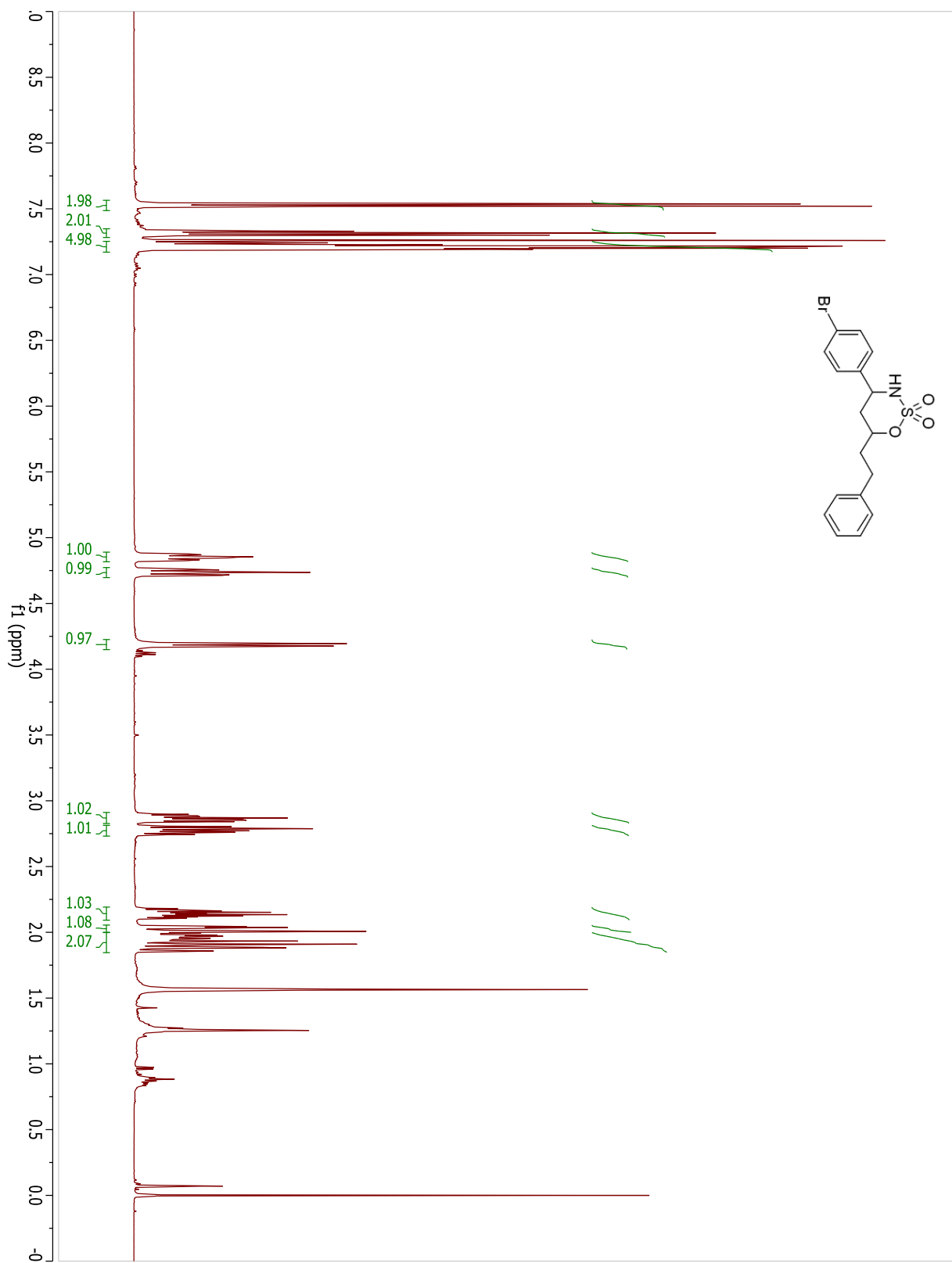
## Compound 3.62a + 3.62b



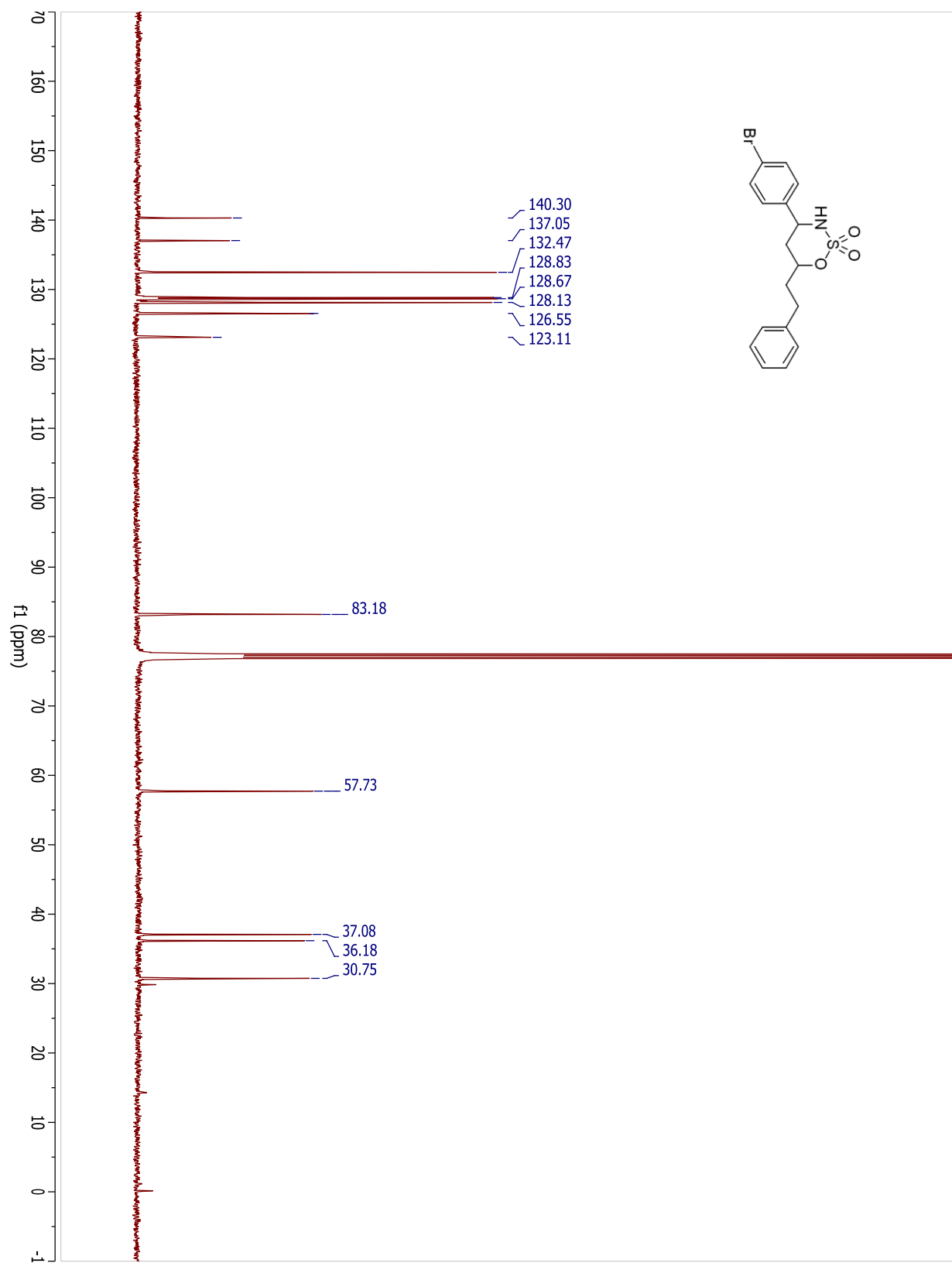
## Compound 3.62a + 3.62b



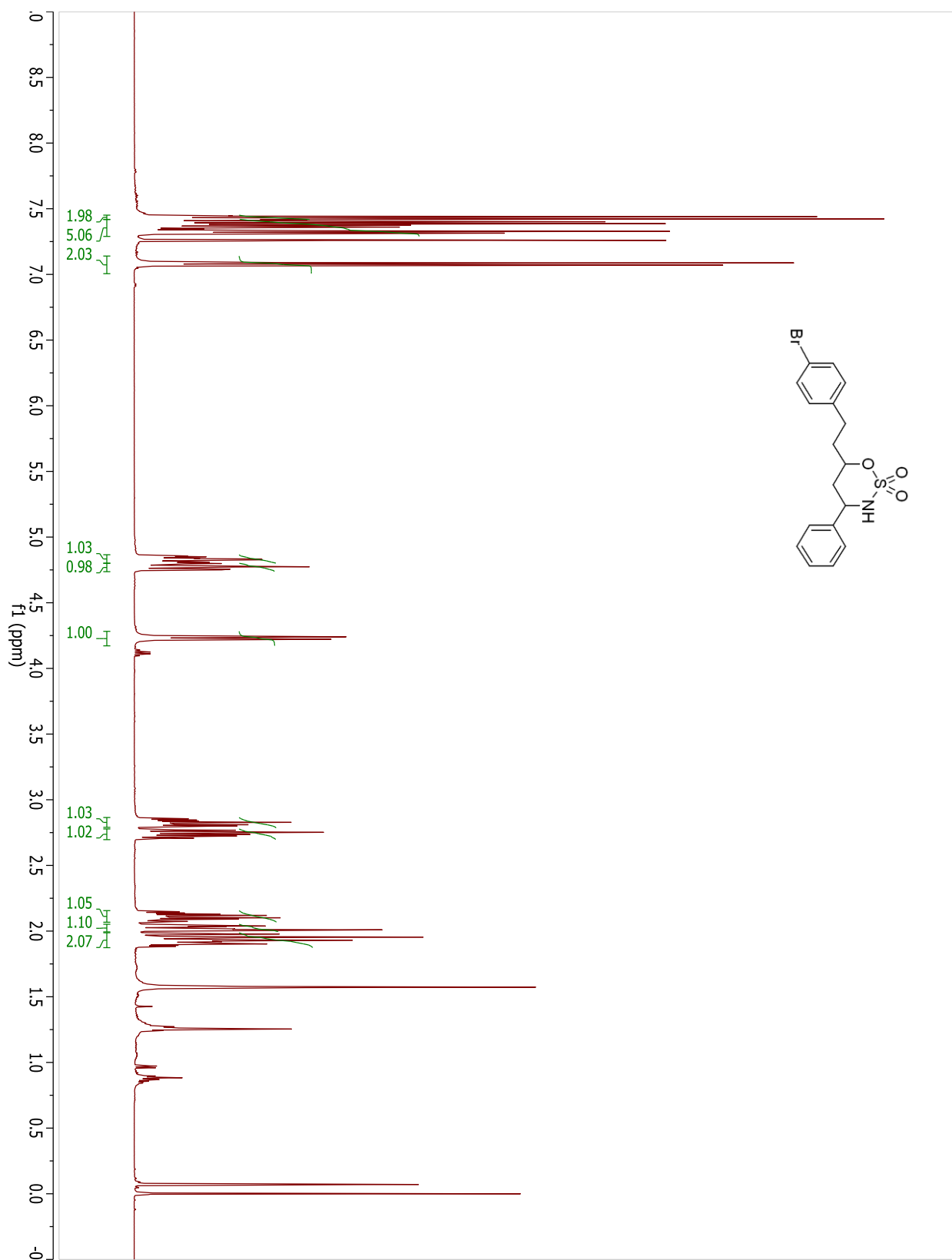
## Compound 3.63a



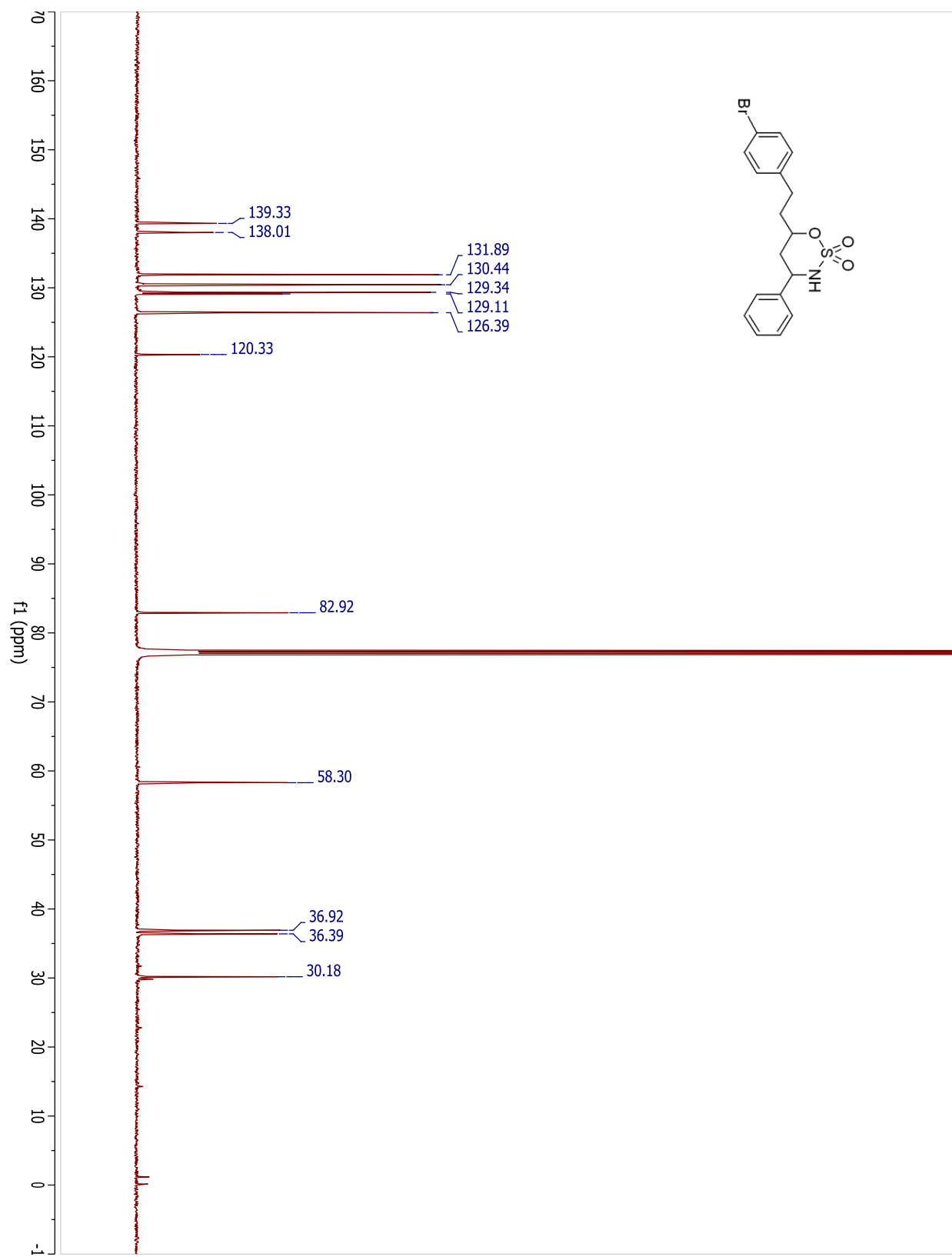
## Compound 3.63a



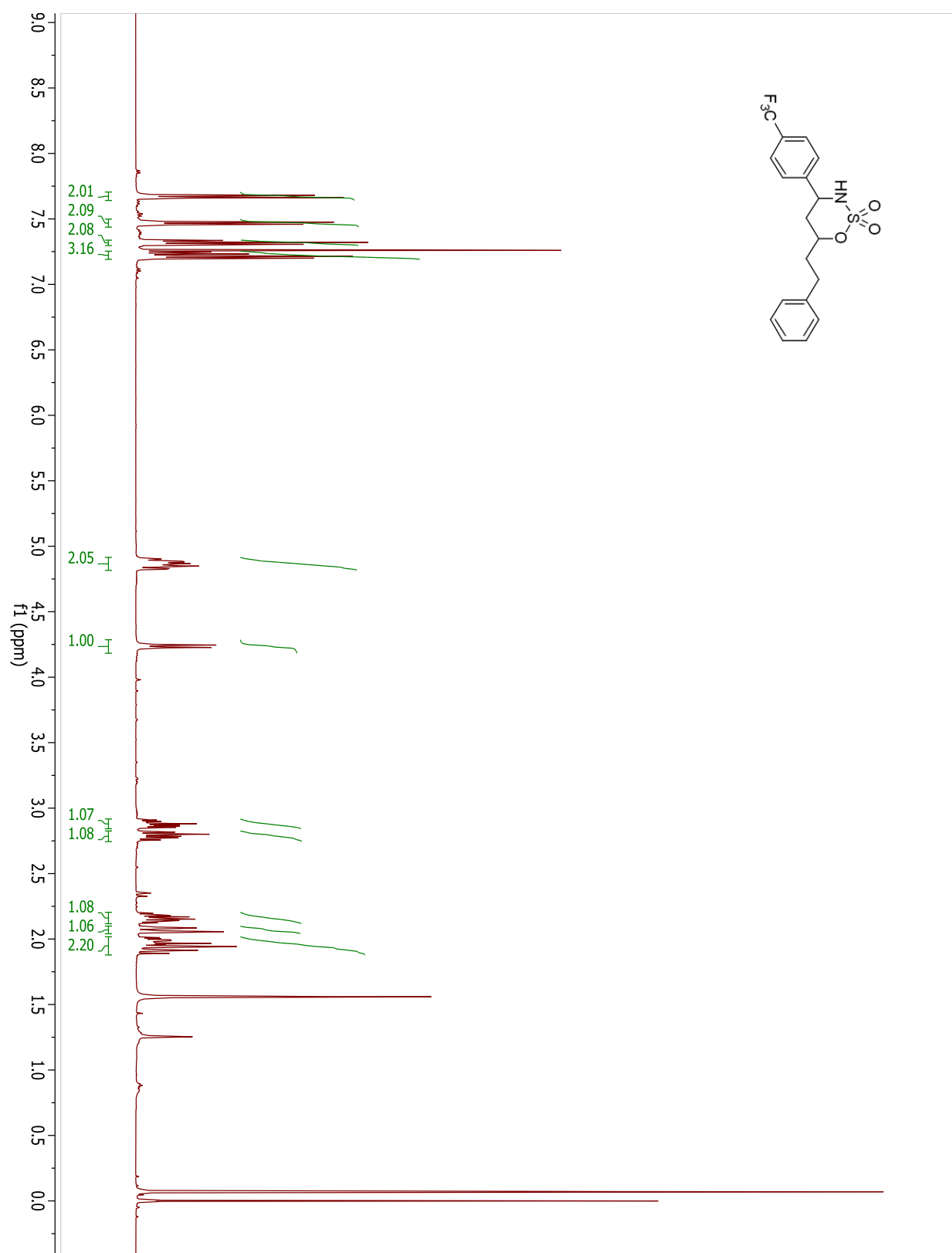
## Compound 3.63b



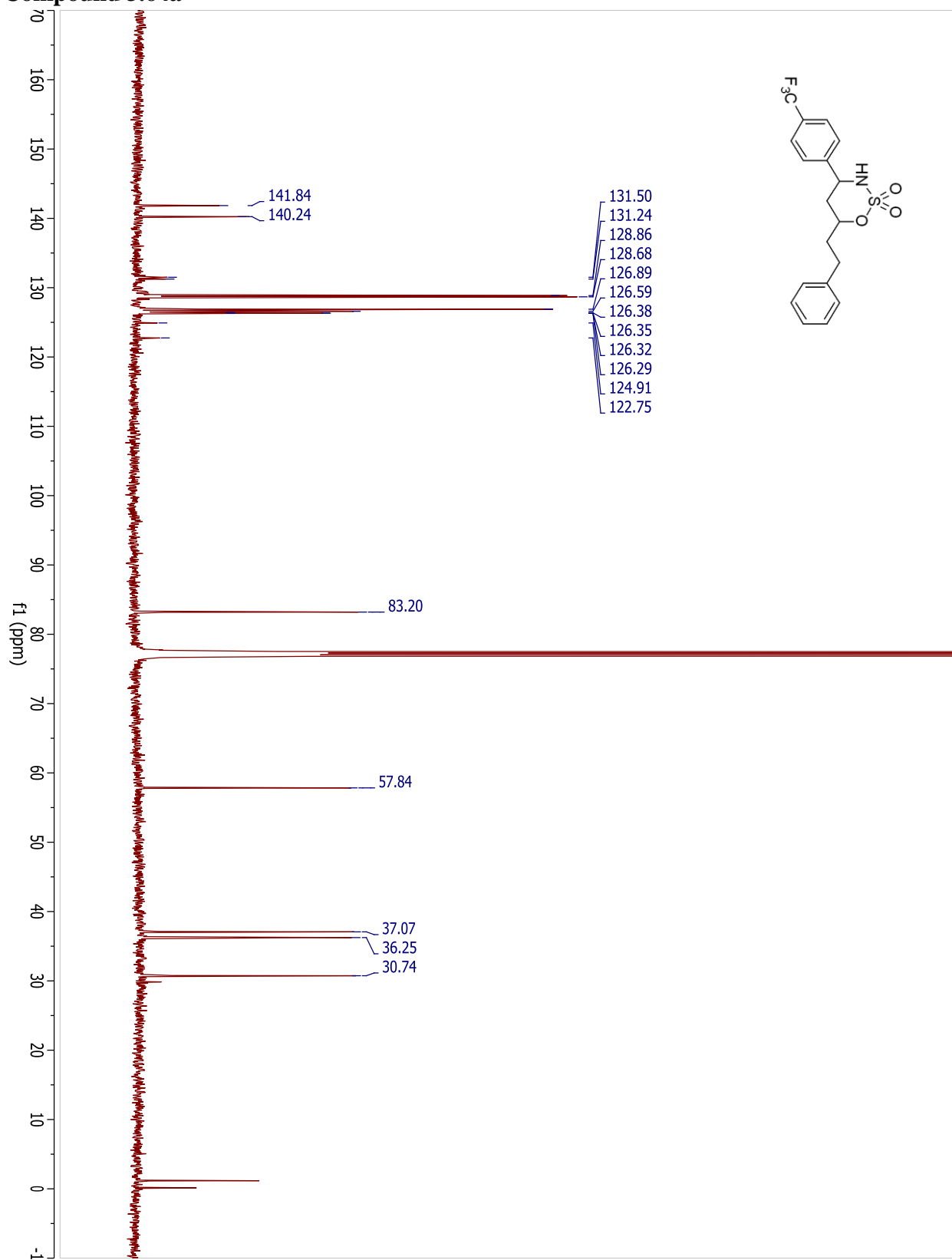
## Compound 3.63b



## Compound 3.64a

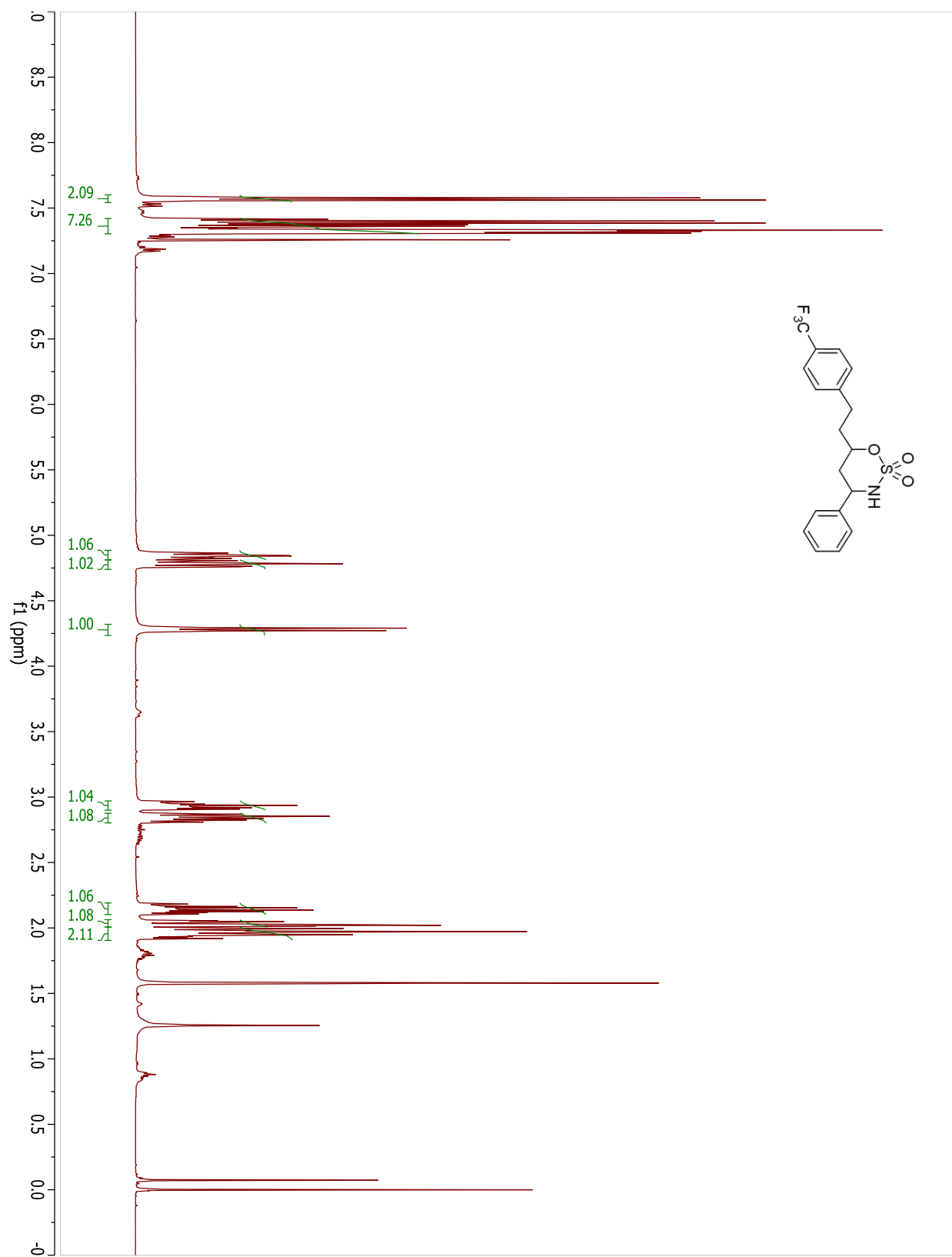


Compound 3.64a

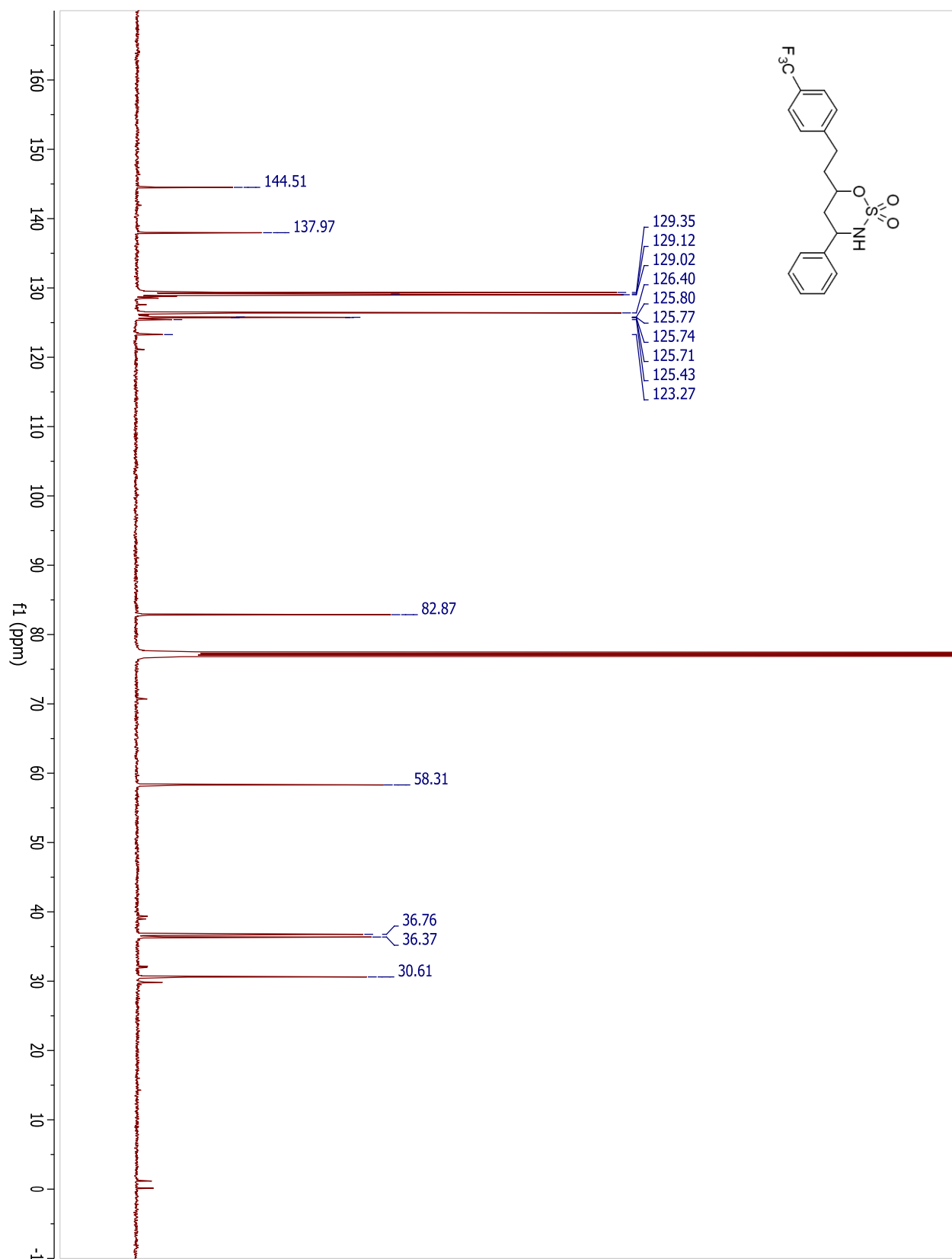




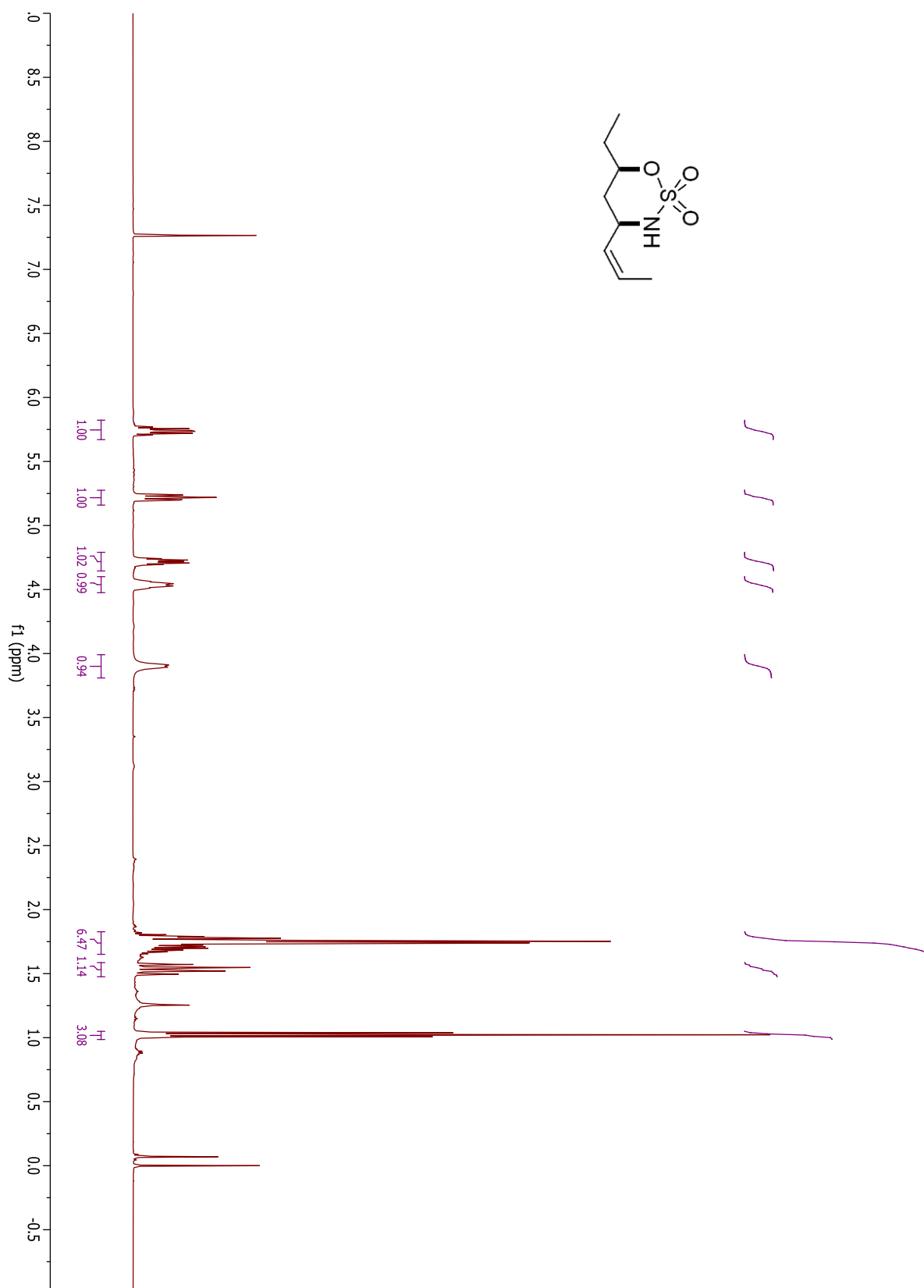
## Compound 3.64b



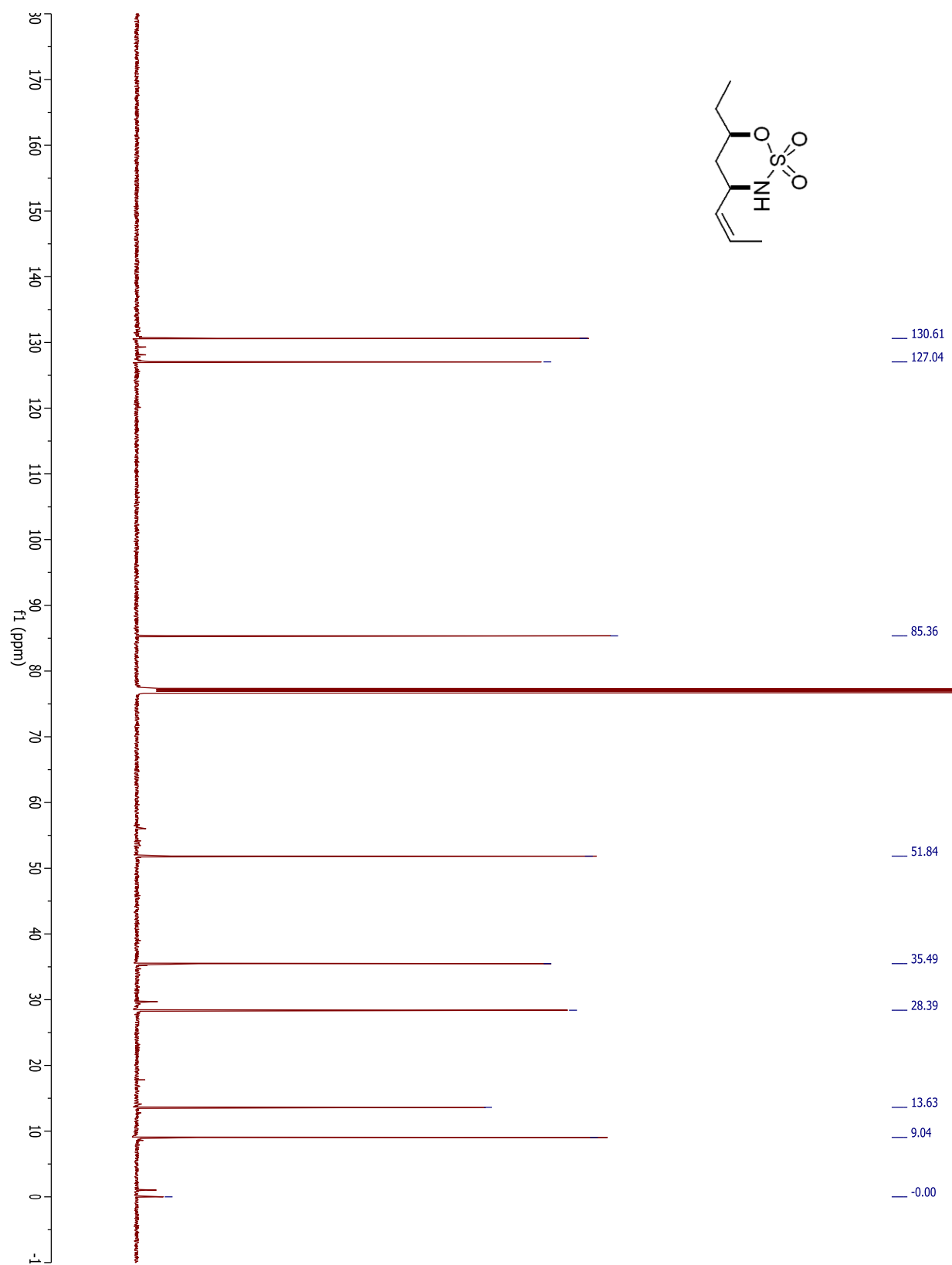
## Compound 3.64b



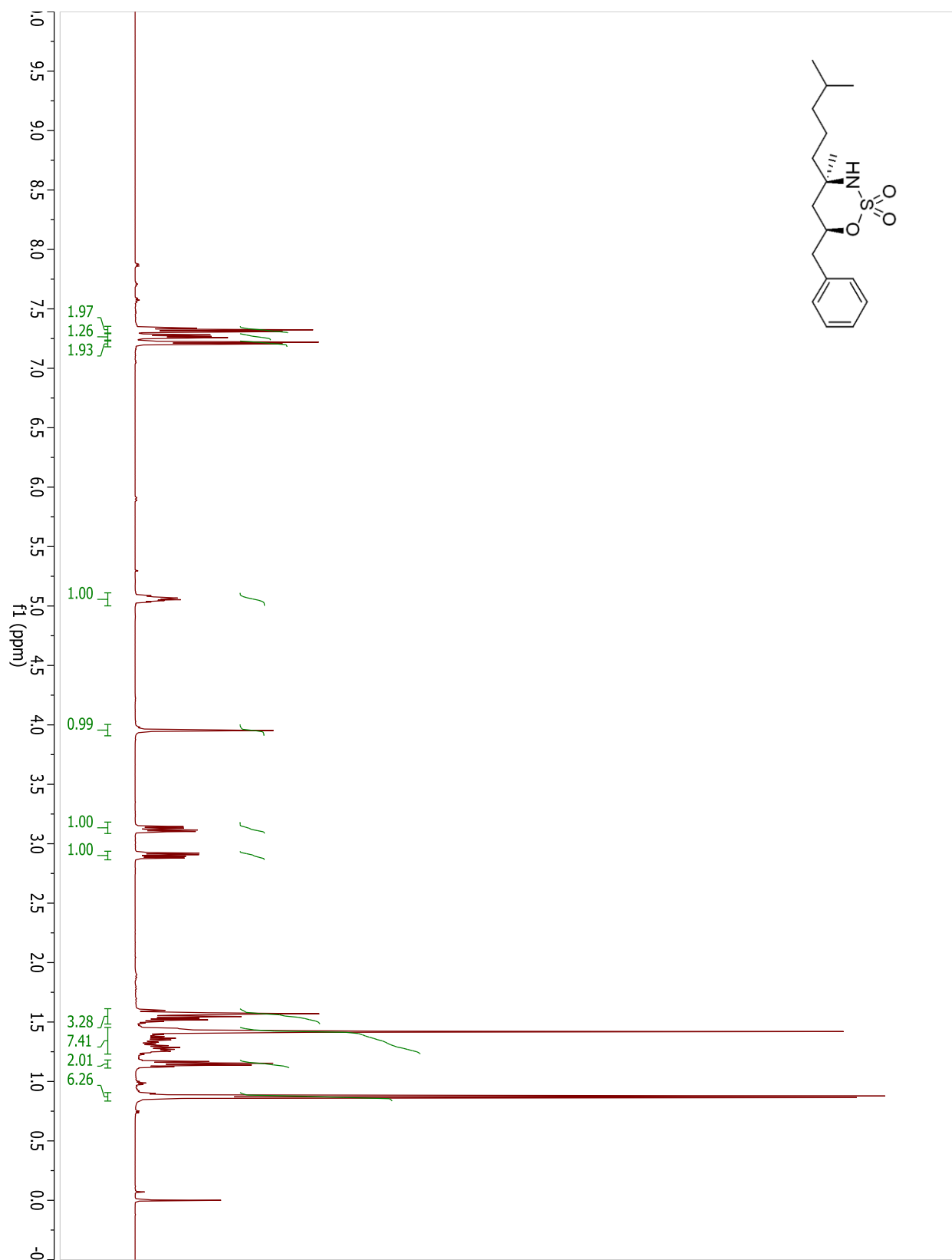
Compound 3.65a



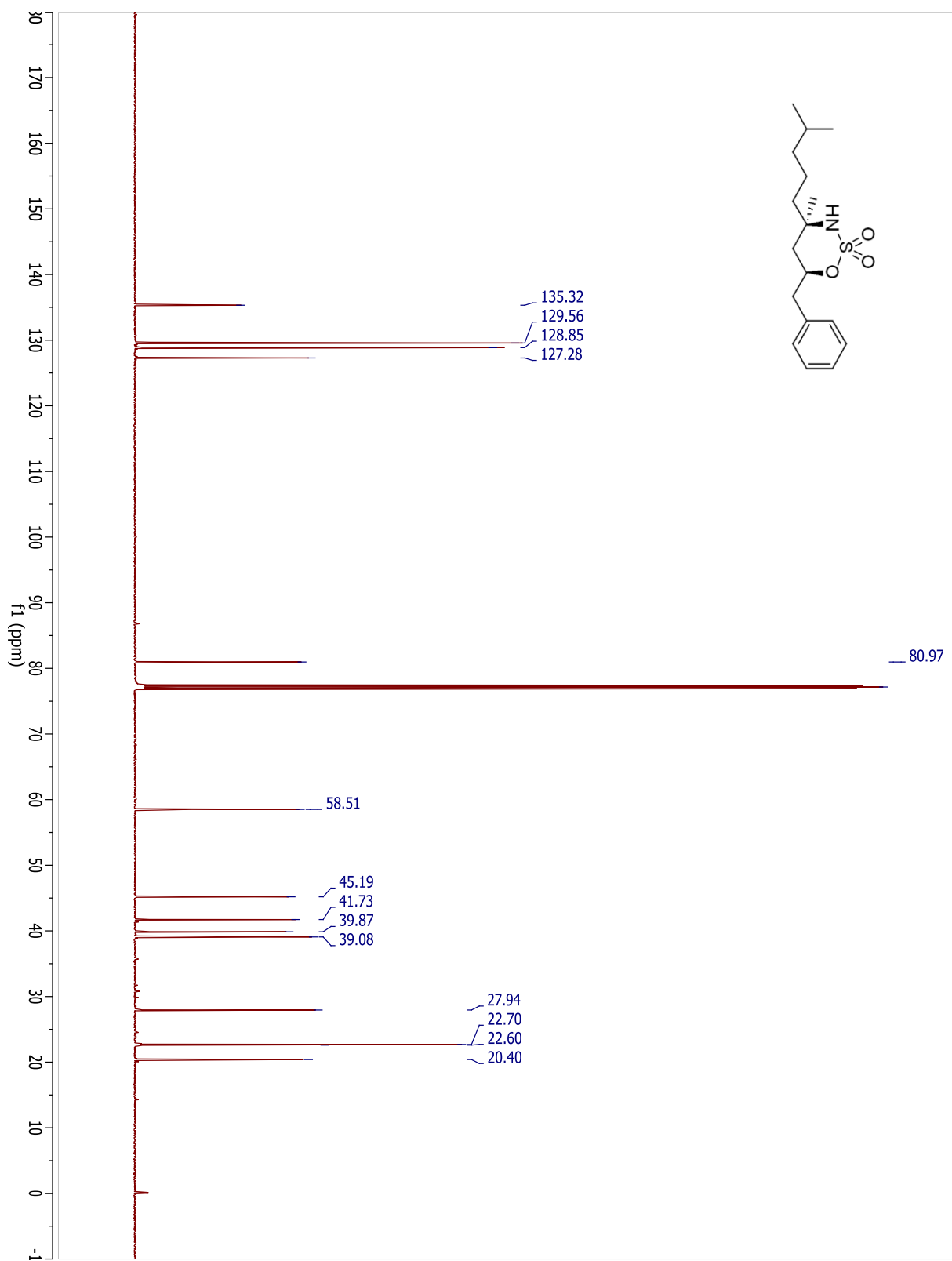
## Compound 3.65a

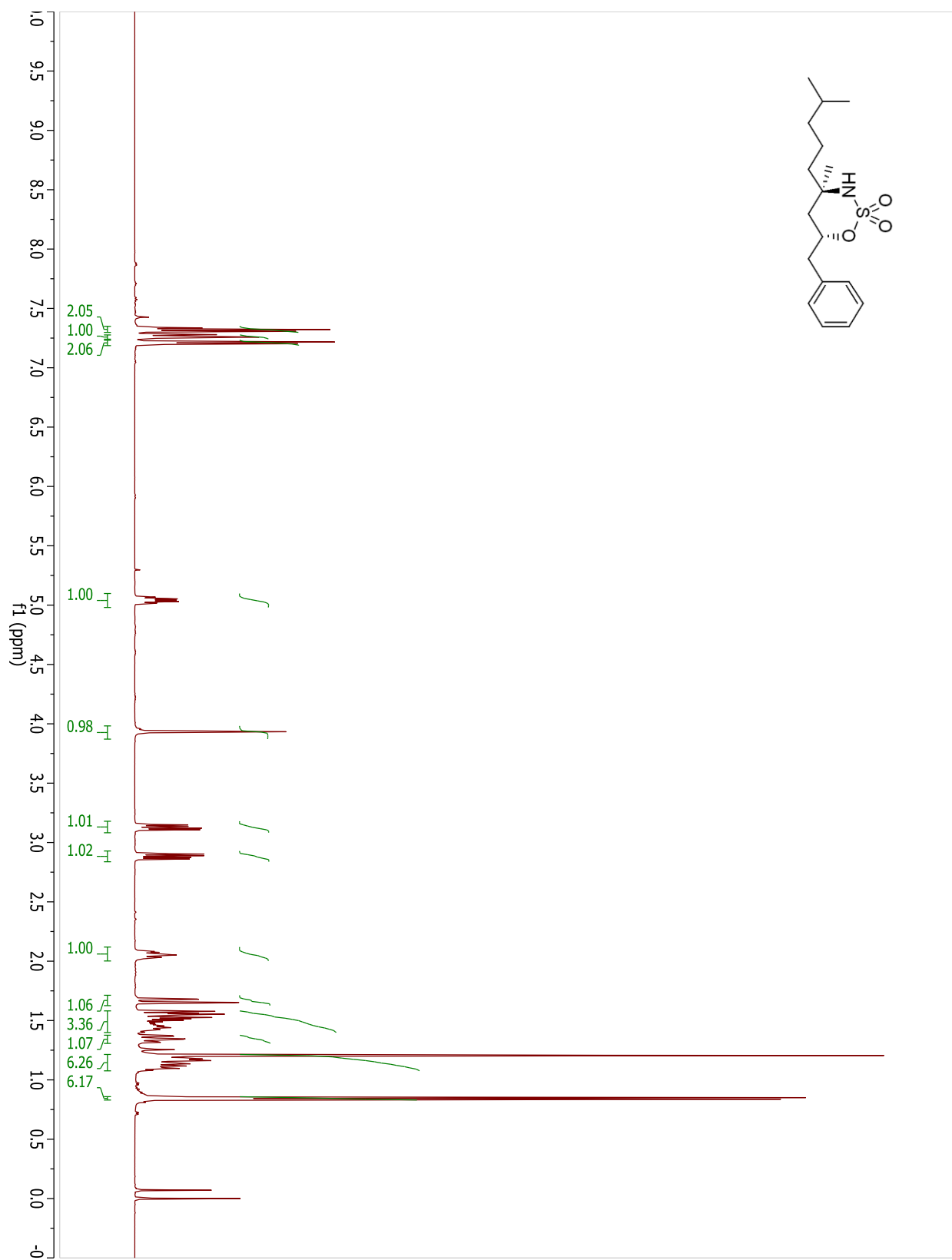


## Compound 3.66a

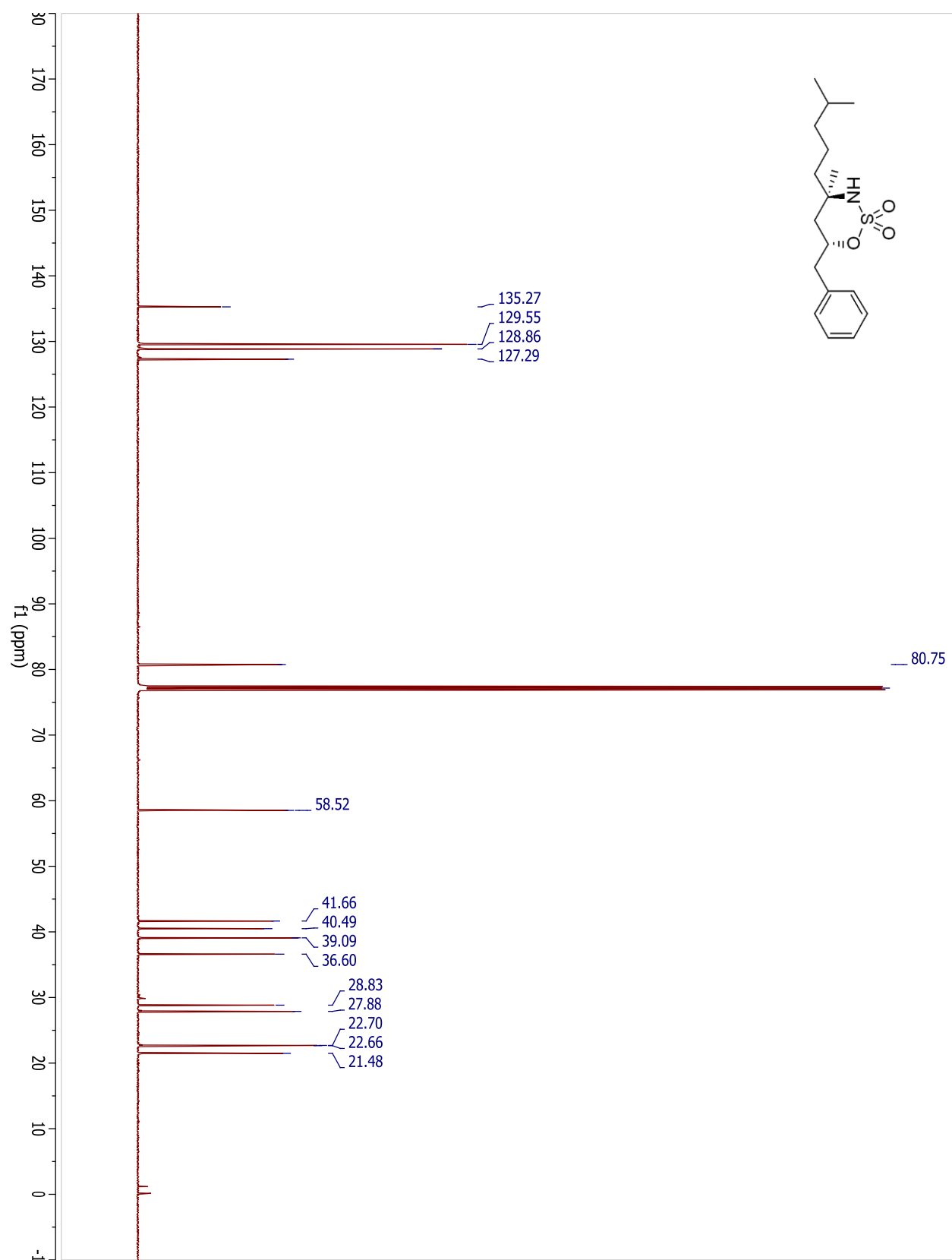


## Compound 3.66a



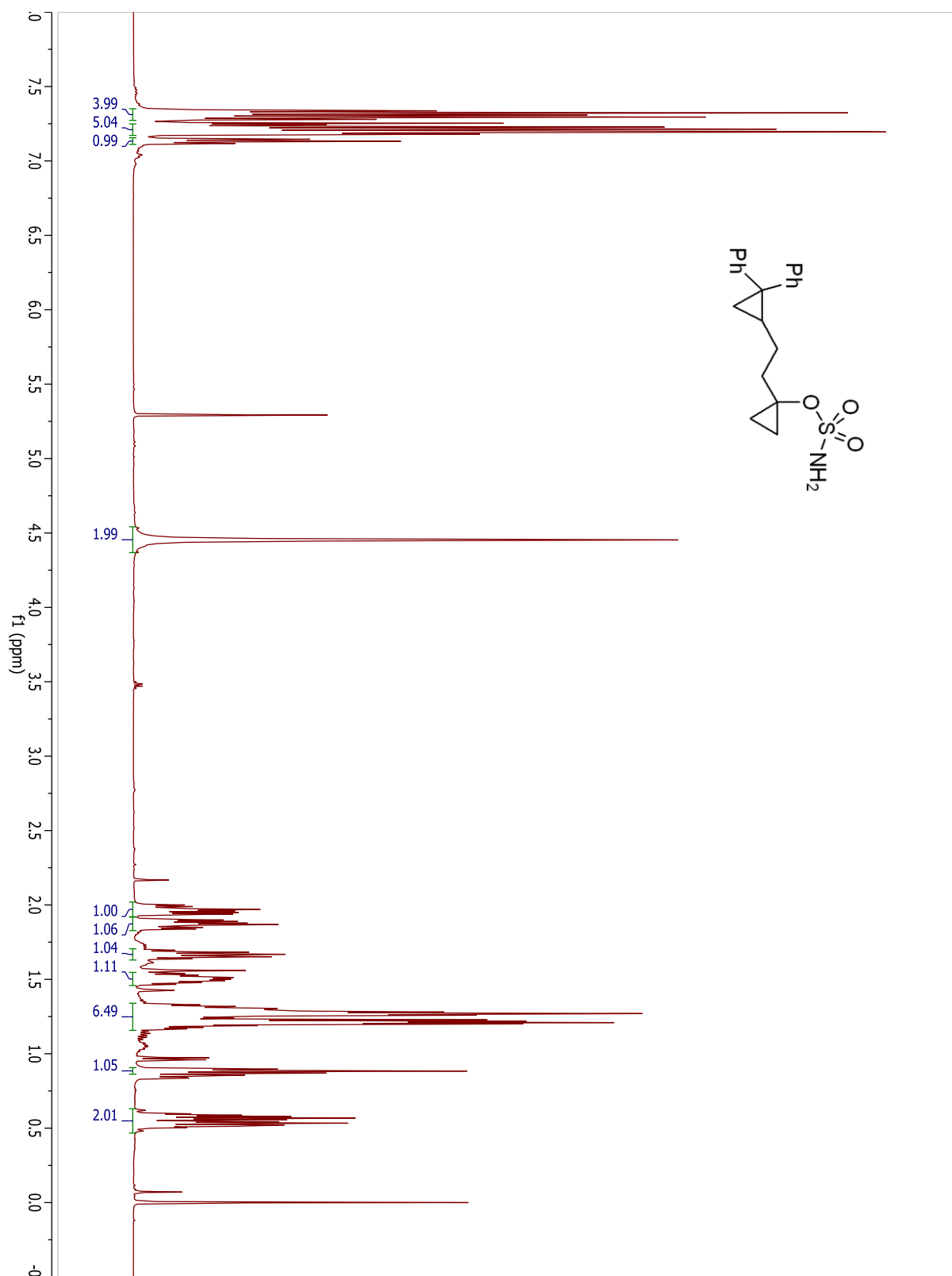
**Compound 3.66b**

## Compound 3.66b





## Compound 3.67a



## Compound 3.67a

